Autoantibodies in PLA2R1-associated membranous nephropathy : epitopes, immunodominance and clinical implication

Joana Justino

UNIVERSITÉ CÔTE D'AZUR

ÉCOLE DOCTORALE
SCIENCES DE LA VIE ET DE LA SANTÉ

THÈSE DE DOCTORAT

Autoanticorps dans la glomérulonéphrite extra-membraneuse associée à PLA2R1: épitopes, immunodominance et implication clinique

Joana JUSTINO

Institut de Pharmacologie Moléculaire et Cellulaire, CNRS, UMR 7275

Présentée en vue de l'obtention du grade de docteur en Interactions Moléculaires et Cellulaires **d'**Université Côte d'Azur

Dirigée par : Gérard Lambeau

Soutenue le : 02 Décembre 2019

Devant le jury, composé de :

Véronique BRAUD, Directrice de recherche, CNRS, IPMC, Valbonne, France. Président du jury.

An DE VRIESE, Professeure, Université de Gand, Gand, Belgique, Rapportrice.

Jérôme NIGOU, Directeur de recherche, CNRS, IPBS, Toulouse, France. Rapporteur.

Noémie JOURDE-CHICHE, Professeure, INRA, INSERM, C2VN-AMU, Marseille, France. Examinatrice.

Jack WETZELS, Professeur, Université de Radboud, Nimègue, Pays-Bas. Examinateur.

Gérard LAMBEAU, Directeur de recherche, CNRS, IPMC, Valbonne, France- Directeur de thèse.

ANR AGENCE NATIONALE DE LA RECHERCHE · FRM FONDATION RECHERCHE MÉDICALE · cnrs · SIGNALIFE · ipmc

Autoanticorps dans la glomérulonéphrite extra-membraneuse associée à PLA2R1: épitopes, immunodominance et implication clinique

Soutenue le 02 Décembre 2019

Devant le jury composé de:

Présidente du jury:
Dr. Véronique Braud, Directrice de recherche, CNRS, IPMC, Valbonne, France

Rapporteurs:
Dr. An DE VRIESE, Professeure, Université de Gand, Gand, Belgique
Dr. Jérôme NIGOU, Directeur de recherche, CNRS, IPBS, Toulouse, France

Examinateurs:
Pr. Noémie JOURDE-CHICHE, Professeure, INRA, INSERM, C2VN, Marseille, France
Pr. Jack WETZELS, Professeur, Université et Centre de Recherche Médicale Radboud, Nimègue (Nijmegen), Pays-Bas

Directeur de thèse:
Dr. Gérard LAMBEAU, Directeur de recherche, CNRS, IPMC, Valbonne, France

Résumé

La glomérulonéphrite extra-membraneuse (GEM) est une maladie auto-immune rénale rare (1,2/100.000 nouveaux cas par an), mais grave. C'est la principale cause de syndrome néphrotique chez l'adulte. L'évolution clinique des patients est variable, de la rémission spontanée à l'insuffisance rénale terminale. Malgré les recommandations internationales (KDIGO), le traitement de la GEM reste controversé et difficile. De meilleurs biomarqueurs sont nécessaires pour identifier les patients à risque de développer une maladie sévère, orienter le traitement et prédire sa réponse.

D'un point de vue physiopathologique, la GEM est caractérisée par la formation de dépôts immuns le long la membrane basale glomérulaire, associés à des lésions podocytaires et une forte protéinurie. La double identification du récepteur des phospholipases A_2 sécrétées (PLA_2R1) comme l'auto-antigène majeur de la GEM pour environ 70% des patients puis de la thrombospondine 7A contenant des domaines de type 1 (THSD7A) comme second autoantigène pour un autre groupe de 2 à 5% des patients est considérée comme une avancée majeure. Ces découvertes ont non seulement apporté une nouvelle base moléculaire pour mieux comprendre la pathogenèse de la GEM, mais ont aussi rapidement fourni des essais cliniques pour mieux diagnostiquer et suivre la maladie. Des titres élevés d'anticorps anti-PLA_2R1 sont associés à la gravité de la maladie et sont de mauvais pronostic.

PLA_2R1 est un récepteur membranaire glycosylé de 180 kDa comprenant 10 domaines extracellulaires dont un domaine riche en cystéine (CysR), un domaine fibronectine de type II (FnII) et huit domaines lectine de type C (CTLD). PLA_2R1 lie et inhibe l'activité enzymatique des $sPLA_2$ et joue un rôle dans différentes conditions inflammatoires. PLA_2R1 pourrait également agir comme suppresseur de tumeurs. Cependant, sa fonction dans les podocytes reste inconnue. Plusieurs types d'autoanticorps ciblant trois domaines distincts de PLA_2R1 (CysR, CTLD1 et CTLD7) ont été identifiés. Ces autoanticorps sont probablement produits par un mécanisme d'étalement épitopique et leur présence simultanée est associée à la gravité de la maladie et à un mauvais prognostic.

L'objectif principal de cette thèse était de caractériser l'ensemble des épitopes PLA_2R1 et d'évaluer leur pertinence clinique, en particulier comme prédicteurs d'évolution de la maladie et de la réponse au traitement. En utilisant différents outils de biologie moléculaire et cellulaire, nous avons montré que les autoanticorps de patients peuvent reconnaître jusqu'à 5 des 10 domaines PLA_2R1. Le criblage par

ELISA d'une cohorte de 142 patients ayant une GEM associée à PLA_2R1 pour leur réactivité contre chacun des 10 domaines de PLA_2R1 révèle différentes prévalences. Le titre des anticorps et la positivité pour certains épitopes apparaissent comme des biomarqueurs pertinents pour prédire le devenir des patients et la réponse au traitement. Nous avons également identifié les domaines CysR et CTLD1 comme deux épitopes immunodominants alternatifs, suggérant que la réponse autoimmune peut progresser de deux façons différentes. D'un intérêt clinique potentiel, les patients présentant une immunodominance CysR semblent avoir une évolution clinique plus favorable et une meilleure réponse au traitement que les patients présentant une immunodominance CTLD1. En conclusion, ces travaux permettent de mieux comprendre comment se développe la réponse auto-immune contre PLA_2R1 et pourraient contribuer au développement de nouveaux tests diagnostiques vers une médecine plus personnalisée de la GEM.

Mots-clés: glomérulonéphrite extra-membraneuse, PLA_2R1, épitopes immunodominance, diagnostic, pronostic.

Abstract

Membranous Nephropathy (MN) is a rare (1.2/100,000 new cases per year) but severe autoimmune kidney disease. It is also a common cause of nephrotic syndrome in adults. The clinical outcome of patients is complex and variable, going from spontaneous remission to end-stage renal disease (ESRD), with persistent high levels of proteinuria. Despite international KDIGO recommendations, MN treatment remains highly controversial and challenging. Better biomarkers are needed to identify patients at risk of severe disease, orient treatment decision and predict response to therapy.

From the pathophysiological point of view, MN is characterized by the formation of immune complex deposits at the glomerular basement membrane leading to podocyte injury and proteinuria. A major breakthrough was the identification of phospholipase A_2 receptor 1 (PLA_2R1) as the main autoantigen of MN for about 70% of the patients, followed by the identification of thrombospondin–type 1 domain containing 7A (THSD7A) as a second autoantigen in another group of 2-5% of patients. These discoveries not only gave a new molecular basis to better understand MN pathogenesis but also rapidly provided clinical assays to diagnose MN and monitor disease activity. Anti–PLA_2R1 titers correlate with disease activity and have a prognostic value. Another major discovery was the identification of three distinct epitope-containing domains in PLA_2R1-associated MN: CysR, CTLD1 and CTLD7. The severity of the disease and poor clinical outcome were found to be associated with multiple autoantibodies targeting these domains. These autoantibodies are likely produced by a mechanism of epitope spreading.

PLA_2R1 is a 180 kDa glycosylated transmembrane receptor with a large extracellular region comprising 10 distinct domains: a cysteine-rich domain (CysR), a fibronectin type II domain (FnII) and eight different C-type lectin-like domains (CTLDs). PLA_2R1 binds $sPLA_2$ and inhibits their enzymatic activity, thereby playing a role in immune and inflammatory conditions. PLA_2R1 may also act as a tumor suppressor in cancer. However, its biological function in podocytes is largely unknown.

The major aim of my thesis was to characterize the full set of PLA_2R1 epitopes, and analyze their clinical relevance, in particular as predictors of clinical outcome and response to treatment. Using different molecular and cellular biology techniques, we have demonstrated that patients' autoantibodies can recognize

multiple epitopes in up to 5 of the 10 PLA_2R1 domains. Further screening of a cohort of 142 PLA_2R1-associated MN patients by ELISA, with each of the 10 individual domains of PLA_2R1 indicated different prevalence towards each domain. In this cohort, anti-PLA_2R1 titer and epitope positivity appear as relevant biomarkers to predict clinical outcome and response to treatment. We also identified the CysR and CTLD1 domains as two alternative immunodominant epitope-domains, suggesting that the driving force of the autoimmune response may progress towards two different pathways. Of potential clinical interest, patients with a CysR versus CTLD1 immunodominance had different response to treatment and clinical outcome. Together, this work provides a better understanding of the trajectory of the PLA_2R1 autoimmune response within the pathogenesis of PLA_2R1–associated MN, and might contribute to the development of specific diagnosis tests towards more personalized medicine.

Keywords: membranous nephropathy, PLA_2R1, epitopes, immunodominance, diagnosis, prognosis.

“Only one who devotes himself to a cause with his whole strength and soul can be a true master. For this reason mastery demands all of a person.”

~Albert Einstein~

To my parents

To my sister

"The value of things is not the time they last, but the intensity with which they occur. That is why there are unforgettable moments, inexplicable things and unique people."

~Fernando Pessoa~

In memory of grandpa

In memory of Pr. Tiago Henriques-Coelho

Acknowledgments

I would like to convey my sincere and deepest gratitude to all the people who in one way or another have contributed to this work. Without each one of these extraordinary persons none of this would have been possible.

I will be forever grateful to Dr. Gérard Lambeau for believing in me and accepting me as his mentee when I was about to give it up. Thank you for your continuous patience, support, dedication and encouragement throughout this PhD. Thank you for your enthusiasm, immense knowledge, for all the discussions, training and guidance, which were essential for this work and have greatly contributed for my growth as research scientist. Your dedication and passion for good science and your efforts to convey it to your mentees are a true inspiration.

I would like to express my deep appreciation to the members of the PhD committee for accepting to evaluate my work and for being part of this committee. I thank Dr. An de Vriese and Dr. Jérôme Nigou for reviewing this manuscript and for their insightful comments. I also thank Dr. Véronique Braud and Pr. Jack Wetzels, not only as member of this committee but also as my PhD advisors, for their collaboration and evaluation of my work during the PhD. I am also thankful to Pr. Noémie Jourde-Chiche for accepting examines this work as well as for her valuable contribution and comments.

I would like to express my gratitude to the Laboratory of Excellence SIGNALIFE program for my PhD fellowship as well as to the *Fondation pour la Recherche Médicale* for the *"Fin de thèse"* fellowship that was granted to me.

I am also grateful to all our collaborators, particularly to Pr. Pierre Ronco, Pr. Jack Wetzels, Dr. Alexandra Rousseau and Dr. Anne-Els van de Logt for their collaboration, for their valuable discussions and advices. Thank you for sharing your knowledge and insights particularly within the nephrology and/or statistical field(s).

I am thankful to all the lab members for the all the delightful shared moments, for their welcome and support. Christelle, thank you for all the support and scientific feedback as well as for the memorable travels and moments that we shared inside and outside the lab. Guillaume, thank you for your welcome in the lab since day one, with your good humour, intensive training and numerous stimulating discussions. Christine, thank you for your gentleness and help. Barbara, thank you for your help in the inclusion of patients and the collection of their clinical data for this study. Agnès, my most recent partner in "crime", thank

you for your patience, kindness and all the insightful discussions and advices. Franck, thank you for your benevolence and fruitful discussions. Alice, thank you for your amiability. Joëlle, thank you for your kindness and interesting discussions. I would also grateful to former members of the lab, particularly, Vesna, for her guidance and shared scientific expertise as well as for her friendliness and good humour. Joël, for his helpfulness even after his departure. Sarah, for her kindness and good humour. Louise and Dominique for their amiability. I also thank to Delphine Viard, a trainee that I had the chance to supervise, for her hard work and enthusiasm.

I am greatly thankful to my long-time friends and to the friendships forged during this adventure. Thank you for the patience, support and wonderful moments that we lived and shall continue living. Without each one of you my life would not be full of *"unforgettable moments, inexplicable things and unique people"*.

Finally, and most importantly, I will forever owe my deepest gratitude to my family. To my parents, thank you for raising me, for your unconditional support and love. Above all, thank you for being *"true masters",* without you, *"your whole strength and soul"*, I would never have become the person who I am today. To my sister for her unconditional love, trust, encouragement and support.

Table of Contents

List of Figures xv
List of Tables xvii
List of Abbreviations xix
Part I – Introduction 1
Chapter 1 – Autoimmune Diseases 3
1.1 Epidemiology 6
1.2 Diagnosis 6
1.3 Aetiology 8
1.3.1 Environmental factors 8
1.3.1.1 Molecular mimicry 9
1.3.1.2 Post-translational modifications 9
1.3.2 Genetic susceptibility 11
1.4 Pathophysiology 12
1.4.1 Epitope spreading 14
1.5 Treatment 17
Chapter 2 – Membranous Nephropathy 19
2.1 Kidney physiology and glomerular diseases 21
2.2 Membranous nephropathy 22
2.2.1 History 23
2.2.2 Clinical classification 24
2.2.3 Clinical features, presentation and natural history 27
2.2.4 Diagnosis and histopathological features 28
2.2.5 Prognosis and treatment 30
2.2.5.1 Conservative treatment 32
2.2.5.2 Immunosuppressive treatment 33
2.2.6 Genetic susceptibility 34
2.3 Autoantigens of human MN 35
2.3.1 Neutral endopeptidase (NEP) 37
2.3.2 Phospholipase A_2 receptor 1 (PLA_2R1) 38
2.3.3 Thrombospondin type–1 domain containing 7A (THSD7A) 39
2.3.4 Cytoplasmic autoantigens 42
2.3.5 Exostosin 1/Exostosin 2 43
2.3.6 Exogenous autoantigens 44
2.4 Animal models of MN 44
2.4.1 Heymann nephritis model in rat 45

2.4.2 Heymann nephritis model in mice 46
2.4.3 cBSA animal model of MN 47
2.4.4 PLA_2R1 animal model of MN 48
2.4.5 THSD7A animal model of MN 48
2.5 Pathophysiology of MN 49
2.5.1 Immunoregulation and initial phase of the autoimmune response 51
2.5.2 Spreading of the autoimmune response 51
2.5.3 Formation and deposition of immune complexes 53
2.5.4 Pathogenic effect of the autoantibodies 55
2.5.4.1 Autoantibodies effect through complement activation 55
2.5.4.2 Direct effect of autoantibodies 59
2.5.5 Protective mechanisms 61
Chapter 3 – PLA_2R1 63
3.1 C-type lectin superfamily 65
3.1.1 The macrophage mannose receptor family 69
3.1.1.1 Biological functions of PLA_2R1 paralogs 70
3.2 The phospholipase A_2 receptor 1 (PLA_2R1) 72
3.2.1 PLA_2R1 structure and expression 73
3.2.2 PLA_2R1 ligands 76
3.2.3 Physiological and pathophysiological roles of PLA_2R1 77
3.2.3.1 PLA_2R1 role in inflammation 77
3.2.3.2 Role of PLA_2R1 in cellular senescence and cancer 78
3.2.3.3 Other roles of PLA_2R1 80
Chapter 4 – PLA_2R1-associated MN 83
4.1 Aetiology of PLA_2R1-associated MN 85
4.2 PLA_2R1 epitopes and epitope spreading 87
4.3 Diagnosis and prognosis of PLA_2R1-associated MN 91
4.3.1 Biopsy staining of the PLA_2R1 autoantigen 92
4.3.2 Autoantibodies detection 93
4.3.3 Clinical value of anti-PLA_2R1 autoantibodies 94
Chapter 5 – Aims 99
Part II – Results 103
Chapter 6 – PLA_2R1 autoantibody response in MN and clinical association 105
6.1 Epitope-containing domains in the N-terminal region CysR-FnII-CTLD1 108
6.2 Epitope-containing domains in the CTLD2–CTLD8 region 110
6.3 Epitope prevalence and correlation with anti-PLA_2R1 titer 111
6.4 Immunodominant epitopes and correlation with anti-PLA_2R1 titer 112

6.5 Clinical relevance of anti-PLA$_2$R1 titer, epitope positivity and immunodominance 112

Article 1 (in preparation) 115

Chapter 7 – Anti-PLA$_2$R1 antibodies as predictors of progression and clinical outcome in MN 199

7.1 Development of ELISAs for the detection of autoantibodies against THSD7A, PLA$_2$R1, CysR, CTLD1 and CTLD7 202

7.2 Patients stratification and selection 202

7.3 Association between the autoimmune response, clinical characteristics and clinical outcome 203

Chapter 8 – Novel ELISA for patients with THSD7A-positive MN 209

Article 2 215

Part III – Discussion and conclusion 259

Chapter 9 – Discussion 261

9.1 From analysis of the autoimmune humoral response to a working model of the autoimmune response in PLA$_2$R1-associated MN 263

9.1.1 The saga of PLA$_2$R1 epitopes' discovery and relationship to titer 264

9.1.1.1 PLA$_2$R1 epitope-containing domains or "macroepitopes" 264

9.1.1.2Towards the identification of the genuine epitopes or "microepitopes" 267

9.1.2 Prevalence and PLA$_2$R1 epitope spreading 270

9.1.3 Driving-forces of the autoimmune response 272

9.2 Biomarkers of PLA$_2$R1-associated MN 276

Chapter 10 – Conclusions and perspectives 279

10.1 Pathophysiology and natural course of MN 281

10.2 Clinical impact in MN 283

Bibliographic References 285

List of Figures

Figure 1.1 Development of an autoimmune disease 5

Figure 1.2 Detection of autoantibodies 7

Figure 1.3 General view of the pathophysiology of an autoimmune immune disease 12

Figure 1.4 The endocytic pathway as the primary mechanism of B cell epitope spreading 15

Figure 1.5 Somatic hypermutation as a mechanism of B cell epitope spreading . 16

Figure 2.1 Physiology of the renal glomerulus in MN 22

Figure 2.2 Representative cases of the different electron-microscopy stages of MN 29

Figure 2.3 Representative cases of glomerular alteration of MN observed under light microscopy and immunofluorescence 30

Figure 2.4 Schematic diagram of the autoantigens found to be implicated in MN until now 36

Figure 2.5 Pathophysiology of MN 50

Figure 2.6 Proposed mechanisms for the formation and deposition of the immune complexes in MN 54

Figure 2.7 Mechanism of activation of the complement cascade 56

Figure 3.1 The C-type lectin domain (CTLD) superfamily 67

Figure 3.2 Ribbon diagrams of representative CTLDs 68

Figure 3.3 Structure of the CysR and FnII domains from members of the macrophage mannose receptor family. 69

Figure 3.4 The phospholipase A_2 receptor 1 (PLA_2R1) 74

Figure 4.1 Renal biopsy staining for PLA_2R1 and THSD7A autoantigens. 92

Figure 4.2 Monitoring and prognostic algorithm as proposed by De Vriese and colleagues (De Vriese et al., 2017). 96

Figure 7.1 Cumulative incidence of progression (plain line) and spontaneous remission (dot line) in a cohort of 168 PLA2R1-positive patients with a median follow-up of 5 years. 205

Figure 9.1 Progression of the autoimmune response in PLA_2R1-associated MN 274

List of Tables

Table 1.1 Geo-epidemiological characteristics of some human autoimmune diseases. 6

Table 7.1 Baseline clinical characteristics and clinical outcome of the 168 PLA_2R1-positive MN patients included in the study. 204

Table 7.2 Baseline clinical characteristics and clinical outcome of patients according to anti-PLA_2R1 tertiles assessed by the commercial Euroimmun ELISA. 206

Table 7.3 Baseline clinical characteristics and clinical outcome according to spreading. 207

Table 7.4 Baseline clinical characteristics of progressors and non-progressors... 207

List of Abbreviations

AR	Aldose reductase
CRD	Carbohydrate-recognition domain
CTLD	C-type lectin-like domain
CysR	Cysteine-rich domain
DEC-205	Dendritic cell-205 kDa or Lymphocyte antigen 75
eGFR	Estimated glomerular filtration rate
ELISA	Enzyme-linked immunosorbent assay
Endo180	Endothelial-180 kDa or Mannose receptor 2
αENO	Alpha-enolase
ESRD	End-stage renal disease
FnII	Fibronectin type II domain
GBM	Glomerular basement membrane
GWAS	genome-wide association study
HEK293	Cellular line of "Human Embryonic Kidney 293"
HLA	Human leukocyte antigen
hPLA$_2$R1	Human phospholipase A$_2$ receptor 1
iC1	Immunodominant CTLD1
iCR	Immunodominant CysR
IgG	Immunoglobulin G
IIFT	Indirect immunofluorescence test
IL	Interleukin
KDIGO	Kidney Disease Improving Global Outcomes
LBD	Ligand binding domain
LPS	Lipopolysaccharide
MBL	Mannose-binding lectin
MHC	Major histocompatibility complex
MN	Membranous nephropathy
MRC1	Mannose receptor 1
mPLA$_2$R1	Mouse phospholipase A$_2$ receptor 1
NEP	Neutral endopeptidase
Non-iDom	Non-immunodominant
PDB	Protein data bank
PLA$_2$R1	Phospholipase A$_2$ receptor 1
PTM	Post-translational modification
rbPLA$_2$R1	Rabbit phospholipase A$_2$ receptor 1
ROS	Reactive oxygen species
RU	Relative unit
SNP	Single nucleotide polymorphism
SOD2	Superoxidase dismutase 2
sPLA$_2$	Secreted phospholipase A$_2$
THSD7A	Thrombospondin type 1 domain-containing 7A
TNF	Tumour necrosis factor
TPS-1	Thrombospondin-1

Part I
Introduction

Chapter 1

Autoimmune Diseases

The primary function of the immune system is to protect and defend the host from infectious agents. This function is highly dependent on the immune system capacity to distinguish self from non–self–molecules. A disruption of this ability, known as breach of tolerance, can lead to an autoimmune disease (Wang et al., 2015). Of note, autoimmune diseases can be broadly classified as organ-specific when the autoimmune response targets a specific tissue, such as in type 1 diabetes and membranous nephropathy (MN), or systemic when the immunological dysfunction targets multiple organs, like in rheumatoid arthritis and systemic lupus erythematous.

The immune system produces T and B cells that can be reactive to self-antigens producing autoantibodies. These autoantibodies can be found under physiological or pathophysiological conditions (Figure 1.1) (Hang et al., 1997; Wang et al., 2015). In physiological conditions, they can be found transiently without clinical signs of a disease. Within this scenario, the autoantibodies actually help to eliminate degraded self-antigens and maintain homeostasis. During central and peripheral tolerance, the majority of self-reactive cells are (1) killed before becoming active within the immune system, (2) cleared from the immune system due to over-activation (cells are rendered anergic), or (3) removed from the immune system by regulatory T cells (Tregs). When one of these mechanisms fails, and tolerance is broken, self-reactive cells become functional within the immune system and an autoimmune response followed by an autoimmune disease can be engaged.

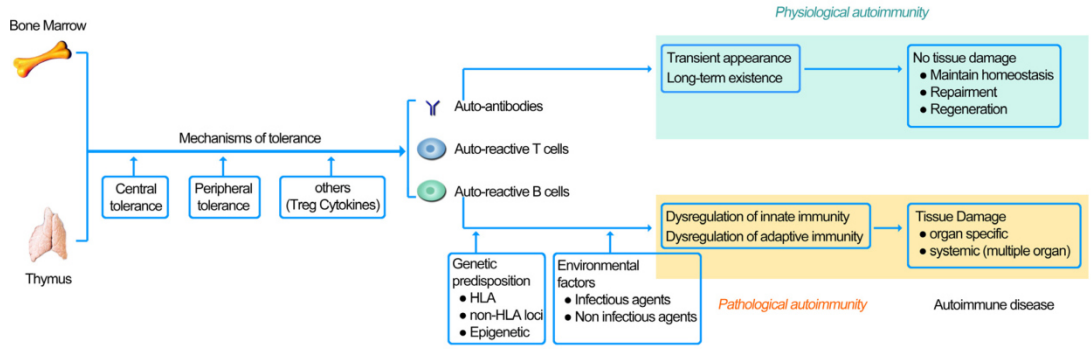

Figure 1.1 – Development of an autoimmune disease. Even though there are strict control mechanisms of tolerance, autoreactive B and T cells can escape them and be found in healthy individuals. They will remain harmless until there is a break in tolerance, due to genetic predisposition or environmental triggers. This latter will lead to a pathological autoimmune state from which an autoimmune disease can develop. *Adapted from (Wang et al., 2015) with copyright permission from "John Wiley & Sons".*

1.1 Epidemiology

Overall, autoimmune diseases have been diagnosed in 3-5% of the population, often starting during adulthood and affecting more women than men (with a 2.7:1 ratio). Certain ethnic groups are more prone to some autoimmune diseases than others, for example lupus is more common in African-American and Hispanic people than Caucasians (Hayter et al., 2012; Wang et al., 2015). Still, naturally, each autoimmune disease has its own geo-epidemiological characteristics (incidence, prevalence, age of onset, female-to-male ratio, etc.) (Table 1.1).

Table 1.1 – Geo-epidemiological characteristics of some human autoimmune diseases. F, female; M, male. *Adapted from (Wang et al., 2015) with copyright permission from "John Wiley & Sons".*

Disease	Onset Age (years)	Gender (F:M)	Incidence (per 100,000 person-years)		
			Europe	North America	Asia and Middle East
Multiple sclerosis	20–40	2:1	0.8–8.7	2.7–7.5	0.7–3.6
Type 1 diabetes	6–13	1:1	> 20	10–20	< 1
Primary biliary cirrhosis	50–60	10:1	1.4–3.1	2.7 (USA)	0.34–0.42
Grave's disease	50–60	5:1	21–50	38	120
Systemic lupus erythematous	30–50	9:1	1.0–5.0	1.2–8.7	0.9–3.1
Rheumatoid arthritis	44–55	2:1	9–36	31–45	8–42

1.2 Diagnosis

Type 1 diabetes and autoimmune thyroid disease are the most common conditions, but there are around 100 different autoimmune diseases. Some of them might share certain common early symptoms such as fatigue, swelling and redness, low-grade fever, trouble concentrating and muscle aches, which makes the initial diagnosis by the physicians quite tricky. Some autoimmune diseases, like psoriasis or rheumatoid arthritis, may also have what is called "flare-ups", meaning that the symptoms get worse or disappear, along with immunological relapse or spontaneous remission.

As referred, diagnosis can be difficult, and usually the physician starts by relaying on the patients symptoms and clinical history. When feasible, biopsy of the affected tissue is performed, providing evidence of the presence or absence of immune tissue injury (Hang et al., 1997). Advances in the understanding of the pathophysiological mechanisms and natural history of each individual disease have allowed the development of several tools to detect and measure specific and non-

specific autoantibodies to better diagnose numerous specific autoimmune diseases and in some cases even monitor them (Figure 1.2) (Ludwig et al., 2017). Indirect immunofluorescence assay (IFA or IIFT) is one of the "gold standard" tests. In this technique, tissue cryosections or cultured cells containing the autoantigen are incubated with samples (usually serum) from patients that are detected with fluorochrome-labeled secondary antibodies (Anderson et al., 1986). A semi-quantification of autoantibody concentration can be estimated by titering out the sample. Western blot (WB) is another technique frequently used to qualitatively detect autoantibodies (Burnette, 1981; Towbin et al., 1979). Patients' samples are incubated with a membrane containing the immobilized target autoantigen previously transferred from a gel electrophoresis. The autoantibodies can then be detected using secondary antibodies coupled to a reporter. Another classical method to detect autoantibodies is the ELISA (enzyme-linked immunosorbent assay) (Engvall et al., 1971; Yalow et al., 1960). A purified antigen of interest is immobilized on a solid phase and it is then incubated with patients' samples followed by the incubation with a secondary antibody coupled to reporter like an enzymatic substrate. Of note, all of these methods can and have been used to diagnose and monitor MN (chapter 4.3.2).

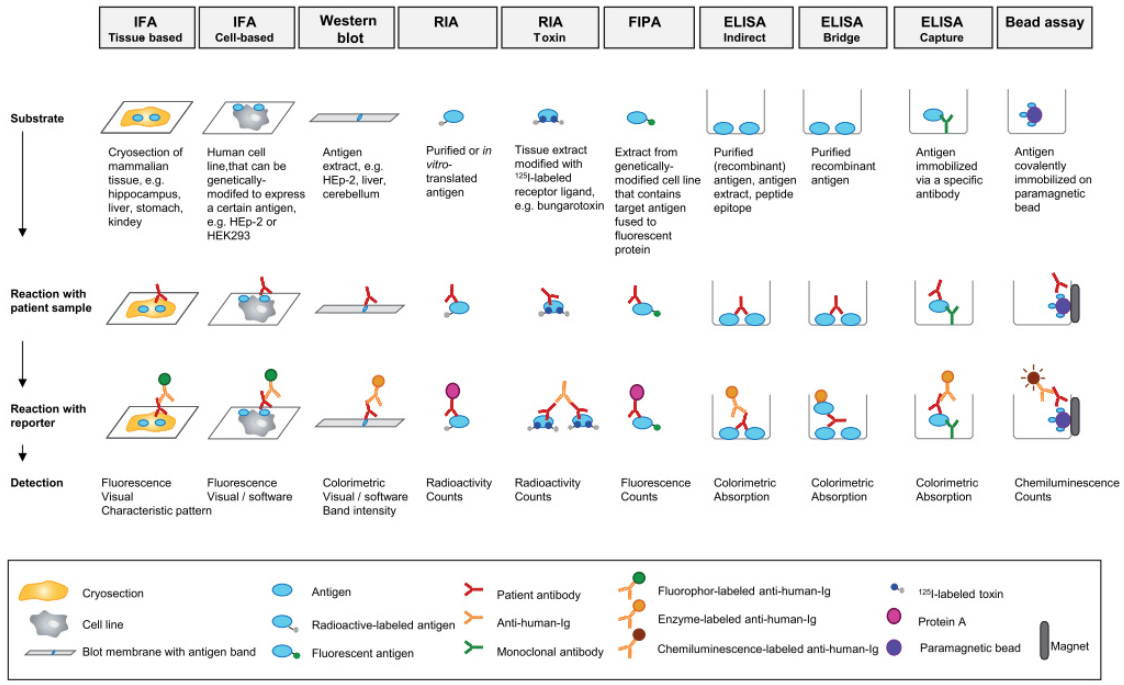

Figure 1.2 – Detection of autoantibodies. Methods to detect and quantify autoantibodies present in patients' samples. ELISA, enzyme-linked immunosorbent assay; FIPA, fluorescence immunoprecipitation assay; IFA, indirect immunofluorescence assay; RIA, radioimmunoassay. *Adapted from* (Ludwig et al., 2017).

1.3 Aetiology

An autoimmune response can be triggered by environmental factors and might be dependent on genetic predisposition. For most autoimmune diseases, the aetiology is not well understood or is even completely unknown.

1.3.1 Environmental factors

Multiple environmental factors, including pathogenic microorganisms, xenobiotics, air pollution, smoking, lifestyle, microbiota and diet, have been suggested to trigger an autoimmune response (Floreani et al., 2016). For instance, under physiological conditions, the microbiota is important for nutrient digestion, xenobiotic degradation, vitamin production and protection from pathogens, among others. However, changes in the microbiome content leading to disruption (dysbiosis) of the symbiotic interaction with the host (symbiosis) have been considered as a trigger of several autoimmune diseases (McLean et al., 2015; Shamriz et al., 2016). Dysbiosis of the gut microbiota can be associated to inflammatory bowel disease, type 1 diabetes and multiple sclerosis. Changes in the oral microbiota may be linked to rheumatoid arthritis and alteration in the skin microbiota might be connected to psoriasis.

The increased incidence of autoimmune diseases over the last decades has led to the hypothesis that exposure to physical and environmental agents, diet and modern lifestyle might be putative triggers of an autoimmune response (Floreani et al., 2016). Smoking and exposure to ultraviolet light have been suggested to be a risk factor for systemic lupus erythematous and rheumatoid arthritis. Smoking might also promote the development of primary biliary cirrhosis, Sjögren's syndrome and autoimmune thyroid disease. Curiously, alcohol consumption has been investigated for its potential role for triggering an autoimmune response although a protective role has also been suggested. Different studies suggested a protective role of light and moderate alcohol ingestion in systemic lupus erythematous. The alcohol benefits were also described in a meta-analysis study for patients with rheumatoid arthritis associated with autoantibodies against a citrullinated protein antigen. However, until now, the deleterious effects of excess alcohol intake were only suggested as a risk factor for psoriasis. Air pollution has also been linked to the development of autoimmune diseases. It has been proposed that air pollution may induce systemic inflammation, increase oxidative stress and epigenetic modifications, all being possible triggers of an autoimmune response. Air pollution has been proposed as a putative risk factor for the development and/or

exacerbation of several diseases, including systemic lupus erythematous, rheumatoid arthritis, multiple sclerosis and type 1 diabetes (Zhao et al., 2019). Finally, personal care products and cosmetics that contain natural and synthetic chemicals might be associated with the development of systemic lupus erythematous and primary biliary cirrhosis (Floreani et al., 2016).

The environmental factors mentioned above will induce a stress or "danger signal", with subsequent activation of host defence mechanisms, including activation of the immune system and inflammation. Within this immunological and inflammatory context to fight against the danger signal, different molecular mechanisms such as molecular epitope mimicry and alterations in the post-translational modifications (PTMs) of endogenous proteins may occur and be at the origin of an autoimmune response.

1.3.1.1 Molecular mimicry

Molecular (or epitope) mimicry is one of the most common mechanisms proposed to activate autoreactive B and T cells. In this scenario, the immune system originally produces antibodies against an antigen from a pathogen or another environmental factor (Cusick et al., 2012). However, these antibodies will cross-react and bind to self-proteins (autoantigens), breaking self-tolerance due to similarities between the two molecules (sequence and/or structure), leading to an autoimmune response. This phenomenon was suggested for the development of systemic lupus erythematous due to infection by Epstein-Barr virus (EBV) (Poole et al., 2006; Poole et al., 2009). The EBV nuclear antigen-1 (EBNA-1) contains a peptide sequence (PPPGRRP) that is quite similar to the Smith (Sm) autoantigen (PPPGMRPP) targeted by the autoantibodies in systemic lupus erythematous patients. Molecular mimicry has also been suggested to trigger several other autoimmune diseases, such as autoimmune thrombocytopenic purpura (*Helicobacter pylori*), type 1 diabetes (Coxsackie B virus, rubella, rotavirus, herpes, rhinovirus, hantavirus, flavivirus, retrovirus), multiple sclerosis (Epstein-Barr virus, measles, human herpes virus 6) and psoriasis (*Streptococcus pyogenes*) (Wang et al., 2015).

1.3.1.2 Post-translational modifications

After biosynthesis, proteins naturally undergo a series of spontaneous or enzymatic post-translational modifications (PTMs) that are necessary for their physiological function but can eventually be also important to promote their degradation, for instance after oxidative modifications (Ahmad et al., 2019; Kurien et al., 2008). The enzymes responsible for such PTMs can be regulated by different

pathological conditions such as inflammation and cancer. Therefore, it is not surprising that deregulation of PTMs and associated enzymes after inflammation and/or other stimuli induces and/or exacerbates autoimmunity through the formation of neo-epitopes followed by epitope spreading and/or alteration of the T cell signalling (Doyle et al., 2001).

One of the most common PTMs described in autoimmunity is citrullination (enzymatic deamination of arginine to citrulline). For instance, citrullination of different autoantigens have been associated with rheumatoid arthritis (rheumatoid factor, filaggrin, fibrin and vimentin autoantigens), multiple sclerosis (myelin basic protein and glial fibrillary acidic protein) and type 1 diabetes (glucose-regulated protein 78). Interestingly, in rheumatoid arthritis, autoanti-peptidylarginine deiminase (an enzyme responsible for the citrullination) seems to be produced; yet they could not inhibit its activity (Anderton, 2004; Bradford et al., 2014; Darrah et al., 2018; Martinez-Prat et al., 2019; Rondas et al., 2015; Valesini et al., 2015). Also in the context of rheumatoid arthritis, fucosylation levels of ficolin-3 are increased, and type II collagen can undergo several different types of PTMs: hydroxylation of proline and lysine as well as glycosylation of hydroxylysine (Corthay et al., 1998; Myers et al., 2004; Roy et al., 2013).

Goodpasture's disease is another example of an autoimmune disease in which PTMs play an important role as a trigger. In this rare autoimmune kidney disease, patients produce circulating autoantibodies against type IV collagen, more specifically against the α3 chain of non-collagenous domain (NC1) (McAdoo et al., 2017; Pedchenko et al., 2010). The conformational structure type IV collagens (NC1 hexamers) is maintained by several hydrophobic and hydrophilic interactions as well as sulphilimine bonds (S=N), a rare PTM that allows the crosslinking of opposing NC1 domains. Lack of sulfilimine bonds unmasks the cryptic epitopes described for Goodpasture's disease (McAdoo et al., 2017; Pedchenko et al., 2011; Vanacore et al., 2011). Of curiosity, autoantibodies against peroxidasin, the enzyme required for the formation of the sulphilimine bond, can be found in patients with Goodpasture's disease before clinical onset as well as during active disease (McCall et al., 2018).

As for MN, even though the aetiology remains unknown, several of the mentioned scenarios (such as molecular mimicry and air pollution) have been proposed as possible triggers of the disease (chapter 4.1).

1.3.2 Genetic susceptibility

Development of autoimmune diseases due to specific gene mutations is rare, but it can occur. For example, autoimmune polyglandular syndrome type I, a multiple organ-specific autoimmune disease, is characterized by a mutation in the autoimmune regulator (*AIRE*) gene, affecting self-antigen presentation (DeVoss et al., 2007). Mutations in *FAS*, *FASLG* and/or *CASP10* gene(s) leads to autoimmune lymphoproliferative syndrome, which is characterized by the accumulation of T cells due to a defective apoptosis of lymphocytes mediated via the Fas/Fas ligand pathway (Shah et al., 2014).

The major histocompatibility complex (MHC) locus (short arm of chromosome 6, 6p21.3), also known as human leukocyte antigen (HLA), encodes molecules involved in antigen presentation, regulation of inflammation, complement system, and innate and adaptive immune responses. Therefore, it is not surprising that variants (polymorphisms) in the MHC have been associated with different autoimmune diseases, even though the mechanisms underlying it remains poorly understood (Matzaraki et al., 2017). For example, six amino acid variants at position 11 in the HLA-DRB1 gene have been strongly associated with rheumatoid arthritis. The valine and leucine variants seem to confer susceptibility to the disease whereas the asparagine, proline, glycine and serine variants appear to be protective (Raychaudhuri et al., 2012). Many other autoimmune diseases have been strongly associated with HLA variants: type 1 diabetes (HLA–DQ2, –DQ8, –A and –DQB1*0602), systemic lupus erythematous (HLA–DR3, –DR2 and –DR8; HLA-III: SCIVaL, CFB, RDBP, DOM3Z, STL19C4A and C4B), autoimmune thyroid disease (HLA–DR3 and –DR4), and psoriasis (HLA–Cw*0602, –Cw1203 and –HCP5). Non-HLA loci also have been described to be linked with autoimmune diseases. For instance, *IRF5-TNPO3* gene, which codes interferon regulatory factor 5 and transportin 3, has been associated to susceptibility for rheumatoid arthritis, systemic lupus erythematous, primary biliary cirrhosis, ulcerative colitis and Sjögren's syndrome (Wang et al., 2015).

Finally, changes in gene expression by epigenetic mechanisms have been associated to the development of autoimmune diseases (Aslani et al., 2016). For example, DNA hypermethylation of the insulin gene INS has been associated with type 1 diabetes while multiple sclerosis has been linked to hypomethylation of peptidylarginine deaminase 2 (*PAD2*) and Src homology region 2 domain-containing phosphatase-1 (*SHP-1*). Acetylation of histone H4 regulates the gene promoter of aquaporin-5 (*AQP5*) and was associated to Sjögren's syndrome while microRNAs, such as miR-326, were linked to multiple sclerosis and type 1 diabetes.

In sum, specific gene mutations, HLA susceptibility, non-HLA loci and epigenetic mechanisms have been implicated in the development of specific autoimmune diseases. Some of these mechanisms have also been proposed to increase the susceptibility of developing MN (chapter 2.2.6 and chapter 4.1).

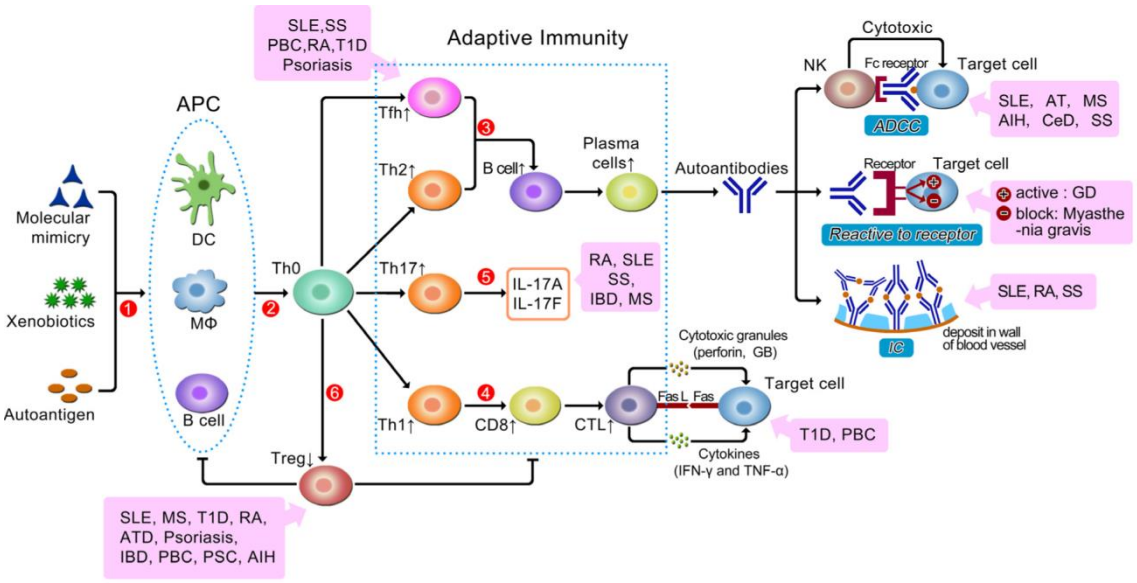

Figure 1.3 – General view of the pathophysiology of an autoimmune immune disease. (1) Environmental factors (molecular mimicry, microbiota, air pollution, etc.) associated or not with genetic susceptibility, activate innate immune cells (dendritic cells (DC), macrophages (MΦ) and natural killer cells (NK)). (2) T-cell immunogenic peptides generated by antigen-presenting cells (APCs) are "presented" to uncommitted T helper lymphocytes (Th0) which will differentiate into Th2 T follicular helper (Tfh), Th17, Th1 and T regulatory cells (Tregs). (3) Th2 and Tfh cells facilitate B-cell activation, maturation and differentiation into plasma cells leading to autoantibody production. (4) Th1 cells stimulate development of autoreactive cytotoxic T lymphocytes (CTLs) that will induce tissue injury through the secretion of cytotoxic granules, activation of Fas-Fas ligand and/or release of cytokines. (5) Increased Th17 have been also described to be correlated with the progression of the autoimmune response. (6) Tregs are responsible for maintaining tolerance by negatively regulating innate and adaptive immunity. A decrease in Treg cells enabling loss of tolerance has been demonstrated in several autoimmune diseases including MN. AIH, autoimmune hepatitis; AITD, autoimmune thyroid disease; CeD, celiac disease; GD, Graves' disease; IBD, inflammatory bowel disease; MS, multiple sclerosis; PBC, primary biliary cirrhosis; PSC, primary sclerosing cholangitis; SLE, systemic lupus erythematous; SS, Sjögren's syndrome; RA, rheumatoid arthritis; T1D, type 1 diabetes. *Adapted from (Wang et al., 2015) with copyright permission from "John Wiley & Sons".*

1.4 Pathophysiology

Beyond variations in the epidemiology and aetiology of autoimmune diseases, the mechanisms underlying the development and progression of the autoimmune response are also different and specific. This section will provide a short snapshot of what is known regarding the pathophysiological mechanisms at play in some

well-documented autoimmune diseases, which might bring new insights to investigate the autoimmune response involved in MN (Figure 1.3).

Under physiological conditions the immune system produces T and B cells in order to achieve one its main functions: protect and defend the host from infectious agents. This function is highly dependent on the ability of T and B cells being able to distinguish self- from non-self-molecules. Disruption of this ability leads to the so-called break of tolerance, in which the B and T cells escape primary and peripheral tolerance (described above) becoming aberrantly self-reactive towards autoantigens (Wang et al., 2015). The causes of this disruption remain poorly understood or even completely unknown for the majority of the autoimmune diseases. Still several environmental factors and genetic susceptibilities or most probably the two factors have been pointed out for the development and progression of several autoimmune conditions. It has been proposed that antigen overexpression, changes in antigen conformation, PTMs and/or molecular mimicry followed by activation and maturation of antigen presenting cells (APCs) and immune cells can lead to break of tolerance and autoimmunity (Melchers et al., 2006; Ohashi et al., 2002).

The autoreactive B and T cells will lead to an increase production of autoantibodies that generally results in persistent inflammation and tissue damage through different mechanisms (Lleo et al., 2010). One of the most common mechanisms of tissue injury occurs through complement activation and antibody-dependent cell-mediated cytotoxicity. This mechanism usually limits the tissue injury to the primary target, thus being highly associated with the development of organ-specific autoimmune diseases such as type 1 diabetes, autoimmune thyroid disease mediated by anti-thyroperoxidase antibodies and likely membranous nephropathy (Kaminitz et al., 2007; Ma et al., 2013; Rodien et al., 1996; Ronco et al., 2017). Cell cytotoxicity will lead to a second mechanism where new autoantibodies target nuclear and intracellular constituents, forming circulating immune complexes, which if not eliminated (for example by phagocytosis) will cause tissue damage at their sites of deposition (glomerulonephritis, vasculitis, cerebritis and arthritis). The circulating immune complexes formed may accumulate in multiple tissues besides the primary target, thus this mechanism usually leads to the development of systemic autoimmune diseases such as systemic lupus, Sjögren's syndrome and rheumatoid arthritis (Derksen et al., 2017; Wahren-Herlenius et al., 2013). In addition to complement-dependent tissue damage, autoantibodies can affect physiological functions by direct interaction to their cognate autoantigen targets, such as by facilitating their phagocytosis (immune thrombocytopenia), or by binding to cell

surface receptors thereby stimulating (Graves' disease) or blocking (Myasthenia Gravis) different signalling pathways (Gomez et al., 2010; Li et al., 2018; Lleo et al., 2010). Finally, a third mechanism, antibody-independent, can lead to tissue damage. In this scenario, autoreactive cytotoxic T lymphocytes (CTLs) recognize the target cells and induce death (apoptosis) through secretion of cytotoxic granules, activation of the Fas/Fas ligand signalling pathway, and/or release of cytokines. This mechanism has been associated to the development of type 1 diabetes, autoimmune thrombocytopenia, and primary biliary cirrhosis (Kaminitz et al., 2007; Li et al., 2018; Wang et al., 2015).

The progression and exacerbation of an autoimmune disease is characterized by persistent inflammatory self-recognition through a continuous acquisition of new self-recognition events (by T and/or B cells), leading to an inflammatory steady-state condition and chronicity. These new events can occur through different mechanisms: molecular mimicry (chapter 1.3.1.1), epitope spreading and post-translational modifications (chapter 1.3.1.2).

1.4.1 Epitope spreading

Epitope (or determinant) spreading is an immune mechanism characterized by the diversification of epitope recognition from an epitope initiating the inflammatory process – immunodominant epitope – to several secondary epitopes – subdominant epitopes. These secondary epitopes can be present within the same antigen (intramolecular spreading), or within an antigenic molecule interacting with the primary target (intermolecular spreading) (Vanderlugt et al., 1996). The epitope spreading mechanism itself can occur through different mechanisms including interaction between B and T cells, endocytic processing of antigens and somatic hypermutation in the B cells (Cornaby et al., 2015).

Indeed, B cell endocytosis and antigen presentation to T cells are important contributors to the mechanism of epitope spreading. After activation through intrastructural T cell help or upon antigen binding to B cells receptors (BCRs), B cells undergo endocytosis, leading to antigen processing and presentation (Figure 1.4) (Amigorena et al., 1998; Cornaby et al., 2015). This will select what peptides will be loaded into the MHC class II molecules and displayed on the cell surface, ultimately determining what epitopes will be presented to T cells and will be targeted by the immune system. Additionally, once a B cell recognizes an antigen, it is stimulated to proliferate. During proliferation, the B cell receptor locus can undergo somatic hypermutation, mainly at the hypervariable regions, which are involved in the antigen recognition, contributing to epitope spreading (Figure 1.5)

(Cornaby et al., 2015). Of note, linear epitopes (six to eight contiguous amino acids from the primary protein structure) are recognized by T cells. These epitopes usually are internal hydrophobic amino acid sequences that are processed and present to T cells. On the other hand, conformational B cell epitopes reacting to the conformational tertiary structure of the folded antigen, relies on B cells maturation by a mechanism which is still not well characterized (Cornaby et al., 2015; McCluskey et al., 1998).

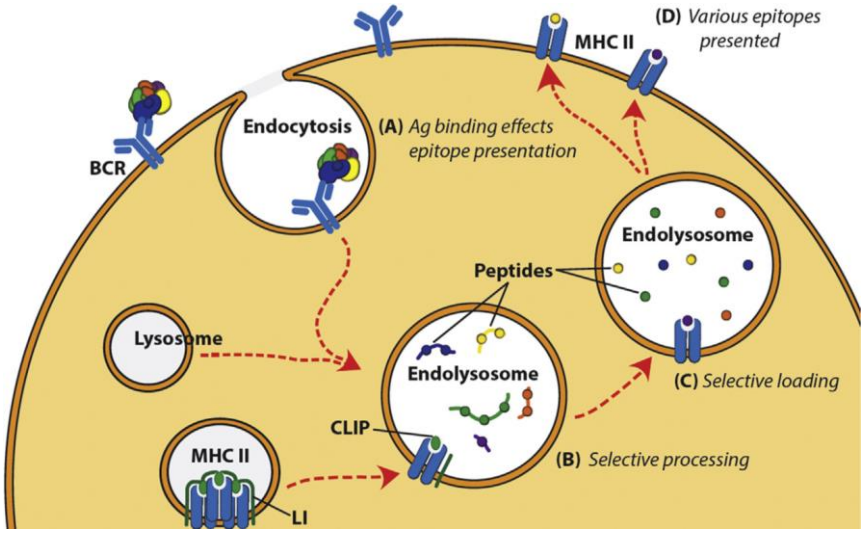

Figure 1.4 – The endocytic pathway as the primary mechanism of B cell epitope spreading. **(A)** Antigens bind to B cells receptors (BCRs) which are composed by surface immunoglobulin (sIg) molecules that will affect the epitope that is selected and loaded into MHC II molecules. How the antigen binding to BCR impacts its processing and consequently affects selection of epitopes presented to T cells remains unclear. Two explanations have been proposed: (1) the binding stability between the antigen and sIg, and/or (2) a selective intracellular targeting by the sIg cytoplasmic tail and/or the Igα/Igß associated chains. **(B)** The endosome fuses with the lysosome, containing GILT (gamma-interferon-inducible lysosomal thiol reductase), cathepsins and other proteases. These proteases selectively digest the antigen into small peptides, providing another point for selection of epitopes and exclusion of others. This selection is based on the cleavage sites of the enzymes, their relative concentration and activity, which in turn is regulated by multiple endogenous cytokines and competitive inhibitors. **(C)** Once CLIP (class II-associated invariant chain peptide) dissociates, peptides are selectively into the MHC class II molecule based on amino acid motifs, pH, the presence or absence of HLA-DM, and other endosomal environmental factors. **(D)** The chosen epitope(s) that resulted from the multiple selective processes is then displayed via the MHC II on the surface of the cell. *Adapted from (Cornaby et al., 2015) with copyright permission from "Elsevier".*

The role of intramolecular epitope spreading for the development of autoimmunity has been demonstrated in pemphigus foliaceus. In this cutaneous autoimmune blistering disease, patients produce autoantibodies against an epidermal cell adhesion molecule, desmoglein-1 (Dsg-1). This is a 160 kDa glycoprotein comprising five extracellular domains (EC1 to EC5). A study realized

by Li and colleagues (Li et al., 2003), using an elegant chimera production approach, demonstrated that patients with pemphigus foliaceus start by developing non-pathogenic autoantibodies against EC5. These autoantibodies could be detected even before the clinical onset of the disease and in healthy donors. Transition from the pre-clinical to the clinical stage of the disease was characterized by the production of autoantibodies through a mechanism of intramolecular epitope spreading from the initial non-pathogenic EC5 to the pathogenic EC1 and EC2.

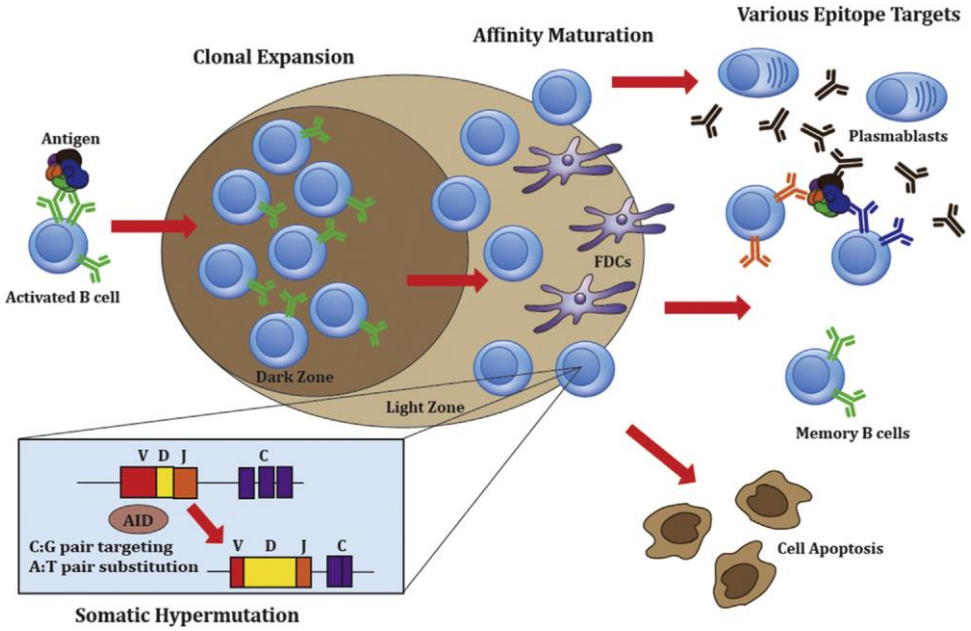

Figure 1.5 – Somatic hypermutation as a mechanism of B cell epitope spreading. After B cell activation upon recognition of an antigen, in secondary lymph tissue, B cells produce large amounts of daughter calls though the process of clonal expansion. These daughter cells independently induce changes in the variable regions of the immunoglobulin gene. The IgV gene will suffer single nucleotides substitutions at a frequency of approximately 10^{-3} per base pair in each B lymphocyte generation. Subsequently an affinity maturation process allows a selection of the B cells with the higher affinity to the antigen, and will then differentiate into plasma cells producing antibody and long-lived memory B cells contributing to an enhanced immune response. The low affinity binding B cells are signalled to apoptosis. *Adapted from (Cornaby et al., 2015) with copyright permission from "Elsevier".*

Type 1 diabetes is an example of an autoimmune disease in which intermolecular epitope spreading is associated with progression. During the development of this condition patients can produce autoantibodies targeting several islet proteins, including islet cell autoantibody, islet cell autoantibody-2, insulin autoantibody and glutamic acid decarboxylase autoantibody. In a clinical study (Brooks-Worrell et al., 2001), 25 volunteers were considered to be at risk of

developing type 1 diabetes due to the presence of at least one of the four autoantibodies just mentioned. Within 30 months of follow-up, 7 of the 25 subjects developed clinical type 1 diabetes. At the initial visit 4 of these 7 subjects were positive for one or two of the referred autoantibodies and by the end of the study they were found positive for all four, highlighting a mechanism of intermolecular epitope spreading in the development of type 1 diabetes.

Depending on the disease process, epitope spreading can either perpetuate (pathogenic epitope spreading, such as in autoimmune diseases) or attenuate (protective epitope spreading, like in tumour clearance) the disease progression. As just exemplified above, in the majority of autoimmune diseases, epitope spreading mechanism is associated with pathogenicity; still, in a few cases it might play a protective role. For instance, in a rat model of rheumatoid arthritis, epitope spreading towards the 65 kDa heat shock protein (hsp65) seems to be involved in natural remission of acute inflammatory arthritis triggered by Mycobacterium tuberculosis (Moudgil, 1998).

1.5 Treatment

Nowadays, the treatment options for autoimmune diseases are still quite limited and most of them rely on the suppression of the immune system (as a whole, like cyclophosphamide) and/or in the neutralization of autoantibody production (for instance an anti-CD20 such as rituximab) (Tavakolpour, 2017; Vanderlugt et al., 2002). A better understanding of epitope spreading underlying the development and progression of the different autoimmune diseases would not only bring better comprehension of the mechanisms of pathogenesis but would help to develop more specific antigen-specific immunotherapies keeping the immune system functional. However, several different mechanisms involving a multitude of different cell populations are at play in autoimmune diseases such as systemic lupus erythematous and rheumatoid arthritis, making their treatment more difficult and complex, requiring a combined therapeutic approach.

Chapter 2
Membranous Nephropathy

Membranous nephropathy (MN) is one of the most common causes of nephrotic syndrome in adults. This rare disease is characterized by the accumulation of subepithelial immune deposits at the glomerular basement membrane (GBM) and persistent high levels of proteinuria (> 3.5 g/day). The structural changes of the podocyte due to the accumulation of immune deposits, classifies MN not only as a glomerular disease but also as an organ-specific autoimmune disease.

2.1 Kidney physiology and glomerular diseases

The main function of kidney is to filter blood. However, kidney is also an endocrine gland responsible for the synthesis of different hormones (such as vitamin D3, erythropoietin, thromboietin, renin, some prostaglandins) and exert metabolic tasks (like formation of ammonium from glutamine and glucogenesis), contributing to homeostasis (such as water, potassium, pH and blood pressure) (Mitchell et al., 2018; Scott et al., 2015). These functions are achieved by approximately one million nephrons (the functional unit of the kidney). The nephrons are composed by the glomerulus and the attached tubular system. The blood is filtrated in the glomerulus forming the primary urine (around 180 L/day) that is directed to the proximal tubule, while the filtered blood returns to circulation. The size-selective glomerular filtration barrier is composed by an innermost fenestrated endothelium, the glomerular basement membrane (GBM), and the slit diaphragm of podocyte foot processes (Figure 2.1–A, B) (Tryggvason et al., 2005). The foot processes from adjacent podocytes interdigitate forming the slit diaphragm, essential for the glomerular filtration, that is composed by several adhesion proteins (actin, podocin, nephrin, P-cadherin, etc.) (Jarad et al., 2009). Any disruption of the integrity of the glomerulus leads to a group of pathological conditions referred to as glomerular diseases that are characterized by a less selective blood filtration which ultimately leads to an important leak of proteins in the urine, referred as proteinuria.

Glomerular diseases are characterized by a dysfunction of the glomerular barrier, accounting for about 20% of the chronic clinical cases. The most common glomerular diseases include immunoglobulin A nephropathy, focal segmental glomerulosclerosis, membranoproliferative glomerulonephritis, minimal change disease and membranous nephropathy (Floege et al., 2016). There is no specific clinical presentation. Depending on the disease and its clinical course, the signs can vary from asymptomatic patients with urinary abnormalities to patients with oedema and nephrotic syndrome. Nevertheless, clinical manifestation of glomerular diseases is characterized by variable amounts of proteinuria and/or haematuria.

Increasing amounts of urinary alpha-1 microglobulin are indicative that the primary glomerular injury spreads to the tubular system. Kidney biopsy is the gold standard procedure for the diagnosis of glomerular diseases (Figure 2.1–C, D).

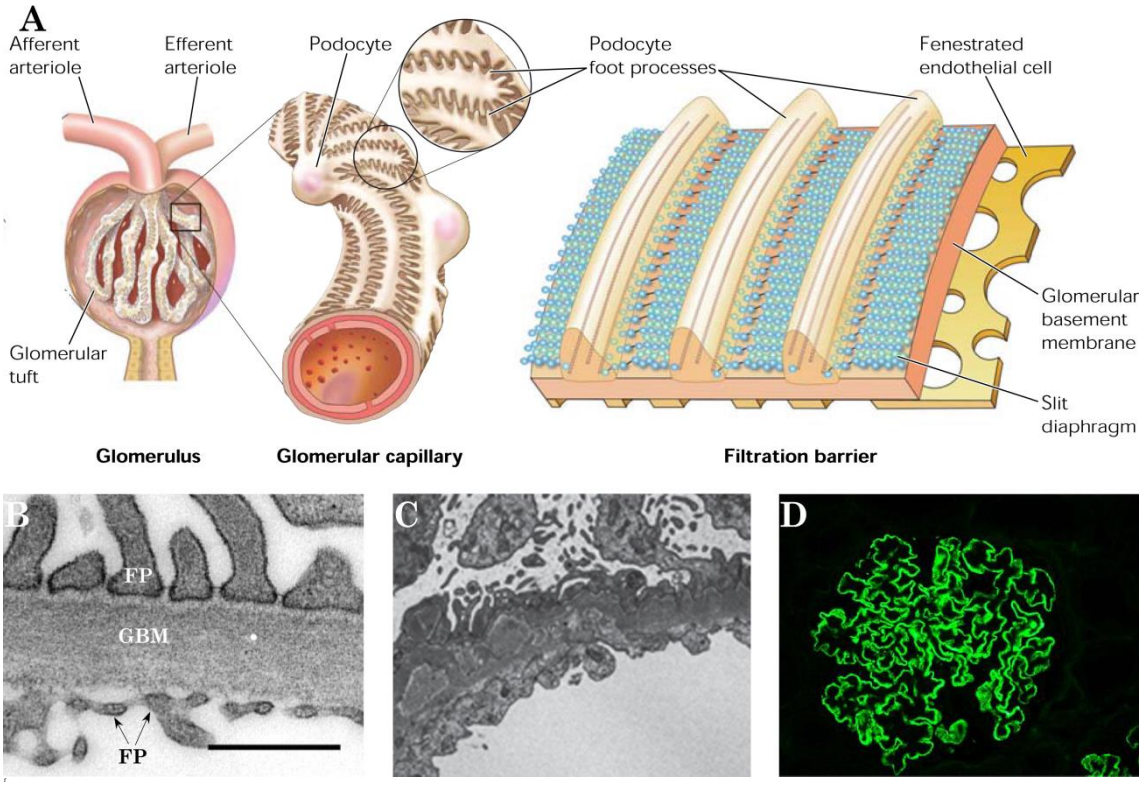

Figure 2.1 – Physiology of the renal glomerulus in MN. (A) Schematic representation of the renal glomerulus and the glomerular filtration barrier. *Adapted from* (Tryggvason et al., 2005) *with copyright permission from "The American Physiological Society"*. **(B)** Electron microscopy of a normal adult glomerular filtration barrier, with a uniform glomerular basement membrane (GBM) located between the fenestrated endothelial cells (FE) and the podocyte foot processes (FP). *Adapted from (Tryggvason et al., 2006) with copyright permission from "American Society of Nephrology"*. **(C)** Electron microscopy showing the alterations of the glomerular filtration barrier due to subepithelial deposits from a representative stage II case of MN. *Adapted from (Morita et al., 2015)*. **(D)** Immunofluorescence staining of a glomerulus showing the granular deposits along the GBM in a representative case of PLA_2R1-associated MN. *Adapted from (Larsen et al., 2013) with copyright permission from "Nature Publishing Group"*.

2.2 Membranous nephropathy

Membranous nephropathy (MN) is an organ-specific autoimmune disease and the most common cause of nephrotic syndrome in non-diabetic adults. It is a rare disease with a worldwide annual incidence of 1.2/100,000 new cases (Couser, 2017; McGrogan et al., 2011). Surprisingly, and contrary to what is observed for many other autoimmune diseases, MN affects more men than women (with a 2:1 ratio). This pathology affects patients of all ages, but is more likely to occur in adults, with a

peak of incidence at 50's and 60's years old, and more rarely diagnosed in children (0.02-0.09/100,000 new cases/year).

MN is characterized by the formation of subepithelial immune deposits with consequent complement system activation, leading to podocyte injury and damage of the glomerular filtration barrier (Doi et al., 1984; Farquhar et al., 1957; Mellors et al., 1957). In the primary form of MN, the immune complexes consist of the target autoantigen co-localized with autoantibodies, mainly IgG4, the complement factor C3 and the C5b-9 complex. A definitive diagnosis of this disease can be made after kidney biopsy, where these complexes are best evidenced by electron microscopy or immunofluorescence (Figure 2.1–C, D).

2.2.1 History

The term membranous glomerulonephritis (MGN) was first proposed in 1946, but, with time, due to the lack of significant glomerular inflammation it has been replaced by membranous nephropathy (MN). In 1957, based on the characteristic structural changes of the glomerular basement membrane (GBM) and capillary wall thickening, MN was recognized as a distinct clinico-pathological entity (Figure 2.1–C) (Jones, 1957). These unique changes were later identified to be due to the deposition of immune complexes between the podocyte and the subepithelial aspect of GBM, leading to a dysfunction of the glomerular filtration barrier with consequent nephrotic syndrome, a main characteristic of this disease.

Shortly after, in 1959, Heymann and colleagues (Heymann et al., 1959) established the first animal model of MN, nowadays referred as the Heymann nephritis model of MN in rat, providing the first major breakthrough in the understanding of MN. In this model, Sprague-Dawley rats were repeatedly immunized with crude kidney extract from the same rat species in the presence of complete Freund's adjuvant with mycobacterium extract. Six to 12 weeks after, animals developed clinical and pathological features similar to the ones observed in human MN: proteinuria, hypoalbuminemia, hyperlipemia and increased creatinine blood levels, accompanied by thickening of the GBM. Initially, it was though that the autoantibodies bound to components from the kidney extract, forming circulating immune complexes that then got trapped and accumulated in the glomerulus. However, in 1978, two different groups demonstrated that autoantibodies would bind to an autoantigen intrinsically present at the surface of podocytes of the glomerular filtration barrier, forming *in situ* immune complexes (Couser et al., 1978; Van Damme et al., 1978). The major target autoantigen in the rat Heymann model of MN was later identified as megalin (gp330), a large 600 kDa transmembrane

protein that belongs to the low-density lipoprotein receptor family (Kerjaschki et al., 1982, 1983; Raychowdhury et al., 1989). Follow-up studies revealed that the megalin-autoantibody complexes induced complement-mediated cytotoxicity (C3 and C5b-9 complex) leading to podocyte injury and proteinuria (Baker et al., 1989; Cybulsky et al., 1986).

The identification of megalin as the autoantigen in the Heymann nephritis experimental rat model of MN further encouraged the scientific community to search for the autoantigen(s) in human MN. For several years, researchers tried to identify anti-megalin autoantibodies in MN patients. However, this search proved to be fruitless, since human podocytes do not seem to express megalin, although this latter is abundantly expressed in human proximal tubules. Ironically, anti-megalin autoantibodies have been recently involved in ABBA (anti-brush border antibody disease), another rare autoimmune kidney disease affecting proximal tubule cells (Larsen et al., 2018). After endless efforts, in 2002, Debiec and colleagues (Debiec et al., 2002) identified neutral endopeptidase (NEP) as the first human MN autoantigen, but in a rare neonatal form of MN called alloimune MN. In this form, renal biopsy from newborns demonstrates a typical severe form of MN with diffuse alterations of the glomerular capillary walls and subepithelial deposits of IgG and complement C3 (more details on chapter 2.2.2). However, alloimmune cases of MN are tremendously rare, and, additionally, NEP turned out not to be the autoantigen in adult MN. Nevertheless, the discovery of this mechanism in alloimmune MN with NEP endogenously present at the surface of podocytes led credence to the scenario of intrinsic podocyte autoantigens targeted by free circulating autoantibodies in human MN (Glassock, 2009). Exactly 50 years after the first description of an experimental model of MN by Walter Heymann, in 2009, another key breakthrough for the understanding of MN occurred, with the identification of PLA_2R1 as the major autoantigen for approximately 70% of patients with adult MN (Beck et al., 2009). Shortly after, in 2014, thrombospondin type 1 domain-containing 7A (THSD7A) was identified as the second autoantigen for another group of 2-5% of patients with adult MN (Tomas et al., 2014). More detailed information concerning the autoantigens of MN is provided in chapter 2.3.

2.2.2 Clinical classification

Historically, MN has been classified as primary or secondary forms. Approximately 20-30% of MN cases are referred as secondary since they occur as a consequence of another systemic disease (KDIGO Guidelines, 2012; Ponticelli et al., 2014; Ronco et al., 2015). In the remaining 70-80% of MN cases the exact cause underlying

the development of the pathology remains fully unknown with no symptoms other than proteinuria, oedema and the presence of immune deposits at the GBM. These cases are thus classified as primary or idiopathic MN (iMN). Contrary to the secondary forms which are more common among children and may even account for the majority of the diagnosed cases, primary MN during childhood cases of nephrotic syndrome are very low (1-5% prevalence among all primary MN cases), with an incidence of 0.02-0.09/100,000 new cases/year. Primary MN is thus considered an adulthood disease (KDIGO Guidelines, 2012; McGrogan et al., 2011; Ponticelli et al., 2014).

Secondary forms of MN occur as a consequence of another disease, and they may be cured by treating the underlying cause of the primary disease. The main causes associated with secondary MN include other autoimmune diseases (including systemic lupus erythematous, autoimmune thyroid disease, rheumatoid arthritis and Sjögren's syndrome), infections (such as viral hepatitis B and C, human immunodeficiency virus, malaria and syphilis), malignancies and medications (like D-penicillamine, cyclooxygenase-2 inhibitors and nonsteroidal anti-inflammatory drugs) (Couser, 2017; KDIGO Guidelines, 2012). However, some controversial cases have been presented, such as for sarcoidosis-associated MN, since it is unclear whether the associated disease is causal or co-incidental with MN (Stehle et al., 2015). Thus, diagnosis of secondary MN is difficult and usually occurs retrospectively once the primary cause is treated and a remission or cure of MN is observed. Still, renal-biopsy might provide some insightful information suggestive of either idiopathic or secondary MN (Huang et al., 2013; Larsen et al., 2013). For instance, even though all IgG subclasses can be found in both forms, IgG1, IgG2 and IgG3 as well as C1q are predominantly observed in immune deposits from secondary MN whereas the predominant presence of IgG4 subclass as well as the absence of C1q is a good indication for primary MN. Also, contrary to what is known and has been observed in primary MN, immune deposits in the secondary form can be found in other places besides the subepithelial space, such as mesangial immune deposits.

After careful examination and evaluation of the patients and after all causes of secondary MN have been eliminated and no underlying cause can be attributed to the development of MN, the patients are diagnosed with the primary form of MN. Recently, PLA_2R1 and THSD7A have been identified as autoantigens in approximately 70% and 3% of the primary MN cases, respectively, linking an autoimmune response against these specific proteins to the MN disease activity, as in alloimmune NEP and the Heymann nephritis model (Beck et al., 2009; Tomas et al., 2014; Zaghrini et al., 2019). Although the exact aetiology of primary MN associated with

PLA_2R1 remains largely unknown, environmental factors (such as molecular mimicry and air pollution) and/or genetic predisposition have been suggested as triggers of the autoimmune response underlying the development of this form of MN (Fresquet et al., 2015; Stanescu et al., 2011; Xu et al., 2016). Additionally, the identification of these autoantigens has led to the development of specific assays to diagnose patients with PLA_2R1- and THSD7A-associated MN, facilitating and/or confirming the diagnosis provided by the renal-biopsy (more details on chapter 2.2.4 and chapter 4.3) (Bobart et al., 2019; Dahnrich et al., 2013; Hoxha et al., 2017; Hoxha et al., 2011; Zaghrini et al., 2019). Finally and hopefully, these identifications will help to bring some more insights regarding the aetiology and physiopathology underlying primary MN. And perhaps they might lead to a change in the current classification, which will likely become serologically-based, leaving the term idiopathic for those cases where no autoantibodies for PLA_2R1 or THSD7A as well as no evidence for a secondary cause are found (Beck, 2017).

An extraordinary rare form of alloimmune MN has been described in newborns who presented oligoanuria (with the need or not for peritoneal dialysis), mild to massive proteinuria, hypoalbuminemia, hypercholesterolemia, arterial hypertension, increased levels of serum creatinine and respiratory distress syndrome that might require mechanical ventilation depending on the severity of the disease. Renal biopsies performed days to few weeks after birth demonstrated slight to marked alterations in the physiology of the glomerulus, with mainly IgG1 and/or IgG4 immune deposits. Of curiosity enlarged kidneys of the foetus can be observed on the ultrasound scan preformed during the last weeks of gestation. In this rare form of MN, the NEP-deficient mother (homozygous for the truncating deletion mutation 466delC) was immunized against NEP during pregnancy or following a previous miscarriage. During pregnancy, anti-NEP autoantibodies produced by the mother are passively transferred through the placenta into the foetus blood flow targeting NEP present in the podocytes of the foetus who strongly expresses it because of heterozygosity from the father. Few days or weeks after birth, the autoantibody titer of the newborn decreased not only due to a possible underlying treatment but mainly because of the short life span of maternal IgG (Debiec et al., 2002; Debiec et al., 2004; Vivarelli et al., 2015). Still, in some cases, the glomerulus damage might be irreversible, and nephron loss can occur as well, which might lead to chronic renal failure or MN diagnosis during adolescence or early adulthood. Based on the study of three of the five known alloimmune cases, two mechanisms were proposed to be involved in the pathophysiology of this form of MN. In the first mechanism, the anti-NEP autoantibodies which are mainly

IgG1, strongly inhibit the enzymatic activity of NEP and activate the complement pathway leading to an extremely severe form of MN. In the second mechanism, anti-NEP autoantibodies, which are mainly IgG4, not only weakly inhibit NEP enzymatic activity but also do not activate the complement pathway leading to a less severe form of MN (Vivarelli et al., 2015).

2.2.3 Clinical features, presentation and natural history

MN is considered an adulthood disease since the average age of diagnosis is above 50 years-old with a higher prevalence in men than women, with a 2:1 ratio. Clinically, at the time of diagnosis, patients can present nephrotic range proteinuria (proteinuria > 3.5 g/day, 60-80%), hypoalbuminemia (60%), oedema (41-60%), hypertension (30-55%) and hyperlipidaemia (50%), depending on the stage of the disease. Despite heavy proteinuria at presentation, most patients seem to have preserved renal function (eGFR > 60 mL/min/1.73 m^2, 71%) (Donadio et al., 1988; Polanco et al., 2010; Schieppati et al., 1993). In a short term, patients might manifest other nephrotic syndrome complications such as development of thrombotic and thrombolytic events (7%), that are usually proportional to the degree of hypoalbuminemia (Lionaki et al., 2012). They might also have a higher risk to develop cardiovascular diseases and infections, the last one being mainly due to loss of IgG in urine (Barbour et al., 2013; Lee et al., 2016). As first described by Jones, thickening of the GBM (without proliferation) due to deposition of immune complexes is the main histopathological feature of MN (Jones, 1957). According to the structural changes observed in the renal biopsy, patients can be diagnosed with stages I to IV (see next chapter for more details).

Overall, the clinical outcome is very variable, going from spontaneous remission to end-stage renal disease (ESRD). If untreated (natural history), 30-35% of the patients can undergo spontaneous remission within 5 years after diagnosis or 40-50% of the patients within at least 10 years of follow-up; whereas the remainder stay in active disease or progress to ESRD with a need for dialysis and/or transplantation (Donadio et al., 1988; Hladunewich et al., 2009; Kanigicherla et al., 2016; Polanco et al., 2010; Schieppati et al., 1993). Ultimately, in some cases, the patient might die from nephrotic syndrome complications (such as cardiovascular diseases, infections, pulmonary embolism), as observed in rats in the Heymann nephritis model. Of note, after remission, 25-40% of patients can recur at any time, and MN can also recur in 35-40% of the transplanted patients (Cosio et al., 2017; Dabade et al., 2008; Kanigicherla et al., 2016; Passerini et al., 2019).

Several clinical features such as age, sex, ethnicity (African American, Caucasian), persistent heavy proteinuria, hypoalbuminemia, persistent hypertension and hyperlipidaemia, decrease eGFR at presentation, C3 staining in the biopsy, and increased excretion of low molecular weight markers (like ß2 microglobulin), C3dg and C5b-9 have been associated with an increased risk for progression of the disease (including development of ESRD) (Donadio et al., 1988; Glassock, 2003; Polanco et al., 2010; Rozenberg et al., 2018; Schieppati et al., 1993). Still, it should be kept in mind that different studies might present contradictory conclusions and/or different numbers regarding risk factors and/or clinical outcome. This might be due to the inherent limitation of retrospective cohorts, such as the number of patients, low number of patients with less severe disease, inclusion of patients with non-nephrotic proteinuria, age and sex bias (Glassock, 2003).

Understanding the mechanisms of the natural history of MN is important not only for pathophysiology but also to help physicians to make the appropriate decision for an optimized therapy and better patients' healthcare. The observations referred above as well as physicians' daily practice have provided international recommendations known as the KIDGO guidelines, which are followed worldwide for management of MN (KDIGO Guidelines, 2012). Finally, the routine use of specific diagnosis assays for the detection of anti-PLA_2R1 and anti-THSD7A autoantibodies in clinical practice has confirmed that these autoantibodies can be found at the time of diagnosis in approximately 70% and 3% of MN patients, respectively. It also has been demonstrated that they might have a predictive value for clinical outcome (more details on chapter 4.3.2 and chapter 4.3.3), which is leading to a paradigm shift in patients' healthcare with improved KDIGO guidelines for MN (Floege et al., 2019).

2.2.4 Diagnosis and histopathological features

The definitive diagnosis of MN relies on the detection of subepithelial immune deposits in renal biopsy, which are best observed and characterized by electron microscopy (Lai et al., 2015; Pozdzik et al., 2018). Based on the ultrastructural changes four stages of the disease can be identified: stage I, which is characterized by small immune complexes scattered in the subepithelial space between the GBM and the podocytes; stage II, which is characterized by spikes of the GBM material around the subepithelial deposits; stage III, characterized by increased spikes and formation of a new GBM layer around the deposits; and stage IV, which is characterized by irregular thickening of the GBM with loss of electro-dense deposits (Figure 2.2).

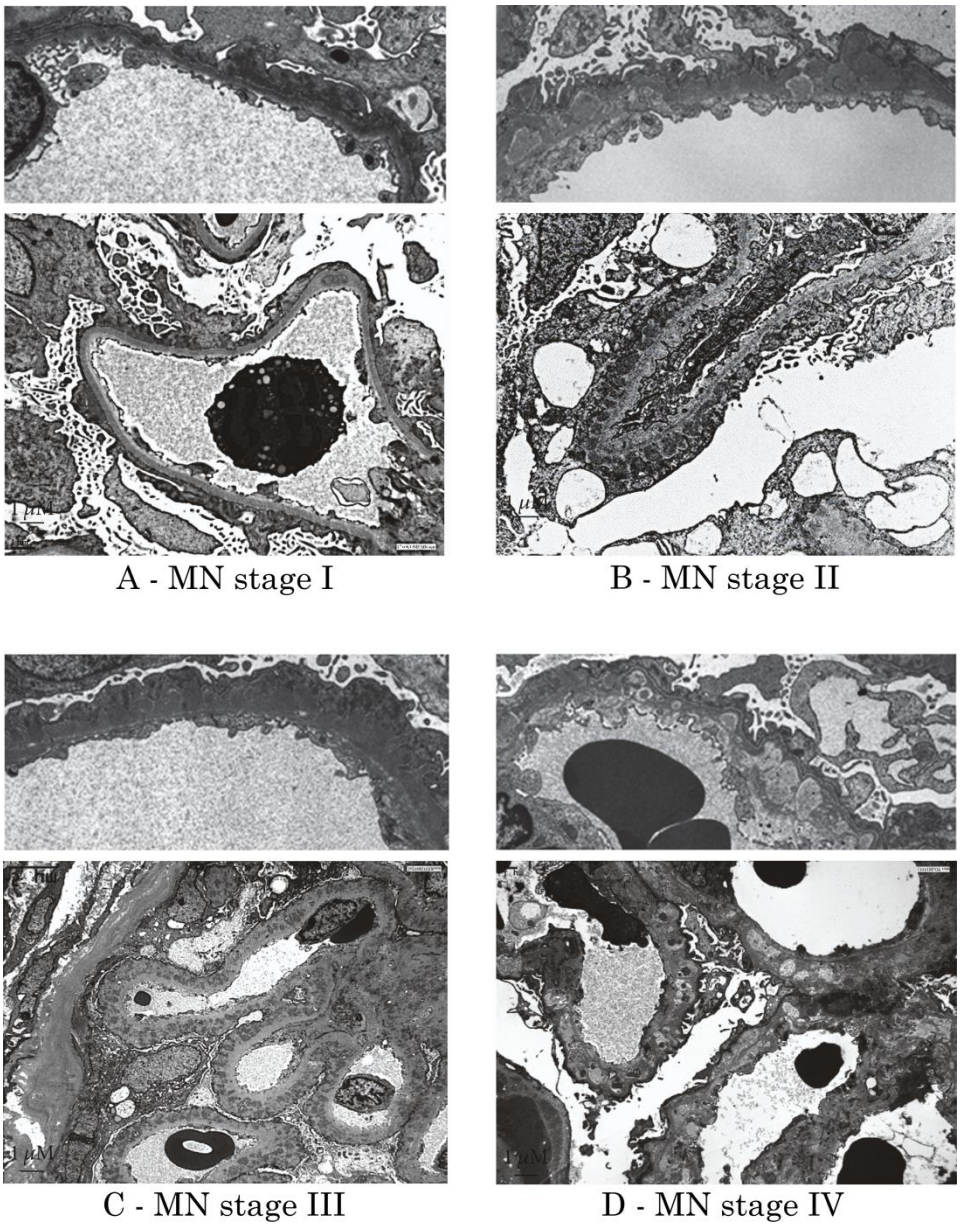

Figure 2.2 – Representative cases of the different electron-microscopy stages of MN. (A) Stage I: small immune-complexes scattered in the subepithelial space. **(B)** Stage II: spikes of the GBM around the subepithelial deposits. **(C)** Stage III: longer spikes incorporate the deposits in a thickened GBM. **(D)** Stage IV: irregular thickening of the GBM with the loss of electro-dense deposits. *Adapted from (Morita et al., 2015) and (Pozdzik et al., 2018).*

When using light microscopy, the glomerulus will appear normal, with no thickening of the GBM during the early stages of MN. No inflammatory or proliferative features are observed during the course of MN. With the progression of MN, immune complexes accumulate, leading to thickening of the membrane that can be observed with periodic acid-Schiff staining (Figure 2.3–A) (Lai et al., 2015). Contrary to periodic acid-Schiff and haematoxylin-eosin staining's which do not highlight well the immune complexes, silver methenamine stain allows a proper

assessment of the GBM spikes that might have formed around the deposits since it stains all the GBM components in black but not the immune complexes (Figure 2.3–B) (Couser, 2017).

Renal biopsy analysis by immunofluorescence will be characterized by diffuse granular staining of the glomerulus for IgG and complement components. Typically, IgG4 predominance and the absence of C1q will further confirm the diagnosis of primary MN (Figure 2.3–C). Contrarily, predominance of IgG1, IgG2 and/or IgG3, as well as a full-pattern of IgG, IgM, IgA, C3 and C1q would be indicative of a secondary form of MN (Huang et al., 2013; Larsen et al., 2013).

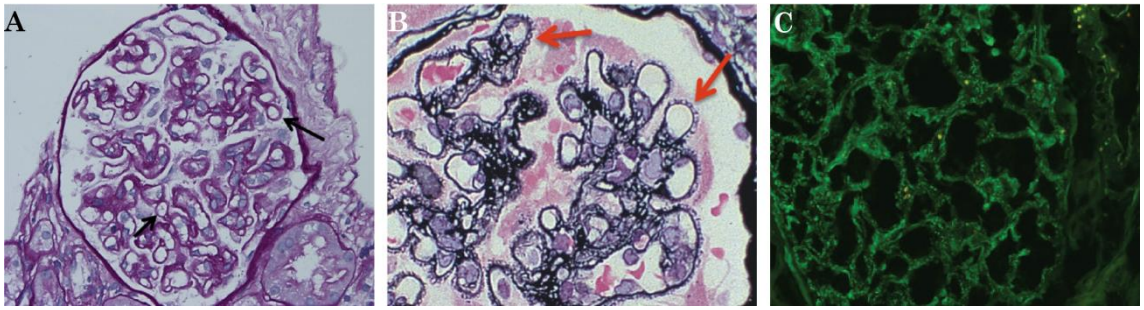

Figure 2.3 – Representative cases of glomerular alteration of MN observed under light microscopy and immunofluorescence. (**A**) Renal biopsy staining with periodic acid-Schiff showing a diffuse thickening of the GBM (arrow). *Adapted from* (Lai et al., 2015) with copyright permission from *"Elsevier Health Science Journals"*. (**B**) Renal biopsy staining with silver-methenamine revealing "spikes" of basement membrane projecting from the outer surface of the GBM (arrows). *Adapted from (Couser, 2017) with copyright permission from "American Society of Nephrology"*. (**C**) Representative staining of IgG observed in immunofluorescence microscopy. *Adapted from (Rodriguez et al., 2012) with copyright permission from "Blackwell Publishing"*.

Historically, confirmation of MN disease by renal biopsy was solely based on characteristic alterations of the glomerulus structure (and the GBM in particular) and the identification of immune deposits by electron-microscopy, light microscopy, and/or immunofluorescence. Nowadays, with the identification of MN autoantigens, kidney staining against PLA_2R1 and THSD7A became of high value in the analysis of renal biopsies (chapter 4.3.1). Finally, even though renal biopsy is still the gold-standard method for diagnosis of MN, detection and measurement of serum autoantibodies against known autoantigens may become a standard procedure in clinical practice (chapter 4.3.2).

2.2.5 Prognosis and treatment

Once a patient is diagnosed with MN, the major goal is to give an effective treatment to lower proteinuria and restore kidney function. Since MN is an

autoimmune disease, in which autoantigens are biological components of the podocyte, the treatment strategy relies on the suppression of the (auto)immune response with concomitant supportive care of the kidney function. Nevertheless, MN treatment remains controversial mainly due to three fundamental questions: when start treating, which therapy (or combine therapy) should be used, and how to avoid secondary effects due to the potential use of toxic drugs?

Differentiating patients with a favourable prognosis from those with a poor prognosis is of outmost importance to guide treatment decision. As discussed above, histological markers, gender, age, blood pressure, urinary complement levels, and HLA type can help to predict clinical outcome. However, these clinical markers are not very reliable. More satisfying parameters have been used to predict diagnosis: persistent proteinuria, initial creatinine clearance, alterations in creatinine clearance over time and urinary low-molecular weight proteins (Reichert et al., 1998; van den Brand et al., 2012). In fact, in 1997, Cattran and colleagues (Cattran et al., 1997) developed a predictive model based on proteinuria and creatinemia levels during the first 6 months after diagnosis and creatinine clearance. This semi-quantitative model, known as the Toronto Risk Score, helps to predict patients' progression with an accuracy of approximately 85%. Based on this model, in general, patients can be considered at: (1) low risk for progression if they present a normal creatinine clearance, proteinuria below 4 g/day and a stable kidney function during a six-months observation period; (2) medium risk for progression if proteinuria is between 4 and 8 g/day with a normal kidney function during the 6 months of observation, and (3) high risk for progression when they have persistent proteinuria superior to 8 g/day independently of kidney dysfunction (Cattran et al., 1997; KDIGO Guidelines, 2012). The Toronto Risk Score seems to be a useful tool to help physicians to decide when to start immunosuppressive treatment.

Thanks to recent advances in the understanding of the pathophysiological mechanisms of MN, both biochemically and immunologically, a consortium of researchers and physicians prepared what is known as the Kidney-Disease-Improving Global Outcomes (KDIGO) guidelines in which they propose the best strategy to evaluate and treat MN patients. The last guidelines (KDIGO Guidelines, 2012), which are widely used worldwide, were prepared in 2012 and recommend that physicians initiate a symptomatic treatment for an observational period of 6 months, in order to evaluate whether the patient will enter into spontaneous remission (i.e. within the natural course of the disease) and avoid unnecessary immunosuppressive treatment. Immunosuppressive treatment is recommended when patients with nephrotic syndrome present at least one of the following

conditions: (1) proteinuria over 4 g/day and remains over 50% of the baseline value and does not progressively decreases during an observational period of least 6 months with conservative treatment (such as anti-hypertensive and anti-proteinuric drugs); (2) presence of severe, disabling or life-threatening nephrotic syndrome complications; (3) increase of serum creatinine levels by 30% or more within 6 to 12 months from diagnosis but with an eGFR not inferior than 25-30 mL/min/1.73 m^2 and not explained by a superimposed complication.

Nevertheless, many MN cases have a complicated clinical history and the decision to treat or not with immunosuppressors remains awfully puzzling for the clinicians, as one can read in clinical forums like the one from the American Society of Nephrology. The upcoming KDIGO guidelines (Floege et al., 2019), which are taking into account the most recent knowledge, will probably help to reply to some questions, but many will remain unanswered. For instance, for the major form of primary MN associated with PLA_2R1, these guidelines might take into account the improved risk assessment of MN using anti-PLA_2R1 titer as a prognosis value as it has been proposed in several studies (De Vriese et al., 2017) (more details in chapter 4.3.3). Still, prospective clinical trials with long-term follow-up are necessary to evaluate the efficacy and safety of treatment regimens as well as identify new biomarkers to recognize patients at risk of severe disease, to guide treatment decision and predict response to therapy, in a more personalized approach.

2.2.5.1 Conservative treatment

Upon diagnosis of MN, patients should receive optimal conservative care during an observational period of at least 6 months and later on if an immunosuppressive treatment is given. The treatment should help to reduce proteinuria and clinical complications associated to a nephrotic syndrome: decrease of blood pressure, reduction of oedema, limitation of risks for cardiovascular events and thromboembolism (Alfaadhel et al., 2015; Bomback et al., 2018). A combined therapy with sodium channel blocker amiloride with loop and thiazide diuretics are suggested as an effective approach to control oedema formation in proteinuric patients. Even though they hardly contribute to a decrease in proteinuria, angiotensin-converting enzyme inhibitors (ACEIs) and angiotensin II receptor blockers (ARBs) are widely recommended to control blood pressure. For patients at high risk of cardiovascular and/or thromboembolic events, due to the hypercholesterolemia and/or hypoalbuminemia, statins (a 3-hydroxy-3-methyl-glutaryl-coenzyme A reductase inhibiter) and/or a prophylactic anticoagulant therapy is recommended.

2.2.5.2 Immunosuppressive treatment

The first randomized controlled clinical trial in patients with MN took place in 1979 to verify the efficacy and safety of corticosteroids (such as prednisone) as first-line therapy for MN (Anonymous, 1979). However corticosteroid monotherapy was not better than symptomatic therapy alone, even though a Japanese study showed that it was associated with better renal survival (Alfaadhel et al., 2015; Xu et al., 2015). Accordingly, KDIGO guidelines do not recommend corticosteroids monotherapy as the first-line therapy in MN, probably due to the fact that long-term high-dose treatments are highly toxic and alternative therapies are now available (Hofstra et al., 2013).

A 6-month regimen known as the "Ponticelli protocol", which proposes the daily intake of oral alkylating agents (cyclophosphamide or chlorambucil) alternating monthly with corticosteroids, was found to be more effective than supportive therapy in nephrotic patients with normal renal function (Ponticelli et al., 1998; Ponticelli et al., 1984; Ponticelli et al., 1995). However, the short-term and potential long-term side effects of alkylating agents (such as infection, infertility and increased risk of cancer) make the physicians reluctant to use this therapy (Hofstra et al., 2010).

Calcineurin inhibitors (such as cyclosporine or tacrolimus) seem to be an effective alternative for patients who were previously unresponsive to other immunosuppressors including steroids and alkylating agents (Cattran et al., 2001; Goumenos, 2008; Praga et al., 2007). Its anti-proteinuric effect is visible quite early, therefore if within 3 months no decrease in proteinuria is observed, it is unlikely that it will occur later (Waldman et al., 2012). Even though the rate of remission is approximately 75%, relapse occurs in 40-50% of patients within one year after drug withdrawal (Cattran et al., 2001; Praga et al., 2007). This might lead to a discontinued long-term use of calcineurin inhibitors with further concerns due to risk of nephrotoxicity associated with the prolonged use of these drugs.

More recently, rituximab, an anti-CD20 drug initially used for non-Hodgkin's lymphoma and rheumatoid arthritis, has emerged as new effective immunosuppressive treatment for MN (Edwards et al., 2001; Remuzzi et al., 2002; Taylor et al., 2008). Proteinuria decreases rapidly or slowly over time and remission occurs in 65 to 80% of patients within 1 to 5 years after therapy, while the rate of relapse is relatively low, approximately 30% (Fervenza et al., 2010; Remuzzi et al., 2002; Ruggenenti et al., 2012). Different randomized controlled clinical trials have recently demonstrated the better safety and efficacy of rituximab in comparison to conservative treatment or other immunosuppressive agents (Dahan et al., 2017; Fervenza et al., 2019). Therefore,

rituximab may become the most recommended therapy and first-line immunosuppressive therapy in MN (Rojas-Rivera et al., 2019).

Of curiosity and without knowledge of the underlying mechanisms, traditional Chinese medicine seems to be often used for MN, in particular among the Asiatic population. One study showed that prescription of *Tripterygium wilfordii* was associated with a remission rate of approximately 45% within 1 year, while in combination with a low-dose of prednisone it was approximately 75% (Xu et al., 2015). Additionally, consumption *Astragalus membranaceus* was associated with proteinuria remission and the prescription of Shenqi particles (composed of 13 herbs including *Astragalus membranaceus*) is associated with a remission rate of about 70% with a significant eGFR improvement within 48 weeks (Ahmed et al., 2007; Chen et al., 2013; Leehey et al., 2010).

2.2.6 Genetic susceptibility

Autoimmune diseases have been commonly linked to variants in the MHC class II (chapter 1.3.2). Thus, without surprise, the same was observed for MN. In 1979, Klouda and colleagues (Klouda et al., 1979) demonstrated that the HLA-DRw3 variant was significantly associated with MN in Caucasian patients versus the control population (75% versus 20%), with a relative risk of 12, associating MHC class II with MN for the first time. This observation was confirmed in other studies with Caucasian patients, whereas it was the HLA-DR2 allele that was associated with MN in the Japanese population (Hiki et al., 1984; Le Petit et al., 1982; Muller et al., 1981; Tomura et al., 1984). These observations were followed by the demonstration of a strong association of the HLA-DQA1 allele with MN (Vaughan et al., 1989).

More recently, in 2011, an independent genome-wide association study (GWAS) with a total of 556 Caucasian patients (from three populations – French, Dutch and British) demonstrated that among the 242,824 common SNPs (single nucleotide polymorphisms) studied only two were strongly associated with MN (Stanescu et al., 2011). On chromosome 6p21, which codes for HLA-DQA1, the SNP rs2187668 is associated with a risk of 20.2; and on chromosome 2q24, which codes for PLA_2R1, the SNP rs4664308 is associated with a risk of 4.2, further confirming by a different and independent approach the key role of PLA_2R1 in MN. Importantly, homozygosity for the four risk alleles has an additive effect, increasing the risk of developing MN to 78.5. Interestingly, the SNP rs4664308 was significantly associated with another coding SNP that leads to a missense mutation in the β2-strand of CTLD1: rs3749117 (Met292Val). A follow-up study identified an additional SNP in each chromosome that was associated with the risk of developing

MN in the British population: rs17830558 in the PLA_2R1 gene and rs9272729 in the HLA-DQA1 gene (Sekula et al., 2017).

Other studies conducted in different populations confirmed the susceptibility associated to the HLA-DQA1 rs2187668 SNP in Caucasian Spanish, South Asians and Han Chinese populations, but not in the Afro-American population (Bullich et al., 2014; Qin et al., 2017; Ramachandran et al., 2016; Saeed et al., 2014; Wang et al., 2018). Additionally, it was observed that another SNP in this gene, rs28383345, was associated with protection against the susceptibility to MN (relative risk of 0.4) in the Chinese Han population (Qin et al., 2017). The risk associated to the PLA_2R1 rs4664308 SNP was also observed in Caucasian Spanish and South Asian populations, and in the South Asian population additional SNPs were associated to the susceptibility of developing MN (rs3749119 and rs3749117) (Bullich et al., 2014; Ramachandran et al., 2016).

HLA-DRB1 variants, and in particular HLA-DRB1*15:01 and HLA-DRB1*03:01, were identified as independent risk alleles for the development of MN in a GWAS of 261 patients from the Chinese Han population (Cui et al., 2017). Another study confirmed that in the Chinese population HLA-DRB1*15:01 as well as HLA-DRB3*02:02 alleles were independently and strongly associated with MN (Le et al., 2017). A study with Japanese patients strongly associated HLA-DRB1*15:01 and HLA-DQB1*06:02 with PLA_2R1-associated MN among this population (Thiri et al., 2016). In this last study, four PLA_2R1 SNPs were associated to MN in Japanese patients: rs3749119 and rs35771982, which were previously identified in other populations, as well as rs2715928 and rs16844715.

Finally, different studies conducted in different populations have also suggested that other genes, such as *IL-4*, *IL-6*, *IL-10*, *TNF-α*, *MBL2*, *TLR-4*, *TLR-9,* and *NPHS1* genes, were also associated with MN (Liu et al., 2019). In sum, a combination of gene polymorphisms might predispose to disease initiation and also modulate progression and severity of MN.

2.3 Autoantigens of human MN

In 1957, MN was recognized as a distinct clinico-pathological entity (Jones, 1957). Shortly after, in 1959, Heymann and colleagues (Heymann et al., 1959) established the first animal model of the disease, the Heymann nephritis rat model, providing a major breakthrough in the understanding of MN. Indeed, most of the knowledge we have today regarding the pathophysiology of human MN was obtained and/or predicted from this model. Later on, in 1982, megalin (gp330, or low density

lipoprotein-related protein 2 – LRP2, Figure 2.4) was identified as the main target autoantigen in the rat model of MN (Kerjaschki et al., 1982). This finding further encouraged the search for the human autoantigen. Disappointingly, megalin was not the human autoantigen and furthermore, it is not expressed in human podocytes.

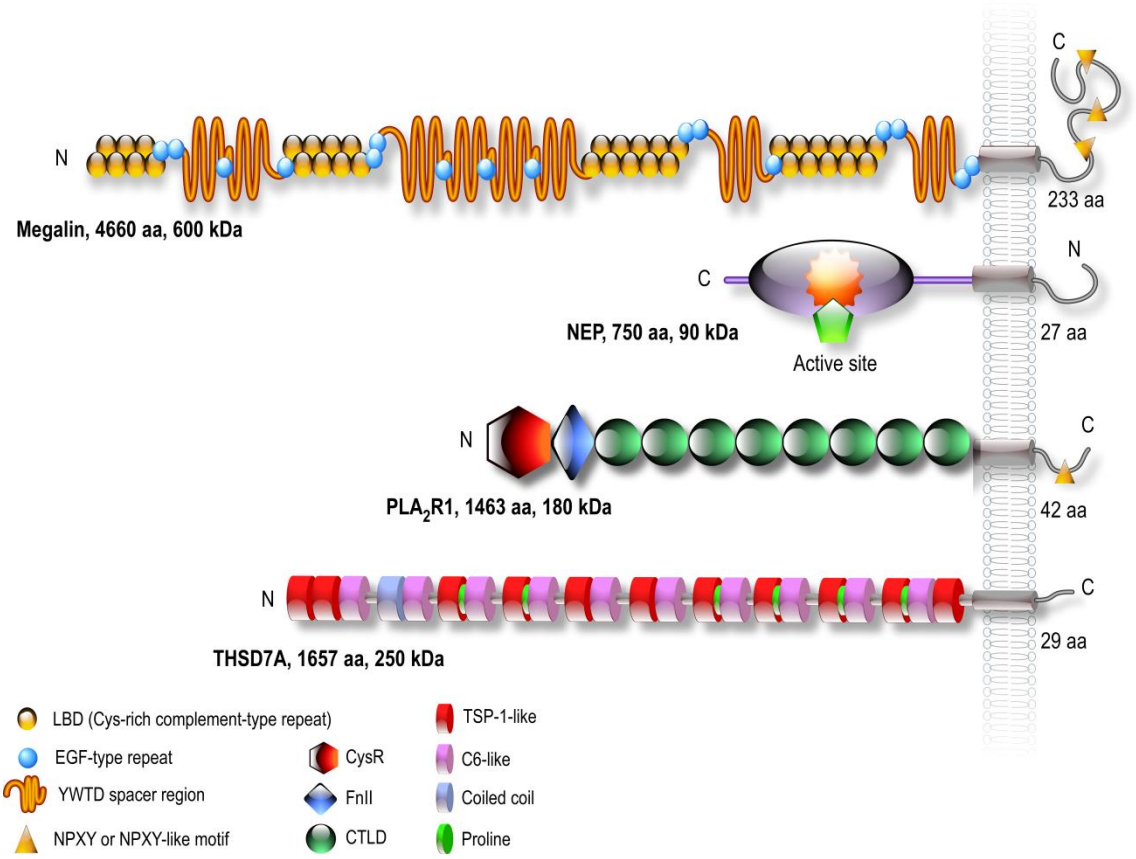

Figure 2.4 – Schematic diagram of the autoantigens found to be implicated in MN until now. Megalin (gp330, LRP2) is a 600 kDa glycotransmembrane protein identified in 1982 as the autoantigen in the Heymann nephritis experimental model of MN. This protein is composed by a large extracellular region, a small transmembrane domain and an intracellular domain. The extracellular region is composed by 36 cysteine-rich complement-type repeats comprising four clusters of ligand-binding domains (LBD) and by 16 epidermal growth factor-like (EGF-like) repeats that are separated by 8 YWTD-containing spacer regions. NEP, a 90 kDa glycosylated zinc-dependent membrane metalloprotease, was identified in 2002 as the autoantigen in the rare alloimmune form of MN. It consists of a short cytoplasmic N-terminal domain, a transmembrane domain and a large extracellular domain containing the active site. In 2009, PLA_2R1, a 180 kDa transmembrane glycoprotein, was identified as the first autoantigen in human adult MN. PLA_2R1 is formed by a large glycosylated extracellular portion, comprising a N-terminal cysteine-rich (CysR) domain, a fibronectin type-II (FnII) domain and 8 different C-type lectin like domains (CTLDs), a transmembrane domain and a short cytoplasmic tail. Finally, in 2014, THSD7A was identified as the second autoantigen in human adult MN. This 250 kDa glycosylated protein is composed by 21 extracellular domains (thrombospondin type-1 (TSP-1) repeat domains alternating with complement 6-like (C6-like) repeats and a coiled coil), as well as a transmembrane domain and a short cytoplasmic tail.

It was only in 2002, 20 years after the identification of megalin, that the first human antigen was identified: NEP (Figure 2.4) (Debiec et al., 2002). However, NEP is the antigen of a rare alloimmune form of MN and it is not the autoantigen in the primary form of MN, which is predominant in adults. In 2009, exactly 50 years after the development of the Heymann nephritis model of MN, PLA_2R1 was identified as the major autoantigen in adult MN for approximately 70% of cases (Beck et al., 2009). This was followed by the identification of THSD7A as the second autoantigen in another group of 3% of patients (Tomas et al., 2014). In some very rare cases, approximately 0.3% of the patients can be positive for both PLA_2R1 and THSD7A. On the contrary, about 27% of patients are double negative for both PLA_2R1 and THSD7A, meaning that they should have autoantibodies targeting a different autoantigen with several hypotheses such as a third or more unknown autoantigens, a complex of proteins, one of the already known autoantigen but in a different conformation, etc. Indeed, more recently, exostosins 1 and 2 as well as NELL-1 (neural epidermal growth factor-like1 protein) were identified as new autoantigens – exostosins seem to be associated with secondary MN, being mainly present in cases of lupus nephritis while NELL-1 seems to be an autoantigen for approximately 7% of primary MN cases (Sethi et al., 2019; Sethi et al., 2019).

2.3.1 Neutral endopeptidase (NEP)

The neutral endopeptidase (NEP, chromosome 3q25.3) is a 90 kDa glycosylated zinc-dependent membrane metalloprotease that cleaves peptides at the amino side of hydrophobic residues, also known by other names: neprilysin, membrane metallo-endopeptidase (MME), enkephalinase, vasopeptidase, atriopeptidase, cluster of differentiation 10 (CD10) and common acute lymphoblastic leukaemia antigen (CALLA) (Maguer-Satta et al., 2011; Malek et al., 2017; Malito et al., 2008; Mishra et al., 2016). It consists of three domains: a short cytoplasmic N-terminal domain, a transmembrane domain and a large extracellular domain containing the active site (Figure 2.4). NEP is highly expressed in the brush border of proximal renal tubular cells, but also in podocytes. It can also be found in the brain, vascular endothelial cells, smooth muscle cells, cardiomyocytes and neutrophils. It has the ability to metabolise several endogenous peptides, such as glucagon, enkephalins, oxytocin, natriuretic peptide and vasoactive peptides (including bradykinin, substance P, vasoactive intestinal peptide, adrenomedullin, endothelin-1 and angiotensin-II). Therefore, it has several regulatory effects in the cardiovascular and renal systems. It also can degrade ß-amyloid peptide, which is well known in Alzheimer's disease. As one of its alternative names indicates, NEP or CALLA is also an antigen in 85%

of cases of acute lymphocytic leukaemia, and is also expressed in several other cancers.

In 2002, Debiec and colleagues (Debiec et al., 2002) identified NEP as the first human antigen in a rare case of MN. A baby boy was born with oligoanuria and massive proteinuria. In addition, the biopsy revealed an atypical form of MN with subepithelial deposits of IgG (more details on chapter 2.2.2). Since the newborn was too young to have produced autoantibodies of his own, and having in mind the passive Heymann nephritis model, it was hypothesized that the mother had passively transferred the autoantibodies to her foetus (Debiec et al., 2002; Ronco et al., 2015). Further investigation confirmed this hypothesis and identified NEP as the autoantigen.

2.3.2 Phospholipase A_2 receptor 1 (PLA_2R1)

After the development of the Heymann nephritis model, for several years, many teams worked hard to identify the human autoantigen in adult patients with MN. It was finally in 2009, that, with a small amount of serendipity, a major breakthrough by Beck and colleagues (Beck et al., 2009) led to the identification of PLA_2R1 as the major autoantigen in adult MN. Their experiments consisted on testing MN patients' serum reactivity against human glomerular extracts by western blot. However, contrary to the most common standard procedure, the western blot experiments were performed under non-reducing conditions. This apparently small but in fact major change was key to detect circulating autoantibodies from MN patients that specifically bind to a 185 kDa glycosylated antigen in a conformational manner. Further analysis of the reactive bands after partial purification and by mass spectrometry provided a list of candidate proteins that were tested by western blot, leading to the identification of PLA_2R1 as the target autoantigen. Immunoprecipitation of human glomerular extracts with serum samples from MN patients followed by western blot with specific anti-PLA_2R1 antibody further confirmed this major and important discovery.

In the original study, 26 out of 37 MN patients (70%) recognized PLA_2R1 as the autoantigen, for both the native protein from the glomerular extract and the recombinant protein expressed in HEK293 cells. In contrast, sera from healthy controls, patients with secondary MN or other glomerular or autoimmune diseases did not react with the autoantigen. Therefore PLA_2R1 has been considered a pathognomonic biomarker for MN disease. After excluding the formation of circulating immune complexes with soluble PLA_2R1, Beck and colleagues confirmed their initial hypothesis: the immune complexes form *in situ* in the

glomerulus where PLA_2R1 is expressed, particularly in the podocyte, as demonstrated by immunofluorescence microscopy. Additionally, PLA_2R1 co-localized with IgG4 in the typical fine granular pattern. Even though IgG4 was the predominant IgG subclass, different amounts of IgG1, IgG2 and IgG3 were observed in MN patients' serum. As referred before, PLA_2R1 autoantibodies from MN patients only recognized the autoantigen in western blot experiments performed under non-reducing conditions, demonstrating that they recognize conformational epitopes, partially explaining the time gap between the identification of megalin and PLA_2R1. Finally, Beck and colleagues were the first to demonstrate that autoantibodies against PLA_2R1 were associated with disease activity, being present during disease activity and declining or disappearing during clinical remission and before decrease of proteinuria. After this landmark study, several other teams confirmed that PLA_2R1 is the autoantigen in 70-80% of MN cases, with IgG4 as the main subclass and anti-PLA_2R1 titer associated with disease activity.

PLA_2R1 was first identified, in 1990, as a receptor for several snake venom secreted phospholipase A_2 ($sPLA_2s$) in rabbit skeletal muscle cells by Lambeau and colleagues (Lambeau et al., 1990). The receptor was thus initially called M-type (muscle-type) receptor and rabbit PLA_2R1 was cloned in 1994 as a second member of the macrophage mannose receptor family (Lambeau et al., 1994). Shortly after, in 1995, human PLA_2R1 was cloned from lung, and interestingly it was found to be highly expressed in adult kidney (Ancian et al., 1995). This highly glycosylated receptor is formed by an extracellular region, a transmembrane domain and a cytoplasmic tail (Figure 2.4). My Ph.D. works focused mainly on PLA_2R1-associated MN, thus chapter 3 of this manuscript has more detail information regarding PLA_2R1 structure and functions. In this chapter and chapter 4, more detailed information regarding PLA_2R1-associated MN can be found.

2.3.3 Thrombospondin type–1 domain containing 7A (THSD7A)

After the identification of PLA_2R1 as the major autoantigen in about 70% of MN patients, the search for the autoantigen(s) responsible for the remaining 30% of cases continued, now having in mind that the autoantibodies may target conformational epitopes. An international collaborative work between three teams (Dr. Beck and Dr. Salant team from USA, Dr. Lambeau team from France and Dr. Stahl team from Germany) led to the identification of THSD7A as the second autoantigen in adult MN. The collaboration was essential for the identification of THSD7A since it has a very low prevalence of about 3-5% among all MN patients.

Dr. Laurence Beck first identified a patient with biopsy-proven MN who had also been diagnosed with prostate cancer two years earlier and had no evidence suggestive of secondary MN (Beck, 2010). When analysed by western blot with human glomerular extract, the patient's serum reacted against an antigen with a size similar to PLA_2R1. However this latter was not the autoantigen for this patient since in further analysis by western blot and immunoprecipitation with recombinant PLA_2R1, the serum did not show any reactivity. Additionally, in the renal biopsy, immunofluorescence staining showed that IgG4 was present within the immune deposits but did not co-localized with PLA_2R1. Thus, the MN autoantigen for this patient was another highly glycosylated protein with a high molecular weight.

At the same time, the laboratory of Dr. Lambeau was also trying to identify this new second autoantigen through a candidate approach experiment based on the hypothesis that it might be one of the three paralogs of PLA_2R1 (Tomas et al., 2014) (more detailed information about PLA_2R1 and its paralogs can be found in chapter 3). In collaboration with the team of Dr. Stahl, they started by screening a small cohort of biopsy-proven MN patients by western blot for the human glomerular extract as well as for PLA_2R1 and its paralogs. With this approach, they first identified a serum from a patient from Nice (France) with MN and HIV and 3 other patients that could also recognize a band of high molecular weight in the human glomerular extract, but did not recognize PLA_2R1 nor its paralogs.

The two teams used two different strategies to identify the new autoantigen using mass spectrometry analysis (Tomas et al., 2014). In one approach, purification of glomerular proteins by gel electrophoresis run in parallel with western blot analysis, pretreated or not with N-glycopeptidase F alone or with both N-glycopeptidase F and neuraminidase, revealed three different discrete bands (250 kDa, 225 kDa and 200 kDa), that were further analysed by mass spectrometry. In the other approach, the glomerular proteins were treated or not with N-glycopeptidase F and partially trypsinized. After electrophoresis the bands that were previously recognized by western blot under non-reducing conditions by an MN patient were excised and analysed by mass spectrometry. Both mass spectrometry analyses generated a list of potential candidates that finally led both teams to identify THSD7A (thrombospondin type-1 domain containing 7A) as the newly autoantigen for MN (Tomas et al., 2014).

A combined cohort of 154 PLA_2R1-negative MN patients from the American, French and German teams was assembled and screened for THSD7A. Fifteen patients showed reactivity against the newly identified antigen suggesting a

prevalence of 2.5-5%. Follow-up studies confirmed that THSD7A is the autoantigen for 2.5-3% of the MN patients (Hoxha et al., 2017; Larsen et al., 2016; Tomas et al., 2014; Zaghrini et al., 2019). Similar to PLA_2R1, anti-THSD7A autoantibodies were conformational and predominantly IgG4. Finally, recent studies identified some rare cases of patients' double positive for anti-PLA_2R1 and anti-THSD7A autoantibodies (Larsen et al., 2016; Wang et al., 2017; Zaghrini et al., 2019).

Thrombospondin type 1 domain-containing 7A (THSD7A, chromosome 7p21.3) is a 250 kDa glycosylated transmembrane protein that belongs to the thrombospondin superfamily. It is expressed in several tissues including cerebral cortex, testis, lung and of course, kidney. Although the overall structural organization of THSD7A is still unclear, it is formed by a large N-terminal extracellular region followed by a transmembrane domain and a short cytoplasmic C-terminal tail. The extracellular region comprises a total of 21 domains: thrombospondin type-1 (TSP-1-like) repeats alternating with complement 6-like (C6-like or F-spondin-like) repeats (Figure 2.4) and a single highly basic coiled-coil region (Seifert et al., 2018; Stoddard et al., 2019).

The exact function of THSD7A remains unknown. Based on its structure, it has been hypothesized that THSD7A might act has an adhesive glycoprotein that can interact with components of the extracellular matrix including fibronectin and collagen, and promote cell adhesion by binding to sulfated glycoconjugates such as heparin, sulfatides and heparin sulphates (Dardik et al., 1989; Galvin et al., 1987; Guo et al., 1992; Stoddard et al., 2019). Studies using human umbilical vascular endothelial cells (HUVECs) and zebrafish suggested that THSD7A may be involved in cytoskeletal organization, endothelial cell migration and tube formation during embryonic angiogenesis and neurogenesis (Kuo et al., 2011; Liu et al., 2016; Wang et al., 2011; Wang et al., 2010). The overexpression of THSD7A has also been described in several human tumours, including renal, colorectal, breast and prostate cancers (Stahl et al., 2017). Upregulation or downregulation of THSD7A has been observed in different tumours: low THSD7A expression in colorectal or renal cancers was associated with adverse clinico-pathological parameters whereas THSD7A overexpression in prostate cancer was associated with poor prognosis, suggesting either different roles of THSD7A in different tumour contexts or that the regulation of THSD7A is a consequence of the cancer microenvironment. It also has been hypothesized that the expression of THSD7A is associated with vascular invasion, metastasis and angiogenesis (Stahl et al., 2017).

In kidney, THSD7A is expressed in the podocytes of human, rodents and zebrafish, in particular in foot processes and split diaphragm (Godel et al., 2015; Meyer-

Schwesinger et al., 2015; Tomas et al., 2014; Tomas et al., 2017). Studies from Tomas and colleagues (Tomas et al., 2016; Tomas et al., 2017) support the idea that THSD7A may be important for the maintenance of the glomerular filtration barrier since disruption of its expression can induce rearrangement of cytoskeleton, alteration of focal adhesion, cell detachment and apoptosis, altered podocyte differentiation and impaired glomerular filtration barrier function. In a very recent study from the same group, Herwig and colleagues (Herwig et al., 2019), using both murine and immortalized culture murine podocytes, demonstrated that the expression of THSD7A was characteristic of late stages of podocyte development. They showed that, in murine and human, THSD7A is expressed at the basal aspect of foot processes, in close proximity to the slit diaphragm and nephrin (Herwig et al., 2019). The authors suggested that THSD7A stabilizes membrane dynamics of human mature podocytes, increasing their adhesion and slowing-down cell motility, since THSD7A expression in human podocytes was associated with increased cell size, enhanced adhesion, reduced detachment from collagen type IV and decreased ability to migrate.

2.3.4 Cytoplasmic autoantigens

In addition to PLA_2R1 and THSD7A, other podocyte autoantigens have been identified in adult MN patients. In 1999, α-enolase (αENO) was first described as an autoantigen in MN patients (Wakui et al., 1999). Autoantibodies against this glycolytic enzyme with multiple functions were identified by western blot and based on its partial amino acid sequence when testing MN patients' serum against human and porcine renal extract. The autoantibodies were mainly IgG1 and IgG3 with a more recent study also reporting IgG4 (Kimura et al., 2017; Wakui et al., 1999). It was also demonstrated that αENO co-localized with IgG4 and C5b-9 in electron-dense subepithelial immune deposits (Bruschi et al., 2011). However, αENO autoantibodies are not exclusive nor specific for MN, since they can be detected in other diseases such as ANCA disease, inflammatory bowel disease, primary biliary cirrhosis and systemic lupus erythematous (Akisawa et al., 1997; Moodie et al., 1993; Pratesi et al., 2000; Roozendaal et al., 1998).

In 2010, Prunotto and colleagues (Prunotto et al., 2010) identified (i) aldose reductase (AR), an oxidoreductase that catalyze the reduction of aldehydes and carbonyls, and (ii) superoxidase dismutase 2 (SOD2), a key antioxidant enzyme, as two other autoantigens in MN. Autoantibodies against these podocyte autoantigens were detected in patients' serum as well as in the glomeruli where they co-localized with IgG4 and C5b-9 within electron-dense subepithelial immune deposits. Like

αENO, autoantibodies against SOD2 are not specific for primary MN since they have also been described in lupus nephritis. However, in primary MN, the autoantibodies are predominantly IgG4 while in lupus nephritis they are mostly IgG2 (Bonanni et al., 2015; Bruschi et al., 2011; Prunotto et al., 2010).

In 2012, Murtas and colleagues (Murtas et al., 2012) screened a cohort of 186 MN patients for all the autoantigens described until then: NEP, PLA_2R1, αENO, AR and SOD2. As expected, no patient presented reactivity against NEP, since this has only been described in alloimmune cases. Autoantibodies against PLA_2R1 were found in 60% of patients, while anti-αENO, anti-AR and anti-SOD2 were detected in 43%, 34% and 28% of the patients, respectively. The autoantibodies against the cytoplasmic autoantigens were mainly IgG4 and they were significantly correlated with the anti-PLA_2R1 titer. Additionally, 20% of the patients were negative for all autoantibodies, which was significantly associated with lower proteinuria after 1 year of follow-up. Conversely, 10% of the patients had autoantibodies against all four autoantigens. The fact that a single patient can produce autoantibodies against several autoantigens suggests a complex and progressive pathophysiological mechanism in the development and progression of MN.

Of note, these cytoplasmic autoantigens are likely not the primary targets in MN. It has been suggested that upon the formation of autoantibodies against the primary target, ie. PLA2R1, THSD7A or other (un)known antigens, and with the progression of the autoimmune response, podocyte injury leads to the exposure to these neoantigens. Thereby, these cytoplasmic autoantigens may represent an immunological marker of advanced renal damage and ESRD.

2.3.5 Exostosin 1/Exostosin 2

More recently, a study by Sethi and colleagues (Sethi et al., 2019) used a combination of laser microdissection, mass spectrometry and immunohistochemistry to identify exostosin 1 (EXT1) and exostosin 2 (EXT2) (glycosyltransferases) as similar autoantigens in 21 out of 209 cases (10%) of PLA_2R1-negative MN patients. The autoantibodies targeting EXT1/EXT2 in the immune complexes were mainly IgG1. Interestingly, the authors were not able to detect circulating anti-EXT1/EXT2 autoantibodies. Kidney biopsy of the EXT1/EXT2 cases revealed positive staining for C3 and C1q within the electron-dense subepithelial immune deposits. However, these new autoantigens seem to be associated with secondary MN, being mainly present in cases of lupus nephritis.

2.3.6 Exogenous autoantigens

In some MN cases, mainly secondary ones, the antibodies target antigens in the subepithelial deposits that are not intrinsically present in the podocyte, but instead have an exogenous origin. This can occur in cases of MN secondary to infections in which the antigen of bacterial or viral origin can be identified in the immune deposits, such as the antigenic protein at the surface of the Hepatitis B and C virus or *Helicobater pylori* (Debiec et al., 2014; Lai et al., 1991; Nakahara et al., 2010). The exogenous antigens can also originate from drug therapy which was the case of recombinant human α-glucosidase or recombinant human arylsulfatase B prescribed for enzymatic replacement therapy for Pompe disease and mucopolysaccharidosis type VI, respectively (Debiec et al., 2014; Hunley et al., 2004). Diet can be another source of exogenous antigens, as it has been well described for the cationic bovine serum albumin (Debiec et al., 2011).

Two scenarios that lead to the deposition of these antigens in the human glomerulus have been proposed (Debiec et al., 2014). One suggests that due to uncommon physiochemical properties, these exogenous antigens may be trapped in the glomerular basement membrane (scenario of planted antigen) where they are targeted by circulating antibodies, leading to the formation of *in situ* immune complexes, as it has been demonstrated for cationic albumin (Debiec et al., 2011). The other proposes that small circulating non-precipitated immune complexes containing IgG4 and the exogenous antigen can deposit in the glomerular basement membrane as it was demonstrated in the chronic serum sickness model (Debiec et al., 2014).

2.4 Animal models of MN

In general, animal models are of great importance to better understand the pathogenesis of human diseases. And membranous nephropathy is not an exception, but it is a particular example of an animal model preceding knowledge of the human molecular pathophysiology. In 1959, long before the identification of any human MN antigen, Heymann and colleagues (Heymann et al., 1959) established the first animal model of MN, nowadays known as the Heymann nephritis MN model. Their pioneering work and the follow-up studies in this model greatly contributed to a better understanding of human MN. In fact, most of the knowledge we have today regarding the pathophysiology of MN was obtained and/or predicted from this model. Additionally, their experimental work further encouraged the

scientific community to search for human autoantigens that culminated with the key identification of NEP, PLA_2R1 and THSD7A (more details on chapter 2.3).

2.4.1 Heymann nephritis model in rat

In the active model of Heymann nephritis, Sprague-Dawley rats were actively immunized with their own crude kidney extract (Fx1A) in complete Freund's adjuvant (containing tubercle bacillus nowadays termed Mycobacterium tuberculosis) during 6 to 12 weeks (Heymann et al., 1959). After this period, the rats presented clinical and immunohistological features similar to the ones described in human MN, including proteinuria and thickening of the glomerular basement membrane due to the presence of electron-dense subepithelial immune deposits. Further studies (using a passive model of Heymann nephritis and perfused rat kidneys) demonstrated that the autoantibodies bind to an intrinsic autoantigen present at the glomerular filtration barrier to form *in situ* immune complexes, with the main autoantigen later identified as megalin (Couser et al., 1978; Feenstra et al., 1975; Kerjaschki et al., 1982, 1983; Kerjaschki et al., 1987; Raychowdhury et al., 1989; Van Damme et al., 1978). Additional studies demonstrated that the autoantigen-autoantibody complexes co-localized with C3 and C5b-9 complexes, and that the podocyte injury and proteinuria observed in this model were complement-mediated (Baker et al., 1989; Cybulsky et al., 1986; Ma et al., 2013).

In passive Heymann nephritis models, rats are actively injected with antibodies against brush border antigens (anti-Fx1A) produced in rabbit or sheep or with antibodies against specific antigens, such as anti-megalin (Couser et al., 1978; Feenstra et al., 1975; Makker et al., 2006; Salant et al., 1980; Salant et al., 1988; Salant et al., 1989; Van Damme et al., 1978). Similar to the active model, immune complexes between the antigen and the injected antibodies can be observed in the subepithelial space and rats develop proteinuria which again is dependent of complement activation. Of curiosity, a study with both active and passive Heymann nephritis models suggested that molecular rearrangement of the slit diaphragm may play a role in the pathogenesis of MN (Nakatsue et al., 2005). Particularly, it is suggested that dissociation of nephrin from podocin with its subsequent urinary excretion as well as a reduced expression of both nephrin and podocin might contribute to the development of proteinuria.

As reviewed and exemplified in chapter 1.4.1, at the beginning of an (auto)immune response, the diversity of epitopes targeted by the immune response is usually limited (Vanderlugt et al., 1996). In the physiological process of maturation of the immune response with optimization of antibodies, a mechanism of epitope

spreading can occur. This mechanism is characterized by the diversification of the epitope recognition pattern from an initial epitope which triggers the inflammatory process (immunodominant epitope) to multiple secondary epitopes (subdominant epitopes) within the same antigen (intramolecular spreading) or other(s) antigenic molecule(s) (intermolecular spreading).

Interestingly, a mechanism of intramolecular epitope spreading has been described in the Heymann nephritis model, in which antibodies targeting different megalin epitopes were associated with the development of glomerular immune deposits and nephrotic syndrome. Immunization of Lewis rats with a recombinant protein referred to as the "L6" fragment – consisting of the first 236 amino acids of the N-terminal LBD-I cysteine-rich ligand-binding domain of megalin (Figure 2.4) – generated over time a cascade of autoantibodies describing a mechanism of epitope spreading towards the C-terminal domains and inducing severe disease (Shah et al., 2007; Tramontano et al., 2006). Four weeks after injection, the rats produced antibodies against the L6 fragment but not the others LBD domains and they did not developed proteinuria. Eight weeks after immunization (with a boost at week 4) the rats generated antibodies against the C-terminal LBD-II, LBD-III and LBD-IV domains highlighting a mechanism of epitope spreading that significantly correlated with the increase of proteinuria (Shah et al., 2007). Additionally, 12 weeks post-injection, proteinuria levels correlated with staining for C3, C5b-9 and IgG1 in the glomerular immune deposits (Tramontano et al., 2006). Of note, conformational epitopes as well as post-translational modifications, in particular glycosylation, seem to be necessary for the pathogenic role of megalin (Tramontano et al., 2004).

2.4.2 Heymann nephritis model in mice

Several groups have tried to establish similar passive models of Heymann nephritis models in mice. Despite the enormous efforts from several groups to achieve this goal, most models that have been established turned out to be of limited use mainly because of the inability to induce long-term complement-dependent proteinuria (Jefferson et al., 2010).

One example is the passive model developed by Assmann and colleagues (Assmann et al., 1983), in 1983, in which they injected C57.B110 mice with rabbit IgG against homologous pronase-digested renal tubular antigens. The immunized mice developed subepithelial immune complexes containing rabbit IgG, mice IgG1 and mice C3. However, histologically the mice presented very few differences compared to the control: they did not present GBM "spikes" nor effacement of podocyte foot processes, both characteristic features of human MN. Additionally, the mice only

presented transient albuminuria without developing nephrotic syndrome. At this time, the weak pathogenic effects were proposed to be due to the presence of mouse IgG1 antibodies (equivalent to human IgG4) in immune deposits which do not activate mouse complement.

Another passive model was developed by the same group, in 1992, in which they injected mouse IgG1 antibodies against mice aminopeptidase A, hoping to induce a more severe and persistent proteinuria (Assmann et al., 1992). Indeed, after immunization the mice immediately developed massive albuminuria for at least 16 days. However glomerular deposition of mice C3 was absent, no glomerular lesions were observed under light microscopy, and activation of the complement was not required for the development of proteinuria. Moreover, even though electron microscopy revealed fusion of the podocyte foot processes and scattered electron-dense immune deposits, there was no thickening of the GBM, one of the main features of human MN.

More recently, in 2011, another passive MN model was also reproduced in C57BL/6N and BALB/c mice to which antibodies against podocyte proteins (produced in sheep) were injected (Meyer-Schwesinger et al., 2011). The mice developed nephrotic syndrome with severe oedema, proteinuria and hypoalbuminemia. They presented swollen podocyte and subepithelial immune complex deposits with effacement of the podocyte foot processes, but no disruption of the GBM. Complement activation was not necessary for podocyte disruption.

2.4.3 cBSA animal model of MN

An alternative model of MN was provided by Border and colleagues (Border et al., 1982) based on the hypothesis that the antigen net charge could be fundamental for the formation of subepithelial deposits. Thus, their model consisted of repeatedly injecting rabbits with cationic bovine serum albumin (cBSA) which would work as a “planted” or exogenous antigen. Immunizations with anionic or native (neutral) BSA mostly led to mesangial deposits while immunization with cBSA led to the formation of subepithelial deposits co-localized with IgG and C3. Further experiments demonstrated that cBSA binds to anionic heparan sulphate proteoglycans of the GBM, which in turn induces the binding of antibodies to the trapped cBSA, leading to *in situ* formation of immune complexes (Adler et al., 1983; Border et al., 1982). This model was later reproduced and established in dogs, mice and rats, and corresponds to the rare cases of childhood human MN with cBSA (Debiec et al., 2011).

2.4.4 PLA$_2$R1 animal model of MN

In 2009, a major breakthrough was achieved with the identification of PLA$_2$R1 as the major autoantigen in human MN with expression in human podocytes. However, PLA$_2$R1 is not expressed in rodent podocytes which has strongly hampered the development of an *in vivo* animal model for PLA$_2$R1-associated MN (Godel et al., 2015; Meyer-Schwesinger et al., 2015).

In a collaborative work, several teams attempt to generate a transgenic mice model by overexpressing human PLA$_2$R1 in the CD1 strain, but unfortunately they did not succeed in expressing the protein in the glomeruli (Borza et al., 2013).

During the ASN Kidney Week 2012, an abstract from Zahner and colleagues (Zahner et al., 2012) described the generation of a tetracycline-inducible human PLA$_2$R1 transgenic mice that could express the human protein in the glomeruli. However, there was no data regarding the animals becoming proteinuric or not upon immunization with anti-PLA$_2$R1. And since there is no publication with such data until today, one can assume that most probably this was another unsuccessful model. Two years later, at the 2014 ASN Kidney week, the same group described the generation of another transgenic mice model specifically expressing human PLA$_2$R1 in podocytes (Zahner et al., 2014).The mice were immunized with recombinant human PLA$_2$R1 developing granular subepithelial immune deposits along the GBM which were positive for mouse IgG. Injection of serum from PLA2R1-positive patients' also led to the development granular deposits along the glomerular capillary wall.

More recently, during the 2018 ASN Kidney Week, Rhoden and colleagues (Rhoden et al., 2018) described a transgenic mice model (BL6/J) where a flagged-tagged N-terminal CysR-CTLD3 region of human PLA2R1 was overexpressed in mouse podocyte as a membrane protein. These mice did not present proteinuria nor any histological differences in comparison with wild-type mice. In future studies, they aim to induce MN using patient IgG subclasses of anti-PLA$_2$R1 autoantibodies and mouse anti-human PLA$_2$R1 antibodies. Hopefully, this work will allow to validate the pathogenicity of the anti-PLA$_2$R1 antibodies and the role of immune complex formation, complement activation and GBM thickening in causing proteinuria.

2.4.5 THSD7A animal model of MN

In contrast to PLA$_2$R1, THSD7A is constitutively expressed in both human and rodent podocytes, enabling conditions to evaluate more directly the pathogenicity of

anti-THSD7A human autoantibodies in a mouse model. Indeed, in 2016, Tomas and colleagues (Tomas et al., 2016) established the first passive THSD7A mice model by injecting human serum containing anti-THSD7A autoantibodies to BALB/c mice. The human anti-THSD7A antibodies were bound to the murine THSD7A present in the podocyte foot processes along the glomerular filtration barrier forming electron-dense subepithelial immune deposits with effacement of podocyte foot processes that resulted in the onset of proteinuria within 3 days. The podocyte injury was accompanied by oxidative stress and enhanced expression of SOD2. Histological analysis revealed positive staining for C3 in a granular subepithelial pattern suggesting complement activation. Similar but weaker results were observed when purified human anti-THSD7A antibodies were injected instead of serum with antibodies. In this case, the effects were more transient, less pronounced and without C3 deposition. Together, data from this model prove that anti-THSD7A antibodies alone or in the presence of serum are sufficient to induce MN.

In subsequent studies, the same group immunized BALB/c mice with purified rabbit anti-THSD7A antibodies that were bound to the podocyte antigen along the glomerular filtration barrier within 2 hours (Tomas et al., 2017). Fourteen days after injection, the mice presented severe nephrotic syndrome and typical histomorphologic signs of human MN, such as subepithelial immune complexes deposition with effacement of podocyte foot processes. However, once again, the anti-THSD7A antibodies did not have the ability to activate the complement in mice. Interestingly, the results were strain-dependent since they could not be obtained in C57BL/6 and DBA/J1 mice nor in Sprague-Dawley rats. The injected rabbit anti-THSD7A antibodies bound along the glomerular filtration barrier but did not induce proteinuria. These latter results suggest that the genetic background might be a key factor for the induction of nephrotic syndrome in this passive THSD7A animal model of MN.

2.5 Pathophysiology of MN

The characteristic histomorphologic markers of MN were first described in 1957. Since then, researchers and physicians have been working together to better understand the pathophysiological mechanisms underlying the development of the disease. Experimental animal models, *in vitro* experiments as well as daily clinical observations have contributed to this aim. This chapter summarizes what is known and/or hypothesized as well as the remaining open questions concerning the pathophysiological mechanism of MN (Figure 2.5).

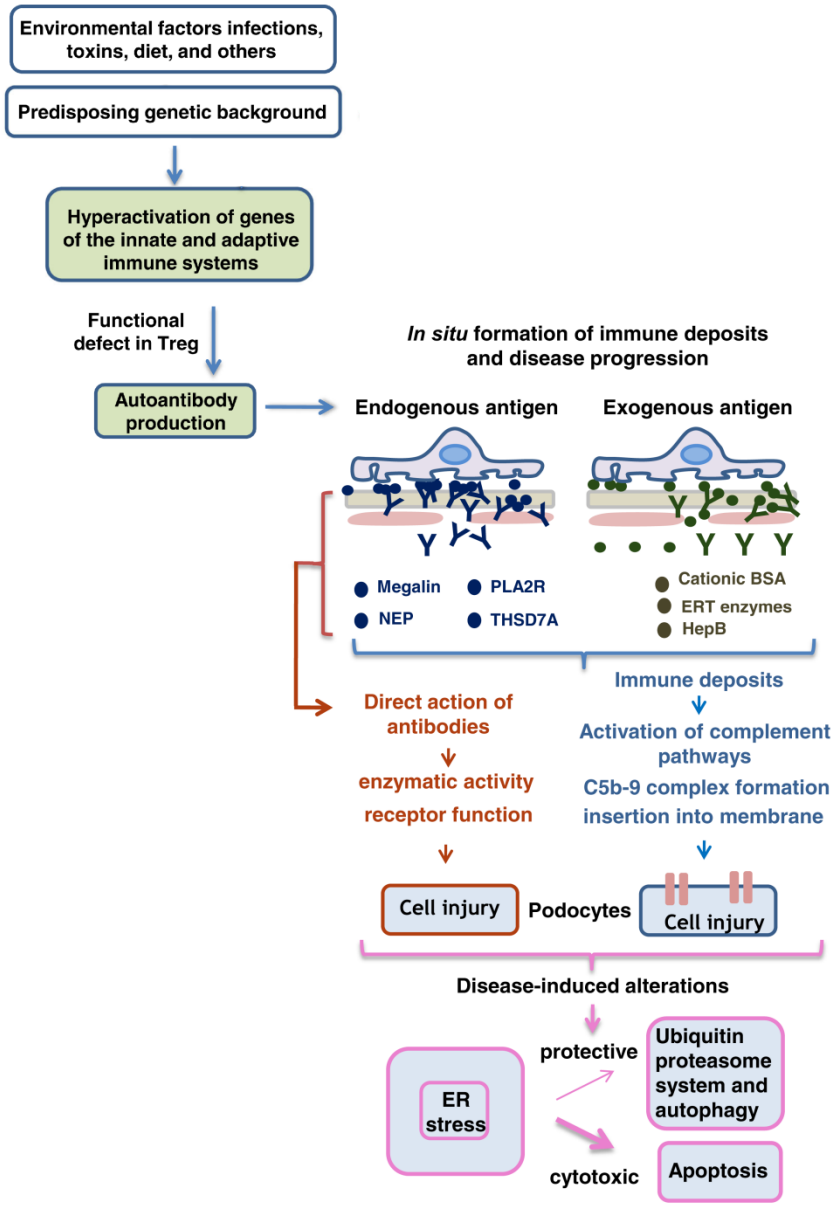

Figure 2.5 – Pathophysiology of MN. The aetiology and pathogenesis of MN is multifactorial, involving the interplay of initiating and predisposing environmental and genetic factors leading to the loss of immune tolerance that result in the production of autoantibodies against podocyte autoantigens. The circulating autoantibodies form *in situ* immune complexes by binding to the membrane-bound podocyte autoantigens in the glomerular basement membrane. The autoantibody-autoantigen membrane-bound complex is shedded into the extracellular space, escaping clearance by endocytosis and activating complement system. Complement activation results in the formation and insertion of the C5b-9 complex into the membrane podocyte playing a major role in sublethal podocyte injury and proteinuria. Additionally, anti-podocyte autoantibodies can directly influence the function of the target autoantigen contributing to podocyte injury. In parallel, distinct cytoprotective responses can be activated over time in cells undergoing endoplasmic reticulum (ER) stress. However, prolonged ER stress beyond some threshold results in apoptosis of the podocyte. *Adapted from (Debiec et al., 2014) and (Ronco et al., 2017) with copyright permissions from "Springe".*

2.5.1 Immunoregulation and initial phase of the autoimmune response

As described in chapter 1.4, loss of central and/or peripheral self-tolerance leads to aberrant self-reactive B and T cells that target self-antigens. The causes of this disruption remain poorly understood in the majority of the autoimmune diseases and in MN in particular. Nonetheless, pollution and epitope mimicry (more details on chapter 4.1) as well as genetic susceptibility (more details on chapter 2.2.6 and chapter 4.1) have been suggested as possible causes of the development and/or progression of MN. Still, the initial phase of the autoimmune response in MN remains one of the more puzzling unanswered questions.

Once an (auto)immune response is initiated, uncommitted T helper lymphocytes (Th0) can differentiate into T helper cells (Th1, Th2, Th17, Tfh) and/or T regulatory cells (Treg). The Th1/Th2 cells facilitate B-cell activation, maturation and differentiation into plasma cells, leading to autoantibody production. Treg cells are responsible for maintaining tolerance by negatively regulating innate and adaptive immunity. A recent study showed that patients with active MN have lower levels of Treg cells, suggesting that the absence of Treg enables loss of tolerance in MN and pathogenesis progression (Rosenzwajg et al., 2017; Wang et al., 2011). This is further supported by the fact that patients clinically responding to rituximab treatment present decreased levels of B cells with concomitant increase of Treg cells whereas patients not responding to treatment maintain low levels of Treg (Roccatello et al., 2016; Rosenzwajg et al., 2017).

MN is characterized by the presence of circulating autoantibodies, mainly IgG4 (at least at a later phase), that bind to specific podocyte autoantigens leading to the formation and deposition of immune complexes. Therefore, it is not surprising that a Th2-immune response plays an important role in the pathogenesis of MN, with patients in active disease presenting elevated levels of Th2 cytokines as well as Tfh (follicular B helper T cells) and plasma cells (Hirayama et al., 2002; Kuroki et al., 2005; Masutani et al., 2004; Zhang et al., 2017).

2.5.2 Spreading of the autoimmune response

As reviewed in chapter 1.4.1, the progression of an (auto)immune response can occur through a mechanism of epitope spreading in which there is an extension of the primary immune response against the immunodominant epitope to other epitopes within the same protein (intramolecular spreading) or neighbouring antigenic molecule(s) that may be partners of the original antigen (intermolecular spreading). This mechanism has been observed in the Heymann nephritis model

suggesting that it might have an important role in the pathogenesis of MN. Indeed, as described in chapter 2.4.1, upon immunization with a fragment (L6, 1-236 aa) of the first domain of megalin (LBD-I), Lewis rats developed antibodies against this fragment but not towards the other LBD domains (Shah et al., 2007). With the progression of the immune response, antibodies towards the other domains (LBD-II, LBD-III and LBD-IV) arisen. Additionally, the onset of proteinuria coincided with epitope spreading, suggesting that multiple antibodies effectors might be required for the full-blown expression of the disease.

A similar mechanism of epitope spreading might occur in PLA_2R1-associated MN. A recent work from our laboratory by Seitz-Polski&Dolla and colleagues (Seitz-Polski et al., 2016) demonstrated that patients have autoantibodies against 3 independent epitope-containing domains of PLA_2R1: CysR, CTLD1 and CTLD7 (more details concerning the identification of PLA_2R1 epitopes can be found in chapter 4.2). The screen of 69 PLA_2R1-positive patients for the identified epitope-containing domains revealed that CysR was the most prevalent one, being recognized by 99% of the patients, followed by CTLD1 and CTLD7. The patients were then stratified according to their epitope profile into three groups: CR (patients to whom only anti-CysR autoantibodies were detected), and CRC1 or CRC1C7 (patients to whom additional anti-CTLD1 or anti-CTLD1 and anti-CTLD7 autoantibodies were detected). Interestingly, patients that only had anti-CysR autoantibodies had lower proteinuria and were more likely to enter into spontaneous remission during follow-up, suggesting that multiple antibodies might be required for expression of a full-blown MN disease. Nevertheless, additional studies are required to validate these findings. Evaluation of the clinical significance of PLA_2R1 epitope spreading in *in vivo* animal models and MN cohorts is of interest to better understand the pathophysiology of MN.

In contrast, in THSD7A-associated MN, epitope-containing domains have been identified but without evidence for a mechanism of epitope spreading (Seifert et al., 2018). Screening of 31 THSD7A-positive MN patients for fragments of THSD7A comprising two to three contiguous domains, such as D1–D2, D3–4, … , D19–D21, revealed that all fragments except D3–D4 and D19–D21 were recognized by at least three patients. Additionally, 90% of the patients recognized multiple fragments, whereas the remainders recognized only one fragment, with different fragments being recognized among these patients. Still, patients reacting only to one or two fragments were more prone to have low proteinuria and were more predisposed to reach remission in comparison with patients with reactivity to more than two fragments, suggesting once again that multiple autoantibodies targeting

multiple domains might be required for expression of a full-blown MN disease. Nonetheless, further studies in *in vivo* animal model and with THSD7A-positive patients with serum obtained at the early steps of the disease are needed to demonstrate whether or not epitope spreading occurs in the early phase of the autoimmune response for THSD7A-associated MN. Noteworthy, it has been described that some patients produce autoantibodies towards both PLA_2R1 and THSD7A autoantigens, suggesting that in these rare cases a mechanism of intermolecular epitope spreading might occur, as described for instance in type 1 diabetes; however this remains highly speculative. (Brooks-Worrell et al., 2001; Csorba et al., 2010; Fresquet et al., 2019; Larsen et al., 2016; Zaghrini et al., 2019). Such a hypothesis of a common epitope should be confirmed in an experimental animal model of MN. For instance, injection of the common nephritogenic immunodominant epitope in animals expressing both PLA_2R1 and THSD7A may lead to the production of autoantibodies against PLA_2R1, THSD7A or both antigens, with the formation of immune deposits, podocyte injury and proteinuria. Injection of the nephritogenic peptide in animals deficient for either PLA_2R1 or THSD7A would only lead to the production of anti-PLA_2R1 or anti-THSD7A antibodies. The dual positivity may also suggest a physical interaction between PLA_2R1 and THSD7A at the podocyte surface and might only occur under certain conditions. Here, injection of each recombinant protein may lead to rare events of intermolecular epitope spreading between one or the other proteins. Such studies have been for instance performed for megalin and RAP in the Heymann's rat model (Hiesberger et al., 1996).

2.5.3 Formation and deposition of immune complexes

Based on the knowledge obtained from different animal models (chapter 2.4) and clinical observations, three different mechanisms have been proposed for the formation of subepithelial immune complexes (Figure 2.6) (Ronco et al., 2015).

In the first scenario, the autoantigen is endogenously expressed at the foot processes of the podocyte and is targeted by circulating autoantibodies leading to formation and deposition of immune complexes *in situ*. This scenario was observed in animal models of passive Heymann nephritis and THSD7A-associated MN, and it applies for the four autoantigens identified in primary MN: megalin in the Heymann nephritis model, NEP in the neonatal alloimmune MN and PLA_2R1 and THSD7A in adult MN (Beck et al., 2009; Debiec et al., 2002; Heymann et al., 1959; Tomas et al., 2014; Tomas et al., 2016). The Heymann nephritis model further demonstrated that the binding of the antibodies to megalin, present at the surface of the podocyte, is followed by shedding of the membrane-bound protein (Kerjaschki et al., 1987). The shed

antibody-megalin complex is not subject to clearance by endocytosis, instead it will cross-react with circulating antibodies and/or other immune complexes already present at the subepithelial space, gradually enlarging the immune deposits through repeated cycles of this mechanism. The same is believed to occur in PLA_2R1- and THSD7A- associated MN, since it has been. proven that both proteins can be shed (Dolla, 2017). The human autoantigens involved in this mechanism (NEP, PLA_2R1 and THSD7A) are further reviewed in chapter 2.3.

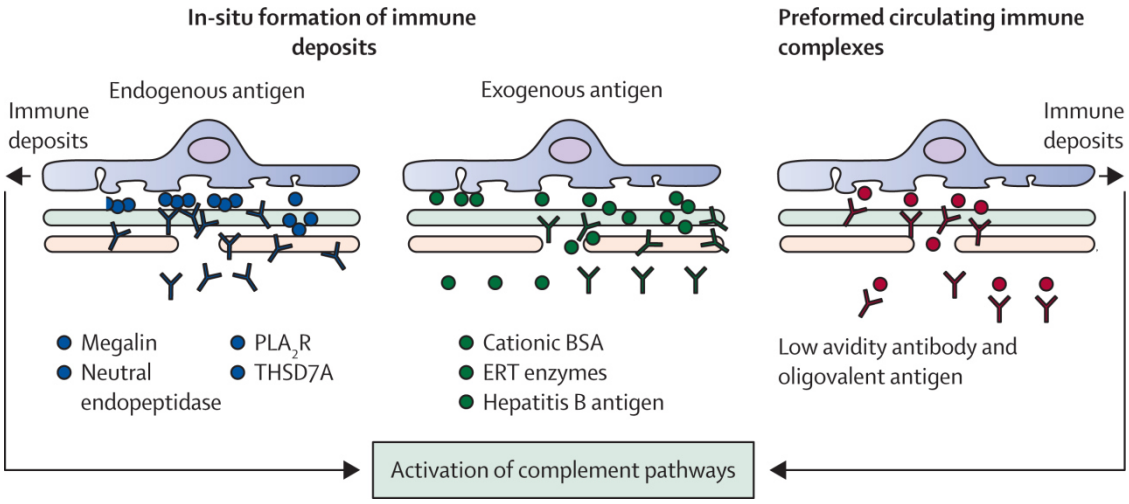

Figure 2.6 – Proposed mechanisms for the formation and deposition of the immune complexes in MN. There are three possible scenarios that can explain the formation and accumulation of IgG immune complexes in the subepithelial space. **On the left:** endogenous proteins expressed on the podocyte surface (megalin, NEP, PLA_2R1, THSD7A) would be directly targeted by circulating autoantibodies. **On the middle:** circulating exogenous antigens (such as cBSA, Hepatitis B antigen or enzymes used in enzyme replacement therapy) would be "planted" in the GBM with subsequent *in situ* binding of circulating antigens. **On the right:** preformed circulating immune complexes would accumulate and form deposits in the subepithelial space. Autoantibodies accumulation would activate complement pathways (classical, alternative or lectin pathway) inducing podocyte injury and proteinuria. *Adapted from (Ronco et al., 2015) with copyright permission from "Elsevier".*

In a second scenario, a circulating exogenous or "planted" antigen, originating from different sources extrinsic to the podocyte, is trapped into the subepithelial space and subsequently targeted by circulating antibodies leading to formation of *in situ* immune complexes. This scenario can occur in secondary cases of MN, such as Hepatitis B virus or cBSA secondary MN, and the antigen is detected in patients' serum (Adler et al., 1983). In these first two scenarios, in which the immune deposits form *in situ*, no circulating immune complexes have been detected in MN patients nor in any of the corresponding animal models of MN, suggesting low affinity between the circulating autoantibodies and the corresponding antigens.

However, one can dispute *in situ* formation of immune deposits in the case of Hepatitis B virus, since these antigens are anionic it would be unlikely that they would deposit within the subepithelial space (Gupta et al., 2015). Given their anionic characteristic it would be expected and more likely that they would deposit within the mesangium and subendothelial spaces. Additionally, a study from Takekoshi and colleagues (Takekoshi et al., 1979) described two cases in which Hepatitis B virus antigens were detected free in the serum or associated with IgG, supporting a third scenario for the formation of the immune deposits. In this scenario, small immune complexes can be formed and circulate in the bloodstream and then they can deposit in the glomerular basement membrane. However, this hypothesis has not yet been confirmed in animal models of MN. In addition, Hepatitis B antigen-IgG antibodiy complex tend to be cationic, facilitating the accumulation of the immune complexes (from the circulation and/or formed *in situ)* within the subepithelial space (Gupta et al., 2015).

2.5.4 Pathogenic effect of the autoantibodies

Once the autoantibodies (mainly IgG subclasses) bind their target autoantigen present at the podocyte, they not only form the immune complexes that deposit and accumulate in the subepithelial space, but they might also induce complement-mediated podocyte injury or directly modify podocyte biology by altering the autoantigen function.

2.5.4.1 Autoantibodies effect through complement activation

The complement cascade is part of the innate immunity being of most importance for host protection against foreign pathogens. It can also be recruited by the antibodies produced through the adaptive immune response. Briefly, the complement system can be activated by the so-called classical, alternative and lectin pathways, all leading to the activation of the C3 component by C3 convertases, and eventually realising C3b opsinin and C5 conversion (Figure 2.7). In turn, C5 convertase cleaves C5 into C5b to form a stable complex with C6 (C5b-6). The C5b-6 complex recruits homologous proteins – C7, C8 and 12 to 18 copies of C9 – forming the C5b-9 complex, also known as the membrane attack complex (MAC) (Borza, 2016; Janeway et al., 2011; Vignesh et al., 2017). Sub-lytic assembly of the C5b-9 complex to podocytes leads to production of reactive oxygen species, which in turn promotes peroxidation of podocyte lipids, membrane proteins and glomerular basement membrane components. In sub-lytic quantities, C5b-9 complex can also activate several mediators including phospholipases A_2, protein

kinases, cyclooxygenases, transcription factors and cytokines, which will influence podocyte cell metabolism, structure and function, such as cytoskeleton rearrangement, destruction of the slit diaphragm and effacement of the foot processes. Injured podocytes can also produce more extracellular matrix proteins which lead to GBM expansion between and around the immune complexes forming the characteristic "spikes" observed by electron microscopy or silver methenamine staining. Additionally, activation of the C5b-9 complex can also induce DNA damage and podocyte detachment resulting in podocytopenia through apoptosis and insufficient proliferation. All these alterations lead to heavy proteinuria (Nangaku et al., 2005; Ronco et al., 2017; Salant et al., 1989).

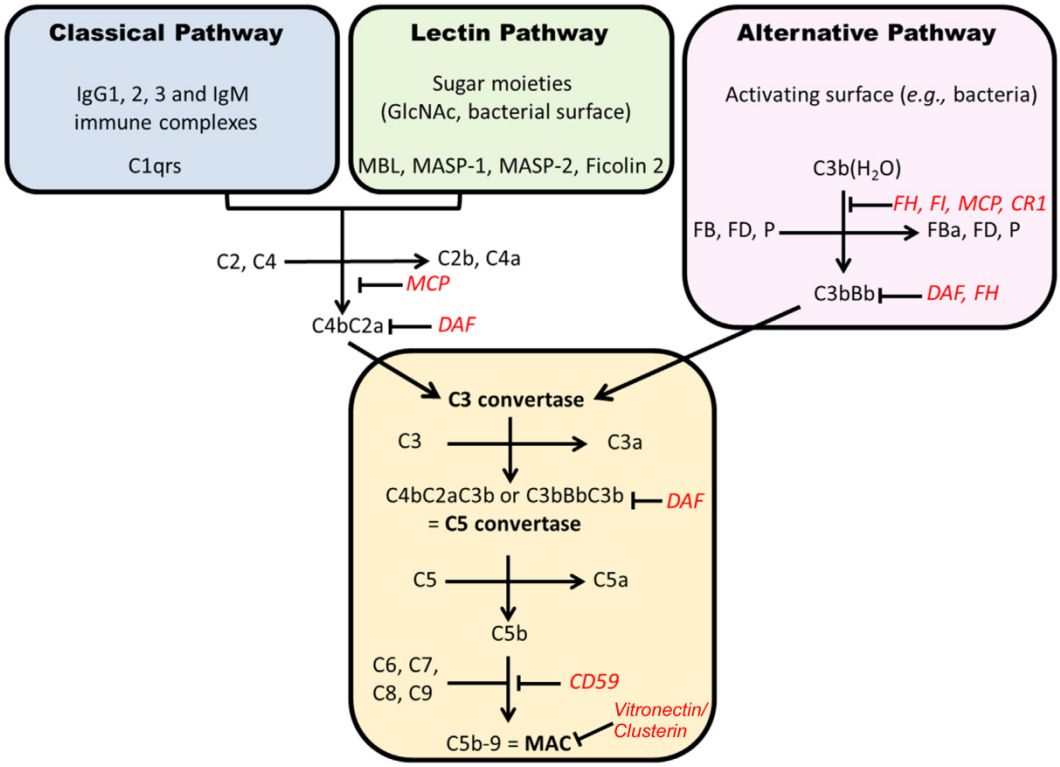

Figure 2.7 – Mechanism of activation of the complement cascade. The complement system can be activated by the classical, alternative or lectin pathways when triggered by different effectors. In human MN, the classical pathway is usually activated in secondary forms, whereas it is most probably the alternative and lectin pathways play a role in primary MN. The three pathways converge towards the formation of C5 convertase which cleaves C5. Cleavage of C5 leads to the formation of C5b that recruits and binds C6, C7, C8 and multiple C9 molecules, forming the C5b-9 complex also known as the membrane attack complex (MAC). MAC insertion on the podocyte membrane, even at sub-lytic levels, can induce cellular injury and proteinuria in the absence of inflammation. The complement cascade is tightly regulated by circulating and podocyte inhibitors: CR1 (complement receptor-1), DAF (or CD55, decay accelerating factor), MCP (or CD46, membrane cofactor protein), FH (factor H) which shorten the half-life of cell surface-assembled C3 and C5 convertase; clusterin, vitronectin and podocyte-expressed CD59 prevent insertion of MAC into the cell membrane. *Adapted from (Knoppova et al., 2016).*

Experimental animal models as well as observations in MN patients have demonstrated that complement might play a crucial role in the pathogenesis of MN. In the Heymann nephritis model, the antibody-antigen immune complexes co-localized with C3 and C5b-9 complex (Ma et al., 2013; Tramontano et al., 2006). In experimental models in which one element from the complement cascade was absent (such as C3, C6 and C8), the formation of the C5b-9 complex was prevented, thus this latter could not be detected or was reduced in the immune deposits and/or proteinuria could not be observed (Baker et al., 1989; Cybulsky et al., 1986; Salant et al., 1980). In primary MN, C3, C4 and C5b-9 complex have also been detected within the immune deposits (Ma et al., 2013). In secondary MN, C1q can also be detected in the immune deposits, suggesting activation of the classical complement pathway. Additionally, plasma and urinary levels of complement components – C3a, C5a and C5b-9 complex – were found to be significantly increased in patients with primary MN (Brenchley et al., 1992; Schulze et al., 1991; Zhang et al., 2019).

The above evidence confirms complement activation in the pathogenesis of MN. However, a question remains: which complement pathway is mainly activated in primary human MN and/or by which IgG subclass? Studies from Ronco and colleagues (Debiec et al., 2012; Seikrit et al., 2018) showed that both classical and alternative complement pathways can be activated in primary MN. Activation of the classical pathway was demonstrated in recurrent PLA_2R1-associated MN case in which a patient produced monoclonal anti-PLA_2R1 IgG3κ autoantibodies that were co-localized with C1q, C3 and C5b-9 in both native and graft kidneys (Debiec et al., 2012). Activation of the alternative pathway was illustrated in another case of PLA_2R1-associated MN in which the patient presented high levels of IgG3 anti-CFH (complement factor H) (Seikrit et al., 2018). Complement factor H is a major regulator of alternative pathway, thereby inhibition of its activity by the autoantibodies led to a hyperactivation of this pathway. Despite these rare cases and even though other IgG subclasses, mainly IgG1 and IgG3 autoantibodies, have been frequently described in patients with primary MN, IgG4 is the predominant IgG subclass detected in both immune deposits and among circulating autoantibodies (Debiec et al., 2014; Doi et al., 1984; Hofstra et al., 2012; von Haxthausen et al., 2018). The absence of C1q in immune deposits is consistent with the inability of IgG4 antibodies to activate the classical complement pathway. Moreover, the detection of C4d in immune deposits suggests activation of the lectin pathway, which is supported by MBL staining in kidney biopsy from patients with primary MN (Espinosa-Hernandez et al., 2012; Hayashi et al., 2018; Lhotta et al., 1999; Val-Bernal et al., 2011). Still, the mechanism by which the lectin pathway might be activated remains

unclear. Recent *in vitro studies* demonstrated that IgG4 anti-PLA_2R1 autoantibodies from MN patients induced time-dependent degradation of synaptopodin and neph-1 that was also dependent on anti-PLA_2R1 titer, suggesting complement activation through the lectin pathway (Haddad et al., 2017). Additionally, it was described that the IgG4 antibodies fraction from MN patients is hypogaloctosylated which might allow the direct binding of the IgG to the MBL thus activating the complement through the lectin pathway (Haddad et al., 2017; Ma et al., 2011). Finally, a study by Huang and colleagues (Huang et al., 2013) demonstrated that in an early phase of MN (stage I) IgG1 was the predominant IgG subclass in the immune deposits whereas in later stages of the disease, IgG4 becomes predominant. These results suggest that a switch in the IgG subclasses might occur during development of MN, with a possibly concomitant switch in the activated pathway of complement. An IgG subclass switch has been described in other autoimmune diseases such as endemic pemphigus foliaceus (Warren et al., 2003). In this disease, it was demonstrated that in the early phase, before clinical onset, the non-pathogenic autoantibodies against EC5 of desmoglein-1 are mainly IgG1. The observed intramolecular epitope spreading mechanism seems to be associated with an IgG isotype switch leading to disease onset with pathogenic autoantibodies targeting the EC1/2 domains of desmoglein-1 and belonging to the IgG4 subclass. If such switch occurs in MN, one can hypothesize that initially the IgG1 and/or IgG3 present at the immune deposits might induce the activation of the classical complement pathway but in a later stage an IgG subclass switch may occur with IgG4 becoming predominant and complement activation mainly occur by the lectin pathway.

In sum, complement activation definitely plays a crucial role in the pathogenesis of primary MN, but it remains unclear whether one or several complement pathway(s) is/are activated and by which IgG subclasses. Several questions remain including the following ones: Since IgG4 is the predominant IgG subclass, does it play a pivotal pathogenic role in MN via complement activation? Or do IgG1 and IgG3 play a crucial role to activate the complement? Does their pathogenic role take place in an early stage of the disease before a switch to IgG4? Or even though IgG4 is predominant in the immune deposits, the low amount of IgG1 and IgG3 are sufficient to activate the complement? In that case does IgG4 play a pathogenic role or its elevated levels are in fact related to a protective mechanism against the other IgG subclasses?

2.5.4.2 Direct effect of autoantibodies

In addition to the role of complement in MN pathogenesis, some studies have demonstrated that podocyte injury and proteinuria can be observed in the absence of the C5b-9 complex, suggesting that autoantibodies may directly alter podocyte biology by changing the function of the targeted autoantigen (Kerjaschki et al., 1997; Spicer et al., 2007; Tomas et al., 2017).

Megalin, a member of the LDL receptor superfamily, is an endocytic multiligand receptor expressed at the sole of podocyte foot processes in clathrin–coated pits (Kerjaschki et al., 1997). In the passive Heymann nephritis model, it was demonstrated that anti-megalin antibodies inhibit the uptake of lipoproteins, including apoE and apoB, which will accumulate within the immune deposits. The concomitant accumulation of lipoproteins within the immune deposits with the production of ROS likely promotes lipid peroxidation inducing and/or contributing to podocyte injury (Debiec et al., 2014).

NEP, which is expressed at the surface of podocytes (chapter 2.3.1) is a metalloprotease responsible for cleaving several peptides such as angiotensin-II, bradykinin and natriuretic peptides, thereby participating in the regulation of blood pressure in nephrons and diuresis. *In vitro* studies demonstrated that anti-NEP antibodies obtained from immunized mothers can inhibit NEP enzymatic activity (Vivarelli et al., 2015). Therefore, NEP inhibition may alter glomerular haemodynamics, endothelial permeability and tubular function (Hu et al., 2013; Ronco et al., 2017). However, the immunized mothers, from who the serum was retrieved in order to perform the *in vitro* experiments, do not express NEP; still they did not present any particular renal function impairment suggesting compensatory mechanism in the absence of NEP(Debiec et al., 2004; Vivarelli et al., 2015). Additionally, IgG1 anti-NEP antibodies were stronger inhibitors of NEP enzymatic activity than IgG4 anti-NEP antibodies (Vivarelli et al., 2015). Moreover, a neonate alloimmunized mainly with IgG1 anti-NEP antibodies seems to present a severe renal failure whereas a baby that mainly alloimmunized IgG4 anti-NEP antibodies appears to develop a mild renal dysfunction (Debiec et al., 2004; Vivarelli et al., 2015). All the previous observations suggest that multiple antibodies, depending on their IgG subclass and antibody titer, act in concert to induce podocyte injury, either directly or via complement activation.

PLA_2R1 is likely a multifunctional and multiligand membrane receptor. Even though PLA_2R1 function in the kidney, and particularly in the podocyte, remains unknown, it has the capacity to bind $sPLA_2$s and collagen (chapter 3.2.2 and

chapter 3.2.3), tentatively suggesting that binding of anti-PLA$_2$R1 autoantibodies may affect its function and promote podocyte injury. Indeed, PLA$_2$R1 seems to increase cell adhesion to collagen IV, which can be disrupted by anti-PLA$_2$R1 autoantibodies, interfering with podocyte adhesion to collagen IV (Ancian et al., 1995; Skoberne et al., 2014). Additionally, even though no mechanism has been proposed, *in vitro* studies demonstrated that, in the absence of complement, purified human anti-PLA$_2$R1 autoantibodies can modulate podocyte cell biology by inducing changes in cell shape and monolayer permeability, activate free radical production and apoptosis (Fresquet et al., 2015). Moreover, PLA$_2$R1 has been described to be involved in cellular senescence (chapter 3.2.3.2). However, podocytes are aberrantly senescent in glomerular renal diseases, including in MN patients, thus it is conceivable that anti-PLA$_2$R1 autoantibodies might reinforce the pro-senescent activity of PLA$_2$R1 contributing to podocyte impairment (Augert et al., 2009; Debiec et al., 2014; Sis et al., 2007). Furthermore, *in vitro* studies demonstrated that upregulation of PLA$_2$R1 in the presence of sPLA$_2$-IB increases apoptosis rate in human podocytes through the PLA$_2$R1-ERK1/2-p53 signalling pathway (Pan et al., 2014). Since, i) PLA$_2$R1 has been described to be overexpressed in podocytes from MN patients, ii) serum levels of sPLA$_2$-IB might be elevated in MN patients and iii) PLA$_2$R1 and serum sPLA$_2$-IB levels correlated positively to kidney apoptosis in MN patients, one can also hypothesize that autoantibodies against PLA$_2$R1 might modulate podocyte apoptosis in MN (Hoxha et al., 2012; Pan et al., 2014; Svobodova et al., 2013). Finally, the ligands and partners of PLA$_2$R1 also remain unknown; therefore the anti-PLA$_2$R1 autoantibodies might not only interfere with the biological function of PLA$_2$R1 but might also disrupt the function of the potential partners contributing to the pathogenesis of MN.

Like for PLA$_2$R1, the physiological role of THSD7A in podocytes remains unclear, even though significant advances have been made since its identification as an autoantigen of primary MN (chapter 2.3.3). *In vitro* and *in vivo* studies have demonstrated a pathogenic effect of anti-THSD7A autoantibodies on podocytes by a mechanism independent of complement activation (Tomas et al., 2016; Tomas et al., 2017). In fact similar to PLA$_2$R1, anti-THSD7A autoantibodies might directly alter focal adhesion leading to cytoskeleton rearrangement and/or by interfering with THSD7A adhesion to collagen resulting in podocyte detachment. Similar to PLA$_2$R1, the ligands and partners of THSD7A remain unknown, leaving open the possibility that anti-THSD7A autoantibodies promote podocyte injury by interfering with one or more components of the THSD7A network.

2.5.5 Protective mechanisms

As reviewed above, activation of the C5b-9 complex leads to podocyte damage, while feedback mechanisms may be activated to promote podocyte recovery. An important protective mechanism is the clearance of the C5b-9 complex from the podocyte membrane by endocytosis and exocytosis being expelled into the urinary space (Debiec et al., 2014; Kerjaschki et al., 1989). This mechanism seems to be activated in patients with primary MN, with elevated urinary excretion of the C5b-9 complex (Brenchley et al., 1992; Kon et al., 1995). The urinary levels of C5b-9 complex correlated with disease activity, thus it can be considered as a useful dynamic marker of the ongoing immunological injury. Additionally, activation of the complement might also upregulate the adaptive unfolded protein response and the ubiquitin-proteasome in response to endoplasmic reticulum (ER) stress due to the accumulation of misfolded proteins in the ER of the injured podocyte (Debiec et al., 2014; Wiebke et al., 2018). However, sustained ER stress might activate pro-apoptotic pathways that will result in the destruction of the podocyte. Finally, IgG4 antibodies have the ability to exchange Fab arms by swapping half of the molecule (a heavy chain and its associated light chain) with another molecule of IgG4 resulting in a bispecific antibody (Ma et al., 2013; van der Neut Kolfschoten et al., 2007). This ability for each IgG4 arm to recognize a different antigen might limit the formation of immune complexes as well as the cross-linking of antigens. IgG4 antibodies also have a non-traditional rheumatoid factor-like activity in which the Fc fragment from IgG4 can interact with the Fc segment from another IgG (Kawa et al., 2008; Ma et al., 2013; Rispens et al., 2009). This atypical IgG4 activity might prevent the binding of IgG1 and/or IgG3 to C1q, thus downregulating the activation of the classical complement pathway. Therefore, besides their potential pathogenicity, IgG4 autoantibodies might also have a protective role in MN.

A better understanding of these and other protective mechanism would be of most interest for the treatment of MN patients and it would help to reply to one of the most intriguing questions: how approximately 30% of the MN patients enter into spontaneous remission?

Chapter 3

PLA_2R1

Originally, lectin referred to non-immunoglobulin agglutinins that have the ability to distinguish erythrocytes from different blood groups. With time, lectin became a broader term referring to proteins that can bind carbohydrates – carbohydrate-binding proteins or glycan-binding proteins. In the late 1960's, the hepatic asialoglycoprotein receptor (ASGPR) was the first mammalian lectin to be identified (Anonymous, 2008; Rigopoulou et al., 2012). After that, more than hundred lectin receptors have been described. Based on protein sequence motifs that are associated with sugar-binding activity (carbohydrate-recognition domains – CRDs) and their 3D structure, glycan-binding receptors can be classified in four different groups: (1) siglecs (I-type lectin), (2) galectins (S-type), (3) R-type lectins (ricin-like) and (4) C-type lectins (Taylor et al., 2019). In this chapter, I will focus my attention on PLA_2R1, a particular member of the C-type lectin superfamily, describing some of its features.

3.1 C-type lectin superfamily

Initially, "C-type lectin" was the term created to identify the group of animal lectins that were structurally similar to the asialoglycoprotein receptor (ASGPR) and had a calcium-dependent carbohydrate-binding activity (Drickamer, 1999; Zelensky et al., 2005). Biochemical studies demonstrated that these proteins structural homology in their carbohydrate-recognition domains (CRDs), with conserved consensus amino acid residues and secondary structural motifs that are required for carbohydrates binding in a calcium-dependent manner. The first crystallographic studies of C-type lectins confirmed that the CRDs shared a unique similar compact globular structure, not observed in any other known protein at that time. With time, it became evident that being a protein containing CRDs is not synonymous of possessing lectin and/or calcium-dependent activities (Drickamer, 1999; Kilpatrick, 2002). In fact, it is frequent to find animal lectins that can bind other structures besides carbohydrates through a protein-protein (e.g.: tumour necrosis factor-α), protein-lipid (such as the mannose-binding lectin (MBL) (Kilpatrick, 1998; Kuroki et al., 1997)) or protein-nucleic acid (e.g.: serum amyloid P component (Pepys et al., 1987)) interactions. Therefore, these domains are no longer classified based on their molecular function, but instead on their structural characteristics, being currently designated as "C-type lectin-like domain" (CTLD). The most recent classification proposed by Drickamer organizes the proteins containing CTLD(s) into 14 different groups (Drickamer et al., 2002). In 2004, Zelensky and colleagues (Zelensky et al., 2004) identified a new set of proteins containing CTLDs, updating the latest classification into 17 different groups, as shown in Figure 3.1, including

PLA2R1 that belongs to the macrophage mannose receptor family (group VI) (Zelensky et al., 2005). More details concerning the macrophage mannose receptor family and PLA2R1 are presented below in chapter 3.1.1 and chapter 3.2 respectively. Of note, the C-type lectins are involved in several biological processes, including intracellular trafficking, cell-adhesion, cell signalling, endocytosis and innate immune response (Taylor et al., 2019). Interestingly, a few of them have also been identified as autoantigens in autoimmune diseases such as calreticulin in Sjögren's Syndrome, ASGPR in autoimmune hepatitis and more recently PLA2R1 in membranous nephropathy (MN) (Beck et al., 2009; Kilpatrick, 2002).

A CTLD consists of 110 to 140 amino acids characteristically folded in a loop with two antiparallel ß-sheets and two α-helices maintained by 2 to 3 disulphide bonds (Figure 3.2) (Drickamer, 1999; Zelensky et al., 2003, 2005). The overall structure can be divided in two lobes: upper and lower. The lower lobe contains a vertical ß-sheet formed by the ß1-, ß5- and ß1'-strands that are flanked by both α1- and α2-helices. A long loop region (with approximately 40 amino acids) and the second antiparallel ß-sheet formed by ß2-, ß3- and ß4-strands constitute the upper lobe. The long loop region is involved in calcium-dependent carbohydrate binding determining the glycan-binding specificity of the CTLDs with lectin activity. Depending on the presence or absence of this region, the CTLDs can also be classified into two structural groups: canonical (Figure 3.2–A) and compact (Figure 3.2–B), respectively. Importantly, the N- and C-terminal ends interact with each other at the bottom of the structure, with the interaction stabilized by a conserved disulphide bridge between the α1-helice (C1) and the ß5-strand (C4). Another highly conserved feature of the domain is a second disulphide bridge between ß3- (C2) and ß5- (C3) strands. Of note, some CTLDs have an additional ß-strand (ß1'-strand) in the extremity of the N-terminal forming a ß-hairpin with the ß1-strand that is stabilized by a third disulphide bridge (C0-C0'). The presence or absence of this extra ß1'-strand allows another subdivision of CTLDs into "long form" or "short form", respectively. As detailed in chapter 3.2, PLA2R1 comprises 8 different CTLDs; six of them are long forms while two are short forms (CTLD5 and CTLD7).

Some crystallographic studies show the calcium ions within the CTLD structure, revealing four possible calcium binding sites (Zelensky et al., 2005). Depending on the particular protein sequence and on the crystallization conditions, the CTLD could contain no or up to three calcium ions. Three calcium binding sites localize in the upper lobe, whereas the fourth binding site is located in the lower lobe. Figure

3.2–C shows the four typical calcium-binding sites in two representative CTLDs, as described in (Zelensky et al., 2005).

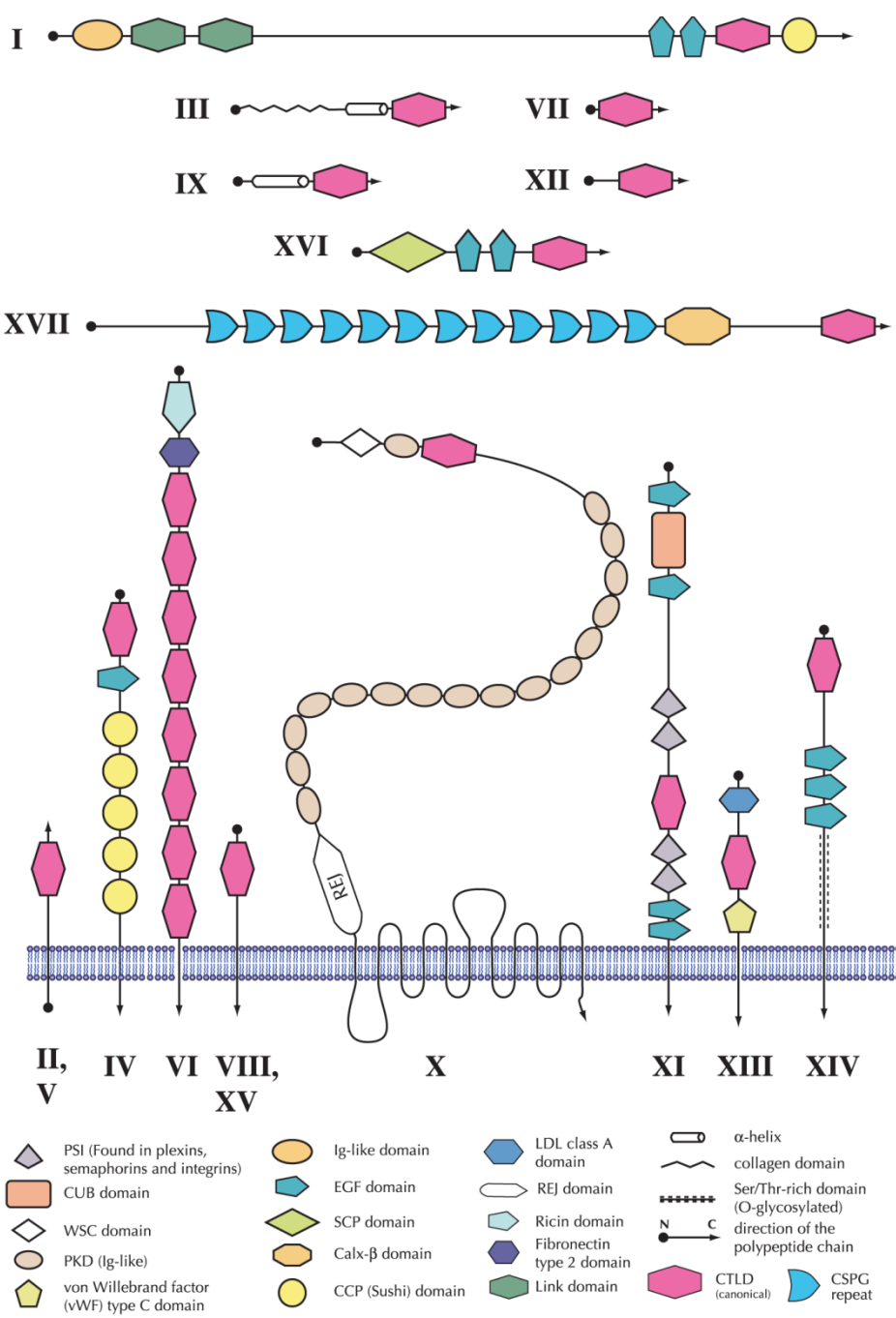

Figure 3.1 – The C-type lectin domain (CTLD) superfamily. Schematic illustration of the structures of the 17 different CTLD groups: 10 groups comprising transmembrane proteins and 7 groups containing soluble proteins. I –lecticans; II – the ASGR (asialoglycoprotein receptor) group; III – collectins; IV – selectins; V – NK (natural killer) receptors; VI – the macrophage mannose receptor group; VII – REG (regenerating) proteins; VIII – the chondrolectin group; IX – the tetranectin group; X – polycystin 1; XI – attractin; XII – EMBP (eosinophil major basic protein); XIII – DGCR2 (integral membrane protein DGCR2/IDD); XIV – the thrombomodulin group; XV – Bimlec (or CD302); XVI – SEEC group, XVII CBCP group. *Adapted from (Zelensky et al., 2005) with copyright permission from "John Wiley and Sons".*

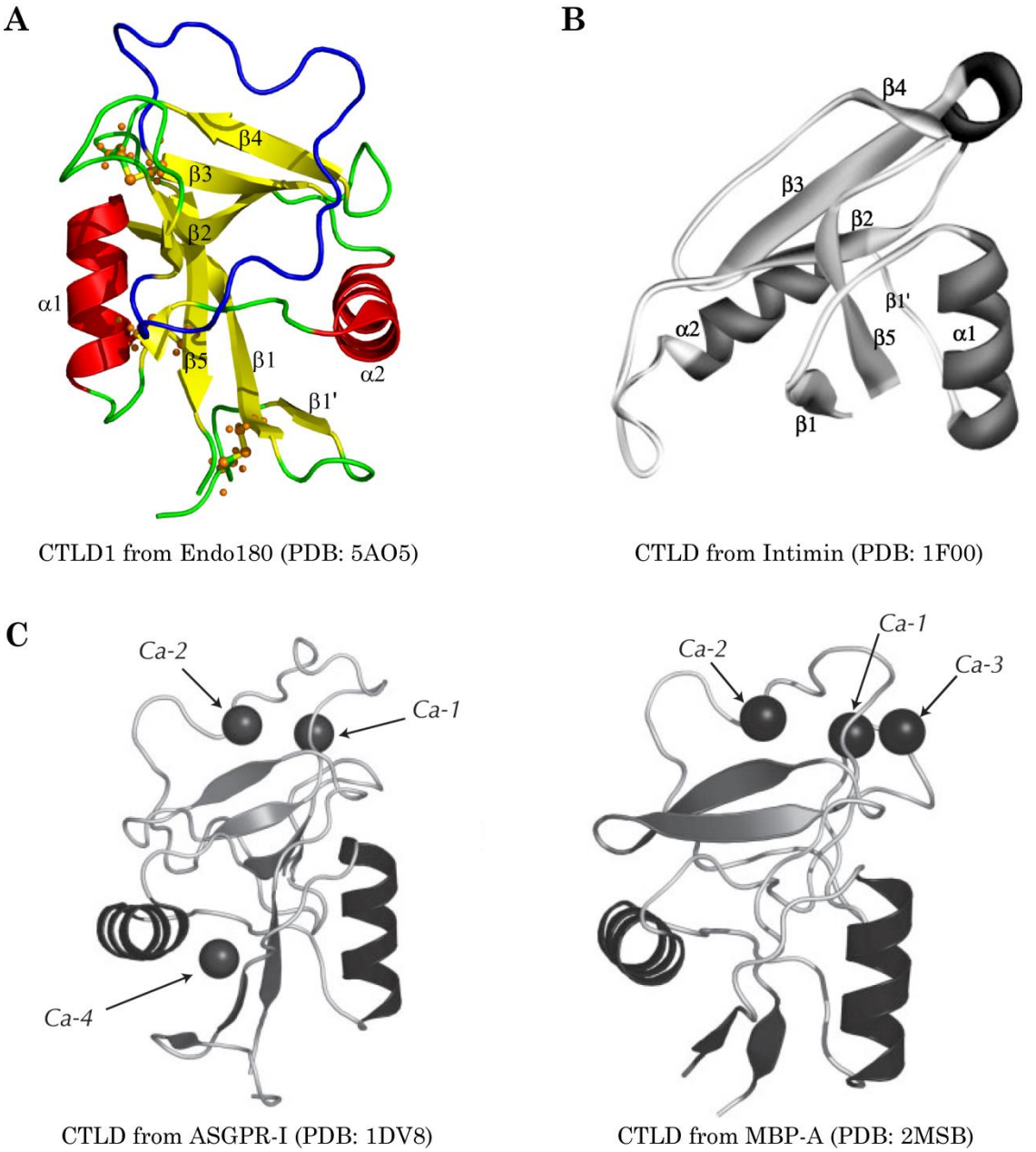

CTLD1 from Endo180 (PDB: 5AO5)

CTLD from Intimin (PDB: 1F00)

CTLD from ASGPR-I (PDB: 1DV8)

CTLD from MBP-A (PDB: 2MSB)

Figure 3.2 – Ribbon diagrams of representative CTLDs. (**A**) Representative 3D structure of a canonical long CTLD: CTLD1 from Endo180 (PDB: 5A05). The long loop region is represented in blue, the α-helices in red, the ß-sheets and the disulphide bridges in yellow. (**B**) Representative 3D structure of a compact long CTLD from intimin (PDB: 1F00). *Adapted from (Zelensky et al., 2005) with copyright permission from "John Wiley and Sons".* (**C**) Ribbon diagram of two representative CTLD structures: the human asialoglycoprotein receptor 1 (ASGR-1) on the left, and the rat mannose-binding protein-A (MBP-A) on the right, showing the four typical calcium-binding sites within the CTLD structure. The black spheres represent the calcium ions, and the numbering of the binding sites is according to (Zelensky et al., 2005) *Adapted from (Zelensky et al., 2005) with copyright permission from "John Wiley and Sons".*

3.1.1 The macrophage mannose receptor family

PLA$_2$R1 belongs to the macrophage mannose receptor family, the group VI within the C-type lectin superfamily, along with mannose receptor 1 (i.e. the founding member of this lectin group: macrophage mannose receptor or MRC1 or CD206), the mannose receptor 2 (MRC2 or Endo180 or CD280) and the lymphocyte antigen 75 (LY75 or DEC-205 or CD205) (East et al., 2002). This is a unique group of four proteins within the C-type lectin superfamily since these are the only proteins that contain multiple CTLDs within a single polypeptide backbone.

All the members from the mannose receptor family are characterized by an extracellular region containing a N-terminal cysteine-rich (CysR) domain followed by a fibronectin-like type-II domain (Fn-II) and 8 different CTLDs (except DEC-205 with 10 CTLDs). They also possess a transmembrane domain and a short cytoplasmic tail. The cytoplasmic domain comprises an endocytic motif that promotes receptor internalization by clathrin-coated vesicles. However, despite having the same overall structural organisation, the four proteins have a low level of sequence identity, down to 40%. For instance, the amino acid sequence identity of the extracellular regions of Endo180 and MRC1 with PLA$_2$R1 is 37% and 31%, respectively.

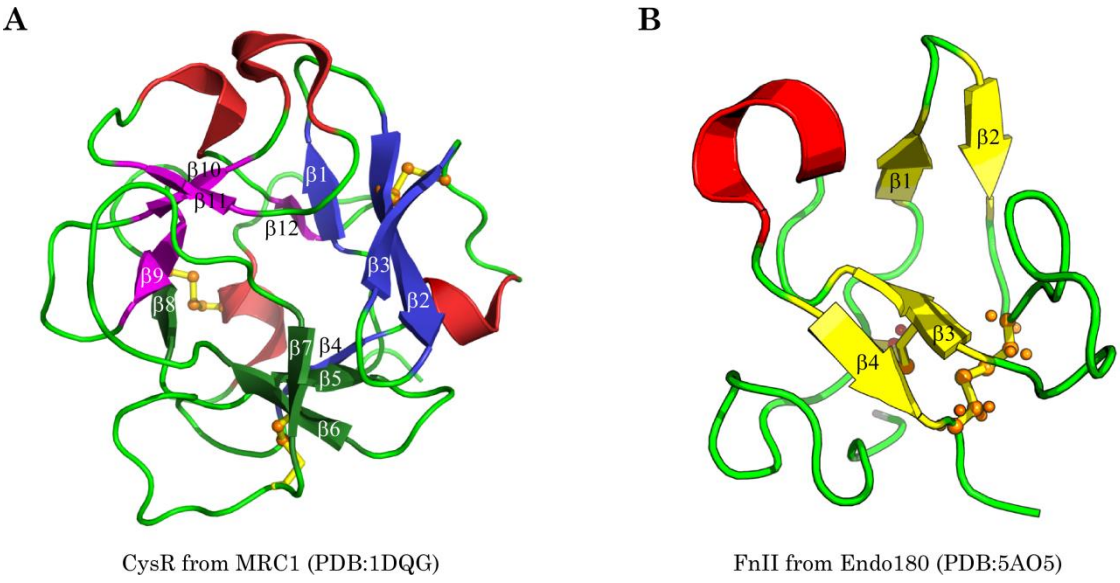

Figure 3.3 – Structure of the CysR and FnII domains from members of the macrophage mannose receptor family. (**A**) Ribbon diagram of the CysR domain from MRC1 (PDB: 1DQG). The lobes I, II and III are represented in blue, dark green and magenta, respectively; the disulphide bridges are in yellow. (**B**) Ribbon diagram of the FnII domain from Endo180 (PDB: 5AO5). The ß-strands and the disulphide bridges are represented in yellow.

The CysR domain was first described in the ricin toxin. In addition to proteins from the macrophage mannose receptor family, it can also be found in fibroblast growth factors (FGFs), interleukin-1α (IL1-α) and interleukin-1ß (IL1-ß). The crystallographic structure of the CysR domain from MRC1 at a 1.7 Å resolution reveals a globular protein comprising 12 antiparallel ß-strands folded into a ß-trefoil structure with a pseudo threefold symmetry (Liu et al., 2000), similar to what was previously observed for the ricin-B chain (at a 2.5 Å resolution) (Rutenber et al., 1991). The CysR domain is composed by three lobes: (a) lobe I containing the ß1-4-strands, (b) lobe II comprising the ß5-8-strands and (c) lobe III having the ß9-12-strands (Figure 3.3–A). The overall structure is maintained by three disulphide bridges. The first binds the ß2-strand with the loop between ß3- and ß4-strands. The second connects the ß6-strand and the loop between ß7- and ß8-strands. The third disulphide bridge, which has only been reported in the MRC1 and PLA2R1 CysR domains, links the ß8-strand to an extended region after the ß12-strand.

The FnII domain, best known within the fibronectin glycoprotein, can be found in a variety of other proteins including the blood coagulation factor XII, insulin-like growth factor 2 receptor (IGF2R) and the matrix metalloproteinases 2 and 9 (MMP2 and MMP9). The solution structure of the FnII domain reveals a total of 4 ß-strands, containing several highly conserved aromatic residues, folded into two double-stranded antiparallel ß-sheets, approximately perpendicular to each other (Figure 3.3–B) (Pickford et al., 1997). The overall structure is maintained by two highly conserved disulphide bridges (between Cys15-Cys41 and Cys29-Cys56). The FnII is the most conserved domain within the mannose receptor family with a 44-63% of sequence identity, while the CTLDs have only 30-45% of identity and the CysR domain is the least conserved, having only 25-30% of sequence identity. Chapter 3.1 presents a detailed description of the CTLD structure.

3.1.1.1 Biological functions of PLA$_2$R1 paralogs

All members of the macrophage mannose receptor family share the same domains in their extracellular region (CysR, FnII and CTLDs), however they are not close paralogs based on amino acid sequence identity. Even though their molecular biology and biological functions are not yet well-defined, they appear to have different ligands, different partners and different patterns of tissue expression; therefore they should have different biological roles. Still some functions seem to be conserved between some members, such as collagen binding. Although some ligands and partners have been identified, it is likely that many of

them remain to be discovered, which should lead to a better understanding of the functions of the mannose receptor family members.

MRC1 (180 kDa) was first identified in rabbit alveolar macrophages and then cloned from human placenta (Stahl et al., 1980; Taylor et al., 1990). It is also expressed in the lymphatic, hepatic and retinal pigment endothelium, tracheal smooth muscle cells and kidney mesangial cells. It recognizes sulphated glycoproteins through the CysR domain, whereas the CTLD4 domain is able to bind in a calcium-dependent manner glycan chains terminating in mannose, fucose or N-acetylglucosamine. These glycans are usually found at the membrane surface of several microorganisms but not in mammalian glycoproteins, allowing MRC1 to distinguish between self- from non-self-partners, thereby playing a role in the innate and adaptive immune system. Like PLA$_2$R1 and Endo180, the FnII domain of MRC1 can bind collagen. Finally, like PLA$_2$R1, a soluble form of MRC1, produced by protease cleavage, has been identified in human and mouse serum, and might play a role in different pathological conditions (Martinez-Pomares, 2012).

DEC-205 (205 kDa) was identified and cloned from dendritic cells (Jiang et al., 1995). It is also expressed in pulmonary and intestinal epithelia as well as in T and B lymphocytes. DEC-205 is involved in the internalization of antigen for processing and presentation to T lymphocytes. DEC-205 also seems to have a modulatory effect on interleukin-4 receptor signal transduction which is involved in the maturation of epithelial cells and anti-proliferating effects on T lymphocytes. Finally, some studies suggested that it might have a tumour suppressor role by enhancing differentiation as well as inhibiting cell division of epithelial cells (East et al., 2002).

Endo180 (180 kDa) was originally cloned from mouse and human heart (Wu et al., 1996). It is expressed in endothelial cells (hence Endo180) but also in some fibroblasts, and macrophages, as well as foetal bone and cartilage cells, being important for bone development and homeostasis. It is able to recognize ligands containing residues of fucose, mannose and N-acetylglucosamine through the CTLD2 domain. Additionally, Endo180 can interact with matrix metalloproteinase-13 (MMP-13) and urokinase-type plasminogen activator (uPA). It can also bind, uptake and degrade collagen as well as promote fibroblast adhesion and migration in collagen matrices. Endo180 is therefore involved in extracellular matrix degradation and remodelling in physiological and pathological conditions such as cancer, in which it is overexpressed (Engelholm et al., 2009; Melander et al., 2015).

3.2 The phospholipase A2 receptor 1 (PLA2R1)

PLA2R1 (180 kDa) was first identified in 1990, thanks to its binding properties for venom secreted phospholipases A2 (sPLA2s) (Lambeau et al., 1990). sPLA2s (13-15 kDa) are enzymes that catalyse the hydrolysis of the sn-2 ester bond of phospholipids releasing free fatty acids (like arachidonic acid) and lysophospholipids (like lysophosphatidylcholine) (Lambeau et al., 2008). They are major components of snake and insect venoms, being responsible for their multiple toxic effects – neurotoxicity, myotoxicity, pro-inflammatory and/or cardiovascular toxic effects (Gutierrez et al., 2013; Kini et al., 1989). The different sPLA2s toxicities seems to be mediated by their enzymatic activity and/or direct binding to soluble and membrane-bound proteins (Kini et al., 1989). In mammals, sPLA2s are also involved in multiple physiological and pathophysiological conditions, such as lipid metabolism, inflammation, reproduction, metabolic syndrome, cancer and many others (Dennis et al., 2011; Lambeau et al., 2008; Murakami et al., 2015; Murakami et al., 2011).

During their search for proteins with binding capacities to sPLA2s, Lambeau and colleagues (Lambeau et al., 1989; Lambeau et al., 1990) identified two new protein receptors using the neurotoxic sPLA2 OS2 present in the venom of the Australian Taipan snake *Oxyuranus scutellatus scutellatus*. The first receptor was called N-type phospholipase A2 receptor because it was identified in rat brain neurons (Lambeau et al., 1989). Despite this early identification and several attempts in Lambeau team, the N-type receptors have not been yet cloned and little advances have been made to characterize their physiological and/or pathophysiological function(s), especially after snake venom envenomation or in neurodegenerative conditions associated to mammalian sPLA2s (Kolko et al., 1999; Pungercar et al., 2007; Sribar et al., 2014; Villanueva et al., 2012). The second sPLA2 receptor was called the M-type phospholipase A2 receptor (now called PLA2R1 and one of the focus of this thesis work), because it was first identified in rabbit skeletal muscle (Lambeau et al., 1990). Shortly after that, the rabbit, human, mouse and bovine PLA2R1s were purified, sequenced and cloned (Ancian et al., 1995; Higashino et al., 1994; Ishizaki et al., 1994; Lambeau et al., 1994). The amino acid identity of human PLA2R1 (hPLA2R1) with its mammalian orthologs is not very high: hPLA2R1 has 74%, 85% and 86% of identity with mouse PLA2R1 (mPLA2R1), bovine (bPLA2R1) and rabbit (rbPLA2R1), respectively. Furthermore, the homology between hPLA2R1 and other orthologs in vertebrates is even lower with for instance a percentage of identity between hPLA2R1 and chicken PLA2R1 (FcRY) as low as 55%, and decreasing to 45% and 41% when compared to xenopus or zebrafish PLA2R1 receptors, respectively.

Finally, PLA2R1 is not expressed in *C. elegans* or in D*rosophila*. Such low levels of identity are getting close to those observed between PLA2R1 paralogs.

3.2.1 PLA2R1 structure and expression

Human PLA2R1 (hPLA2R1, UniProt Q13018) is a 180 kDa type I transmembrane glycoprotein of 1463 amino acids encoded by a 131 kbp gene mapped into the q23-q24 bands of chromosome 2 (Entrez gene: 22925) (Ancian et al., 1995). It contains a signal peptide of 20 amino acids, followed by a large extracellular region, a single transmembrane segment and a short C-terminal cytoplasmic tail (Figure 3.4–A). The extracellular region contains a N-terminal cysteine-rich domain (CysR) followed by a fibronectin type-II domain (FnII) and 8 different C-type lectin-like domains (CTLD1-CTLD8) separated by short linker regions of 5 to 16 amino acids. The cytoplasmic region of 42 amino acids comprises the endocytosis motifs "NP(X)Y" and "LI" or "LL" which allows the internalization of ligand-receptor complexes via clathrin-coated vesicles, suggesting a function of hPLA2R1 in the clearance of circulating sPLA2s (Ancian et al., 1995; Zvaritch et al., 1996). The main structural characteristics of PLA2R1 indicate that it belongs to the C-type lectin superfamily (chapter 3.1), particularly to the macrophage mannose receptor family (chapter 3.1.1). Detailed information concerning the individual structure of PLA2R1 extracellular domains are shortly presented in chapter 3.1 (CTLDs) and chapter 3.1.1 (CysR and FnII).

While cloning membrane-bound hPLA2R1, Ancian and colleagues (Ancian et al., 1995) identified a second mRNA coding for a soluble secreted form. This soluble form is truncated within the CTLD8 domain, and it is generated by a non-usual alternative splicing within an intron. Similar amounts of mRNA coding for membrane-bound and soluble forms were found in human kidney, suggesting that they have an important physiological role (and share the same binding activities). Besides humans, it is unknown if this splice variant mRNA also exists. Furthermore, in mouse species, another form of soluble PLA2R1 can be generated by proteolysis of the membrane form (Dolla, 2017; Higashino Ki et al., 2002; Yokota et al., 2000). This is in line with our recent yet unpublished data. Indeed, after transfecting HEK293 cells with the membrane-bound form of PLA2R1, we could detect the membrane-bound form in cell lysates as well as a soluble form in culture medium. This observation and additional unpublished data from our laboratory, mainly obtained by Guillaume Dolla, supports the hypothesis that a soluble form of human PLA2R1 is also produced by proteolysis of the membrane form through a

proteolytic mechanism commonly called shedding and that operates for many type I and type II receptors (Dolla, 2017).

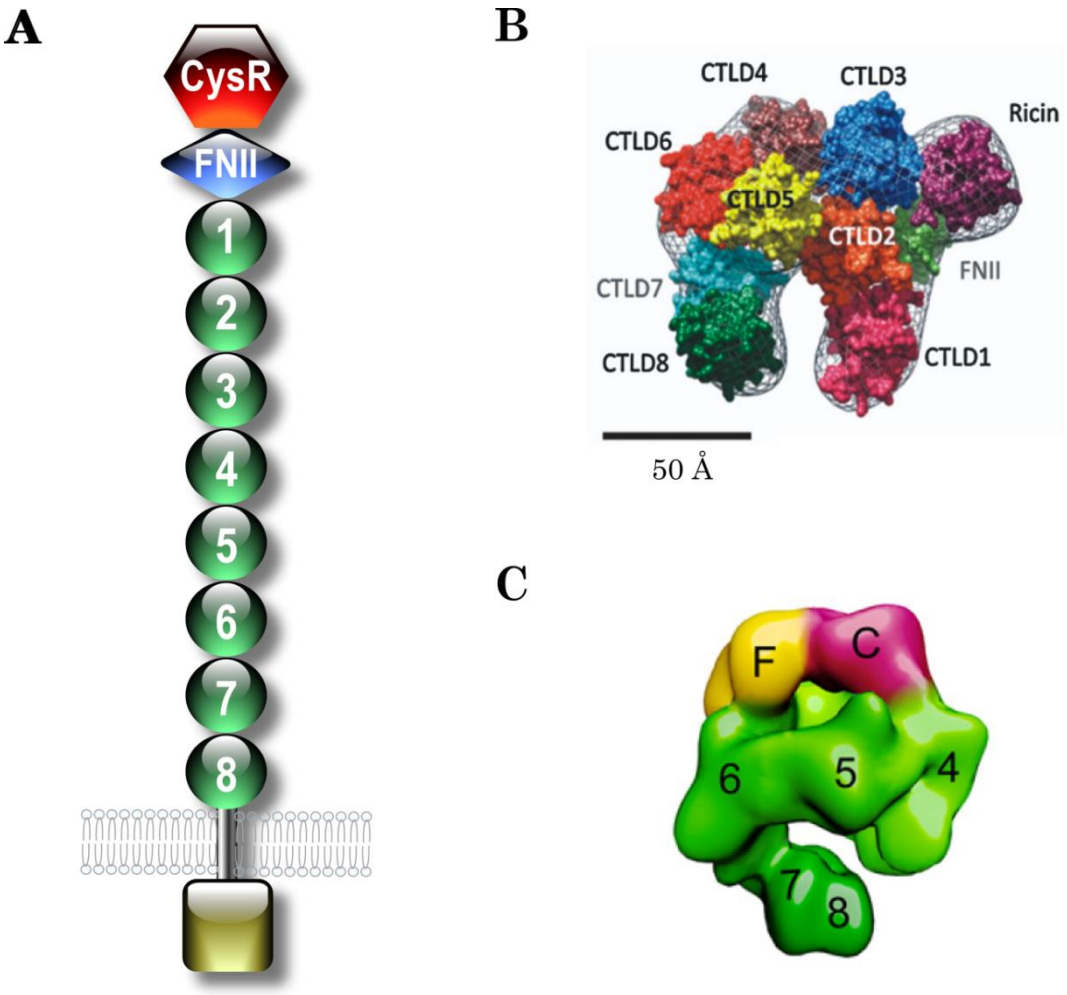

Figure 3.4 – The phospholipase A2 receptor 1 (PLA2R1). (**A**) Schematic diagram of the domains of PLA2R: an N-terminal cysteine-rich domain (CysR), a fibronectin type-II domain (Fn-II) and 8 different C-type lectin-like domains (CTLD1-CTLD8), followed by a transmembrane segment and a short C-terminal cytoplasmic tail. (**B**) Low resolution 3D modelling of the ectodomain structure of the hPLA2R1 obtained after transmission electron microscopy (Cryo-EM) and proposed by (Fresquet et al., 2015). *Adapted from (Fresquet et al., 2015) with copyright permission from "American Society of Nephrology".* (**C**) 3D modelling of the extracellular region of the hPLA2R1 obtained by cryo-EM and proposed by (Dong et al., 2017). *Adapted from (Dong et al., 2017) with copyright permission from "Elsevier".*

Although PLA2R1 was first identified almost 30 years ago, little is known about its detailed structure, with models mainly extrapolated from its paralogs, with only one high resolution structure until now. In 2015, Fresquet and colleagues (Fresquet et al., 2015) proposed the first low resolution (20 Å) structural model for the entire extracellular region (CysR–CTLD8) of human PLA2R1 using transmission electron

microscopy and single-particle averaging. They suggested that the CysR and CTLD3 domains are close together to form a ring-like configuration, with the overall hPLA2R1 3D structure resembling the Greek character "π" (pi, Figure 3.4-B). Shortly after, Dong and colleagues (Dong et al., 2017) proposed a different and more detailed 3D modelling of the ectodomain of hPLA2R1 (Figure 3.4-C). The 10 Å resolution cryo-electron microscopy revealed that the overall PLA2R1 structure can be divided into a head and a tail. The head region is formed by two rings almost parallel (a smaller and a larger one), with one on the top of the other. The smaller ring comprises the CysR, FnII, CTLD1 and CTLD2 domains, while the larger ring is formed by FnII and CTLD1-6. The tail region contains the CTLD7 and CTLD8 domains. Bio-layer interferometry binding assays suggested inter-domain interactions between (i) CysR and CTLD2, (ii) FnII and CTLD6 and (iii) CysR and CTLD4. Interestingly, both studies (Dong et al., 2017; Fresquet et al., 2015) demonstrated that the hPLA2R1 structure may be pH-dependent, with a more compact structure at acidic pH and an extended conformation at neutral to basic conditions, thereby adopting a similar pH-dependent behaviour to that described for its paralogs (Boskovic et al., 2006; Cao et al., 2015; Llorca, 2008; West et al., 2004). Additionally, the inter-domain interactions above described between CysR-CTLD2 and FnII-CTLD6 were pH-dependent, further supporting the pH-dependent extended and bent conformational changes. Furthermore, as observed for its paralogs (Boskovic et al., 2006; Cao et al., 2015; West et al., 2004), mPLA2R1 ligand-binding was also described to be pH-dependent (Dong et al., 2017). These results suggest that the pH-dependent conformational change might be important for the physiological and/or pathophysiological role(s) of PLA2R1, including its role in internalization and degradation or presentation of antigen, similar to the original macrophage mannose receptor (Cao et al., 2015; Napper et al., 2001; West et al., 2004).

In addition to the kidney, but depending on species, PLA2R1 is also expressed in placenta, lungs, skeletal muscle, spleen, liver, pancreas, colon, thyroid, ovaries and testis (Ancian et al., 1995; Cupillard et al., 1999; Granata et al., 2005; Higashino et al., 1994). It is noteworthy that its tissue distribution is variable among species. For example, PLA2R1 is constitutively expressed in human kidney at relatively high levels, including podocytes, while in rat and mice, podocytes do not express PLA2R1, even though it is present in the kidney but in other cells (Ancian et al., 1995; Beck et al., 2009; Cupillard et al., 1999; Meyer-Schwesinger et al., 2015). The absence of PLA2R1 in rodent podocytes has been a major step-back in the development of a small animal model of PLA2R1-associated MN (chapter 2.4.4).

3.2.2 PLA2R1 ligands

As mentioned previously, PLA2R1 was first identified as a receptor for snake venom sPLA2s, in particular OS1 and OS2 (Lambeau et al., 1990). It has been shown that PLA2R1 can bind several venom and mammalian sPLA2s, with (i) CTLD5 domain playing a central role (yet CTLD3, 4 and 6 are required for stabilization of the interaction and high affinity), (ii) N-glycosylation being required for high affinity binding, and (iii) calcium being quite surprisingly dispensable despite the fact that both sPLA2s and CTLDs have calcium-binding sites and sPLA2s bind to PLA2R1 via residues of their calcium-binding loop (Cupillard et al., 1999; Lambeau et al., 1995; Nicolas et al., 1995; Rouault et al., 2007). PLA2R1-sPLA2 interactions might display opposite regulatory functions for sPLA2s. In one hand, sPLA2 binding to PLA2R1 can neutralize the sPLA2 biological function by inhibiting their enzymatic activity or by favouring their clearance and degradation through PLA2R1 endocytic activity. On the other hand, binding of sPLA2 to PLA2R1 might activate several signalling pathways explaining some sPLA2 physiological functions, but these possibilities have never been confirmed using PLA2R1 knock-out mice (Hanasaki et al., 2002).

In addition to the protein-protein interaction with sPLA2s, CTLDs from PLA2R1 might also have carbohydrate-binding activity. In particular, PLA2R1 can bind mannose- and galactose-residues in a calcium-independent manner via its CTLD4 domain, even though CTLDs 5-8 are required to provide a full affinity (Lambeau et al., 1994; Nicolas et al., 1995). PLA2R1 also has the capacity to bind collagen through its FnII and CTLD1-2 domains, suggesting that it may play a role in cell adhesion and collagen-dependent cell migration (Ancian et al., 1995; Takahashi et al., 2015).

Recently, the annexin A2-S100A10 complex was identified as a new binding partner of hPLA2R1 in the podocyte, regulating its cellular trafficking, and with a possible role of PLA2R1 in actin cytoskeleton reorganisation and tight junction assembly (Fresquet et al., 2017). No specific binding-site was identified, but the interaction occurs through the CysR-CTLD3 domains. This region contains at least two epitope-containing domains targeted by anti-PLA2R1 autoantibodies (chapter 4.2), but whether binding of autoantibodies to PLA2R1 alters the interaction of PLA2R1 with annexin A2-S100A10 is still unknown (Fresquet et al., 2015; Seitz-Polski et al., 2016). Despite advances in the identification of some PLA2R1 ligands and their putative physiological roles, the complete set of ligands for PLA2R1, in particular in humans, is still unclear. For instance, while it is clear that in the mouse species, PLA2R1 can bind seven out of 12 sPLA2s, the binding profile of human sPLA2s to human PLA2R1 needs to be characterized in more details (Rouault et al., 2007). Also, an unbiased search for ligands of hPLA2R1 and

partners should be done, for instance using a PLA2R1 affinity column and several body fluids or tissues where human PLA2R1 is expressed.

3.2.3 Physiological and pathophysiological roles of PLA2R1

PLA2R1 is likely a multifunctional and multiligand receptor with diverse ligand-associated biological functions. It has been shown that PLA2R1 can bind, inhibit and act as an endogenous receptor for several sPLA2s. Since its discovery, PLA2R1 has been successively proposed to have a role in inflammation, in cellular senescence, apoptosis and finally as the major autoantigen in the primary form of MN. However, in all of these settings, the physiological and pathophysiological roles of PLA2R1 are still not well-defined at the molecular level.

3.2.3.1 PLA2R1 role in inflammation

Some key lipid mediators such as eicosanoids, which can be tightly regulated by sPLA2 enzymatic activity, are involved in multiple physiological and pathophysiological conditions of sPLA2s including pathogenesis of airway inflammation such as asthma (Murakami et al., 2013; Murakami et al., 2015). For instance, sPLA2-X was found to play an important role in asthma in the well-known ovalbumin mouse model of asthma. Knockout mouse for sPLA2-X had reduced levels of eicosanoids and T helper type 2 cell cytokines in comparison with wild-type mouse (Henderson et al., 2007). Additionally, several sPLA2s (in particular sPLA2-X) and PLA2R1 have been identified and overexpressed in the airways of patients with asthma (Hallstrand et al., 2007; Hallstrand et al., 2012; Hallstrand et al., 2011; Nolin et al., 2016). These findings and the fact that PLA2R1 might participate in the clearance of sPLA2s led to the investigation of the role of PLA2R1 in the disease using the same mouse model of asthma (Nolin et al., 2016; Tamaru et al., 2013). PLA2R1 knockout mice had a stronger inflammatory response, characterized by a higher infiltration of inflammatory cells around the airways and blood vessels, compared to the wild-type mice. Additionally, bronchoalveolar lavage fluid from PLA2R1 knockout mice presented higher levels of group IB and group X sPLA2s, eicosanoids and T helper type 2 cell cytokines in comparison with the fluid obtained from wild-type mice. These results support the idea that PLA2R1 might have an anti-inflammatory role in asthma by inhibiting and facilitating the clearance of sPLA2s such as group IB and X which might be pro-inflammatory mediators in the lung.

Contrary to its anti-inflammatory role in asthma, PLA2R1 appears to promote inflammation during sepsis. In a model of endotoxic shock, PLA2R1 exacerbates

lipopolysaccharide (LPS)-induced lethality, with wild-type mice having a lower rate of survival than knockout mice after injection of a lethal or sublethal dose of LPS (Hanasaki et al., 1997). The injection of sPLA2-IB, a ligand of PLA2R1, induced a lower rate of survival after inducing endotoxic shock with a sublethal dose of LPS in wild-type but not PLA2R1 knockout mice, confirming a possible role of PLA2R1 in sepsis. Additionally, LPS injection induces the production of several pro-inflammatory cytokines and inflammatory factors, such as tumour necrosis factor-α (TNF-α) and interleukin-1-ß (IL1-ß), however their plasma levels were significantly lower in PLA2R1 knockout mice than wild-type mice. Finally, an up-regulation of PLA2R1 expression in lung alveolar type II epithelial cells and in spleen was observed in LPS-treated wild-type mice, followed by a delayed transient increase of circulating soluble PLA2R1 (Higashino Ki et al., 2002; Yokota et al., 2000). Overall, these results suggest that in the inflammatory model of endotoxic shock, PLA2R1 might have a dual antagonistic effect. A sPLA2s-PLA2R1 interaction (or interaction of PLA2R1 with other unknown ligands) may lead to the production of pro-inflammatory factors, such as TNF-α and IL1-ß, favouring the progression of sepsis. During endotoxic shock and progression of the inflammatory response, increased levels of circulating PLA2R1 may counterbalance the effects evoked by the cell surface PLA2R1.

The above studies revealed that PLA2R1 might play both anti- and pro-inflammatory roles, modulating various inflammatory conditions, such as asthma and endotoxic shock. It is tempting to speculate that its opposite anti- and pro-inflammatory roles might be tissue-dependent (and species), ligand/partner-dependent and/or microenvironment-dependent. More studies are required to better understand its role in inflammation.

3.2.3.2 Role of PLA2R1 in cellular senescence and cancer

In 2009, it was shown for the first time that PLA2R1 could play an anti-tumoural role. Oncogene-induced cellular senescence (OIS) is a tumour suppression mechanism that is activated in the early stages of tumourigenesis arresting permanently the cell-cycle. On their search for new tumour suppressive genes, Augert and colleagues (Augert et al., 2009) initially found that knockdown of PLA2R1 in normal primary human fibroblasts or mammary epithelial cells delayed the onset of replicative senescence, i.e. increasing cell lifespan, while forced overexpression of PLA2R1 during cell proliferation induces premature cellular senescence. Similarly, experiments using cellular models of oncogene-induced senescence and cancer cells confirmed the role of PLA2R1 as a potential gene

suppressor (Augert et al., 2013; Vindrieux et al., 2013). For instance, PLA_2R1 ectopic expression in normal breast epithelial cells challenged with oncogenes triggers premature senescence whereas PLA_2R1 ectopic expression in PLA_2R1-negative cancer cells leads to apoptosis (Augert et al., 2009; Augert et al., 2013). In line with these findings, PLA_2R1 expression is increased at replicative cellular senescence while it is decreased in cancer cell lines compared to normal cells (Augert et al., 2009; Augert et al., 2013). *In vivo* experiments confirmed the anti-oncogenic properties of PLA_2R1 (Vindrieux et al., 2013; Vindrieux et al., 2014). PLA_2R1 knockout mice were more sensitive to RAS-induced skin tumours due to decreased ability to enter into senescence.

The mechanism by which PLA_2R1 induces cellular senescence and in particular the role of $sPLA_2$s or other possible ligands are still elusive. The role of $sPLA_2$s in the effect of PLA_2R1 on senescence and cancer cell death (apoptosis) is not clear. On one hand cellular knockdown of $sPLA_2$-IIA in human normal fibroblasts also induces replicative senescence, an effect also observed in dermal human fibroblasts (Augert et al., 2009; Kim et al., 2009). On the other hand, addition of $sPLA_2$s to cells expressing PLA_2R1 and undergoing cellular senescence does not trigger an additional effect (unpublished data). During cellular senescence, PLA_2R1 appears to regulate the production and accumulation of reactive oxygen species (ROS) that (i) in normal cells, due to DNA damage, will activate the p53 pathway promoting senescence, and (ii) in cancer cells, due to mitochondrial increase content, will promote cell death (apoptosis) through the JAK2/STAT5/ERRα pathway (janus kinase 2 / signal transducer and activator of transcription proteins / estrogen-related receptor alpha1 pathway) (Augert et al., 2009; Augert et al., 2013; Griveau et al., 2016; Vindrieux et al., 2013).

Finally, a study by Vindrieux and colleagues (Vindrieux et al., 2014) suggested that in human renal cell carcinoma (RCC), PLA_2R1 expression is regulated by the Von Hippel-Lindau gene (VHL). RCC occurs due to the loss of function of VHL, which will stabilize HIFα proteins (hypoxia-inducible factor alpha), in particular HIF2α. HIF2α will increase c-MYC transcriptional activity, leading to methylation of PLA_2R1 promotor. This result in the repression of PLA_2R1 expression promoting cancer growth, probably through the mechanisms previously described. These results are in line with previous studies on the regulation of the PLA_2R1 gene in cancer cells by Menschikowski and colleagues (Menschikowski et al., 2015; Menschikowski et al., 2012) and Denizot and colleagues (Amin et al., 2011; Fiancette et al., 2009) showing a tight regulation of PLA_2R1 expression in mammary and lymphoma cancer cells by epigenetic mechanisms and cytokines.

Senescence is not only a tumour suppressive mechanism, but it is also involved in the pathogenesis of chronic obstructive pulmonary disease (COPD) (Barnes, 2017). mRNA and protein levels of PLA2R1 were increased in the pulmonary vessels of COPD patients (Huang et al., 2016). Additionally, cultured primary endothelial cells and pulmonary smooth muscle cells from COPD patients expressed elevated levels of PLA2R1 mRNA and protein, inducing senescence. Therefore, PLA2R1-mediated senescence seems to be key for the development of COPD.

3.2.3.3 Other roles of PLA2R1

Recently, a potential protective role of PLA2R1 after myocardial infarction (MI) was proposed using knockout mice (Mishina et al., 2014). After inducing MI, PLA2R1 knockout mice present impaired healing of the infarcted region probably due to reduced recruitment of myofibroblasts contributing to a significant lower survival rate after cardiac rupture. Additionally, myofibroblasts from PLA2R1-deficient mice showed reduced collagen-dependent migration and proliferation in response to sPLA2-IB. The regeneration effect observed after MI seems to be independent of the catalytic activity of sPLA2-IB, and it might be mediated by the interaction sPLA2-IB–PLA2R1–integrin β1.

Additionally, expression of PLA2R1 in HEK293 cells increases cell adhesion to collagens type I and IV, as well as mediates collagen internalization (Ancian et al., 1995; Takahashi et al., 2015). Moreover, podocyte adhesion to collagen is decreased in the presence of anti-PLA2R1 autoantibodies (Skoberne et al., 2014). These data suggest that PLA2R1 might modulate cell adhesion and be implicated in extracellular matrix remodelling.

A referred before, PLA2R1 is expressed in podocytes and likely in other cells in the kidney where its physiological and pathophysiological role remains largely unknown. It was showed that podocyte adhesion to collagen is decreased in the presence of anti-PLA2R1 autoantibodies (Skoberne et al., 2014). Also, sPLA2-IB seems to induce human podocyte apoptosis through PLA2R1–ERK1/2–cPLA2α–AA–p53 signalling pathway (Pan et al., 2014). Additionally, anti-PLA2R1 autoantibodies in the absence of complement activation seemed to alter podocyte shape and permeability, and activate free radical production and apoptosis (Fresquet et al., 2015). These data allows us to hypothesise that PLA2R1 might modulate podocyte cell biology and adhesion to the GBM, being of importance for the structure of the glomerular filtration barrier. Moreover, both *in vitro* and *in vivo* studies in a model of rat glomerulonephritis suggest that sPLA2-IB, sPLA2-IIA and PLA2R1 may be involved

in inflammatory conditions in the kidney (Beck et al., 2006; Beck et al., 2003; Scholz-Pedretti et al., 2002).

Finally, as further discussed in chapter 2 and chapter 4, in 2009, PLA_2R1 was identified as the major autoantigen in primary MN with 70% of patients having circulating autoantibodies (Beck et al., 2009). PLA_2R1 is expressed at the podocyte surface from where it is likely shedded to form immune-complexes with anti-PLA_2R1 IgG4 autoantibodies at the GBM. The identification of PLA_2R1 as the major autoantigen in MN not only contributed to a better understanding of MN pathogenesis but also rapidly provided clinical assays to better diagnose and monitor this disease.

Chapter 4

PLA_2R1-associated MN

The identification of PLA2R1 as the autoantigen in adult primary membranous nephropathy (MN) was considered as a milestone in the MN field. It has provided a molecular basis to better understand MN pathogenesis. For instance, to better understand the autoimmune phase of the disease, from aetiology with pollution as a possible environmental factor or infection and a possible mechanism of epitope mimicry impacting on PLA2R1 as the initial target up to the identification of PLA2R1 epitopes targeted by autoantibodies. At the clinical level, the identification of anti-PLA2R1 autoantibodies and then of epitope-containing domains have contributed to a better management of patients' healthcare.

4.1 Aetiology of PLA2R1-associated MN

Long before the identification of the autoantigens involved in MN, polymorphisms in MHC class II genes have been linked to the development of the disease (Klouda et al., 1979) (chapter 2.2.6). More recently, an independent genome-wide association study (GWAS) showed that the SNP rs4664308 in the gene coding for PLA2R1 was associated with the development of MN (a risk of 4.2) (Stanescu et al., 2011). Additionally they showed that homozygosity for the four risk alleles in the PLA2R1 (SNP rs4664308) and HLA-DQA1 (SNP rs2187668) genes increased the odd-ratio for MN to 78.5. Interestingly, sequence variants were described in regions that later on were identified as containing epitopes: SNP rs4665143 (S87S in the CysR domain), SNP rs3749117 (Met292Val in the CTLD1 domain), SNP rs3577182 (His300Asp in the CTLD1 domain) and SNP rs3828323 (Gly1106Ser in the linker region between CTLD6 and CTLD7) (Coenen et al., 2013; Kim et al., 2011; Liu et al., 2010; Stanescu et al., 2011). These polymorphisms were frequent and are insufficient to explain MN by themselves; however, we simply do not know how they might affect PLA2R1 biological properties and/or antigenicity and/or progression of the autoimmune response. Of note, until the moment there is no genetic evidence supporting THSD7A as an autoantigen in MN.

Molecular mimicry (chapter 1.3.1) has been suggested as a possible initiation factor of PLA2R1-associated MN. Following their work on the identification of PLA2R1 epitopes (chapter 4.2), Fresquet and colleagues (Fresquet et al., 2015) observed that a seven amino acid peptide (LTLENCK) – within the identified immunodominant epitope peptide of 31 amino acids – shares complete sequence identity with the enzyme D-alanyl-D alanine carboxypeptidase present in the cell wall of many bacteria including *Clostridium* species. Therefore, they proposed that

a mechanism of molecular mimicry could lead to loss of tolerance, explaining immunization against the immunodominant epitope of PLA_2R1.

More recently, Fresquet and colleagues (Fresquet et al., 2019) claimed to have identified an immunodominant epitope in THSD7A-associated MN within the first domain of THSD7A (TSR1 or D1): T28mer. This T28mer peptide would share some conserved amino acids with the immunodominant epitope of PLA_2R1-associated MN (31-mer) which was identified in their previous work and is now referred to as P28mer. It was shown that the mature anti-PLA_2R1 and anti-THSD7A autoantibodies were able to recognize both P28mer and T28mer peptides, but not each entire autoantigen (i.e. anti-PLA_2R1 autoantibodies do not recognize THSD7A and anti-THSD7A autoantibodies do not recognize PLA_2R1). Thus, the authors suggested that P28mer and T28mer share a common immunodominant epitope that triggers the autoimmune response in both PLA_2R1- and THSD7A-associated MN. Interestingly, P28mer (SVLTLENCKQA) and T28mer (TLHTNCKQA) peptides contain a C-terminal sequence which shares sequence homology with *Clostridium* peptidase S11 (LTENCK) and other organism *(*such as *Saccharomyces cerevisiae* and *Pseudomonas HrcC Type II* containing the sequence SVLTLEN) supporting the authors' hypothesis published in previous works of molecular mimicry playing an important role in the development of MN (Fresquet et al., 2015; Fresquet et al., 2019). However, this study remains under debate as the level of sequence identity between P28mer, T28mer and the bacterial peptide is small and on short sequences, with in fact no significant p-values between proteins when tested in a blast search, suggesting a random sequence alignment. Furthermore, it remains to be demonstrated that these peptides can be "nephritogenic" by injecting them into animals and inducing an autoimmune response with antibodies targeting either PLA_2R1 and/or THSD7A and triggering MN, as shown in other diseases such as encephalomyelitis or ANCA diseases or in experimental autoimmune glomerulonephritis (Land et al., 2014; Venkatesha et al., 2015).

The increase in incidence of autoimmune diseases over the last decades had led to hypothesize that exposition to physical and environmental agents might be putative triggers of an autoimmune response. Interestingly, a study from Xu and colleagues (Xu et al., 2016) analysed the association between long-term exposure to fine particulate matter with less than 2.5 μm in diameter ($PM_{2.5}$ particles) with the incidence of glomerulopathies. By studying 17,151 cases of biopsy-proven glomerular diseases obtained from 2004 to 2014 across 282 Chinese cities, they observed that the frequency of MN increased over time, while the frequency of other major glomerulopathies remained stable. Thus, the authors attributed the

increased incidence of MN to an increased exposure to air pollution, in particular to $PM_{2.5}$ particles (Xu et al., 2016). Even though the mechanism by which prolonged exposure to air pollution might increase the risk of MN remains to be elucidated, it is hypothesized that it might be due to environmental and genetic interactions with the production of inflammatory cytokines (Zhang et al., 2018). In this scenario, cytokines production in the airways in response to air pollution could upregulate PLA_2R1 expression (and/or change its conformation) which could potentiate an interaction with the antigen presenting cells in the inflamed airways culminating in an autoimmune response to PLA_2R1 expressed in the podocytes (Ritz, 2010; Salant, 2019).

In sum, even though the overall aetiology of MN remains to be completely elucidated, almost certainly it is multifactorial, involving the interplay of initiating and predisposing environmental and genetic factors.

4.2 PLA_2R1 epitopes and epitope spreading

After the identification of PLA_2R1 as the major autoantigen in MN and eager to bring new insights into the pathophysiology of the disease, several teams have worked hard to identify the epitopes that are targeted by the anti-PLA_2R1 autoantibodies. This has led to the publication of four articles in this topic within three years.

In 2013, using a peptide array scanning approach and SPOT technology, Behnert and colleagues (Behnert et al., 2013) first proposed that patients' serum could recognize up to 7 putative epitopes suggesting that a mechanism of intermolecular epitope spreading could occur during the course of the disease. The authors synthesized on nitrocellulose membrane 276 peptides, each comprising 15 amino acids overlapping by a window of 5 amino acids and covering the full extracellular region of PLA_2R1. Serum from 7 different PLA_2R1-positive MN patients presented reactivity against 7 peptides: one present in the CysR domain, one within CTLD1, one within CTLD2, two within CTLD6, one within CTLD8 and one between CTLD8 and the transmembrane segment. However, ELISA screen using these peptides as coated antigens did not confirm the screening results since the ELISA signal was not significantly different between sera from PLA_2R1-positive MN patients and various controls (PLA_2R1-negative MN patients, unrelated inflammatory disease controls and healthy donors). Such results can be explained by the fact that the authors used linear peptides whereas anti-PLA_2R1 autoantibodies are known to recognize only conformational epitopes, meaning that the recognized epitope motif

may comprise several amino acids in a discontinuous primary structure (Beck et al., 2009). In addition, the sequence of one putative epitope supposed to be within the CysR domain was actually within the signal peptide which is absent in the mature form of PLA2R1 (membrane-bound or soluble forms) and thus has a small chance to be presented as an autoantigen (Ancian et al., 1995).

In 2015, Kao and colleagues (Kao et al., 2015) suggested that an immunodominant epitope is comprised within the CysR-FnII-CTLD1 region, and that the absence of either CysR or CTLD1 domains prevents autoantibodies recognition of the triple domain. The authors expressed a series of recombinant soluble proteins in which they successively removed one by one the PLA2R1 domains from the C-terminal region. The autoantibodies of one patient serum presented reactivity towards all recombinant proteins except for the constructs in which CTLD1 was absent (CysR-FnII and CysR). To further investigate the possibility of CTLD1 being an epitope-containing domain, they tried to express the CTLD1 domain alone but were unsuccessful. Thus, the authors expressed the triple domain CysR-FnII-CTLD1 introducing a thrombin cleavage site between the CysR and FnII domains or between the FnII and CTLD1 domains. They observed that the patient serum reacted to the three-domain construct before but not after thrombin digestion, with no reactivity towards the proteolyzed fragments, leading them to conclude that the CysR-FnII-CTLD1 region contained a single intramolecular epitope overlapping between at least two domains. However, as further detailed in chapter 6.1, this apparently elegant strategy was weakened by the erroneous insertion of the thrombin cleavage site, leading to inappropriate conclusions. Nevertheless, using a western blot competition assay, the authors were able to demonstrate that the CysR-FnII-CTLD1 region contained the immunodominant epitope, in other words the autoantibodies present in the 10 patients' sera analysed mainly target this region.

Also in 2015, using a pool of serum from five different patients and then a cohort of 43 patients, Fresquet and colleagues (Fresquet et al., 2015) proposed that the CysR domain contains the immunodominant epitope. They confirmed that the identified epitope within CysR was sensitive to reduction and suggested that it might also be sensitive to SDS denaturation due to contrasting reactivity between western blot and slot blot. The approach they followed was based on partial trypsin digestion of the CysR-CTLD3 region of PLA2R1 followed by identification of the resulting fragments reactive to patients' sera by mass spectrometry. Mass spectrometry analysis of the reactive fragments of about 14 kDa after standard reduction/alkylation of the fragments and full proteolysis to generate peptides for

MS/MS led to the identification of 8 peptides spanning the different domains within the CysR-CTLD3 region, but with more peptides in the CysR domain. The identified peptides were thought to be part of the immunodominant epitope, thus the authors synthetized them to evaluate their potential to inhibit the binding between the autoantibody and PLA_2R1. Among the eight identified peptides, 2 of them ($_{39}$GIFVIQSESLKKC$_{51}$ and $_{57}$SVLTLENCK$_{65}$, both within the CysR domain) appeared to compete with the CysR-CTLD3 for recognition of anti-PLA_2R1 autoantibodies obtained from a serum pool of 5 patients. By extending peptide 1 to peptide 2, the authors designed a new N-terminal peptide of 31-mer ($_{35}$WQDKGIFVIQSESLKKCIQAGKSVLTLENCK$_{65}$) that could inhibit 85% of autoantibodies recognition to the CysR-CTLD3 region. These results were in agreement with competition assay where the CysR-CTLD3 region inhibits most of the reactivity of the anti-PLA_2R1 autoantibodies to the complete extracellular domain of PLA_2R1, suggesting that the 31-mer comprises most of the immunodominant epitope of PLA_2R1-associated MN. Finally, the competition assay with the CysR-CTLD3 region led the authors to conclude that the CysR domain contained the immunodominant epitope (31-mer peptide) but also allowed them to suggest that patients' serum could have autoantibodies towards other epitopes present in the distal region of PLA_2R1.

Indeed, in 2016, Seitz-Polski&Dolla and colleagues (Seitz-Polski et al., 2016) suggested that CysR, CTLD1, and CTLD7 are three epitope-containing domains. The authors expressed a series of recombinant membrane proteins in which they successively removed one by one the PLA_2R1 domains from the N-terminal end. Screening by western blot with 50 individual patients led to the conclusion that patients' sera can differentially recognize one, two or three distinct epitope-containing domains: CysR, CTLD1 and CTLD7. Following the same strategy from Kao and colleagues, the authors also expressed the N-terminal triple domain CysR-FnII-CTLD1 and inserted a thrombin cleavage site either between the CysR and FnII domains or between the FnII and CTLD1 domains. However, after proteolysis with thrombin they showed that the patients' serum presented reactivity towards the individual fragments thereby confirming that the two domains are recognized by distinct anti-PLA_2R1 autoantibodies. The contradictory findings were due to the insertion of the thrombin cleavage site at different amino acid positions, a key point that is further discussed on chapter 6.1. An ELISA screen with a cohort of 69 patients against the three individual domains confirmed the previous results and revealed that CysR was the most prevalent epitope-containing domain followed by CTLD1 and CTLD7. These findings led the authors to hypothesize that the anti-

PLA2R1 autoantibodies might be initially raised against CysR with progression of the autoimmune response towards the CTLD1 and/or CTLD7 domains by a mechanism of epitope spreading (chapter 2.5.2).

In sum, the above works provide a better view of the epitope-containing domains and/or discrete epitopes present within the complex structure of PLA2R1 that might be targeted by anti-PLA2R1 autoantibodies. They all converge to the notion that anti-PLA2R1 autoantibodies target one or more predominant epitope(s) present within the CysR-FnII-CTLD1 region (Fresquet et al., 2015; Kao et al., 2015; Seitz-Polski et al., 2016). Furthermore, studies by Fresquet and colleagues (Fresquet et al., 2015) and Kao and colleagues (Kao et al., 2015) demonstrated that the CysR-FnII-CTLD1 region contains one or more immunodominant epitopes. Nevertheless, controversies remained regarding the exact number and location of the epitopes, in particular, whether the CysR-FnII-CTLD1 region can contain a single "interdomain" epitope or two independent epitope-containing domains (Kao et al., 2015; Seitz-Polski et al., 2016). To lend credence to the mechanism of epitope spreading proposed by Seitz-Polski&Dolla and colleagues (Seitz-Polski et al., 2016) which involve individual reactivities from CysR to CTLD1 and/or CTLD7, it was important to clarify this last, as I did during my PhD (chapter 6.1).

As for THSD7A, several groups have also tried to identify the conformational epitopes. Initially, Ma and colleagues (Ma et al., 2015) tested patients' serum reactivity against N- and C-terminally truncated forms of recombinant THSD7A as well as constructs containing single or multiple adjacent domains by western blot, dot blot and immunoprecipitation. The majority of patients' sera presented reactivity towards 2 or more distinct domains in the C-terminal region, but a few patients also had additional autoantibodies targeting epitopes in domains at the N-terminal end. Later, the works from Seifert and colleagues (Seifert et al., 2018) confirmed that anti-THSD7A autoantibodies present reactivity towards multiple domains. By screening 31 patients' serum against several recombinant constructs comprising two to three adjacent domains of THSD7A (D1–D2, D3–D4, … , D19–D21) the authors showed that all domains, except D3–D4 and D19–D21, comprised epitopes recognized by at least three patients. These results were confirmed by Stoddard and co-workers (Stoddard et al., 2019). Using an *in silico* structural model of THSD7A and epitope prediction algorithms, they suggested that THSD7A contains up to 18 domains comprising epitopes whereas 3 domains were predicted to have no immunogenicity. Finally, as reviewed in the previous chapter, Fresquet and colleagues (Fresquet et al., 2019) proposed that PLA2R1 and THSD7A share a common

epitope motif within the T28mer present in the D1 domain of THSD7A and the P28mer present in the CysR domain of PLA_2R1.

4.3 Diagnosis and prognosis of PLA_2R1-associated MN

Historically, confirmation of MN disease was solely based on renal biopsy diagnosis ("biopsy-proven MN"), with (i) the characteristic alterations of the glomerular structure (ii) the detection of immune deposits by electron-microscopy, light microscopy, and/or immunofluorescence, (iii) the detection of different predominant IgG subclasses as a possible indicator of primary (mainly IgG4) versus secondary MN (mainly IgGs other than IgG4) and (iv) no detection of any of the possible different autoantigens, which were unknown until 2009 in adult MN (chapter 2.2.4). In addition, prognosis was mostly predicted through the Toronto Risk Score which is based on variation in proteinuria levels and creatinine clearance over at least six months after diagnosis (chapter 2.2.5). If available, clinicians could also use urinary excretion of ß2-microglobulin or α1-microglobulin to predict prognosis. If the nephrotic syndrome persisted beyond the 6 months observational period and/or the renal function got deteriorated, the patient would receive immunosuppressive treatment otherwise symptomatic conservative therapy would be maintained. However, this approach was not ideal for patients' follow-up and healthcare. Indeed, approximately 30-35% of patients reach spontaneous remission within 5 years after diagnosis, i.e. without receiving immunosuppressive therapy, meaning that they might have been overtreated if recommendations were to give immunosuppressors at 6 months with apparent signs of disease worsening at early stages. Conversely, for some patients with a strong overt disease observed at diagnosis, the 6 months observational period might be too long, and once the immunosuppressive treatment would be prescribed at 6 months, the disease may be too advanced, and the patient may no longer respond.

The identification of both PLA_2R1 and THSD7A as autoantigens in MN led to the development of specific tests to detect the autoantibodies. These tests not only allow a better diagnosis of MN, in addition to a renal biopsy, but they also have prognostic and theragnostic values. In a few years, these tests may change (i) the classification of MN forms which may become based on serology, (ii) the diagnosis of patients (with less need for an invasive kidney biopsy) and (iii) patients' healthcare based on serological levels of autoantibodies to monitor disease activity and treatment efficacy.

4.3.1 Biopsy staining of the PLA2R1 autoantigen

Renal biopsy of healthy individuals shows a very weak stain for PLA2R1 at the external side of the GBM with a typical fine granular pattern (Figure 4.1), contrasting with a stronger pseudo-linear staining along the GBM for THSD7A (Figure 4.1) but also NEP, suggesting different expression levels of the three autoantigens in normal podocytes (Hoxha et al., 2012; Larsen et al., 2016; Svobodova et al., 2013; Tomas et al., 2014; Vivarelli et al., 2015). Typically, biopsies from patients with PLA2R1-associated MN present a specific enhanced PLA2R1 staining with a more granular pattern in the sub-epithelial deposits along the glomerular capillary loops but not enhanced staining for THSD7A (Figure 4.1). Conversely, biopsies from patients with THSD7A-associated MN show enhanced diffuse global granular staining of THSD7A along the capillary loops but no enhanced staining for PLA2R1 (Figure 4.1). Biopsies from patients with both PLA2R1- and THSD7A-associated MN presented enhanced staining for both antigens (Larsen et al., 2016; Zaghrini et al., 2019). The increased staining, and therefore the presence of higher amount of autoantigenic protein, does not seem to be due to an increase of transcription, and no real explicative (patho)physiological mechanism has been proposed, except the likely shedding of the membrane-bound protein that accumulates in immune deposits over time because of cross-linking with autoantibodies (Hoxha et al., 2012; Kerjaschki et al., 1987).

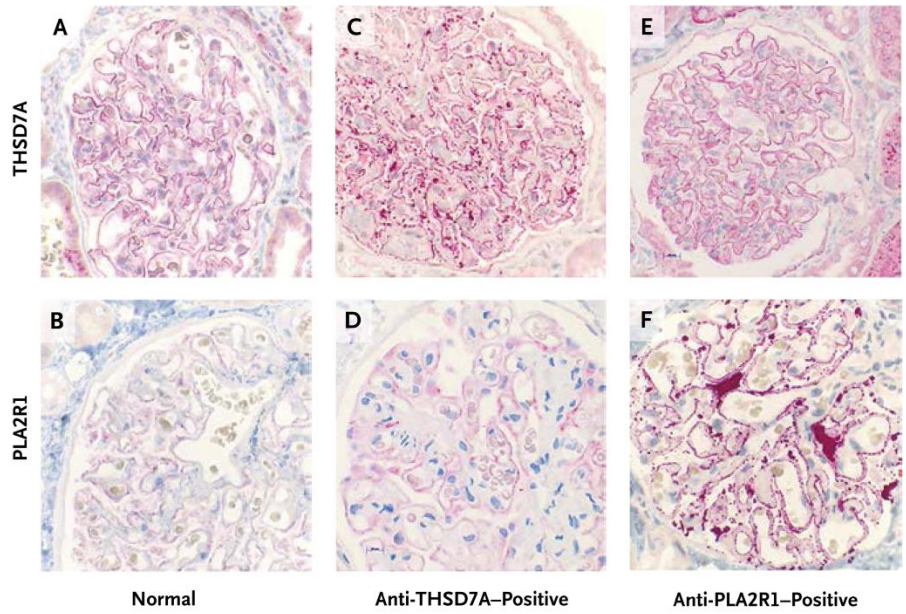

Figure 4.1 – Renal biopsy staining for PLA2R1 and THSD7A autoantigens. Renal immunohistochemical staining for THSD7A (**upper panels**) and PLA2R1 (**lower panels**) in healthy individuals (**A,B**), in patients with THSD7A-associated MN (**C,D**) and in patients with PLA2R1-associated MN (**E,F**). *Adapted and reproduced with permission from* (Tomas et al., 2014), *"Copyright Massachusetts Medical Society"*.

The renal biopsy staining can be used in the daily clinical practice to differentially diagnose patients with PLA2R1- or THSD7A-associated MN, as well as to document retrospective diagnosis (Pourcine et al., 2017; Svobodova et al., 2013). This technique is more sensitive than the detection of circulating autoantibodies, which is of particular interest for patients presenting very low or undetectable autoantibody titer (Debiec et al., 2011; Qin et al., 2016; Svobodova et al., 2013). The discrepancies can be explained by (i) an initial rapid clearance of the autoantibodies from the blood to the glomeruli in a phenomenon known as the "kidney sink hypothesis" (the kidney serves as a sponge); (ii) detection of antibodies during immunological remission, since there is a time lag between immunological and clinical remission and (iii) irreversible podocyte injury even though there is no longer immunological response, which leads to later referral of patients due to persistent high proteinuria. Nonetheless, an increased staining for the autoantigen in the glomeruli can correlate with the presence of circulating autoantibodies in the serum (Debiec et al., 2011; Hoxha et al., 2012). On the contrary, detection of circulating autoantibodies is not always associated with immune deposits of the autoantigen, yet patients have MN disease. Several explanations are possible: (i) serum and biopsy were not collected and analysed at the same time, explaining the apparent discrepancy, (ii) some circulating autoantibodies are not highly nephritogenic and do not form strong immune deposits as revealed by staining of increased amount of the PLA2R1 autoantigen, and not by the actual presence of those autoantibodies in the biopsy, and (iii) immune deposits are in fact formed but the specific PLA2R1 epitope recognized by the commercial antibody used to detect enhanced PLA2R1 staining is not accessible in these particular kidney biopsies and the detection method used (Debiec et al., 2011). Therefore, sometimes assessment of both autoantigen in the kidney biopsy and circulating autoantibodies might provide complementary information for diagnosis, treatment follow-up and relapse (Debiec et al., 2014; Pourcine et al., 2017; Qin et al., 2016).

4.3.2 Autoantibodies detection

Historically, anti-PLA2R1 circulating autoantibodies were detected by western blot which was in fact the same technique used for the identification of the autoantigen (Beck et al., 2009). It is still currently used and considered as the most sensitive technique, especially when using IgG4 detection; however, it is only semi-quantitative and the procedure is just too long for the daily clinical practice. The identification of PLA2R1 as a specific autoantigen of MN quickly led to the

development of commercial assays for the detection of circulating autoantibodies: IIFT and ELISA.

The commercial IIFT is a semi-quantitative cell-based assay (Chapter 1.2) that measures the anti-PLA2R1 titer against the membrane-bound protein using total IgG (Hoxha et al., 2011). The assay was validated with a cohort of 117 patients with MN, 90 patients with non-membranous glomerulonephritis and 153 healthy donors, and showed 100% specificity and 52% sensitivity compared to biopsy. A commercial standardized ELISA is also available for the quantification of anti-PLA2R1 antibodies targeting the full extracellular region of the receptor using total IgG (Dahnrich et al., 2013). The assay was validated with a cohort of 200 patients with primary MN, 230 patients with other glomerular diseases, 316 patients with other autoimmune diseases and 291 healthy donors, and presented 99.9% specificity and 96.5% sensitivity with respect to the IIFT. Additional homemade ELISAs have also been developed with detection of anti-PLA2R1 antibodies using different species of PLA2R1 as antigen source and different secondary antibodies to detect either total or IgG4 specific antibodies (Hofstra et al., 2012; Seitz-Polski et al., 2015). Despite the disadvantages of the IIFT assay (semi-quantitative and observer-dependent/bias) versus ELISA assay (use of different positivity threshold for anti-PLA2R1 or use of total IgG versus IgG4), both commercial IIFT and ELISA are currently widely use on the daily clinical practice, and are now important for diagnosis, monitoring and prognosis of PLA2R1-associated MN.

As for the detection of anti-THSD7A antibodies, the same techniques can be used. A commercial IIFT assay is currently available and used on the clinical practice. The assay was validated with a cohort of 1276 patients with MN from whom 40 were THSD7A-associated MN, and it presents 92% specificity and 100% sensitivity in comparison to western blot (Hoxha et al., 2017). A homemade ELISA has been developed and may be commercially available soon, since similar to PLA2R1, the detection of anti-THSD7A antibodies is important for diagnosis, monitoring and prognosis of THSD7A-associated MN (chapter 7).

4.3.3 Clinical value of anti-PLA2R1 autoantibodies

Anti-PLA2R1 autoantibodies have been detected in approximately 70% of MN patients and they have not been described to be present in any other disease nor in healthy individuals, thus emerging as pathognomonic biomarker for MN. The assays to detect anti-PLA2R1 antibodies are highly sensitive (78%) and specific

(99%) which is leading the clinicians to re-evaluate the need to perform renal biopsy, especially when there is contra-indications (Du et al., 2014).

In fact, a new diagnosis method and a new algorithm for patient management, both based on serological analysis of antibody and titer were recently suggested for diagnosis and monitoring of MN (Bobart et al., 2019; De Vriese et al., 2017). The serology-based diagnosis method proposes to determine the presence of circulating anti-PLA2R1 in addition to a thorough screen for possible secondary causes. If anti-PLA2R1 autoantibodies are positive with no evidence for secondary causes, the patient should be treated for PLA2R1-associated MN according to the KIDGO guidelines. If anti-PLA2R1 autoantibodies are undetectable, kidney biopsy should be performed, with staining for PLA2R1 and IgG subclasses. If the renal biopsy reveals positivity for PLA2R1 antigen with predominance for IgG4 over other IgG subclasses, the patient should be treated for PLA2R1-associated MN. Furthermore, if the patient is negative for PLA2R1 while IgG4 is predominant, staining for THSD7A and detection of circulating autoantibodies should be performed. Finally, if the renal biopsy is PLA2R1 negative while IgG1, IgG2 and/or IgG3 subclasses are predominant, then secondary causes of MN due to other antigens (including the most recent ones) should be considered.

Once MN patients have been diagnosed with PLA2R1-associated MN, the new algorithm method for patient management proposes to determine anti-PLA2R1 titers during follow-up to monitor disease activity and help for the decision to treat with conservative versus immunosuppressive treatments (Figure 4.2). Indeed, anti-PLA2R1 autoantibodies titer reflects the immunological activity of the disease, thus being useful to monitor disease activity and predict clinical outcome and/or relapse (Bech et al., 2014; Beck et al., 2009; Beck et al., 2011; Hofstra et al., 2011; Seitz-Polski et al., 2014). It has been shown that circulating anti-PLA2R1 autoantibodies can disappear at least 9 months before clinical remission of the nephrotic syndrome (spontaneous or treatment-induced) and become detectable before clinical relapse, reflecting the time lag between immunological and clinical remission. Thus, accurate follow-up of patients' anti-PLA2R1 titer can avoid unnecessary immunosuppressive treatment since reduction of autoantibody titer in untreated patients might indicate spontaneous remission (Francis et al., 2016). Similarly, in patients under immunosuppressive therapy, treatment withdrawal can be considered if no autoantibodies are detected. Additionally, anti-PLA2R1 antibodies are prognostic biomarkers since high anti-PLA2R1 titers have been associated with lower chance for spontaneous remission, higher risk for renal function deterioration and/or longer time to reach remission (Dahan et al., 2017; Hoxha et al., 2014; Kanigicherla et al.,

2013; Pourcine et al., 2017; Rodas et al., 2019; Ruggenenti et al., 2015; Timmermans et al., 2015). Finally, close follow-up of anti-PLA2R1 titer up to non-detectable levels after immunosuppressive treatment may be needed to avoid relapse (Dahan et al., 2018; Georges et al., 2019).

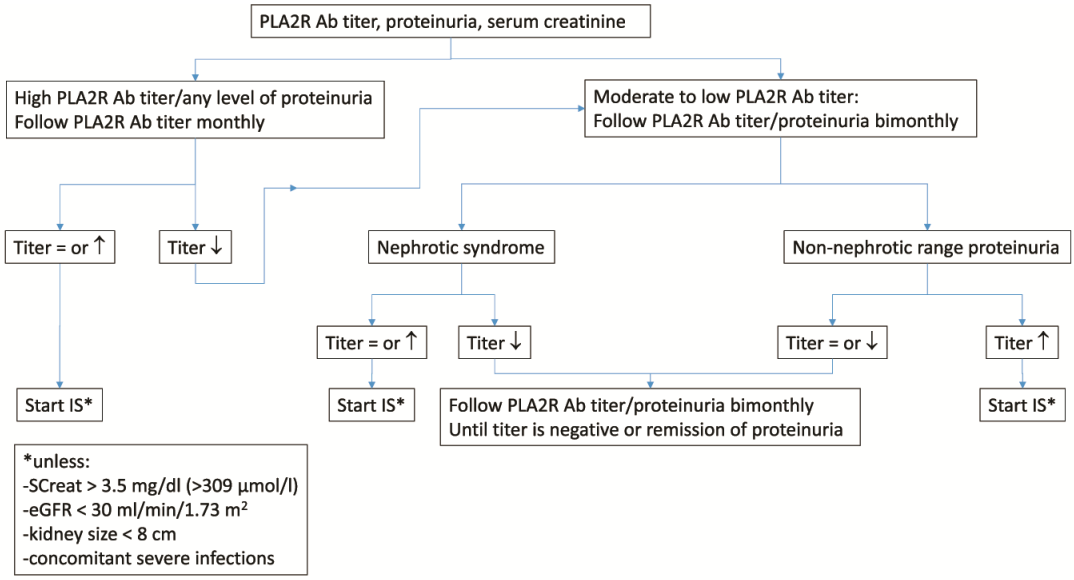

Figure 4.2 – Monitoring and prognostic algorithm as proposed by De Vriese and colleagues (De Vriese et al., 2017). The temporal relationship between anti-PLA2R1 titer and disease activity is well established, however there is a time lag of months between immunological and clinical response that should be taken into account during managment of patients healthcare. Measurment of the anti-PLA2R1 autoantibodies levels may avoid the 6 months observational period recommended by the KDIGO guidelines and allow more rapid treatment decisions. Similarly, serial measurements of the anti-PLA2R1 titer may guide decision to start immunosuppressive therapy (IS). Patients with initial high anti-PLA2R1 titers should be followed monthly, whereas those with moderate to low anti-PLA2R1 levels should be re-evaluated bimonthly. This recommendation does not apply to patients with rapidly declining renal function, in whom prompt initiation of immunosuppressive treatments may be warranted. Anti-PLA2R1 autoantibody levels as measured by the commercial Euroimmun ELISA: low=14–86 RU/mL; moderate=87–204 RU/mL; and high 204 RU/mL. SCreat, serum creatinine. *Adapted from (De Vriese et al., 2017) with permission from, "American Society of Nephrology".*

Beyond measuring anti-PLA2R1 titers, epitope spreading defined by the presence of multiple autoantibodies at presentation or before treatment has also been associated with disease severity and poor outcome (Seitz-Polski et al., 2018; Seitz-Polski et al., 2016). However, its usefulness to help predict clinical outcome is under intensive debate and more prospective clinical studies are required to validate its usefulness, as also further demonstrated during my PhD.

Finally, anti-THSD7A autoantibodies seem to present similar clinical value as anti-PLA2R1 (chapter 7); however more clinical studies are required to validate their clinical usefulness.

It is clear that detection of anti-PLA$_2$R1 autoantibodies is important for definitive diagnosis of PLA$_2$R1-associated MN, but the techniques and methods of detection vary between the different departments of immunology and nephrology around the world. For the commercial ELISA, different cut-off values are now used around the world, which might be a problem to define the severity of MN, once diagnosed (De Vriese et al., 2017; Liu et al., 2018; Tampoia et al., 2018). It is also clear that the determination of anti-PLA$_2$R1 titer is important to evaluate clinical outcome and adapt treatment, but there are pitfalls. Low-titer is better associated with clinical spontaneous remission and high chance of response to immunosuppressors, but there are cases with worsening of the disease during follow-up. Conversely, there are patients with high anti-PLA$_2$R1 titer who will reach spontaneous remission but the tendency is to treat those patients. In addition, similar observations can be made regarding the clinical usefulness for the evaluation of epitope spreading to predict clinical outcome, yet more studies are required. Indeed, some non-spread patients may stay in active disease while spread patients may be able to reach remission. Finally, we talk about "low" versus "high" titers of anti-PLA$_2$R1 autoantibodies, but actually we do not have a precise idea of what that means. Despite standardization, titer values measured around the world may not be identical as the current commercial ELISA has not been validated between different immunological laboratories worldwide, and we don't know what cut-off values should be considered for weak (or even smouldering), mild or severe MN disease, and what threshold may be considered to start immunosuppressive therapy, and up to what upper value there is a high chance for efficient therapy with one or another immunosuppressor. For instance, what are the thresholds tertiles for anti-PLA$_2$R1 titer? Is it a titer of 100 or 200 RU/mL? And what about 50 RU/mL when the detection threshold titer is supposed to be 20 RU/mL according to the manufacturer's protocol, but can be re-defined to 14 RU/mL and as low as 2 RU/mL for anti-PLA$_2$R1 positivity in various laboratories around the world (Liu et al., 2018; Tampoia et al., 2018)? Is anti-PLA$_2$R1 titer or epitope spreading enough by themselves to predict outcome or would it be better a combined assessment? Which other biomarkers in addition to the ones already considered (age, sex, proteinuria levels, anti-PLA$_2$R1 titer) may be used to better stratify patients and provide the best clinical care, towards personalized medicine?

Chapter 5

Aims

As reviewed in the introduction, in 2009, PLA_2R1 was identified as the major autoantigen in membranous nephropathy (MN). Quickly after, specific diagnosis tests for the detection of anti-PLA_2R1 autoantibodies were developed and are currently used in daily clinical practice. In addition to being a specific biomarker for the diagnosis of MN, anti-PLA_2R1 titer is important for monitoring disease activity, prognosis and evaluation of response to therapy. Finally, at the time I was starting my PhD, several studies had been just published regarding the epitopes targeted by anti-PLA_2R1 autoantibodies and their possible clinical value. However, there were a lot of controversies and intensive debate regarding the exact number and location of the epitopes as well as their clinical significance.

Therefore, the major goal of my thesis was to identify in details the PLA_2R1 epitopes and analyse their clinical relevance in MN in a step-by-step approach. To do so, the first aim of my project was to clarify the number of epitope-containing domains within the CysR-FnII-CTLD1 region at the N-terminal end of PLA_2R1. Towards this goal, several soluble recombinant proteins containing the CysR-FnII-CTLD1 region as well as chimeras between PLA_2R1 and its paralog MRC2 were produced and tested with serum from different PLA_2R1-associated MN patients. Additionally, among the remaining 7 PLA_2R1 domains (CTLD2-CTLD8), only CTLD7 was known to contain epitopes. Thus, my second aim was to further investigate the distal region of PLA_2R1 for additional epitopes. Collectively, the work realized towards these two objectives led us to identify 5 epitope-containing domains spreading from the N-terminal to the C-terminal ends of PLA_2R1. The next step aimed to determine the prevalence of each epitope-containing domain, to identify which one(s) was (were) the driving-force of the humoral autoimmune response (immunodominance) and provide a comprehensive view for the association between anti-PLA_2R1 titer, epitope positivity, immunodominance and disease activity including prognosis. In order to reach this goal, a multicenter French cohort of 142 PLA_2R1-positive MN patients was established. All the serum samples were investigated for anti-PLA_2R1 titer, epitope-containing domain reactivity against the 10 individual domains of PLA_2R1 and immunodominance of epitope-containing domains. This work contributed to (i) a better understanding of the pathophysiological mechanism in MN associated with the development of the humoral autoimmune response and ii) unveiled immunodominance as a possible new biomarker to predict response to treatment, in particular to rituximab.

Finally, I also participated in a collaborative study that aims to evaluate the added value of anti-PLA_2R1 titer and epitope spreading to predict clinical outcome

in PLA_2R1-positive MN patients. To do so, quantitative homemade ELISAs to determine anti-PLA_2R1 titer as well as titers of single epitope-containing domains were established and used to screen a cohort of 318 MN patients (baseline samples and available follow-up samples). The cohort included both PLA_2R1-positive and PLA_2R1-negative MN patients. Finally, I also screened these patients for THSD7A positivity and found 9 novel THSD7A-positive patients. These samples were included in an ongoing parallel study from the laboratory to establish a quantitative ELISA assay to screen patients for anti-THSD7A autoantibodies and to assess the usefulness of anti-THSD7A titer to evaluate disease activity, response to treatment and prediction of clinical outcome.

Part II
Results

Chapter 6

PLA_2R1 autoantibody response in MN and clinical association

While the identification of PLA2R1 as an autoantigen of MN provided a rapid paradigm shift for clinical care one "hot" question, more biochemical at first sight, was about the location of PLA2R1 epitopes within the complex structure of PLA2R1, with the fact that autoantibodies purely recognize conformational epitopes. Just before arriving to the laboratory, different works had been published regarding the identification of PLA2R1 epitopes: (i) Behnert and colleagues (Behnert et al., 2013) identified several linear peptides as potential epitopes spanning the full extracellular region of PLA2R1, (ii) Kao and colleagues (Kao et al., 2015) suggested that CysR and CTLD1 domains form an unique overlapping epitope region, (iii) Fresquet and colleagues (Fresquet et al., 2015) proposed that the CysR domain contains the immunodominant epitope, whose conformation would depend on assisted folding by neighbouring domains and (iv) Seitz-Polski&Dolla and colleagues (Seitz-Polski et al., 2016), our laboratory, identified CysR, CTLD1 and CTLD7 as three independent epitope-containing domains. Additionally, we proposed that the multiple autoantibodies were produced through a mechanism of epitope spreading which also presented a predictive clinical value: reactivity limited to the CysR domain was associated to lower proteinuria and a higher chance to enter into spontaneous remission during follow-up, whereas additional reactivity towards CTLD1 and/or CTLD7 was an independent risk factor for poor prognosis. However, controversies regarding the exact number and location of the PLA2R1 epitopes do exist and the predictive value of epitope spreading versus anti-PLA2R1 titer is under intensive debate. Indeed, Hoxha and colleagues (Hoxha et al., 2018) and Reinhard and colleagues (Reinhard et al.) claim that C-terminal epitope recognition and/or PLA2R1 domain-specific antibody level no longer predict clinical outcome of patients with MN, especially after adjustement for the total anti-PLA2R1 titer.

Considering the above points, the first aim of my project was to identify in detail the PLA2R1 epitope-containing domains in a step-by-step approach. Subsequently, by screening a cohort of PLA2R1-positive MN patients, we wanted to (i) determine the prevalence of each epitope-containing domain, (ii) identify which epitope-containing domain(s) comprise(s) the immunodominant epitope(s) driving the humoral autoimmune response, (iii) better understand the relationship between anti-PLA2R1 titer, epitope positivity and immunodominance, and (iv) analyse the clinical association with each of the different features of anti-PLA2R1 autoantibodies (anti-PLA2R1 titer, epitope profile and immunodominance) to evaluate their potential value as biomarkers for monitoring and/or prognosis of PLA2R1-associated MN.

6.1 Epitope-containing domains in the N-terminal region CysR-FnII-CTLD1

To clarify the controversial findings regarding the epitope-containing domains in the N-terminal CysR-FnII-CTLD1 region, we followed the strategy previously described by Kao and colleagues (Kao et al., 2015). Briefly, we expressed several recombinant proteins containing the triple domain CysR-FnII-CTLD1 with tags at both ends (construct A) in which we inserted different protease cleavage sites at different positions (constructs B to G). Then, we tested the WB reactivity of a set of MN patients' sera with known epitope profiles as determined by ELISA (Figure S1 from article 1) on the different constructs before and after protease cleavage.

We started by introducing a thrombin cleavage site between the CysR and FnII domains (construct B, Figure S2A from article 1) as well as between the FnII and CTLD1 domains as described in Kao and colleagues (Kao et al., 2015) (construct C, Figure S3A from article 1). However, we realized that in construct C, Kao and colleagues did not introduce the thrombin cleavage site between the FnII and the CTLD1 domains at the proper position to allow release of the fragments after proteolysis. Indeed, the cleavage site was inserted within the first disulphide bridge of the CTLD1 domain. To further demonstrate this was the basis of the controversy between the two studies, we prepared constructs D and E (Figure S5A from article 1). In construct D, we maintained the thrombin cleavage site within the CTLD1 domain but inserted a factor Xa (F_{Xa}) cleavage site at the appropriate place in the linker region between the FnII and the CTD1 domains, whereas in construct E we added only the F_{Xa} cleavage site in the linker region between the FnII and CTLD1 domains. The 7 soluble constructs were stably expressed in HEK293 cells.

While constructs A and B were well expressed and actively secreted (as expected), constructs C and D were barely detectable in the culture medium and cell lysates (Figure S4B from article 1), which was quite unexpected since the work from Kao and colleagues did not mention this as a limitation. Analysis of the cell lysates further demonstrated that most of the recombinant protein was present in the solubilized detergent fraction with no detection in the soluble cell fraction, indicating serious misfolding of the protein, most probably due to poor pairing of the cysteines forming the CTLD1 disulphide bridge. The folding and the associated low level of expression were partially rescued by lowering the temperature of cell growth to 30°C (Figure S4B from article 1) (Cestele et al., 2013; Farinha et al., 2013; Morello et al., 2000; Syam et al., 2016) and/or by adding chemical chaperones to cell culture (Chen

et al., 2011; Chen et al., 2013; Frump et al., 2013; Morello et al., 2000) (Figure S4C from article 1). No additive/synergistic effect was observed (Figure S4D from article 1). Lowering the temperature was the most cost-effective approach to rescue folding and expression, yet it was not sufficient to produce large amount of proteins (Figure S3B from article 1). Culture medium containing the proteins of interest was thus obtained in large volumes and the proteins were purified by affinity chromatography on His-tag resin and concentrated to perform the proteolysis experiments.

Cleavage of construct B by thrombin followed by western blot analysis with serum from 7 different PLA_2R1-positive MN patients (Figure 1B from article 1) revealed that, according to their epitope profile determined by ELISA, patients had reactivity towards the CysR or the CTLD1 domain or both domains, suggesting two independent epitope domains. To further confirm this finding, we wanted to verify the presence of a possible overlapping epitope that might be more sensitive to cleavage between the FnII and the CTLD1 domains. Despite low expression level, cleavage of construct C by thrombin was validated and both fragments could be separated under reducing conditions. However, under non-reducing conditions, the fragments were still maintained by the disulphide bridge surrounding the thrombin cleavage site, and they were thus not dissociated despite actual cleavage (Figure S3C from article 1). Consequently, serum from eight different PLA_2R1-positive MN patients recognized the full triple domain instead of any digested fragments (Figure 1C from article 1). Afterwards, we tested the cleavage of constructs D and E with F_{Xa}. Unfortunately, we were unsuccessful, even when using different partially denaturing conditions for construct E which was well expressed and folded (Figure S5B from article 1). Cleavage of construct D with F_{Xa} was also ineffective, even when preceded by thrombin digestion. Thus, we expressed construct F, which was already available in the laboratory and contains a TEV (Tobacco Etch Virus) cleavage site in the extended linker region between the FnII and the CTLD1 domains. However, once again, protease cleavage of this construct with different sources of enzyme was ineffective (Figure S5D from article 1). These negative results were most probably due to limited access of the proteolytic site between the FnII and the CTLD1 domains with a highly packed structure and steric hindrance by the globular domains preventing the access of the different proteases to the recognition site. Therefore, since these experiments were by far too time-consuming, we decided to give a last chance to this approach through the production of construct G in which we inserted a thrombin cleavage site within an artificially extended linker region between the FnII and the CTLD1

domains (Figure S3 from article 1). Although the yield of cleavage was not 100%, we were able to confirm that the serum reactivity of 5 different PLA2R1-positive patients presented independent reactivity towards the CysR and the CTLD1 domain (Figure 1D from article 1).

To further demonstrate that CysR and CTLD1 contain independent epitopes in the context of a full-size molecule such as PLA2R1, we prepared two membrane-bound MRC2–PLA2R1 chimeras. By introducing either the CysR or CTLD1 domain of PLA2R1 into the MRC2 backbone, we could definitely show that serum from eight different PLA2R1-positive MN patients recognize independently CysR and/or CTLD1 domains, depending on their epitope profile, and in line with ELISA data on single epitope domains (Figure 2 from article 1).

In sum, using two different approaches, we could clearly demonstrate that the CysR and CTLD1 domains are two independent epitope-containing domains recognized by distinct anti-PLA2R1 autoantibodies. The FnII domain was also investigated as a possible epitope-containing domain, using different techniques, but none of the sera tested could recognize this latter. Demonstrating this was time-consuming but important, as the CysR and CTLD1 turned out to be the two key immunodominant epitope-containing domains (see below).

6.2 Epitope-containing domains in the CTLD2–CTLD8 region

The CTLD2-8 region is known to contain epitopes in the CTLD7 domain (Seitz-Polski et al., 2018; Seitz-Polski et al., 2016). However, CTLD6-7 appeared to be more reactive than CTLD7, particularly by western blot analysis, suggesting assisted folding of the CTLD7 conformational epitope by CTLD6 or the presence of additional epitopes in CTLD6. Additionally, preliminary results obtained in the laboratory prior to my arrival indicated that CTLD8 could be another epitope-containing domain. Thus, we dissected the CTLD6-8 region by producing individual domains as well as by expressing soluble chimeras between MRC2 and PLA2R1 for the CTLD6-7 double domain. Moreover, to further investigate the presence of other epitope-containing domains, we also prepared the recombinant protein CTLD2-CTLD6. A preliminary screen by ELISA of 28 randomly selected PLA2R1-positive MN patients demonstrated that 36% of them were able to recognize CTLD7 but not CTLD6. Additionally, 7% presented reactivity against CTLD8 and interestingly 25% against CTLD2-6 (Figure S6 from article 1). To further confirm CTLD8 as an epitope-containing domain and better identify the epitope-containing domain(s) in

the CTLD2-6 region, we expressed additional isolated soluble constructs from each domain and tested them by ELISA. These experiments confirmed CTLD7 and CTLD8 as epitope-containing domains, but also allowed to identify CTLD5 as a new fifth epitope-containing domain (Figure 3 from article 1). Additional slot blot and immunoprecipitation experiments confirmed CTLD5 and CTLD8 as new independent epitope-containing domains (Figure S7 from article 1). Interestingly, CTLD5 was found to be reactive by ELISA but not by WB, explaining why this epitope domain was not detected before, despite its high prevalence (see below).

6.3 Epitope prevalence and correlation with anti-PLA2R1 titer

To evaluate the prevalence of each epitope-containing domain, we build up a multicenter French cohort of 197 MN patients and screened patients against PLA2R1 as well as each of the 10 individual domains by ELISA with IgG4 detection. From these patients, 24 did not present circulating autoantibodies towards any of the antigens when detected with IgG4 subclass nor towards PLA2R1 when detected with other IgG subclasses. In parallel to the screening, we were collecting clinical data to correlate the autoimmune response of patients with their clinical characteristics and history (such as treatment and outcome). The lack of clinical information or the fact that patients received immunosuppressive treatment before sampling led to the exclusion of another 31 patients, leaving us with a final cohort of 142 PLA2R1-positive MN patients. To better compare our results and observations with other studies, and with the aim to possibly translate novel biomarkers to clinical practice, we also measured anti-PLA2R1 titer using the commercial Euroimmun ELISA kit which is commonly used in clinical practice.

In our cohort, anti-PLA2R1 autoantibodies could recognize up to 5 different epitope-containing domains with different prevalence and epitope profiles (Figure 4 from article 1). The CysR domain was clearly the most prevalent, recognized by 100% of patients, unexpectedly followed by CTLD5, then CTLD1, CTLD7 and CTLD8. By ranking patients according to their Euroimmun ELISA titer, we observed that the CTLD5-positive patients were equally distributed over the full range of anti-PLA2R1 titers while the CTLD1-positive patients were more present at high titer, in the last tertile range, even though some are present in the lower tertiles. The CTLD7-positive patients were mainly present in the medium and high tertiles of anti-PLA2R1 (Figure 5A from article 1). Additionally, as expected by nature of an autoimmune response, the anti-PLA2R1 titer increased as the positivity for epitope-containing domains increased (Figure S10 from article 1).

Similarly, when we ranked patients according to epitope prevalence and positivity or not to CTLD1, we could observe a relationship between the complexity of the epitope profile and the increase in anti-PLA2R1 titer (Figure 5B from article 1).

6.4 Immunodominant epitopes and correlation with anti-PLA2R1 titer

After identifying the most prevalent epitope-containing domains and the relationship to full anti-PLA2R1 titer, we wanted to determine which epitope-containing domain(s) is(are) the driving force of the humoral autoimmune response, meaning which one(s) is(are) the major contributor(s) to the anti-PLA2R1 titer. For this, we set-up competition assays in which we tested the ELISA reactivity of patients' serum towards the entire PLA2R1 receptor as antigen after preincubation of serum with saturating amounts of different recombinant soluble proteins including the individual epitope-containing domains CysR and CTLD1.

Our competition assays clearly demonstrated that for the majority of patients, the immunodominant epitope(s) was/were comprised within the CysR-FnII-CTLD1 region, which was in agreement with previous studies (Fresquet et al., 2015; Kao et al., 2015). By integrating the full set of competition assays and the epitope profile, we stratified the patients into three different groups: immunodominant CysR (iCR), immunodominant CTLD1 (iC1) and non-immunodominant (non-iDom) (Figure 6 from article 1). The iCR group represented 55% of the cohort while iC1 and non-iDom represented 36% and 9% of the cohort, respectively. By ranking the patients according to their anti-PLA2R1 titer as before, we observed that the iCR patients were more distributed in the first and second tertiles of anti-PLA2R1 titer whereas the iC1 patients were more present in the high tertile, yet both types of immunodominance could be observed in the different tertiles (Figure 7A from article 1). Interestingly, all non-iDom patients had similar middle range anti-PLA2R1 titer, indicating that the absence of "positive immunodominance" to either CysR or CTLD1 prevents patients to reach a maximal humoral response with the highest measurable titers.

6.5 Clinical relevance of anti-PLA2R1 titer, epitope positivity and immunodominance

With immunodominance as a new factor in the humoral autoimmune response, we analysed the association between the immunodominant profile and patients' clinical characteristics at presentation (Table 1 from article 1). iC1 patients had

higher anti-PLA2R1 titer compared to iCR and non-iDom patients. Proteinuria levels were also significantly higher in iC1 patients than iCR patients, but all the remaining clinical parameters were comparable. Interestingly, a majority of iCR patients reached remission whereas it was the opposite for iC1 patients, staying in active disease or progressing to ESRD during follow-up.

Anti-PLA2R1 titer is known to reflect the immunological activity of MN and low levels are usually associated with a higher chance to reach remission. Thus, we wanted to verify if we could make the same observation in our cohort. Indeed, patients who reached remission had a significantly lower anti-PLA2R1 titer (Table 2 from article 1). Additionally, as expected from our previous findings on epitope spreading, these patients were significantly less spread on CTLD1 and/or CTLD7 epitope-containing domains and were more often iCR (Seitz-Polski et al., 2016). In univariable analysis and in an adjusted model, anti-PLA2R1 titer was significantly associated with clinical outcome after first-line therapy, with patients having anti-PLA2R1 titer above the median also having a reduced chance of reaching remission, irrespective of treatment (Table 3 from article 1).

We then observed that immunodominance was also significantly associated with clinical outcome after first treatment in a univariable analysis, where iCR and non-iDom patients had similar features and outcomes (Table 3 from article 1). In adjusted models, iC1 patients had a lower chance to reach remission in comparison with the pooled group of iCR/non-iDom patients (Table 3 and Table S3 from article 1). In particular, iCR/non-iDom patients treated with rituximab had 6-fold more chance to enter into remission than iC1 patients (OR=5.99 [1.77-20.31]). We and others have shown that high anti-PLA2R1 titer (such as above 200 RU/mL as proposed by Ruggenenti and colleagues (Ruggenenti et al., 2015) and De Vriese and coworkers (De Vriese et al., 2017)) is associated with poor prognosis and a reduced response to rituximab. Moreover, we demonstrated that iC1 patients have a significantly higher titer. Therefore, one could argue that the previous observations might be due to the fact that the anti-PLA2R1 titer was significantly higher for iC1 patients. Thus, since our multivariable model cannot include anti-PLA2R1 and immunodominance, which are two variables likely linearly correlated, while selecting only patients treated with rituximab or conservative treatment, we compared the clinical outcome for patients with an anti-PLA2R1 titer below 200 RU/mL at presentation and analysed whether immunodominance might help to refine the likelihood of response overall or after rituximab (Table 4 from article 1). We observed that for patients with an anti-PLA2R1 titer below 200 RU/mL, a vast majority of iCR patients reached clinical remission while most

iC1 patients remained in active disease or progressed to ESRD. This was especially true among those treated with rituximab, with 90% of iCR reaching remission as compared to only 39% for iC1. Interestingly, when comparing the clinical outcome of patients with an anti-PLA$_2$R1 titer above 200 RU/mL, we observed that the majority of patients had a poor outcome, independent of their immunodominant profile (Table S4 from article 1).

In sum, we showed that anti-PLA$_2$R1 autoantibodies can target up to five distinct epitope-containing domains (CysR, CTLD1, CTLD5, CTLD7 and CTLD8), with CysR and CTLD1 harboring the immunodominant epitopes and acting as the drivingforce of the humoral autoimmune response for the majority of patients (more than 90% in this cohort). We demonstrated that anti-PLA$_2$R1 titer, epitope spreading towards CTLD1 and/or CTLD7 as well as a switch of immunodominance are all significantly associated with clinical outcome after first-line therapy. In particular, we propose that immunodominance combined to anti-PLA$_2$R1 titer might be a potential new biomarker to identify patients who will best respond to rituximab treatment versus patients who will need a stronger immunosuppressive treatment or higher doses of rituximab (Seitz-Polski et al., 2019; van de Logt et al., 2018).

Article 1
(in preparation)

Circulating autoantibodies in PLA2R1-associated membranous nephropathy: epitopes, immunodominance and clinical association

Joana Justino[1*], Vesna Brglez[1*], Guillaume Dolla[1], Alexandra Rousseau[2], Christelle Zaghrini[1], Christine Payré[1], Franck Bihl[1], Agnès Petit-Paitel[1], Noémie Jourde-Chiche[5,6], Karine Dahan[7], Christophe Mariat[8,9], Hanna Debiec[10], Pierre Ronco[7,10,11], Gérard Lambeau[1]

[1] Université Côte d'Azur (UCA), Centre National de la Recherche Scientifique (CNRS), Institut de Pharmacologie Moléculaire et Cellulaire (IPMC), UMR7275, Valbonne Sophia Antipolis, France;
[2] Assistance Publique – Hôpitaux de Paris (AP-HP), Unité de Recherche Clinique de l'Est Parisien, Sorbonne Université, Hôpital Saint-Antoine, Paris, France.
[3] Assistance Publique – Hôpitaux de Marseille, Centre de Néphrologie et Transplantation Rénale, Hôpital de la Conception, Marseille, France;
[4] Aix-Marseille Université, Centre Recherche en Cardiovasculaire et Nutrition, Institut National de la Recherche Agronomique 1260, Institut National de la Santé et de la Recherche Médicale INSERM U1263, Marseille, France;
[5] Assistance Publique – Hôpitaux de Paris, Hôpital de jour de Néphrologie, Hôpital Tenon, Paris, France;
[6] Département de Néphrologie, Dialyse et Transplantation Rénale, Hôpital Nord, CHU Saint-Etienne, France;
[7] EA3064 GIMAP, Université Jean Monnet Saint-Etienne, Université de Lyon, Lyon, France;
[8] Institut National de la Santé et de la Recherche Médicale (INSERM), UMR-S 1155, Paris, France;
[9] Sorbonne Université, Université Pierre et Marie Curie Paris 06, Paris, France.

*Contributed equally

Running Title: Comprehensive analysis of the anti-PLA2R1 humoral response and clinical association

Corresponding Author: Dr. Gérard Lambeau, Institut de Pharmacologie Moléculaire et Cellulaire, UMR 7275 CNRS et Université Côte d'Azur, 660 Route des Lucioles, Sophia-Antipolis, 06560 Valbonne, France. Email: lambeau@ipmc.cnrs.fr

Keywords: Membranous nephropathy, autoimmune response, circulating autoantibody, PLA2R1, epitope, immunodominance, biomarker, prognosis, immunosuppressor

Abbreviations: CTLD or C, C-type lectin-like domain; **CysR or CR**, cysteine-rich domain; **ELISA**, enzyme-linked immunosorbent assay; **ESRD,** end-stage renal disease **FnII**, fibronectin type II domain; **iC1**, immunodominance for CTLD1; **iCR**, immunodominance for CysR; **IS**, immunosuppressors/immunosuppressive treatment; **MN**, membranous nephropathy; **MRC2**, C-type mannose receptor 2; **NIAT**, non-immunosuppressive anti-proteinuric treatment; **non-iDom**, no immunodominance for CysR nor CTLD1; **PLA2R1**, M-type phospholipase A2 receptor; **WB**, western blot; **Δ7**, membrane-bound CTLD8 domain.

ABSTRACT

Background: Membranous nephropathy (MN) is a rare autoimmune kidney disease in which 70% of patients have circulating autoantibodies against phospholipase A2 receptor 1 (PLA2R1). These autoantibodies are useful biomarkers for diagnosis and prognosis. However, there are controversies regarding the number of epitopes and relationships to titer. This study provides a comprehensive analysis of the anti-PLA2R1 humoral response, from characterization of epitope-containing domains with different prevalence and immunodominance features to their clinical relevance.

Methods: We tested the serum reactivity of 142 patients against multiple PLA2R1 recombinant proteins and identified conformational epitopes spreading all over the extracellular region of PLA2R1. We determined their prevalence and immunodominant features by ELISA and analyzed their association with clinical characteristics and outcome.

Results: Anti-PLA2R1 autoantibodies target independent epitopes in five of 10 domains: CysR, CTLD1, CTLD5, CTLD7 and CTLD8. Epitope prevalence decreases from N-terminal to C-terminal ends while the two N-terminal CysR and CTLD1 domains are immunodominant and drive the anti-PLA2R1 humoral response, thereby stratifying patients into three groups: iCR, iC1 and non-iDom. Patients with high anti-PLA2R1 titer or a CTLD1 immunodominant profile (iC1) have worse clinical outcome and reduced likelihood of response to rituximab, one of the main immunosuppressors used to treat MN.

Conclusion: Combined evaluation of anti-PLA2R1 titer and immunodominance helps to predict clinical outcome and response to rituximab in PLA2R1-associated MN, as a further step towards personalized medicine.

Funding: Fondation Maladies Rares, Agence Nationale de la Recherche, Fondation de la Recherche Médicale, Direction Générale de l'Offre de Soins and European Research Council.

INTRODUCTION

Membranous nephropathy (MN) is a rare but severe autoimmune kidney disease (1-3). It is a common cause of nephrotic syndrome in adults affecting both native and transplanted kidneys. The clinical evolution is complex, ranging from spontaneous remission to persistent proteinuria and end-stage renal disease (ESRD).

In 2009, Beck and colleagues identified the M-type phospholipase A2 receptor (PLA2R1) as the major autoantigen in MN, with approximately 70% of patients having circulating anti-PLA2R1 autoantibodies, associated with *in situ* immune complex deposits in the glomerulus, podocyte injury and high proteinuria (4).

PLA2R1 is a 180 kDa type I transmembrane glycoprotein consisting of an extracellular region comprising 10 domains: a N-terminal cysteine-rich domain (CysR), a fibronectin type II domain (FnII) and eight distinct C-type lectin-like domains (CTLDs) (5, 6). Several studies demonstrated that anti-PLA2R1 autoantibodies recognize multiple conformational epitopes within PLA2R1. Behnert and colleagues first identified several linear peptides as potential epitopes, but this was not confirmed on the native PLA2R1 protein (7). Kao and colleagues then proposed an overlapping epitope between the CysR and CTLD1 domains (8). Next, Fresquet and colleagues showed that the CysR domain contains a major epitope, whose conformation would depend on assisted folding by the neighboring domains (9). Finally, Seitz-Polski&Dolla and colleagues identified CysR, CTLD1 and CTLD7 as three distinct epitope-containing domains that may be linked by a mechanism of epitope spreading (10). Despite the above advances in the identification of PLA2R1 epitopes, the total number of epitopes and the ones most prevalent and immunodominant are still uncertain.

Commercial assays based on the detection of anti-PLA2R1 autoantibodies are now used in clinical practice for PLA2R1-associated MN diagnosis, prognosis and theragnosis (11-15). Anti-PLA2R1 titer at presentation helps to predict clinical outcome, with low titer associated with spontaneous remission, and high titer associated with progression to severe disease and ESRD (16-20). Likewise, the presence of anti-PLA2R1 autoantibodies against multiple epitopes is associated with disease severity and poor clinical outcome (10, 21). Furthermore, anti-PLA2R1 titer and epitope profiling help to predict response to immunosuppressive therapy including treatment of severe MN cases with rituximab (21-27). However, the relationship between anti-PLA2R1 titer and epitope profiling, and their respective usefulness at predicting clinical outcome are debated (26, 28-30). Treatment options with conservative treatment or various

immunosuppressors based on anti-PLA2R1 titer or epitope analysis are also not well-defined (14, 21, 23, 25-27, 31-34). For instance, despite recent studies to better diagnose and predict outcome in patients with PLA2R1-associated MN based on levels of anti-PLA2R1 autoantibodies as measured with the standardized commercial assay (14, 15, 34), there is no definitive studies to establish low and high cut-off values that might help to guide treatment with immunosuppressors and predict the likelihood of a response. Thus, better biomarkers based on the nature of the anti-PLA2R1 circulating autoantibodies are required to identify patients at risk of poor clinical outcome and to monitor the efficacy of therapy.

The aim of this study was four-fold: 1) to investigate in more detail how many PLA2R1 domains are targeted by patients' autoantibodies, 2) to identify which of these epitope-containing domains are immunodominant and drive the humoral response, 3) to provide a comprehensive analysis of the relationships between anti-PLA2R1 titer, epitopes and immunodominance, and 4) to analyze the clinical association with full titer, epitope profiling and immunodominance in a well-defined cohort of 142 PLA2R1-positive MN patients.

CONCISE METHODS

Patients — Baseline serum samples from 142 patients with biopsy-proven primary MN were collected from eight French Departments of Nephrology (10, 21, 26, 35-37). We analyzed the clinical outcome of patients according to the 2012 KDIGO recommendations from baseline to first-line therapy outcome (median follow-up of 12 months, IQR: 6 – 22 months). Partial remission was defined as proteinuria below 3.5 g/day and less than 50% of baseline value, accompanied by an increase or return to normal albuminemia and stable creatininemia. Complete remission was defined as proteinuria lower than 0.5 g/day and normal albuminemia and creatininemia. Remissions were considered as spontaneous if they occurred without administration of immunosuppressive drugs during follow-up. Clinically active disease was defined as proteinuria above 3.5 g/day and/or serum creatinine increase over 30% compared to baseline in the absence of any other cause. The study was approved by institutional review boards and conducted according to the principles of the Declaration of Helsinki. Written informed consent was obtained from all participants.

Production of PLA2R1 mutants and membrane-bound chimeras of PLA2R1-MRC2 — Soluble, membrane-bound and chimera constructs of PLA2R1 with N-terminal Flag and/or 6xHis tags and a C-terminal HA tag were generated as described in the supplementary methods. All constructs were transfected into HEK293 cells using Ca/PO4 (10). The expression of recombinant proteins was validated by WB and/or ELISA using anti-HA, anti-Flag antibodies and MN patients' sera, as described in supplementary methods. Protease digestion of the triple domain CysR-FnII-CTLD1 constructs is also described in supplementary methods.

Immunoblotting and immunoprecipitation of PLA2R1 recombinant proteins — Recombinant proteins were analyzed by western blot under reducing or non-reducing conditions or by dot-blot as described in supplementary methods. Primary antibodies (mouse monoclonal anti-HA antibody (1:5,000, Sigma-Aldrich, St. Louis, USA), mouse monoclonal anti-Flag antibody (1:1,000, Sigma-Aldrich, St. Louis, USA) and MN patients' serum (1:100 unless stated otherwise) were all diluted in 0.5% low-fat milk in PBS-Tween 0.05% while secondary antibodies (anti-mouse antibody (1:20,000, Cambridge, UK) and anti-human IgG4 (1:7,500, Southern Biotech, Birmingham, USA)) were diluted in PBS-Tween 0.05%. Immunoprecipitation of PLA2R1 epitope-containing domains is described in supplementary methods.

ELISA assays — For HA-based antigen capture ELISA assays, 96-well microplates (Thermo Fisher Scientific, Waltham, USA) were coated with anti-HA antibody

(1:5,000, Sigma-Aldrich, St. Louis, USA) diluted in 20 mM Tris pH 8.0 overnight at 4°C. Plates were blocked with SeramunBlock (Seramun Diagnostica GmbH, Heidesee, Germany) for two hours and then washed with PBS-Tween 0.05%. HA-tagged PLA2R1 antigens (10–100 µl of cell culture medium diluted in PBS) were captured by incubation for two hours and then washed. Patients' sera diluted in 0.1% (m/v) low-fat milk in PBS were added to wells and incubated for two hours. Plates were then washed and incubated for one hour with anti-human IgG4 horseradish peroxidase (HRP)-conjugated secondary antibody (1:7,500, Southern Biotech, Birmingham, USA) diluted in SeramunStab ST (Seramun Diagnostica GmbH, Heidesee, Germany). After three washes, tetramethylbenzidine peroxidase substrate (TMB, Interchim, Montluçon, France) was added and developed for 15 minutes before stopping the reaction with 1.2 N HCl. Optical density (OD) was read at 450 nm using a Multiskan FC plate reader (Thermo Scientific, Waltham, USA). Serum-free medium from mock-transfected HEK293 cells was used as a negative control for each patient, providing individual background. Cut-off OD values were determined as twice the background value for each individual patient.

Autoantibody titers for full PLA2R1, CysR and CTLD1 domains were determined by performing ELISA in which a standard curve was added. The standard curve consisted of seven dilutions of a highly PLA2R1-, CysR- or CTLD1-positive serum allowing the conversion of optical density into RU/mL using a 5-parameter logistic curve (GraphPad Prism 7 Software, San Diego, USA). Anti-PLA2R1 titer was also measured with anti-total IgG using the commercial ELISA from Euroimmun (Medizinische Labordiagnostika AG, Lübeck, Germany).

For ELISA competition assays, microplates (Thermo Fisher Scientific, Waltham, USA) were coated with the purified full extracellular domain of PLA2R1 expressed as a recombinant secreted protein from HEK293 cells (12) (10 ng diluted in 20 mM Tris pH 8.0) overnight at 4°C, then blocked with SeramunBlock (Seramun Diagnostica GmbH, Heidesee, Germany) for two hours and washed with PBS-Tween 0.05%. Patients' sera were preincubated for 30 minutes with cell culture medium containing saturating amounts of different recombinant proteins (PLA2R1, CysR-FnII-CTLD1, CysR, CTLD1, CTLD5, CTLD7, CysR+CTLD2-8, CTLD1+CTLD2-8, or mock as a negative control), then added to the wells containing full PLA2R1 antigen and incubated for two hours. Preliminary dose-response experiments were performed to determine the appropriate patients' serum dilutions as well as the volumes of cell culture medium sufficient to ensure full competition for each recombinant protein (data

not shown). The plates were then washed, incubated with secondary antibody and revealed as described above. Results of competition assays are expressed as the percentage of maximal signal measured in the absence of competitor, taking into account the non-specific signal for individual patient.

Patients were classified as immunodominant for CysR (iCR) when competition with CysR-FnII-CTLD1 was higher than 65% while competition with CTLD1 was lower than 20%. Patients were classified as immunodominant for CTLD1 (iC1) when competition with Cys-FnII-CTLD1 was higher than 65% while competition with CTLD1 was higher than 20%. Patients were classified as non-immunodominant (non-iDom) when competition with CysR-FnII-CTLD1 was lower than 65% while competition with any individual domain was too low to determine any specific immunodominance, meaning that no specific domain was driving the signal of the humoral autoimmune response. For 17 of 142 patients, serum was not available to perform competition assays. Among them, 11 were positive only for the CysR domain, and assigned as iCR. The last 6 patients were positive for CysR and other epitope-containing domains, and no immunodominant profile could be assigned. These 6 patients were excluded from further immunodominance analyses.

Statistical analysis — Patients characteristics are presented as frequencies and percentages for qualitative variables, and medians and interquartile ranges for continuous variables. Wilcoxon-Mann-Whitney or Kruskal-Wallis rank test were used to assess the relationship between continuous and qualitative variables; Pearson Chi-Squared or Fisher Exact test for qualitative variables and Spearman rank correlation for continuous variables. Unadjusted and adjusted analyses were performed using logistic regression. Selection of variables for multivariate analysis was based on a threshold at 0.20. As age, gender and serum creatinine, were linked, we choose to used eGFR in multivariate analysis. Treatment and multivariate analysis was also adjusted on proteinuria, anti-PLA2R1 titer according to median level and treatment. Two variables were built combining treatment and anti-PLA2R1 titer according to median level or immunodominance, respectively, and were used in a second model to assess the interaction with treatment. Data are expressed among the population with no missing value for eGFR, proteinuria, treatment, anti-PLA2R1 titer and immunodominance. Hosmer and Lemeshow test was used to assess goodness of fit. All tests were two-sided and p-values < 0.05 indicated statistical significance. Analyses were performed using SAS v.9.3 software (SAS Institute, Cary, USA) or GraphPad Prism 7 Software (San Diego, USA).

RESULTS

Anti-PLA2R1 autoantibodies can target up to 5 independent epitope-containing domains spreading all over the extracellular region of PLA2R1

CysR and CTLD1 are two N-terminal independent epitope-containing domains – We first clarified the controversy between overlapping (8) versus independent epitopes (10) within the N-terminal CysR-FnII-CTLD1 region by building up on the approach based on site-directed mutagenesis coupled to serial insertion of thrombin cleavage sites between domains, as originally described by Kao and coworkers (8). Importantly, we noticed that in their original 1-2T construct (construct C in Figure 1A), the thrombin cleavage site was inserted within the first disulfide bond of CTLD1 and not in the small linker region between FnII and CTLD1 (8). In total, we produced seven soluble constructs expressing CysR-FnII-CTLD1 recombinant proteins with N-terminal 6xHis/3xFlag and C-terminal HA tags, and harboring either no protease cleavage site (construct A, used as a control) or different protease cleavage sites (constructs B-G) between PLA2R1 domains. We then cleaved the recombinant proteins by proteases and tested the WB reactivity of sera from MN patients with different epitope profiles determined by indirect ELISA (Figure S1). The detailed production, expression and analysis of patients' serum reactivity towards the different constructs before and after protease cleavage are shown as supplementary materials (Figures S2 to S5). Figure 1 presents a summary of the key findings. Construct B harbors a thrombin cleavage site between CysR and FnII and provided straightforward results (Figure 1). It clearly shows that patients' sera react with independent epitopes on the thrombin-cleaved fragments CysR and FnII-CTLD1 domains (Figure 1B), a finding in contrast with previous data suggesting an overlapping epitope (8). We next produced construct C (Figure 1A) as described (8). In our hands, construct C was hardly expressed in HEK293 cells, likely because of insertion of the thrombin cleavage between the CTLD1 disulfide bond, which may produce a structural clash. Expression was rescued by growing cells at 30°C and thrombin cleavage was effective when western blot detection with both tags were performed under reducing conditions (see supplementary data). However, western blot analysis under non-reducing conditions showed no apparent cleavage, in fact because the two PLA2R1 fragments are maintained in a covalent manner by the CTLD1 disulfide bond, despite actual cleavage of the amino acid peptide bond by thrombin. As a result, serum from different MN patients could only react with the triple domain instead of any cleaved fragments (Figure 1C), a finding which could have been

interpreted as an overlapping epitope between the different domains (8). To demonstrate that patients could recognize cleaved fragments from constructs similar to C but with the protease cleavage site inserted between FnII and CTLD1 domains, we prepared several other constructs (see supplementary data) and end up with construct G where a thrombin cleavage site was inserted within an extended linker region between FnII and CTLD1 (Figure 1A). Construct G could be only partially cleaved by thrombin, but this was sufficient to demonstrate that patients' sera had reactivity to either CysR-FnII or CTLD1 or both cleaved domains (Figure 1D).

Collectively, the above results suggest the presence of distinct epitopes in the CysR and CTLD1 domains without evidence of overlapping epitopes. To ascertain this finding and further demonstrate that CysR and CTLD1 contain independent epitopes in the context of a full-size molecule such as PLA2R1, we prepared two MRC2-PLA2R1 membrane-bound chimeras where the CysR and CTLD1 domains of PLA2R1 are respectively introduced into the MRC2 backbone in place of the corresponding domains (Figure 2A). Of note, MRC2 is the closest paralog of PLA2R1 and has the same overall structural organization, but is not reactive with MN patients, positive or not for PLA2R1 (38). We validated the expression of chimeras versus wild-type paralogs (Figure 2B) and tested the reactivity of eight different MN patients (Figure 2C). Both ELISA and WB data confirmed that patients could independently recognize CysR and/or CTLD1 domains (Figure 2C), in good accordance with their epitope profile (Figure S1). Of note, the FnII domain was investigated as a possible independent epitope-containing domain after expression as a single domain and was found to be not reactive to all MN sera tested (see below).

CTLD5, CTLD7 and CTLD8 are three C-terminal independent epitope-containing domains — To investigate whether the remaining large C-terminal region of PLA2R1 (CTLD2 to CTLD8) contains epitope-containing domains beyond the known CTLD7 domain (10), we produced various PLA2R1 recombinant proteins spanning the CTLD2-CTLD8 region (Figure S6A) validated their expression by WB (Figure S6B) and tested the reactivity of a subset of 28 MN patients by ELISA. Figure S6C shows representative data for four patients having different reactivities to CTLD7 but also other CTLDs.

We first confirmed reactivity to CTLD7 as a single domain. Ten of the 28 patients (35.7%) were positive for CTLD7. In previous studies, CTLD6-7 appeared to be more reactive than CTLD7, especially by western blot analysis (10). This would suggest assisted folding of the CTLD7 conformational epitope by CTLD6 or the presence of

additional epitopes in CTLD6. We thus verified that CTLD7 but not CTLD6 was reactive as an independent epitope-containing domain when expressed as soluble chimeras between PLA2R1 and MRC2. The C6M-C7P chimera containing the PLA2R1 CTLD7 domain was clearly reactive while the C6P-C7M chimera containing the PLA2R1 CTLD6 domain was not reactive, indicating reactivity restricted to CTLD7 (Figure S6C).

Interestingly, among the 28 patients, we found additional reactivities to CTLD2-6 for seven patients (25%) and to CTLD8 for two patients (7.1%), suggesting other epitopes (Figure S6C). To further investigate the reactivity within the CTLD2-6 region and confirm CTLD8 as an independent epitope-containing domain, we produced a series of single domains from CTLD2 to CTLD8 as well as Δ7, the longer membrane-bound form of CTLD8 (Figures 3A and 3B). Among the four above representative patients, the three reacting to CTLD2-6 also recognize CTLD5 but none of the other single domains within this region (Figure 3C). To confirm these results by another technique, we tested the reactivity of patients against the same recombinant proteins by WB. CTLD2-8, but not CTLD2-6 and CTLD3-5 was reactive (Figure 3C), despite efficient transfer of all three proteins under non-reducing conditions (Figure 3B). When expressed as single domains, CTLD3, CTLD5 and Δ7 but not CTLD2, CTLD4, CTLD6, CTLD7 and CTLD8 were efficiently transferred under non-reducing conditions but none of these domains was recognized by patients (Figures 3B and 3C). WB conditions with better transfer and lower serum dilution showed reactivity to CTLD8 but not CTLD5 (Figure S7A). Together, the above data suggest that patients' sera 1) are reactive to CTLD2-8 by WB because of reactivity to CTLD7 and/or CTLD8 but not CTLD5 (with CTLD2-8 allowing efficient transfer of CTLD7 and CTLD8) and 2) are not reactive to CTLD5 by WB when presented either as a single domain or as CTLD2-6 and CTLD3-5 larger fragments (with all three proteins transferring efficiently). This indicates that CTLD5 is reactive only in its native conformation, i.e. in ELISA but not WB. Interestingly, we found that the CTLD5 reactivity by ELISA was more sensitive to temperature and DTT than the other CTLDs or the CysR domain (see supplementary results and Figures S8 and S9). Further analysis by immunoprecipitation (Figure S7B) and dot-blot (Figure S7C) confirmed the reactivity of patients to CTLD5 and CTLD8, identifying them as two novel independent epitope-containing domains. Conversely, neither CTLD2, CTLD3, CTLD4 nor CTLD6 were recognized by patients by ELISA or immunoprecipitation (data not shown).

Prevalence, immunodominance and relationship with anti-PLA2R1 titer

Collectively, the above findings indicate that the autoimmune response against PLA2R1 is polyclonal and leads to the presence of multiple circulating anti-PLA2R1 autoantibodies targeting up to five distinct PLA2R1 domains that spread the entire extracellular region from the N-terminal to the C-terminal ends. Interestingly, all epitopes were found to be conformational (4, 9, 10), including the novel epitopes present in CTLD5 and CTLD8 (not shown). The next question we wanted to address was the prevalence and immunodominance properties of the five epitope-containing domains relative to the anti-PLA2R1 titer as measured with the commercial ELISA.

CysR and CTLD5 are the most prevalent epitope-containing domains — To determine which epitope-containing domains are most prevalent, we screened a cohort of 142 PLA2R1-positive MN patients against the 10 single PLA2R1 domains by ELISA. As expected, the five epitope-containing domains were recognized with different prevalence (Figure 4A). None of the other single domains, namely FnII, CTLD2, CTLD3, CTLD4 and CTLD6 were recognized. CysR was recognized by all patients (Figure 4A), thereby appearing as the most prevalent epitope-containing domain. Interestingly, CTLD5 was the second most prevalent domain with 65.5% reactivity followed by CTLD1 (46.5%), CTLD7 (36.6%) and CTLD8 (3.5%) (Figure 4A). Based on the combined prevalence, patients could be stratified into different epitope profiles, with CRC5 being the most abundant (Figure 4B).

Epitope positivity increases with anti-PLA2R1 titer — To analyze the relationship between epitope positivity and anti-PLA2R1 titer, we ranked patients by titer as measured with the commercial ELISA and plotted the positivity for each epitope-containing domain (Figure 5A). While all patients were positive for CysR, CTLD5-positive patients were equally distributed over the full range of anti-PLA2R1 titer. In contrast, CTLD1-positive patients were more present at high titers, even though some are present in the low tertile. CTLD7-positive patients were also more abundant in the second and third tertiles of anti-PLA2R1 titer, and the rare CTLD8-positive patients were only found at medium to high titers. Overall, anti-PLA2R1 titer increases as the number of positive epitope-containing domains also increases (Figure S10). Finally, when we ranked patients by epitope prevalence and the complexity of their epitope profile while considering positivity or not for CTLD1, we observed a relationship between the complexity of epitope profile and the increase in anti-PLA2R1 titer (Figure 5B).

CysR and CTLD1 are the immunodominant epitope-containing domains – Beyond prevalence, we aimed to determine which PLA2R1 domains contain the major immunodominant epitopes that would contribute to most of the signal measured by ELISA on the full PLA2R1 antigen. Towards this aim, we developed competition ELISA assays between full PLA2R1 (complete extracellular region) as target antigen and various PLA2R1 recombinant proteins as competitors (PLA2R1, CysR-FnII-CTLD1, CysR, CTLD1, CTLD5, CTLD7, mix of CysR and CTLD2-8, and mix of CTLD1 and CTLD2-8). In these experiments, all patients' sera were preincubated with an excess of competitor and then tested against full PLA2R1 antigen to measure the remaining anti-PLA2R1 reactivity. As expected, competition with homologous PLA2R1 was total for all patients' sera, validating our assay conditions (Figure S11). For the majority of patients, the N-terminal CysR-FnII-CTLD1 triple domain could inhibit from 65 to 100% of the PLA2R1 signal, indicating that the autoimmune response is mostly driven by autoantibodies targeting CysR and/or CTLD1 epitope-containing domains (Figure S11). Further competition with CysR or CTLD1 as single domains (Figure S11) as well as with CysR or CTLD1 mixed with CTLD2-8 (Figure S12) demonstrated that both CysR and CTLD1 are major contributors of anti-PLA2R1 reactivity. In contrast, the C-terminal CTLD5 and CTLD7 epitope-containing domains appeared as minor contributors for most patients (Figure S11). We did not perform competition assays for CTLD8 because of its low prevalence and likely minor contribution, as inferred from competition data measured with single CTLD5 and CTLD7 domains mixed or not with the CTLD2-8 region (Figure S12).

The above experiments indicate that patients' sera exhibit different patterns of circulating autoantibodies based on epitope positivity and competition profiles, with CysR and CTLD1 containing the immunodominant epitopes and driving the humoral autoimmune response for most patients. Taking into account both competition assays and epitope prevalence, we stratified patients into three groups: immunodominant CysR (iCR, where the PLA2R1 signal is mostly driven by reactivity to CysR), immunodominant CTLD1 (iC1, where the PLA2R1 signal is mostly driven by reactivity to CTLD1 over CysR or both domains) and non-immunodominant (non-iDom, where the PLA2R1 signal is spread over different domains without indication of immunodominance for a single epitope domain). This is further defined in methods with patients from each group illustrated in Figure 6A. Interestingly, patients having the same epitope profile (for instance CRC1C5C7) can belong to different immunodominant groups (Figure 6A). As shown in Figure 6B, the majority of patients

was iCR (55.1%) while a significant number was iC1 (36.0%), and a minority was non-iDom (8.8%).

Anti-PLA2R1 titer and immunodominance — As above, we ranked patients by anti-PLA2R1 titer as measured by the commercial ELISA and displayed their immunodominant profile (Figure 7A). We observed that iCR patients were more present in the first and second tertiles of anti-PLA2R1 titer while iC1 patients were mostly in the third tertile and non-iDom patients in the second tertile (Figure 7A). When combining epitope and immunodominant profiles, we could rank non-iDom, iCR and iC1 patients according to the increasing complexity of their epitope profiles, and observed that the anti-PLA2R1 titer increases as epitope positivity develops towards the C-terminal region of PLA2R1 up to CTLD7 and CTLD8, for both types of immunodominance (Figure 7B). Interestingly, the few non-iDom patients had relatively low anti-PLA2R1 titer despite having complex epitope profiles up to CTLD7, and could be best positioned between the iCR and iC1 groups (Figure 7B). This supports the view that the highest anti-PLA2R1 titers (third tertile) can only be observed when CysR and/or CTLD1 act as immunodominant epitope-containing domains and drive most of the anti-PLA2R1 signal.

Correlation between anti-PLA2R1 titers for full PLA2R1 and immunodominant epitope-containing domains — Since CysR and CTLD1 were identified as the immunodominant epitope-containing domains, we measured anti-PLA2R1 titers for these latter domains versus full PLA2R1 antigen for all patients (detection of anti-PLA2R1 IgG4), and analyzed the correlations with anti-PLA2R1 titer measured with the commercial ELISA assay (detection of anti-PLA2R1 total IgG). Highly positive correlations were observed between anti-PLA2R1 titers measured for full PLA2R1 with total IgG versus IgG4 when analyzing the cohort as a whole (r=0.89) or after stratification into iCR or iC1 patients (r=0.85 and r=0.86, respectively) (Figure 8A). Highly positive correlations were also observed between full anti-PLA2R1 titer (total IgG) and anti-CysR titers for the whole population as well as iCR and iC1 patients (r=0.82, r=0.81 and r= 0.90, respectively, Figure 8B). However, the correlation between full anti-PLA2R1 titer and anti-CTLD1 titer was higher for iC1 patients (r=0.80) than for the full cohort or iCR patients (r=0.58 and r=0.50, respectively, Figure 8C). Similar observations were made for correlations between full anti-PLA2R1 titer with detection of IgG4 antibodies and anti-CysR or anti-CTLD1 titers (Figure S13). Interestingly, non-iDom patients had anti-PLA2R1 titers for full PLA2R1, CysR and CTLD1 scattered in a relatively narrow range, with low to medium values. As observed for anti-PLA2R1 titer,

the anti-CysR and anti-CTLD1 titers increased as the number of positive epitope-containing domains increased (Figure S14). Finally, we also analyzed the anti-PLA2R1, anti-CysR and anti-CTLD1 titers for the different immunodominant groups. Overall, median titers for the iCR and non-iDom groups were similar and lower than those for iC1 patients, suggesting an additional immunodominant effect of CTLD1 over CysR immunodominance (Figure S15).

Clinical association with immunodominance, epitopes and anti-PLA2R1 titer

Having in hands the various patterns of anti-PLA2R1 circulating autoantibodies for 142 MN patients, we analyzed their association with clinical presentation and outcome.

Clinical presentation and outcome by immunodominance — We first compared the clinical characteristics at baseline and clinical outcome after first-line therapy according to the stratification of patients into the iCR, iC1 and non-iDom groups (Table 1). Patients did not present any differences in age, gender or clinical parameters, except for proteinuria which was lower in iCR than in iC1 patients (5.3 vs 6.8 g/day, p=0.02). The majority of iCR and non-iDom patients reached remission (64.0 and 75.0%, respectively) whereas the opposite was observed for iC1 patients, with the majority remaining in active disease or progressing to ESRD (59.2%) (Table 1 and Table S1). iCR and iC1 patients did not differ for treatment with immunosuppressors (IS) or conservative therapy (NIAT) (Table S1). iC1 patients had a higher anti-PLA2R1 titer at baseline (178.0 RU/mL) compared to iCR and non-iDom patients (56.5 RU/mL and 59.7 RU/mL, respectively) (Table 1 and Figure S15). Positivity towards the various epitope-containing domains and spreading to CTLD1 and/or CTLD7 domains (10, 21, 26) was more frequent in iC1 than iCR patients (Table 1).

Exploration of associations between baseline characteristics and clinical outcome — We analyzed the baseline clinical parameters and anti-PLA2R1 features that may differ between patients entering or not into remission. Patients reaching remission were younger, had a better renal function and lower proteinuria at presentation (Table 2). In agreement with previous studies, patients reaching spontaneous or IS-induced remission had a lower anti-PLA2R1 titer at baseline (16-18, 22, 23), differed in epitope positivity and were less spread on CTLD1 and/or CTLD7 epitope-containing domains (10, 21, 26). As for immunodominance, patients reaching

remission were more often iCR or non-iDom than iC1, suggesting that immunodominance may be a novel predicting factor of clinical outcome (Table 2).

Anti-PLA2R1 titer predicts clinical outcome in adjusted analysis — Several previous studies have shown that anti-PLA2R1 titer predicts clinical outcome (16-18, 21-23). Thus, before testing immunodominance as a novel predictive factor, we validated that this could be observed in our cohort when considering the same population of 135 patients for which we had all the relevant data. In unadjusted analysis, anti-PLA2R1 titer was associated with clinical outcome when comparing patients with anti-PLA2R1 titer below and above the median (64.8 RU/mL, Table 3). Patients with a titer above the median had worse clinical outcome (OR=0.237 [0.114-0.492], p=0.0001, Table 3). In adjusted analysis, patients with titers above 64.8 RU/mL had a 4-fold lower chance to reach remission, independently from baseline eGFR and proteinuria levels as well as treatment (NIAT versus IS) (Table 3, model 1). Considering the combination of anti-PLA2R1 titer and treatment, we observed that, as compared to NIAT-treated patients with an anti-PLA2R1 titer below 64.8 RU/mL, patients who received the same conservative therapy but had anti-PLA2R1 titer above 64.8 RU/mL had a 5-fold lower chance to reach remission, independently from eGFR and proteinuria (Table 3, model 2). Similarly, IS-treated patients with an anti-PLA2R1 titer below 64.8 RU/mL had a 3-fold higher chance to reach remission as compared to IS-treated patients with an anti-PLA2R1 titer above 64.8 RU/mL (OR=3.149 [1.142-8.686], p=0.03, Table S2, model 2).

Immunodominance predicts clinical outcome in a multivariable model — We then tested whether the type of immunodominance can also predict clinical outcome. Since non-iDom patients had clinical and immunological characteristics more similar to iCR than iC1 patients (Tables 1 and 2) and similar chance of remission (data not shown), we compared immunodominance between iCR/non-iDom patients combined as a single group versus iC1 patients (Table 3). In unadjusted analysis, immunodominance was associated with clinical outcome (Table 3). In adjusted analysis, iC1 patients had about 3-fold lower chance to reach remission than iCR/non-iDom patients, independently from baseline eGFR and proteinuria levels as well as treatment (NIAT vs IS) (Table 3, model 3). When combining immunodominance and treatment, iCR/non-iDom patients treated with immunosuppressors had about 3-fold more chance to reach remission than NIAT-treated patients (Table 3, model 4). Furthermore, iCR/non-iDom patients treated with immunosuppressors had 4.5-fold more chance to enter into remission than iC1

patients also treated with immunosuppressors (OR=4.467 [1.605-12.432], p=0.004, Table S2, model 4). Of note, the same observations were made when iCR and non-iDom patients were considered as separate groups, yet with lower to barely significant p-values (Tables S3).

Immunodominance may help to refine the likelihood of response to rituximab — Since rituximab was the main immunosuppressor given to patients in our cohort (Table S1), we performed a sensitivity analysis excluding patients treated with immunosuppressors other than rituximab (i.e 20 patients among 142). Results were quite similar. On one hand, among iCR/non-iDom patients, those treated with rituximab had 4.5-fold higher chance to reach remission than NIAT-treated patients (OR=4.615 [1.486-14.329], data not shown). On the other hand, among patients treated with rituximab, iCR/non-iDom patients had 6-fold higher chance to reach remission than iC1 patients, suggesting that iC1 patients are more resistant to treatment (OR=5.998 [1.771-20.311], data not shown).

Together, this suggests that iCR/non-iDom patients have a higher chance to respond to rituximab than iC1 patients, but this might be associated with their lower anti-PLA2R1 titer. Indeed, it is known that the response to rituximab decreases in patients with very high anti-PLA2R1 titer, above a certain cut-off value which is not clearly defined (21-24, 27, 32, 34, 39). Considering the above observation and the recent proposal for a serology-based approach of MN with 204 RU/mL as a possible upper cut-off value (14), we selected patients with baseline anti-PLA2R1 titers below 200 RU/mL, who may need rituximab therapy and may have a better chance of response, and we analyzed whether immunodominance might help to refine the likelihood of response to rituximab in this population (Table 4). Within this range of anti-PLA2R1 titer, 51.2% of patients were treated with rituximab while others (48.9%) were NIAT-treated., iCR/non-iDom and iC1 patients presented differences in proteinuria, but not other clinical characteristics, including anti-PLA2R1 titer (Table 4). iC1 patients had an overall worse clinical outcome, and among those treated with rituximab, a majority did not respond to treatment while more iCR patients responded and reached remission (61.5% in no remission for the iC1 group versus 89.7% in remission for the iCR/non-iDom group, p=0.001). Despite the limited number of patients, we analyzed for comparison the clinical outcome of patients with an anti-PLA2R1 titer above 200 RU/mL (Table S4). As expected from previous studies (14, 23, 24), the majority of these patients had poor clinical outcome (Table S4). In contrast to patients below 200 RU/mL, besides age, no differences in clinical characteristics, anti-PLA2R1 titer and clinical outcome were

observed between iCR/non-iDom and iC1 patients. Finally, we analyzed the clinical outcome of patients with titers below 50 RU/mL, because these patients may have a higher chance for spontaneous remission and may not need rituximab treatment (14, 16, 17) (Table S5). As expected in this subgroup, the majority of patients were NIAT-treated. Albuminemia and proteinuria appeared higher in iC1 patients, but no difference in clinical outcome was observed between iCR/non-iDom and iC1 patients (Table S5).

In summary, the combined evaluation of anti-PLA2R1 titer and immunodominance profile may help to better predict the clinical response to rituximab treatment.

DISCUSSION

The present study had two major objectives: 1) To provide a comprehensive analysis of the anti-PLA2R1 humoral response, focusing on the description of conformational PLA2R1 epitopes recognized by circulating autoantibodies from a large retrospective cohort of 142 patients with PLA2R1-associated MN; and 2) To evaluate how the specific characteristics of individual anti-PLA2R1 response observed among patients may be translated to the clinics to predict clinical outcome and response to therapy.

Comprehensive analysis of the anti-PLA2R1 response: epitopes, prevalence, immunodominance and relationship to anti-PLA2R1 titer

In summary, our series of biochemical experiments provide new information about the number of PLA2R1 epitope-containing domains, their prevalence and immunodominance (Figure 9). Specifically, we now show that in PLA2R1-positive MN patients: i) Circulating anti-PLA2R1 autoantibodies can recognize up to 5 epitope-containing domains, including CysR, CTLD1, CTLD5, CTLD7 and CTLD8, indicating that 50% of the PLA2R1 extracellular region is targeted by autoantibodies; ii) The epitope prevalence decreases from the N-terminal to the C-terminal epitope-containing domains; iii) The N-terminal CysR and CTLD1 domains harbor the major immunodominant epitopes which contribute to most of the anti-PLA2R1 titer measured by the commercial ELISA; and iv) The C-terminal domains CTLD5, CTLD7 and CTLD8 harbor non-immunodominant epitopes which collectively have a minor contribution to the anti-PLA2R1 titer measured by the commercial ELISA. Together, the overall humoral autoimmune response appears to be mostly driven by the N-terminal CysR and/or CTLD1 domains functioning as two key immunodominant epitope-containing domains while the distal spreading to the C-terminal other domains contributes little to the full titer.

Our work first clearly shows that the five PLA2R1 domains containing independent epitopes are not equivalent in terms of immunological reactivity. Among them, the N-terminal CysR domain plays a central role and is undoubtedly the major immunodominant epitope-containing domain, based on both its highest prevalence (100%) and its highest contribution to the anti-PLA2R1 signal as measured by competition ELISA (up to 100%). This is in line with previous findings from Fresquet et al. (9). Interestingly, while all patients were positive for CysR, not all of them were

iCR, and can be iC1 or non-iDom. Of note, iCR patients were quite uniformly distributed among the three tertiles of anti-PLA2R1 titer.

We next clearly identified the N-terminal CTLD1 domain as a second immunodominant epitope-containing domain with specific features. Because previous studies led to controversial conclusions about independent versus overlapping epitopes within the N-terminal CysR-FnII-CTLD1 region (8, 10), we re-investigated the site-directed mutagenesis approach coupled to proteolysis initially developed by Kao and colleagues (8) and demonstrated that CysR and CTLD1 domains contain in fact independent epitopes, while the FnII domain does not harbor any. We confirmed these results in the context of a full-size molecule by preparing new chimeras between PLA2R1 and MRC2. Our findings are also consistent with cryo-EM studies showing that CysR and CTLD1 are N-terminal neighboring domains but without physical interaction, arguing for the absence of overlapping epitopes between these domains (9, 40). In contrast to CysR, we observed that the prevalence for CTLD1 positivity was only 46.5%, with positivity more often observed in the second and third tertiles of anti-PLA2R1 titer. Also in contrast to CysR, we observed that iC1 patients were more often present in the high tertile with an opposite trend for iCR. Together, this suggests a switch from iCR to iC1 among patients as the anti-PLA2R1 titer increases.

We next identified CTLD5 as a new independent and predominant but not immunodominant epitope-containing domain, with features clearly different from CTLD1 and CysR. First, CTLD5 was the second most prevalent epitope-containing domain with 65.5% positivity, irrespective of positivity for CTLD1 or other domains. Accordingly, patients with a CRC5 profile were most prevalent. Second, like CysR but unlike CTLD1, CTLD5 positivity was spread all over the three anti-PLA2R1 tertiles. Third, in contrast to both CysR and CTLD1, CTLD5 had a very minor contribution to the anti-PLA2R1 titer as measured by competition ELISA. Finally, CTLD5 differs from other epitope-containing domains by its particular reactivity to patients' autoantibodies. CTLD5 was detectable by techniques where the antigenic domain is presented in its native conformation such as ELISA, immunoprecipitation and dot blot but not WB. Of note, CTLD5 reactivity was very sensitive to temperature and reducing agents.

We previously identified CTLD7 as an epitope-containing domain (10). Based on expression of CTLD7 as a single domain or as a chimera with the CTLD6 domain of MRC2, we confirmed that this C-terminal domain functions as a fourth independent epitope-containing domain. Its prevalence and pattern of positivity was comparable to CTLD1, with positivity associated to high titer. However, in contrast to CTLD1, the

contribution of CTLD7 to the anti-PLA2R1 titer was modest, and positivity to CTLD7 was independent of positivity to CTLD1 or immunodominance for iCR versus iC1.

Last, we identified CTLD8 as the most C-terminal but minor epitope-containing domain. Like CTLD1 and CTLD7, positivity for CTLD8 was associated with high titer, and CTLD8 likely contributes very little to anti-PLA2R1 titer.

Together, our data show that the anti-PLA2R1 humoral response observed among patients is in most cases polyclonal but variable, with the presence of multiple autoantibodies differing in prevalence and immunodominance. Collectively, the observed humoral autoimmune response may be reminiscent of a mechanism of epitope spreading that may have started before overt disease, i.e. during the smoldering phase of the disease, with progression over months or even years from the early onset of the autoimmune response to the clinical signs of the disease; and that may still progress during overt disease, with fluctuation of the autoimmune humoral response during phases of relapse and remission. In this mechanism of epitope spreading, it is tempting to speculate that the autoimmune response would have been initiated on the N-terminal CysR domain and would have matured by epitope spreading up to the C-terminal CTLD8 domain, with CysR and CTLD1 becoming immunodominant domains and the CTLD5, CTLD7 and CTLD8 domains harboring only non-immunodominant epitopes. As expected from this scenario and in line with data from patients' sera, the anti-PLA2R1 titer increases as the number of positive epitopes increases, and the highest titers can only be observed when either CysR or CTLD1 or both play their immunodominant role and maximally drive the humoral autoimmune response (as shown in figures 5 and 7). The non-iDom group of patients would correspond to the rare cases where neither CysR nor CTLD1 are immunodominant, explaining the relatively lower anti-PLA2R1 titers measured in those patients. This view is in agreement with previous data showing that the anti-PLA2R1 titer is mainly due to autoantibodies targeting the CysR-CTLD1 (8) or the CysR-CTLD3 regions (9). Finally, although the rise of the autoimmune response seems to occur as a continuum of sequential immunoreactivities from CysR to other epitope-containing domains with CysR acting as the major immunodominant domain our data suggest a switch of immunodominance from CysR to CTLD1 once this latter becomes positive, associated to a maximal autoimmune reaction for epitope spreading and titer, and associated with worsening of disease activity (see below). Whether the different single nucleotide polymorphisms present in PLA2R1, especially those within the CysR and CTLD1 domains, play a role in the initiation and/or progression of the autoimmune response towards the different

paths of immunodominance with both PLA2R1 intradomain and interdomain epitope spreading remain to be determined (41, 42).

Importantly, all patients had anti-CysR autoantibodies but only about half of them (46.5%) had anti-CTLD1 autoantibodies. Furthermore, 55.1% of all patients were iCR and 36% were iC1. This implies an "imbalance" between the two groups and may be important at the pathophysiological level. For the major group of iCR patients, the autoimmune response is mostly driven by anti-CysR autoantibodies acting as a "single class" of autoantibodies and targeting PLA2R1 at a single binding domain that is CysR. In contrast, for iC1 patients, the autoimmune response is in fact driven by different ratios of anti-CysR and anti-CTLD1 autoantibodies, acting as a "dual class" of autoantibodies and targeting PLA2R1 at two different binding domains, which might lead to larger immune deposits, more podocyte injury and increased pathogenicity. Interestingly, this hypothesis fits with pioneering studies from i) Allegri and colleagues in the Heymann nephritis model of MN in rats showing that polyclonal but not monoclonal antibodies against megalin produce larger electron-dense immune deposits (43) and ii) Mentzel and colleagues showing that injection of two monoclonal antibodies targeting different domains of aminopeptidase A has a synergistic effect on pathogenicity as compared to injection with a single antibody in a mouse model of glomerulonephritis (44). Finally, our overall scenario is simply in agreement with the general mechanism of epitope spreading that occurs by nature for many immune or autoimmune responses (45, 46). For instance, a mechanism of epitope spreading associated to worsening of the disease has been clearly documented in previous studies for megalin in the Heymann nephritis model (47) and for desmogleins in *Pemphigus vulgaris* (48, 49). However, our model remains speculative and should be confirmed by additional experimental evidence, including not only the development of *bona fide in vivo* animal models, but also further analysis in MN patients, for instance by testing patients' sera obtained during the smoldering phase of the disease, as recently documented by Joshi and colleagues (50). We also need cohorts of patients with follow-up sera to longitudinally analyze the fluctuations or "waves" of the humoral autoimmune response for both epitope and immunodominance profiles during overt disease.

Clinical relevance of anti-PLA2R1 autoantibodies: from titer to immunodominance

As stated above, multiple studies have demonstrated the clinical value of measuring anti-PLA2R1 titer to better predict clinical outcome, with low titer associated with a higher chance to reach remission, either spontaneous or after immunosuppressive treatment, and high titer associated with an increased risk of progression to severe disease and ESRD, as well as resistance to treatment (16-20, 22-24, 27, 34). Our previous studies with epitope profiling of patients towards a single (CysR) or multiple (CysR and CTLD1 and/or CTLD7) epitope-containing domains (reminiscent of a mechanism of epitope spreading, as explained above) may also help to better predict clinical outcome and guide efficient therapy (10, 21, 26). In this study, we established a retrospective but well-characterized cohort of patients with PLA2R1-associated MN and tested side-by-side whether anti-PLA2R1 titer, epitope profiling and immunodominance can be used as predictors of clinical outcome. Search for predictors of outcome showed that anti-PLA2R1 titer, epitope profiling such as spreading to CTLD1 and/or CTLD7 and immunodominance are all associated to clinical outcome (Table 2). We next validated that anti-PLA2R1 titer can predict clinical outcome in two multivariable models adjusted for clinical characteristics and when testing the interaction with treatment. Similar multivariable models considering immunodominance as two groups (iCR/non-iDom and iC1) or three separate groups also showed that immunodominance can predict clinical outcome. Moreover, in a multivariable model testing the specific interaction between immunodominance and rituximab treatment, we observed that treatment was less effective in iC1 than iCR/non-iDom patients.

Since i) the above observation could be related to the higher anti-PLA2R1 titer observed in iC1 patients and ii) patients become more resistant to rituximab therapy when they have high anti-PLA2R1 titer, for instance above 200 RU/mL as observed in recent studies (23, 24), we compared the clinical outcome of patients treated with rituximab and with an anti-PLA2R1 titer below or above 200 RU/mL according to their immunodominant profile. Below 200 RU/mL, we observed that clinical remission in iCR/non-iDom patients was higher than in iC1 patients, either when considering overall outcome or the one after rituximab treatment. In contrast, when analyzing patients with titers above 200 RU/mL, clinical outcome was not different between the two immunodominant groups. This suggests that under a certain cut-off for anti-PLA2R1 titer, immunodominance may be clinically useful to guide therapy and identify patients as responders versus non-responders to rituximab. For patients with very high anti-

PLA2R1 titer, rituximab treatment might be less effective and independent of the type of immunodominance, requiring higher doses of rituximab, or alternative or combined therapies (14, 26, 32, 34).

Our above clinical findings have limitations. First, our data are based on a retrospective cohort with low numbers of patients when divided in groups and subgroups, and the impact of immunodominance profiling combined with anti-PLA2R1 titer should be validated in larger prospective cohorts or randomized clinical trials. Furthermore, patients were treated with different doses of rituximab, with about two thirds of them treated with the original protocol (23, 24) and the other third with higher doses (26). Finally, it remains to be determined whether immunodominance (and epitope spreading) might be of additive value to anti-PLA2R1 titer to predict clinical outcome for immunosuppressive treatments such as cyclophosphamide that appears to induce a faster disappearance of anti-PLA2R1 antibodies than rituximab (32).

In summary, our findings not only contribute to a better understanding of the different phases in the development of the PLA2R1 autoimmune response but also highlight the type of immunodominance as a potential new biomarker for PLA2R1-associated MN. We have shown that circulating anti-PLA2R1 autoantibodies can target up to five distinct PLA2R1 domains but those targeting CysR and CTLD1 constitute the main driving force of the autoimmune response and are also those mainly measured by the commercial anti-PLA2R1 ELISA, irrespective of immunodominance and further spreading to distal epitope domains. Consequently, we highlight the notion of two main "classes" of immunodominant autoantibodies targeting either CysR or CTLD1 or both, and propose that these two classes of autoantibodies may play synergistic roles in the pathogenesis of MN. Whether injection of the two classes of immunodominant antibodies produce more pathogenicity than a single class should be performed in an appropriate yet currently not available animal model of PLA2R1-associated MN. Whether the different types of immunodominance and the possible switch from iCR to iC1 (immunodominant spreading?) are associated with genetics or environmental factors and/or different etiologies remains to be determined. Future investigations should also be conducted to identify the genuine epitopes present in each PLA2R1 epitope-containing domains and analyze the subclasses of anti-PLA2R1 IgGs with a possible IgG subclass switch during follow-up. In this context, our initial definition of "spreaders" and "non-spreaders" (21) should be redefined once we will have a more complete mechanism of epitope spreading targeting PLA2R1, but our data already argue that the autoimmune response to PLA2R1 is not gambling, as previously stated (51).

Finally, even though additional studies are required to validate our clinical conclusions, we believe that immunodominance can be a new biomarker *per se* and also when combined with anti-PLA2R1 titer. In particular, stratifying patients according to immunodominance can be useful to guide and optimize therapy with different regimens of rituximab, and for a better likelihood of response to treatment.

AUTHORS CONTRIBUTION

G.L. and P.R. designed the study; J.J., V.B., G.D., C.Z., C.P., F.B and A.P.P. carried out experiments; J.J., V.B., G.D., A.R. and G.L. analyzed the data and performed statistical analyses; J.J., V.B. and G.L. made the figures and tables; J.J., V.B., P.R. and G.L. drafted and revised the paper; H.D., P.R., K.D., N.J.C. and C.M. had a major role in the inclusion of patients; all authors revised and approved the final version of the manuscript.

ACKNOWLEDGMENT AND FINANCIAL DISCLOSURE

We are grateful to the physicians who participated to the inclusion of patients in this study: Barbara Seitz-Polski and Vincent Esnault (CHU de Nice, France); Stéphane Burtey, Laurent Samson, Laurent Daniel and Sophie Jego-Desplat (CHU la Conception, Marseille, France); Thomas Crépin, Nadège Devillard and Cécile Courivaud (CHU de Besançon, France). We would like to thank Eva Compérat and all staff members of the Tenon Hospital Biological Resource Center (BRC cancer HUEP- Paris) for their help in centralizing and managing biological data collection and participants of the GEMRITUX study. We thank Dr W. Schlumberger and colleagues (Euroimmun, Lübeck) for providing purified recombinant human PLA2R1.

Supported by grants to GL from CNRS, the Fondation Maladies Rares (LAM-RD_20170304), the National Research Agency (grants MNaims (ANR-17- CE17-0012-01, also to PR) and “Investments for the Future” Laboratory of Excellence SIGNALIFE, a network for innovation on signal transduction pathways in life sciences (ANR-11-LABX-0028-01) with allocated PhD fellowships for CZ and JJ), and the Fondation de la Recherche Médicale (DEQ20180339193 to GL, FDT201805005509 to JJ and SPF20150934219 to VB). Supported by grants to GL from the Centre Hospitalier Universitaire de Nice and the Direction Générale de l’Offre de Soins of the French Ministry of Health (PLA2R1 autoantibodies in Membranous Nephropathy in Kidney Transplantation Programme, PRAM-KT PHRC2011-A01302-39, NCT01897961). Supported by grants from the European Research Council ERC-2012 ADG_20120314 no. 322947 and the Seventh Framework Programme of the European Community contract no. 2012-305608 (European Consortium for High-Throughput Research in Rare Kidney Diseases) to PR.

DISCLOSURES

Some coauthors are coinventors on the patents “Diagnostics for membranous nephropathy” (GL), “Methods and kits for monitoring membranous nephropathy” (GL), and “Prognosis and monitoring of membranous nephropathy based on the analysis of PLA2R1 epitope profile and spreading” (GD and GL).

REFERENCES

1. Glassock RJ. Diagnosis and natural course of membranous nephropathy. *Semin Nephrol.* 2003;23(4):324-32.
2. Ponticelli C, and Glassock RJ. Treatment of membranous nephropathy in patients with renal insufficiency: what regimen to choose? *J Nephrol.* 2013;26(3):427-9.
3. Ronco P, and Debiec H. Pathophysiological advances in membranous nephropathy: time for a shift in patient's care. *Lancet.* 2015;385(9981):1983-92.
4. Beck LH, Jr., Bonegio RG, Lambeau G, Beck DM, Powell DW, Cummins TD, Klein JB, and Salant DJ. M-type phospholipase A2 receptor as target antigen in idiopathic membranous nephropathy. *N Engl J Med.* 2009;361(1):11-21.
5. Lambeau G, Ancian P, Barhanin J, and Lazdunski M. Cloning and expression of a membrane receptor for secretory phospholipases A2. *J Biol Chem.* 1994;269(3):1575-8.
6. Ancian P, Lambeau G, Mattéi MG, and Lazdunski M. The human 180-kDa receptor for secretory phospholipases A2. Molecular cloning, identification of a secreted soluble form, expression, and chromosomal localization. *J Biol Chem.* 1995;270(15):8963-70.
7. Behnert A, Fritzler MJ, Teng B, Zhang M, Bollig F, Haller H, Skoberne A, Mahler M, and Schiffer M. An anti-phospholipase A2 receptor quantitative immunoassay and epitope analysis in membranous nephropathy reveals different antigenic domains of the receptor. *PloS one.* 2013;8(4):e61669.
8. Kao L, Lam V, Waldman M, Glassock RJ, and Zhu Q. Identification of the immunodominant epitope region in phospholipase A2 receptor-mediating autoantibody binding in idiopathic membranous nephropathy. *J Am Soc Nephrol.* 2015;26(2):291-301.
9. Fresquet M, Jowitt TA, Gummadova J, Collins R, O'Cualain R, McKenzie EA, Lennon R, and Brenchley PE. Identification of a major epitope recognized by PLA2R autoantibodies in primary membranous nephropathy. *J Am Soc Nephrol.* 2015;26(2):302-13.
10. Seitz-Polski B, Dolla G, Payre C, Girard CA, Polidori J, Zorzi K, Birgy-Barelli E, Jullien P, Courivaud C, Krummel T, et al. Epitope Spreading of Autoantibody Response to PLA2R Associates with Poor Prognosis in Membranous Nephropathy. *J Am Soc Nephrol.* 2016;27(5):1517-33.
11. Hoxha E, Harendza S, Zahner G, Panzer U, Steinmetz O, Fechner K, Helmchen U, and Stahl RA. An immunofluorescence test for phospholipase-A2-receptor antibodies and its clinical usefulness in patients with membranous glomerulonephritis. *Nephrol Dial Transplant.* 2011;26(8):2526-32.
12. Dahnrich C, Komorowski L, Probst C, Seitz-Polski B, Esnault V, Wetzels JF, Hofstra JM, Hoxha E, Stahl RA, Lambeau G, et al. Development of a standardized ELISA for the determination of autoantibodies against human M-type phospholipase A2 receptor in primary membranous nephropathy. *Clin Chim Acta.* 2013;421C(213-8.
13. Glassock RJ. Antiphospholipase A2 receptor autoantibody guided diagnosis and treatment of membranous nephropathy: a new personalized medical approach. *Clin J Am Soc Nephrol.* 2014;9(8):1341-3.
14. De Vriese AS, Glassock RJ, Nath KA, Sethi S, and Fervenza FC. A Proposal for a Serology-Based Approach to Membranous Nephropathy. *J Am Soc Nephrol.* 2017;28(2):421-30.

15. Bobart SA, De Vriese AS, Pawar AS, Zand L, Sethi S, Giesen C, Lieske JC, and Fervenza FC. Noninvasive diagnosis of primary membranous nephropathy using phospholipase A2 receptor antibodies. *Kidney Int.* 2019;95(2):429-38.
16. Hofstra JM, Debiec H, Short CD, Pelle T, Kleta R, Mathieson PW, Ronco P, Brenchley PE, and Wetzels JF. Antiphospholipase A2 receptor antibody titer and subclass in idiopathic membranous nephropathy. *J Am Soc Nephrol.* 2012;23(10):1735-43.
17. Kanigicherla D, Gummadova J, McKenzie EA, Roberts SA, Harris S, Nikam M, Poulton K, McWilliam L, Short CD, Venning M, et al. Anti-PLA2R antibodies measured by ELISA predict long-term outcome in a prevalent population of patients with idiopathic membranous nephropathy. *Kidney Int.* 2013;83(5):940-8.
18. Hoxha E, Thiele I, Zahner G, Panzer U, Harendza S, and Stahl RA. Phospholipase A2 receptor autoantibodies and clinical outcome in patients with primary membranous nephropathy. *J Am Soc Nephrol.* 2014;25(6):1357-66.
19. Timmermans SA, Abdul Hamid MA, Cohen Tervaert JW, Damoiseaux JG, van Paassen P, and Limburg Renal R. Anti-PLA2R Antibodies as a Prognostic Factor in PLA2R-Related Membranous Nephropathy. *Am J Nephrol.* 2015;42(1):70-7.
20. Rodas LM, Matas-Garcia A, Barros X, Blasco M, Vinas O, Llobell A, Martin N, and Quintana LF. Antiphospholipase 2 receptor antibody levels to predict complete spontaneous remission in primary membranous nephropathy. *Clinical kidney journal.* 2019;12(1):36-41.
21. Seitz-Polski B, Debiec H, Rousseau A, Dahan K, Zaghrini C, Payre C, Esnault VLM, Lambeau G, and Ronco P. Phospholipase A2 Receptor 1 Epitope Spreading at Baseline Predicts Reduced Likelihood of Remission of Membranous Nephropathy. *J Am Soc Nephrol.* 2018;29(2):401-8.
22. Beck LH, Jr., Fervenza FC, Beck DM, Bonegio RG, Malik FA, Erickson SB, Cosio FG, Cattran DC, and Salant DJ. Rituximab-induced depletion of anti-PLA2R autoantibodies predicts response in membranous nephropathy. *J Am Soc Nephrol.* 2011;22(8):1543-50.
23. Ruggenenti P, Debiec H, Ruggiero B, Chianca A, Pelle T, Gaspari F, Suardi F, Gagliardini E, Orisio S, Benigni A, et al. Anti-Phospholipase A2 Receptor Antibody Titer Predicts Post-Rituximab Outcome of Membranous Nephropathy. *J Am Soc Nephrol.* 2015;26(10):2545-58.
24. Dahan K, Debiec H, Plaisier E, Cachanado M, Rousseau A, Wakselman L, Michel PA, Mihout F, Dussol B, Matignon M, et al. Rituximab for Severe Membranous Nephropathy: A 6-Month Trial with Extended Follow-Up. *J Am Soc Nephrol.* 2017;28(1):348-58.
25. Ruggenenti P, Fervenza FC, and Remuzzi G. Treatment of membranous nephropathy: time for a paradigm shift. *Nat Rev Nephrol.* 2017;13(9):563-79.
26. Seitz-Polski B, Dahan K, Debiec H, Rousseau A, Andreani M, Zaghrini C, Ticchioni M, Rosenthal A, Benzaken S, Bernard G, et al. High-Dose Rituximab and Early Remission in PLA2R1-Related Membranous Nephropathy. *Clin J Am Soc Nephrol.* 2019;14(8):1173-82.
27. Fervenza FC, Appel GB, Barbour SJ, Rovin BH, Lafayette RA, Aslam N, Jefferson JA, Gipson PE, Rizk DV, Sedor JR, et al. Rituximab or Cyclosporine in the Treatment of Membranous Nephropathy. *N Engl J Med.* 2019;381(1):36-46.
28. Hoxha E, Zahner G, Reinhard L, and Stahl RAK. PLA2R1 Epitope Recognition Patterns and Clinical Outcome in Patients with Membranous Nephropathy. . *J Am Soc Nephrol.* 2018;29(823.

29. Salant DJ. Unmet challenges in membranous nephropathy. *Current opinion in nephrology and hypertension.* 2019;28(1):70-6.
30. Salant DJ. Does Epitope Spreading Influence Responsiveness to Rituximab in PLA2R-Associated Membranous Nephropathy? *Clin J Am Soc Nephrol.* 2019;14(8):1122-4.
31. van den Brand J, Ruggenenti P, Chianca A, Hofstra JM, Perna A, Ruggiero B, Wetzels JFM, and Remuzzi G. Safety of Rituximab Compared with Steroids and Cyclophosphamide for Idiopathic Membranous Nephropathy. *J Am Soc Nephrol.* 2017;28(9):2729-37.
32. van de Logt AE, Dahan K, Rousseau A, van der Molen R, Debiec H, Ronco P, and Wetzels J. Immunological remission in PLA2R-antibody-associated membranous nephropathy: cyclophosphamide versus rituximab. *Kidney Int.* 2018;93(4):1016-7.
33. Stahl RA, Reinhard L, and Hoxha E. Characterization of autoantibodies in primary membranous nephropathy and their clinical significance. *Expert review of clinical immunology.* 2019;15(2):165-75.
34. Floege J, Barbour SJ, Cattran DC, Hogan JJ, Nachman PH, Tang SCW, Wetzels JFM, Cheung M, Wheeler DC, Winkelmayer WC, et al. Management and treatment of glomerular diseases (part 1): conclusions from a Kidney Disease: Improving Global Outcomes (KDIGO) Controversies Conference. *Kidney Int.* 2019;95(2):268-80.
35. Seitz-Polski B, Dolla G, Payre C, Tomas NM, Lochouarn M, Jeammet L, Mariat C, Krummel T, Burtey S, Courivaud C, et al. Cross-reactivity of anti-PLA2R1 autoantibodies to rabbit and mouse PLA2R1 antigens and development of two novel ELISAs with different diagnostic performances in idiopathic membranous nephropathy. *Biochimie.* 2015;118(104-15.
36. Jullien P, Seitz Polski B, Maillard N, Thibaudin D, Laurent B, Ollier E, Alamartine E, Lambeau G, and Mariat C. Anti-phospholipase A2 receptor antibody levels at diagnosis predicts spontaneous remission of idiopathic membranous nephropathy. *Clinical kidney journal.* 2017;10(2):209-14.
37. Pourcine F, Dahan K, Mihout F, Cachanado M, Brocheriou I, Debiec H, and Ronco P. Prognostic value of PLA2R autoimmunity detected by measurement of anti-PLA2R antibodies combined with detection of PLA2R antigen in membranous nephropathy: A single-centre study over 14 years. *PloS one.* 2017;12(3):e0173201.
38. Tomas NM, Beck LH, Jr., Meyer-Schwesinger C, Seitz-Polski B, Ma H, Zahner G, Dolla G, Hoxha E, Helmchen U, Dabert-Gay AS, et al. Thrombospondin type-1 domain-containing 7A in idiopathic membranous nephropathy. *N Engl J Med.* 2014;371(24):2277-87.
39. Alfaadhel T, and Cattran D. Management of Membranous Nephropathy in Western Countries. *Kidney diseases.* 2015;1(2):126-37.
40. Dong Y, Cao L, Tang H, Shi X, and He Y. Structure of Human M-type Phospholipase A2 Receptor Revealed by Cryo-Electron Microscopy. *J Mol Biol.* 2017;429(24):3825-35.
41. Coenen MJ, Hofstra JM, Debiec H, Stanescu HC, Medlar AJ, Stengel B, Boland-Auge A, Groothuismink JM, Bockenhauer D, Powis SH, et al. Phospholipase A2 receptor (PLA2R1) sequence variants in idiopathic membranous nephropathy. *J Am Soc Nephrol.* 2013;24(4):677-83.
42. Stanescu HC, Arcos-Burgos M, Medlar A, Bockenhauer D, Kottgen A, Dragomirescu L, Voinescu C, Patel N, Pearce K, Hubank M, et al. Risk HLA-DQA1 and PLA2R1 alleles in idiopathic membranous nephropathy. *N Engl J Med.* 2011;364(7):616-26.

43. Allegri L, Brianti E, Chatelet F, Manara GC, Ronco P, and Verroust P. Polyvalent antigen-antibody interactions are required for the formation of electron-dense immune deposits in passive Heymann's nephritis. *Am J Pathol.* 1986;125(1):1-6.
44. Mentzel S, van Son JP, Dijkman HB, Wetzels JF, and Assmann KJ. Induction of albuminuria in mice: synergistic effect of two monoclonal antibodies directed to different domains of aminopeptidase A. *Kidney Int.* 1999;55(4):1335-47.
45. Vanderlugt CL, and Miller SD. Epitope spreading in immune-mediated diseases: implications for immunotherapy. *Nat Rev Immunol.* 2002;2(2):85-95.
46. Cornaby C, Gibbons L, Mayhew V, Sloan CS, Welling A, and Poole BD. B cell epitope spreading: mechanisms and contribution to autoimmune diseases. *Immunol Lett.* 2015;163(1):56-68.
47. Shah P, Tramontano A, and Makker SP. Intramolecular epitope spreading in Heymann nephritis. *J Am Soc Nephrol.* 2007;18(12):3060-6.
48. Grando SA. Pemphigus autoimmunity: hypotheses and realities. *Autoimmunity.* 2012;45(1):7-35.
49. Didona D, and Di Zenzo G. Humoral Epitope Spreading in Autoimmune Bullous Diseases. *Front Immunol.* 2018;9(779.
50. Joshi MR, Burbelo PD, Waldman MA, Gordon SM, Thurlow JS, and Olson SW. Pre-Diagnostic Evaluation of Anti-Phospholipase A2 Receptor Antibodies in Primary Membranous Nephropathy. *J Am Soc Nephrol.* 2018;29(Abstract ASN Kidney Week 2018):823.
51. Debiec H, and Ronco P. Immune Response against Autoantigen PLA2R Is not Gambling: Implications for Pathophysiology, Prognosis, and Therapy. *J Am Soc Nephrol.* 2016;27(5):1275-7.

LEGEND TO FIGURES

Figure 1 – Sera from MN patients have independent reactivity to CysR and CTLD1 after cleavage of the N-terminal CysR-FnII-CTLD1 triple domain by thrombin. (A) Schematic diagram of soluble constructs for the CysR-FnII-CTLD1 triple domain with a thrombin (Thr) cleavage site inserted at different positions: between CysR and FnII (construct B), within the first disulfide bridge in CTLD1 (construct C) or in the extended linker region between FnII and CTLD1 (construct G). All constructs were N-terminally 6xHis- and 3xFlag-tagged and C-terminally HA-tagged. The expected mass is calculated without the contribution of glycosylation. Expression level in HEK293 cells and cleavage efficiency is indicated. **(B)** Western blots showing the reactivity of seven MN patients to construct B before and after cleavage with thrombin under non-reducing conditions. Data demonstrate that CysR and CTLD1 can be independently detected after cleavage. **(C)** Western blots showing the reactivity of eight MN patients to construct C before and after cleavage with thrombin under non-reducing conditions. Data suggest the absence of cleavage by thrombin and show patients' sera reactivity only to the triple domain before and after cleavage. However, cleavage was done (refer to figure S3) and fragments containing either CysR or CTLD1 domains were maintained by the disulfide bridge within CTLD1. **(D)** Western blots showing the reactivity of five MN patients to construct G before and after cleavage with thrombin under non-reducing conditions. Data show that CysR and CTLD1 can be independently detected after thrombin cleavage (even though the cleavage is only partial).

Figure 2 – Sera from MN patients have independent reactivity to CysR and CTLD1 when expressed as chimeras between PLA2R1 and MRC2. (A) Schematic diagram of the two wild-type membrane-bound proteins (PLA2R1 and MRC2) and chimeras (M2/P-CysR and M2/P-C1) where the CysR and CTLD1 domains of PLA2R1 are respectively introduced into the structural backbone of MRC2. All proteins are N-terminally 6xHis- and 3xFlag-tagged and C-terminally HA-tagged, and were expressed in HEK293 cells. The expected mass is calculated without the contribution of glycosylation. (**B**) Expression of the four membrane-bound proteins was validated by western blot under both reducing and non-reducing conditions using anti-HA antibody (1:5,000). **(C)** Western blots under non-reducing conditions and ELISA with eight MN patients show independent reactivity against CysR and CTLD1 introduced as single domain in the M2/P-CysR and M2/P-C1 chimeras.

Figure 3 – CTLD5 and CTLD8 are two novel independent epitope-containing domains recognized by PLA2R1-positive MN patients. **(A)** Schematic diagram of C-terminally HA-tagged soluble and membrane-bound recombinant proteins spanning the CTLD2–CTLD8 region of PLA2R1. All proteins were expressed in HEK293 cells. The expected mass is calculated without the contribution of glycosylation. **(B)** Western blot under reducing conditions with anti-HA antibody (1:5,000) validate the expression of all PLA2R1 recombinant proteins. However, the single domains C2, C4, C6, C7 and C8 were not detected by anti-HA antibody (1:5,000) under non-reducing conditions due to poor transfer of the small likely hydrophilic proteins. **(C)** ELISA with four representative MN patients (1:100) shows the recognition of CTLD5 and CTLD8 as single domains. In contrast, the same patients do not recognize CTLD5 (C5) and CTLD8 single domains (C8, Δ7) by western blot because of denaturation of the epitope(s) for C5 (see also Figure S8B) and weak reactivity for C8 (see also Figure S7A).

Figure 4 – Prevalence and epitope profile in a cohort of 142 PLA2R1-positive MN patients. **(A)** Screening of 142 PLA2R1-positive patients by ELISA (IgG4 detection) with the 10 individual domains of PLA2R1 shows reactivity against 5 domains with decreasing prevalence: CysR, CTLD5, CTLD1, CTLD7 and CTLD8. None of the five remaining domains were recognized. **(B)** Patients' reactivity to single domains can be combined to provide different epitope profiles among which CRC5, CRC1C5C7, CRC1, CR, CRC5C7 and CRC1C5 are the most prevalent.

Figure 5 – Relationship between epitope positivity and anti-PLA2R1 titer. **(A)** Patients (n=142) were ranked by increasing anti-PLA2R1 titer (commercial ELISA, total IgG) and positivity to the different domains was superimposed to display the different patterns. All patients were positive for CysR. In the first tertile, 29.8% of patients were CTLD1, 53.2% CTLD5, 8.5% CTLD7 and 0% CTLD8. In the second tertile, 35.4% of patients were CTLD1, 75.0% CTLD5, 35.4% CTLD7 and 4.2% CTLD8. In the third tertile, 74.5% of patients were CTLD1, 68.1% CTLD5, 66.0% CTLD7 and 6.4% CTLD8. **(B)** Patients (n=142) were ranked according to the complexity of their epitope profile from the CysR domain to the C-terminal end of PLA2R1 and positivity or not for CTLD1. The increased complexity of epitope profiles appears to be associated with anti-PLA2R1 titer.

Figure 6 – CysR and CTLD1 are two immunodominant PLA2R1 domains and define different groups of PLA2R1-positive MN patients. (A) Representative competition assays by ELISA (IgG4 detection) for three patients allowing classification in three distinct groups: iCR, iC1 and non-iDom (see methods for a complete definition). Note that the chosen representative patients have the same epitope profile CRC1C5C7 but different immunodominant profiles. **(B)** Stratification of patients (n=136) according to their immunodominant profile shows that the majority of them (n=75, 55.1%) have CysR as immunodominant PLA2R1 domain (iCR) while a significant number (n=49, 36.0%) have CTLD1 as immunodominant domain (iC1). A small group of patients (n=12, 8.8%) are classified as non-iDom. The immunodominant profile could not be assigned for 6 patients from the original cohort of 142 patients because of lack of serum.

Figure 7 – Relationship between immunodominance and anti-PLA2R1 titer. (A) Patients (n=136) were ranked by increasing anti-PLA2R1 titer (commercial ELISA, total IgG detection) and their immunodominance was displayed. In the first tertile 66.7% of patients were iCR, 24.4% iC1 and 8.9% non-iDom. In the second tertile, 60.9% of patients were iCR, 21.7% iC1 and 17.4% non-iDom. In the third tertile, 37.8% of patients were iCR, 62.2% were iC1 and 0% non-iDom. **(B)** Patients (n=136) were ranked according to their immunodominant profile (iCR, non-iDom or iC1) combined with the complexity of their epitope profile from the CysR domain to the C-terminal region of PLA2R1. CR and C1 are indicated in bold when they become immunodominant. The increased complexity of epitope profiles appears to be associated with anti-PLA2R1 titer for both iCR and iC1 groups. Note that patients from the non-iDom group have relatively low titers, in line with the notion that high titers are increased with immunodominance to CysR or CTLD1. The star above titer indicates positivity for CTLD7 and/or CTLD8.

Figure 8 – Correlation between anti-PLA2R1 (commercial total IgG ELISA) and anti-PLA2R1 titer (in-house IgG4 ELISA), anti-CysR or anti-CTLD1 titers (in-house IgG4 ELISA) for PLA2R1-positive MN patients overall (n=141) or according to immunodominance (n=135). (A) Correlations between anti-PLA2R1 titer measured by commercial ELISA (total IgG) and in-house ELISA (IgG4). **(B and C)** Correlations between anti-PLA2R1 titer measured by commercial ELISA (total IgG) and anti-CysR titer **(B)** or anti-CTLD1 titer **(C)**. Note the weaker correlations between anti-PLA2R1 and anti-CTLD1 titers for the whole population and iCR patients as compared to iC1 patients.

Figure 9 – Schematic drawing of PLA2R1 showing the novel findings of the study: serum from PLA2R1-positive MN patients can recognize up to 5 epitope-containing domains among which CysR and CTLD1 are immunodominant. Before this study (left panel), PLA2R1-positive MN patients were known to contain circulating autoantibodies targeting the CysR, CTLD1 and/or CTLD7 domains. There were also controversies about the independent reactivity of autoantibodies to CysR and CTLD1. Finally, potential additional epitopes as well as epitope prevalence and immunodominance as a driving-force of the autoimmune response were not well-established. The present study (right panel) demonstrates that PLA2R1-positive MN patients contain circulating autoantibodies that can recognize independently up to 5 epitope-containing domains (CysR, CTLD1, CTLD5, CTLD7 and CTLD8). Competition assays show that CysR and/or CTLD1 function as the immunodominant epitope-containing domains in the majority of patients, thereby being responsible for most of the anti-PLA2R1 signal and the associated titer, suggesting their major role in the humoral autoimmune response.

Table 1 – Baseline characteristics, treatment and clinical outcome of PLA2R1-positive patients as a whole (overall) and according to immunodominant profile. Values are present as n (%) or median [IQR]. eGFR was calculated according to the Chronic Kidney Disease Epidemiology Collaboration (CKD-EPI) Equation. NIAT, non- immunosuppressive anti-proteinuric treatment; IS, immunosuppressive treatment; ESRD, end-stage renal disease.

Characteristics	**Overall** (n=142)	**iCR** (n=75)[A]	**iC1** (n=49)[A]	**non-iDom** (n=12)[A]	**p-value**
Age (years)	55.5 [41.0-64.0]	52.0 [41.0-64.0]	58.0 [41.5-64.0]	58.5 [37.0-71.0]	0.6789
Gender (M/F), n (%)	104 (73.2)/38 (26.8)	57 (76.0)/ 18(24.0)	35 (71.4)/14 (28.6)	8 (66.7)/4 (33.3)	0.7274
Clinical parameters					
Serum albumin (g/L) [B]	23.0 [19.0-28.0]	24.0 [20.0-29.2]	22.0 [17.9-26.9]	25.0 [19.4-28.2]	0.4503
Serum creatinine (µmol/L)	95.0 [80.0-119.0]	94.0 [80.0-113.0]	95.0 [81.0-122.5]	95.0 [69.5-124.5]	0.8233
Calculated eGFR (mL/min/1.73 m^2)	72.5 [53.0-92.0]	76.0 [57.0-95.0]	66.0 [54.0-90.5]	71.0 [45.8-105.3]	0.4664
Proteinuria (g/day) [C]	6.3 [3.5-9.0]	5.3 [3.2-8.0]	6.8 [4.8-10.0]	6.0 [3.3-11.4]	0.0277
Treatment (n (%))					0.2064
NIAT	61 (43.0)	37 (49.3)	19 (38.8)	3 (25.0)	
IS	81 (57.0)	38 (50.7)	30 (61.2)	9 (75.0)	
Clinical outcome (n (%))					0.0158
Combined remission	82 (57.7)	48 (64.0)	20 (40.8)	9 (75.0)	
NIAT-induced	31 (21.8)	20 (26.7)	8 (16.3)	2 (16.7)	
IS-induced	51 (35.9)	28 (37.3)	12 (24.5)	7 (58.3)	
Active disease or ESRD	60 (42.3)	27 (36.0)	29 (59.2)	3 (25.0)	
Anti-PLA2R1 autoantibodies					
Anti-PLA2R1 titer (RU/mL)					
Commercial ELISA (total IgG)	64.8 [27.0-210.3]	56.5 [19.7-133.5]	178.0 [38.9-344.4]	59.7 [29.3-64.1]	0.0026
Homemade ELISA (IgG4) [D]	70.9 [30.4-355.4]	50.5 [20.6-199.0]	346.8 [62.1-804.5]	57.5 [36.1-72.7]	<0.0001
Epitope titer (IgG4, RU/mL) [D]					
CysR	224.2 [122.0-873.5]	223.3 [133.7-902.0]	417.9 [149.4-1108.0]	159.5 [98.1-325.8]	0.1591
CTLD1	5.1 [3.6-33.0]	3.8 [3.2-5.4]	36.2 [13.2-114.2]	4.1 [3.4-4.7]	<0.0001
Spreading to CTLD1 and/or CTLD7 (n (%))	86 (60.1)	26 (34.7)	49 (100.0)	9 (75.0)	<0.0001
Epitope positivity (n (%))					<0.0001
CysR	142 (100.0)	75 (100.0)	49 (100.0)	12 (100.0)	
CTLD1	66 (46.5)	13 (17.3)	49 (100.0)	2 (16.7)	<0.0001
CTLD5	93 (65.5)	51 (68.0)	26 (53.1)	11 (91.7)	0.0289
CTLD7	52 (36.6)	22 (29.3)	20 (40.8)	9 (75.0)	0.0035
CTLD8 (n(%)) [E]	5 (3.5)	3 (4.0)	2 (4.1)	0 (0.0)	
Number of epitopes (n(%))					<0.0001
1	19 (13.4)	19 (13.4)	0 (0.0)	0 (0.0)	
2	63 (44.4)	34 (45.3)	20 (40.8)	4 (33.3)	
3	29 (20.4)	12 (16.0)	11 (22.4)	6 (50.0)	
>3	31 (21.8)	10 (13.2)	18 (36.7)	2 (16.7)	

[A] For six patients, there was not enough serum available to determine their immunodominance. [B] Serum albumin values were missing for 21 patients (8 iCR patients, 10 iC1 patients and 3 non-iDom patients).
[C] Proteinuria value was missing for one iCR patient. [D] Values for one iCR patient were missing due to lack of serum. [E] Due to its low frequency, the CTLD8 distribution according to immunodominance was analyzed separately from the other epitope-containing domains.

Table 2 – Exploration of baseline characteristics of PLA2R1-positive patients as possible predictors of clinical outcome after first treatment. Values are presented as n(%) or median [IQR]. eGFR was calculated according to the Chronic Kidney Disease Epidemiology Collaboration (CKD-EPI) Equation. NIAT, non-immunosuppressive anti-proteinuric treatment.

Characteristics	**Overall** (n=142)	**Combined remission** (n=82)	**No remission** (n=60)	**p-value**
Age (years)	55.5 [41.0-64.0]	52.0 [41.0-61.3]	58.5 [46.0-70.0]	0.0282
Gender (M/F), n(%)	104 (73.2)/38 (26.8)	60 (73.2)/22 (26.)	44 (73.3)/16 (26.7)	>0.9999
Clinical parameters				
Serum albumin (g/L) [A]	23.0 [19.0-28.0]	23.0 [19.3-28.0]	23.0 [18.5-27.0]	0.7874
Serum creatinine (µmol/L)	95.0 [80.0-119.0]	92.0 [73.8-113.5]	102.0 [85.0-135.0]	0.0172
Calculated eGFR (mL/min/1.73m^2)	72.5 [53.0-92.0]	78.5 [57.0-97.5]	65.5 [39.3-88.8]	0.0359
Proteinuria (g/day) [B]	6.3 [3.5-9.0]	5.5 [3.3-8.3]	6.8 [4.6-10.0]	0.0410
Treatment (n(%))				0.1714
NIAT	61 (43.0)	31 (37.8)	30 (50.0)	
Immunosuppressive	81 (57.0)	51 (62.2)	30 (50.0)	
Rituximab	61 (43.0)	42 (51.2)	19 (31.7)	
Ponticelli	10 (7.0)	5 (6.1)	5 (8.3)	
Corticosteroids	9 (6.3)	4 (4.9)	5 (8.3)	
Immunoglobulin therapy	1 (0.7)	0 (0.0)	1 (1.7)	
Anti-PLA2R1 autoantibodies				
Anti-PLA2R1 titer (RU/mL)				
Commercial ELISA (Total IgG)	64.8 [27.0-210.3]	39.7 [19.3-107.5]	152.1 [56.4-394.5]	<0.0001
Homemade ELISA (IgG4) [C]	70.9 [30.4-355.4]	47.8 [22.3-118.3]	257.7 [54.7-840.2]	<0.0001
Epitope titer (IgG4, RU/mL) [C]				
CysR	224.2 [122.0-873.5]	186.4 [98.5-414.4]	652.8 [180.9-1335.0]	0.0001
CTLD1	5.1 [3.6-33.0]	4.4 [3.3-8.7]	21.7 [4.4-68.5]	<0.0001
Spreading to CTLD1 and/or CTLD7 (n(%))	86 (60.6)	39 (47.6)	47 (78.3)	0.0002
Epitope positivity (n(%))				0.0910
CysR	142 (100.0)	82 (100.0)	60 (100.0)	
CTLD1	66 (46.5)	27 (32.9)	39 (65.0)	
CTLD5	93 (65.5)	54 (65.9)	39 (65.0)	
CTLD7	52 (36.6)	23 (28.0)	29 (48.3)	
CTLD8	5 (3.5)	2 (2.4)	3 (5.0)	
Number of epitopes (n(%))				0.0020
1	19 (13.4)	13 (15.9)	6 (10.0)	
2	63 (44.4)	43 (52.4)	20 (33.3)	
3	29 (20.4)	15 (18.3)	14 (23.3)	
>3	31 (21.8)	11 (13.4)	20 (33.3)	
Immunodominance (n(%)) [D]				0.0158
iCR	75 (52.8)	48 (58.5)	27 (45.0)	
non-iDom	12 (8.5)	9 (11.0)	3 (5.0)	
iC1	49 (34.5)	20 (24.4)	29 (48.3)	

[A] Serum albumin values were missing for 21 patients (10 in remission and 11 not in remission). [B] Proteinuria value was missing for one patient in non-remission. [C] Value for a patient in remission was missing due to lack of serum. [D] Immunodominance was not tested for 6 patients due to lack of serum (5 patients in remission and 1 in non-remission). For 11 more patients, no serum was available to perform assays for immunodominance. A iCR profile was assumed since their epitope profile was only CysR.

Table 3 – Anti-PLA2R1 and immunodominance as prognostic factors of clinical remission (unadjusted and adjusted analyses).

Variable	Unadjusted	Adjusted Model 1	Adjusted Model 2	Adjusted Model 3	Adjusted Model 4
	Odds Ratio (95% Confidence Interval)	Odds Ratio (95% Confidence Interval)	Odds Ratio (95% Confidence Interval)	Odds Ratio (95% Confidence Interval)	Odds Ratio (95% Confidence Interval)
Calculated eGFR (mL/min/1.73 m^2)	1.014 (1.002-1.027)	1.010 (0.997-1.024)	1.010 (0.996-1.023)	1.012 (1.000-1.026)	1.013 (1.000-1.026)
Proteinuria (g/day)	0.922 (0.846-1.005)	0.952 (0.866-1.047)	0.956 (0.868-1.052)	0.933 (0.852-1.021)	0.929 (0.848-1.018)
Treatment					
NIAT	1	1		1	
Immunosuppressive (IS)	1.567 (0.787-3.120)	1.999 (0.921-4.340)		1.892 (0.895-4.001)	
Anti-PLA2R1 median (RU/mL, total IgG)					
< 64.8	1	1			
≥ 64.8	0.237 (0.114-0.492)	0.255 (0.117-0.558)			
Anti-PLA2R1 titer and treatment combined					
NIAT + anti-PLA2R1 < 64.8	1		1		
NIAT + anti-PLA2R1 ≥ 64.8	0.137 (0.043-0.435)		0.190 (0.056-0.639)		
IS + anti-PLA2R1 < 64.8	1.272 (0.421-3.841)		1.515 (0.482-4.763)		
IS + anti-PLA2R1 ≥ 64.8	0.391 (0.147-1.042)		0.481 (0.171-1.354)		
Immunodominance					
iCR/non-iDom	1			1	
iC1	0.351 (0.170-0.724)			0.365 (0.171-0.781)	
Immunodominance and treatment combined					
NIAT + iCR/non-iDom	1				1
NIAT + iC1	0.595 (0.197-1.794)				0.696 (0.224-2.168)
IS + iCR/non-iDom	2.603 (1.037-6.535)				2.912 (1.114-7.613)
IS + iC1	0.545 (0.209-1.425)				0.652 (0.238-1.783)

Number of observations analyzed: 135, 77 clinical remissions.

eGFR was calculated according to the Chronic Kidney Disease Epidemiology Collaboration (CKD-EPI) Equation. NIAT, non-immunosuppressive anti-proteinuric treatment; IS, immunosuppressive treatment.

Table 4 – Baseline characteristics and clinical outcome of NIAT- or rituximab-treated patients according to their immunodominance and with an anti-PLA2R1 titer equal or below 200 RU/mL. Values are present as n (%) or median [IQR]. eGFR was calculated according to the Chronic Kidney Disease Epidemiology Collaboration (CKD-EPI) Equation. NIAT, non-immunosuppressive anti-proteinuric treatment; ESRD, end-stage renal disease.

Characteristics	Overall (n=82)	iCR/non-iDom (n=59)	iC1 (n=23)	p-value
Age (years)	52.0 [41.0-61.3]	52.0 [40.0-62.0]	59.0 [41.0-61.0]	0.5096
Gender (M/F), n (%)	66 (80.5)/16 (19.5)	47 (79.7)/12 (20.3)	19 (82.6)/4 (17.4)	>0.9999
Clinical parameters				
Serum albumin (g/L) [A]	23.0 [20.0-28.0]	24.0 [20.2-28.5]	21.3 [17.0-24.3]	0.0623
Serum creatinine (µmol/L)	95.0 [79.8-115.3]	95.0 [80.0-115.0]	92.0 [79.0-116.0]	0.9001
Calculated eGFR (mL/min/1.73 m^2)	77.5 [55.0-101.0]	78.0 [53.0-101.0]	77.0 [57.0-99.0]	0.8790
Proteinuria (g/day)	5.8 [3.3-8.8]	4.8 [3.2-8.4]	7.2 [5.7-10.0]	0.0073
Anti-PLA2R1 autoantibodies				
Anti-PLA2R1 titer (RU/mL)				
Commercial ELISA (total IgG)	39.1 [18.6-77.2]	39.2 [19.6-73.2]	38.9 [17.0-122.9]	0.4116
Treatment (n(%))				0.6268
NIAT	40 (48.9)	30 (50.8)	10 (43.5)	
Rituximab	42 (51.2)	29 (49.2)	13 (56.5)	
Clinical outcome (n (%))				0.0069
Combined remission	58 (70.7)	47 (79.7)	11 (47.8)	
Active disease or ESRD	24 (29.3)	12 (20.3)	12 (52.2)	
Clinical outcome after NIAT (n (%))				0.7004
Combined remission	27 (67.5)	21 (70.0)	6 (60.0)	
Active disease or ESRD	13 (32.5)	9 (30.0)	4 (40.0)	
Clinical outcome after rituximab (n (%))				0.0012
Combined remission	31 (73.8)	26 (89.7)	5 (38.5)	
Active disease or ESRD	11 (26.2)	3 (10.3)	8 (61.5)	

[A] Serum albumin values were missing for 11 patients (6 iCR patients and 5 iC1 patients).

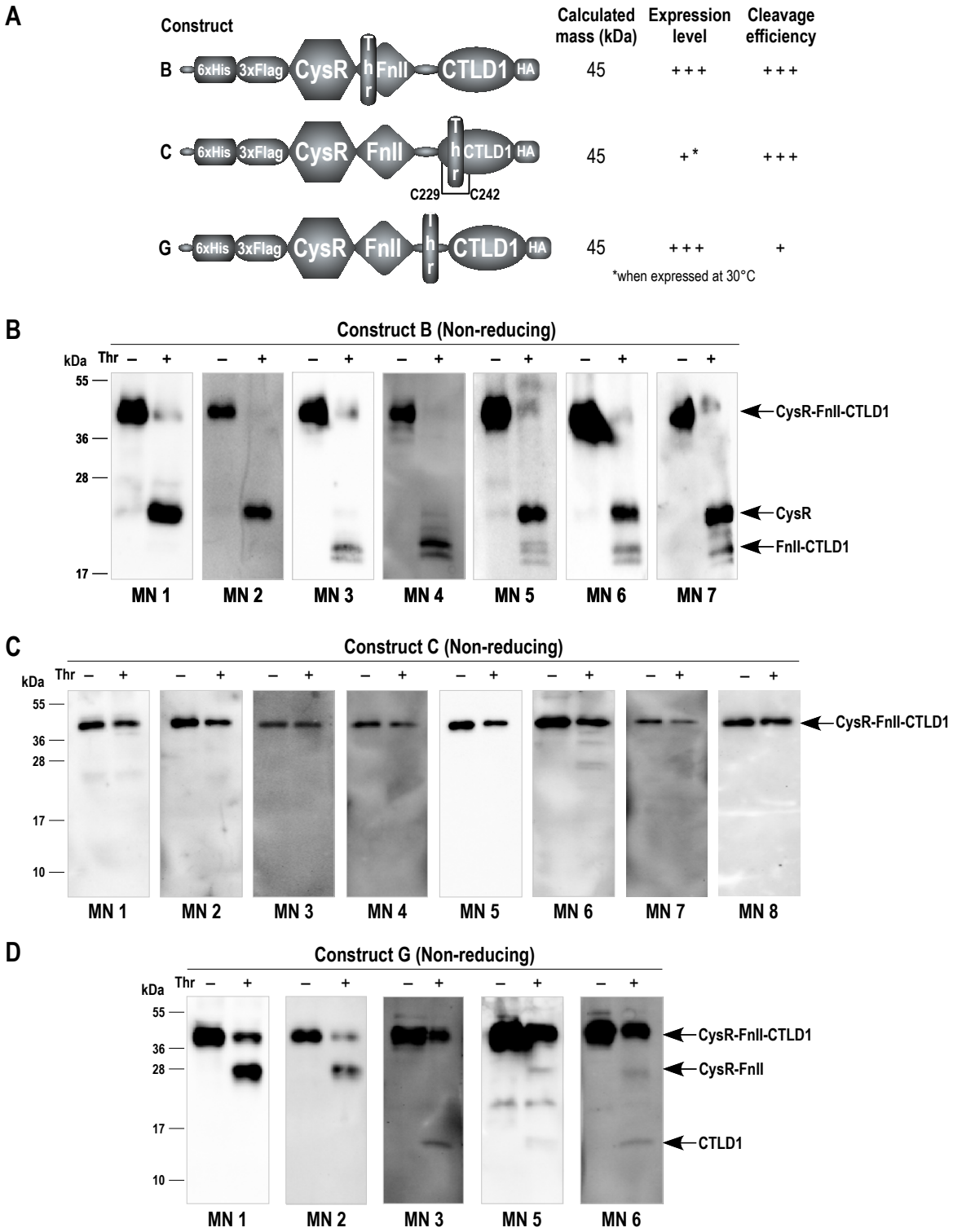

Figure 1 - Sera from MN patients have independent reactivity to CysR and CTLD1 after cleavage of the N-terminal CysR-FnII-CTLD1 triple domain by thrombin. (A) Schematic diagram of soluble constructs for the CysR-FnII-CTLD1 triple domain with a thrombin (Thr) cleavage site inserted at different positions: between CysR and FnII (construct B), within the first disulfide bridge in CTLD1 (construct C) or in the extended linker region between FnII and CTLD1 (construct G). All constructs were N-terminally 6xHis- and 3xFlag-tagged and C-terminally HA-tagged. The expected mass is calculated without the contribution of glycosylation. Expression level in HEK293 cells and cleavage efficiency is indicated. **(B)** Western blots showing the reactivity of seven MN patients to construct B before and after cleavage with thrombin under non-reducing conditions. Data demonstrate that CysR and CTLD1 can be independently detected after cleavage. **(C)** Western blots showing the reactivity of eight MN patients to construct C before and after cleavage with thrombin under non-reducing conditions. Data suggest the absence of cleavage by thrombin and show patients' sera reactivity only to the triple domain before and after cleavage. However, cleavage was done (refer to figure S3) and fragments containing either CysR or CTLD1 domains were maintained by the disulfide bridge within CTLD1. **(D)** Western blots showing the reactivity of five MN patients to construct G before and after cleavage with thrombin under non-reducing conditions. Data show that CysR and CTLD1 can be independently detected after thrombin cleavage (even though the cleavage is only partial).

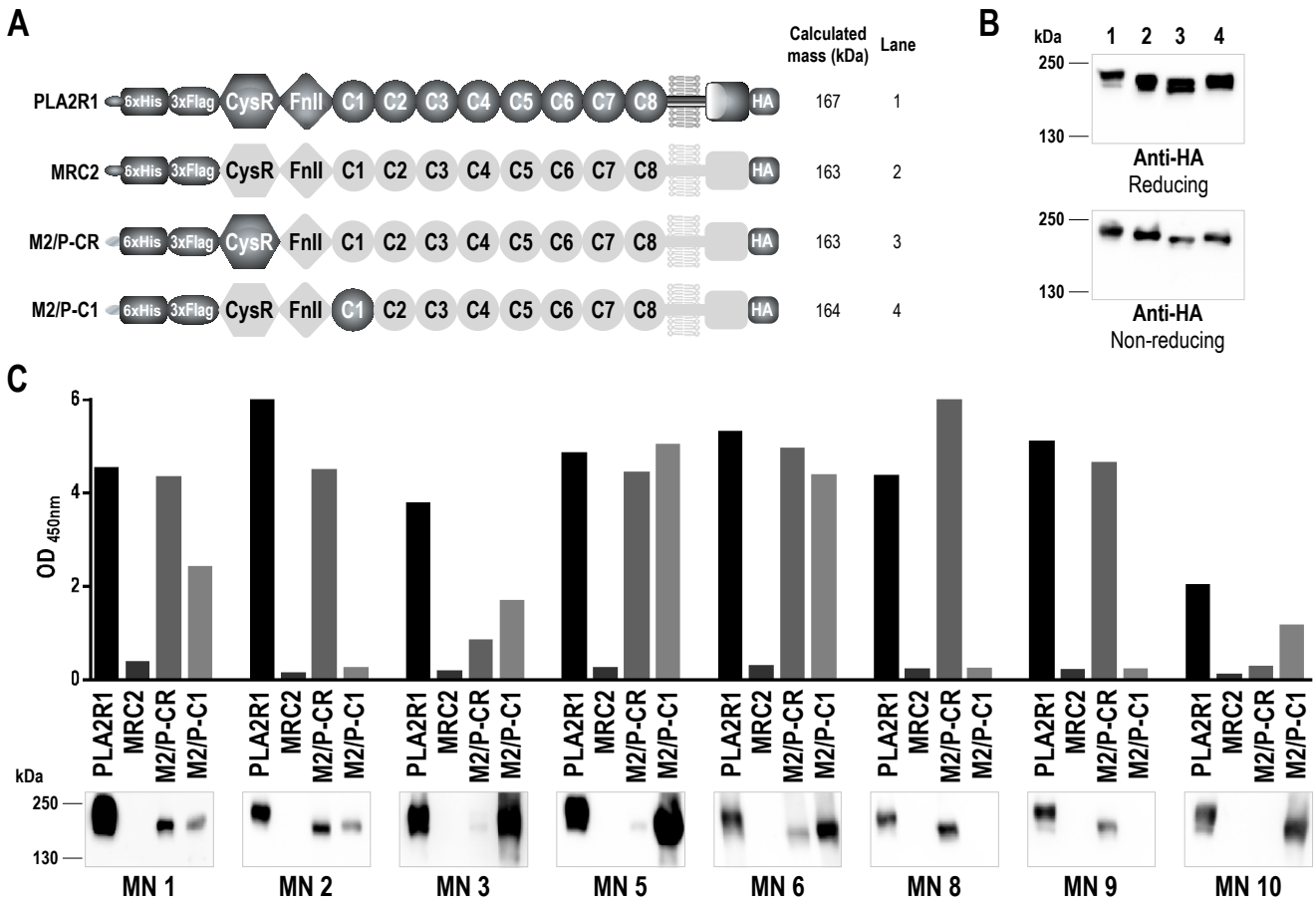

Figure 2 - Sera from MN patients have independent reactivity to CysR and CTLD1 when expressed as chimeras between PLA2R1 and MRC2. (A) Schematic diagram of the two wild-type membrane-bound proteins (PLA2R1 and MRC2) and chimeras (M2/P-CysR and M2/P-C1) where the CysR and CTLD1 domains of PLA2R1 are respectively introduced into the structural backbone of MRC2. All proteins are N-terminally 6xHis- and 3xFlag-tagged and C-terminally HA-tagged, and were expressed in HEK293 cells. The expected mass is calculated without the contribution of glycosylation. **(B)** Expression of the four membrane-bound proteins was validated by western blot under both reducing and non-reducing conditions using anti-HA antibody (1:5,000). **(C)** Western blots under non-reducing conditions and ELISA with eight MN patients show independent reactivity against CysR and CTLD1 introduced as single domain in the M2/P-CysR and M2/P-C1 chimeras.

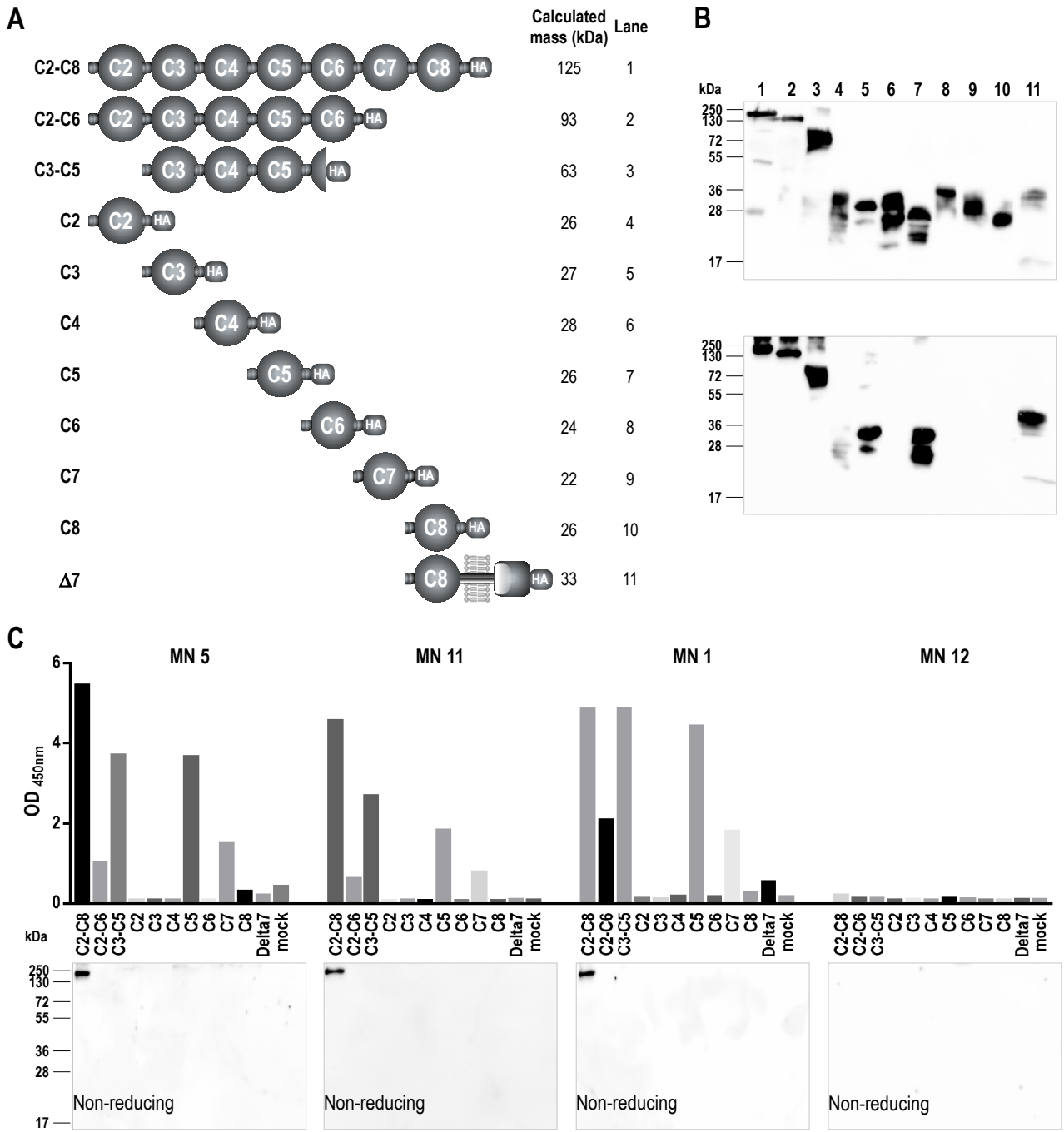

Figure 3 - CTLD5 and CTLD8 are two novel independent epitope-containing domains recognized by PLA2R1-positive MN patients. (A) Schematic diagram of C-terminally HA-tagged soluble and membrane-bound recombinant proteins spanning the CTLD2-CTLD8 region of PLA2R1. All proteins were expressed in HEK293 cells. The expected mass is calculated without the contribution of glycosylation. **(B)** Western blot under reducing conditions with anti-HA antibody (1:5,000) validate the expression of all PLA2R1 recombinant proteins. However, the single domains C2, C4, C6, C7 and C8 were not detected by anti-HA antibody (1:5,000) under non-reducing conditions due to poor transfer of the small likely hydrophilic proteins. **(C)** ELISA with four representative MN patients (1:100) shows the recognition of CTLD5 and CTLD8 as single domains. In contrast, the same patients do not recognize CTLD5 (C5) and CTLD8 single domains (C8, D7) by western blot because of denaturation of the epitope(s) for C5 (see also Figure S8B) and weak reactivity for C8 (see also Figure S7A).

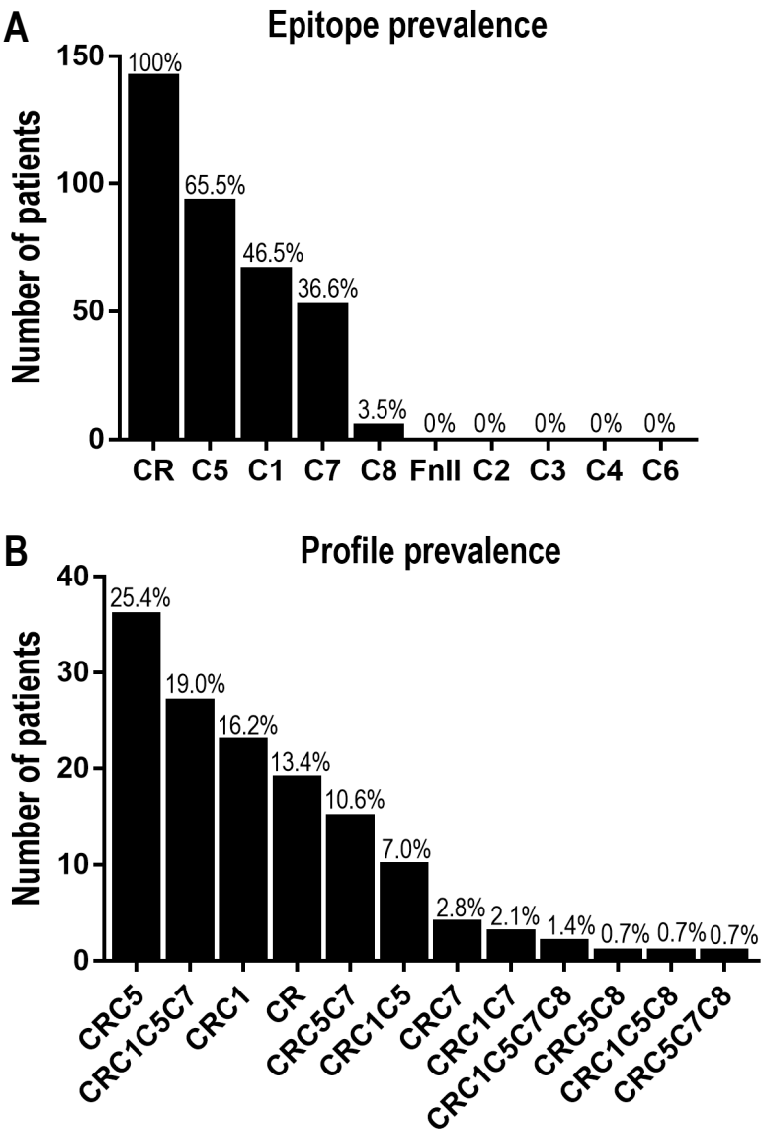

Figure 4 - Prevalence and epitope profile in a cohort of 142 PLA2R1-positive MN patients. (A) Screening of 142 PLA2R1-positive patients by ELISA (IgG4 detection) with the 10 individual domains of PLA2R1 shows reactivity against 5 domains with decreasing prevalence: CysR, CTLD5, CTLD1, CTLD7 and CTLD8. None of the five remaining domains were recognized. **(B)** Patients' reactivity to single domains can be combined to provide different epitope profiles among which CRC5, CRC1C5C7, CRC1, CR, CRC5C7 and CRC1C5 are the most prevalent.

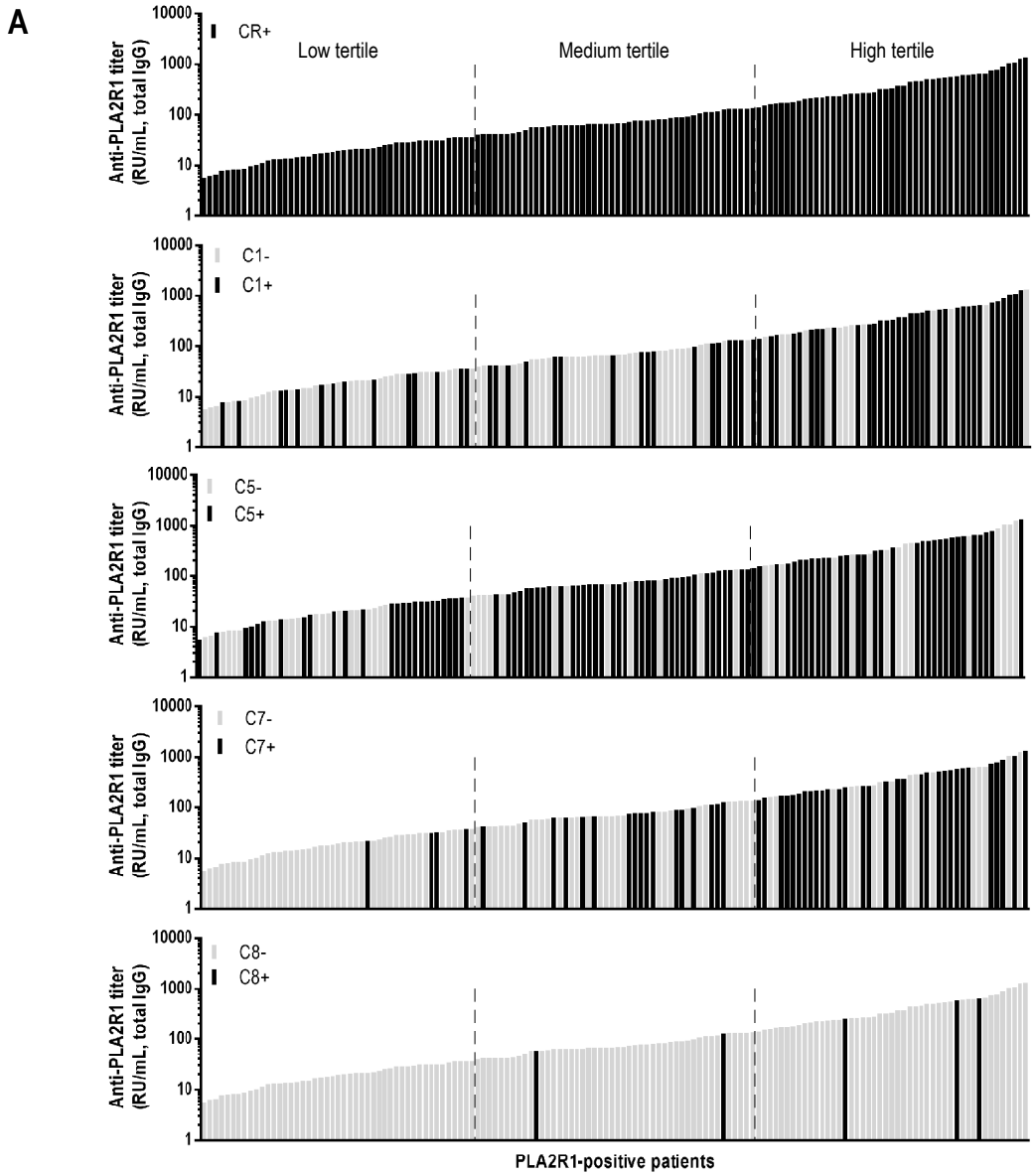

Figure 5 - Relationship between epitope positivity and anti-PLA2R1 titer. (A) Patients (n=142) were ranked by increasing anti-PLA2R1 titer (commercial ELISA, total IgG) and positivity to the different domains was superimposed to display the different patterns. All patients were positive for CysR. In the first tertile, 29.8% of patients were CTLD1, 53.2% CTLD5, 8.5% CTLD7 and 0% CTLD8. In the second tertile, 35.4% of patients were CTLD1, 75.0% CTLD5, 35.4% CTLD7 and 4.2% CTLD8. In the third tertile, 74.5% of patients were CTLD1, 68.1% CTLD5, 66.0% CTLD7 and 6.4% CTLD8. (B) Patients (n=142) were ranked according to the complexity of their epitope profile from the CysR domain to the C-terminal end of PLA2R1 and positivity or not for CTLD1. The increased complexity of epitope profiles appears to be associated with anti-PLA2R1 titer.

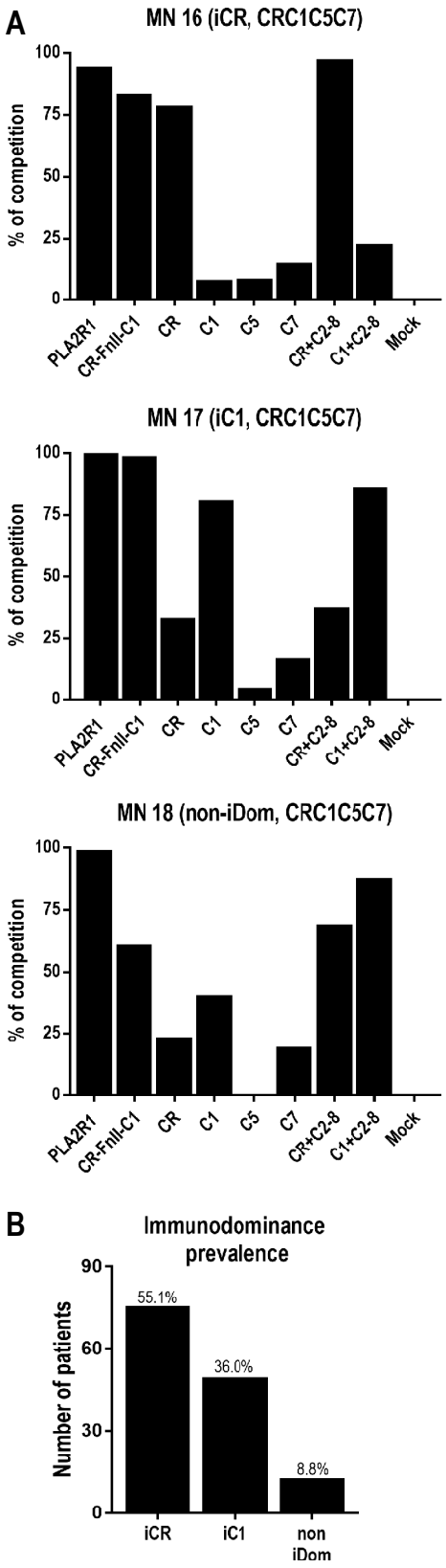

Figure 6 - CysR and CTLD1 are two immunodominant PLA2R1 domains and define different groups of PLA2R1-positive MN patients. (A) Representative competition assays by ELISA (IgG4 detection) for three patients allowing classification in three distinct groups: iCR, iC1 and non-iDom (see methods for a complete definition). Note that the chosen representative patients have the same epitope profile CRC1C5C7 but different immunodominant profiles. **(B)** Stratification of patients (n=136) according to their immunodominant profile shows that the majority of them (n=75, 55.1%) have CysR as immunodominant PLA2R1 domain (iCR) while a significant number (n=49, 36.0%) have CTLD1 as immunodominant domain (iC1). A small group of patients (n=12, 8.8%) are classified as non-iDom. The immunodominant profile could not be assigned for 6 patients from the original cohort of 142 patients because of lack of serum.

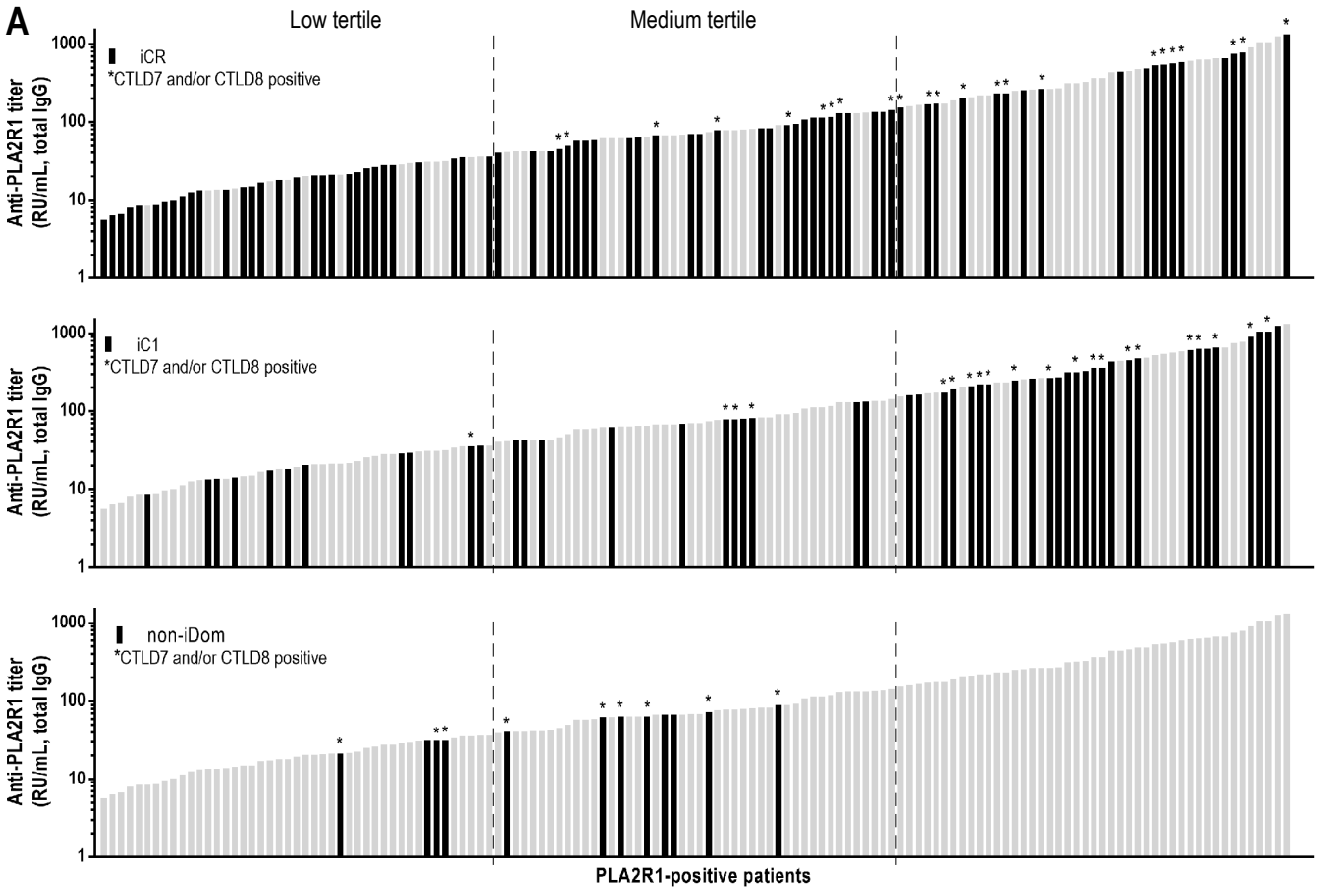

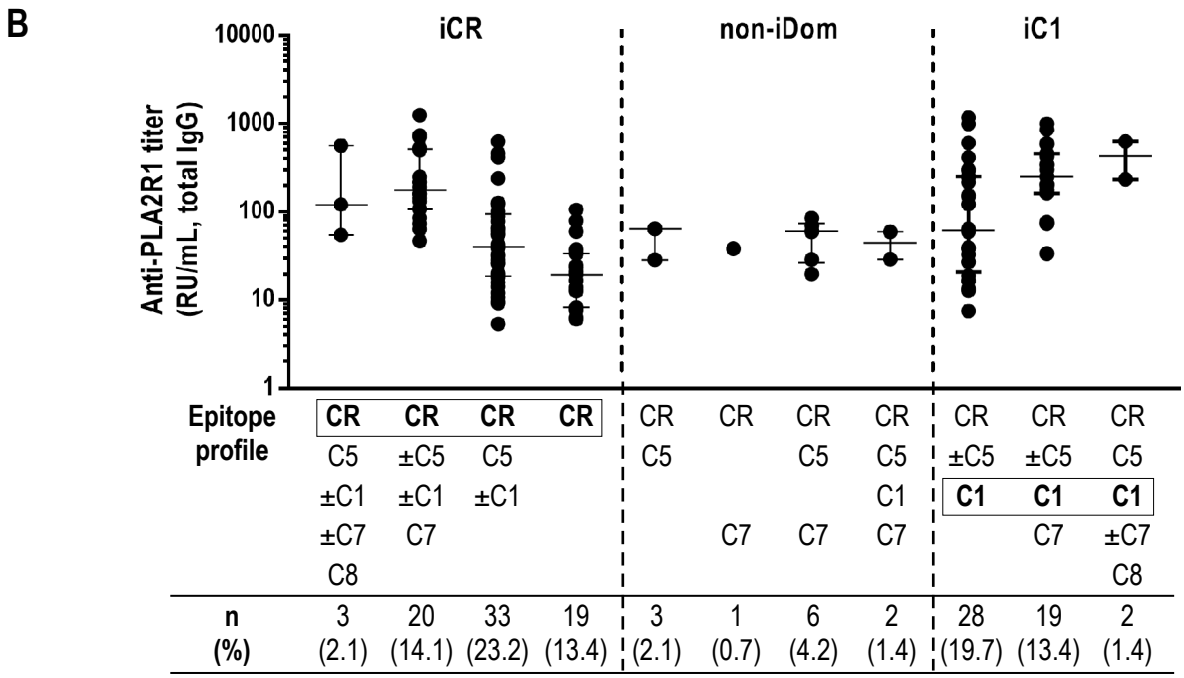

Epitope profile	CR	CR	CR	CR	CR	CR	CR	CR	CR	CR	CR
	C5 ±C1 ±C7 C8	±C5 ±C1 C7	C5 ±C1		C5		C5	C5 C1 C7	±C5 **C1**	±C5 **C1** C7	C5 **C1** ±C7 C8
n	3	20	33	19	3	1	6	2	28	19	2
(%)	(2.1)	(14.1)	(23.2)	(13.4)	(2.1)	(0.7)	(4.2)	(1.4)	(19.7)	(13.4)	(1.4)

Figure 7 - Relationship between immunodominance and anti-PLA2R1 titer. (A) Patients (n=136) were ranked by increasing anti-PLA2R1 titer (commercial ELISA, total IgG detection) and their immunodominance was displayed. In the first tertile 66.7% of patients were iCR, 24.4% iC1 and 8.9% non-iDom. In the second tertile, 60.9% of patients were iCR, 21.7% iC1 and 17.4% non-iDom. In the third tertile, 37.8% of patients were iCR, 62.2% were iC1 and 0% non-iDom. **(B)** Patients (n=136) were ranked according to their immunodominant profile (iCR, non-iDom or iC1) combined with the complexity of their epitope profile from the CysR domain to the C-terminal region of PLA2R1. CR and C1 are indicated in bold when they become immunodominant. The increased complexity of epitope profiles appears to be associated with anti-PLA2R1 titer for both iCR and iC1 groups. Note that patients from the non-iDom group have relatively low titers, in line with the notion that high titers are increased with immunodominance to CysR or CTLD1. The star above titer indicates positivity for CTLD7 and/or CTLD8.

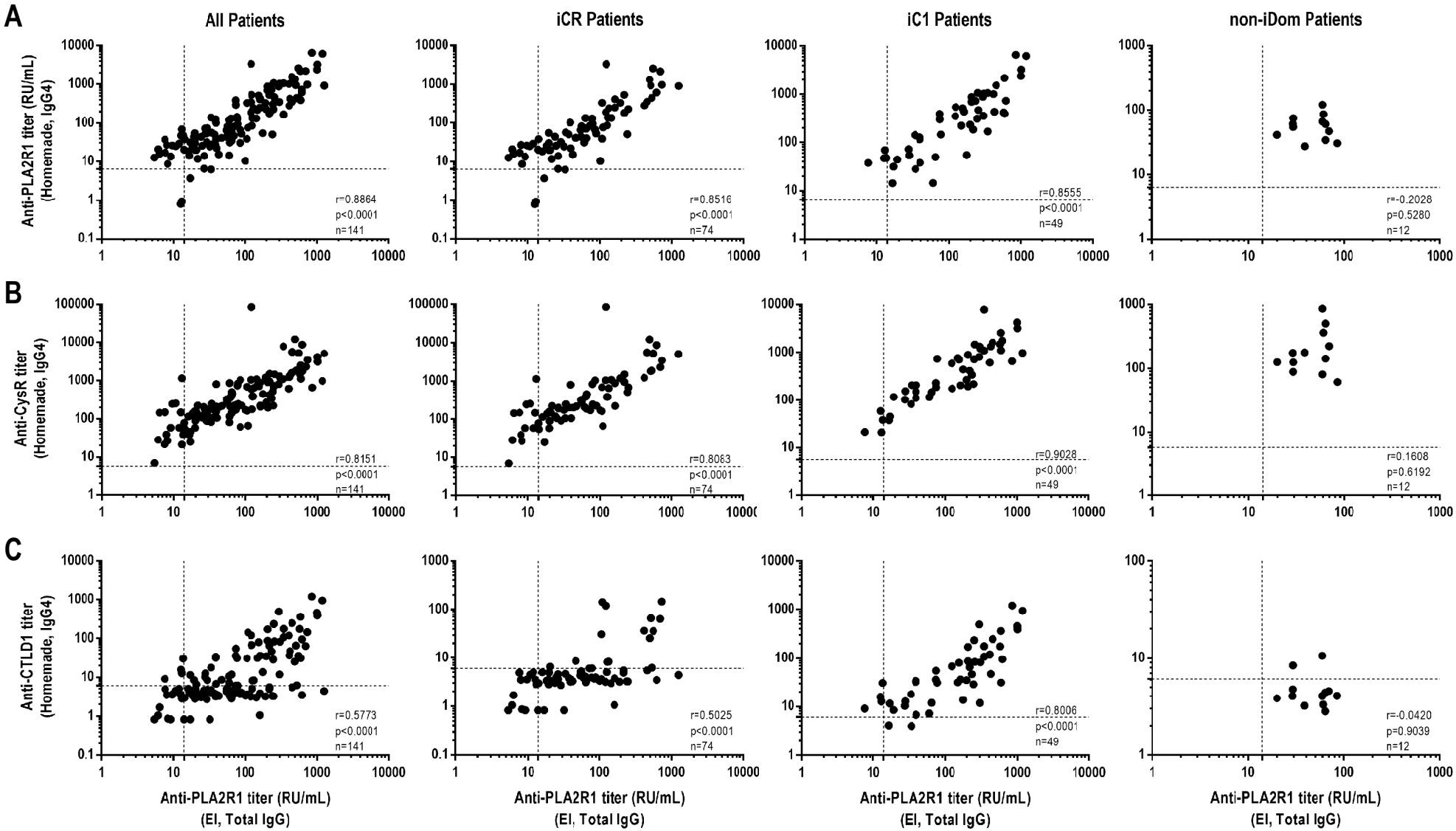

Figure 8 - Correlation between anti-PLA2R1 (commercial total IgG ELISA) and anti-PLA2R1 titer (in-house IgG4 ELISA), anti-CysR or anti-CTLD1 titers (in-house IgG4 ELISA) for PLA2R1-positive MN patients overall (n=141) or according to immunodominance (n=135). (A) Correlations between anti-PLA2R1 titer measured by commercial ELISA (total IgG) and in-house ELISA (IgG4). **(B and C)** Correlations between anti-PLA2R1 titer measured by commercial ELISA (total IgG) and anti-CysR titer **(B)** or anti-CTLD1 titer **(C)**. Note the weaker correlations between anti-PLA2R1 and anti-CTLD1 titers for the whole population and iCR patients as compared to iC1 patients.

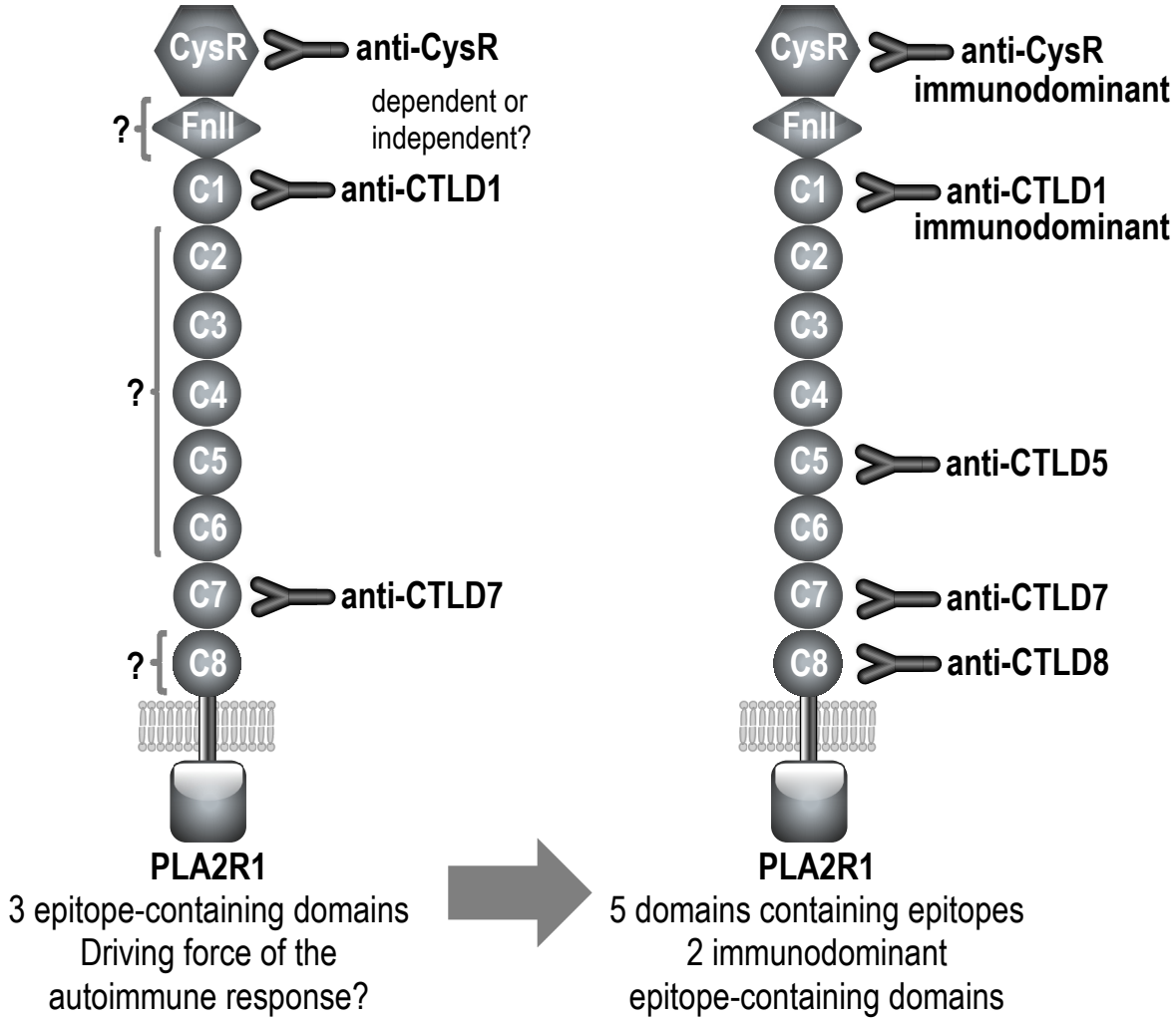

Figure 9 - Schematic drawing of PLA2R1 showing the novel findings of the study: serum from PLA2R1-positive MN patients can recognize up to 5 epitope-containing domains among which CysR and CTLD1 are immunodominant. Before this study (left panel), PLA2R1-positive MN patients were known to contain circulating autoantibodies targeting the CysR, CTLD1 and/or CTLD7 domains. There were also controversies about the independent reactivity of autoantibodies to CysR and CTLD1. Finally, potential additional epitopes as well as epitope prevalence and immunodominance as a driving-force of the autoimmune response were not well-established. The present study (right panel) demonstrates that PLA2R1-positive MN patients contain circulating autoantibodies that can recognize independently up to 5 epitope-containing domains (CysR, CTLD1, CTLD5, CTLD7 and CTLD8). Competition assays show that CysR and/or CTLD1 function as the immunodominant epitope-containing domains in the majority of patients, thereby being responsible for most of the anti-PLA2R1 signal and the associated titer, suggesting their major role in the humoral autoimmune response.

SUPPLEMENTARY INFORMATION

Circulating autoantibodies in PLA2R1-associated membranous nephropathy: epitopes, immunodominance and clinical association

Joana Justino[1*], Vesna Brglez[1*], Guillaume Dolla[1], Alexandra Rousseau[2], Christelle Zaghrini[1], Christine Payré[1], Franck Bihl[1], Agnès Petit-Paitel[1], Noémie Jourde-Chiche[5,6], Karine Dahan[7], Christophe Mariat[8,9], Hanna Debiec[10], Pierre Ronco[7, 10, 11], Gérard Lambeau[1]

[1] Université Côte d'Azur (UCA), Centre National de la Recherche Scientifique (CNRS), Institut de Pharmacologie Moléculaire et Cellulaire (IPMC), UMR7275, Valbonne Sophia Antipolis, France;
[2] Assistance Publique – Hôpitaux de Paris (AP-HP), Unité de Recherche Clinique de l'Est Parisien, Sorbonne Université, Hôpital Saint-Antoine, Paris, France.
[3] Assistance Publique – Hôpitaux de Marseille, Centre de Néphrologie et Transplantation Rénale, Hôpital de la Conception, Marseille, France;
[4] Aix-Marseille Université, Centre Recherche en Cardiovasculaire et Nutrition, Institut National de la Recherche Agronomique 1260, Institut National de la Santé et de la Recherche Médicale INSERM U1263, Marseille, France;
[5] Assistance Publique – Hôpitaux de Paris, Hôpital de jour de Néphrologie, Hôpital Tenon, Paris, France;
[6] Département de Néphrologie, Dialyse et Transplantation Rénale, Hôpital Nord, CHU Saint-Etienne, France;
[7] EA3064 GIMAP, Université Jean Monnet Saint-Etienne, Université de Lyon, Lyon, France;
[8] Institut National de la Santé et de la Recherche Médicale (INSERM), UMR-S 1155, Paris, France;
[9] Sorbonne Université, Université Pierre et Marie Curie Paris 06, Paris, France.

*Contributed equally

SUPPLEMENTARY METHODS

Generation and expression of PLA2R1 mutants and membrane-bound chimeras of PLA2R1-MRC2

All soluble and membrane-bound PLA2R1 mutants as well as chimeras were generated by PCR and cloned into the pcDNA3.1/Zeo (–) expression vector (Life Technologies, Carlsbad, USA). Soluble and membrane-bound PLA2R1 constructs were generated using the Phusion Site-Directed Mutagenesis Kit (Thermo Fisher Scientific, Waltham, USA). Membrane-bound and soluble chimeras between MRC2 (Uniprot Q9UBG0) and PLA2R1 were generated using recombination-assisted megaprimer cloning essentially as described (1).

A series of 6 mutants containing the CysR-FnII-CTLD1 triple domain (Q36 to N359 – constructs A to G except D) and various protease cleavage sites was designed based on previous work (2). All 6 constructs comprised the PLA2R1 signal peptide (M1 to A20) followed by its N-terminal linker sequence (E21 to W35), the N-terminal 6xHis and 3xFlag tags, the triple PLA2R1 domains with or without protease cleavage sites and a C-terminal HA-tag (except for construct F which was only HA-tagged). Protease cleavage sites were introduced at different amino acid positions as follows: construct A, no protease cleavage site; construct B, thrombin cleavage site (LVPRGS) inserted between CysR and FnII (replacing amino acids L166 to G171); construct C, thrombin cleavage site within the first disulfide bond of CTLD1 (replacing amino acids T231 to D236); construct D, same as construct C but with an additional factor Xa cleavage site (IEGR) within the linker region between FnII and CTLD1 (replacing amino acids T223 to E226); construct E, only factor Xa cleavage site (IEGR) within the linker region between FnII and CTLD1 (replacing amino acids T223 to E226); construct F, extended TEV protease cleavage site (GLENLYFQG) inserted in the linker region between FnII and CTLD1 (between D221 and P222), thereby extending the linker region between the two domains; construct G, thrombin cleavage site inserted in the linker region between FnII and CTLD1 (T223 to S224), thereby extending the region between the two domains. For construct D, a human codon-optimized synthetic gene was designed (Genecust, Dudelange, Luxembourg). The synthetic gene comprises the signal peptide of human group IIA secreted phospholipase A2 (M1 to N20, Uniprot P14555) which has been shown to drive high expression level of various proteins (3)) followed by the N-terminal linker sequence of PLA2R1 (E21 to W35), N-terminal 6xHis and 3xFlag tags, the triple domain CysR-FnII-CTLD1 (Q36 to H377) with factor Xa and thrombin cleavage sites and a C-terminal HA tag.

All other soluble and membrane-bound PLA2R1 constructs comprised the PLA2R1 signal peptide (M1 to A20) followed by its N-terminal linker sequence (E21 to W35) and the human PLA2R1 sequence coding for the different PLA2R1 recombinant proteins: soluble PLA2R1 (Q36 to S1397, full extracellular domain), CTLD2-8 (C2-C8: Y-357 to S1397), CTLD2-6 (C2-C6: Y357 to P1114), CTLD3-5 (C3-C5: V507 to S979), CTLD6-8 (C6-C8: K947 to S1397), CTLD6-7 (C6-C7: K947 to L1246), CTLD7-8 (C7-C8: E1097 to S1397), CysR (CR: Q36 to K164), FnII (H163 to G228), CTLD1 (C1: P222 to A375), CTLD2 (C2: H360 to E512), CTLD3 (C3: V507 to F661), CTLD4 (C4: N649 to W809), CTLD5 (C5: K797 to T957), CTLD6 (C6: K947 to P1114), CTLD7 (C7: E1097 to L1246), CTLD8 (C8: P1235 to S1397), Δ7 (P1235 to Q1463, membrane-bound CTLD8). All recombinant proteins were C-terminally HA-tagged (YPYDVPDYA). Soluble PLA2R1, CR, FnII, C1, C2, C3, C4, C5, C8 and Δ7 constructs were also N-terminally 3x-Flag-tagged (DYKDDDDK); soluble PLA2R1, CR, FnII, C1, C2, C3, C4 and C5 were also N-terminally 6x-His-tagged.

PLA2R1/MRC2 chimeras were produced in the open reading frame of membrane-bound mature MRC2 protein (G31 to E1479). The CysR or CTLD1 domain of MRC2 was replaced by the corresponding domain of PLA2R1 (E21 to H167 for CysR and D221 to H377 for CTLD1). Soluble chimeras of the CTLD6-CTLD7 region from MRC2 (T956 to H1258) were constructed by replacing either CTLD6 or CTLD7 with the corresponding domain from PLA2R1 (W943 to D1111 and T1102 to P1244, respectively). All constructs were prepared in pcDNA3.1/Zeo (–) expression vector with a PLA2R1 signal peptide and were C-terminally HA-tagged and N-terminally 6xHis- and 3xFlag-tagged.

After sequencing of all cDNA constructs, the expression plasmids were transfected into HEK293 cells using a homemade calcium phosphate transfection kit (4) or Exgen (Biomol GmbH, Hamburg, Germany). HEK293 cells were cultured in DMEM medium containing 1% penicillin/streptomycin solution and 10% heat-inactivated FBS (all from Gibco, Waltham, USA) at 37°C in a humidified atmosphere of 5% CO_2. Transfected cells were selected with 0.2 mg/mL Zeocin (InvivoGen, San Diego, USA). For larger-scale production of recombinant proteins, single clones or mixed populations stably selected were cultured to sub-confluency in complete medium at 37°C, then switched to serum-free medium (OptiMEM) and incubated at 37°C. For PLA2R1 constructs with low expression at 37°C, cells were grown at 30°C with or without tauroursodeoxycholic acid (TUDCA, Sigma-Aldrich, St. Louis, USA) or 4-phenyl butyric acid (PBA, Sigma-Aldrich, St. Louis, USA) to enhance expression, trafficking and/or folding of recombinant proteins as previously described for various mutated proteins (5-9). After seven days of expression, cell culture medium was collected and cells were washed with PBS, scrapped and lyzed in 20 mM Tris pH 7.4, 2 mM EDTA and protease inhibitor cocktail

(Roche Diagnosis, Basel, Swizterland). Cells were sonicated and centrifuged in a microcentrifuge apparatus at 14,000 rpm for five minutes at 4°C. The supernatant corresponding to the cytosolic fraction (CF) was collected and the pellet resuspended and solubilized in 50 mM Tris pH 7.4, 2 mM EDTA, 100 mM NaCl, 1% Triton X-100, 0.5% sodium deoxycholate with protease inhibitors. The suspension was sonicated, incubated for one hour at 4°C under rotation and centrifuged for 15 minutes at 14,000 rpm at 4°C. The supernatant corresponding to the solubilized fraction (SF) was recovered. Total protein concentration of each fraction was determined by BCA protein assay (Thermo Fisher Scientific, Waltham, USA). When the recombinant proteins were expressed at very low levels, culture medium was either precipitated with trichloroacetic acid (TCA) using standard protocol or purified by affinity chromatography on complete His-tag beads according to the manufacturer's protocol (Roche, Basel, Switzerland). Eluted purified proteins were concentrated and buffer-exchanged with Fxa buffer (50 mM Tris pH 8.0, 1 mM $CaCl_2$, 10 mM NaCl) and 5 mM N-dodecyl-N-N-dimethyl-3-ammonio-1-propanesulfonate (SB12) using a centricon centrifugal filter device (Amicon, Millipore, Bedford, USA) equipped with an YM-30 membrane.

Protease digestion of the triple domains CysR-FnII-CTLD1 constructs

Purified protein or culture medium from constructs B to G were digested overnight at 37°C with thrombin (Thr, Calbiochem, San Diego, USA), factor Xa (F_{Xa}, Amersham Biosciences, UK) or tobacco etch virus (TEV, Sigma-Aldrich, St. Louis, USA) proteases according to purchasers' recommendations. Cleaved products were immunodetected by WB.

Immunodetection of PLA2R1 recombinant proteins

Recombinant proteins were run on SDS-PAGE gels under reducing or non-reducing conditions as originally described by Laemmli (10). Proteins were transferred to a methanol-soaked poly-vinylidene difluoride membrane (PerkinElmer, Waltham, USA) under semi-dry conditions (25 mM Tris, 192 mM glycine, pH 8.5, 20% ethanol) using Trans-blot Turbo (Bio-rad laboratories, Hercules, USA) at 25 V constant for 30 minutes. Culture medium containing the proteins of interest was slot-blotted onto a nitrocellulose membrane (Whatman, Maidstino, UK). For both western and slot blots, non-specific binding was blocked with 5% (w/v) low-fat milk in PBS-Tween 0.05% for one hour or overnight at 4°C. Membranes were then incubated with primary antibody under agitation for two hours or overnight at 4°C. After three washes for five minutes each, the membranes were incubated with horseradish peroxidase (HRP)-

conjugated secondary antibody, under agitation for one hour. The membranes were washed three times for five minutes and the immunoreactive bands were detected with enhanced chemiluminescence substrate (ECL, PerkinElmer, Waltham, USA) and a Fusion-FX digital imager.

Immunoprecipitation of PLA2R1 epitope-containing domains

Proteins of interest were pulled-down from cell culture medium with MN patients' serum overnight at 4°C followed by incubation with anti-IgG4 affinity beads (Thermo Fisher Scientific, Waltham, USA) for one hour at 4°C. After three washes with Tris-buffered saline (TBS+: 20 mM Tris/HCl pH 7.2, 150 mM NaCl, 5 mM $CaCl_2$) and centrifugation in a microcentrifuge apparatus at 14,000 rpm for 15 minutes at 4°C, bound protein was eluted with 2x Laemmli buffer and analyzed by WB.

SUPPLEMENTARY RESULTS

CysR and CTLD1 are two N-terminal independent epitope-containing domains – We first clarified the controversy between overlapping (2) versus independent epitopes (4) within the N-terminal CysR-FnII-CTLD1 region by building up on the approach originally described by Kao and coworkers based on site-directed mutagenesis coupled to serial insertion of protease cleavage sites between domains (2). In total, we produced seven soluble constructs expressing CysR-FnII-CTLD1 recombinant proteins with N-terminal 6xHis/3xFlag and C-terminal HA tags, and harboring either no protease cleavage site (construct A, used as a control) or different protease cleavage sites (constructs B-G) between PLA2R1 domains. We then cleaved the recombinant proteins by proteases and tested the WB reactivity of sera from MN patients with different epitope profiles determined by indirect ELISA (Figure S1).

In construct B, we introduced a thrombin cleavage site between CysR and FnII for which the analysis was straightforward (Figures 1A and S2A). The expression as a folded protein was as good as construct A (Figure S2B) and cleavage by thrombin was validated by detection of the expected fragments under both reducing and non-reducing conditions with anti-tag antibodies (Figure S2C). Among seven patients with different epitope profiles (Figure S1), two reacted to CysR (MN1-2), two reacted to FnII-CTLD1 (MN3-4) and the last three reacted to cleaved CysR and FnII-CTLD1 (MN5-7) domains (Figure 1B). This suggests the presence of independent epitopes in the CysR and CTLD1 domains, a finding in contrast with previous data suggesting an overlapping epitope (2).

To further test the presence of an overlapping epitope between the CysR and CTLD1 domains that might be sensitive to a specific cleavage between FnII and CTLD1, we produced construct C (Figures 1A, S3A and S4A) exactly as described (2). Noticeably, the thrombin cleavage site was inserted within the first disulfide bond of CTLD1 and not in the small linker region between FnII and CTLD1 (2). Therefore, we designed two additional constructs. Construct D was identical to C but with an additional factor Xa (F_{Xa}) cleavage site introduced between FnII and CTLD1 (Figure S4A). Construct E had the F_{Xa} cleavage site between the FnII and CTLD1 domains but without the thrombin cleavage site within CTLD1 (Figure S5A). Constructs C and D were hardly expressed in both culture medium and cell lysate (Figure S4B) while construct E was well expressed (Figure S5B), indicating misfolding of constructs C and D likely due to poor pairing of the cysteines forming the CTLD1 disulfide bridge. The expression and folding of these constructs could be partially rescued by growing cells at 30°C (Figure S4B) or by adding chemical chaperones to cell culture (Figures S4C and S4D). No additive/synergistic effect was observed (Figure S4D). Growth at low temperature

was most effective but still insufficient to produce enough proteins for a direct analysis (Figure S3B) and constructs had to be His-tag purified before analysis.

Efficient cleavage of construct C by thrombin was validated by the presence of two fragments under reducing conditions detected with anti-tag antibodies (Figure S3C). However, construct C appeared uncleaved under non-reducing conditions (Figure S3C). This is consistent with the two PLA2R1 fragments being maintained by the CTLD1 disulfide bond in a covalent manner, despite actual cleavage of the amino acid peptide bond by thrombin (Figure S3A). Consequently, under non-reducing conditions, serum from different MN patients could only react with the triple domain instead of any cleaved fragments, which may be interpreted as an overlapping epitope between the different domains (Figure 1C). We next tried to cleave constructs D and E with F_{Xa}. Cleavage of construct E was ineffective under both native and partially denaturing conditions (Figure S5B). Cleavage of construct D was also ineffective before (Figure S5C) or after thrombin cleavage (data not shown). We thus prepared construct F where a TEV protease cleavage site was introduced within an extended linker region between FnII and CTLD1 (Figure S5A). Cleavage of this construct was also unsuccessful with different sources of TEV enzyme (Figure S5D).

Finally, construct G was prepared with a thrombin cleavage site inserted within the extended linker region between FnII and CTLD1 (Figure S3A). Construct G was expressed at higher levels than construct C, and could be cleaved by thrombin, even though the digestion was incomplete (Figure S3C). However, this was sufficient to demonstrate that several patients' sera had preferential reactivity to either CysR-FnII or CTLD1 or the two cleaved domains (Figure 1D), in accordance with their epitope profile determined by ELISA (Figure S1).

Reactivity of patients' sera to CTLD5 is temperature- and DTT-sensitive — To better understand the differential reactivity of CTLD5 to patient's sera by ELISA versus WB, we tested the effect of heat denaturation (Figure S8) and reduction with DTT for CTLD5 and the four other epitope-containing domains (Figure S9). Heat denaturation showed that CTLD5 is the most sensitive among CTLDs, with a 50% denaturing temperature around 55°C, while CysR is less sensitive (Figure S8). CTLD1 and CTLD8 contain three disulfides while CTLD5 and CTLD7 contain only two (Figure S9A). Reduction with DTT at the denaturing temperature of 56°C had a strong effect on all domains. In contrast, increasing concentrations of DTT at non-denaturing temperatures (RT and 30°C) had little effect on CTLD5, CTLD7 and CTLD8, but were partially effective on CysR and CTLD1 (Figures S9B and S9C).

LEGEND TO SUPPLEMENTARY FIGURES

Figure S1 – Epitope profile of MN patients used to demonstrate independent reactivity to CysR and CTLD1 epitope-containing domains. The indicated epitope profiles were determined by indirect ELISA on wells coated with CysR-FnII-CTLD1, CysR or CTLD1 single domains, or mock medium (HA-capture ELISA assays). MN patients' sera were incubated at a dilution of 1:100. The same set of patients was used for experiments using the triple domain CysR-FnII-CTLD1 cleaved by various proteases (as depicted in Figure 1 and main text) as well as in experiments with chimeras between MRC2 and PLA2R1 (as depicted in Figure 2 and main text).

Figure S2 – Structure, expression and cleavage of construct B. (A) Schematic diagram showing the structure of soluble CysR-FnII-CTLD1 triple domains with N-terminal 6xHis and 3xFlag tags and C-terminal HA-tag: construct A has no thrombin cleavage site while construct B has a thrombin (Thr) cleavage site inserted between the CysR and FnII domains. The expected mass is calculated without the contribution of glycosylation. Both constructs were well expressed in HEK 293 cells. **(B)** Expression of the constructs was validated by western blot with anti-HA antibody (1:5,000, under reducing and non-reducing conditions) and with patient MN1 (1:100, non-reducing conditions). **(C)** Cleavage of construct B by thrombin was validated by WB using anti-Flag (1:1,000) and anti-HA (1:5,000) antibodies under both reducing and non-reducing conditions. N.A.: not applicable.

Figure S3 – Structure, expression and cleavage of constructs C and G. (A) Schematic diagram showing the structure of soluble CysR-FnII-CTLD1 triple domains with N-terminal 6xHis and 3xFlag tags and C-terminal HA-tag: Construct A has no thrombin cleavage site, construct C has a thrombin (Thr) cleavage site inserted within the first disulfide bond of CTLD1 by replacing 6 amino acids, and construct G has a thrombin (Thr) cleavage site inserted in the linker region between the FnII and CTLD1 domains, thereby extending the linker. Expected mass is calculated without the contribution of glycosylation. Constructs A and G are well expressed in HEK293 cells, while construct C was poorly expressed at 37°C. Expression was rescued by growing cells at 30°C (see methods and Figure S4). **(B)** Relative expression in cell medium of construct A at 37°C and construct C at 30°C as measured by WB with anti-HA antibody (1:5,000, under reducing and non-reducing conditions) and with patient MN1 (1:100, non-reducing conditions). **(C)** Cleavage of construct C and G by thrombin was validated with anti-Flag (1:1,000) and anti-HA (1:5,000) antibodies by WB under reducing conditions. Cleavage of construct G by thrombin was also validated under non-reducing conditions. However, the actual cleavage by thrombin could not be evidenced

for construct C under non-reducing conditions, because of insertion of the thrombin cleavage site within the first disulfide bridge of CTLD1, with that disulfide maintaining the two cleaved fragments (CysR-FnII and CTLD1). N.A.: not applicable.

Figure S4 – Misfolding of constructs C and D was partially rescued by growing HEK293 cells at low temperature or by the addition of chemical chaperones. **(A)** Schematic diagram showing the structure of soluble CysR-FnII-CTLD1 triple domains N-terminally 6xHis- and 3xFlag-tagged and C-terminally HA-tagged expressed in HEK 293 cells: construct C is as in Figure S3 while construct D has an additional factor Xa (F_{Xa}) cleavage site introduced in the linker region between FnII and CTLD1. Both constructs were poorly expressed in cell medium from HEK293 cells at 37°C because of insertion of the thrombin (Thr) cleavage site within the first disulfide bond in CTLD1. **(B)** Detection of recombinant proteins after expression of constructs C and D in HEK293 cells grown at 37°C and 30°C. Cytosolic (CF) and solubilized (SF) cellular fractions as well as medium (M) were analyzed by WB under reducing and non-reducing conditions using anti-HA antibody (1:5,000). No or weak expression was observed in cell lysates and medium at 37°C, while higher expression was seen in medium at 30°C. **(C)** Detection of constructs C and D with MN1 (1:100) by ELISA (anti-HA capture assays) in cell lysate and culture medium of HEK293 cells grown at 37°C in the presence of TUDCA or PBA at different concentrations. **(D)** Expression of constructs C and D in culture medium of HEK 293 cells incubated at 37°C versus 30°C in the presence of TUDCA or PBA at different concentrations as detected by ELISA with MN1 (1:100). N.A.: not applicable; Thr: thrombin; F_{Xa}: factor Xa; CF: cytosolic fraction; SF: solubilized fraction; M: culture medium; TUDCA: tauroursodeoxycholic acid; PBA: 4-phenyl butyric acid.

Figure S5 – Proteolysis of the CysR-FnII-CTLD1 triple domain by F_{Xa} and TEV proteases is likely prevented by steric hindrance and poor access to the recognition sites. **(A)** Schematic diagram showing the structure of soluble CysR-FnII-CTLD1 triple domains N-terminally 6xHis- and 3xFlag-tagged and C-terminally HA-tagged expressed in HEK 293 cells: constructs A and D are as in Figure S4. Constructs E and F have F_{Xa} and TEV protease cleavage sites inserted in the linker region between the FnII and CTLD1 domains, respectively. The expected mass is calculated without the contribution of glycosylation and cleavage efficiency is indicated. **(B)** Absence of cleavage of construct E by F_{Xa} protease under various denaturing conditions as seen by WB under reducing conditions using anti-HA antibody (1:5,000). **(C)** Absence of cleavage of construct D by F_{Xa} even though it is efficiently cleaved by thrombin, as observed by WB under reducing conditions using anti-HA antibody(1:5,000). **(D)** Absence of cleavage of construct F by different sources of commercial

TEV proteases as seen by WB (reducing conditions) with anti-HA antibody (1:5,000). N.A.: not applicable; F_{Xa}: factor Xa, TEV: Tobacco Etch Virus; DOC: sodium deoxycholate.

Figure S6 – Sera from different MN patients recognized two novel epitope-containing domains in the CTLD2–CTLD8 region of PLA2R1. **(A)** Schematic diagram of several C-terminally HA-tagged soluble and membrane-bound constructs within the CTLD2–CTLD8 region of PLA2R1. The expected mass is calculated without the contribution of glycosylation. **(B)** Expression of PLA2R1 recombinant proteins in HEK293 cells was validated with anti-HA antibody (1:5,000) by WB under reducing conditions. **(C)** Representative results of four patients (1:100) from a preliminary ELISA screen of 28 patients. Patients MN5, MN11 and MN1 recognize the CTLD2-6 region of PLA2R1 while patient MN1 is also recognizing CTLD8 and Δ7. Patient MN12 recognizes only the CysR domain, and is negative on all constructs within the C2-C8 region.

Figure S7 – WB, immunoprecipitation and dot-blot experiments confirming that single domains CTLD5 and CTLD8 contain independent epitopes recognized by PLA2R1-positive patients. **(A)** WB (non-reducing conditions) with anti-HA antibody (1:5,000) validating the expression and transfer of CTLD5 and CTLD8 as single domains. Representative WB (non-reducing conditions) with patients' sera used at 1:25 showed that patients could not detect CTLD5 while several patients could detect CTLD8. **(B)** Immunoprecipitation of CTLD5 and CTLD8 with different patients' sera followed by WB detection under reducing conditions with anti-HA antibody (1:5,000). In these conditions, both CTLD5 and CTLD8 could be detected. **(C)** Dot-blot transfer of single domains CTLD5 and CTLD8 under non-denaturing conditions was validated with anti-HA antibody (1:5,000). Representative dot-blots showing reactivity of patients against both CTLD5 and CTLD8 domains versus mock-negative control.

Figure S8 – Heating of the epitope-containing domains shows that reactivity of patients' sera is more rapidly lost for CTLD5 than other PLA2R1 domains. **(A)** ELISA reactivity of four MN patients' sera against CysR, CTLD1, CTLD5, CTLD7 and CTLD8 single domains which have been exposed to different temperatures (no treatment (room temperature), 56°C for 30 minutes or 95°C for 10 min) before ELISA. **(B)** ELISA reactivity of MN 1 against the various epitope-containing domains which have been exposed to different temperatures for 10 minutes before ELISA.

Figure S9 – Reactivity of patients' sera to CTLD5 and other PLA2R1 domains is sensitive to DTT when combined to heat. **(A)** Sequence alignment of the four CTLD epitope-containing domains showing the presence of two conserved disulfides in all CTLDs and a third disulfide only present in CTLD1 and CTLD8. The CysR domain contains three disulfides (not shown). **(B)** ELISA reactivity for four MN patients against the epitope-containing domains after treatment with 10 mM DTT at different temperatures (no treatment: no DTT/room temperature). **(C)** ELISA reactivity of MN 1 against the epitope-containing domains treated with different concentrations of DTT for 30 minutes at room temperature (RT) or 10 minutes at 30°C before ELISA.

Figure S10 – Anti-PLA2R1 titer increases as the number of positive epitope-containing domains increases. Distribution of anti-PLA2R1 titer (commercial ELISA, total IgG) according to the number of positive epitope-containing domains (IgG4, n=142).

Figure S11 – Competition assays by ELISA (IgG4 detection) between recombinant PLA2R1 (full extracellular region) and different domains of PLA2R1 for all PLA2R1-positive MN patients with available serum (n=136). PLA2R1-positive MN patients were ranked by decreasing percentage of competition with recombinant proteins: PLA2R1 (full extracellular region), CysR-FnII-CTLD1, CysR, CTLD1, CTLD5 and CTLD7. The total competition with PLA2R1 (full extracellular region) for all patients validated the assay conditions. For a majority of patients (113/142, 79.6%), competition with CysR-FnII-CTLD1 was higher than 65%, indicating that CysR and/or CTLD1 domains contribute to most of the PLA2R1 signal. On the other hand, CTLD5 and CTLD7 have a minor contribution to the PLA2R1 signal for most patients since they contribute to a significant part of the PLA2R1 signal for only a few patients (12/142), which are classified as non-iDom. Importantly, note that the percentage of competition for each individual patient and individual domain are different, and consequently, patients are not ranked in the same order in each panel (but by decreasing values of competition for each recombinant PLA2R1 competing protein).

Figure S12 – Competition assays by ELISA (IgG4 detection) between recombinant PLA2R1 (full extracellular region) and CysR or CTLD1 domains mixed with the large C-terminal region CTLD2-8 for all PLA2R1-positive MN patients with available serum (n=136). Patients were ranked by decreasing percentage of competition with CysR (**A, upper panel**), CysR mixed with CTLD2-8 (**A, lower panel**), CTLD1 (**B, upper panel**) and CTLD1 mixed with CTLD2-8 (**B, lower panel**). The comparison between lower and upper graphics in both panels A and B shows a minor contribution of the C-terminal epitope-containing domains (CTLD5, CTLD7 and CTLD8) to the PLA2R1 signal. In mirror, the remaining

signal for each patient (empty space in the lower graphics) can also be seen as the actual contribution of anti-CTLD1 (**A**) or anti-CysR (**B**) signal relative to the anti-PLA2R1 titer, in line with data shown in Figure S11. Importantly, note that the percentage of competition for each individual patient and individual domain are different, and consequently, patients are not ranked in the same order in each panel (but by decreasing values of competition for each recombinant PLA2R1 competing protein).

Figure S13 – Correlation between anti-PLA2R1 titer (in-house IgG4 ELISA) and anti-PLA2R1 titer (commercial total IgG ELISA), anti-CysR or anti-CTLD1 titers (in-house IgG4 ELISA) for PLA2R1-positive MN patients as a whole (n=141) or according to their immunodominant profile (n=135). (A) Correlations between the anti-PLA2R1 titers obtained with the commercial ELISA (total IgG) and in-house ELISA (IgG4) **(B and C)** Correlations between anti-PLA2R1 titer (in-house IgG4 ELISA) and anti-CysR **(B)** or anti-CTLD1 **(C)** titers (in-house IgG4 ELISA).

Figure S14 – Anti-CysR and anti-CTLD1 titers increase as the number of positive epitope-containing domains increases. (A) Distribution of anti-CysR titer (IgG4) according to the number of positive epitope-containing domains for the cohort as a whole (n=141) or considering positivity or not for CTLD1, showing lower increase of anti-CysR titer in the CTLD1 positive patients. **(B)** Anti-CTLD1 titer (IgG4) according to the number of positive epitope-containing domains for the cohort as a whole (n=141).

Figure S15 Anti-PLA2R1, anti-CysR and anti-CTLD1 titers vary according to the immunodominant profile of PLA2R1-positive MN patients. (A) Anti-PLA2R1 titer (commercial ELISA, total IgG) is higher in the iC1 group, as compared to the iCysR and non-iDom groups. **(B and C)** Anti-CysR **(B)** and anti-CTLD1 **(C)** titers (in-house ELISA, IgG4) according to the immunodominant profile. Note that similarly to anti-PLA2R1 titer, anti-CysR and anti-CTLD1 titers are higher in iC1 patients as compared to iCR and non-iDom patients. All anti-PLA2R1 titers are similar between iCR and non-iDom patients.

REFERENCES

1. Mathieu J, Alvarez E, and Alvarez PJ. Recombination-assisted megaprimer (RAM) cloning. *MethodsX.* 2014;1(23-9.
2. Kao L, Lam V, Waldman M, Glassock RJ, and Zhu Q. Identification of the immunodominant epitope region in phospholipase A2 receptor-mediating autoantibody binding in idiopathic membranous nephropathy. *J Am Soc Nephrol.* 2015;26(2):291-301.
3. Valentin E, Ghomashchi F, Gelb MH, Lazdunski M, and Lambeau G. On the diversity of secreted phospholipases A2. Cloning, tissue distribution, and functional expression of two novel mouse group II enzymes. *J Biol Chem.* 1999;274(44):31195-202.
4. Seitz-Polski B, Dolla G, Payre C, Girard CA, Polidori J, Zorzi K, Birgy-Barelli E, Jullien P, Courivaud C, Krummel T, et al. Epitope Spreading of Autoantibody Response to PLA2R Associates with Poor Prognosis in Membranous Nephropathy. *J Am Soc Nephrol.* 2016;27(5):1517-33.
5. Denning GM, Anderson MP, Amara JF, Marshall J, Smith AE, and Welsh MJ. Processing of mutant cystic fibrosis transmembrane conductance regulator is temperature-sensitive. *Nature.* 1992;358(6389):761-4.
6. Morello JP, Petaja-Repo UE, Bichet DG, and Bouvier M. Pharmacological chaperones: a new twist on receptor folding. *Trends in pharmacological sciences.* 2000;21(12):466-9.
7. Gora S, Perret C, Jemel I, Nicaud V, Lambeau G, Cambien F, Ninio E, Blankenberg S, Tiret L, and Karabina SA. Molecular and functional characterization of polymorphisms in the secreted phospholipase A2 group X gene: relevance to coronary artery disease. *J Mol Med.* 2009;87(7):723-33.
8. Cortez L, and Sim V. The therapeutic potential of chemical chaperones in protein folding diseases. *Prion.* 2014;8(2).
9. Chen YM, Zhou Y, Go G, Marmerstein JT, Kikkawa Y, and Miner JH. Laminin beta2 gene missense mutation produces endoplasmic reticulum stress in podocytes. *J Am Soc Nephrol.* 2013;24(8):1223-33.
10. Laemmli UK. Cleavage of structural proteins during the assembly of the head of bacteriophage T4. *Nature.* 1970;227(259):680-5.

Table S1 – Detailed information concerning treatment and outcome after first-line of therapy of the PLA2R1-positive patients as a whole (overall) and according to immunodominance. Values are present as n (%). NIAT, non-immunosuppressive anti-proteinuric treatment; IS, immunosuppressive treatment; ESRD, end-stage renal disease.

Event	Overall (n=142)	iCR (n=75)[A]	iC1 (n=49)[A]	non-iDom (n=12)[A]
Treatment (n (%))				
NIAT	61 (43.0)	37 (49.3)	19 (38.8)	3 (25.0)
IS	81 (57.0)	38 (50.7)	30 (61.2)	9 (75.0)
Rituximab	61 (43.0)	27 (36.0)	25 (51.0)	6 (50.0)
Ponticelli	10 (7.0)	7 (9.3)	1 (2.0)	2 (16.7)
Corticosteroids	9 (6.3)	3 (4.0)	4 (8.2)	1 (8.3)
Immunoglobulin therapy	1 (0.7)	1 (1.3)	0 (0.0)	0 (0.0)
Type of response (n (%))				
Combined remission	82 (57.7)	48 (64.0)	20 (40.8)	9 (75.0)
NIAT-induced	31 (21.8)	20 (26.7)	8 (16.3)	2 (16.7)
Rituximab-induced	42 (29.6)	22 (29.3)	11(22.4)	6 (50.0)
Ponticelli-induced	5 (3.5)	5 (6.7)	0 (0.1)	0 (0.0)
Corticosteroids-induced	4 (2.8)	1 (1.3)	1 (2.0)	1 (8.3)
Immunoglobulin therapy induced	0 (0.0)	0 (0.0)	0 (0.0)	0 (0.0)
No remission	60 (42.3)	27 (36.0)	29 (59.2)	3 (25.0)
Active disease	48 (33.8)	22 (29.3)	25 (51.0)	1 (8.3)
ESRD	12 (8.5)	5 (6.7)	5 (8.2)	2 (16.7)

[A] For six patients, there was not enough serum available to determine their immunodominance.

Table S2 – Anti-PLA2R1 and immunodominance as prognostic factors of clinical remission (unadjusted and adjusted analyses, change of reference).

Variable	Unadjusted	Adjusted Model 1	Adjusted Model 2	Adjusted Model 3	Adjusted Model 4
	Odds Ratio (95% Confidence Interval)	Odds Ratio (95% Confidence Interval)	Odds Ratio (95% Confidence Interval)	Odds Ratio (95% Confidence Interval)	Odds Ratio (95% Confidence Interval)
Calculated eGFR (mL/min/1.73 m^2)	1.014 (1.002-1.027)	1.010 (0.997-1.024)	1.010 (0.996-1.023)	1.012 (1.000-1.026)	1.013 (1.000-1.026)
Proteinuria (g/day)	0.922 (0.846-1.005)	0.952 (0.866-1.047)	0.956 (0.868-1.052)	0.933 (0.852-1.021)	0.929 (0.848-1.018)
Treatment					
NIAT	1	1		1	
Immunosuppressive (IS)	1.567 (0.787-3.120)	1.999 (0.921-4.340)		1.892 (0.895-4.001)	
Anti-PLA2R1 median (RU/mL, total IgG)					
< 64.8	1	1			
≥ 64.8	0.237 (0.114-0.492)	0.255 (0.117-0.558)			
Anti-PLA2R1 titer and treatment combined					
IS + anti-PLA2R1 ≥ 64.8	1		1		
IS + anti-PLA2R1 < 64.8	3.250 (1.199-8.807)		3.149 (1.142-8.686)		
NIAT + anti-PLA2R1 ≥ 64.8	0.350 (0.122-1.002)		0.395 (0.135-1.156)		
NIAT + anti-PLA2R1 < 64.8	3.250 (1.199-8.807)		2.079 (0.738-5.854)		
Immunodominance					
iCR/non-iDom	1			1	
iC1	0.351 (0.170-0.724)			0.365 (0.171-0.781)	
Immunodominance and treatment combined					
IS + iC1	1				1
IS + iCR/non-iDom	4.773 (1.762-12.925)				4.467 (1.605-12.432)
NIAT + iC1	1.091 (0.339-3.506)				1.068 (0.323-3.535)
NIAT + iCR/non-iDom	1.833 (0.702-4.788)				1.534 (0.561-4.196)

Number of observations analyzed: 135, 77 clinical remissions.

eGFR was calculated according to the Chronic Kidney Disease Epidemiology Collaboration (CKD-EPI) Equation. NIAT, non-immunosuppressive anti-proteinuric treatment; IS, immunosuppressive treatment.

Table S3 – Immunodominance as prognostic factor of clinical remission with iCR and non-iDom patients being considered as separate groups (unadjusted and adjusted analyses).

Variable	Univariable	Multivariable Model 1	Multivariable Model 2
	Odds Ratio (95% Confidence Interval)	Odds Ratio (95% Confidence Interval)	Odds Ratio (95% Confidence Interval)
Calculated eGFR (mL/min/1.73 m^2)	1.014 (1.002-1.027)	1.013 (1.000-1.026)	1.013 (1.000-1.027)
Proteinuria (g/day)	0.922 (0.846-1.005)	0.929 (0.848-1.018)	0.923 (0.839-1.016)
Treatment			
NIAT	1	1	
IS	1.567 (0.787-3.120)	1.822 (0.856-3.880)	
Immunodominance			
iCR	1	1	
non-iDom	1.625 (0.404-6.531)	1.686 (0.384-7.407)	
iC1	0.374 (0.178-0.785)	0.394 (0.180-0.863)	
Immunodominance and treatment combined			
NIAT + iCR	1		1
NIAT + non-iDom	1.700 (0.142-20.422)		1.066 (0.084-13-472)
NIAT + iC1	0.618 (0.202-1.889)		0.706 (0.224-2.231)
IS + iCR	2.644 (0.982-7.124)		2.642 (0.955-7.312)
IS + non-iDom	2.975 (0.544-16.273)		4.748 (0.738-30.539)
IS + iC1	0.567 (0.214-1.503)		0.663 (0.238-1.841)
Immunodominance and treatment combined (change of reference)			
IS + iC1	1		1
IS + iCR	4.667 (1.637-13.304)		3.988 (1.360-11.693)
IS + non-iDom	5.250 (0.928-29.700)		7.165 (1.115-46.067)
NIAT + iC1	1.091 (0.339-3.506)		1.066 (0.321-3.537)
NIAT + iCR	1.765 (0.665-4.681)		1.509 (0.543-4.193)
NIAT + non-iDom	3.000 (0.244-36.883)		1.609 (0.121-21.400)

Number of observations analyzed: 135, 77 clinical remissions.

eGFR was calculated according to the Chronic Kidney Disease Epidemiology Collaboration (CKD-EPI) Equation. NIAT, non-immunosuppressive anti-proteinuric treatment; IS, immunosuppressive treatment.

Table S4 – Baseline characteristics and clinical outcome of NIAT- or rituximab-treated patients according to their immunodominance and with an anti-PLA2R1 titer above 200 RU/mL. Values are present as n (%) or median [IQR]. eGFR was calculated according to the Chronic Kidney Disease Epidemiology Collaboration (CKD-EPI) Equation. NIAT, non-immunosuppressive anti-proteinuric treatment; ESRD, end-stage renal disease.

Characteristics	Overall (n=35)	iCR/non-iDom (n=14)	iC1 (n=21)	p-value
Age (years)	63.0 [49.0-71.0]	70.0 [58.8-76.3]	58.0 [47.0-64.0]	0.0392
Gender (M/F), n (%)	19 (54.3)/16 (45.7)	7 (50.0)/7 (50.0)	12 (57.1)/9 (42.9)	0.7391
Clinical parameters				
Serum albumin (g/L) [A]	21.0 [17.9-26.8]	21.0 [18.0-27.0]	22.0 [17.0-26.0]	0.8440
Serum creatinine (µmol/L)	100.0 [80.0-128.0]	100.5 [78.0-183.5]	95.0 [82.0-126.0]	0.8746
Calculated eGFR (mL/min/1.73 m^2)	66.0 [40.0-86.0]	63.0 [33.5-75.8]	66.0 [39.5-86.5]	0.7460
Proteinuria (g/day) [B]	6.8 [4.3-9.3]	7.4 [4.2-8.0]	6.4 [4.3-10.6]	0.9170
Anti-PLA2R1 autoantibodies				
Anti-PLA2R1 titer (RU/mL)				
Commercial ELISA (total IgG)	454.4 [251.2-621.4]	506.4 [247.6-643.8]	411.0 [254.1-610.3]	0.6778
Treatment (n(%))				0.1662
NIAT	19 (54.3)	10 (71.4)	9 (42.9)	
Rituximab	16 (45.7)	4 (28.5)	12 (57.1)	
Clinical outcome (n (%))				0.4606
Combined remission	11 (31.4)	3 (21.4)	8 (38.1)	
Active disease or ESRD	24 (68.6)	11 (78.6)	13 (61.9)	
Clinical outcome after NIAT (n (%))				0.5820
Combined remission	3 (15.8)	1 (10.0)	2 (22.2)	
Active disease or ESRD	16 (84.2)	9 (90.0)	7 (77.8)	
Clinical outcome after rituximab (n (%))				>0.9999
Combined remission	8 (50.0)	2 (50.0)	6 (50.0)	
Active disease or ESRD	8 (50.0)	2 (50.0)	6 (50.0)	

[A] Serum albumin values were missing for 7 patients (3 iCR patients and 4 iC1 patients). [B] Proteinuria value was missing for one iC1 patient.

Table S5 – Baseline characteristics and clinical outcome of NIAT- or rituximab-treated patients according to their immunodominant profile and with an anti-PLA2R1 titer below 50 RU/mL. Values are present as n (%) or median [IQR]. eGFR was calculated according to the Chronic Kidney Disease Epidemiology Collaboration (CKD-EPI) Equation. NIAT, non-immunosuppressive anti-proteinuric treatment; ESRD, end-stage renal disease.

Characteristics	Overall (n=45)	iCR/non-iDom (n=32)	iC1 (n=13)	p-value
Age (years)	52.0 [23.0-61.5]	53.5 [44.5-63.5]	42.0 [41.0-60-5]	0.3748
Gender (M/F), n (%)	37 (82.2)/8 (17.8)	26 (81.3)/6 (18.7)	11 (84.6)/2 (15.4)	>0.9999
Clinical parameters				
Serum albumin (g/L) [A]	25.0 [207-29.5]	27.0 [22.0-30.7]	19.5 [16.6-24.4]	<0.0063
Serum creatinine (µmol/L)	95.0 [72.5-114.5]	95.5 [72.5-118.0]	88.0 [70.5-110.0]	0.4240
Calculated eGFR (mL/min/1.73 m^2)	80.0 [53.0-105.0]	75.0 [46.5-105.5]	80.0 [62.5-105.0]	0.5649
Proteinuria (g/day)	4.9 [3.2-8.3]	3.6 [1.4-7.1]	7.7 [5.3-10.1]	0.0096
Anti-PLA2R1 autoantibodies				
Anti-PLA2R1 titer (RU/mL)				
Commercial ELISA (total IgG)	19.7 [12.6-30.6]	19.8 [11.0-29.0]	19.1 [13.27-36.4]	0.3923
Treatment (n(%))				>0.9999
NIAT	26 (57.8)	18 (56.3)	8 (61.5)	
Rituximab	19 (42.2)	14 (43.7)	5 (38.5)	
Clinical outcome (n (%))				0.4411
Combined remission	35 (77.8)	26 (82.3)	9 (69.2)	
Active disease or ESRD	10 (22.2)	6 (18.7)	4 (30.8))	
Clinical outcome after NIAT (n (%))				0.6673
Combined remission	18 (69.2)	13 (72.2)	5 (62.5)	
Active disease or ESRD	8 (30.8)	5 (27.8)	3 (37.5)	
Clinical outcome after rituximab (n (%))				0.4678
Combined remission	17 (89.5)	13 (92.9)	4 (80.0)	
Active disease or ESRD	2 (10.5))	1 (7.1)	1 (20.0)	

[A] Serum albumin values were missing for 3 iC1 patients

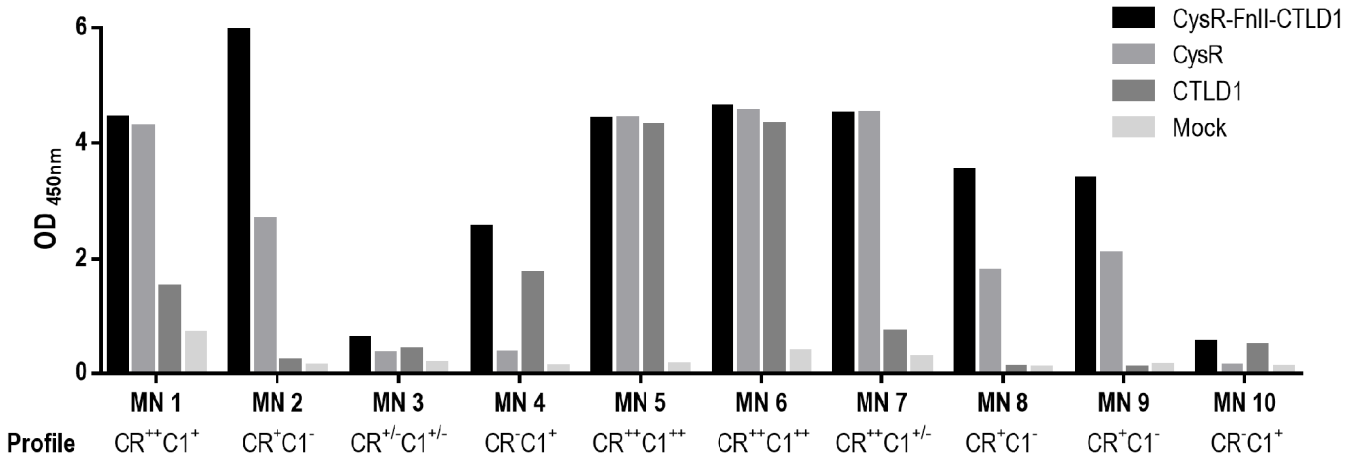

Figure S1 - Epitope profile of MN patients used to demonstrate independent reactivity to CysR and CTLD1 epitope-containing domains. The indicated epitope profiles were determined by indirect ELISA on wells coated with CysR-FnII-CTLD1, CysR or CTLD1 single domains, or mock medium (HA-capture ELISA assays). MN patients' sera were incubated at a dilution of 1:100. The same set of patients was used for experiments using the triple domain CysR-FnII-CTLD1 cleaved by various proteases (as depicted in Figure 1 and main text) as well as in experiments with chimeras between MRC2 and PLA2R1 (as depicted in Figure 2 and main text).

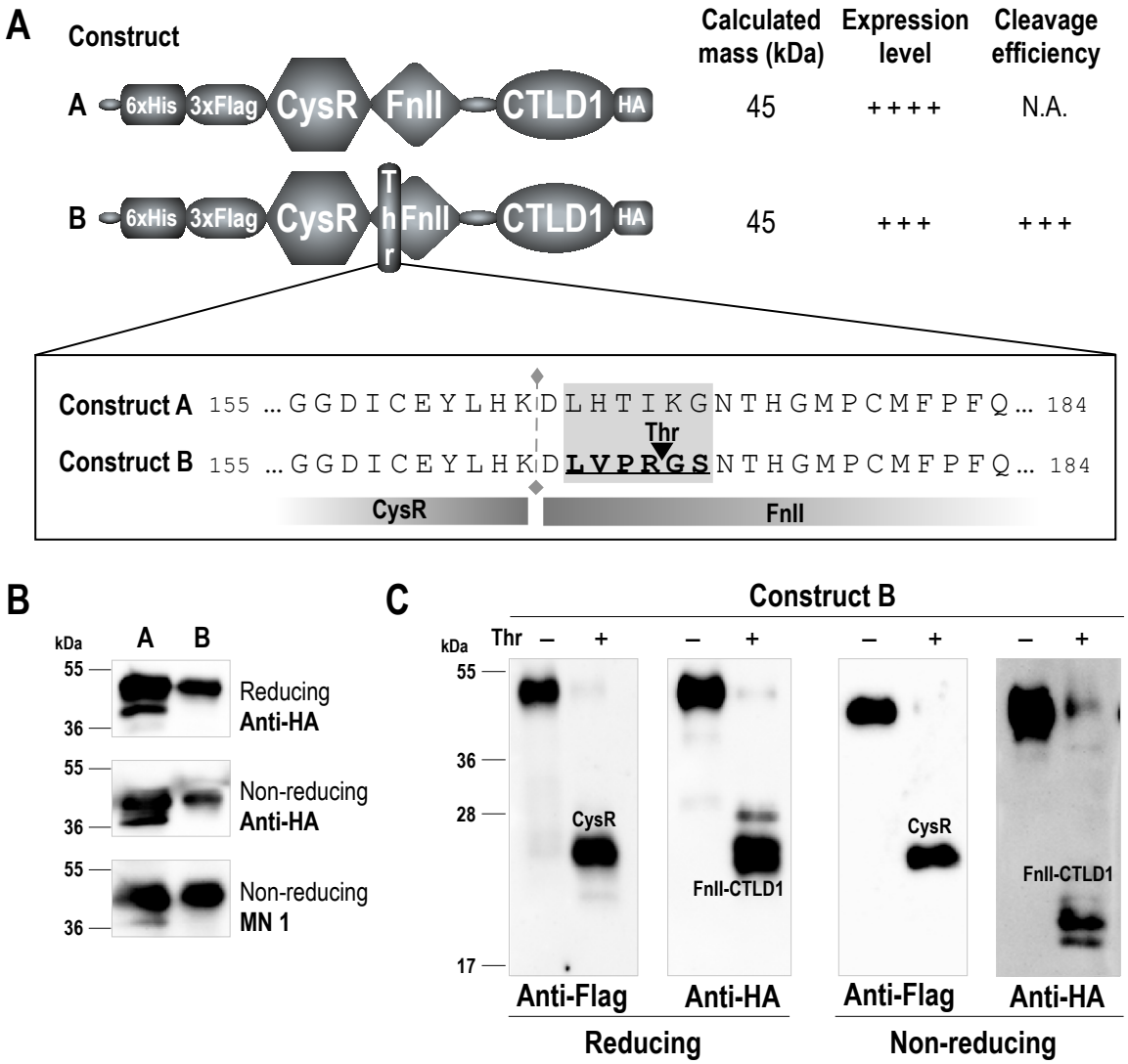

Figure S2 - Structure, expression and cleavage of construct B. (A) Schematic diagram showing the structure of soluble CysR-FnII-CTLD1 triple domains with N-terminal 6xHis and 3xFlag tags and C-terminal HA-tag: construct A has no thrombin cleavage site while construct B has a thrombin (Thr) cleavage site inserted between the CysR and FnII domains. The expected mass is calculated without the contribution of glycosylation. Both constructs were well expressed in HEK 293 cells. **(B)** Expression of the constructs was validated by western blot with anti-HA antibody (1:5,000, under reducing and non-reducing conditions) and with patient MN1 (1:100, non-reducing conditions). **(C)** Cleavage of construct B by thrombin was validated by WB using anti-Flag (1:1,000) and anti-HA (1:5,000) antibodies under both reducing and non-reducing conditions. N.A.: not applicable.

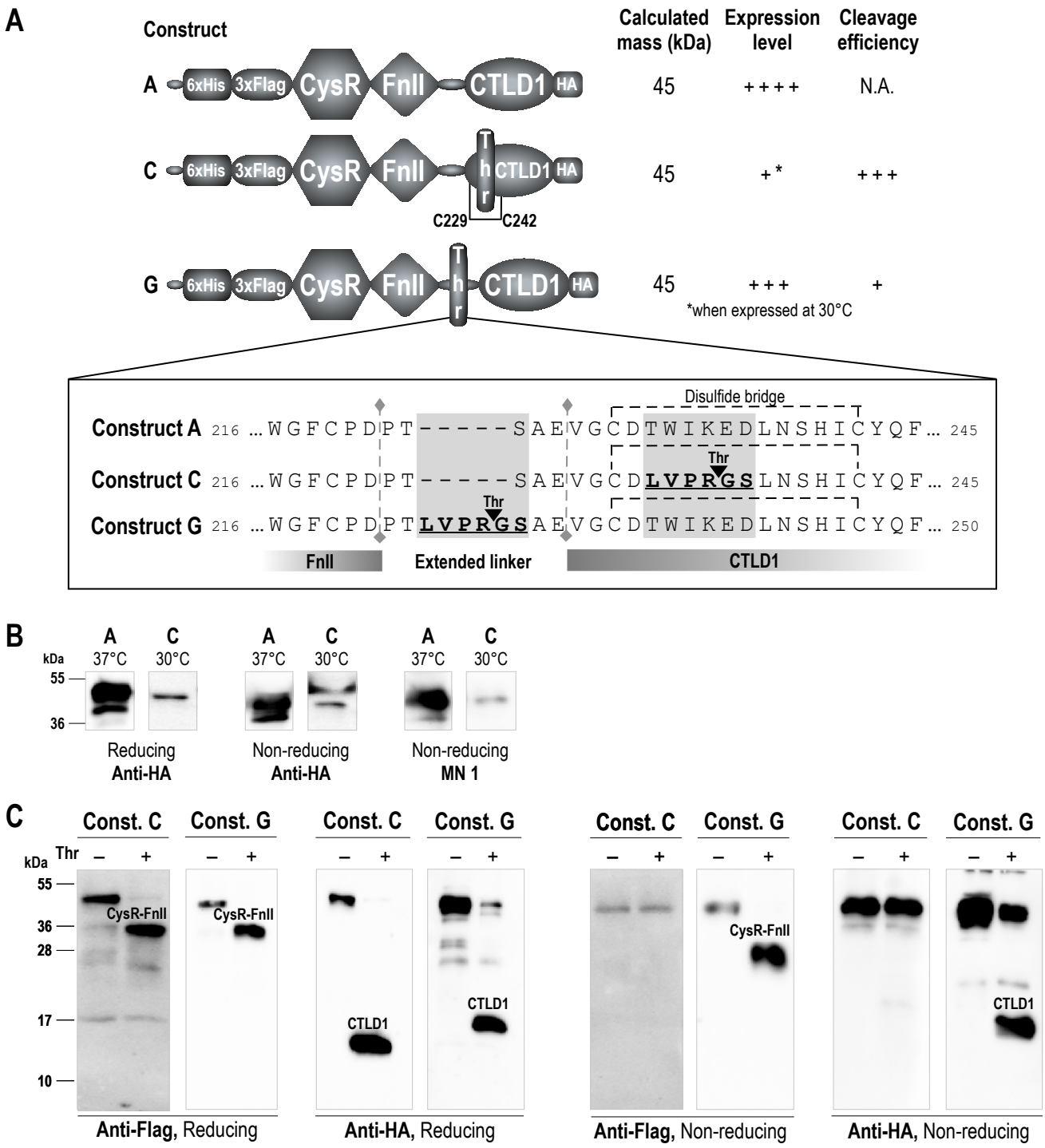

Figure S3 - Structure, expression and cleavage of constructs C and G. (A) Schematic diagram showing the structure of soluble CysR-FnII-CTLD1 triple domains with N-terminal 6xHis and 3xFlag tags and C-terminal HA-tag: Construct A has no thrombin cleavage site, construct C has a thrombin (Thr) cleavage site inserted within the first disulfide bond of CTLD1 by replacing 6 amino acids, and construct G has a thrombin (Thr) cleavage site inserted in the linker region between the FnII and CTLD1 domains, thereby extending the linker. Expected mass is calculated without the contribution of glycosylation. Constructs A and G are well expressed in HEK293 cells, while construct C was poorly expressed at 37°C. Expression was rescued by growing cells at 30°C (see methods and Figure S4). **(B)** Relative expression in cell medium of construct A at 37°C and construct C at 30°C as measured by WB with anti-HA antibody (1:5,000, under reducing and non-reducing conditions) and with patient MN1 (1:100, non-reducing conditions). **(C)** Cleavage of construct C and G by thrombin was validated with anti-Flag (1:1,000) and anti-HA (1:5,000) antibodies by WB under reducing conditions. Cleavage of construct G by thrombin was also validated under non-reducing conditions. However, the actual cleavage by thrombin could not be evidenced for construct C under non-reducing conditions, because of insertion of the thrombin cleavage site within the first disulfide bridge of CTLD1, with that disulfide maintaining the two cleaved fragments (CysR-FnII and CTLD1). N.A.: not applicable.

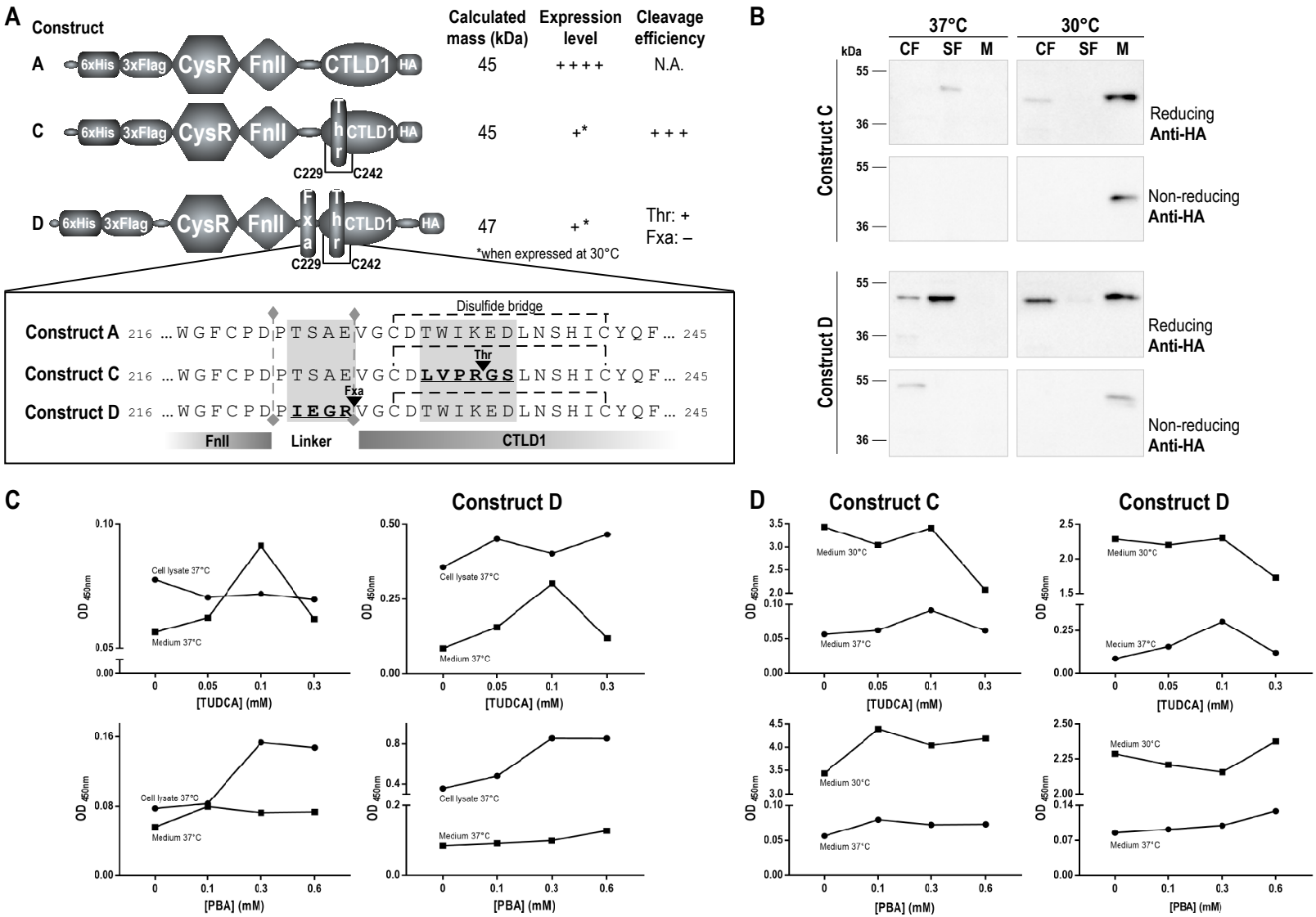

Figure S4 - Misfolding of constructs C and D was partially rescued by growing HEK293 cells at low temperature or by the addition of chemical chaperones. (A) Schematic diagram showing the structure of soluble CysR-FnII-CTLD1 triple domains N-terminally 6xHis- and 3xFlag-tagged and C-terminally HA-tagged expressed in HEK 293 cells: construct C is as in Figure S3 while construct D has an additional factor Xa (FXa) cleavage site introduced in the linker region between FnII and CTLD1. Both constructs were poorly expressed in cell medium from HEK293 cells at 37°C because of insertion of the thrombin (Thr) cleavage site within the first disulfide bond in CTLD1. **(B)** Detection of recombinant proteins after expression of constructs C and D in HEK293 cells grown at 37°C and 30°C. Cytosolic (CF) and solubilized (SF) cellular fractions as well as medium (M) were analyzed by WB under reducing and non-reducing conditions using anti-HA antibody (1:5,000). No or weak expression was observed in cell lysates and medium at 37°C, while higher expression was seen in medium at 30°C. **(C)** Detection of constructs C and D with MN1 (1:100) by ELISA (anti-HA capture assays) in cell lysate and culture medium of HEK293 cells grown at 37°C in the presence of TUDCA or PBA at different concentrations. **(D)** Expression of constructs C and D in culture medium of HEK 293 cells incubated at 37°C versus 30°C in the presence of TUDCA or PBA at different concentrations as detected by ELISA with MN1 (1:100). N.A.: not applicable; Thr: thrombin; FXa: factor Xa; CF: cytosolic fraction; SF: solubilized fraction; M: culture medium; TUDCA: tauroursodeoxycholic acid; PBA: 4-phenyl butyric acid.

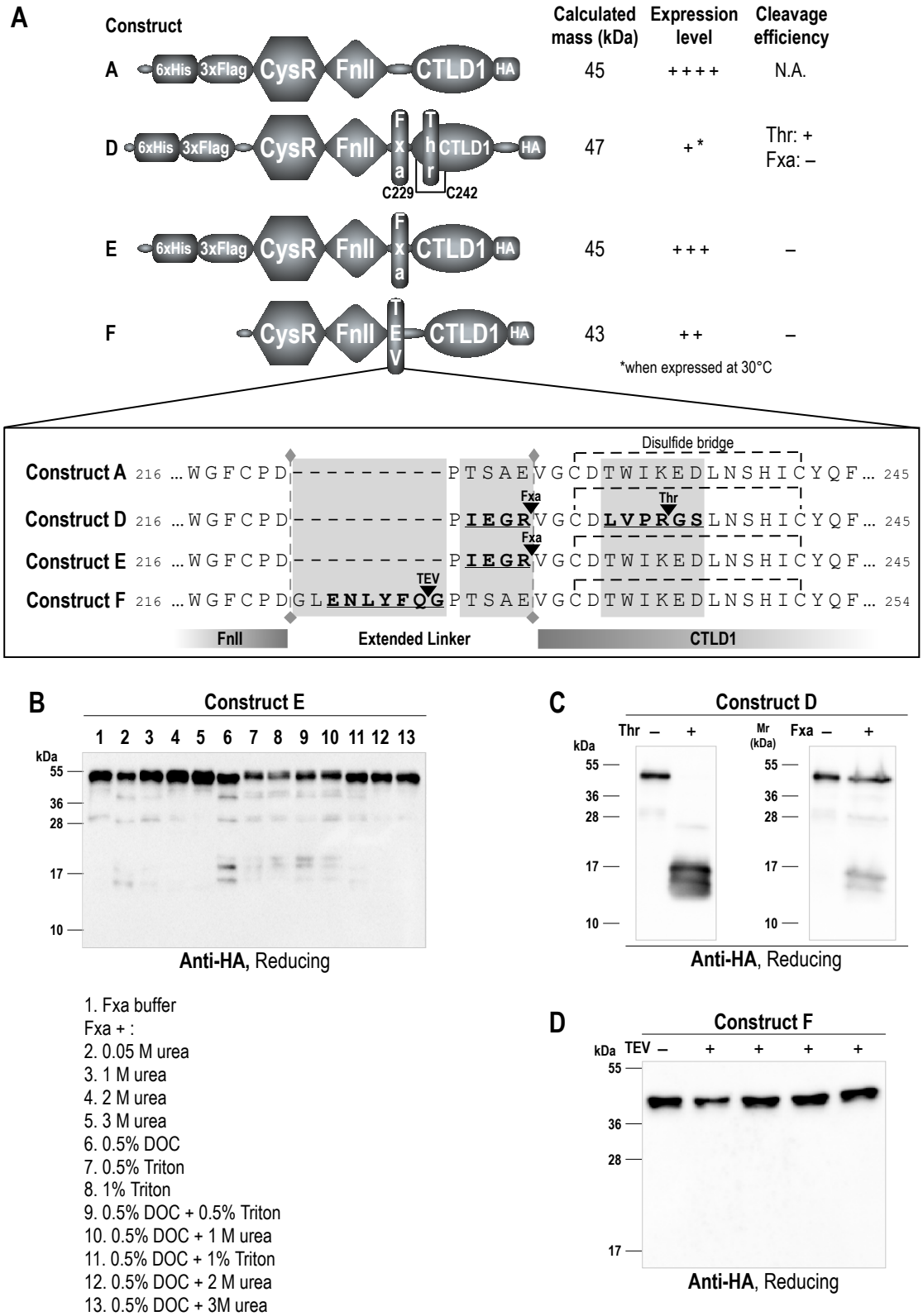

Figure S5 - Proteolysis of the CysR-FnII-CTLD1 triple domain by FXa and TEV proteases is likely prevented by steric hindrance and poor access to the recognition sites. (A) Schematic diagram showing the structure of soluble CysR-FnII-CTLD1 triple domains N-terminally 6xHis- and 3xFlag-tagged and C-terminally HA-tagged expressed in HEK 293 cells: constructs A and D are as in Figure S4. Constructs E and F have FXa and TEV protease cleavage sites inserted in the linker region between the FnII and CTLD1 domains, respectively. The expected mass is calculated without the contribution of glycosylation and cleavage efficiency is indicated. **(B)** Absence of cleavage of construct E by FXa protease under various denaturing conditions as seen by WB under reducing conditions using anti-HA antibody (1:5,000). **(C)** Absence of cleavage of construct D by FXa even though it is efficiently cleaved by thrombin, as observed by WB under reducing conditions using anti-HA antibody(1:5,000). **(D)** Absence of cleavage of construct F by different sources of commercial TEV proteases as seen by WB (reducing conditions) with anti-HA antibody (1:5,000). N.A.: not applicable; FXa: factor Xa, TEV: Tobacco Etch Virus; DOC: sodium deoxycholate.

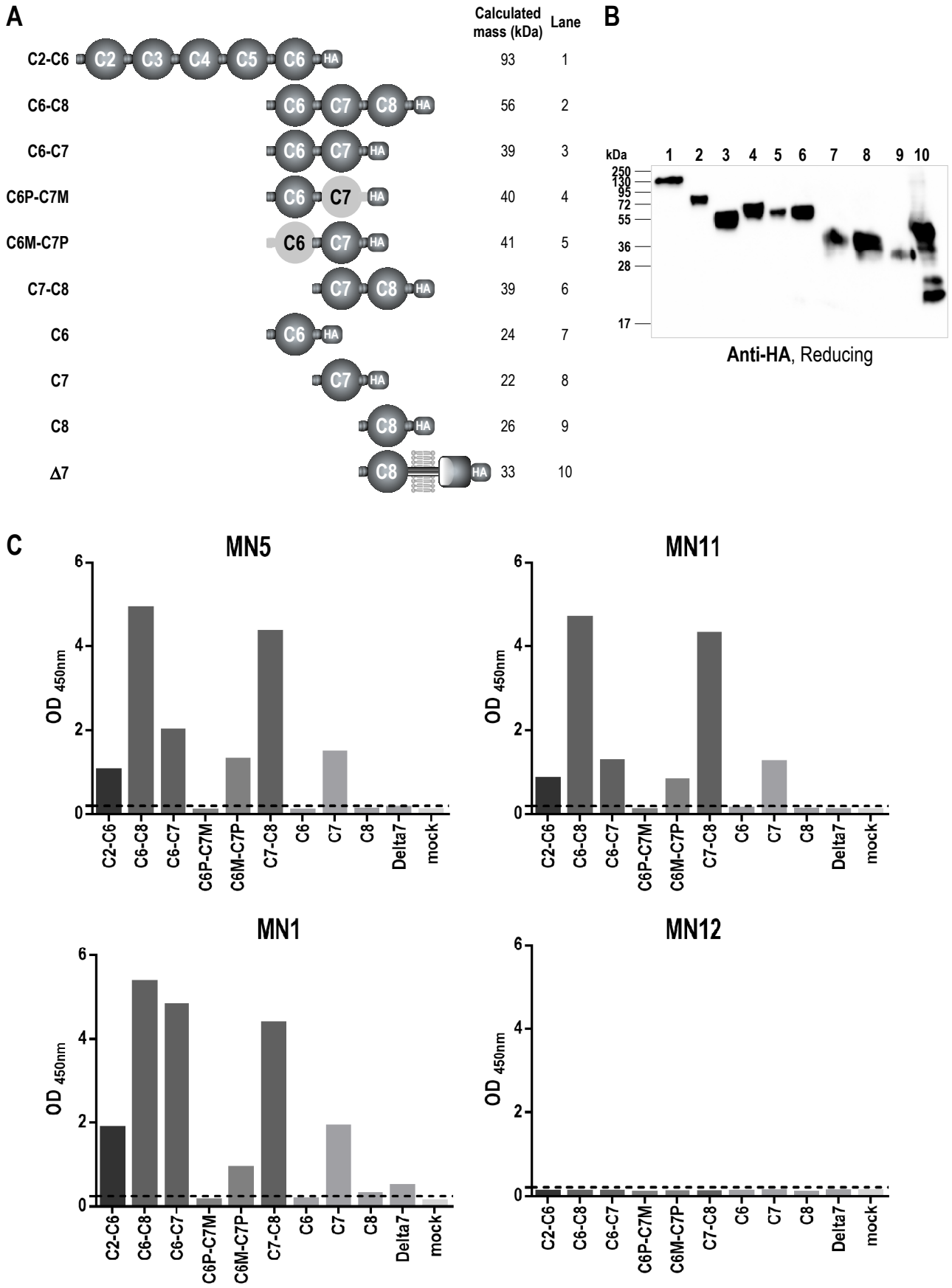

Figure S6 - Sera from different MN patients recognized two novel epitope-containing domains in the CTLD2-CTLD8 region of PLA2R1. (A) Schematic diagram of several C-terminally HA-tagged soluble and membrane-bound constructs within the CTLD2-CTLD8 region of PLA2R1. The expected mass is calculated without the contribution of glycosylation. **(B)** Expression of PLA2R1 recombinant proteins in HEK293 cells was validated with anti-HA antibody (1:5,000) by WB under reducing conditions. **(C)** Representative results of four patients (1:100) from a preliminary ELISA screen of 28 patients. Patients MN5, MN11 and MN1 recognize the CTLD2-6 region of PLA2R1 while patient MN1 is also recognizing CTLD8 and D7. Patient MN12 recognizes only the CysR domain, and is negative on all constructs within the C2-C8 region.

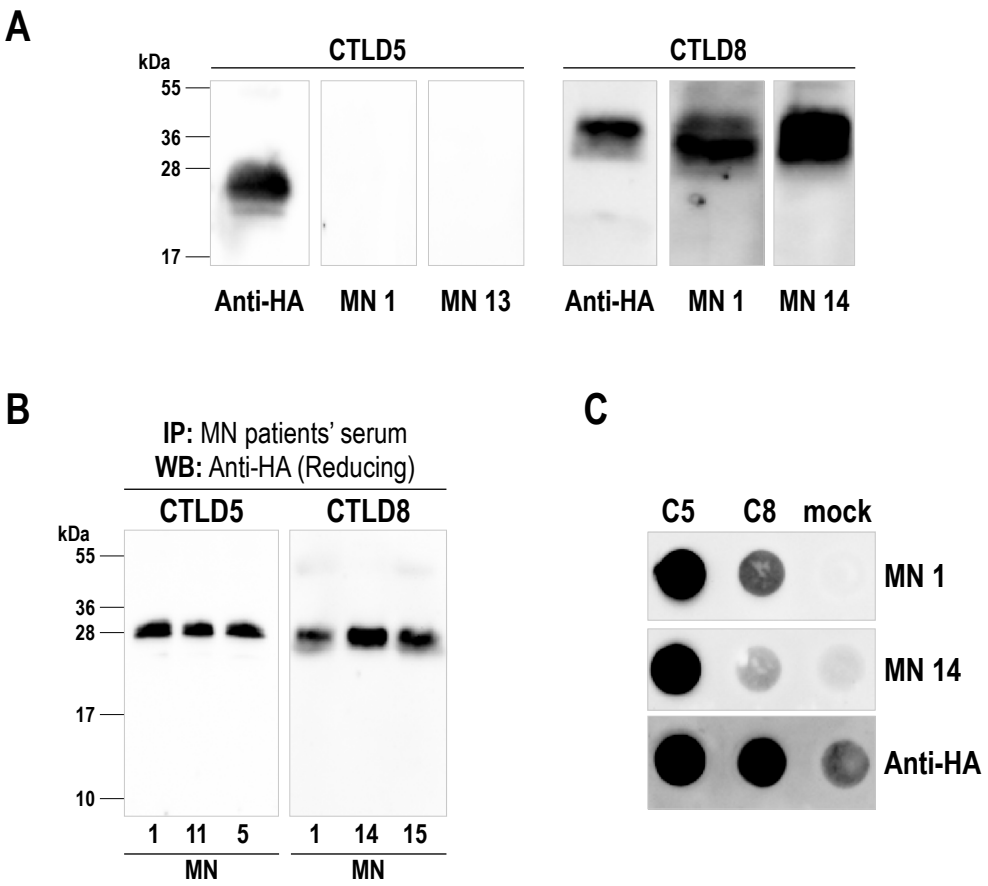

Figure S7 - WB, immunoprecipitation and dot-blot experiments confirming that single domains CTLD5 and CTLD8 contain independent epitopes recognized by PLA2R1-positive patients. (A) WB (non-reducing conditions) with anti-HA antibody (1:5,000) validating the expression and transfer of CTLD5 and CTLD8 as single domains. Representative WB (non-reducing conditions) with patients' sera used at 1:25 showed that patients could not detect CTLD5 while several patients could detect CTLD8. **(B)** Immunoprecipitation of CTLD5 and CTLD8 with different patients' sera followed by WB detection under reducing conditions with anti-HA antibody (1:5,000). In these conditions, both CTLD5 and CTLD8 could be detected. **(C)** Dot-blot transfer of single domains CTLD5 and CTLD8 under non-denaturing conditions was validated with anti-HA antibody (1:5,000). Representative dot-blots showing reactivity of patients against both CTLD5 and CTLD8 domains versus mock-negative control.

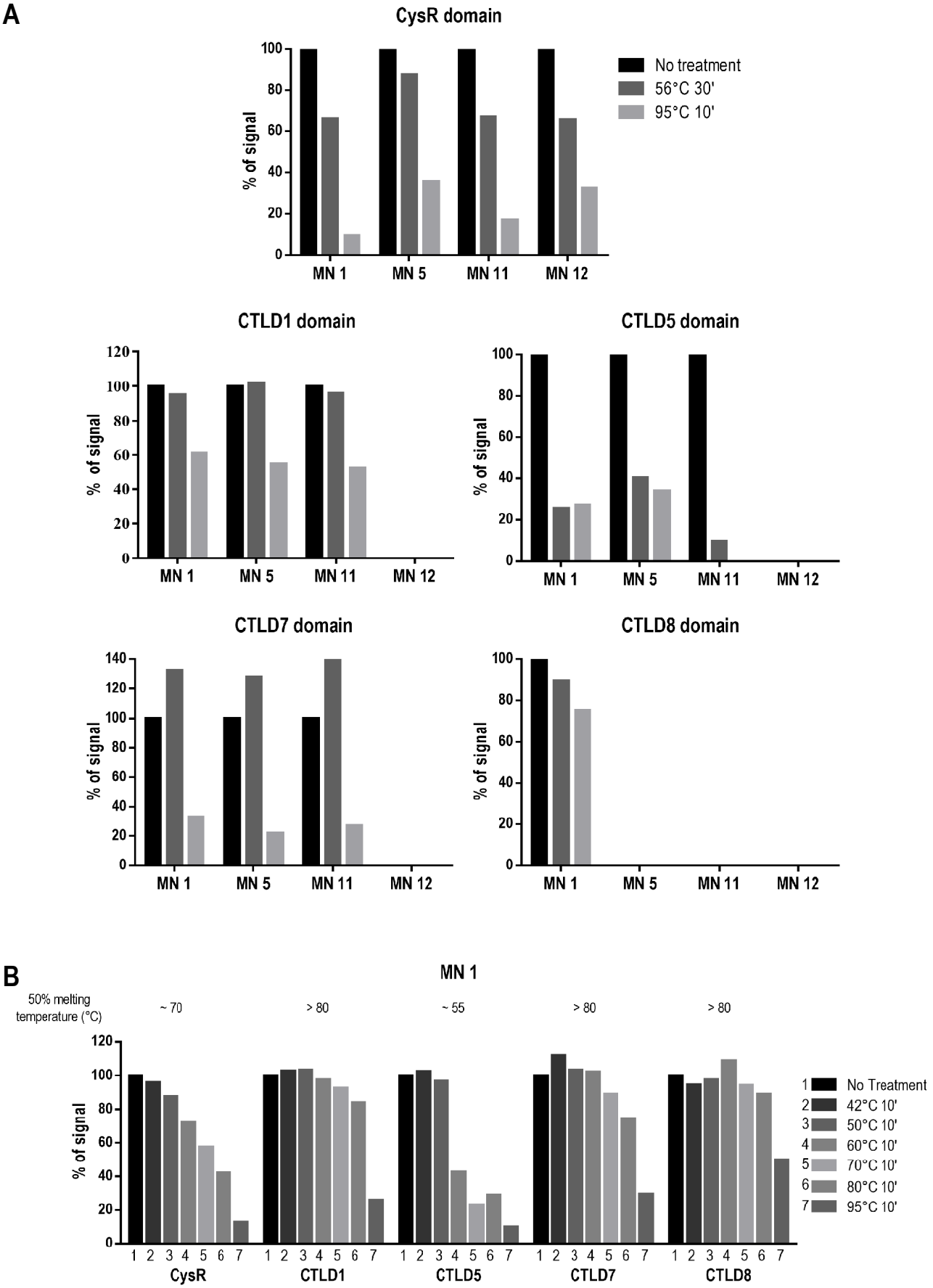

Figure S8 - Heating of the epitope-containing domains shows that reactivity of patients' sera is more rapidly lost for CTLD5 than other PLA2R1 domains. (A) ELISA reactivity of four MN patients' sera against CysR, CTLD1, CTLD5, CTLD7 and CTLD8 single domains which have been exposed to different temperatures (no treatment (room temperature), 56°C for 30 minutes or 95°C for 10 min) before ELISA. **(B)** ELISA reactivity of MN 1 against the various epitope-containing domains which have been exposed to different temperatures for 10 minutes before ELISA.

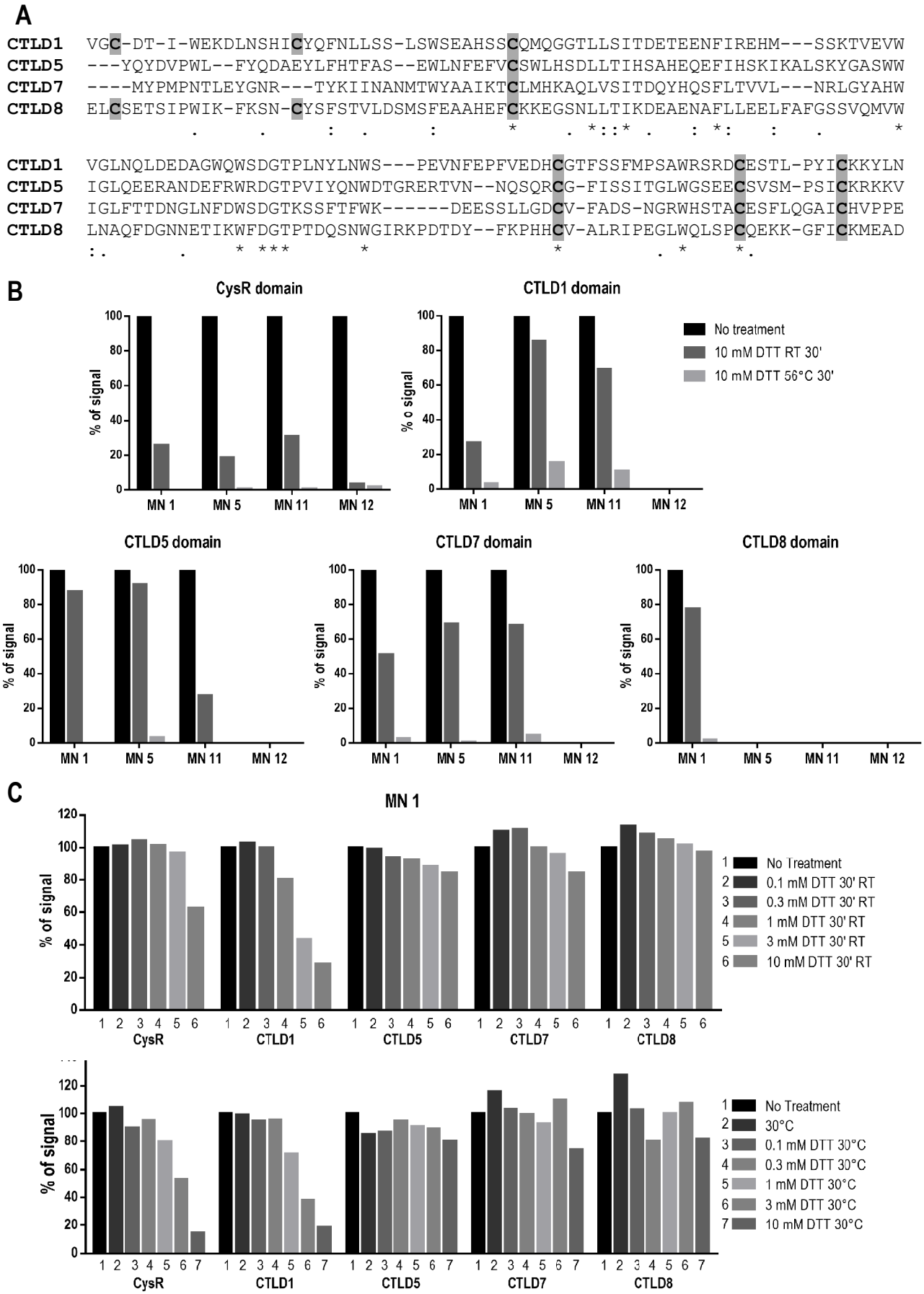

Figure S9 - Reactivity of patients' sera to CTLD5 and other PLA2R1 domains is sensitive to DTT when combined to heat. (A) Sequence alignment of the four CTLD epitope-containing domains showing the presence of two conserved disulfides in all CTLDs and a third disulfide only present in CTLD1 and CTLD8. The CysR domain contains three disulfides (not shown). **(B)** ELISA reactivity for four MN patients against the epitope-containing domains after treatment with 10 mM DTT at different temperatures (no treatment: no DTT/room temperature). **(C)** ELISA reactivity of MN 1 against the epitope-containing domains treated with different concentrations of DTT for 30 minutes at room temperature (RT) or 10 minutes at 30°C before ELISA.

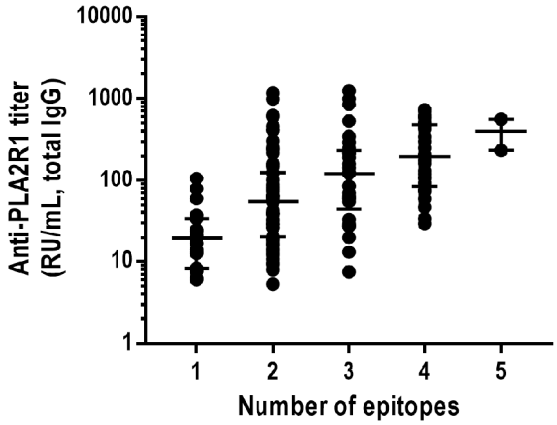

Figure S10 - Anti-PLA2R1 titer increases as the number of positive epitope-containing domains increases. Distribution of anti-PLA2R1 titer (commercial ELISA, total IgG) according to the number of positive epitope-containing domains (IgG4, n=142).

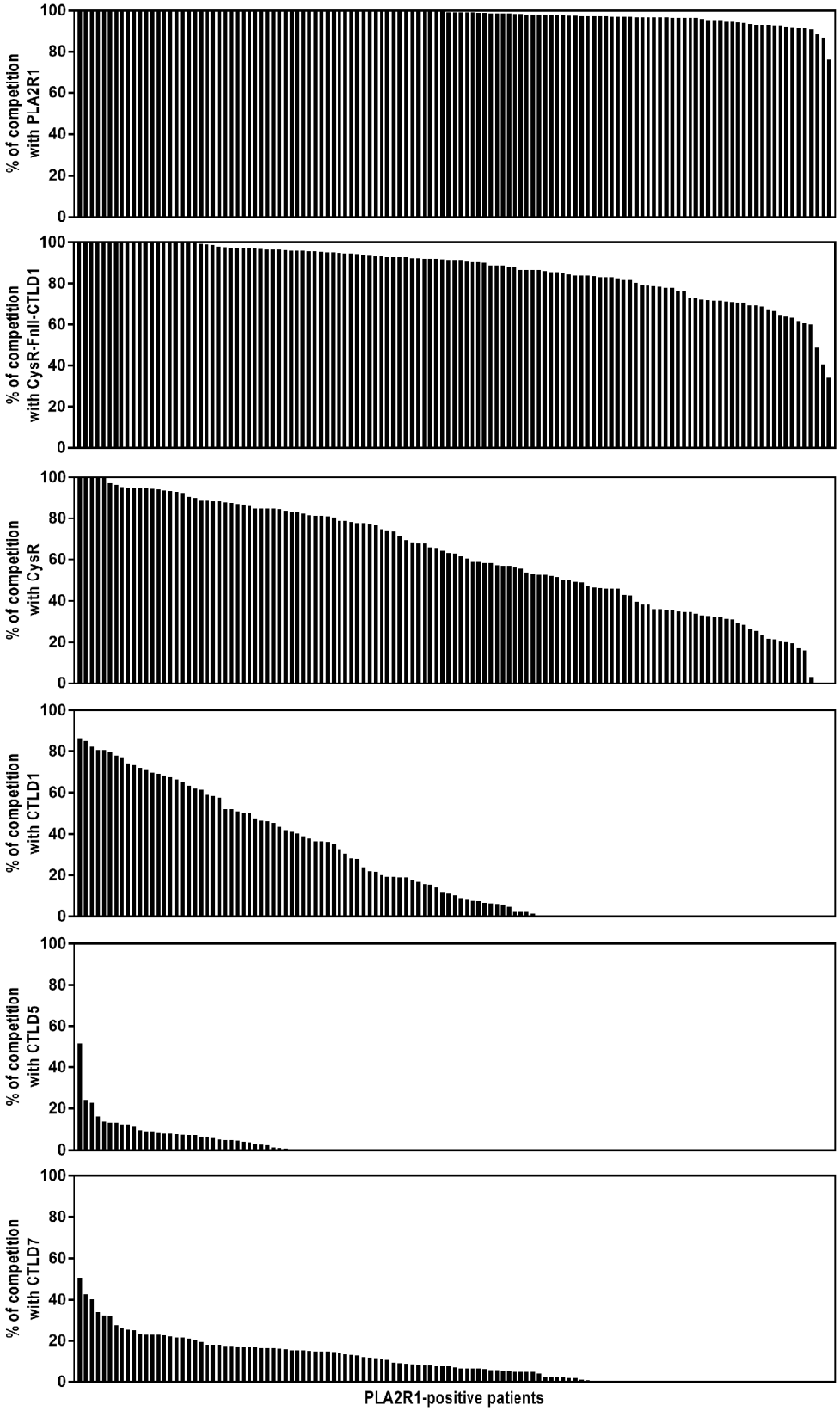

Figure S11 - Competition assays by ELISA (IgG4 detection) between recombinant PLA2R1 (full extracellular region) and different domains of PLA2R1 for all PLA2R1-positive MN patients with available serum (n=136). PLA2R1-positive MN patients were ranked by decreasing percentage of competition with recombinant proteins: PLA2R1 (full extracellular region), CysR-FnII-CTLD1, CysR, CTLD1, CTLD5 and CTLD7. The total competition with PLA2R1 (full extracellular region) for all patients validated the assay conditions. For a majority of patients (113/142, 79.6%), competition with CysR-FnII-CTLD1 was higher than 65%, indicating that CysR and/or CTLD1 domains contribute to most of the PLA2R1 signal. On the other hand, CTLD5 and CTLD7 have a minor contribution to the PLA2R1 signal for most patients since they contribute to a significant part of the PLA2R1 signal for only a few patients (12/142), which are classified as non-iDom. Importantly, note that the percentage of competition for each individual patient and individual domain are different, and consequently, patients are not ranked in the same order in each panel (but by decreasing values of competition for each recombinant PLA2R1 competing protein).

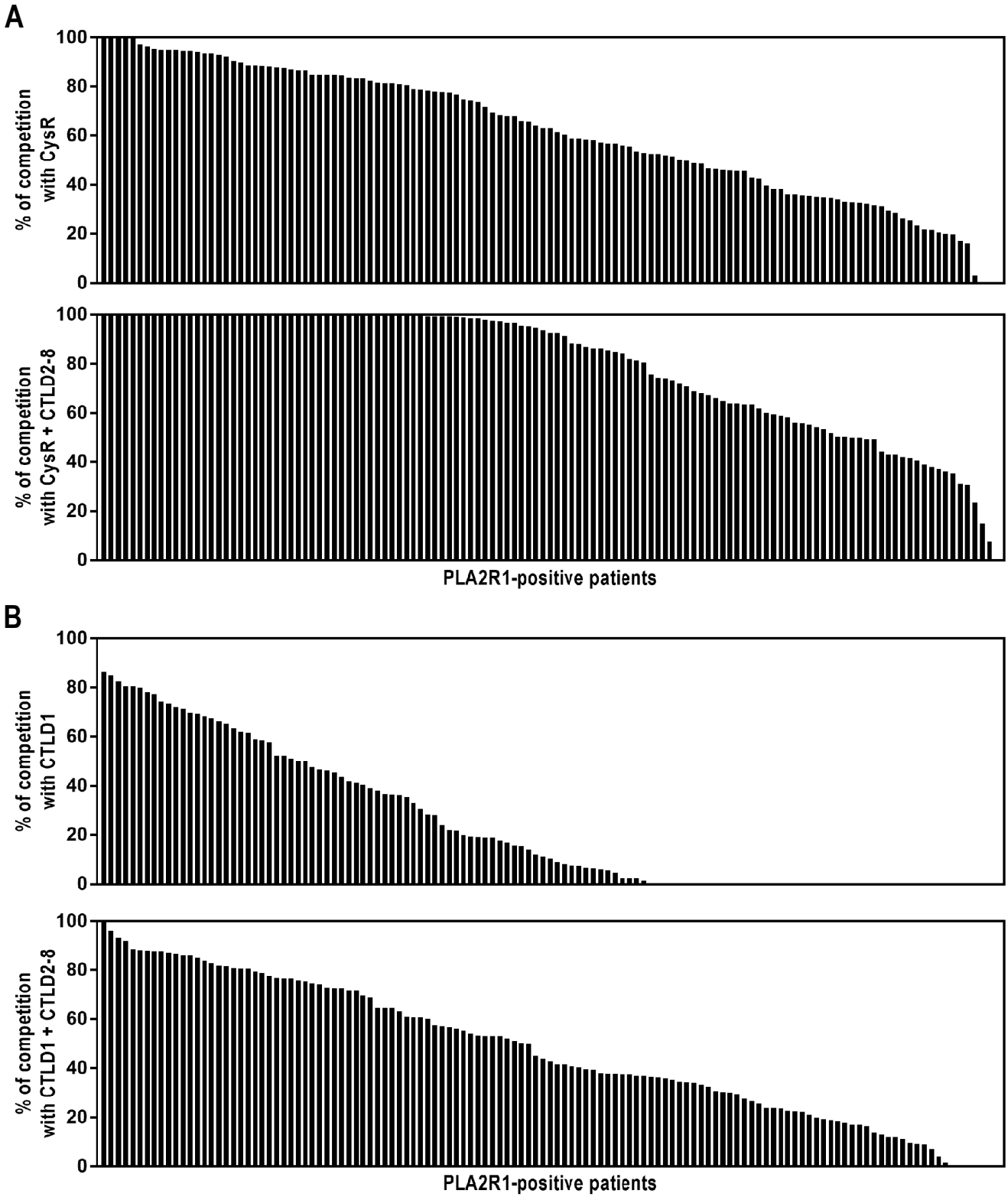

Figure S12 - Competition assays by ELISA (IgG4 detection) between recombinant PLA2R1 (full extracellular region) and CysR or CTLD1 domains mixed with the large C-terminal region CTLD2-8 for all PLA2R1-positive MN patients with available serum (n=136). Patients were ranked by decreasing percentage of competition with CysR (A, upper panel), CysR mixed with CTLD2-8 (A, lower panel), CTLD1 (B, upper panel) and CTLD1 mixed with CTLD2-8 (B, lower panel). The comparison between lower and upper graphics in both panels A and B shows a minor contribution of the C-terminal epitope-containing domains (CTLD5, CTLD7 and CTLD8) to the PLA2R1 signal. In mirror, the remaining signal for each patient (empty space in the lower graphics) can also be seen as the actual contribution of anti-CTLD1 (A) or anti-CysR (B) signal relative to the anti-PLA2R1 titer, in line with data shown in Figure S11. Importantly, note that the percentage of competition for each individual patient and individual domain are different, and consequently, patients are not ranked in the same order in each panel (but by decreasing values of competition for each recombinant PLA2R1 competing protein).

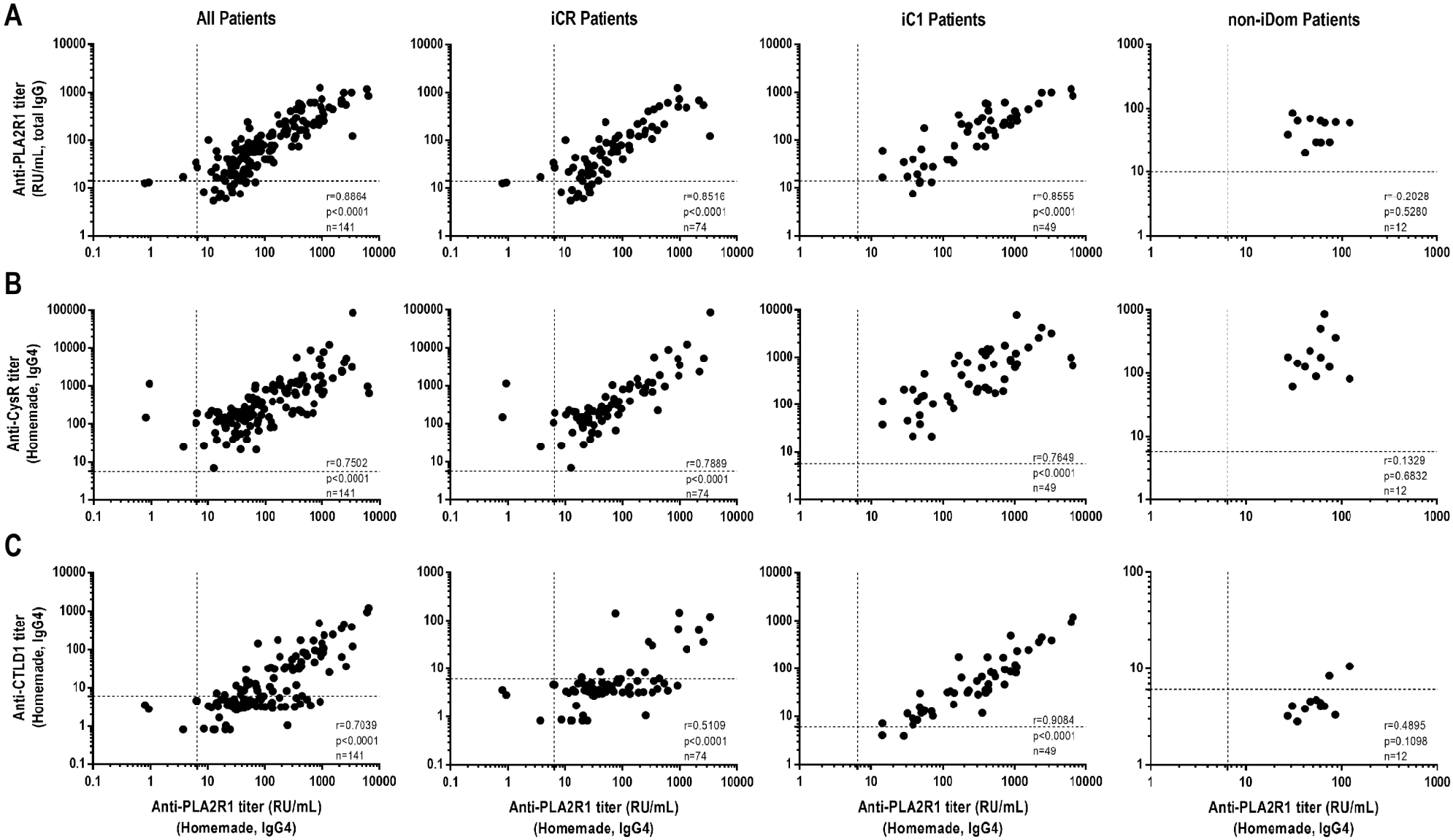

Figure S13 - Correlation between anti-PLA2R1 titer (in-house IgG4 ELISA) and anti-PLA2R1 titer (commercial total IgG ELISA), anti-CysR or anti-CTLD1 titers (in-house IgG4 ELISA) for PLA2R1-positive MN patients as a whole (n=141) or according to their immunodominant profile (n=135). (A) Correlations between the anti-PLA2R1 titers obtained with the commercial ELISA (total IgG) and in-house ELISA (IgG4) (**B and C**) Correlations between anti-PLA2R1 titer (in-house IgG4 ELISA) and anti-CysR (**B**) or anti-CTLD1 (**C**) titers (in-house IgG4 ELISA).

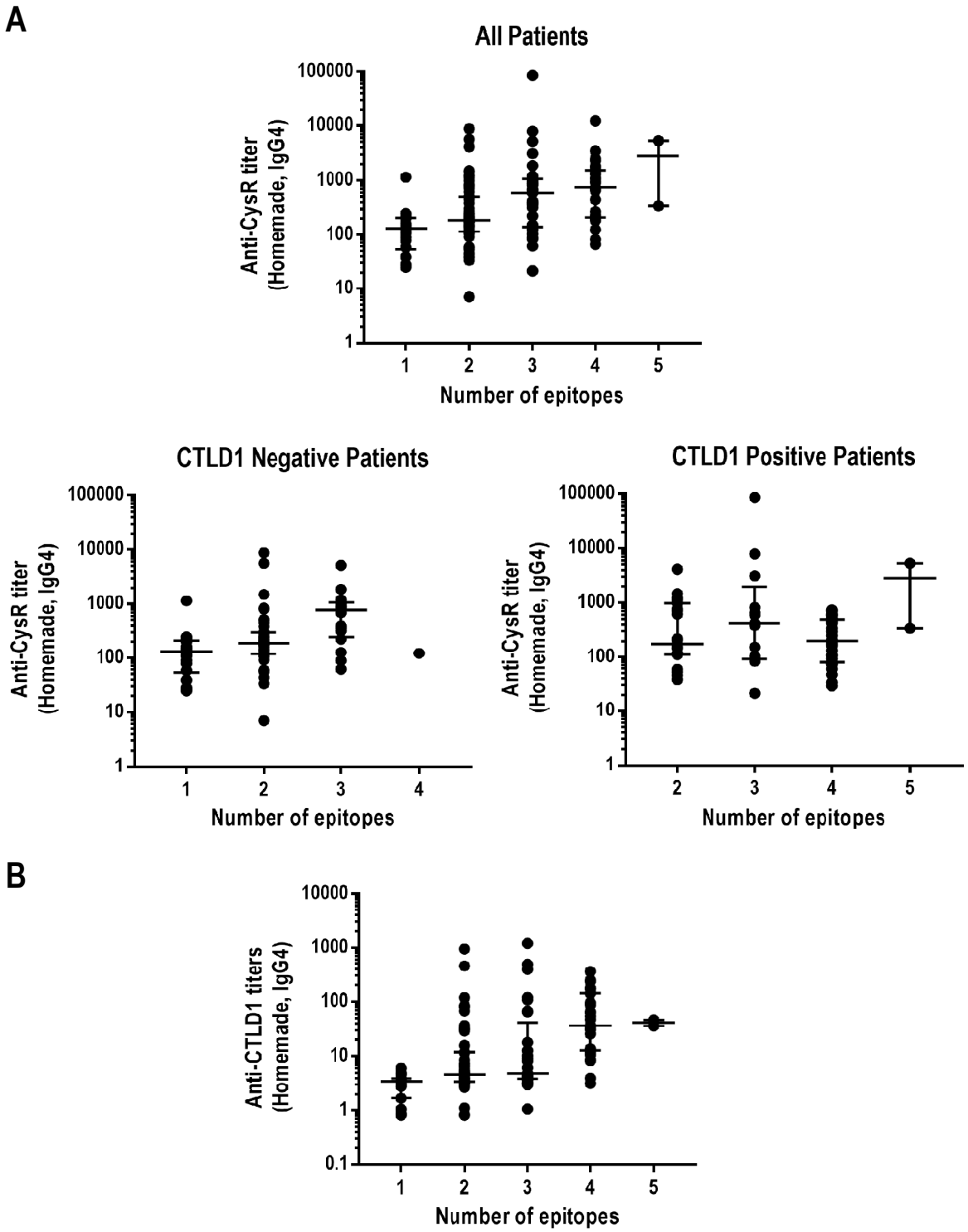

Figure S14 - Anti-CysR and anti-CTLD1 titers increase as the number of positive epitope-containing domains increases. (**A**) Distribution of anti-CysR titer (IgG4) according to the number of positive epitope-containing domains for the cohort as a whole (n=141) or considering positivity or not for CTLD1, showing lower increase of anti-CysR titer in the CTLD1 positive patients. (**B**) Anti-CTLD1 titer (IgG4) according to the number of positive epitope-containing domains for the cohort as a whole (n=141).

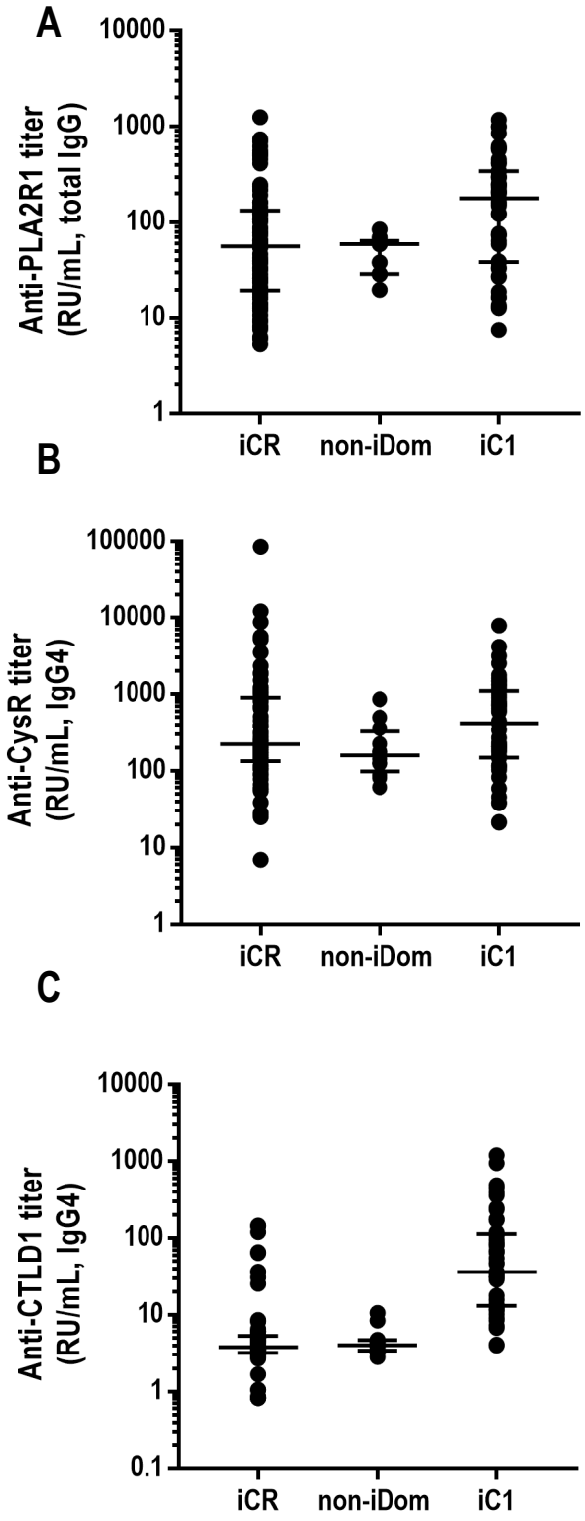

Figure S15 Anti-PLA2R1, anti-CysR and anti-CTLD1 titers vary according to the immunodominant profile of PLA2R1-positive MN patients. (**A**) Anti-PLA2R1 titer (commercial ELISA, total IgG) is higher in the iC1 group, as compared to the iCysR and non-iDom groups. (**B and C**) Anti-CysR (**B**) and anti-CTLD1 (**C**) titers (in-house ELISA, IgG4) according to the immunodominant profile. Note that similarly to anti-PLA2R1 titer, anti-CysR and anti-CTLD1 titers are higher in iC1 patients as compared to iCR and non-iDom patients. All anti-PLA2R1 titers are similar between iCR and non-iDom patients.

Chapter 7

Anti-PLA_2R1 antibodies as predictors of progression and clinical outcome in MN

The natural course of MN is variable with 40-50% of patients reaching spontaneous remission within 5-10 years after diagnosis, whereas the remainder progress to ESRD. Differentiating between patients with favourable versus poor prognosis as early as possible is of upmost importance to prescribe them the most optimized therapy and in particular avoid unnecessary treatment with immunosuppressors which are toxic and/or costly. Currently, the Toronto Risk Score or urinary low-molecular weight proteins levels are predictive markers used by physicians (Cattran et al., 1997; Reichert et al., 1998; van den Brand et al., 2012). However, their predictive value is at best 80%. There is thus a need for better predictive biomarkers.

As mentioned several times throughout this manuscript, anti-PLA$_2$R1 titer has been used to monitor disease activity at baseline and during the clinical course of the disease, with low titer predicting spontaneous remission and high titer predicting poor prognosis (Bech et al., 2014; Beck et al., 2009; Beck et al., 2011; Hofstra et al., 2012; Hoxha et al., 2014; Kanigicherla et al., 2013; Rodas et al., 2019; Ruggenenti et al., 2015). However, without validation studies and defined cut-off values for anti-PLA$_2$R1 levels, it still unclear how to use the anti-PLA$_2$R1 titer in clinical practice. Furthermore, using first a retrospective cohort of 69 PLA$_2$R1-positive patients, and then a subgroup of 58 PLA$_2$R1-positive patients from the clinical trial GEMRitux, our laboratory suggested that epitope spreading (or epitope profiling) can also help to predict clinical outcome (Seitz-Polski et al., 2018; Seitz-Polski et al., 2016). Still, both studies used a small number of patients and evaluated the predictive outcome value of epitope spreading in a mixed population of treated and untreated patients.

Soon after my arrival to the laboratory, i.e. before the identification of CTLD5 and CTLD8 as new epitope-containing domains and before the immunodominance study, we established a collaboration with Pr. Jack Wetzels with the aim to evaluate whether anti-PLA$_2$R1 titer and/or epitope spreading (as defined with CysR versus CTLD1/CTLD7 positivity) can help to predict clinical outcome and "natural progression" in a large retrospective cohort of PLA$_2$R1-associated MN patients which have not been treated by immunosuppressors. A manuscript, in which I should be second author, is currently in preparation as detailed below.

7.1 Development of ELISAs for the detection of autoantibodies against THSD7A, PLA$_2$R1, CysR, CTLD1 and CTLD7

We started by setting-up standardized homemade ELISA assays for the detection and quantification of autoantibodies against human THSD7A, PLA$_2$R1, CysR, CTLD1 and CTLD7 using anti-IgG4 secondary antibodies. For detection of anti-THSD7A and anti-PLA$_2$R1 autoantibodies, we used purified recombinant soluble proteins directly coated in ELISA plates overnight followed by blocking for 2 h at room temperature. For epitope-containing domains, we used HA-tagged soluble recombinant proteins which were HA-captured for 2 h incubation on ELISA plates previously coated with anti-HA antibody and blocked for 2 h at room temperature. To reduce inter-assay variability, a single coating solution was prepared and after blocking (PLA$_2$R1 and THSD7A ELISAs) or antigen capture (epitope-domain ELISAs) the plates were lyophilized and stored in a dried place at 4°C. The exception was the ELISA used to detect CTLD7, since lyophilisation of this domain prevents high sensitivity detection of antibody binding, likely by altering its conformation.

Each ELISA had appropriate negative controls of the respective antigens to allow accurate assessment of serum background for each patient. We used BSA as a negative control for the pure antigens (PLA$_2$R1 and THSD7A) and OptiMEM medium from non-transfected HEK293 cells as negative control for the epitope-containing domains (CysR, CTLD1 and CTLD7). Each ELISA plate also contained a negative control for the primary antibody: a serum sample consisting of a pool of healthy donors. The cut-off value of each antigen was determined based on optical density (OD) values as the mean value obtained for the negative control (healthy donor pool) in all the plates plus three times the standard deviation value. For each antigen, a standard curve consisting of seven dilutions of a highly THSD7A-, PLA$_2$R1-, CysR- CTLD1- or CTLD7-positive serum (different for THSD7A and PLA2R1) was designed, allowing the conversion of OD values into RU/mL using a 5-parameter logistic curve.

7.2 Patients stratification and selection

A total of 525 serum samples, including 318 baseline samples and 207 follow-up samples of adult patients with biopsy-proven primary MN were blind tested. At baseline, 226 patients (71.1%) presented reactivity against PLA$_2$R1, 9 patients (2.8%) were positive for THSD7A and 83 patients (26.1%) were double negative. No

cases of double positivity were identified. The 9 patients THSD7A-positive at baseline and the corresponding follow-up samples were extracted for a parallel ongoing study in the laboratory establishing a novel ELISA for patients with THSD7A-associated MN (chapter 8). Among the 226 PLA$_2$R1-positive patients, 74 (32.7%) were qualified as non-spreaders because of limited reactivity towards CysR. The other 152 PLA$_2$R1-positive patients (67.3%) were qualified as spreaders because of additional reactivity against CTLD1 and/or CTLD7: 48 patients (21.2%) had a CRC1 profile, 55 (24.3%) were CRC7 and 49 (21.9%) were CRC1C7. Of note, patients were additionally screened using the commercial Euroimmun ELISA (total IgG detection). A cut-off of 14 RU/mL was used to determine patients' positivity against PLA$_2$R1. Discrepant results were found between the two assays: 16 patients were positive using the homemade IgG4 ELISA whereas they had a titer inferior to 14 RU/mL with the commercial ELISA, with some patients even having undetectable autoantibodies (0 RU/mL). Conversely, one patient was PLA$_2$R1-positive with the commercial ELISA while negative with the homemade assay, which was due to the fact that this patient only had anti-PLA$_2$R1 autoantibodies from the IgG3 subclass. These observations are in agreement with other studies suggesting lower cut-off to determine PLA$_2$R1 positivity (Liu et al., 2018; Tampoia et al., 2018). This is raising the question whether the double negative patients can actually be false-negative patients for anti-PLA$_2$R1? Will other assays used in the clinical practice be in agreement with the commercial ELISA assay results? These questions have led to an ongoing second study, not present in this manuscript, which aims to re-evaluate the double negative patients.

7.3 Association between the autoimmune response, clinical characteristics and clinical outcome

For the next step of this project, which aimed to evaluate the added value of anti-PLA$_2$R1 titer and epitope spreading to predict progression and clinical outcome, only anti-PLA$_2$R1-positive patients at baseline with the homemade ELISA were included in the study. Additionally, only patients with nephrotic range proteinuria (proteinuria-creatinine ratio (uPCR) $\geq$ 3 g/10 mmol/L) and serum creatinine levels lower than 135 µmol/L were considered.

A total of 168 patients fulfilled the above criteria and were included in the study. The baseline characteristics of patients are described in Table 7.1. All patients were treated with angiotensin-converting enzyme inhibitors and/or angiotensin receptor blockers to decrease blood pressure as a conservative

treatment. Anti-coagulant drugs were given if serum albumin levels were below 20 g/L. Patients were considered as "progressors" if they had the need for immunosuppressive therapy due to an increase of serum creatinine levels above 30% from baseline or due to severe persistent nephrotic syndrome (uPCR ≥ 3.0 g/10 mmol/L and serum albumin below 30 g/L) A patient under only conservative therapy was considered to have reached spontaneous remission if uPCR was lower than 3.0 g/10 mmol/L with stable kidney function (less than 30% increase of serum creatinine level from baseline).

Table 7.1 – Baseline clinical characteristics and clinical outcome of the 168 PLA$_2$R1-positive MN patients included in the study.

Characteristic	PLA$_2$R1-Positive (n=168)
Age (years)	52 ± 13
Gender (M/F, n (%))	118 (70)/50 (30)
Disease duration (months) [1]	2.5 [1.2-7.8]
Serum creatinine (µmol/L)	91 [80-105]
Serum albumin (g/L)	21 [17-25]
Serum IgG (g/L)	4.4 [3.2-5.5]
Proteinuria (g/10 mmol)	7.2 [5.6-10.7]
Anti-PLA$_2$R1 titer Euroimmun (RU/mL)	106 [45-230]
Urinary β2m (ng/min) [2]	1016 [282-3264]
Urinary α1m (µg/min) [3]	45 [27-81]
IgG excretion (mg/24h) [4]	306 [158-520]
Previous disease episode (n (%))	10 (6)
Previous immunosuppressive treatment (n (%))	7 (4)
Spreading (n (%))	116 (69)
Outcomes (n (%))	
Spontaneous remission	55 (33)
Persisting proteinuria	1 (1)
Progression	112 (67)
Patients treated with immunosuppressives	112 (67)
Follow-up duration	
Until spontaneous remission (months)	18 [11-27]
Until spontaneous complete remission (months)	51 [35-76]
Until progression (months)	5 [2-12]
Total duration of follow-up (years)	5.0 [2.0-9.0]

Results are presented as mean ± SD, median [IQR], frequency (percentage).
[1] Disease duration is the interval between kidney biopsy and first measurement.
[2] Information missing for 10 patients. [3] Information missing for 1 patient. [4] Information missing for 2 patients.

During follow-up under only conservative treatment, 55 patients (33%) developed spontaneous remission (non-progressors) whereas 112 patients (67%) had disease progression (progressors) and started immunosuppressive therapy within a median of 5 months (IQR=[2.0-12]) after evaluation. As shown in Figure 7.1, it can take up to two to three years to achieve spontaneous remission whereas progression of the disease tends to occur faster. It is important to note that anti-PLA$_2$R1 titer was measured in stored samples; therefore the physicians were not aware of the anti-PLA$_2$R1 levels at the time of clinical decision to treat with immunosuppressors.

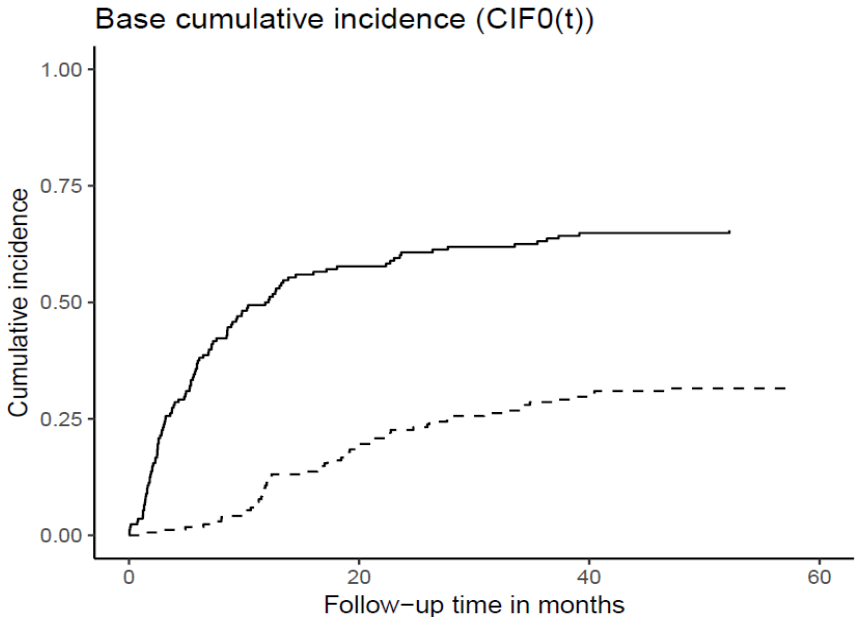

Figure 7.1 – Cumulative incidence of progression (plain line) and spontaneous remission (dot line) in a cohort of 168 PLA2R1-positive patients with a median follow-up of 5 years.

In agreement to others studies, in this cohort, patients in the highest tertile of anti-PLA$_2$R1 titer had poor kidney function, more severe nephrotic syndrome and higher levels of urinary low molecular weight proteins (Table 7.2). Spreading was associated with high anti-PLA$_2$R1 titers, with all patients with an anti-PLA$_2$R1 titer above 176 RU/mL (as measured by the Euroimmun ELISA) being spreaders. Additionally, spontaneous remission occurs significantly more often in the first tertile (54%) in comparison to the second and third tertiles (29% and 16% respectively) of anti-PLA$_2$R1. If we compare patient characteristics' based on epitope spreading (Table 7.3), we confirmed that spreaders had higher anti-PLA$_2$R1 titer, worst kidney function, more severe nephrotic syndrome and higher levels of

urinary low molecular weight proteins. Additionally, spreaders were less likely to reach spontaneous remission. These results demonstrated that epitope spreading is significantly associated with an increase of anti-PLA$_2$R1 titer, disease severity and progression.

Table 7.2 – Baseline clinical characteristics and clinical outcome of patients according to anti-PLA$_2$R1 tertiles assessed by the commercial Euroimmun ELISA.

Characteristics	First tertile 0-54 RU/mL (n=56)	Second tertile 55-173 RU/mL (n=56)	Third tertile 176-1239 RU/mL (n=56)	p-value
Age (years)	51 ± 12	52 ± 15	54 ± 12	0.423
Gender (M/F, (n (%))	41 (73)/15 (27)	42 (75)/14 (25)	35 (62.5)/21 (37.5)	0.294
Disease duration (months)	3.4 [1.6-8.9]	2.2 [1.1-8.8]	2.2 [1.2-5.7]	0.285
Serum creatinine (µmol/L)	90 [80-105]	91 [83-104]	95 [77-111]	0.711
Serum albumin (g/L)	24 [18-27]	21 [17-24]	19 [15-22]	0.001
Serum IgG (g/L)	4.9 [3.8-6.0]	4.2 [3.1-5.5]	4.0 [3.1-5.1]	0.108
Proteinuria (g/10 mmol)	6.1 [4.5-8.4]	7.6 [5.9-10.8]	9.3 [6.0-11.3]	0.002
Urinary β2m (ng/min)	541 [186-2558]	934 [233-3090]	2233 [382-8106]	0.010
Urinary α1m (µg/min)	38 [25-65]	48 [26-95]	59 [37-89]	0.020
IgG excretion (mg/24h)	246 [122-391]	306 [138-554]	387 [229-613]	0.011
Previous disease episode (n (%))	7 (12.5)	3 (5.4)	0 (0)	0.020
Previous immunosuppressive treatment (n (%))	6 (10.7)	0 (0)	1 (1.8)	0.010
Spreading (n (%))	28 (50)	39 (70)	49 (88)	0.000
Spontaneous remission (n (%))	30 (54)	16 (29)	9 (16)	0.000
Total duration of follow-up (months)	90 [36-129]	36 [27-96]	36 [24-96]	0.024

Results are presented as mean ± SD, median [IQR], frequency (percentage).

Table 7.3 – Baseline clinical characteristics and clinical outcome according to spreading.

Characteristics	Non-spreaders n=52	Spreaders n=116	p-value
Age (years)	52 ± 12	52 ± 14	0.827
Gender (M/F, n (%))	42 (81)/10 (19)	76 (66)/40 (44)	0.047
Disease duration (months)	3.4 [1.7-10.8]	2.1 [1.2-6.8]	0.133
Serum creatinine (µmol/L)	89 [82-97]	93 [79-109]	0.133
Serum albumin (g/L)	23 [19-27]	19 [16-24]	0.010
anti-PLA$_2$R1 titer by Euroimmun (RU/mL)	48 [25-99]	145 [54-297]	0.000
Serum IgG (g/l)	4.7 [3.8-5.8]	4.3 [3.0-5.4]	0.546
Proteinuria (g/10 mmol)	6.2 [4.7-9.3]	7.4 [5.9-10.9]	0.066
Urinary β2M (ng/min)	518 [204-2376]	1469 [314-5019]	0.119
Urinary α1M (µg/min)	37 [21-67]	50 [30-88]	0.074
IgG excretion (mg/24h)	257 [117-482]	311 [182-535]	0.403
Previous disease episode (n (%))	7/52 (14)	3/116 (3)	0.010
Previous immunosuppressive treatment (n (%))	4/52 (8)	3/116 (3)	0.205
Spontaneous remission (n (%))	25/52 (48)	30/116 (26)	0.007
Total duration of follow-up (months)	90 [24-120]	42 [24-96]	0.033

Results are presented as mean ± SD, median [IQR], frequency (percentage).

Table 7.4 – Baseline clinical characteristics of progressors and non-progressors.

Characteristics	Progressors N= 112	Non-progressors N= 56	p-value
Age (years)	53 ± 13	51 ± 14	0.380
Gender (M/F, n (%))	76 (68)/36 (32)	42 (75)/14 (25)	0.380
Serum creatinine (µmol/L)	95 [81-110]	86 [80-93]	0.005
Serum albumin (g/L)	19 [16-24]	24 [20-27]	0.000
Proteinuria (g/10 mmol)	8.6 [6.2-11.3]	5.9 [4.4-7.8]	0.000
Anti-PLA$_2$R1 titer by Euroimmun (RU/mL)	127 [60-311]	51 [31-129]	0.000
Urinary β2m (ng/min)	2258 [444-7575]	315 [156-794]	0.000
Urinary α1m (µg/min)	61 [38-101]	27 [15-43]	0.000
Serum IgG (g/L)	4.0 [3.0-5.1]	5.1 [4.1-6.2]	0.000
IgG excretion (mg/24h)	389 [228-567]	185 [100-315]	0.000
Disease duration (months)	2.4 [1.2-7.5]	3.0 [1.4-8.4]	0.695
Previous disease episode (n (%))	8(7.1)	2(3.6)	0.499
Previous IS treatment (n (%))	5 (4.5)	2 (3.6)	1.000
Spreading (n (%))	25 (46)	86 (77)	0.003
Partial remission (n (%))[1]	105 (94)	55 (98)	0.188
Complete remission (n (%))[1]	47 (42)	22 (39)	0.435

Results are presented as mean ± SD, median [IQR], frequency (percentage).

[1] Remission rate is the total amount of remissions achieved with (in progressors) or without (in non-progressors) immunosuppressive therapy

At presentation progressors had higher levels of proteinuria, urinary low molecular weight proteins, anti-PLA$_2$R1 titer and were more often spreaders (Table 7.4). Additionally, in preliminary multivariable analyses where anti-PLA$_2$R1 titer, epitope spreading or urinary α1m excretion were individually adjusted for baseline levels of serum creatinine as well as uPCR, these individual variables improved the risk prediction of disease progression (data not shown). However, in a multivariable model where the three variables (anti-PLA$_2$R1 titer, epitope spreading and urinary α1m excretion) were again adjusted for baseline levels of serum creatinine as well as uPCR, urinary α1m excretion was the strongest predictive parameter, with limited added value of anti-PLA$_2$R1 titer and epitope spreading (data not shown).

In sum, even though anti-PLA$_2$R1, epitope spreading and urinary α1m excretion predict outcome with reasonable accuracy, the calculated AUCs (area under the curves) are all below 0.80, indicating that there is still a large margin of error. Therefore, more complex prognostic models, which might include serum creatinine, proteinuria, urinary α1m excretion, anti-PLA$_2$R1 titer, epitope spreading, gender and age, are required to better predict progression and clinical outcome within the natural history of MN. Additionally, it would be interesting to test in such prediction models the novel potential biomarker identified in the previous chapter 6.5, immunodominance.

Chapter 8

Novel ELISA for patients with THSD7A-positive MN

In 2014, THSD7A was identified as the second autoantigen of MN, with circulating autoantibodies recognizing conformational epitopes and predominantly of the IgG4 subclass, similar to PLA2R1 (Tomas et al., 2014). With this discovery, it became essential to develop assays that would allow the detection of the autoantigen in kidney biopsy and/or the circulating autoantibodies to identify patients with THSD7A-associated MN. The assay should be simple and quantitative for clinical practice. In 2017, while this project was in progress, an IIFT assay was established and is currently commercially available (Hoxha et al., 2017). However, this method is only semi-quantitative and observer-dependent. Thus, we believed that it was important to continue the development of a sensitive, robust and quantitative ELISA that would not only allow the detection of anti-THSD7A antibodies, but also evaluate their potential clinical value as a titer.

The development of such an ELISA required the production of large amounts of purified recombinant THSD7A protein properly folded and able to detect antibodies recognizing only conformational epitopes. An expression plasmid coding for a recombinant soluble form of THSD7A corresponding to the full extracellular region with a 6xHis tag was stably transfected into HEK293 cells, the best cell clone was selected with antibiotics and several liters of culture medium containing the protein were collected. THSD7A was purified by affinity chromatography on His-tag purification beads (Figure S1 from article 2). The final yield of production of purified soluble THSD7A was 1mg per liter of cell culture medium.

Then, an optimized ELISA for the detection of IgG4 anti-THSD7A antibodies was set-up by screening patients with biopsy-proven primary MN, other diseases and healthy donors (Figure 1 from article 2). A cut-off for THSD7A positivity of 16 RU/mL was established from a ROC curve analysis and using the above-mentioned serum samples. The screen of an international multicenter cohort comprising 1012 biopsy-proven primary MN patients led to the identification of 28 THDS7A-positive patients, indicating a prevalence of 2.8% for THSD7A-associated MN. Interestingly, three of these patients were double positive since they were also PLA_2R1-positive, demonstrating a prevalence of 0.3% for double-positive MN cases. Additional serum samples referred to the different nephrology centers mostly due to negativity for PLA_2R1 were also screened for THSD7A antibodies leading to the identification of 21 more cases. Thus, we end-up with a final cohort of 49 THSD7A-associated MN patients, the largest cohort established at that time, and of great value, considering the low prevalence of THSD7A-associated MN.

Next, we compared the positivity of the 49 THSD7A-positive patients (as measured by ELISA) with the recently commercially available IIFT as well as western blot (Figure 2, Figure S4 and Figure S5 from article 2). Forty-three of the forty-nine patients were positive for all 3 techniques, while among the six remainders, three were positive with at least one technique and the three others were negative by the three techniques but positive for THSD7A staining in the kidney biopsy. Nevertheless, the sensitivity of the ELISA was similar to that of IIFT and the titers measured by both techniques were significantly correlated. Additionally, the 49 patients were also tested for other IgG subclasses by ELISA: IgG1, IgG2 and IgG3 anti-THSD7A autoantibodies were detected in 14%, 18% and 20% of the patients, respectively (Figure S3C from article 2).

We next analysed the clinical characteristics of THSD7A-positive patients (Table 2 and Table S1 from article 2) and found them comparable to those of PLA_2R1-positive patients. However, a 1.3:1 male to female ratio was observed for THSD7A-positive patients, which contrasts with the typical 2:1 ratio observed in the overall MN population and in PLA_2R1-positive patients. Additionally, THSD7A-positive female patients were significantly younger than male patients (Figure 4A from article 2). In particular, we identified a subgroup of younger female patients with a median age below the one estimated for menopause. By comparing the two subgroups of female patients (Table S2 from article 2), we noticed that they only differ in age but not in any other feature, suggesting a possible aetiology of MN related to pregnancy or preeclampsia, as described in a few case reports (Al-Rabadi et al., 2016; Iwakura et al., 2016; Luo et al., 2016). THSD7A-associated MN has been suggested to be linked to malignancy (Stahl et al., 2017). However, only 8 patients from our cohort had a history of malignancy, with only 3 of them diagnosed within 2 years of MN diagnosis. Additionally, these patients did not differ in their clinical features besides age (Table S3 from article 2), with patients with history of cancer being significantly older. Moreover, no particular IgG subclass pattern was observed in these patients (Table S5 from article 2). These results suggest that in our cohort, the cases of malignancy were most likely co-incidental rather than causative of MN. Furthermore, we also carefully analysed the clinical characteristics of patients with double positivity for THSD7A and PLA_2R1 autoantibodies compared to those with single positivity towards THSD7A, and no significant differences were observed (Table S6 from article 2).

We then compared anti-THSD7A titer at baseline and during follow-up to assess the association between anti-THSD7A titer and disease activity. Overall, patients in active disease have higher anti-THSD7A titer compared with patients in partial

or complete remission (Figure 5 from article 2). Finally, we investigated the association between anti-THSD7A autoantibodies levels and clinical outcome as well as response to treatment. By analysing 36 patients with a median follow-up of 37 months, we observed that patients with anti-THSD7A titer in the lowest tertile (titer below 134 RU/mL) had a better clinical outcome than patients with higher titer (Figure 6B from article 2).

In sum, we developed a robust, reproducible and quantitative ELISA that allows detection of anti-THSD7A antibodies. Similar to what was observed for PLA_2R1, anti-THSD7A titer appeared to reflect the immunological activity of MN, allowing careful monitoring of disease activity, evaluation of the response to treatment as well as prediction of clinical outcome.

Article 2

Novel ELISA for thrombospondin type 1 domain-containing 7A autoantibodies in membranous nephropathy

Christelle Zaghrini[1], Barbara Seitz-Polski[1,2,3], Joana Justino[1], Guillaume Dolla[1], Christine Payré[1], Noémie Jourde-Chiche[4,5], Anne-Els Van de Logt[6], Caroline Booth[7], Emma Rigby[7], Jennie Lonnbro-Widgren[8], Jenny Nystrom[9], Christophe Mariat[10,11], Zhao Cui[12], Jack F.M. Wetzels[6], GianMarco Ghiggeri[13], Laurence H. Beck Jr[14], Pierre Ronco[15,16,17], Hanna Debiec[15,16] and Gérard Lambeau[1]

[1]*Université Côte d'Azur, Centre National de la Recherche Scientifique, Institut de Pharmacologie Moléculaire et Cellulaire, UMR7275 Valbonne Sophia Antipolis, France;* [2]*Laboratoire d'Immunologie, Centre Hospitalier Universitaire de Nice, Université Côte d'Azur, Nice, France;* [3]*Service de Néphrologie, Centre Hospitalier Universitaire de Nice, Université Côte d'Azur, Nice, France;* [4]*Aix-Marseille Université, Centre Recherche en Cardiovasculaire et Nutrition, Institut National de la Recherche Agronomique 1260, Institut National de la Santé et de la Recherche Médicale 1263, Marseille, France;* [5]*Assistance Publique–Hôpitaux de Marseille, Centre de Néphrologie et Transplantation Rénale, Hôpital de la Conception, Marseille, France;* [6]*Department of Nephrology, Radboud Institute for Health Sciences, Radboud University Medical Center, Nijmegen, the Netherlands;* [7]*Evelina London Children's Hospital, Lambeth, London, United Kingdom;* [8]*Institute of Medicine, Sahlgrenska University Hospital, University of Gothenburg, Gothenburg, Sweden;* [9]*Institute of Neuroscience and Physiology, University of Gothenburg, Gothenburg, Sweden;* [10]*Service de Néphrologie Dialyse, Transplantation Rénale, Hôpital Nord, Lyon, France;* [11]*CHU de Saint-Etienne, GIMAP, EA 3065, Université Jean Monnet, Saint-Etienne, Comue Université de Lyon, Lyon, France;* [12]*Renal Division, Department of Medicine, Peking University First Hospital, Beijing, China;* [13]*Division of Nephrology, Dialysis and Transplantation, Laboratory of Molecular Nephrology, G. Gaslini Children Hospital, Genoa, Italy;* [14]*Renal Section, Department of Medicine, Boston University School of Medicine, Boston, Massachusetts, USA;* [15]*Sorbonne Université, Université Pierre et Marie Curie, Université Paris 6, Paris, France;* [16]*Institut National de la Santé et de la Recherche Médicale, Unité Mixte de Recherche_S1155, Paris, France; and* [17]*Service de Néphrologie et Dialyses, Assistance Publique–Hôpitaux de Paris, Hôpital Tenon, Paris, France*

Autoantibodies against phospholipase A2 receptor 1 (PLA2R1) and thrombospondin type 1 domain-containing 7A (THSD7A) are emerging as biomarkers to classify membranous nephropathy (MN) and to predict outcome or response to treatment. Anti-THSD7A autoantibodies are detected by Western blot and indirect immunofluorescence test (IIFT). Here, we developed a sensitive enzyme-linked immunosorbent assay (ELISA) optimized for quantitative detection of anti-THSD7A autoantibodies. Among 1012 biopsy-proven MN patients from 6 cohorts, 28 THSD7A-positive patients were identified by ELISA, indicating a prevalence of 2.8%. By screening additional patients, mostly referred because of PLA2R1-unrelated MN, we identified 21 more cases, establishing a cohort of 49 THSD7A-positive patients. Twenty-eight patients (57%) were male, and male patients were older than female patients (67 versus 49 years). Eight patients had a history of malignancy, but only 3 were diagnosed with malignancy within 2 years of MN diagnosis. We compared the results of ELISA, IIFT, Western blot, and biopsy staining, and found a significant correlation between ELISA and IIFT titers. Anti-THSD7A autoantibodies were predominantly IgG4 in all patients. Eight patients were double positive for THSD7A and PLA2R1. Levels of anti-THSD7A autoantibodies correlated with disease activity and with response to treatment. Patients with high titer at baseline had poor clinical outcome. In a subgroup of patients with serial titers, persistently elevated anti-THSD7A autoantibodies were observed in patients who did not respond to treatment or did not achieve remission. We conclude that the novel anti-THSD7A ELISA can be used to identify patients with THSD7A-associated MN and to monitor autoantibody titers during treatment.

Kidney International (2019) **95,** 666–679; https://doi.org/10.1016/j.kint.2018.10.024

KEYWORDS: clinical outcome; ELISA; malignancy; membranous nephropathy; sex; THSD7A

Correspondence: *Gérard Lambeau, Institut de Pharmacologie Moléculaire et Cellulaire, Unité Mixte de Recherche 7275, Centre National de la Recherche Scientifique et Université Côte d'Azur, 660 Route des Lucioles, Sophia-Antipolis, 06560 Valbonne, France. E-mail: lambeau@ipmc.cnrs.fr*

Received 2 July 2018; revised 18 September 2018; accepted 11 October 2018

The primary form of membranous nephropathy (MN) is an autoimmune kidney disease in which circulating autoantibodies target podocyte autoantigens, leading to deposition of immune complexes in the glomerular capillary wall, podocyte injury, and proteinuria.[1–3] Overall, MN affects more men than women (sex ratio 2:1), with a peak incidence at 50 to 55 years.[4,5] Clinical outcome varies from spontaneous remission to persistent proteinuria and end-stage renal disease in about 30% of cases.

In 2009, phospholipase A2 receptor 1 (PLA2R1) was identified as the major target autoantigen with circulating autoantibodies present in about 70% of MN patients.[6] In 2014, thrombospondin type 1 domain-containing 7A (THSD7A) was identified as a second autoantigen for another group of 2% to 5% MN patients.[7] Most cases of PLA2R1- and THSD7A-associated MN are mutually exclusive, yet rare cases of dual positivity have been described.[8–10]

Both PLA2R1 and THSD7A autoantigens are expressed in human podocytes and are membrane-bound proteins (180 and 250 kDa, respectively) with a long extracellular region comprising multiple but distinct domains with disulfide bonds.[6,7] Anti-PLA2R1 and anti-THSD7A autoantibodies exclusively bind to conformational epitopes present in 1 or more respective domains and are predominantly of the IgG4 subclass.[11–16] Epitope spreading associated with disease worsening has been suggested for PLA2R1.[13,14]

Although the pathogenic role of anti-PLA2R1 autoantibodies is still a matter of debate, multiple studies have shown that anti-PLA2R1 autoantibodies are specific and sensitive biomarkers for 50% to 80% of MN patients, depending on the studied cohorts.[17,18] Anti-PLA2R1 autoantibodies are nowadays measured by robust biological assays such as indirect immunofluorescence test (IIFT)[19] and enzyme-linked immunosorbent assay (ELISA).[20,21] Furthermore, PLA2R1 antigen accumulated in glomerular immune deposits is detected by standardized biopsy staining protocols.[22–24] These assays are now routinely used in clinical practice to identify and diagnose patients with PLA2R1-associated MN, predict clinical outcome, and improve clinical management from conservative therapy to treatment with potent immunosuppressors.[20,25–36] Other specific assays have also been described.[37,38]

Concerning THSD7A, patients' autoantibodies have recently been shown to be pathogenic in a mouse model.[39,40] However, the detection of circulating autoantibodies is currently possible by Western blot (WB)[7] and IIFT,[41] which provide only semi-quantitative titers. As for PLA2R1-related MN, standardized biopsy staining protocols that can detect THSD7A antigen in glomerular immune deposits have been reported.[8,9,42,43] Developing more robust and rapid assays such as ELISA for the sensitive and quantitative measurement of autoantibody levels in THSD7A-associated MN patients would be helpful for both diagnosis and clinical follow-up.

In this study, we describe the setup of the first ELISA for the sensitive and quantitative detection of anti-THSD7A autoantibodies. We used the assay to screen a combined cohort of 1012 MN patients and identified 28 THSD7A-positive patients, indicating a prevalence of 2.8%. We also screened additional PLA2R1-negative patients and included in total 49 THSD7A-positive MN cases. We tested all cases by WB and IIFT, characterized the anti-THSD7A IgG subclasses and analyzed their reactivity for PLA2R1. We finally described the clinical characteristics of this population for age, sex, disease activity, and possible links to etiology including malignancy. Our results show that this ELISA is rapid, sensitive, and specific to measure anti-THSD7A autoantibodies and will be useful for better diagnosis and clinical follow-up of MN patients.

RESULTS

ELISA setup

We prepared the full extracellular domain of human THSD7A in human embryonic kidney (HEK) 293 cells (Supplementary Figure S1) as soluble antigen and set up an ELISA that can specifically detect anti-THSD7A autoantibodies in serum from a subset of patients with MN but not from patients with other diseases or from healthy donors (Figure 1). Because many studies have shown that IgG4 is the predominant IgG subclass in MN patients[6,7,20,21,24,42,44,45] and is more sensitive than total IgG to measure anti-PLA2R1 autoantibodies,[6,7,13,46,47] we optimized the ELISA for detection of IgG4 anti-THSD7A autoantibodies. Using the above-mentioned serum samples and receiver-operating characteristics curve analysis, we defined a cutoff value of 16 relative units (RU)/ml above which serum samples are considered positive for anti-THSD7A (Figure 1 and Supplementary Figure S2A). We also established a standard curve for conversion of optical density values into RU/ml (Supplementary Figure S2B).

Identification of THSD7A-positive patients

Screening by ELISA of baseline serum from a total of 1012 biopsy-proven MN patients from 6 national and international cohorts[14,20,32,33,48–51] led to the identification of 28 THSD7A-positive patients, indicating an overall prevalence of 2.8% for THSD7A-associated MN (Table 1). Three of these patients were also positive for anti-PLA2R1 autoantibodies, indicating a prevalence of about 0.3% for double-positive MN patients (Table 1).

Additionally, our consortium screened for THSD7A positivity in baseline serum or biopsy from other MN patients (mostly referred to our different nephrology centers because of PLA2R1-unrelated MN over the last 4 years) by any of the 4 techniques available to identify THSD7A-associated MN: ELISA, IIFT, WB, or enhanced THSD7A staining in biopsy.[8,9,14,33,41] This led to the inclusion of 21 additional THSD7A-positive patients, among which 5 were double positive. Collectively, our cohort thus included 49 THSD7A-positive MN patients (Figure 1, Supplementary Figure S3, Table 2, and Supplementary Table S1).

Comparison of THSD7A positivity by ELISA, WB, and IIFT and analysis of IgG subclasses

We then compared the positivity for THSD7A in baseline serum from the 49 patients by the 3 techniques: ELISA, WB, and IIFT (Figure 2, Supplementary Table S1). In total, 43 of 49 patients were fully positive by ELISA (Figure 1, Supplementary Table S1 for IgG4 detection), IIFT (Supplementary Figure S4, Supplementary Table S1 for total IgG detection), and WB (Supplementary Figure S5, Supplementary Table S1 for IgG4 detection). Among the 6

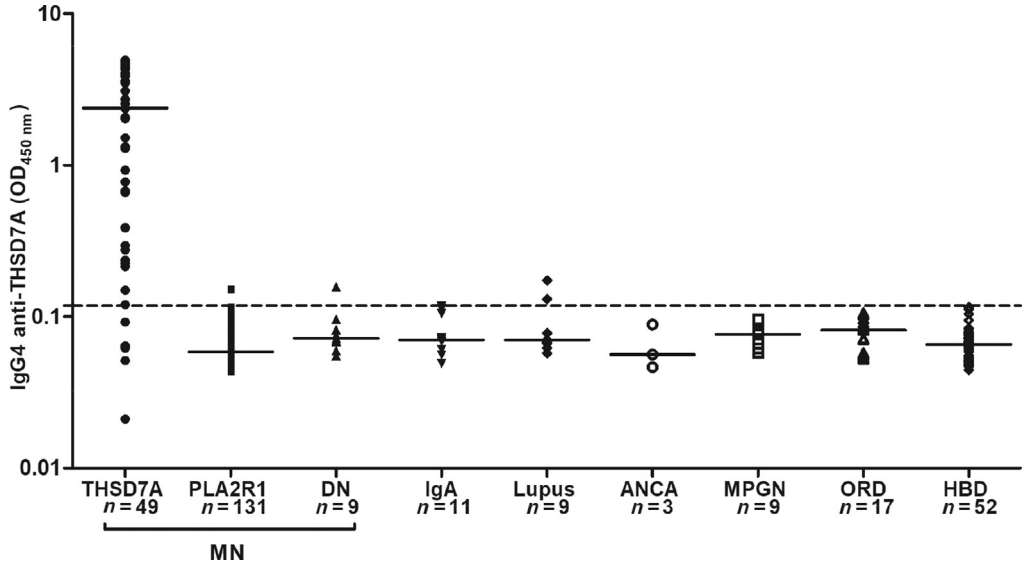

Figure 1 | Comparative analysis of IgG4 reactivity against thrombospondin type 1 domain-containing 7A (THSD7A) determined by enzyme-linked immunosorbent assay (ELISA). IgG4 anti-THSD7A reactivity was validated using THSD7A-positive membranous nephropathy (MN) patients (with respect to positivity by indirect immunofluorescence test and Western blot) versus THSD7A-negative MN patients (phospholipase A2 receptor 1 [PLA2R1]–positive and double-negative [DN] patients) and other control subjects (other diseases and healthy blood donors, $n = 101$). The data are expressed as optical density $(OD)_{450\ nm}$ and presented as medians. The dotted line represents the cutoff ($OD_{450\ nm}$ of 0.12 corresponding to 16 relative units/ml) at a defined specificity of 97% with respect to immunofluorescence test by receiver-operating characteristic curve analysis (Supplementary Figure S2). ANCA, anti-neutrophil cytoplasmic autoantibodies; HBD, healthy blood donor; IgA, IgA nephropathy; Lupus, lupus nephritis; MPGN, membranoproliferative glomerulonephritis; ORD, other renal diseases.

remaining patients, membranous nephropathy patient 40 (MN40) and MN41 were positive by IIFT when assayed at a 1:10 dilution with detection of total IgG (Supplementary Figure S4) but negative by WB and ELISA when detected for IgG4 (Supplementary Table S1). On the other hand, MN46 was positive by ELISA and WB but negative by IIFT (Figure 3). The last 3 patients (MN47, MN48, and MN49) were negative in serum by all 3 techniques but were positive based on THSD7A biopsy staining (Figure 3, Supplementary Figure S6).[9]

Because ELISA titers ranged over several logs (Figure 2, Supplementary Figure S3), we compared the different assays for 3 representative patients having low- to high-range anti-THSD7A titers and analyzed the correlation of titers measured by ELISA and IIFT for the whole cohort. Figure 2 shows that the 3 patients can be detected by ELISA at a 1:100 serum dilution (Figure 2a), by WB at the same dilution or lower (Figure 2b) and by IIFT, where appropriate dilution ranging from 1:10 to 1:1000 gave a specific signal (Figure 2c). The autoantibody titers measured by ELISA and IIFT correlated significantly ($r = 0.8592$, $P < 0.0001$) (Figure 2d for IgG4 ELISA and Supplementary Figure S3B for total IgG ELISA).

We also tested the positivity of the 49 patients by ELISA when detection of anti-THSD7A autoantibodies was performed with secondary antibodies specific for other IgG subclasses or total IgG. In our conditions, we detected IgG1, IgG2, and IgG3 anti-THSD7A autoantibodies in only 14%, 18%, and 20% of patients, respectively (Supplementary Figure S3C). As for total IgG, 38 of the 49 patients (78%) were positive, with autoantibody titers spanning 3 log units and correlating significantly with IgG4 titers ($r = 0.925$,

Table 1 | THSD7A and PLA2R1 reactivity of patients' sera from the different MN cohorts screened in this study

	Patients				THSD7A-positive		THSD7A-negative	
Cohort	All	Male	Female	THSD7A-positive	PLA2R1-positive	PLA2R1-negative	PLA2R1-positive	PLA2R1-negative
Nice	275	183 (67)	92 (33)	8 (2.9)	1	7	150 (54.6)	117 (42.5)
Saint-Etienne	68	45 (66)	23 (34)	2 (2.9)	0	2	41 (60.3)	25 (36.8)
Gemritux	75	52 (69)	23 (31)	2 (2.7)	0	2	61 (81.3)	12 (16.0)
Sweden	25	16 (64)	9 (26)	1 (4.0)	0	1	16 (64.0)	8 (32.0)
Italy	251	175 (70)	76 (30)	6 (2.4)	2	4	182 (72.5)	63 (25.1)
Netherlands	318	219 (69)	99 (31)	9 (2.8)	0	9	234 (73.6)	75 (23.6)
Total	1012	690 (68.2)	322 (31.8)	28 (2.8)	3 (0.3)	25 (2.5)	684 (67.6)	300 (29.6)

MN, membranous nephropathy; PLA2R1, phospholipase A2 receptor 1; THSD7A, thrombospondin type 1 domain-containing 7A.
Values are shown as *n* (%).
The main clinical characteristics of each cohort can be found elsewhere: Nice,[14] Saint-Etienne,[49] Gemritux,[32] Sweden,[50] Italy,[48] and the Netherlands.[51]

Table 2 | Epidemiological and clinical baseline characteristics of anti-THSD7A positive patients

Characteristics of THSD7A-positive patients	All (n = 49)	Male (n = 28)	Female (n = 21)	P value
Sex, M/F	28/21	28 (57)	21 (43)	
Age at diagnosis (yr)	59.9 (48.5–75.0)	67.0 (54.3–75.0)	48.8 (36.5–64.5)	0.003
Proteinuria (g/d)	6.1 (4.1–10.2)	6.6 (5.3–11.2)	5.0 (3.0–7.7)	0.106
Serum creatinine (μmol/l)	89.0 (70.7–121.0)	112.0 (88.0–145.0)	70.7 (64.7–86.6)	0.0004
eGFR (CKD-EPI) (ml/min per 1.73 m^2)	76.5 (49.8–90.0)	60.0 (39.8–80.0)	85.5 (64.5–91.8)	0.017
Serum albumin (g/l)	21.0 (16.5–25.3)	21.0 (15.3–25.8)	22.2 (17.5–25.3)	0.681
Anti-THSD7A titer (RU/ml)	278.0 (40.5–835.0)	256.0 (27.5–857.8)	302 (55.5–1035.0)	0.585
Cancer incidence	8 (16)	6 (21)	2 (10)	0.264

CKD-EPI, Chronic Kidney Disease Epidemiology Collaboration; eGFR, estimated glomerular filtration rate; RU, relative units; THSD7A, thrombospondin type 1 domain-containing 7A.
Values are n (%) or median (interquartile range).
The 49 patients were positive for THSD7A by at least 1 technique of detection: enzyme-linked immunosorbent assay (44 of 49 positive patients with IgG4 detection and 1 additional patient with total IgG detection), indirect immunofluorescence test (45 of 49 positive patients, total IgG detection), Western blot (44 of 49 positive patients, IgG4 detection), or biopsy staining (11 of 11 positive patients).

$P < 0.0001$) (Supplementary Figure S3D and E). More careful analysis showed that 37 of the 38 patients positive with total IgG were among the 44 patients positive for IgG4 while the last patient was negative for IgG4. Among the 7 patients negative for total IgG but positive for IgG4, 6 had low IgG4 anti-THSD7A titers and were negative for IgG1, IgG2, and IgG3 subclasses while the last one was positive for both IgG4 and IgG3. The higher number of patients detected with anti-IgG4 secondary antibodies is likely due to the better signal-to-noise ratio of these antibodies as compared with that of anti-total IgG (Supplementary Figure S3) and the fact that anti-THSD7A autoantibodies are mostly IgG4, like for anti-PLA2R1 autoantibodies.[7,46,47,52,53]

Among the 5 patients negative with IgG4 detection, 4 were also negative for total IgG, IgG1, IgG2, and IgG3. However, the last patient, MN40, illustrated a unique case in our cohort because it was negative for IgG4 but positive for total IgG. We carefully double-checked the positivity of this patient when using total IgG versus IgG4 and other IgG subclasses by ELISA, WB, and IIFT, and we confirmed that this patient was clearly positive for anti-THSD7A total IgG as well as IgG1, but not IgG2, IgG3, and IgG4 (Supplementary Figures S3, S4, and S5).

MN patients double positive for THSD7A and PLA2R1

We carefully evaluated the 49 patients for their double positivity for THSD7A and PLA2R1 by detection of anti-THSD7A and anti-PLA2R1 autoantibodies in baseline serum by ELISA, WB, and IIFT, and of THSD7A and PLA2R1 antigens in immune deposits (when biopsies were available). In total, 8 patients (MN42 to MN49) were found to be double positive

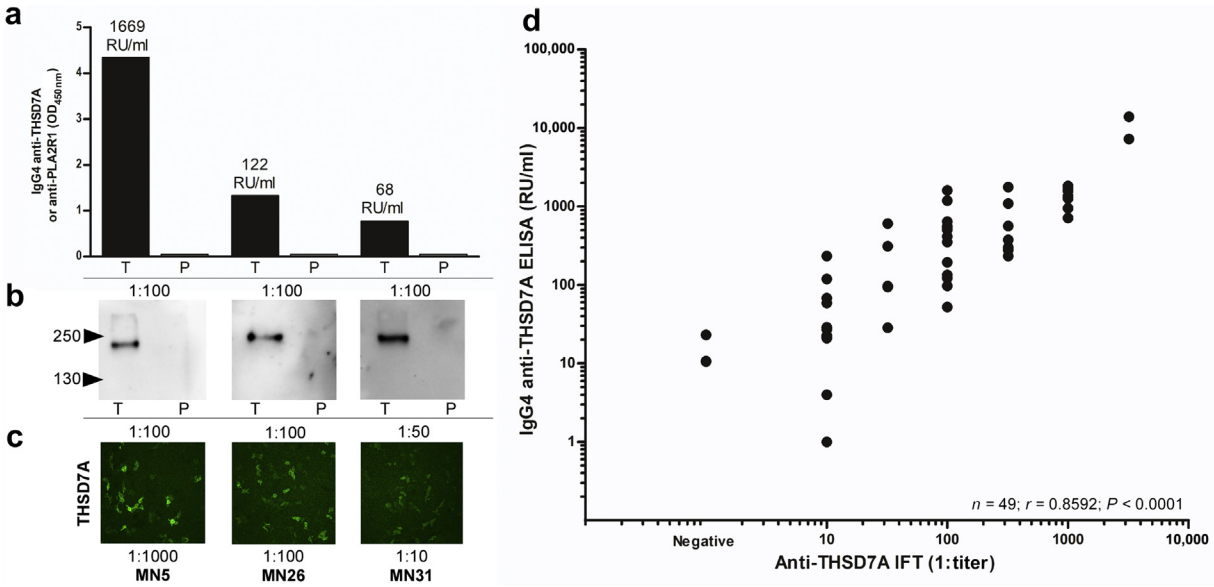

Figure 2 | Comparison of anti-thrombospondin type 1 domain-containing 7A (THSD7A) detection in serum by enzyme-linked immunosorbent assay (ELISA), Western blot, and indirect immunofluorescence test (IIFT). (**a**) ELISA reactivity for 3 membranous nephropathy (MN) patients (MN5, MN26, and MN31) with low- to high-range titers detected at a dilution of 1:100. MN5 was further diluted to determine the ELISA titer with accuracy. (**b**) Western blot reactivity of the same patients tested at optimal serum dilution against purified recombinant THSD7A (T) and phospholipase A2 receptor 1 (PLA2R1) (P) (50 ng each). Blots were exposed for different times. (**c**) IIFT reactivity at optimal serum dilution. (**d**) Correlation between anti-THSD7A levels of MN patients (n = 49) as measured by IIFT (detection for total IgG) and ELISA (detection for IgG4). The correlation is significant (r = 0.8592, $P < 0.0001$). OD, optical density; RU, relative units. To optimize viewing of this image, please see the online version of this article at www.kidney-international.org.

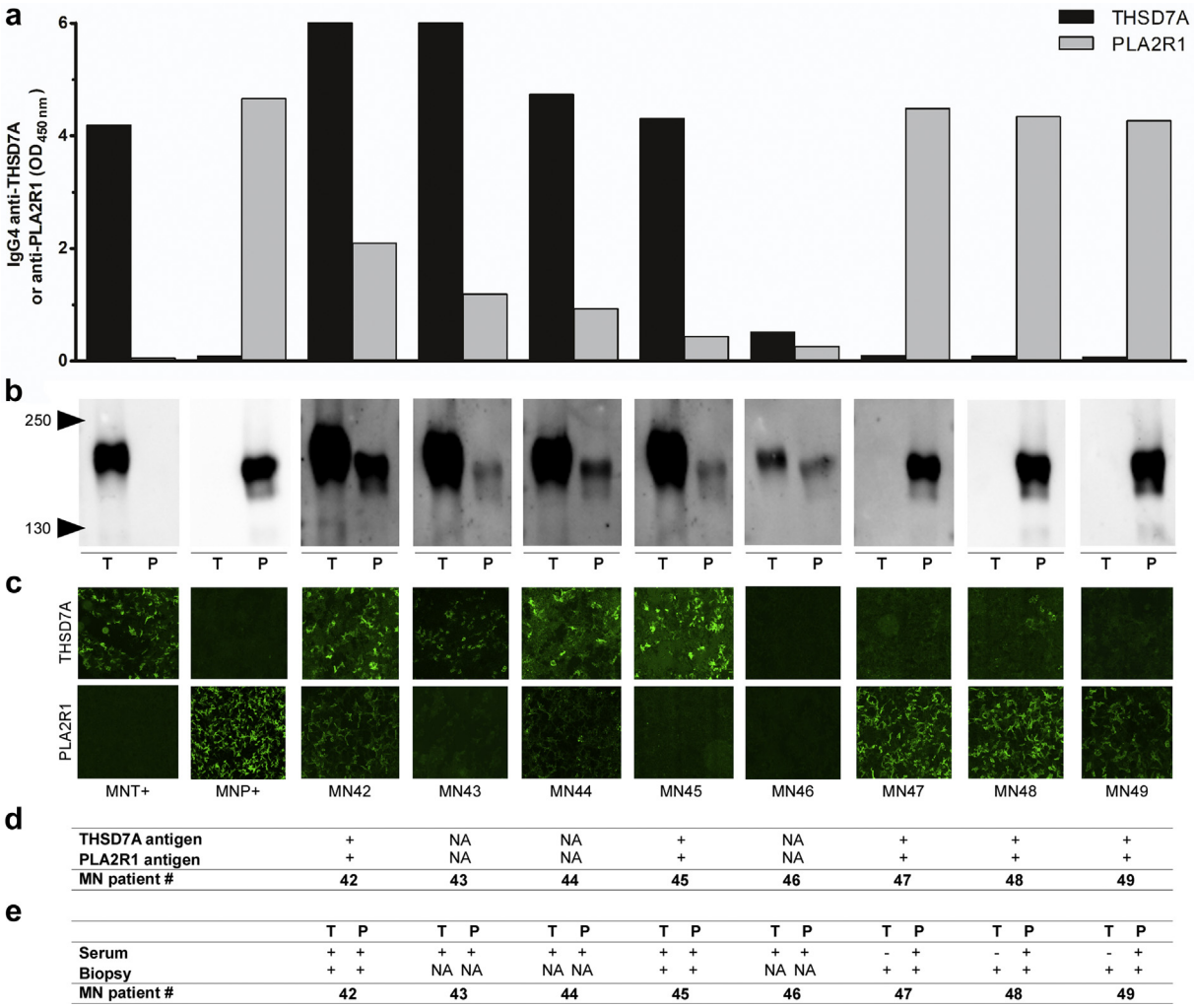

Figure 3 | Detection of anti-thrombospondin type 1 domain-containing 7A (THSD7A) and anti-phospholipase A2 receptor 1 (PLA2R1) autoantibodies in double-positive membranous nephropathy (MN) patients. (**a**) Reactivity of sera from double-positive MN patients (MN42 to MN49) and single-positive MN control subjects (MNT+ and MNP+) against THSD7A and PLA2R1 antigens in enzyme-linked immunosorbent assay (ELISA). All sera were diluted at 1:100 except MN46 (1:25). (**b**) Western blot reactivity of sera from double-positive MN patients (MN42 to MN49) against THSD7A (T) and PLA2R1 (P) antigens (50 ng each) loaded on sodium dodecylsulfate polyacrylamide gel electrophoresis (SDS-PAGE) (6%) under nonreducing conditions. All sera were used at a dilution of 1:25. Soluble forms of THSD7A and PLA2R1 have molecular masses of about 230 kDa and 170 kDa, respectively. (**c**) Indirect immunofluorescence test showing the reactivity of MN42 to MN49 against HEK 293 cells transfected with THSD7A or PLA2R1 expression vectors. Sera were tested at a dilution of 1:10 or higher depending on titer. (**d**) Summary of positivity by biopsy staining for THSD7A and PLA2R1 antigens (biopsies were available for 5 patients: MN49 staining is shown in Supplementary Figure S6; for other patients, the original data can be found elsewhere[8,9]). (**e**) Summary of positivity for THSD7A and PLA2R1 autoantibody or antigen in serum or on biopsy, respectively. NA, not available; OD, optical density. To optimize viewing of this image, please see the online version of this article at www.kidney-international.org.

(Figure 3). Four of these patients were previously reported from an American cohort (MN42 and MN45)[8] and a Chinese cohort (MN47 and MN48),[9] but none of them were compared for levels of anti-THSD7A and anti-PLA2R1 autoantibodies by quantitative ELISA. Analysis with baseline serum showed that double-positive patients can have different titers of anti-THSD7A and anti-PLA2R1 autoantibodies (Figure 3a). Four patients had relatively higher titers of anti-THSD7A than anti-PLA2R1; 1 patient had low titers of both autoantibodies; and the last 3 patients had no detectable levels of anti-THSD7A but high anti-PLA2R1 titers. The first 5 patients (MN42 to MN46) were clearly double positive in serum by ELISA and WB (Figure 3a and b), but some of them appeared less positive by IIFT, which may be explained, at least in part, by the low titers measured by ELISA (Figure 3c). The last 3 patients (MN47, MN48, and MN49) were positive in serum by all 3 techniques (ELISA, WB, and IIFT) for PLA2R1 but not for THSD7A (Figure 3a to c).

Among the 49 patients, renal biopsies were available for a total of 11 patients and were tested for THSD7A and PLA2R1 staining. This includes data previously published for MN42, MN45, MN47, and MN48.[8,9] In agreement with ELISA, 6 patients (MN5, MN6, MN13, MN26, MN34, and MN41) were positive for THSD7A but negative for PLA2R1 on biopsy

(Supplementary Figure S6). The other 5 patients had enhanced staining for both THSD7A and PLA2R1 (for MN42, MN45, MN47, MN48, and MN49, see Larsen *et al.*[8] and Wang *et al.*[9]; see also Supplementary Figure S6 for MN49; data for MN42 to MN49 are summarized in Figure 3d).

Taken together, we conclude that 8 patients are double positive for THSD7A and PLA2R1 (Figure 3e). Our analyses also illustrate the need of using all available techniques for detection of anti-THSD7A and anti-PLA2R1 in serum and antigen staining in biopsy to identify these rare cases of double-positive MN patients.

Clinical characteristics of THSD7A-associated MN patients

Overall, the baseline clinical characteristics of the 49 THSD7A-associated MN patients (Table 2, Supplementary Table S1) did not strongly differ from patients with PLA2R1-associated MN including those from the cohorts listed in Table 1.[23,27,33,34,41,49,54] At baseline, the median age of the 49 anti-THSD7A-positive patients was 59.9 years. Median proteinuria and estimated glomerular filtration rate (eGFR) were 6.1 g/d (interquartile range [IQR]: 4.1–10.2) and 76.5 ml/min per 1.73 m^2 (IQR: 49.8–90.0), respectively. There was no significant correlation between anti-THSD7A titer and proteinuria (Supplementary Figure S7).

Because we previously observed a high proportion of women in THSD7A-positive patients as compared to PLA2R1-positive patients,[7] we investigated the influence of sex on the clinical parameters and anti-THSD7A titers in our cohort (Table 2). Among the 49 patients, 28 were male (57%) and 21 were female (43%), giving a sex ratio of 1.3:1, which contrasts with the 2:1 ratio typically observed in the general MN population (e.g., it is 2.1:1 in our combined cohort of 1012 patients) (Table 1) or the PLA2R1-associated MN-specific subgroup.[15] Interestingly, female patients were significantly younger than male patients (48.8 vs. 67.0 years, $P = 0.003$). Data for age of menopause were lacking in our cohort. The average age at menopause of women with CKD is 51 years,[55,56] which suggests that a significant number of women developed MN before menopause (Figure 4a, Table 2). However, the levels of anti-THSD7A titers did not significantly differ between male and female patients, nor with age when analyzed by tertiles or when female patients were compared as 2 subgroups, below and above 51 years (Figure 4b, Supplementary Figure S8A, Supplementary Table S2). Titers separated by sex did not correlate with proteinuria (Supplementary Figure S7). Proteinuria and serum albumin did not differ between male and female patients, irrespective of age (Table 2, Supplementary Figure S8B). Serum creatinine was higher and eGFR was lower in male patients, which might be partly age-related or due to more severe disease in these men (Table 2).

It has been reported that THSD7A-associated MN may be linked to malignancy.[41] In our cohort, only 8 patients (16%) had a history of malignancy, including 6 male and 2 female patients (Table 2, Supplementary Table S3). Clinical parameters were similar between these patients and others, except for serum albumin, which was lower, possibly due to superimposed malnutrition.[57] Interestingly, all 8 patients with malignancy were significantly older, and only 3 of them were diagnosed for malignancy within 2 years of MN diagnosis (Supplementary Tables S3 and S4). Titers of anti-THSD7A autoantibodies tended to be higher in patients with associated malignancy but the difference did not reach statistical significance (Supplementary Table S3). Although the pattern of IgG subclass may differ between primary and secondary MN associated with malignancy,[24,45,58] no differences in the relative levels of anti-THSD7A IgG subclasses were observed between patients with and without malignancy (Supplementary Table S5).

We finally compared the clinical characteristics of patients with single positivity to THSD7A ($n = 41$) versus double positivity to THSD7A and PLA2R1, which included 4 male and 4 female patients ($n = 8$). No significant differences were observed for age, sex, and baseline clinical values nor for percentage of malignancy-associated MN between the 2 groups (Supplementary Table S6).

Association of anti-THSD7A titer with disease activity

We compared anti-THSD7A titers at baseline and during follow-up to test the association between anti-THSD7A titers and disease activity, including response to treatment or spontaneous remission. Overall, we observed higher titers of anti-THSD7A autoantibodies in patients with active disease as compared to those in partial or complete remission (Figure 5a). We only had follow-up sera for 12 patients with a median follow-up of 17 months (IQR: 7.0–31.3), but this number was sufficient to demonstrate that the anti-THSD7A titer is a relevant biomarker of the immunological autoimmune response and helps to monitor response to treatment (Figure 5b and c). At baseline, the 12 patients had nephrotic to subnephrotic range proteinuria (median: 5.9 g/d [IQR: 3.0–6.6]) and relatively high anti-THSD7A titers (median: 206 RU/ml [IQR: 68.8–472.8]). At the last follow-up of patients with available serum samples, patients who had reached spontaneous remission or remission after conservative or immunosuppressive treatment had non-nephrotic proteinuria levels (median: 1 g/d [IQR: 0.8–2.7]) and no detectable or strongly decreased anti-THSD7A titers (IQR: 16–26.5 RU/ml). In contrast, patients who did not reach remission, either untreated or resistant to immunosuppressive treatment, had nephrotic range proteinuria (median: 10.8 g/d [IQR: 6.5–14.0]) and persistently high anti-THSD7A titers (median: 709 RU/ml [IQR: 381.3–993.3]).

The utility of anti-THSD7A titer to monitor disease activity and response to treatment was further illustrated by the clinical follow-up of patient MN13, a 4-year-old girl treated twice with rituximab over 27 months (Supplementary Figure S9). At baseline, the patient had high proteinuria (6.1 g/d) and anti-THSD7A titer (715 RU/ml). Treatment with rituximab led to a progressive decrease of anti-THSD7A titer that was followed by fluctuating but finally decreasing proteinuria down to the subnephrotic range at month 18. Between months 18 and 27, anti-THSD7A titer and

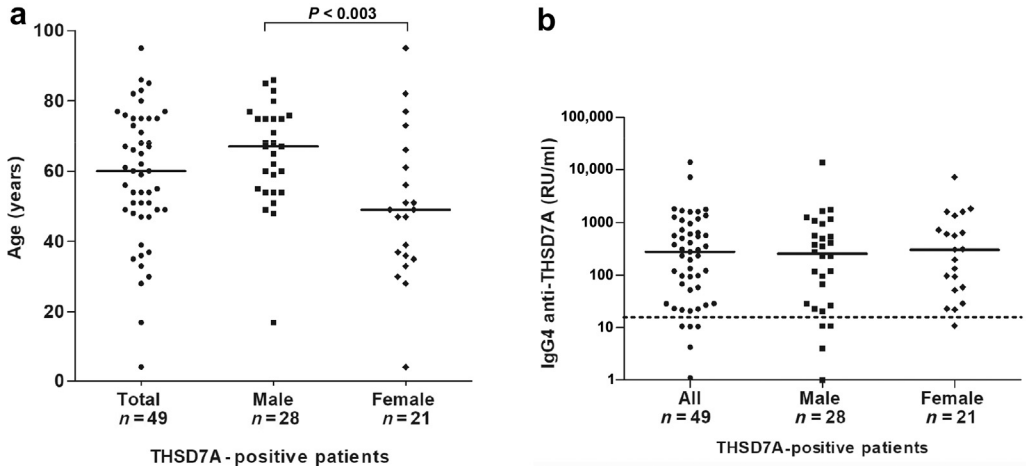

Figure 4 | Distribution of age and anti-thrombospondin type 1 domain-containing 7A (THSD7A) titers among THSD7A-positive patients as a whole or by sex. (**a**) Age distribution of anti-THSD7A-positive patients ($n = 49$). The data are presented as medians. Female patients were significantly younger than male patients using the Mann-Whitney *U* test ($P < 0.003$). (**b**) Distribution of anti-THSD7A titers for THSD7A-positive patients, as measured with anti-IgG4 secondary antibodies. The dotted line represents the threshold value for IgG4 detection. RU, relative units.

proteinuria increased again, suggesting an ongoing relapse. Comparison of anti-THSD7A autoantibody levels by ELISA, WB, and IIFT showed that ELISA was the most accurate assay to detect subtle changes of anti-THSD7A levels, with IgG4 and IgG3 appearing as the most relevant IgG subclasses to monitor disease activity.

Anti-THSD7A titer and clinical outcome of THSD7A-associated MN patients

Among the 49 THSD7A-associated MN patients, we had clinical outcome and detectable anti-THSD7A autoantibodies at baseline for 36 patients during a median follow-up of 37 months (range 6.5–180 months) (Supplementary Tables S1 and S7). During follow-up, 10 patients (28%) were untreated or treated with antiproteinuric therapy (angiotensin-converting enzyme inhibitors or angiotensin 2 receptor blockers and diuretics or all 3) while 24 (67%) patients received an additional immunosuppressive treatment (cyclosporine A, cyclophosphamide, rituximab, or adrenocorticotropic hormone). Treatment information was not available for 2 patients. Twelve patients (33%) remained in active disease among which 2 reached end-stage kidney disease, while 24 (67%) reached complete ($n = 16$) or partial ($n = 8$) remission. Two patients (MN29 and MN33) experienced relapse after partial remission (one after spontaneous remission and the other after treatment with cyclosporine A). Among the 12 patients who remained in active disease, 10 patients (83%) had received an immunosuppressive treatment (Supplementary Tables S1 and S7). Among the 24 patients who reached remission, 14 (58%) had received an immunosuppressive treatment (Supplementary Tables S1 and S7).

We evaluated the association between anti-THSD7A titer at baseline and clinical outcome. Overall, baseline anti-THSD7A titer significantly differs between patients reaching remission or not during follow-up (134 [IQR: 52; 955] vs. 536 [IQR: 250; 1671] RU/ml, respectively, $P = 0.04$) (Figure 6a), while these 2 groups were comparable for age, sex ratio, proteinuria, albuminemia, eGFR, and immunosuppressive treatment (Supplementary Table S7).

We then divided the patients into tertiles based on anti-THSD7A titer and analyzed outcome. Patients in the lowest tertile (titers 23–122 RU/ml) tended to have a higher rate of remission (11 of 12, 92%) compared with patients in the middle (titers 134–566 RU/ml) and highest (titers 606–13,920 RU/ml) tertiles (6 of 12, 50% and 7 of 12, 58%, respectively, $P = 0.07$), while persistent proteinuria and renal failure tended to be more frequent in patients with high anti-THSD7A titer, but none of these trends reached statistical significance (not shown). Because of the small sample size, we combined the middle and highest tertiles and compared renal survival during the first 3 years after diagnosis to the lowest tertile. Patients from the lowest tertile had better renal survival with more remission compared with patients from the medium and highest tertiles (Figure 6b, $P = 0.006$).

DISCUSSION

This study had 2 major aims: (i) the development of a robust ELISA allowing the sensitive and quantitative measurement of anti-THSD7A autoantibodies, and (ii) the analysis of a relatively large retrospective cohort of THSD7A-positive patients from which we may identify clinical characteristics specific for THSD7A-associated MN.

We set up an ELISA to detect anti-THSD7A autoantibodies in serum with characteristics and performance similar to those previously reported for PLA2R1, using the purified full extracellular region of THSD7A as antigen for the solid-phase assay, validation of the ELISA with MN patients versus negative control subjects and detection for either total IgG or IgG4 secondary antibodies.[20,21] Using this ELISA to screen a combined cohort of 1012 MN patients, we identified 28

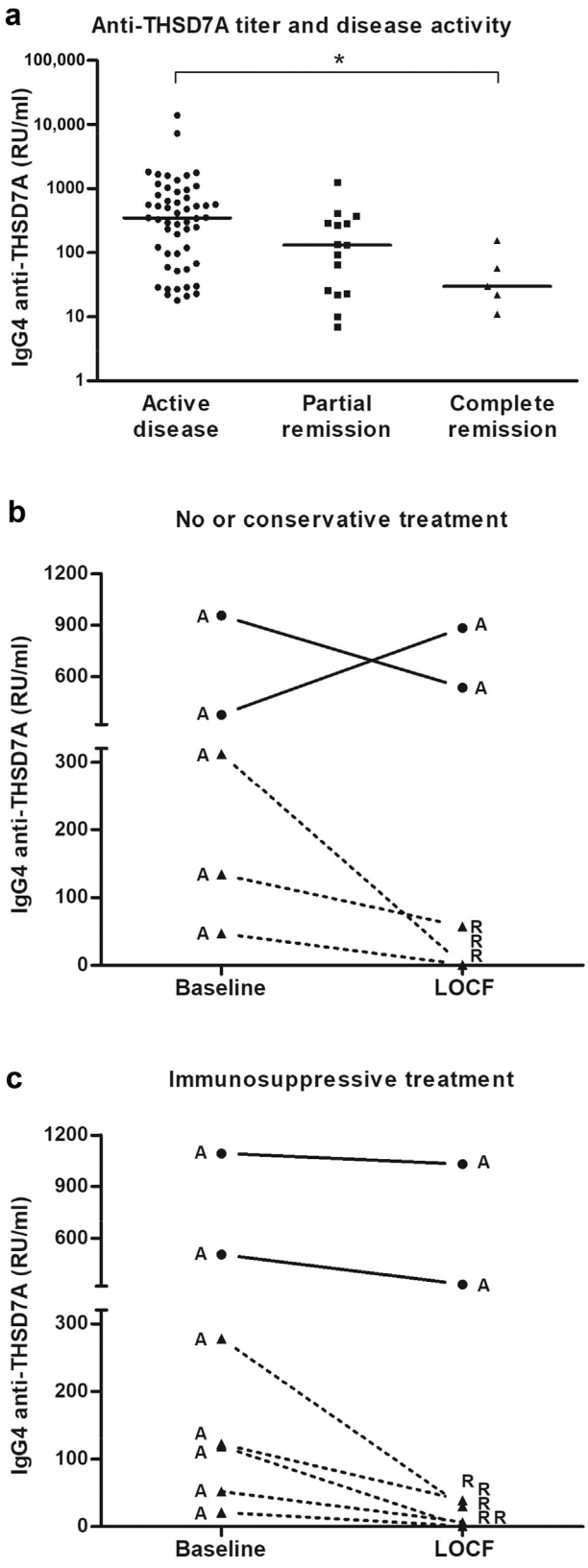

Figure 5 | Relationships between anti-thrombospondin type 1 domain-containing 7A (THSD7A) titers and clinical status in THSD7A-positive patients. (**a**) Anti-THSD7A titers were measured from baseline and follow-up sera of anti-THSD7A patients with active disease (53 baseline and follow-up serum samples with a mean proteinuria of 7.4 g/d), partial remission (15 follow-up serum samples with a mean proteinuria of 1.9 g/d), or complete remission (5 follow-up serum samples with a mean proteinuria of 0.3 g/d). The anti-THSD7A titer was significantly lower in patients with complete remission than in those in active disease. The difference in titer between patients in active disease versus partial remission did not reach significance. (**b**) Anti-THSD7A titers during follow-up of patients who received no or conservative treatment and (**c**) immunosuppressive treatment. Anti-THSD7A titers of patients who reached remission are shown with dotted lines. A, active disease; LOCF, last observation carried forward; R, remission; RU, relative units.

patients, indicating a prevalence of 2.8%, in accordance with the prevalence range of 2% to 5% previously reported for Caucasian or Asian cohorts (data are summarized in Supplementary Table S8).[7,9,41–43,59,60] By screening additional patients mostly referred because of PLA2R1-unrelated MN, we included 21 more cases, providing a cohort of 49 patients with THSD7A-associated MN. We validated the novel ELISA by comparing its sensitivity against the 49 MN patients with the original WB method[7] and the commercially available IIFT assay.[41] We found similar levels of sensitivity by ELISA and WB, and a significant correlation between anti-THSD7A titers measured by IIFT and ELISA. Among the 49 patients, 43 were positive by the 3 techniques: ELISA (IgG4 detection), WB (IgG4 detection), and IIFT (total IgG detection). One was positive by ELISA, WB, and IIFT (total IgG detection). One was only positive by ELISA (IgG4 detection) and WB (IgG4 detection). One was only positive by IIFT (total IgG detection). The last 3 were negative in serum by all 3 techniques. These discrepancies may be explained by the different autoantibody detection systems and presentation of antigens in solid-phase ELISA, WB, and IIFT cell-based assay. We also found that the ELISA is more sensitive when detection of anti-THSD7A autoantibodies is made with anti-IgG4 as compared to anti-total IgG. Indeed, 6 patients could be detected only with anti-IgG4 while 1 patient could be detected only with anti-total IgG. It is thus preferable to use anti-IgG4 as a secondary antibody to detect the highest number of MN patients with THSD7A-associated disease and avoid false-negative cases, yet further screening with anti-total IgG may help to identify additional patients.

The 3 patients who had no circulating anti-THSD7A autoantibodies detected by ELISA, WB, and IIFT were positive on biopsy with the presence of immune deposits containing the THSD7A antigen. Such discrepancies have been initially observed for PLA2R1-associated MN[22] and more recently for THSD7A-associated MN.[41] We conclude that the new ELISA is reliable and in accordance with available methods of detection such as WB and IIFT.[7,41]

Among the 49 patients, we identified 8 patients who were double positive for THSD7A and PLA2R1. No major clinical differences were observed between the single- and double-positive patients. Four double-positive cases were novel and from Europe while 2 were already reported from an American cohort[8] and two from a Chinese cohort.[9] Three of the new cases were identified from the screening of 1012 MN patients,

indicating an overall prevalence of about 0.3%. However, these 3 double-positive cases actually represent about 10% of the 28 THSD7A-positive patients (identified from 1012 patients) but only about 0.4% of the 684 patients identified with PLA2R1-associated MN (Table 1). With the observed respective prevalence of about 70% and 3% for PLA2R1 and THSD7A in our combined cohort, and assuming that the respective production of anti-PLA2R1 and anti-THSD7A autoantibodies is a random event, one would have expected many more double-positive patients in the PLA2R1-positive group than in the negative one, suggesting a negative association between the 2 events. However, we could not determine from these studies whether the presence of both anti-PLA2R1 and anti-THSD7A autoantibodies is coincidental or associated one to another (for instance by intermolecular epitope spreading),[61] nor could we determine what autoantibody would precede the other during the natural history of the disease.

Careful analysis of the 8 double-positive patients led us to make 2 additional observations. First, the respective circulating levels of anti-THSD7A and anti-PLA2R1 could be very different between patients, with all scenarios observed, that is, lower titer of anti-THSD7A than anti-PLA2R1 and vice versa, or similar titers of both autoantibodies. Second, among the 5 patients with available serum and biopsy, 2 were fully positive, in other words, for both antigens in serum and biopsy (MN42 and MN45), while 3 (MN47, MN48, and MN49) were positive in both serum and biopsy for PLA2R1 but only positive for THSD7A in biopsy. This different pattern of positivity in serum versus biopsy is reminiscent of what was previously observed for MN patients with single positivity for PLA2R1 or THSD7A.[22,41]

In this study, we also present the clinical analysis of the largest cohort of patients with THSD7A-associated MN with quantitative analysis of anti-THSD7A titers for the different IgG subclasses. First, we observed that the titer of anti-THSD7A autoantibodies is heterogeneous and can vary by up to 3 orders of magnitude in both sexes. Second, we showed that IgG4 is the predominant IgG subclass for anti-THSD7A autoantibodies in most patients, regardless of coincidental diseases. Third, we observed no strong correlation between anti-THSD7A titer and levels of proteinuria, as previously observed for PLA2R1-associated MN.[20] Nonetheless, the anti-THSD7A titer appears to be a relevant biomarker to monitor disease activity during follow-up and treatment with immunosuppressors, as exemplified for the 12 patients with available follow-up. Fourth, we showed that patients with low anti-THSD7A titer at baseline had better clinical outcome, as was previously observed for PLA2R1-associated MN.[20,25,27,28,31,35,62] In addition to anti-PLA2R1 titer, PLA2R1 epitope spreading was recently identified as a prognosis biomarker to predict outcome in MN.[14,34] Despite the recent identification of several epitopes in THSD7A,[16] it remains to determine whether epitope spreading also occurs in patients with THSD7A-associated MN and may be a relevant biomarker of disease activity and clinical outcome.

The relatively large size of our cohort allowed stratification of patients by sex and comparison of their epidemiological and clinical parameters. First, we observed a male-female ratio of 1.3:1 that contrasts with the 2:1 ratio typically reported when considering all MN cases or PLA2R1-associated MN.[2–5,63] Second, we observed that female patients were younger than male patients at diagnosis, suggesting different etiologies. To confirm our findings, we compiled the available data on sex and age from all previous studies identifying cases of THSD7A-associated MN (Supplementary Table S8) and observed that female patients were indeed more preponderant and younger in THSD7A-associated MN than in PLA2R1-associated MN. Third, we observed that female patients had on average similar levels of anti-THSD7A autoantibodies, yet the levels seemed to vary with age. However, we could not find evidence of significant differences in disease activity, response to treatment, and clinical outcome between male and female patients.

The underlying etiologies leading to PLA2R1- and THSD7A-associated MN are currently unknown.[2,3,64] We observed many associated diseases in our cohort of THSD7A-associated diseases (Supplementary Table S1). Recent studies reported that 8 of 40 THSD7A-positive MN patients (20%) had an associated malignancy within a median time of 3 months from diagnosis of MN, suggesting that THSD7A-positive patients are at higher risk of having an underlying malignant disease and may be intensively screened for cancer as a possible etiology.[41,65] In our cohort, we found that 8 of the 49 THSD7A-positive MN patients (16%) had a history of cancer, including 1 double-positive patient. However, only 3 patients had cancer (gastric, colonic, and prostatic) within 2 years of MN diagnosis. Furthermore, we observed that 7 of the 8 patients were older than 65 years, with 6 male and 2 female patients. These observations are in line with the study by Hoxha *et al.*[41] where 5 of the 8 patients were older than 65 years, with 5 male and 3 female patients. We also observed that the 8 THSD7A-positive patients with associated cancer tended to have higher anti-THSD7A titers, but no significant differences in IgG subclasses. Earlier studies reported that the prevalence of malignancy in MN patients is higher than in the general population, while it increases with age,[66–69] but our data converge to the point that most cases of THSD7A-associated MN with malignancy were likely coincidental in our subgroup of 8 patients.

Another cause of MN may be associated with pregnancy and preeclampsia,[70–73] including recent observations for THSD7A-associated MN.[74,75] In line with this hypothesis, we observed a significant subgroup of young THSD7A-positive female patients (before menopause) (Figure 4b) in our cohort but we could not find evidence of a relationship between MN and pregnancy or preeclampsia.

We also described 2 cases of pediatric and adolescent MN with no associated underlying disease: a 4-year-old girl who was treated with rituximab and reached partial remission, and a 17-year-old boy who had high anti-THSD7A titer at baseline and was resistant to rituximab.

In conclusion, we have reported a novel ELISA that is useful to diagnose MN patients for THSD7A-associated disease, to

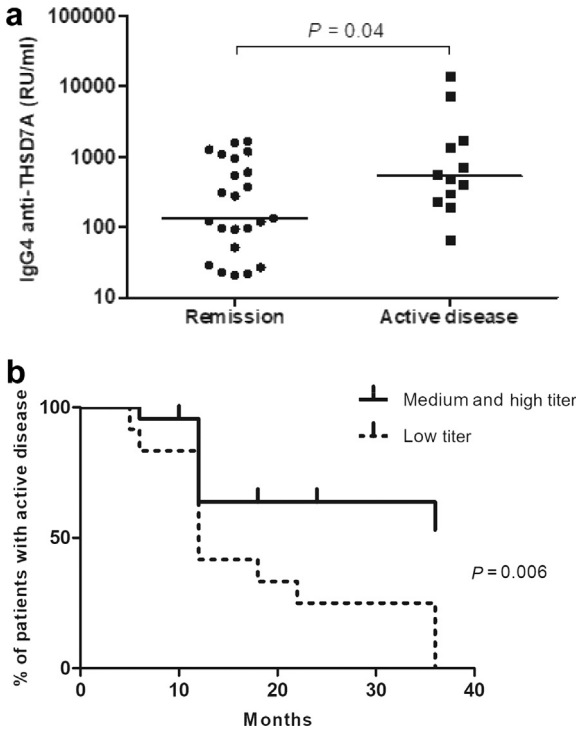

Figure 6 | Anti-thrombospondin type 1 domain-containing 7A (THSD7A) titer at baseline predicts clinical outcome. (**a**) Anti-THSD7A titers at baseline significantly differ between patients with remission versus active disease at last follow-up ($n = 36$, $P = 0.04$). (**b**) Renal survival at last follow-up. Renal event is defined by partial or complete remission within 3 years after anti-THSD7A enzyme-linked immunosorbent assay (ELISA) measured at baseline. Patients with a low titer of anti-THSD7A (titers 23–122 relative units [RU]/ml, first tertile) had a higher incidence of renal events as compared to patients with medium and high titer (titers 134–13,920, middle and high tertiles together) ($n = 36$, $P = 0.006$).

carefully monitor disease activity and response to treatment during follow-up, and predict clinical outcome. We also described new cases of patients with THSD7A-associated MN supporting the hypothesis that THSD7A-associated MN differs from PLA2R1-associated MN in the natural history and epidemiological features, such as sex, age at onset, and associated etiologies.[15,76] Interestingly, this situation appears reminiscent to that observed for myasthenia gravis, a neuromuscular autoimmune disease with multiple autoantigens and different paths and etiologies toward the same disease entity.[77,78]

METHODS

Patients

Because the prevalence of THSD7A-associated MN is low, we included patients from several national and international nephrology centers. Baseline serum samples of patients with biopsy-proven MN were collected within 6 months from renal biopsy. A total of 1012 patients originating from 6 independent retrospective cohorts and additional patients who were referred to us mostly for PLA2R1-unrelated MN were screened for anti-THSD7A autoantibodies. eGFR was calculated by applying the Chronic Kidney Disease Epidemiology Collaboration (CKD-EPI) formula. Disease activity was defined as no remission of nephrotic syndrome. Partial remission was defined as proteinuria lower than 3.5 g/d and at least 50% reduction from the time of inclusion in the study with normalization of the serum albumin concentration and stable serum creatinine. Complete remission of proteinuria was defined as proteinuria lower than 0.5 g/d, normal albuminemia, and stable eGFR. Remissions were classified as spontaneous if they were occurring without the administration of immunosuppressive agents during follow-up. The negative control groups included serum samples from patients with other diseases such as lupus nephritis ($n = 9$), membranoproliferative glomerulonephritis ($n = 9$), anti-neutrophil cytoplasmic autoantibodies vasculitis ($n = 3$), IgA nephropathy ($n = 11$), other renal diseases ($n = 18$) and from healthy blood donors ($n = 52$). The studies were approved by the relevant institutional review boards in the different countries and were conducted according to the principles of the Declaration of Helsinki. Written informed consent was obtained from participants in all studies.

ELISA for the detection of anti-THSD7A and anti-PLA2R1 autoantibodies

Purified recombinant THSD7A protein (prepared as described in the Supplementary Methods) or the full extracellular domain of human PLA2R1 prepared as described[21] were used as antigens to coat 96-well ELISA microplates (Thermo Fisher Scientific, Waltham, MA) in 20 mmol/l tris(hydroxymethyl)-aminomethane pH 8.0 overnight at 4 °C. Plates were blocked with SeramunBlock (Seramun Diagnostica, Heidesee, Germany) for 2 hours. Patients' serum samples diluted at 1:100 in 0.1% low-fat dry milk phosphate-buffered saline were incubated for 2 hours. Plates were washed 3 times with phosphate-buffered saline–Tween 0.02%. Bound human antibodies were detected with either anti-human horseradish peroxidase–conjugated IgG1, IgG2, IgG3, IgG4, or total IgG (Southern Biotech, Birmingham, AL) diluted in SeramunStab ST (Seramun Diagnostica) at 1:5000, 1:5000, 1:20,000, 1:30,000, and 1:200,000, respectively. Secondary antibodies were all incubated for 1 hour. After washes, tetramethylbenzidine peroxidase substrate was added and developed for 15 minutes. The reaction was stopped by adding 1.2 N HCl. All incubation steps were carried out at room temperature on a plate shaker. The optical density was read at 450 nm using a plate reader. A standard curve for IgG4 detection was made using a highly THSD7A-positive serum that was assigned a value of 99,000 RU/ml when not diluted. A standard curve consisting of 8 dilutions covering the range from 990 RU to 9.9 RU/ml was plotted using the GraphPad Prism software and applied to each plate to convert optical density values into RU/ml (Supplementary Figure S2B). Samples that were out of range were diluted at 1:500 and 1:1000 and reanalyzed. The interassay variation was measured by incorporating a borderline positive serum sample on each plate. Results from 10 different plates showed a coefficient of interassay variation lower than 20% (not shown). Normal range for IgG1, IgG2, IgG3, and total IgG detection were defined using serum samples from disease control subjects and healthy donors (not shown).

WB and IIFT for the detection of circulating anti-THSD7A and anti-PLA2R1 autoantibodies and kidney biopsy staining for THSD7A and PLA2R1 antigens

Detailed procedures for WB[7] and biopsy staining[22] are provided in the Supplementary Methods. We used the commercial cell-based IIFT kit from Euroimmun AG containing a mosaic biochip of formalin-fixed HEK293 cells overexpressing full-length human THSD7A or PLA2R1 or mock-transfected HEK293 as a negative control.

Statistical analysis

Baseline characteristics of the patients in the study were expressed as percentages for qualitative variables and medians and IQRs for quantitative variables. Nonparametric correlations between several parameters were calculated using the Spearman test. Quantitative variables were compared by Mann-Whitney U or 1-way analysis of variance (ANOVA) tests and categorical variables were compared by a Pearson chi-squared test or a Fisher exact test. P values lower than 0.05 were considered as statistically significant. Statistics were performed using the GraphPad Prism version 6 software. Renal survival curves were calculated using Kaplan-Meyer estimates for survival distribution. The endpoint was the time where patients entered into remission (partial or complete) from baseline. Differences between groups based on tertiles of anti-THSD7A titer were analyzed with the log-rank test.

DISCLOSURE

Some coauthors are coinventors on the patents "Diagnostics for membranous nephropathy" (LHB and GL), "Methods and kits for monitoring membranous nephropathy" (BSP and GL), and "Prognosis and monitoring of membranous nephropathy based on the analysis of PLA2R1 epitope profile and spreading" (BSP, GD, and GL).

ACKNOWLEDGMENTS

We are grateful to the following physicians who participated in the inclusion of patients in this study: Vincent L. M. Esnault (Centre Hospitalier Universitaire [CHU], Nice, France); Stéphane Burtey, Laurent Samson, Laurent Daniel, and Sophie Jego-Desplat (CHU la Conception, Marseille, France); Karine Dahan (Hôpital Tenon, Paris, France); Aude Servais (Hôpital Necker, Paris, France); Michel Delahousse (Hôpital Foch, Suresnes, France); Corinne Bagnis (Hôpital de la Pitié-Salpêtrière, Paris, France); Thomas Crépin, Nadège Devillard, and Cécile Courivaud (CHU de Besançon, France); Arnaud Lionet (Centre Hosptialier Régional Universitaire, Lille, France); Coralien Vink (Radboudumc, Nijmegen, The Netherlands); Christopher Larsen (Arkana Laboratories, Little Rock, AR, USA); Meryl Waldman (National Institutes of Health/National Institute of Diabetes and Digestive and Kidney Diseases, Bethesda, MD, USA); Jai Radhakrishnan (Columbia University, New York, NY, USA); Tanuja Mishra (Baltimore, MD, USA); and Ming-Hui Zhao (University of Peking, China). HD and PR thank the Centre de Ressources Biologiques (Hôpital Tenon) for the preparation and storing of samples.

Supported by grants to GL from Centre National de la Recherche Scientifique, the Fondation Maladies Rares (LAM-RD_20170304), the National Research Agency (grants MNaims ANR-17- CE17-0012-01), and "Investments for the Future" Laboratory of Excellence SIGNALIFE, a network for innovation on signal transduction pathways in life sciences (ANR-11-LABX-0028-01) with allocated PhD fellowships for CZ and JJ), and the Fondation de la Recherche Médicale (DEQ20180339193 to GL and FDT201805005509 to JJ); grants from the Centre Hospitalier Universitaire de Nice and the Direction Générale de l'Offre de Soins of the French Ministry of Health (PLA2R1 autoantibodies in Membranous Nephropathy in Kidney Transplantation Programme, PRAM-KT PHRC2011-A01302-39, NCT01897961) to GL and BSP; grants from the European Research Council ERC-2012 ADG_20120314 no. 322947 and the Seventh Framework Programme of the European Community contract no. 2012-305608 (European Consortium for High-Throughput Research in Rare Kidney Diseases) to PR; grants from the Dutch Kidney Foundation (Nierstichting Nederland 17PhD12 program) to JFMW and AEvdL; grants from the National Institutes of Health/National Institute of Diabetes and Digestive and Kidney Diseases (R01 DK097053) to LHB; and grants from the Sahlgrenska University Hospital ALF, The Swedish Kidney Foundation and The Swedish Medical Research Council grant 14764 to JN and JLW.

SUPPLEMENTARY MATERIAL

Supplementary Methods.

Figure S1. Cloning, expression, and purification of recombinant human soluble thrombospondin type 1 domain-containing 7A 6X histidine (THSD7A-6xHis). (**A**) Schematic representation of the pCMV6-entry expression vector coding for human soluble THSD7A-6xHis. The cDNA insert encodes for the signal peptide followed by the full extracellular region of THSD7A (from Met-1 to Thr-1606, Uniprot Q9UPZ6) and a C-terminal 6xHis Tag. (**B**) Western blot after HisTag purification from human embryonic kidney 293 cell medium containing soluble THSD7A-6xHis and probed with membranous nephropathy patient 8 (MN8) under nonreducing conditions at a 1:100 dilution. We loaded 400 ml of cell medium onto 4 ml of Ni-NTA resin. The resin was washed once with 40 ml of washing equilibrium buffer and then with 40 ml of washing buffer containing 10 mmol/l imidazole. Bound protein was eluted with 28 ml (in 7 fractions) of elution buffer containing 400 mmol/l imidazole. Aliquots of cell medium (CM), flow-through (FT), washes (W), and eluate (1 to 7) fractions were separated by sodium dodecylsulfate polyacrylamide gel electrophoresis (10%), transferred to polyvinylidene difluoride membranes and analyzed by Western blot. (**C**) Silver staining of the purified THSD7A-6xHis (100 ng) after buffer exchange with 1X phosphate-buffered saline. (**D**) Western blots to validate the purified THSD7A-6xHis as a native folded protein. Purified recombinant THSD7A-6xHis (50 ng) was loaded on sodium dodecylsulfate polyacrylamide gel electrophoresis (10%) under reducing or nonreducing conditions and probed with 2 commercially available anti-THSD7A antibodies and 2 representative anti-THSD7A-positive patients (MN8 and MN10; dilution 1:100).

Figure S2. Receiver-operating characteristic curve and calibration curve for IgG4 anti-thrombospondin type 1 domain-containing 7A (THSD7A) enzyme-linked immunosorbent assay (ELISA). (**A**) Receiver-operating characteristic curve analysis of IgG4 anti-THSD7A detection in 44 anti-THSD7A-positive patients and 242 negative control subjects by ELISA. The area under the curve was 0.9982 (95% confidence interval: 0.9957–1.0, $P < 0.0001$). (**B**) Calibration curve covering the range of 9.9 relative units (RU)/ml to 990 RU/ml used to convert optical density (OD) values into RU/ml.

Figure S3. Levels of IgG subclasses and total IgG for anti-thrombospondin type 1 domain-containing 7A (THSD7A) autoantibodies, and correlation between anti-THSD7A titers by enzyme-linked immunosorbent assay (ELISA) and indirect immunofluorescence test (IIFT). (**A**) Scatter plot showing the distribution of anti-THSD7A titers for the 49 THSD7A-positive patients, as measured with total IgG as a secondary antibody. Titer for membranous nephropathy patient (MN40) is shown with asterisk (*). (**B**) Correlation between total IgG anti-THSD7A titers measured by IIFT versus ELISA. The correlation is highly significant ($n = 49$, $r = 0.8359$, $P < 0.0001$). (**C**) Distribution of anti-THSD7A IgG subclasses measured by ELISA for the THSD7A-positive patients ($n = 49$) versus control subjects (other diseases and healthy donors, $n = 101$). The anti-THSD7A titer for IgG3 and IgG4 subclasses was significantly different from that of control subjects using 1-way analysis of variance test (**<0.01, ***<0.001). Optical density (OD) values for MN40 are shown with asterisk (*). (**D**) Correlation between anti-THSD7A titers measured by ELISA using IgG4 and total IgG secondary antibodies ($n = 49$, $r = 0.9251$, $P < 0.0001$). (**E**) Zoom on the low to middle range titers of anti-THSD7A titers measured by ELISA using IgG4 and total IgG secondary antibodies ($n = 47$).

Figure S4. Indirect immunofluorescence test (IIFT) data for thrombospondin type 1 domain-containing 7A (THSD7A)-positive patients. Autoantibody titers were estimated by the fluorescence intensity at various dilutions. Data are shown at the dilution titer. Data for membranous nephropathy patient 5 (MN5), MN13, MN26, MN31, and MN42 to MN49 are presented in the main figures.

Figure S5. Western blot analysis of purified recombinant thrombospondin type 1 domain-containing 7A (THSD7A) and

phospholipase A2 receptor 1 (PLA2R1) antigens (50 ng each) probed with all sera from THSD7A-positive patients under nonreducing conditions. Serum reactivity of patients was tested at optimal serum dilution (1:10 to 1:100). The blots were exposed for different times. Results for membranous nephropathy patient 5 (MN5), MN13, MN26, MN31, and MN42 to MN49 are presented in the main figures.

Figure S6. Immunofluorescence staining of thrombospondin type 1 domain-containing 7A (THSD7A) and phospholipase A2 receptor 1 (PLA2R1) antigens for available patients' biopsies. (**A**) Available immunofluorescence biopsy staining for THSD7A antigen for the anti-THSD7A-positive patients included in this study (membranous nephropathy patient 5 [MN5], MN6, MN13, MN26, MN34, MN41) and for 1 double-positive patient (MN49). An anti-PLA2R1 positive serum (MNP+) was used as a positive control for PLA2R1 staining. Bar = 50 μm.

Figure S7. Correlation of proteinuria with IgG4 and total IgG anti-thrombospondin type 1 domain-containing 7A (THSD7A) titers measured by enzyme-linked immunosorbent assay for anti-THSD7A-positive patients as a whole or by sex. (**A**) Correlation between proteinuria and IgG4 anti-THSD7A titers for all ($n = 49$, $r = 0.2767$, $P = 0.0542$), male or female THSD7A-positive patients. (**B**) Correlation between proteinuria and total IgG anti-THSD7A titers for all ($n = 49$, $r = 0.2711$, $P = 0.0595$), male or female THSD7A-positive patients. Proteinuria levels show no significant correlation with anti-THSD7A titers.

Figure S8. Relationship between anti-thrombospondin type 1 domain-containing 7A (THSD7A) titer, proteinuria, and age of anti-THSD7A-positive patients by tertiles. (**A**) Relationship between anti-THSD7A median titer (relative units [RU]/ml) and age of patients in tertiles for all, male, or female THSD7A-positive patients. (**B**) Relationship between proteinuria levels (g/d) and age of patients in tertiles for all male or female THSD7A-positive patients. Anti-THSD7A and proteinuria levels show no significant correlation with age.

Figure S9. Anti-thrombospondin type 1 domain-containing 7A (THSD7A) titer and proteinuria levels during clinical follow-up for membranous nephropathy patient 13, a THSD7A-positive pediatric patient (4 years old at baseline) treated with rituximab. The patient had nephrotic range proteinuria at baseline and received 2 courses of rituximab (RTX) at months 2 and 7. See more clinical details in the Supplementary Methods. (**A**) Respective levels of anti-THSD7A autoantibodies measured by enzyme-linked immunosorbent assay for the different IgG subclasses and proteinuria during a follow-up of 27 months. (**B,C**) Anti-THSD7A levels measured by Western blot and indirect immunofluorescence test. Enzyme-linked immunosorbent assay and indirect immunofluorescence test detect the fluctuation of serum anti-THSD7A levels more quantitatively than Western blot. Bar = 70 μm. There is a significant correlation between anti-THSD7A titers measured by enzyme-linked immunosorbent assay and indirect immunofluorescence test (not shown). (**D**) IgG4 anti-THSD7A titer shown in relative units (RU)/ml while it is shown as optical density (OD) values in panel A.

Table S1. Detailed clinical characteristics of the 49 thrombospondin type 1 domain-containing 7A (THSD7A)-associated membranous nephropathy patients, ranked by titers from highest to lowest and by sex. Double-positive patients are listed at the end for each sex. Enzyme-linked immunosorbent assay (ELISA) titer <16 relative units (RU)/ml were measured at dilution 1:25 or 1:10 when serum was available. A, active disease; CR, complete remission; CP, cyclophosphamide; ESKD, end-stage kidney disease; NA, not available; PR, partial remission; RTX, rituximab.

Table S2. Clinical characteristics of females below and above 51 years (chosen as average age for menopause).[55,56] No differences were observed.

Table S3. Clinical characteristics of anti-thrombospondin type 1 domain-containing 7A (THSD7A)-positive patients with and without associated malignancy. Values are shown as *n* or median (interquartile range).

Table S4. Time gap between malignancy and membranous nephropathy (MN) diagnosis. *Negative values indicate prior diagnosis of malignancy.

Table S5. Distribution of anti-thrombospondin type 1 domain-containing 7A (THSD7A) IgG subclasses in THSD7A-positive patients. Values are shown as *n* (%).

Table S6. Clinical baseline characteristics of double-positive patients. No major difference was observed between patients with single positivity for anti-THSD7A versus double positivity for anti-thrombospondin type 1 domain-containing 7A (THSD7A) and anti-phospholipase A2 receptor 1 (PLA2R1). Values are shown as *n* (%) or median (interquartile range).

Table S7. Baseline characteristics of thrombospondin type 1 domain-containing 7A (THSD7A)-positive patients in remission versus active disease during follow-up. Only anti-THSD7A titer differs between the 2 subgroups of patients.

Table S8. Characteristics of all anti-thrombospondin type 1 domain-containing 7A (THSD7A)-positive patients published to date. Values are shown as *n* and mean (or median [*][S1,S2]) for age. ND, not defined.

Supplementary material is linked to the online version of the paper at www.kidney-international.org.

REFERENCES

1. Ponticelli C, Glassock RJ. Glomerular diseases: membranous nephropathy—a modern view. *Clin J Am Soc Nephrol*. 2014;9:609–616.
2. Beck LH Jr, Salant DJ. Membranous nephropathy: from models to man. *J Clin Invest*. 2014;124:2307–2314.
3. Ronco P, Debiec H. Pathophysiological advances in membranous nephropathy: time for a shift in patient's care. *Lancet*. 2015;385:1983–1992.
4. Schieppati A, Mosconi L, Perna A, et al. Prognosis of untreated patients with idiopathic membranous nephropathy. *N Engl J Med*. 1993;329:85–89.
5. Cattran DC, Reich HN, Beanlands HJ, et al. The impact of sex in primary glomerulonephritis. *Nephrol Dial Transplant*. 2008;23:2247–2253.
6. Beck LH Jr, Bonegio RG, Lambeau G, et al. M-type phospholipase A2 receptor as target antigen in idiopathic membranous nephropathy. *N Engl J Med*. 2009;361:11–21.
7. Tomas NM, Beck LH Jr, Meyer-Schwesinger C, et al. Thrombospondin type-1 domain-containing 7A in idiopathic membranous nephropathy. *N Engl J Med*. 2014;371:2277–2287.
8. Larsen CP, Cossey LN, Beck LH. THSD7A staining of membranous glomerulopathy in clinical practice reveals cases with dual autoantibody positivity. *Mod Pathol*. 2016;29:421–426.
9. Wang J, Cui Z, Lu J, et al. Circulating antibodies against thrombospondin type-I domain-containing 7A in Chinese patients with idiopathic membranous nephropathy. *Clin J Am Soc Nephrol*. 2017;12:1642–1651.
10. Hayashi N, Okada K, Matsui Y, et al. Glomerular mannose-binding lectin deposition in intrinsic antigen-related membranous nephropathy. *Nephrol Dial Transplant*. 2018;33:832–840.
11. Kao L, Lam V, Waldman M, et al. Identification of the immunodominant epitope region in phospholipase A2 receptor-mediating autoantibody binding in idiopathic membranous nephropathy. *J Am Soc Nephrol*. 2015;26:291–301.
12. Fresquet M, Jowitt TA, Gummadova J, et al. Identification of a major epitope recognized by PLA2R autoantibodies in primary membranous nephropathy. *J Am Soc Nephrol*. 2015;26:302–313.
13. Seitz-Polski B, Dolla G, Payre C, et al. Cross-reactivity of anti-PLA2R1 autoantibodies to rabbit and mouse PLA2R1 antigens and development of two novel ELISAs with different diagnostic performances in idiopathic membranous nephropathy. *Biochimie*. 2015;118:104–115.
14. Seitz-Polski B, Dolla G, Payre C, et al. Epitope spreading of autoantibody response to PLA2R associates with poor prognosis in membranous nephropathy. *J Am Soc Nephrol*. 2016;27:1517–1533.
15. Beck LH Jr. PLA2R and THSD7A: disparate paths to the same disease? *J Am Soc Nephrol*. 2017;28:2579–2589.

16. Seifert L, Hoxha E, Eichhoff AM, et al. The most N-terminal region of THSD7A is the predominant target for autoimmunity in THSD7A-associated membranous nephropathy. *J Am Soc Nephrol*. 2018;29:1536–1548.
17. Du Y, Li J, He F, et al. The diagnosis accuracy of PLA2R-AB in the diagnosis of idiopathic membranous nephropathy: a meta-analysis. *PLoS One*. 2014;9:e104936.
18. Hu SL, Wang D, Gou WJ, et al. Diagnostic value of phospholipase A2 receptor in idiopathic membranous nephropathy: a systematic review and meta-analysis. *J Nephrol*. 2014;27:111–116.
19. Hoxha E, Harendza S, Zahner G, et al. An immunofluorescence test for phospholipase-A2-receptor antibodies and its clinical usefulness in patients with membranous glomerulonephritis. *Nephrol Dial Transplant*. 2011;26:2526–2532.
20. Hofstra JM, Debiec H, Short CD, et al. Antiphospholipase A2 receptor antibody titer and subclass in idiopathic membranous nephropathy. *J Am Soc Nephrol*. 2012;23:1735–1743.
21. Dahnrich C, Komorowski L, Probst C, et al. Development of a standardized ELISA for the determination of autoantibodies against human M-type phospholipase A2 receptor in primary membranous nephropathy. *Clin Chim Acta*. 2013;421C:213–218.
22. Debiec H, Ronco P. PLA2R autoantibodies and PLA2R glomerular deposits in membranous nephropathy. *N Engl J Med*. 2011;364:689–690.
23. Hoxha E, Kneissler U, Stege G, et al. Enhanced expression of the M-type phospholipase A2 receptor in glomeruli correlates with serum receptor antibodies in primary membranous nephropathy. *Kidney Int*. 2012;82:797–804.
24. Larsen CP, Messias NC, Silva FG, et al. Determination of primary versus secondary membranous glomerulopathy utilizing phospholipase A2 receptor staining in renal biopsies. *Mod Pathol*. 2013;26:709–715.
25. Beck LH Jr, Fervenza FC, Beck DM, et al. Rituximab-induced depletion of anti-PLA2R autoantibodies predicts response in membranous nephropathy. *J Am Soc Nephrol*. 2011;22:1543–1550.
26. Hofstra JM, Fervenza FC, Wetzels JF. Treatment of idiopathic membranous nephropathy. *Nat Rev Nephrol*. 2013;9:443–458.
27. Kanigicherla D, Gummadova J, McKenzie EA, et al. Anti-PLA2R antibodies measured by ELISA predict long-term outcome in a prevalent population of patients with idiopathic membranous nephropathy. *Kidney Int*. 2013;83:940–948.
28. Hoxha E, Thiele I, Zahner G, et al. Phospholipase A2 receptor autoantibodies and clinical outcome in patients with primary membranous nephropathy. *J Am Soc Nephrol*. 2014;25:1357–1366.
29. Ruggenenti P, Debiec H, Ruggiero B, et al. Anti-phospholipase A2 receptor antibody titer predicts post-rituximab outcome of membranous nephropathy. *J Am Soc Nephrol*. 2015;26:2545–2558.
30. van de Logt AE, Hofstra JM, Wetzels JF. Pharmacological treatment of primary membranous nephropathy in 2016. *Expert Rev Clin Pharmacol*. 2016;9:1463–1478.
31. Ruggenenti P, Fervenza FC, Remuzzi G. Treatment of membranous nephropathy: time for a paradigm shift. *Nat Rev Nephrol*. 2017;13:563–579.
32. Dahan K, Debiec H, Plaisier E, et al. Rituximab for severe membranous nephropathy: a 6-month trial with extended follow-up. *J Am Soc Nephrol*. 2017;28:348–358.
33. Pourcine F, Dahan K, Mihout F, et al. Prognostic value of PLA2R autoimmunity detected by measurement of anti-PLA2R antibodies combined with detection of PLA2R antigen in membranous nephropathy: a single-centre study over 14 years. *PLoS One*. 2017;12:e0173201.
34. Seitz-Polski B, Debiec H, Rousseau A, et al. Phospholipase A2 receptor 1 epitope spreading at baseline predicts reduced likelihood of remission of membranous nephropathy. *J Am Soc Nephrol*. 2018;29:401–408.
35. De Vriese AS, Glassock RJ, Nath KA, et al. A proposal for a serology-based approach to membranous nephropathy. *J Am Soc Nephrol*. 2017;28:421–430.
36. Cattran DC, Brenchley PE. Membranous nephropathy: integrating basic science into improved clinical management. *Kidney Int*. 2017;91:566–574.
37. Behnert A, Schiffer M, Muller-Deile J, et al. Antiphospholipase A(2) receptor autoantibodies: a comparison of three different immunoassays for the diagnosis of idiopathic membranous nephropathy. *J Immunol Res*. 2014;2014:143274.
38. Huang B, Wang L, Zhang Y, et al. A novel time-resolved fluoroimmunoassay for the quantitative detection of antibodies against the phospholipase A2 receptor. *Sci Rep*. 2017;7:46096.
39. Tomas NM, Hoxha E, Reinicke AT, et al. Autoantibodies against thrombospondin type 1 domain-containing 7A induce membranous nephropathy. *J Clin Invest*. 2016;126:2519–2532.
40. Tomas NM, Meyer-Schwesinger C, von Spiegel H, et al. A heterologous model of thrombospondin type 1 domain-containing 7A-associated membranous nephropathy. *J Am Soc Nephrol*. 2017;28:3262–3277.
41. Hoxha E, Beck LH Jr, Wiech T, et al. An indirect immunofluorescence method facilitates detection of thrombospondin type 1 domain-containing 7A-specific antibodies in membranous nephropathy. *J Am Soc Nephrol*. 2017;28:520–531.
42. Iwakura T, Ohashi N, Kato A, et al. Prevalence of enhanced granular expression of thrombospondin type-1 domain-containing 7A in the glomeruli of Japanese patients with idiopathic membranous nephropathy. *PLoS One*. 2015;10:e0138841.
43. Sharma SG, Larsen CP. Tissue staining for THSD7A in glomeruli correlates with serum antibodies in primary membranous nephropathy: a clinicopathological study. *Mod Pathol*. 2018;31:616–622.
44. Huang CC, Lehman A, Albawardi A, et al. IgG subclass staining in renal biopsies with membranous glomerulonephritis indicates subclass switch during disease progression. *Mod Pathol*. 2013;26:799–805.
45. Lonnbro-Widgren J, Ebefors K, Molne J, et al. Glomerular IgG subclasses in idiopathic and malignancy-associated membranous nephropathy. *Clin Kidney J*. 2015;8:433–439.
46. Liu Y, Li X, Ma C, et al. Serum anti-PLA2R antibody as a diagnostic biomarker of idiopathic membranous nephropathy: the optimal cut-off value for Chinese patients. *Clin Chim Acta*. 2018;476:9–14.
47. Tampoia M, Migliucci F, Villani C, et al. Definition of a new cut-off for the anti-phospholipase A2 receptor (PLA2R) autoantibody immunoassay in patients affected by idiopathic membranous nephropathy. *J Nephrol*. 2018;31:899–905.
48. Murtas C, Bruschi M, Candiano G, et al. Coexistence of different circulating anti-podocyte antibodies in membranous nephropathy. *Clin J Am Soc Nephrol*. 2012;7:1394–1400.
49. Jullien P, Seitz Polski B, Maillard N, et al. Anti-phospholipase A2 receptor antibody levels at diagnosis predicts spontaneous remission of idiopathic membranous nephropathy. *Clin Kidney J*. 2017;10:209–214.
50. Lonnbro-Widgren J, Molne J, Haraldsson B, et al. Treatment pattern in patients with idiopathic membranous nephropathy-practices in Sweden at the start of the millennium. *Clin Kidney J*. 2016;9:227–233.
51. van den Brand JA, van Dijk PR, Hofstra JM, et al. Long-term outcomes in idiopathic membranous nephropathy using a restrictive treatment strategy. *J Am Soc Nephrol*. 2014;25:150–158.
52. Obrisca B, Ismail G, Jurubita R, et al. Antiphospholipase A2 receptor autoantibodies: a step forward in the management of primary membranous nephropathy. *BioMed Res Int*. 2015;2015:249740.
53. Dou Y, Zhang L, Liu D, et al. The accuracy of the anti-phospholipase A2 receptor antibody in the diagnosis of idiopathic membranous nephropathy: a comparison of different cutoff values as measured by the ELISA method. *Int Urol Nephrol*. 2016;48:845–849.
54. Akiyama S, Akiyama M, Imai E, et al. Prevalence of anti-phospholipase A2 receptor antibodies in Japanese patients with membranous nephropathy. *Clin Exp Nephrol*. 2015;19:653–660.
55. Baker FC, de Zambotti M, Colrain IM, et al. Sleep problems during the menopausal transition: prevalence, impact, and management challenges. *Nat Sci Sleep*. 2018;10:73–95.
56. Vellanki K, Hou S. Menopause in CKD. *Am J Kidney Dis*. 2018;71:710–719.
57. Gyan E, Raynard B, Durand JP, et al. Malnutrition in patients with cancer: comparison of perceptions by patients, relatives, and physicians—results of the NutriCancer2012 Study. *JPEN J Parenter Enteral Nutr*. 2018;42:255–260.
58. Ohtani H, Wakui H, Komatsuda A, et al. Distribution of glomerular IgG subclass deposits in malignancy-associated membranous nephropathy. *Nephrol Dial Transplant*. 2004;19:574–579.
59. Lin L, Wang WM, Pan XX, et al. Biomarkers to detect membranous nephropathy in Chinese patients. *Oncotarget*. 2016;7:67868–67879.
60. Qin HZ, Zhang MC, Le WB, et al. Combined assessment of phospholipase A2 receptor autoantibodies and glomerular deposits in membranous nephropathy. *J Am Soc Nephrol*. 2016;27:3195–3203.
61. Vanderlugt CL, Miller SD. Epitope spreading in immune-mediated diseases: implications for immunotherapy. *Nat Rev Immunol*. 2002;2:85–95.
62. Bech AP, Hofstra JM, Brenchley PE, et al. Association of anti-PLA2R antibodies with outcomes after immunosuppressive therapy in idiopathic membranous nephropathy. *Clin J Am Soc Nephrol*. 2014;9:1386–1392.

63. Dai H, Zhang H, He Y. Diagnostic accuracy of PLA2R autoantibodies and glomerular staining for the differentiation of idiopathic and secondary membranous nephropathy: an updated meta-analysis. *Sci Rep*. 2015;5:8803.
64. Xu X, Wang G, Chen N, et al. Long-term exposure to air pollution and increased risk of membranous nephropathy in China. *J Am Soc Nephrol*. 2016;27:3739–3746.
65. Hoxha E, Wiech T, Stahl PR, et al. A mechanism for cancer-associated membranous nephropathy. *N Engl J Med*. 2016;374:1995–1996.
66. Ronco PM. Paraneoplastic glomerulopathies: new insights into an old entity. *Kidney Int*. 1999;56:355–377.
67. Lefaucheur C, Stengel B, Nochy D, et al. Membranous nephropathy and cancer: epidemiologic evidence and determinants of high-risk cancer association. *Kidney Int*. 2006;70:1510–1517.
68. Beck LH Jr. Membranous nephropathy and malignancy. *Semin Nephrol*. 2010;30:635–644.
69. Cambier JF, Ronco P. Onco-nephrology: glomerular diseases with cancer. *Clin J Am Soc Nephrol*. 2012;7:1701–1712.
70. Malik GH, Al-Harbi AS, Al-Mohaya S, et al. Repeated pregnancies in patients with primary membranous glomerulonephritis. *Nephron*. 2002;91:21–24.
71. Surian M, Imbasciati E, Cosci P, et al. Glomerular disease and pregnancy: a study of 123 pregnancies in patients with primary and secondary glomerular diseases. *Nephron*. 1984;36:101–105.
72. Al-Rabadi L, Ayalon R, Bonegio RG, et al. Pregnancy in a patient with primary membranous nephropathy and circulating anti-PLA2R antibodies: a case report. *Am J Kidney Dis*. 2016;67:775–778.
73. O'Shaughnessy MM, Jobson MA, Sims K, et al. Pregnancy outcomes in patients with glomerular disease attending a single academic center in North Carolina. *Am J Nephrol*. 2017;45:442–451.
74. Luo R, Wang Y, Xu P, et al. Hypoxia-inducible miR-210 contributes to preeclampsia via targeting thrombospondin type I domain containing 7A. *Sci Rep*. 2016;6:19588.
75. Iwakura T, Fujigaki Y, Katahashi N, et al. Membranous nephropathy with an enhanced granular expression of thrombospondin type-1 domain-containing 7A in a pregnant woman. *Intern Med*. 2016;55:2663–2668.
76. Hoxha E, von Haxthausen F, Wiech T, et al. Membranous nephropathy—one morphologic pattern with different diseases. *Pflugers Arch*. 2017;469:989–996.
77. Phillips WD, Vincent A. Pathogenesis of myasthenia gravis: update on disease types, models, and mechanisms. *F1000Res*. 2016;5:F1000. Faculty Rev-1513.
78. Berrih-Aknin S, Frenkian-Cuvelier M, Eymard B. Diagnostic and clinical classification of autoimmune myasthenia gravis. *J Autoimmun*. 2014;48–49:143–148.

SUPPLEMENTARY INFORMATION

Novel ELISA for Thrombospondin type 1 domain-containing 7A autoantibodies in membranous nephropathy: analysis of a cohort of 49 patients

Christelle Zaghrini, Barbara Seitz-Polski, Joana Justino, Guillaume Dolla, Christine Payré, Noémie Jourde-Chiche, Anne-Els Van de Logt, Caroline Booth, Emma Rigby, Jennie Lonnbro-Widgren, Jenny Nystrom, Christophe Mariat, Zhao Cui, Jack F. M. Wetzels, GianMarco Ghiggeri, Laurence H. Beck Jr, Pierre Ronco, Hanna Debiec and Gérard Lambeau

SUPPLEMENTARY METHODS

Cloning and expression of recombinant soluble human THSD7A in *HEK293* cells — The entire extracellular domain of human THSD7A (NP_056019, a. a. 47-1606) was produced in HEK293 cells essentially as described for full-length membrane-bound THSD7A [1]. The full-length cDNA coding for human THSD7A with a Myc-Flag tag and inserted into the pCMV6-entry expression vector (Origene RC213616) was used as a PCR template to delete the transmembrane domain and replace the Myc-Flag tag by a 6x histidine tag (Figure S1A) using the Phusion Site-Directed Mutagenesis Kit (Thermo Fisher Scientific). The THSD7A-6xHis insert was fully sequenced. For production of recombinant soluble THSD7A protein, HEK293 cells were cultured in DMEM medium containing 10% heat-inactivated FBS, 50 units/mL penicillin G, 100 µg/mL streptomycin (all from Gibco) at 37°C in a humidified atmosphere of 5% CO_2. The pCMV6-entry vector coding for soluble THSD7A-6xHis was transfected in HEK293 cells using Exgen (Biomol GmbH) according to the manufacturer's instructions. Transfected cells were selected with 1 mg/mL geneticin (Gibco). Single cell cloning was done by serial dilution in 96-well plates and the best expressing cell clones were selected. For large-scale production, cell clones were cultured to sub-confluency in complete medium, then switched to serum-free medium and the cell culture medium was harvested after expression for 7 days. The recombinant protein was purified by affinity chromatography on complete His-tag purification beads according the manufacturer's protocol (Roche). Cell culture medium containing the recombinant THSD7A protein was incubated with the beads for capture at 4°C overnight on a rocker. The column was washed with equilibrium buffer (300 mM NaCl, 20 mM Tris pH 7.4) followed by washes with equilibrium

buffer containing 10 mM imidazole. The bound protein was eluted stepwise with 400 mM imidazole (Figure S1B). The yield of production was 1 mg of purified soluble THSD7A/L of cell medium. Elutions were concentrated and buffer-exchanged with 1X PBS using an ultrafiltration cell system (Amicon) equipped with an YM-30 membrane. The purity and folding of THSD7A was validated by SDS-PAGE silver staining and WB with commercially available anti-THSD7A antibodies and THSD7A-associated MN sera (Figure S1C and D).

WB analysis for the detection of anti-THSD7A and anti-PLA2R1 autoantibodies — The detection of anti-THSD7A and anti-PLA2R1 autoantibodies was evaluated by WB after running SDS-PAGE (6 or 10%) under reducing or non-reducing conditions as specified in figure legends. Fifty ng/well of THSD7A or PLA2R1 antigens were run on SDS-polyacrylamide gel and transferred to methanol-soaked polyvinylidene difluoride membranes (Bio-Rad) under semi-dry conditions with 0.05% SDS in the transfer buffer using Trans-blot Turbo (Bio-Rad) at 25 V constant for 30 min. Membranes were blocked for 1 hour at RT with 5% milk in PBS-Tween 0.05%. The primary and secondary antibodies (diluted with 0.5% milk in PBS-T or PBS-T, respectively) were incubated at room temperature for 2 and 1 h, respectively. The purity and folding of the purified recombinant THSD7A antigen was initially validated using two commercial antibodies (a rabbit polyclonal THSD7A antibody from Atlas antibodies AB, Sweden, working dilution 1:500; and a goat polyclonal THSD7A antibody from Santa Cruz Biotechnologies, working dilution 1:250) and 2 THSD7A-positive MN sera at a working dilution of 1:100 (Figure S1D). The secondary antibodies used were HRP-conjugated goat anti-rabbit IgG (working dilution 1:5000, Southern Biotech, Birmingham, USA), rabbit anti-goat (working dilution 1: 20,000, Southern Biotech, Birmingham, USA) and HRP-conjugated mouse anti-human IgG4 (working dilution 1:30,000, Southern Biotech, Birmingham, USA), respectively. To test the positivity of the

THSD7A-associated MN patients, 50 ng/well of THSD7A and PLA2R1 antigens were loaded on a 10% SDS-polyacrylamide gel under non-reducing conditions. Membranes were probed with serum samples at a dilution ranging from 1:10 to 1:100 depending on the anti-THSD7A titer measured by ELISA (Figure S5). Serum samples from double positive patients were tested at a 1:25 dilution by WB from 6% SDS-polyacrylamide gel loaded with 50 ng/well of THSD7A and PLA2R1 antigens under non-reducing conditions. The secondary antibody was HRP-conjugated mouse anti-human IgG4 at 1:7,500 dilution. The detection of protein bands was performed with an enhanced chemiluminescent substrate (Perkin Elmer) and a Fuji LAS3000 digital imager.

IIFT for the detection of anti-THSD7A and anti-PLA2R1 autoantibodies — We used the cell–based IIFT kit from Euroimmun AG containing a mosaic biochip of formalin-fixed HEK293 cells overexpressing full-length human THSD7A or PLA2R1 or mock-transfected HEK293 as a negative control. Anti-THSD7A and anti-PLA2R1 titers were measured in a semi-quantitative manner by diluting serum samples at 1:10, 1:100 and 1: 1,000 in PBS-Tween 0.2% and incubating them with the biochip for 30 min. Bound IgG antibodies were then detected using a fluorescein isothiocyanate-conjugated goat anti-human IgG antibody (Euroimmun) as secondary antibody. Slides were examined using a confocal microscope at 460-490 nm LED excitation. Antibody titers were estimated by the fluorescence intensity at each dilution according to the manufacturer's instructions.

Kidney biopsy staining for THSD7A and PLA2R1 antigens — Patients' kidney biopsies were fixed in a solution containing ethanol (75%), formol (3%) and acetic acid (5%). Fixed biopsy specimens were paraffin-embedded according to standard techniques. Dewaxed sections (4-µm thickness) were hydrated and antigens were retrieved by Heat Induced Epitope Retrieval (HIER) at pH 6.0 and 95°C (Diagnostic BioSystems ref KO35). HIER was followed by 5 min incubation

with HistoReveal (Abcam). Biopsies were stained by immunofluorescence using rabbit polyclonal anti-THSD7A at x100 or anti-PLA2R1 at x500 (both from Atlas antibodies AB, Sweden) as primary antibodies and goat conjugated rabbit Fab IgG antibody Alexa 488 (Molecular Probes) at 1:250 (Invitrogen) as secondary antibody.

Detailed follow-up for patient MN13 — At baseline, the patient had high proteinuria (6.1 g/day) associated with high anti-THSD7A titer (especially for IgG4 and IgG3 subclasses) detected by both ELISA and IIFT At month 2, the patient was treated with rituximab (2 doses at 375 mg/m^2), which led to a rapid decrease of anti-THSD7A titers for both IgG3 and IgG4 subclasses followed by gradually decreasing levels of proteinuria from months 3 to 7 (5.2 to 1.4 g/day). At month 7, proteinuria suddenly increased up to 5.5 g/day at months 10 to 13. A renal biopsy performed at month 13 showed enhanced staining of THSD7A antigen on the glomerular basement membrane suggesting a still active MN disease (Figure S9). The patient was treated with a second course of rituximab (2 doses at 375 mg/m^2) which led to further decrease but not disappearance of anti-THSD7A autoantibodies at month 10, as measured by ELISA and IIFT, and was followed by decreased proteinuria to the sub-nephrotic range at month 18, down to 1.9 g/day. Overall, we concluded that the first and second rituximab treatments were effective and led to partial immunological remission, with a significant but slow decrease of anti-THSD7A autoantibodies. This was followed by a global decrease of proteinuria from months 0 to 18, despite a transient increase of proteinuria over 5 months. Finally, between months 18 and 27, there was a slight increase in anti-THSD7A titer with a concomitant increase in proteinuria up to 3.4 g/day, suggesting a possible MN relapse associated with anti-THSD7A autoantibodies. We also compared anti-THSD7A autoantibody levels by ELISA, WB and IIFT during follow-up and treatment (Figure S9). By WB, anti-THSD7A levels were also detected throughout the follow-up

period but it was difficult to evaluate the titer variation over time. Both IIFT and ELISA could measure the change in titer, yet ELISA was more accurate to detect subtle changes. We also monitored by ELISA the changes in anti-THSD7A IgG subclasses. Levels of anti-THSD7A IgG1 and IgG2 were barely detectable at baseline and during follow-up and were thus not useful to monitor the anti-THSD7A immunological response. In contrast, both IgG3 and IgG4 autoantibodies could be robustly monitored throughout follow-up, and both IgG subclasses appeared to vary simultaneously, yet ELISA assay measuring IgG4 anti-THSD7A titers was more reliable (Figure S9).

Table S1: Detailed clinical characteristics of the 49 THSD7A-associated MN patients, ranked by titers from highest to lowest and by sex. Double-positive patients are listed at the end for each gender. ELISA titer <16 RU/mL were measured at dilution 1:25 or 1:10 when serum was available. A, active disease; CR, complete remission; CP, cyclophosphamide; ESKD, end stage kidney disease; NA, not available; PR, partial remission; RTX, rituximab.

Patient ID	ELISA (RU/mL)	WB	IIFT	Anti-PLA2R1	Gender	Age (years)	UProt. (g/day)	SAlb. (g/L)	Screat. (µmol/L)	eGFR (CKD-EPI) (mLmin/1.73 m^2)	Associated disease	Follow-up (months)	Treatment	Outcome
	Anti-THSD7A													
1	13920	+	3200	–	M	68	25.9	13	88	77	Colon adenocarcinoma	5	RTX	A
4	1776	+	320	–	M	71	14.6	14	108	59	None	54	None	A
5	1669	+	1000	–	M	54	9.1	15	89	84	None	150	Prednisone ACTH Cyclosporine A, RTX	CR
9	1270	+	1000	–	M	17	2.7	29	120	76	None	6.5	RTX	PR
10	1188	+	100	–	M	85	3.0	14	80	77	Prostate cancer	36	RAS blockers	PR
11	1092	+	320	–	M	67	10.6	NA	116	56	Diabetes Mellitus	85	CP Prednisone	PR
12	955	+	1000	–	M	59	5.9	23	89	81	None	84	None	CR
14	505	+	100	–	M	55	12.2	15	235	26	Hypothyroidism, diabetes, psoriasis	10	RTX	ESKD
15	566	+	320	–	M	49	9.0	NA	212	31	Discoid lupus	NA	Alternating months of prednisone and CP followed by RTX	A
17	545	+	100	–	M	68	6.0	16	88	77	Cheek intra-epidermal carcinoma Pityriasis rosea, Biermer's disease	48	RAS blockers	PR
18	416	+	100	–	M	62	5.5	18	115	58	None	180	Steroids + CP	ESKD
19	376	+	320	–	M	54	2.9	27	131	53	None	102	CP Prednisone	CR

Patient ID	ELISA (RU/mL)	WB	IIFT	Anti-PLA2R1	Gender	Age (years)	UProt. (g/day)	SAlb. (g/L)	Screat. (μmol/L)	eGFR (CKD-EPI) (mLmin/1.73 m^2)	Associated disease	Follow-up (months)	Treatment	Outcome
	Anti-THSD7A													
21	278	+	320	–	M	80	5.9	26	80	80	Parotitis, Warthin's tumor	14	ACTH	CR
22	234	+	10	–	M	76	8.0	25	150	38	None	NA	Steroids + CP diuretics	CR
23	233	+	320	–	M	75	10.3	NA	89	73	COPD	24	CP Prednisone	A (Persistent proteinuria)
26	122	+	100	–	M	67	5.4	19	122.8	53	Polymyalgia rheumatica,	18	RTX	CR
27	119	+	10	–	M	75	12.0	24	152	38	Pancreatic carcinoma	90	Cyclosporine A, CP Prednisone	CR
28	97	+	100	–	M	75	5.3	31	103	61	None	37	None	CR
31	68	+	10	–	M	75	6.3	20	120	51	None	32	NA	A
35	29	+	32	–	M	83	14.5	15	202.4	25	None	NA	NA	NA
36	27	+	10	–	M	60	10.0	21	90	80	HBV	NA	Steroids + CP RAS blockers diuretics	CR
39	21	+	10	–	M	51	4.0	26	87	88	HIV, HCV	62	RTX	CR
40	<16	–	10	–	M	77	7.0	21	129.9	45	Prostate cancer, diabetes	3	RAS blockers	A
41	<16	–	10	–	M	60	13.2	5	184	34	Gastric carcinoma,	NA	None	NA (Death)
45	353	+	100	+	M	54	11.4	19	72.5	100	NA	NA	NA	NA
46	23	+	–	+	M	86	5.3	21	190	27	None	NA	NA	PR
47	<16	–	–	+	M	48	4.0	25	47	125	NA	NA	ACE and RAS blockers	A
48	<16	–	–	+	M	65	6.0	28	52	106	None	NA	ACE and RAS blockers	CR

Patient ID	ELISA (RU/mL)	WB	IIFT	Anti-PLA2R1	Gender	Age (years)	UProt. (g/day)	SAlb. (g/L)	Screat. (µmol/L)	eGFR (CKD-EPI) (mLmin/1.73 m^2)	Associated disease	Follow-up (months)	Treatment	Outcome
		Anti-THSD7A												
2	7255	+	3200	–	F	95	6.5	10	67	67	Breast cancer, hypothyroidism	12	Corticosteroids Cyclosporine A	A
3	1827	+	1000	–	F	61	20.0	17	66.3	86	Hypothyroidism	NA	NA	NA
6	1605	+	100	–	F	73	4.3	18	74	69	None	72	RAS blockers	CR
7	1586	+	1000	–	F	51	14.9	NA	NA	NA	None	NA	NA	NA
8	1354	+	1000	–	F	37	7.0	18	59	113	Monoclonal IgG Kappa, multiple sclerosis	10	RTX	A
13	715	+	1000	–	F	4	6.1	22	NA	NA	Haemolytic anaemia, thrombocytopenia	32	RTX	A
16	606	+	32	–	F	49	19.6	10	71	86	None	23	CP, Prednisone	CR
20	302	+	320	–	F	66	3.5	24	141.4	33	None	29	Cyclosporine A Prednisone Tacrolimus	A
24	194	+	100	–	F	36	5.0	25	80	82	None	NA	ACTH, RAS blockers	A
25	134	+	100	–	F	33	1.57	39	82.2	81	Hypothyroidism, alopecia areata, latent tuberculosis	44	RAS blockers	CR
29	97	+	32	–	F	51	3.0	36	70.7	86	NA	50	Cyclosporine A plasmapheresis RTX	PR
30	94	+	32	–	F	35	1.8	26	53	119	NA	12	RAS blockers	PR
32	59	+	10	–	F	30	3.7	NA	NA	NA	NA	NA	None	NA

Patient ID	ELISA (RU/mL)	WB	IFT	Anti-PLA2R1	Gender	Age (years)	UProt. (g/day)	SAlb. (g/L)	Screat. (µmol/L)	eGFR (CKD-EPI) (ml/min/1.73 m^2)	Associated disease	F-up (Months)	Treatment	Outcome
	Anti-THSD7A													
33	52	+	100	–	F	47	3.0	NA	70.7	88	Iritis	120	Cyclosporine A Prednisone RTX Tacrolimus ACTH, CP	PR
34	29	+	10	–	F	47	6.6	24	69	91	NA	12	RAS blockers	A
37	23	+	10	–	F	82	1.0	23	110	40	None	46	None	NA
38	22	+	10	–	F	39	6.5	21	70	94	None	22	RAS blockers Steroids + CP	CR
42	642	+	100	+	F	56	3.0	NA	114.9	46	NA	NA	NA	NA
43	561	+	100	+	F	49	8.4	14	100	57	None	NA	Steroids diuretics	NA
44	312	+	32	+	F	77	10	22	60	85	Rectal cancer and thymoma, Goujerot-Sjogren syndrome, monoclonal IgG lambda, HBV	60	None Tumorectomy	CR
49	<16	–	–	+	F	28	4.7	26	53	124	Goujerot-Sjogren syndrome	38	ACE blockers	CR

Table S2. Clinical characteristics of females below and above 51 years (chosen as average age for menopause).[55-56] No differences were observed

Clinical characteristics	Females <51 (n=14)	Females >51 (n=7)	P Value
Age at diagnosis (year)	38.0 [32.3–49.0]	73.0 [61.0–82.0]	0.003
Proteinuria (g/day)	5.6 [3.0–7.4]	4.3 [3.0–10.0]	0.881
Serum Albumin (g/L)	24.0 [18.0–26.0]	20.1 [15.3–23.0]	0.208
Serum Creatinine (µmol/L)	70.7 [59.0–80.0]	74.0 [66.3–115.0]	0.319
eGFR (CKD-EPI) (mL/min/1.73 m^2)	88.0 [82–113.0]	67.0 [40.0–85.0]	0.145
Anti-THSD7A titer (RU/mL)	115.5 [46.3–633.3]	642.0 [302.0–1827.0]	0.079

References

55. Baker FC, de Zambotti M, Colrain IM, *et al.* Sleep problems during the menopausal transition: prevalence, impact, and management challenges. *Nature and science of sleep* 2018; **10:** 73-95.

56. Vellanki K, Hou S. Menopause in CKD. *Am J Kidney Dis* 2018; **71:** 710-719.

Table S3: Clinical characteristics of anti-thrombospondin type 1 domain-containing 7A (THSD7A)-positive patients with and without associated malignancy. Values are shown as n or median (interquartile range).

Clinical characteristics	No malignancy (n=41)	Malignancy (n=8)	P value
Gender M/F (n)	22/19	6/2	0.264
Age at diagnosis (year)	54 [47–69]	76 [69–83]	0.002
Proteinuria (g/day)	6.0 [3.9–9.6]	8.5 [6.1–12.9]	0.117
Serum creatinine (µmol/L)	89.0 [70.7–120.0]	88.0 [70.3–146.0]	0.873
eGFR (CKD-EPI) (mL/min/1.73 m^2)	78.0 [52.5–88.0]	72.0 [39.8–77.0]	0.296
Serum albumin (g/L)	22.3 [18.0–26.0]	15.0 [10.9–21.9]	0.016
Anti-THSD7A titer (RU/mL)	234.0 [40.5–679.0]	429.0 [32.8–5738]	0.635

Table S4: Time gap between malignancy and membranous nephropathy (MN) diagnosis. *Negative values indicate prior diagnosis of malignancy.

MN patient	Gender	Age (year)	Malignancy	Time of diagnosis of tumor to MN diagnosis (months)*
1	M	68	Colon adenocarcinoma	-18*
10	M	85	Prostate cancer	0
17	M	68	Cheek intra-epidermal cancer	96
27	M	75	Pancreatic cancer	84
40	M	77	Prostate cancer	-22
41	M	60	Gastric cancer	0
2	F	95	Breast cancer	-108*
44	F	77	Rectal cancer and thymoma	0

Table S5: Distribution of anti-thrombospondin type 1 domain-containing 7A (THSD7A) IgG subclasses in THSD7A-positive patients. Values are shown as n(%).

Anti-THSD7A IgG subclass	No malignancy (n=41)	Malignancy (n=8)	P value
IgG1 n (%)	5 (12.2)	1 (12.5)	0.981
IgG2 n (%)	8 (19.5)	0 (0)	0.172
IgG3 n (%)	7 (17.0)	2 (25.0)	0.596
IgG4 n (%)	38 (93.0)	6 (75.0)	0.131

Table S6: Clinical baseline characteristics of double-positive patients. No major difference was observed between patients with single positivity for anti-THSD7A versus double positivity for anti-thrombospondin type 1 domain-containing 7A (THSD7A) and anti-phospholipase A2 receptor 1 (PLA2R1). Values are shown as n (%) or median (interquartile range).

Clinical characteristics	THSD7A positive (n=41)	Double positive (n=8)	P value
Gender M/F (n)	24/17	4/4	0.655
Age at diagnosis (year)	60.0 [48.0–75.0]	55.0 [48.3–74.0]	0.828
Proteinuria (g/day)	6.3 [3.9–10.4]	5.7 [4.2–9.6]	0.715
Serum creatinine (µmol/L)	89.0 [73.3–125.0]	66.3 [52.3–111.0]	0.082
eGFR (CKD-EPI) (mL/min/1.73 m^2)	74.5 [49.5–84.5]	92.5 [48.8–120.0]	0.159
Serum albumin (g/L)	21.0 [15.0–25.0]	22.2[19.0–25.6]	0.591
Anti-THSD7A titer (RU/mL)	278.0 [63.5–1140.0]	167.5 [16.0–509.0]	0.136
Cancer incidence n (%)	7 (17)	1 (13)	0.748

Table S7. Baseline characteristics of thrombospondin type 1 domain-containing 7A (THSD7A)-positive patients in remission versus active disease during follow-up. Only anti-THSD7A titer differs between the 2 subgroups of patients.

Clinical characteristics	Remission n=24	Active n=12	P value
Age (years)	59.6 ± 3.928	57.8 ± 6.868	0.82
Sex ratio F/M	9/15	5/7	1.00
Proteinuria (g/day)	5.7 [3–8.825]	6.8 [5.7–11.71]	0.06
Serum creatinine (µmol/L)	87.5 [70.8–119.0]	108.0 [80.0–141.4]	0.33
Serum albumin (g/L)	23.4 [18.8–26.3]	18.0 [13.4–22.5]	0.03
Time of Follow-up (months)	48.0 [18.0–85.0]	29.0 [11.0–43.0]	0.196
Treatment with immunosuppressors	14*	9*	0.27
Anti-THSD7A titer (RU/mL)	134.0 [52.0–955.0]	536.0 [250.0–1671.0]	0.04

*Data for treatment was unavailable for 1 patient in each subgroup.

Table S8: Characteristics of all anti-thrombospondin type 1 domain-containing 7A (THSD7A)-positive patients published to date. Values are shown as n and mean (or median [*] [S1-S13]) for age. ND, not defined.

Reference	Year	Origin	All		Male		Female		Cancer (n)
			Patients (n)	Age (years)	Patients (n)	Age (years)	Patients (n)	Age (years)	
s3	2014	USA, France, Germany	17	49.9	6	54	11	47	1
s4	2015	Japan	5	42.4	2	–	3	–	0
s5	2016	Japan	1	–	–	–	1	30	0
s6	2016	China	5	39.8	2	54	3	32	1
s7	2016	China	4	–	–	–	–	–	ND
s8	2016	USA	9	62	7	–	2	–	ND
s1	2017	USA, Germany	40	60.5*	17	–	23	–	8
s9	2017	France	2	–	–	–	–	–	0
s10	2017	China	12	51.5	8	62.5	4	44.5	1
s11	2017	Japan	2	–	–	–	–	–	ND
s12	2017	USA	31	62.0	19	–	12	–	2
s13	2017	France	2	–	–	–	–	–	1
s2	2018	Germany	31	37*	19	–	12	–	9
This study	2018	France	49	58.4	28	67	21	48.8	8

References

s1. Hoxha E, Beck LH, Jr., Wiech T, *et al.* An Indirect Immunofluorescence Method Facilitates Detection of Thrombospondin Type 1 Domain-Containing 7A-Specific Antibodies in Membranous Nephropathy. *J Am Soc Nephrol* 2017; **28:** 520-531.

s2. Seifert L, Hoxha E, Eichhoff AM, *et al.* The Most N-Terminal Region of THSD7A Is the Predominant Target for Autoimmunity in THSD7A-Associated Membranous Nephropathy. *J Am Soc Nephrol* 2018.

s3. Tomas NM, Beck LH, Jr., Meyer-Schwesinger C, *et al.* Thrombospondin type-1 domain-containing 7A in idiopathic membranous nephropathy. *N Engl J Med* 2014; **371:** 2277-2287.

s4. Iwakura T, Ohashi N, Kato A*, et al.* Prevalence of Enhanced Granular Expression of Thrombospondin Type-1 Domain-Containing 7A in the Glomeruli of Japanese Patients with Idiopathic Membranous Nephropathy. *PloS one* 2015; **10:** e0138841.

s5. Iwakura T, Fujigaki Y, Katahashi N*, et al.* Membranous Nephropathy with an Enhanced Granular Expression of Thrombospondin Type-1 Domain-containing 7A in a Pregnant Woman. *Internal medicine (Tokyo, Japan)* 2016; **55:** 2663-2668.

s6. Lin L, Wang WM, Pan XX*, et al.* Biomarkers to detect membranous nephropathy in Chinese patients. *Oncotarget* 2016; **7:** 67868-67879.

s7. Qin HZ, Zhang MC, Le WB*, et al.* Combined Assessment of Phospholipase A2 Receptor Autoantibodies and Glomerular Deposits in Membranous Nephropathy. *J Am Soc Nephrol* 2016; **27:** 3195-3203.

s8. Larsen CP, Cossey LN, Beck LH. THSD7A staining of membranous glomerulopathy in clinical practice reveals cases with dual autoantibody positivity. *Mod Pathol* 2016; **29:** 421-426.

s9. Dahan K, Debiec H, Plaisier E*, et al.* Rituximab for Severe Membranous Nephropathy: A 6-Month Trial with Extended Follow-Up. *J Am Soc Nephrol* 2017; **28:** 348-358.

s10. Wang J, Cui Z, Lu J*, et al.* Circulating Antibodies against Thrombospondin Type-I Domain-Containing 7A in Chinese Patients with Idiopathic Membranous Nephropathy. *Clin J Am Soc Nephrol* 2017; **12:** 1642-1651.

s11. Hayashi N, Okada K, Matsui Y*, et al.* Glomerular mannose-binding lectin deposition in intrinsic antigen-related membranous nephropathy. *Nephrol Dial Transplant* 2017.

s12. Sharma SG, Larsen CP. Tissue staining for THSD7A in glomeruli correlates with serum antibodies in primary membranous nephropathy: a clinicopathological study. *Mod Pathol* 2017.

s13. Pourcine F, Dahan K, Mihout F*, et al.* Prognostic value of PLA2R autoimmunity detected by measurement of anti-PLA2R antibodies combined with detection of PLA2R antigen in membranous nephropathy: A single-centre study over 14 years. *PloS one* 2017; **12:** e0173201.

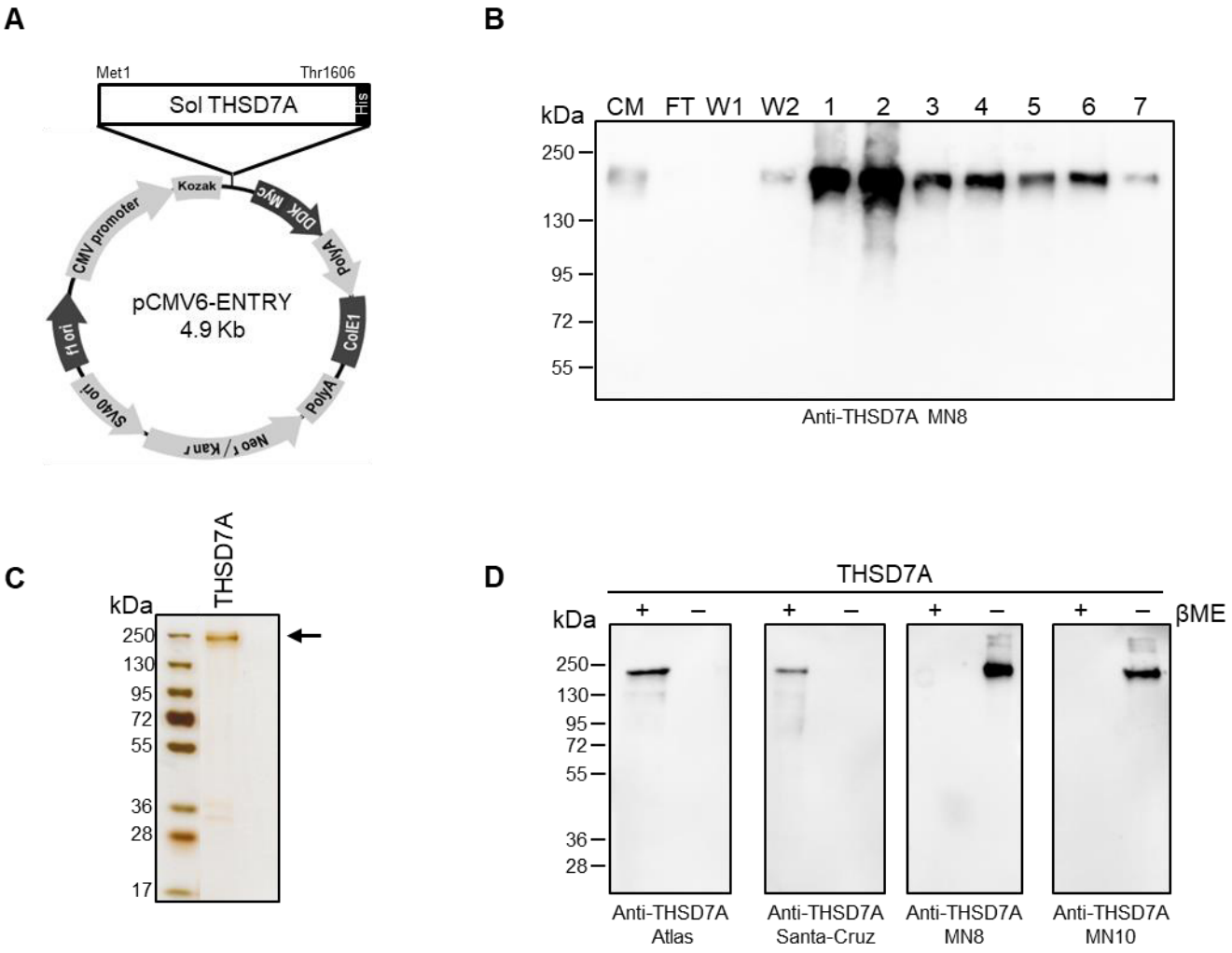

Figure S1: Cloning, expression, and purification of recombinant human soluble thrombospondin type 1 domain-containing 7A 6X histidine (THSD7A-6xHis). (A) Schematic representation of the pCMV6-entry expression vector coding for human soluble THSD7A-6xHis. The cDNA insert encodes for the signal peptide followed by the full extracellular region of THSD7A (from Met-1 to Thr-1606, Uniprot Q9UPZ6) and a C-terminal 6xHis Tag. **(B)** Western blot after His Tag purification from human embryonic kidney 293 cell medium containing soluble THSD7A-6xHis and probed with membranous nephropathy patient 8 (MN8) under nonreducing conditions at a 1:100 dilution. We loaded 400 ml of cell medium onto 4 ml of Ni-NTA resin. The resin was washed once with 40 ml of washing equilibrium buffer and then with 40 ml of washing buffer containing 10 mmol/l imidazole. Bound protein was eluted with 28 ml (in 7 fractions) of elution buffer containing 400 mmol/l imidazole. Aliquots of cell medium (CM), flow-through (FT), washes (W), and eluate (1 to 7) fractions were separated by sodium dodecylsulfate polyacrylamide gel electrophoresis (10%), transferred to polyvinylidene membranes and analyzed by Western blot. **(C)** Silver staining of the purified THSD7A-6xHis (100 ng) after buffer exchange with 1X phosphate-buffered saline. **(D)** Western blots to validate the purified THSD7A-6xHis as a native folded protein. Purified recombinant THSD7A-6xHis (50 ng) was loaded on sodium dodecylsulfate polyacrylamide gel electrophoresis (10%) under reducing or nonreducing conditions and probed with 2 commercially available anti-THSD7A antibodies and 2 representative anti-THSD7A-positive patients (MN8 and MN10; dilution 1:100).

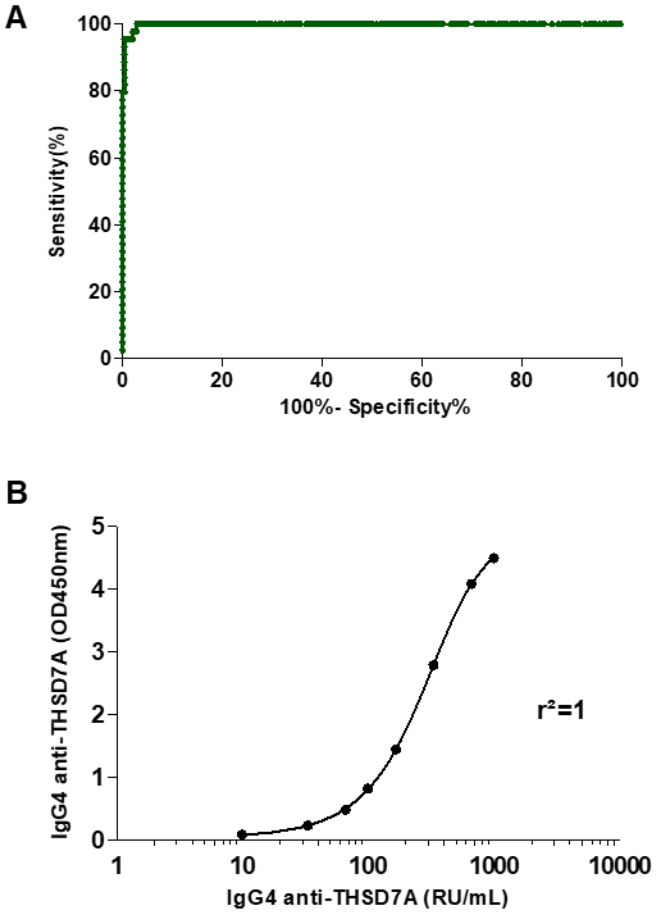

Figure S2: Receiver-operating characteristic curve and calibration curve for IgG4 anti-thrombospondin type 1 domain-containing 7A (THSD7A) enzyme-linked immunosorbent assay (ELISA). (A) Receiver-operating characteristic curve analysis of IgG4 anti-THSD7A detection in 44 anti-THSD7A-positive patients and 242 negative control subjects by ELISA. The area under the curve was 0.9982 (95% confidence interval: 0.9957–1.0, $P < 0.0001$). **(B)** Calibration curve covering the range of 9.9 relative units (RU)/ml to 990 RU/ml used to convert optical density (OD) values into RU/ml.

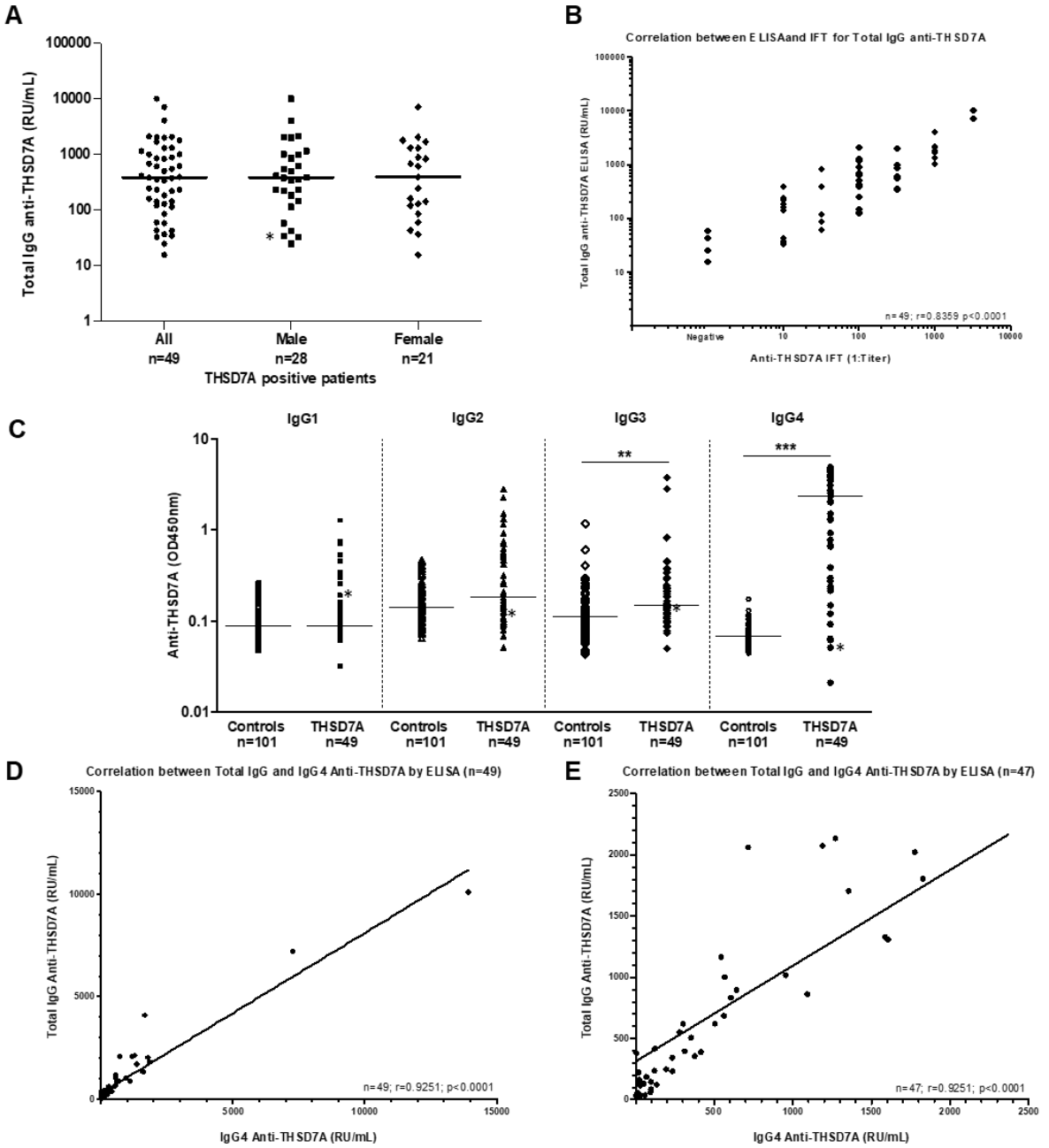

Figure S3: Levels of IgG subclasses and total IgG for anti-thrombospondin type 1 domain-containing 7A (THSD7A) autoantibodies, and correlation between anti-THSD7A titers by enzyme-linked immunosorbent assay (ELISA) and indirect immunofluorescence test (IIFT). (**A**) Scatter plot showing the distribution of anti-THSD7A titers for the 49 THSD7A-positive patients, as measured with total IgG as a secondary antibody. Titer for membranous nephropathy patient (MN40) is shown with asterisk (*). **(B)** Correlation between total IgG anti- THSD7A titers measured by IIFT versus ELISA. The correlation is highly significant (n=49, r=0.8359, P < 0.0001). **(C)** Distribution of anti-THSD7A IgG subclasses measured by ELISA for the THSD7A-positive patients (n=49) versus control subjects (other diseases and healthy donors, n=101). The anti-THSD7A titer for IgG3 and IgG4 subclasses was significantly different from that of control subjects using one-way analysis of variance test (**<0.01, ***<0.001). Optical density (OD) values for MN40 are shown with asterisk (*). **(D)** Correlation between anti-THSD7A titers measured by ELISA using IgG4 and total IgG secondary antibodies (n = 49, r = 0.9251, P < 0.0001). (E) Zoom on the low to middle range titers of anti-THSD7A titers measured by ELISA using IgG4 and total IgG secondary antibodies (n = 47).

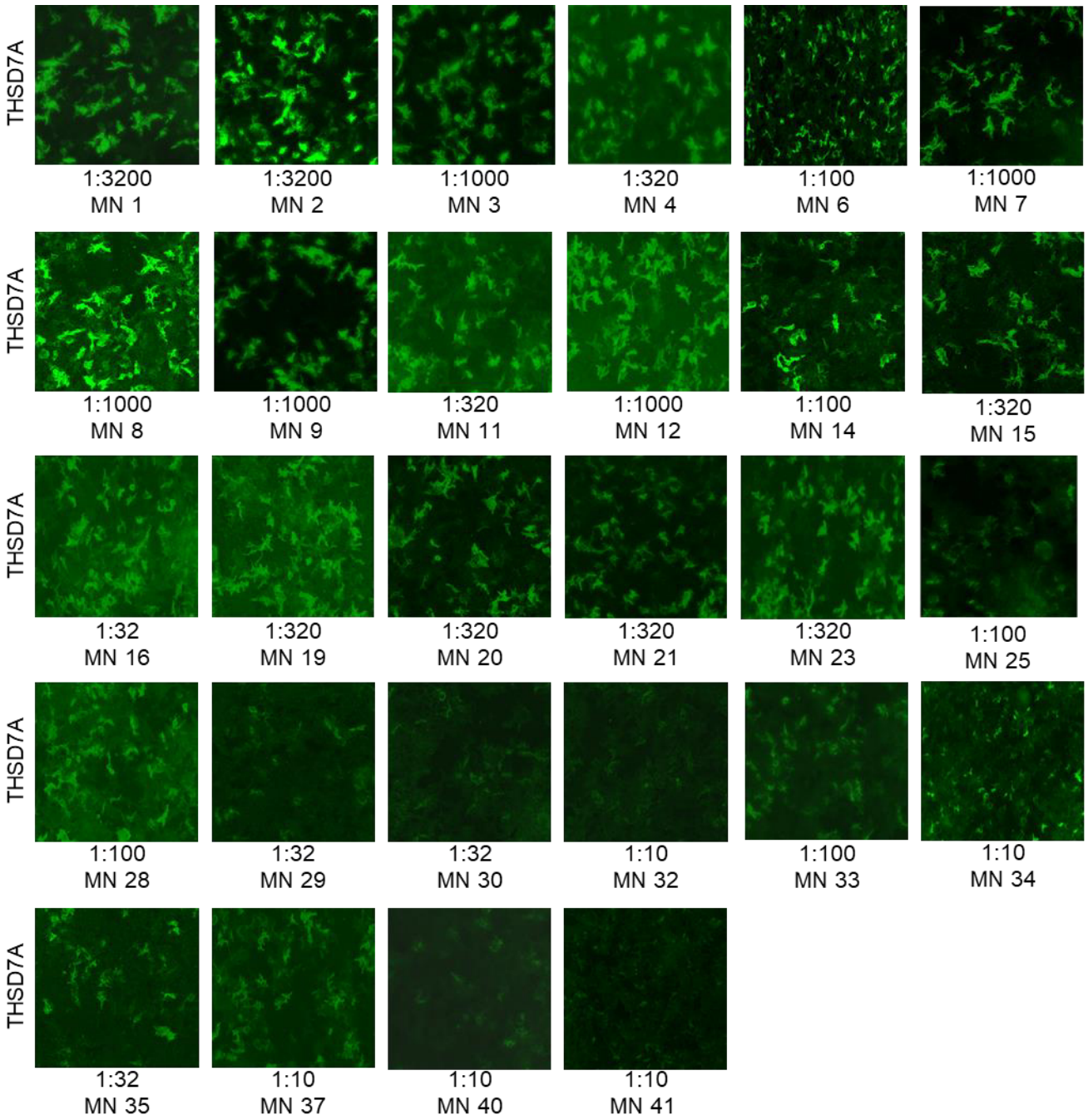

Figure S4: Indirect immunofluorescence test (IIFT) data for thrombospondin type 1 domain-containing 7A (THSD7A)-positive patients. Autoantibody titers were estimated by the fluorescence intensity at various dilutions. Data are shown at the dilution titer. Data for membranous nephropathy patient 5 (MN5), MN13, MN26, MN31, and MN42 to MN49 are presented in the main figures.

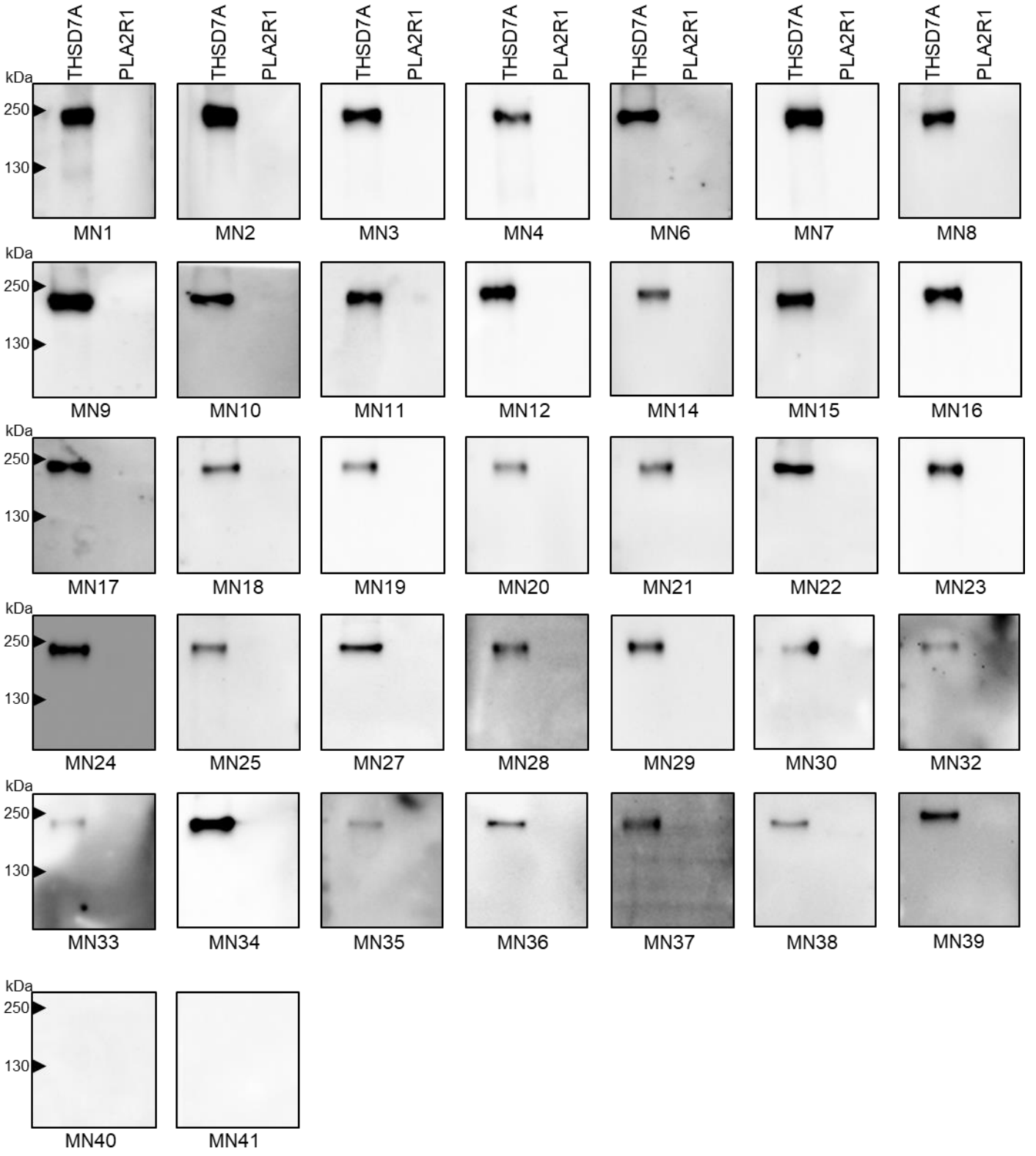

Figure S5: Western blot analysis of purified recombinant thrombospondin type 1 domain-containing 7A (THSD7A) and phospholipase A2 receptor 1 (PLA2R1) antigens (50 ng each) probed with all sera from THSD7A-positive patients under nonreducing conditions. Serum reactivity of patients was tested at optimal serum dilution (1:10 to 1:100). The blots were exposed for different times. Results for membranous nephropathy patient 5 (MN5), MN13, MN26, MN31, and MN42 to MN49 are presented in the main figures.

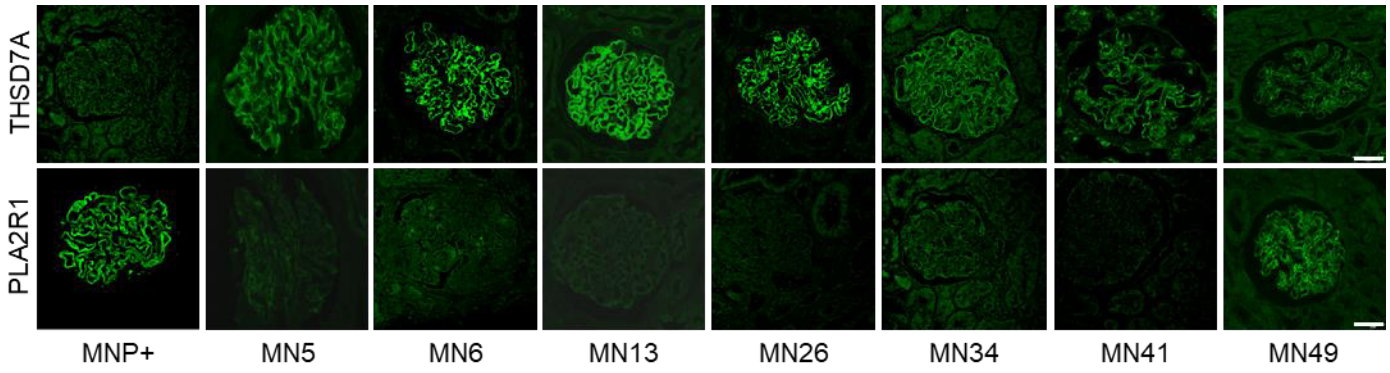

Figure S6: Immunofluorescence staining of thrombospondin type 1 domain-containing 7A (THSD7A) and phospholipase A2 receptor 1 (PLA2R1) antigens for available patients' biopsies. **(A)** Available immunofluorescence biopsy staining for THSD7A antigen for the anti-THSD7A-positive patients included in this study (membranous nephropathy patient 5 MN5, MN6, MN13, MN26, MN34, MN41) and for 1 double-positive patient (MN49). An anti-PLA2R1 positive serum (MNP+) was used as a positive control for PLA2R1 staining. Bar=50 µm.

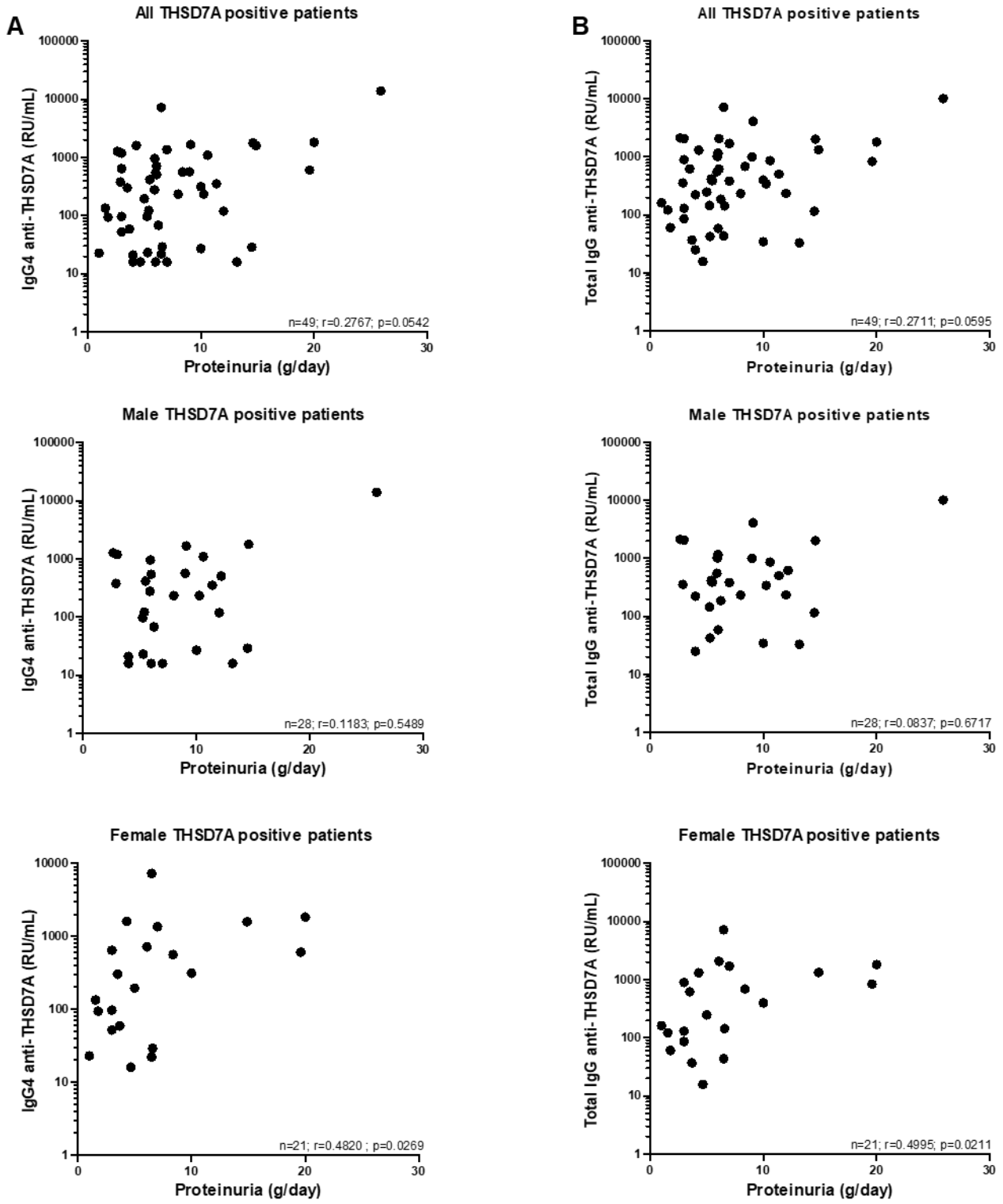

Figure S7: Correlation of proteinuria with IgG4 and total IgG anti-thrombospondin type 1 domain-containing 7A (THSD7A) titers measured by enzyme-linked immunosorbent assay for anti-THSD7A-positive patients as a whole or by sex. (A) Correlation between proteinuria and IgG4 anti-THSD7A titers for all (n=49, r=0.2767, P=0.0542), male or female THSD7A-positive patients. **(B)** Correlation between proteinuria and total IgG anti-THSD7A titers for all (n=49, r=0.2711, P=0.0595), male or female THSD7A-positive patients. Proteinuria levels show no significant correlation with anti-THSD7A titers.

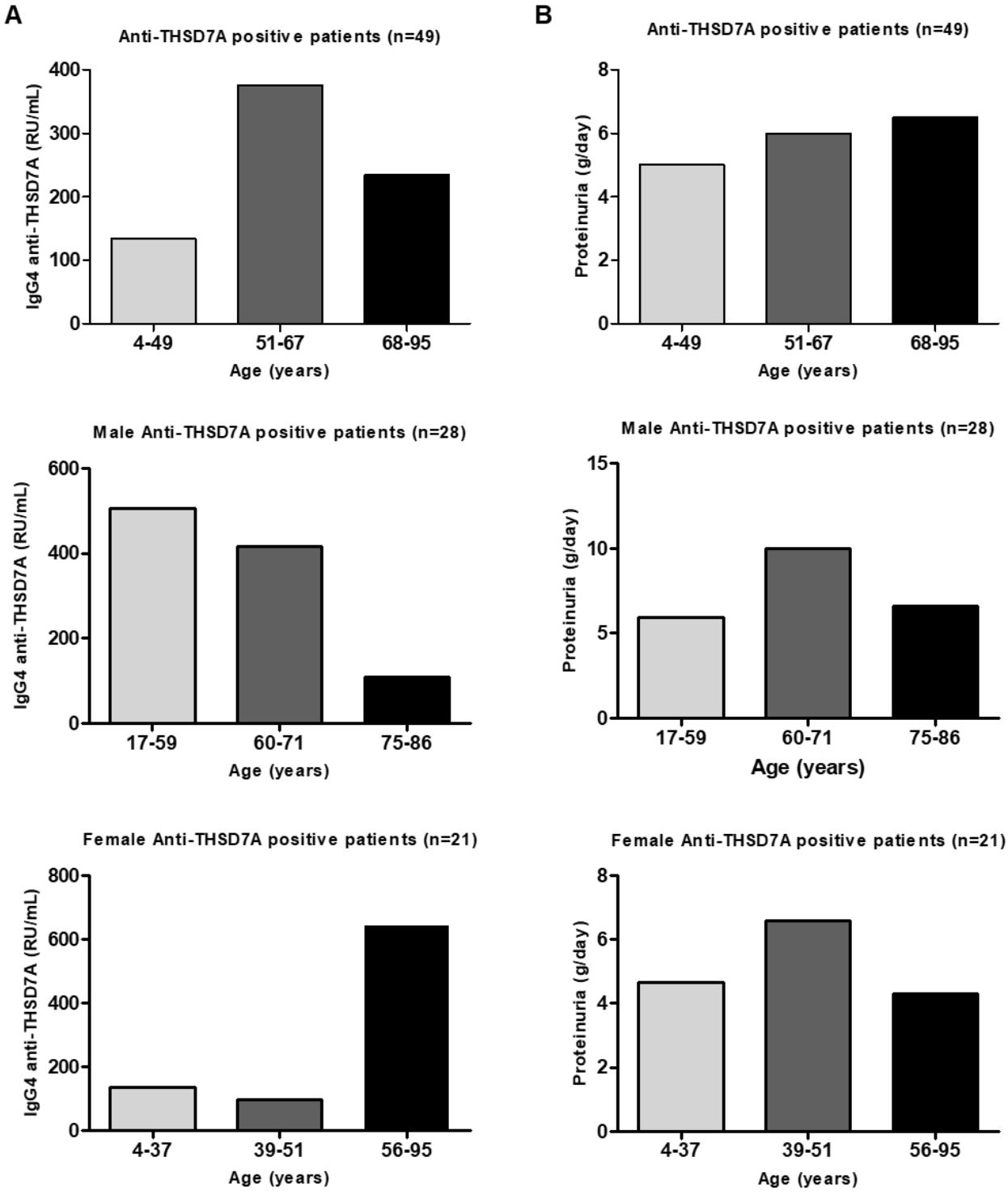

Figure S8: Relationship between anti-thrombospondin type 1 domain-containing 7A (THSD7A) titer, proteinuria, and age of anti-THSD7A-positive patients by tertiles. (A) Relationship between anti-THSD7A median titer (relative units [RU]/ml) and age of patients in tertiles for all, male, or female THSD7A-positive patients. **(B)** Relationship between proteinuria levels (g/d) and age of patients in tertiles for all, male, or female THSD7A-positive patients. Anti-THSD7A and proteinuria levels show no significant correlation with age.

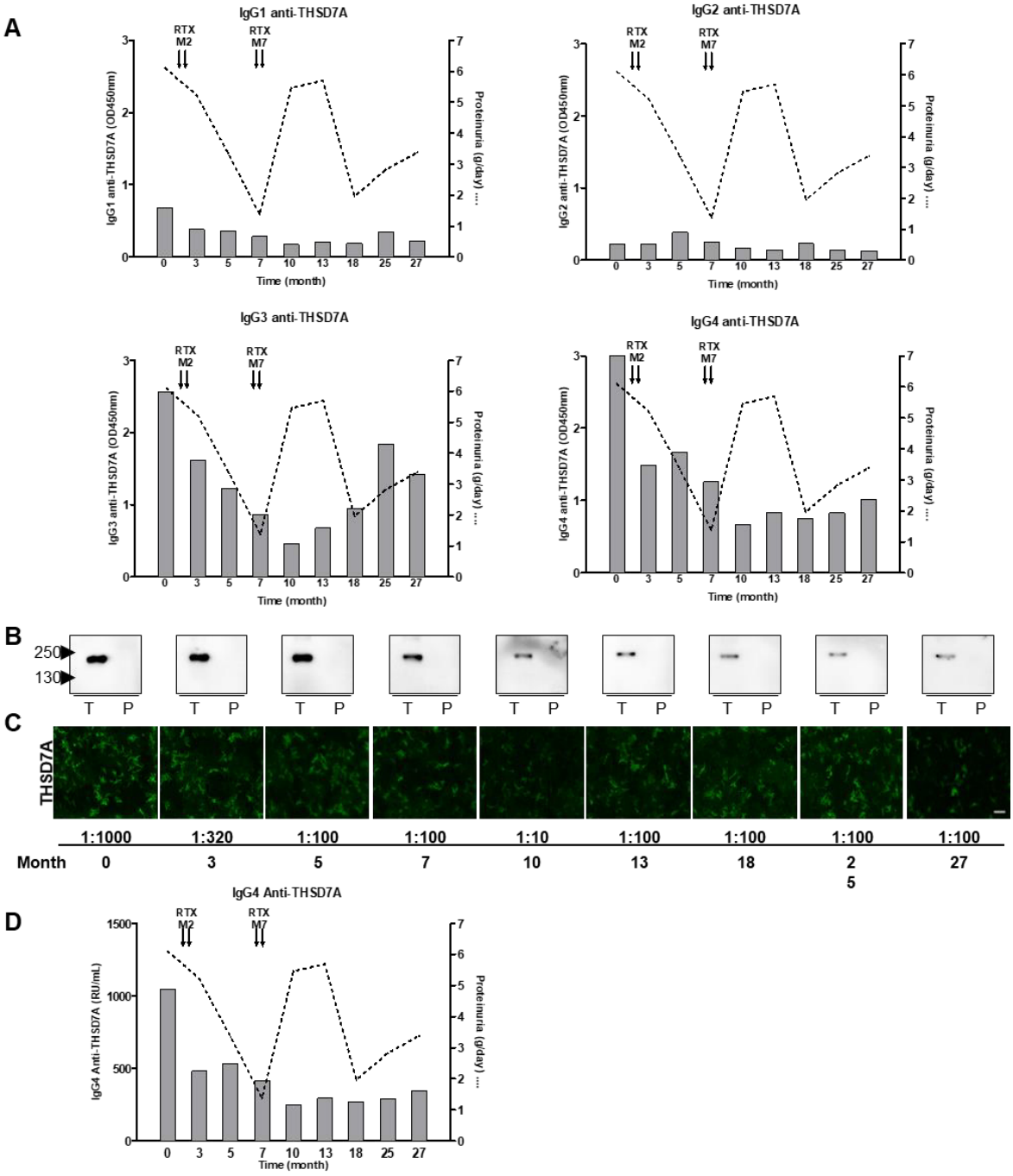

Figure S9: Anti-thrombospondin type 1 domain-containing 7A (THSD7A) titer and proteinuria levels during clinical follow-up for membranous nephropathy patient 13, a THSD7A-positive pediatric patient (4 years old at baseline) treated with rituximab. The patient had nephrotic range proteinuria at baseline and received 2 courses of rituximab (RTX) at months 2 and 7. See more clinical details in the Supplementary Methods. **(A)** Respective levels of anti-THSD7A autoantibodies measured by enzyme-linked immunosorbent assay for the different IgG subclasses and proteinuria during a follow-up of 27 months. **(B,C)** Anti-THSD7A levels measured by Western blot and indirect immunofluorescence test. Enzyme-linked immunosorbent assay and indirect immunofluorescence test detect the fluctuation of serum anti-THSD7A levels more quantitatively than Western blot. Bar=70 um. There is a significant correlation between anti-THSD7A titers measured by enzyme-linked immunosorbent assay and indirect immunofluorescence test (not shown). **(D)** IgG4 anti-THSD7A titer shown in relative units (RU)/ml while it is shown as optical density (OD) values in panel A.

Part III

Discussion and conclusion

Chapter 9
Discussion

At the beginning of this PhD, controversial works had just identified several epitopes in PLA_2R1, with seemingly complex relationships to anti-PLA_2R1 titer and an hypothetical mechanism of epitope spreading, possibly unifying the two factors. At first sight, this gave the impression of a conundrum in the PLA_2R1 autoimmune response, which may differ either because studies were using different methodologies on heterogeneous and limited patients' serum samples, or because of true differences in the natural course of MN for individual patients, from aetiology to smouldering and overt disease, resulting in different patterns of autoantibodies as observed in clinical serum samples.

The main work of this PhD project helped to clarify our view on the anti-PLA_2R1 autoimmune response observed in patients, i.e. during the overt phase of MN disease. Using a well-defined large cohort of MN patients, we identified in detail which PLA_2R1 domains contain epitopes and which ones are the most prevalent and immunodominant, and thus act as the main drivers of the autoimmune humoral response. Hopefully, our work will bring new insights into the pathogenesis of PLA_2R1-associated MN and will help to provide new ways to look at the anti-PLA_2R1 autoantibody humoral response by monitoring not only titer but also specific autoantibodies and profiles such as immunodominance, for a better stratification of patients in the daily clinical practice, towards more personalized medicine.

9.1 From analysis of the autoimmune humoral response to a working model of the autoimmune response in PLA_2R1-associated MN

Specifically, my PhD work definitely demonstrated that (i) CysR and CTLD1 are two independent epitope-containing domains, (ii) CTLD5 and CTLD8 are two novel epitope-containing domains, and (iii) CysR and CTLD1 domains contain the immunodominant epitopes which are the driving force of the autoimmune humoral response and might also be at the origin of the disease, leading us to propose a working model for a step-by-step development of the autoimmune response, resulting in the production of pathogenic autoantibodies that lead to podocyte injury and kidney failure.

9.1.1 The saga of PLA$_2$R1 epitopes' discovery and relationship to titer

"Macroepitopes" versus "microepitopes" in PLA$_2$R1 – It is important to keep in mind that PLA$_2$R1 is a large protein with an extracellular region comprising 10 globular domains, each folded with disulphide bonds while the conformational genuine or true epitopes are expected to consist of less than 10 surface-exposed residues, in a non-linear sequence manner. Thus we can distinguish the so-called "epitope-containing domains" that we routinely call in the laboratory the "macroepitopes" and the genuine epitopes that we call "microepitopes".

9.1.1.1 PLA$_2$R1 epitope-containing domains or "macroepitopes"

With the identification of PLA$_2$R1 as the major autoantigen in MN, several groups worked hard towards the identification of the epitopes targeted by the autoantibodies (chapter 4.2). In 2013, Behnert and colleagues (Behnert et al., 2013) suggested that patients' autoantibodies may target seven specific epitopes within CysR, CTLD1, CTLD2, CTLD6, CTLD7 and CTLD8, i.e. spanning the full extracellular region of PLA$_2$R1. However, their results relied on the use of linear peptides while previous works had demonstrated that anti-PLA$_2$R1 autoantibodies only recognize conformational epitopes. Naturally, we cannot exclude the hypothesis that some other autoantibodies recognizing these non-conformational epitopes might be produced during the course of the autoimmune response or in certain patients. Their low titer or affinity may also prevent their detection by techniques using the full receptor, when the signal is due to multiple autoantibodies, with most of them being conformational. However, our screen with 142 patients against the 10 individual domains did not highlight any epitope in the CTLD2 nor CTLD6 domains which were proposed by the authors to exhibit 3 of the 7 epitopes described. Therefore, we believe that the epitopes identified in this study do not represent any of the major epitopes in PLA$_2$R1-associated MN.

In 2015, Kao and colleagues (Kao et al., 2015) suggested that the CysR-FnII-CTLD1 region contains a single interdomain epitope where deletion of either CysR or CTLD1 apparently prevents patients' autoantibodies recognition. Shortly after, Fresquet and colleagues (Fresquet et al., 2015) showed that CysR may be sufficient for autoantibody binding, yet assistance by other domains may be needed to maintain the conformation of the epitope, while not suggesting epitopes in the CTLD1 domain, but more distant ones. In 2016, our laboratory showed that in fact patients' serum could react to single CysR or CTLD1 domains in the absence of each other (Seitz-Polski et al., 2016). The contradictory results raised doubts regarding

the exact number and location of the epitopes in the N-terminal region of PLA_2R1. My PhD work definitely demonstrated, through two different techniques, that patients' autoantibodies present distinct reactivities towards either CysR and/or CTLD1 expressed as single epitope-containing domains or as chimera with MRC2 or after appropriate cleavage of the CysR-FnII-CTLD1 region (Figure 1 and Figure 2 from article 1). Part of the conflicting results were in fact due to errors in the strategy used by Kao and colleagues, both at the design of PLA_2R1 constructs and by the fact that they used a small number of patients to probe epitopes. First, after verifying that their single serum sample was able to recognize the CysR-FnII-CTLD1 region, the authors tried to dissect this region by producing the soluble forms for single CysR and CTLD1 domains. Facing expression problems for the CTLD1 domain while no reactivity was observed for the CysR-FnII domain with that particular patient's serum, the authors designed an apparently elegant technique in which they introduced a thrombin cleavage site between CysR and FnII domains or FnII and CTLD1 domains, and tested the reactivity of their patient's serum before and after protease digestion. However, instead of introducing the protease cleavage site in the linker region between FnII and CTLD1 domains, they placed it within the first disulphide bridge of the CTLD1 domain (Figure S3 from article 1). This technical error prevented the separation of CysR and CTLD1 domains after digestion under non-reducing conditions, since the disulphide bridge will still maintain together the three domains in a covalent manner, despite actual cleavage of the peptide bond. Additionally, irrespective of the disulphide problem, protease cleavage may lead to the destruction of the epitope recognized by a patient or alter its conformation by a bystander effect, preventing its detection. Indeed, in the study by Kao and colleagues, it appears that their patient's serum no longer recognized the CysR-FnII-CTLD1 domain after thrombin cleavage, even though it would have been maintained as a triple domain by the CTLD1 disulphide bond. However, in our study, all eight patients' sera tested could recognize the triple domain after protease cleavage of the same construct where the cleavage site was inserted in the wrong place. These discrepant results can be best explained by the unfortunate case that the authors used a single patient to test their hypothesis, with this patient likely having more (or exclusively) autoantibodies targeting CTLD1 than CysR. Thus, our data provide step-by-step and detailed explanation about the reason of these discrepancies. Nevertheless, our strategy cannot completely exclude the hypothesis that patients might produce autoantibodies towards conformational interdomain epitopes. However, if present, they do not represent major epitopes in the anti-PLA_2R1

humoral response, as our competition assays suggest that single CysR and CTLD1 compete for most of the signal. Finally, demonstrating that CysR and CTLD1 domains comprise independent epitopes was important as it turned out that they are the major immunodominant domains.

Concerning the more distal part of PLA_2R1 beyond CTLD1, the work from Fresquet and colleagues suggested that a few patients may have epitopes within the region CTLD3-CTLD8 while our work indicated epitopes within CTLD7±CTLD6 and possibly CTLD8 (unpublished data from Dolla and colleagues) (Dolla, 2017; Seitz-Polski et al., 2016). During this PhD, we either confirmed or identified CTLD5, CTLD7 and CTLD8 as three additional PLA_2R1 domains containing independent epitopes.

Together, the humoral autoantibody response to PLA_2R1 is thus polyclonal, with in total 5 of the 10 (50% of the structure) PLA_2R1 domains targeted by autoantibodies, with the possibility for several epitopes within each domain. By screening a cohort of 142 patients with PLA_2R1-associated MN we demonstrated that the prevalence was very different between each domain, as high as 100% for CysR and as low as 3.5% for CTLD8 (Figure 4 from article 1). The low prevalence of CTLD8 might explain why this epitope-containing domain was not identified in previous works. As for CTLD5, while we observed that CTLD5 is the second most prevalent epitope-containing domain, its late discovery was probably due to its unique sensitivity to temperature and denaturation, as it is only recognized in its most native conformation, by ELISA or immunoprecipitation techniques, but not by western blot, even under non-reducing conditions (Figure S8 from article 1). Indeed, previous works mainly used western blot to identify the epitopes targeted by the autoantibodies, a technique that requires denaturation in SDS (usually after boiling at 95°C) and thereby altering the conformation of the CTLD5 domain. Our attempts to sort out what makes CTLD5 sensitive to denaturation and not recognized by western blot was only partially successful. We could indeed demonstrate that the CTLD5 epitope(s) is/are sensitive to temperature and DTT. However, for western blot experiments, we could not demonstrate that SDS is sufficient by itself to denature the epitope(s). Indeed, direct loading of CTLD5 (in Laemmli SDS buffer but without heat denaturation), followed by electrophoresis and transfer of the gel in ice-cold buffers did not maintain CTLD5 reactivity. Furthermore, attempts to renature the CTLD5 epitope(s) by incubating the western blot membrane in semi-chaotropic conditions like urea buffers did not rescue the conformation and patient's reactivity (data not shown). The very sensitive loss of epitope reactivity of CTLD5 was further observed when the

antigen was coated on ELISA plates and lyophilized, with absence of patients' autoantibodies reactivity after lyophilisation (data not shown). In fact, this was also observed for CTLD7 but not CTLD1 and CTLD8 (data not shown). Interestingly, the globular structure of both CTLD5 and CTLD7 domains is maintained by two disulphide bonds whereas that of CTLD1 and CTLD8 domains is maintained by three disulphides, partially explaining their different resistance to temperature- and/or SDS-dependent denaturation. Our findings further underline that PLA_2R1 epitopes are highly conformational and those technical approaches maintaining as much as possible the conformation of the native antigen should be used to detect patient's reactivity. Other factors such as glycosylation or the quaternary structure of PLA_2R1 may also alter the reactivity of patients' autoantibodies. Indeed, the overall structure of PLA_2R1 is pH-dependent, presenting a compact conformation at acidic pH and a more flat extended conformation at basic pH (Dong et al., 2017; Fresquet et al., 2015; He et al., 2011; West et al., 2004). Moreover, PLA_2R1 ligands may alter its overall structural organization and autoantibody reactivity, either inhibiting this latter or unmasking new epitopes. Therefore, even though up to five epitope-containing domains have already been identified, we cannot exclude that other epitopes might be revealed by using different and more specific approaches taking into account the specific complex structure of PLA_2R1. As an example of such a complexity in autoantibody reactivity, about 5% of patients with *myasthenia gravis* have autoantibodies targeting exclusively the acetylcholine receptor when expressed as a multimer of pentamers (Jacob et al., 2012). Last but not least, the particular sensitivity of CTLD5 and CTLD7 to lyophilisation (when lyophilized as single domain) indicates that the commercial Euroimmun ELISA assay which uses lyophilized full PLA_2R1 may not measure the full reactivity to these domains, but the one due to CysR and CTLD1, and in fact underestimate the full titer.

9.1.1.2 Towards the identification of the genuine epitopes or "microepitopes"

When investigating the correlation between anti-PLA_2R1 titer and epitope profile, and as one could expect "by nature of the autoimmune response", we observed that the anti-PLA_2R1 titer increases as more and more epitope-containing domains become positive. However, exceptions are observed, with patients having low anti-PLA_2R1 titer and presenting reactivity towards 3 or 4 epitopes, and vice-versa with patients having high titer but presenting limited reactivity towards 1 or 2 epitope-containing domains. Plots displaying the relationships between anti-

PLA_2R1 titer and epitope profiles revealed these factors, meaning that patients with the same number of epitopes but different profiles (for example CRC5 versus CRC7) or even patients with the same profile might present distinct anti-PLA_2R1 titers (Figure 5 from article 1). The differences observed may also be due to the presence of more than one "microepitope" within the same domain due to "intradomain spreading", associated with different titers for each corresponding autoantibody. In fact, a mechanism of intramolecular (intradomain) spreading is observed for myeloperoxidase (MPO) and proteinase 3 (PR3), which are the two globular autoantigens involved in anti-neutrophil cytoplasmic autoantibody (ANCA)-associated vasculitis (AAV) (Land et al., 2014; Roth et al., 2013). Several studies have been performed to map the epitopes of both MPO and PR3. A study from Bruner and colleagues (Bruner et al., 2010) identified seven epitopes at the surface of PR3 that could be commonly recognized by patients. Similar observations were made by the same group for MPO, in which screening of overlapping peptides (10 amino acids each) allowed to verify that patients could present reactivity to multiple regions of MPO (Bruner et al., 2011). Systemic evaluation of epitope profiles by mass spectrometry showed patients' reactivity to multiple portions of MPO, and the number and specificity of certain "microepitopes" is associated with smouldering or overt disease activity (Roth et al., 2013). Thus, a similar scenario of intradomain spreading may also occur in each domain of PLA_2R1, increasing the complexity of the autoimmune response from five "macroepitopes" or epitope-containing domains to likely much more "microepitopes" or genuine epitopes.

The detailed analysis of these "microepitopes" would be important for a better understanding of the autoimmune response but their identification will be challenging as they are conformational. In fact, the first possible "microepitope" would be the one identified by Fresquet and colleagues (Fresquet et al., 2015) in the N-terminal 35 amino acids of CysR but it is likely still preliminary. Our data in fact could not confirm that the identified peptide has reactivity with several patients known to react with the CysR domain. Furthermore, our preliminary data from a cross-reactivity study testing patients' sera reactivity against epitope-containing domains from human, mouse and rabbit PLA_2R1 showed that the positivity towards a specific domain is not always conserved among species (data not shown). For instance, while serum from a patient reacts against a specific epitope-containing domain from the three PLA_2R1 species, another serum presents reactivity towards the same human epitope-containing domain but not against one or more PLA_2R1 orthologs. Although indirect, these data suggest that patients' sera probably contain different autoantibodies targeting different "microepitopes"

within the same "macroepitope" PLA_2R1 domain. To elucidate the different epitopes within each domain, several strategies can be used among the three strategies listed below.

One strategy would rely on pursuing the comparative analysis of cross-reactivity of PLA_2R1 domains from different species to pinpoint different stretches of amino acids which may be part of the specific "microepitopes". Swapping of these sequences between for instance mouse and human CysR may reveal gain or loss of reactivity.

Similarly, a second strategy, more "all or none", may be elaborated by the production of chimeras between PLA_2R1 and its paralog MRC2, which do not react at all with patients' autoantibodies while being the closest paralog. In parallel with the above cross-reactivity studies to display epitopes, we have already started to prepare a series of chimeras in which we have swapped a domain region of MRC2 by the corresponding portion from PLA_2R1 and vice-versa. However, the detailed PLA_2R1 structure is not yet elucidated which makes difficult to predict which regions of the domain could be swapped without structural clashes, i.e. how this would affect the conformation of the domain relative to the potential "microepitope" region. Indeed, when introducing a full domain of PLA_2R1 and MRC2, the patients' serum could recognize it, which was considered as a proof-of-concept of this strategy between PLA_2R1 and MRC2 (Figure 2 from article 1). However, when we started to swap only partial sequence segments of a domain, we could either not express the protein or we lost patient's reactivity in most of the cases, indicating the limitation of this strategy without a good model of the structures (data not shown).

A third strategy can rely on performing single point site-directed mutagenesis by alanine scanning of each epitope-containing domain. ELISA screen of these mutants may allow to identify the location of the "microepitopes", assuming that a single point mutation is sufficient to significantly decrease or even abolish the epitope recognition, and of note, this would work if the epitope contributes to the signal in that PLA_2R1 domain.

Finally, when performing the cross-reactivity studies just referred above, we used recombinant proteins expressed in HEK293 cells and *E. coli*. During these experiments, we observed that serum reactivity was detected for the epitope-containing domain produced in HEK293 cells but sometimes lost for the recombinant protein produced in *E. coli* (data not shown), suggesting that some post-translational modifications (PTMs) are also involved in epitope reactivity and

maybe in the development of the autoimmune response. Interestingly, Tramontano and colleagues (Tramontano et al., 2004) demonstrated that N-glycosylation of megalin is important for induction of MN in the Heymann nephritis rat model. More work with "elegant techniques" is clearly needed to identify these so-called "microepitopes" within each PLA_2R1 domain.

9.1.2 Prevalence and PLA_2R1 epitope spreading

Screening of 142 patients with PLA_2R1-associated MN for each epitope-containing domain established the prevalence towards these domains. We confirmed that CysR is the most prevalent epitope-containing domain while other domains become less and less positive, roughly from the N-terminal to the C-terminal end, except for CTLD1 versus CTLD5 (Figure 4 from article 1) (Seitz-Polski et al., 2018; Seitz-Polski et al., 2016). These observations further support the hypothesis that the autoimmune response progresses from the CysR domain to the other domains by a mechanism of epitope spreading. However, our hypothesis still needs to be experimentally proven. Ideally, we would like to analyse the natural course of the humoral autoimmune response by testing the reactivity of patients' serum obtained at the very early stages of the disease, i.e. during the smouldering phase of MN and before the clinical onset or diagnosis of MN, after which the MN disease is in its overt phase. This strategy has been used to demonstrate a mechanism of epitope spreading in the development of the autoimmune response for pemphigus foliaceus and for type 1 diabetes (Brooks-Worrell et al., 2001; Li et al., 2003) (chapter 1.4.1). However, so far we only have analysed patients' sera during the overt phase of MN, with the first serum samples collected at the time of diagnosis or later, when the patient is already in an advanced stage of the disease, and likely with a mature autoimmune response in which the mechanism of epitope spreading may have already occurred. What we see might thus probably be "reminiscent" of the early steps of the autoimmune response leading to the formation of immunodominant and non-immunodominant epitopes, with "waves" of autoantibody titers depending on the stage of the immunological response, from remission to relapse phases. A new hope for the analysis of serum from patients during the smouldering phase arose with the recent work from Joshi and colleagues (Joshi et al., 2018) with a cohort of patients from the US army, demonstrating the presence of circulating anti-PLA_2R1 autoantibodies months to years before MN diagnosis and even before the earliest documentation of non-nephrotic range proteinuria. Future studies of this cohort regarding epitope profile but also immunodominance (see below chapter 9.1.3) or anti-PLA_2R1 IgG

subclasses would significantly contribute to a better understanding of the early phase of the autoimmune response.

Another approach to experimentally demonstrate the phenomenon of PLA_2R1 epitope spreading in MN would be by establishing an *in vivo* animal model. Preferentially, this could be done in a rat or mouse model of MN as previously demonstrated for megalin in the Heymann nephritis rat model (Shah et al., 2007). However, PLA_2R1 is not expressed in rodent podocytes which has been a major drawback in the development of an animal model for PLA_2R1-associated MN. Nevertheless, we have started to establish a model of experimental epitope spreading for PLA_2R1 by immunizing rabbits.

Initially, in an immunization protocol of 95 days, we injected two rabbits with human PLA_2R1 in Freund's adjuvant with boosts every 21 days. Analysis of serum samples collected at several time points showed that the immune response initiates by developing antibodies against the CysR domain followed by spreading to other domains with the exception of FnII and CTLD5 for the first rabbit (data not shown). The second rabbit presented a weaker immune response (lower anti-human-PLA_2R1 titer) with antibodies already targeting several domains at the first time point of sampling. By day 95, the rabbit sera recognized all the domains except FnII. Considering that 0.3% of MN patients are positive for both THSD7A and PLA_2R1 and that patients' may share a common immunodominant epitope (Fresquet et al., 2019; Zaghrini et al., 2019), we tested the cross-reactivity of rabbits' serum against THSD7A, which was negative at all time points. In parallel, we injected two rabbits with recombinant rabbit PLA_2R1 in Freund's adjuvant with the hope to initiate an autoimmune response, but no autoantibodies were detected in the serum at any time point (data not shown).

In a second series of experiments, we injected rabbits with human PLA_2R1, but with different adjuvants. The strength of the immune response was adjuvant-dependent as well as the way it developed. With certain adjuvants, the immune response progressed from the N-terminal to the C-terminal, whereas with others it seemed to develop from the C-terminal to the N-terminal (data not shown). Interestingly, in most cases, the antibody response was conformational, as expected.

These projects provide preliminary data in favour of a mechanism of epitope spreading occurring during the progression of the PLA_2R1 autoimmune response. However, which domain contains the immunodominant epitope in this rabbit experimental model remains unclear since several trends have been observed

depending on the adjuvant, suggesting that different aetiologies might lead to different responses by the immune system. We also have to take in consideration that this model involves an immune response and not an autoimmune one; therefore it will not exactly mimic what happens in the pathogenesis of human autoimmune MN. Finally, the observations obtained within each rabbit project are quite preliminary: they are only based on the few experiments performed until now and mostly rely on the response of two rabbits/group. Future projects should involve the injection of the individual epitope-containing domains, in particular CysR and CTLD1 (see below chapter 9.1.3), which hopefully would bring more insights into the pathogenesis of PLA_2R1-associated MN, in particular the identification of the domains containing the immunodominant epitopes and a better view of the mechanism of epitope spreading.

9.1.3 Driving-forces of the autoimmune response

After the identification of the most prevalent epitope-containing domains, we wanted to know which one(s) is(are) the driving force of the humoral autoimmune response, i.e. the major contributor(s) of the anti-PLA_2R1 titer. In their previous works, using a western blot competition assay for 10 patients, Kao and colleagues (Kao et al., 2015) showed that the major driving force of the autoimmune response was the triple domain CysR-FnII-CTLD1. Similarly, by performing ELISA competition assays with the CysR-CTLD3 region for 43 patients, Fresquet and colleagues (Fresquet et al., 2015) demonstrated that the CysR-CTLD3 region contained the epitopes mainly contributing to the anti-PLA_2R1 titer for most patients. Thus, within CysR-FnII-CTLD1 or CysR-CTLD3 regions, is CysR the major contributor as suggested by Fresquet and colleagues (Fresquet et al., 2015) or is it CTLD1? Finally, Fresquet and colleagues also observed that for a few cases there was another more distal epitope-containing domain also contributing to the autoimmune response.

To better define which “macroepitope” domain(s) is/are mainly contributing to the anti-PLA_2R1 titer, we performed ELISA competition assays for all patients from our cohort with available serum with several regions of PLA_2R1 as competing domains against the full PLA_2R1 extracellular domain. Our competition assays confirmed that for 91% of the patients CysR-FnII-CTLD1 is the major contributor of the anti-PLA_2R1 titer (Figure S11 from article 1). By performing competition assays with the individual epitope-containing domains or a combination of them, we clearly demonstrated that CysR is immunodominant and represents the main driving force of the autoimmune response for a significant number of patients.

However, CTLD1 appears as another major immunodominant domain for a significant group of patients, likely at the expense of CysR immunodominance (Figure S11 and Figure S12 from article 1). Conversely, the more distal domains CTLD5, CTLD7 and CTLD8 have only a modest contribution to the anti-PLA_2R1 titer. Of note, all patients produced autoantibodies against the CysR domain and as observed from competition assays, anti-CysR autoantibodies always contributed to some extent to the anti-PLA_2R1 signal. This implies that a patient cannot have an humoral autoimmune response 100% driven by another epitope-containing domain. From a pathophysiological point of view, we also considered previous studies showing that (i) injection of two monoclonal antibodies targeting the podocyte aminopeptidase A is more pathogenic than each antibody injected separately, and (ii) injection of a polyclonal serum versus monoclonal antibodies targeting megalin produces more dense immune deposits (Allegri et al., 1986; Mentzel et al., 1999). These studies suggest that the presence in serum of a significant proportion of two main classes of autoantibodies may be more pathogenic than a single class of antibody. Thus we reasoned that the presence of circulating anti-CysR autoantibodies as a main single class of antibodies may be less pathogenic than the presence of both anti-CysR and anti-CTLD1, when each present at a significant titer and ratio. With this in mind, we defined three groups of patients based on competition assays. For iCR patients, binding to CysR-FnII-CTLD1 should account for at least 65% of the anti-PLA_2R1 signal with most of this binding due to CysR reactivity, i.e. less than 20% due to CTLD1. For iC1 patients, binding to CysR-FnII-CTLD1 should also account for at least 65% of the anti-PLA_2R1 signal but at least 20% of binding should be due to CTLD1 reactivity. For non-iDom patients, no particular PLA_2R1 domain is driving the autoimmune response and the anti-PLA_2R1 signal is distributed over all domains (Figure 6 from article 1). In our cohort, 55% of patients were iCR, 36% were iC1 and 9% were non-iDom.

Interestingly, most patients (74%) who are CTLD1-positive are also iC1. This suggests that as soon as a patient becomes CTLD1-positive the autoimmune response "switches" and starts to be driven by CTLD1. Analysis of a patient with two available follow-up serum samples allowed us to obtain preliminary evidence for this hypothesis of immunodominance switch. In the first serum sample, patient's serum presented reactivity only towards the CysR domain, defining CysR immunodominance. Three months later and in the absence of treatment, patient's serum targeted CysR, CTLD1 and CTLD5 with a CTLD1 immunodominance. After another 3 months, the patient was in spontaneous remission with a CysR profile and a CysR immunodominance (data not shown). If the observation is correct, why

and when this switch of immunodominance occurs may be better documented. It might be associated with genetics or other environmental factors. Our data first need to be confirmed in longitudinal cohorts of patients with analysis of baseline and follow-up samples from patients either untreated or treated with immunosuppressors. Analysis of immunodominance in our models of experimental epitope spreading in rabbits may also bring some insights. Finally, the analysis of the above specific patient illustrates how quick the immune response may switch, or be "plastic".

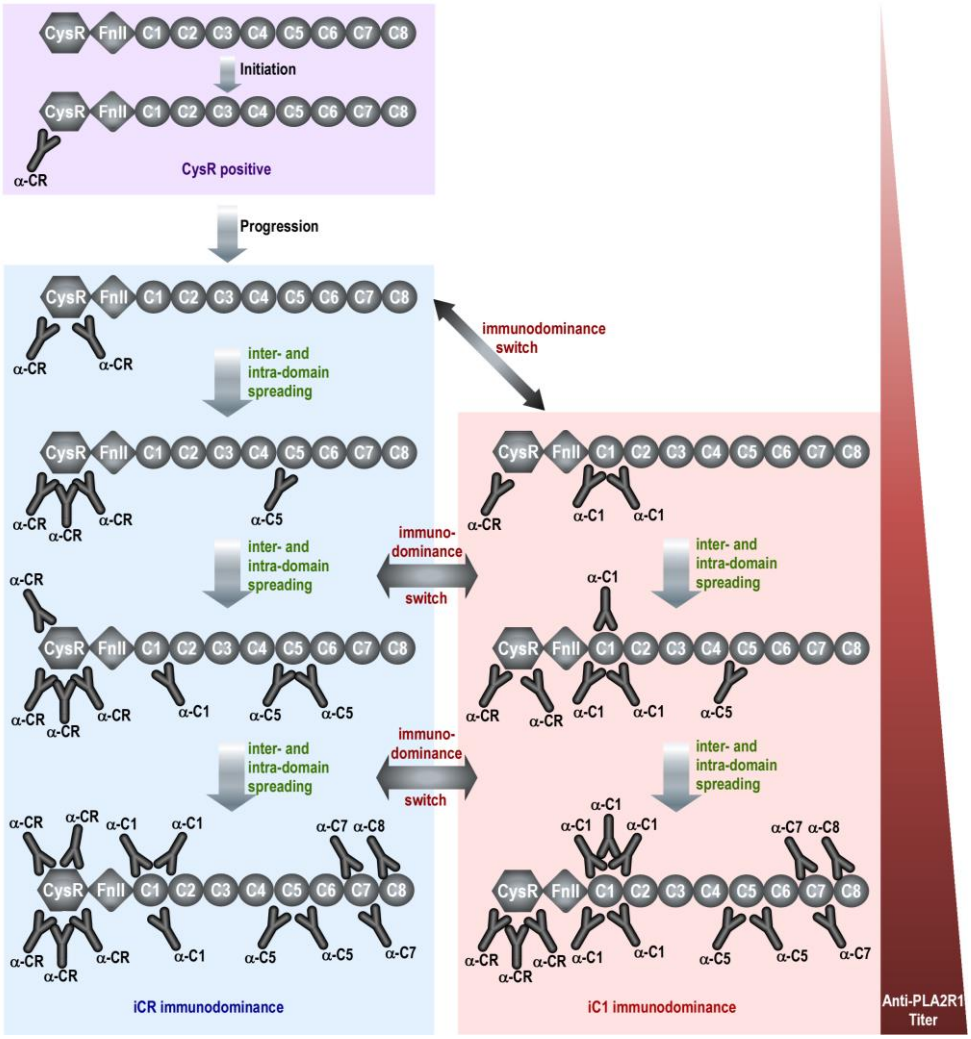

Figure 9.1 – Progression of the autoimmune response in PLA$_2$R1-associated MN. By integrating several results obtained throughout this project we proposed that once tolerance is broken, patients will produce autoantibodies against the CysR domain, starting as iCR at this stage. Via a mechanism of intradomain and interdomain epitope spreading, the autoimmune response will develop from the CysR domain towards other domains with a possible switch of immunodominance from the CysR to the CTLD1 domain at different stages. The development of the autoimmune response is associated with an overall increase in anti-PLA$_2$R1 titer, which may be maximal when all epitope-containing domains become positive and only when either CysR or CTLD1 or both are immunodominant. The non-iDom patients (not represented) cannot reach such high anti-PLA$_2$R1 levels and remain "stucked" in middle range titers.

Our results based on epitope positivity and immunodominance lead us to propose a working model of the humoral autoimmune response as shown in Figure 9.1. In this model, patients initiate the autoimmune response by producing autoantibodies against the CysR domain. As the autoimmune response matures, they will produce autoantibodies towards other epitope-containing domains by a mechanism of interdomain epitope spreading. The increase of the anti-PLA_2R1 titer observed will result not only from interdomain spreading, but also from intradomain spreading, as discussed above, with immunodominance to CysR or CTLD1 starting to appear. Based on "macroepitope" prevalence, interdomain spreading occurs from the CysR domain to the CTLD5 and/or CTLD1 and at a later stage to the CTLD7 and CTLD8 domains. While autoantibodies are produced towards several epitope-containing domains, the patient may stay on the CysR pathway with an autoimmune response driven by the CysR domain, or the patient can switch to the CTLD1 immunodominant pathway. What makes the autoimmune response being driven by one or the other pathway remains unclear, but one can hypothesize that different aetiologies or genetic variants are involved. Of note, the small group of non-iDom patients presenting a low anti-PLA_2R1 titer and an autoimmune response not (or not yet) driven by CysR or CTLD1 may be patients (i) at the beginning of the autoimmune response (low titer and no defined immunodominance), (ii) in transition from iCR to iC1 pathways, (iii) in the process of immunological remission or (iv) presenting an autoimmune response that resulted from a different aetiology without a trigger to progress into the immunodominant CysR or CTLD1 pathways. As said above, our model and the molecular mechanisms involved should be demonstrated by longitudinal follow-up of patients during the smouldering and overt phases of MN and by *in vivo* experiments in animals mimicking the anti-PLA_2R1 autoimmune response.

It is also important to note that progresses have been made towards the identification of epitopes and immunominant profiles in THSD7A-associated MN (Seifert et al., 2018; Zaghrini, 2019). Preliminary results have demonstrated that patients' autoantibodies can target several epitope-containing domains spanning all over the extracellular region of THSD7A (Seifert et al., 2018; Zaghrini, 2019). In contrast to PLA_2R1, no THSD7A epitope-containing domain was found to be 100% prevalent and two of these domains were found to be immunodominant in similar proportions, while other epitopes may represent interdomain spreading associated with low titers (Zaghrini, 2019). These preliminary observations suggest common features but variation on the theme for the autoimmune response observed in PLA_2R1- and THSD7A-associated MN patients, such as a preferential

immunodominance towards one domain versus another (PLA_2R1) or not (THSD7A) and a mechanism of epitope spreading, both interdomain and intradomain.

9.2 Biomarkers of PLA_2R1-associated MN

As mentioned several times throughout this manuscript, detection of anti-PLA_2R1 autoantibodies is nowadays used not only to diagnose MN, but also to monitor disease activity. Anti-PLA_2R1 titer reflects the immunological activity of the disease, with circulating autoantibodies disappearing from circulation months before clinical signs of remission (Beck et al., 2011; Beck et al., 2010; Hofstra et al., 2011; Kanigicherla et al., 2013; Seitz-Polski et al., 2014). Monitoring of anti-PLA_2R1 titer might prevent the unnecessary prescription of immunosuppressive treatment, as well as it might allow earlier treatment withdrawal once autoantibodies are undetectable. Similarly, a sudden rise of anti-PLA_2R1 titer while the patient is in remission likely indicates relapse before observation of clinical features. Finally, anti-PLA_2R1 titer can predict clinical outcome, with low titer associated with spontaneous remission and high titer associated with progression to severe disease and ESRD as well as resistance to immunosuppressive treatment (Beck et al., 2011; Dahan et al., 2017; Hofstra et al., 2012; Hoxha et al., 2014; Kanigicherla et al., 2013; Rodas et al., 2019; Ruggenenti et al., 2015; Timmermans et al., 2015).

During this thesis, we confirmed that high anti-PLA_2R1 titers were associated with poor renal outcome and less chance of spontaneous remission in two different retrospective cohorts of PLA_2R1-associated MN patients, using both univariable and multivariable models. Additionally, in the cohort of 142 patients, we also confirmed that resistance to immunosuppressive therapy was associated to high anti-PLA_2R1 titers. Nevertheless, thresholds for what might be considered as the low cut-off value of anti-PLA_2R1 titer for decision to treat with immunosuppressors and high cut-off value for likelihood of a response remains unclear, despite the first studies trying to address this question (Bobart et al., 2019; De Vriese et al., 2017). Future studies are needed to better define these cut-off values and help clinicians to better manage patients' healthcare.

Previous studies from our laboratory also have demonstrated that epitope spreading might help to better predict clinical outcome and treatment efficacy in combination to anti-PLA_2R1 titer (Seitz-Polski et al., 2019; Seitz-Polski et al., 2018; Seitz-Polski et al., 2016). In our retrospective cohorts, epitope spreading to CTLD1 and/or CTLD7 was also associated with worse clinical outcome in both univariable and multivariable analyses (data not shown). These analyses were done without

considering positivity to CTLD5 which (i) was not yet identified at the time of the screen or (ii) appears to not contribute by itself as a biomarker of pathogenicity. Indeed, when we compared the clinical features of CTLD5-negative and CTLD5-positive patients, no differences in clinical parameters except a lower eGFR were observed (data not shown). Additionally, both groups of patients equally reach remission or remain in active disease or progress to ESRD (data not shown). Therefore, we hypothesize that in contrast to CTLD1 and CTLD7, CTLD5 autoantibodies might not be as pathogenic, and thus might be less useful to predict clinical outcome.

Finally, my PhD work introduced a new stratification of patients based on their immunodominant profile that also appears as a new potential biomarker to predict clinical outcome and possibly the likelihood of response to rituximab therapy. In a multivariable model adjusted for clinical characteristics (proteinuria and eGFR) in which the interaction between immunodominance and treatment was taken into account, we demonstrated that iC1 patients had a poorer clinical outcome and that rituximab treatment was less effective than for iCR/non-iDom patients. Since iC1 patients had a significantly higher anti-PLA_2R1 titer than iCR/non-iDom patients, one could argue that the association to clinical outcome is due to the higher anti-PLA_2R1 titer rather than immunodominance. Since previous studies have demonstrated that patients respond less to rituximab treatment when their anti-PLA_2R1 titer is higher than 200 RU/mL (Dahan et al., 2017; Ruggenenti et al., 2015), we compared the clinical outcome of patients with different immunodominant profiles, having an anti-PLA_2R1 titer below 200 RU/mL and being treated with rituximab or with conservative therapy. We observed that half of iC1 patients (52%) remained in active disease or progressed to ESRD as compared to only 20% of iCR/non-iDom patients. When considering only patients treated with rituximab, the difference between the two immunodominant groups was even more clear, with most iCR patients (90%) responding to rituximab and the majority of iC1 patients (62%) not responding. In contrast, clinical outcome of patients with a high anti-PLA_2R1 titer, above 200 RU/mL in our analysis, showed that patients had poor renal outcome and did not respond to rituximab, independently of their immunodominant profile. Overall, our data suggest that until a certain cut-off of anti-PLA_2R1 titer, immunodominance can be a potential new biomarker to guide immunosuppressive treatment and identify patients that might best respond to rituximab therapy.

In sum, our data confirmed the clinical value of anti-PLA_2R1 titer and epitope spreading to predict clinical outcome. Additionally, we identify immunodominance as a potential new biomarker to predict clinical outcome, in particular the response

to rituximab treatment. Despite the encouraging results, our clinical findings need to be confirmed in larger prospective cohorts and randomized clinical trials. Nevertheless, we propose that a close follow-up and evaluation of anti-PLA_2R1 titer in combination with immunodominance profiling might be of importance for better healthcare of PLA_2R1-associated MN patients.

During my PhD work, I also participated in the development of a novel ELISA for the quantitative detection of anti-THSD7A autoantibodies. Like for PLA_2R1, we observed that anti-THSD7A titer reflects the immunological activity of MN allowing to monitor disease activity and response to treatment as well as predicting clinical outcome. Specifically, patients with anti-THSD7A titers in the lower tertile range were more prone to reach clinical remission, either spontaneous or after immunosuppressive treatment. Therefore, similar to what is observed for PLA_2R1-associated MN, we believe that a close follow-up and evaluation of anti-THSD7A autoantibodies is highly relevant for better healthcare of THSD7A-associated MN patients.

Finally, studies which I started during this PhD and are still ongoing in collaboration with Pr. Jack Wetzels, may help to identify patients at risk of progression to severe disease by monitoring anti-PLA_2R1 titer during follow-up and before any immunosuppressive treatment.

Chapter 10

Conclusions and perspectives

Membranous nephropathy (MN) is a rare but severe autoimmune kidney disease characterized in 1957 as a new entity but for which the autoantigen targets involved in the major adult form of the disease have remained elusive for many years. Exactly 10 years ago, PLA_2R1 was identified as the major autoantigen for approximately 70% of adult MN patients. Five years ago, this was followed by the identification of THSD7A as a second autoantigen of adult MN for another 3-5% of the patients. These discoveries provided a new impetus for a better understanding of the molecular basis underlying the development of MN. Likely and more importantly, they have produced a paradigm shift in clinical practice, providing new clinical assays to diagnose MN and monitor disease activity, leading to a significant improvement of patients' healthcare (Beck et al., 2014; Francis et al., 2016; Ronco et al., 2015; Salant, 2019). During this thesis, I worked towards a better understanding of the humoral autoimmune response observed in PLA_2R1-associated MN as well as the clinical value of the different combinations of anti-PLA_2R1 autoantibodies to improve patients' healthcare towards a more personalized medicine. Nevertheless, several key questions regarding the natural course of the disease and its main pathophysiological steps remain to be addressed (Salant, 2019; van de Logt et al., 2019). At the clinical level, the current knowledge and future research should help clinicians to better classify MN into different forms with improved diagnosis, monitoring and guided therapy, all of this leading to better healthcare with personalized therapy.

10.1 Pathophysiology and natural course of MN

How many autoantigens at the molecular basis of MN forms? After the identification of PLA_2R1 and THSD7A as two key autoantigens, approximately 27% of idiopathic MN cases remained double negative, i.e. "orphans" for a putative "third" autoantigen causing the autoimmune disease. At first, one can ask whether the prevalence for PLA_2R1- and THSD7A-associated MN is accurate, with 70-75% and 3-5%, respectively. Indeed, are all patients PLA_2R1- or THSD7A-negative at diagnosis truly negative? Or would it be possible that they turn out to be positive if the detection assays were more sensitive in line with the use of lower cut-off values in ELISA assays, or if autoantibody levels are measured later during the course of MN, with examples of patients turning positive during follow-up (Liu et al., 2018; Tampoia et al., 2018; van de Logt et al., 2015). Even considering this hypothesis, there is no doubt that a significant proportion of patients (about 20-25%) should have an MN disease due to other autoantigens (Beck, 2017). Besides exostosins, while writing this

conclusion, NELL-1 (neural epidermal growth factor-like1 protein) was identified as a new likely third autoantigen in another small group of 3% of MN patients (Sethi et al., 2019), suggesting that a fourth, fifth and so on autoantigens may be identified. Future studies should keep targeting these questions.

What are the actual genetic, immunological and biological factors triggering the autoimmune response? Are they the same among patients with the same or different autoantigens? The identification of several autoantigens in MN raises questions about the respective aetiology and the possible links between these latters. In myasthenia gravis and pemphigus vulgaris, several autoantigens have been identified, and interestingly, they belong to the same large protein complex (Gilhus et al., 2019; Schmidt et al., 2019). However, the disease onset, male to female ratio and severity of the disease vary between patients positive for one or the other autoantigens. In MN, the typical male to female ratio is 2:1 but it may be different for THSD7A-associated MN (Zaghrini et al., 2019). What is the cause of loss of self-tolerance: epitope mimicry or changes in the structure of the autoantigens, possibly associated with different genetics? In what context: cancer, inflammation or infections which may depend on the autoantigen? During the smouldering phase of MN, how does the autoimmune response progress? What is the dynamics of autoantibody production: is it via a mechanism of epitope spreading with a switch of immunodominance? Or is the "spreading route and immunodominance" due to different causes initiated at the origin of the autoimmune response with also genetic factors (predisposing SNPs are present in both CysR and CTLD1)? What about the IgG subclass switch that seems to occur during the different stages of the autoimmune response: is it associated with immunodominance? Is it possible that epitope spreading and immunodominance transitions still progress during the overt phase of MN, in phases of remission and relapse? How B, T and Treg cells dialog to orchestrate this autoimmune response? And why patients only develop conformational autoantibodies (predominantly IgG4) in both PLA_2R1 and THSD7A? Finally, what complement pathways are activated relative to the set of autoantibodies targeting podocytes and how does podocyte injury occur? More work in patients during the smouldering disease and in *bona fide* animal models carefully mimicking human MN are definitely needed to better understand the key steps of the autoimmune response.

10.2 Clinical impact in MN

Should we re-classify MN forms? After the identification of at least 5 human autoantigens or alloantigens specifically defining different forms of MN – NEP, PLA_2R1, THSD7A, exostosins and NELL-1 – the time may come to classify MN based on serology or staining of the specific antigens in kidney biopsy. This has somehow started for PLA_2R1 by Bobart and colleagues (Bobart et al., 2019) who propose to use a serology-based diagnosis instead of kidney biopsy. For patients having no antigen positivity as a cause of MN, antigens towards intracellular podocyte targets may be used as a surrogate or marker of MN severity (Bruschi et al., 2011; Murtas et al., 2012; Prunotto et al., 2010).

Should we consider personalized medicine based on the different characteristics of the anti-PLA_2R1 autoimmune response? Once the patient is diagnosed with PLA_2R1-associated MN (the same applies to THSD7A-associated MN), monitoring of anti-PLA_2R1 titer and epitope spreading will help to predict clinical outcome, decision to treat with immunosuppressors and orientation for the most adapted treatment with likelihood of a response (Beck et al., 2011; De Vriese et al., 2017; Floege et al., 2019; Kanigicherla et al., 2013; Rodas et al., 2019; Ruggenenti et al., 2015; Seitz-Polski et al., 2018; Seitz-Polski et al., 2014). However, cut-off values for what is considered as low versus high titers of anti-PLA_2R1 titers should be more clearly defined. In that regard, epitope spreading to CTLD1 and/or CTLD7 may better predict clinical outcome and decision to treat. Based on our work, patients with iCR immunodominance would best respond to low or high doses of rituximab while higher doses of rituximab or other more efficient combined therapies may be needed for iC1 patients or patients with titers above 200 RU/mL (Seitz-Polski et al., 2019; van de Logt et al., 2018). The use of second generation anti-CD20 antibodies may also need to be considered (Du et al., 2017).

Finally, more studies are clearly needed in many directions. For instance, my PhD project led to the identification of five main "macroepitope" domains with a first thorough analysis of prevalence, immunodominance and clinical associations in a large cohort of patients. The next studies may tackle the hot question of "microepitopes" as well as the progression of the autoimmune response backwards. What happens during the smouldering phase of PLA_2R1-associated MN, up to the molecular events that trigger the start of the autoimmune response to PLA2R1, i.e. when PLA_2R1 meets MN, caught by the immune system as the culprit autoantigen while on the course of one of its physiological and pathophysiological roles in inflammation, cancer or infection, these latters being in fact still mostly elusive.

Bibliographic References

A

Adler, S. G., Wang, H., Ward, H. J., Cohen, A. H., &Border, W. A. (1983). Electrical charge. Its role in the pathogenesis and prevention of experimental membranous nephropathy in the rabbit. *J Clin Invest, 71*(3), 487-499. doi:10.1172/jci110793

Ahmad, R., Hussain, A., &Ahsan, H. (2019). Peroxynitrite: cellular pathology and implications in autoimmunity. *J Immunoassay Immunochem, 40*(2), 123-138. doi:10.1080/15321819.2019.1583109

Ahmed, M. S., Hou, S. H., Battaglia, M. C., Picken, M. M., &Leehey, D. J. (2007). Treatment of idiopathic membranous nephropathy with the herb Astragalus membranaceus. *Am J Kidney Dis, 50*(6), 1028-1032. doi:10.1053/j.ajkd.2007.07.032

Akisawa, N., Maeda, T., Iwasaki, S., &Onishi, S. (1997). Identification of an autoantibody against alpha-enolase in primary biliary cirrhosis. *J Hepatol, 26*(4), 845-851.

Al-Rabadi, L., Ayalon, R., Bonegio, R. G., Ballard, J. E., Fujii, A. M., Henderson, J. M., Salant, D. J., &Beck, L. H., Jr. (2016). Pregnancy in a Patient With Primary Membranous Nephropathy and Circulating Anti-PLA2R Antibodies: A Case Report. *Am J Kidney Dis, 67*(5), 775-778. doi:10.1053/j.ajkd.2015.10.031

Alfaadhel, T., &Cattran, D. (2015). Management of Membranous Nephropathy in Western Countries. *Kidney Dis (Basel), 1*(2), 126-137. doi:10.1159/000437287

Allegri, L., Brianti, E., Chatelet, F., Manara, G. C., Ronco, P., &Verroust, P. (1986). Polyvalent antigen-antibody interactions are required for the formation of electron-dense immune deposits in passive Heymann's nephritis. *Am J Pathol, 125*(1), 1-6.

Amigorena, S., &Bonnerot, C. (1998). Role of B-cell and Fc receptors in the selection of T-cell epitopes. *Curr Opin Immunol, 10*(1), 88-92. doi:10.1016/s0952-7915(98)80037-x

Amin, R., Fiancette, R., Bordessoule, D., Turlure, P., Guerin, E., Trimoreau, F., &Denizot, Y. (2011). Phospholipase A2 receptors in human leukemic blasts. *Leuk Lymphoma, 52*(5), 908-909. doi:10.3109/10428194.2010.551160

Ancian, P., Lambeau, G., &Lazdunski, M. (1995). Multifunctional activity of the extracellular domain of the M-type (180 kDa) membrane receptor for secretory phospholipases A2. *Biochemistry, 34*(40), 13146-13151.

Ancian, P., Lambeau, G., Mattei, M. G., &Lazdunski, M. (1995). The human 180-kDa receptor for secretory phospholipases A2. Molecular cloning, identification of a secreted soluble form, expression, and chromosomal localization. *J Biol Chem, 270*(15), 8963-8970. doi:10.1074/jbc.270.15.8963

Anderson, D. A., Coulepis, A. G., Chenoweth, M. P., &Gust, I. D. (1986). Indirect immunofluorescence assay for the detection of hepatitis A virus-specific serum immunoglobulins. *J Clin Microbiol, 24*(1), 163-165.

Anderton, S. M. (2004). Post-translational modifications of self antigens: implications for autoimmunity. *Curr Opin Immunol, 16*(6), 753-758. doi:10.1016/j.coi.2004.09.001

Anonymous. (1979). A controlled study of short-term prednisone treatment in adults with membranous nephropathy. Collaborative Study of the Adult Idiopathic Nephrotic Syndrome. *N Engl J Med, 301*(24), 1301-1306. doi:10.1056/NEJM197912133012401

Anonymous. (2008). Gilbert Ashwell: sweet on science. *Nat Med, 14*(6), 608. doi:10.1038/nm0608-608

Aslani, S., Mahmoudi, M., Karami, J., Jamshidi, A. R., Malekshahi, Z., &Nicknam, M. H. (2016). Epigenetic alterations underlying autoimmune diseases. *Autoimmunity, 49*(2), 69-83. doi:10.3109/08916934.2015.1134511

Assmann, K. J., Tangelder, M. M., Lange, W. P., Tadema, T. M., &Koene, R. A. (1983). Membranous glomerulonephritis in the mouse. *Kidney Int, 24*(3), 303-312. doi:10.1038/ki.1983.159

Assmann, K. J., van Son, J. P., Dijkman, H. B., &Koene, R. A. (1992). A nephritogenic rat monoclonal antibody to mouse aminopeptidase A. Induction of massive albuminuria after a single intravenous injection. *J Exp Med, 175*(3), 623-635. doi:10.1084/jem.175.3.623

Augert, A., Payre, C., de Launoit, Y., Gil, J., Lambeau, G., &Bernard, D. (2009). The M-type receptor PLA2R regulates senescence through the p53 pathway. *EMBO Rep, 10*(3), 271-277. doi:10.1038/embor.2008.255

Augert, A., Vindrieux, D., Girard, C. A., Le Calve, B., Gras, B., Ferrand, M., Bouchet, B. P., Puisieux, A., de Launoit, Y., Simonnet, H., Lambeau, G., &Bernard, D. (2013). PLA2R1 kills cancer cells by inducing mitochondrial stress. *Free Radic Biol Med, 65*, 969-977. doi:10.1016/j.freeradbiomed.2013.08.177

B

Baker, P. J., Ochi, R. F., Schulze, M., Johnson, R. J., Campbell, C., &Couser, W. G. (1989). Depletion of C6 prevents development of proteinuria in experimental membranous nephropathy in rats. *Am J Pathol, 135*(1), 185-194.

Barbour, S., Reich, H., &Cattran, D. (2013). Short-term complications of membranous nephropathy. *Contrib Nephrol, 181*, 143-151. doi:10.1159/000349976

Barnes, P. J. (2017). Senescence in COPD and Its Comorbidities. *Annu Rev Physiol, 79*, 517-539. doi:10.1146/annurev-physiol-022516-034314

Bech, A. P., Hofstra, J. M., Brenchley, P. E., &Wetzels, J. F. (2014). Association of anti-PLA(2)R antibodies with outcomes after immunosuppressive therapy in idiopathic membranous nephropathy. *Clin J Am Soc Nephrol, 9*(8), 1386-1392. doi:10.2215/CJN.10471013

Beck, L. H., Jr. (2010). Membranous nephropathy and malignancy. *Semin Nephrol, 30*(6), 635-644. doi:10.1016/j.semnephrol.2010.09.011

Beck, L. H., Jr. (2017). PLA2R and THSD7A: Disparate Paths to the Same Disease? *J Am Soc Nephrol, 28*(9), 2579-2589. doi:10.1681/ASN.2017020178

Beck, L. H., Jr., Bonegio, R. G., Lambeau, G., Beck, D. M., Powell, D. W., Cummins, T. D., Klein, J. B., &Salant, D. J. (2009). M-type phospholipase A2 receptor as target antigen in idiopathic membranous nephropathy. *N Engl J Med, 361*(1), 11-21. doi:10.1056/NEJMoa0810457

Beck, L. H., Jr., Fervenza, F. C., Beck, D. M., Bonegio, R. G., Malik, F. A., Erickson, S. B., Cosio, F. G., Cattran, D. C., &Salant, D. J. (2011). Rituximab-induced depletion of anti-PLA2R autoantibodies predicts response in membranous nephropathy. *J Am Soc Nephrol, 22*(8), 1543-1550. doi:10.1681/ASN.2010111125

Beck, L. H., Jr., &Salant, D. J. (2010). Membranous nephropathy: recent travels and new roads ahead. *Kidney Int, 77*(9), 765-770. doi:10.1038/ki.2010.34

Beck, L. H., Jr., &Salant, D. J. (2014). Membranous nephropathy: from models to man. *J Clin Invest, 124*(6), 2307-2314. doi:10.1172/JCI72270

Beck, S., Beck, G., Ostendorf, T., Floege, J., Lambeau, G., Nevalainen, T., Radeke, H. H., Gurrieri, S., Haas, U., Thorwart, B., Pfeilschifter, J., &Kaszkin, M. (2006). Upregulation of group IB secreted phospholipase A(2) and its M-type receptor in rat ANTI-THY-1 glomerulonephritis. *Kidney Int, 70*(7), 1251-1260. doi:10.1038/sj.ki.5001664

Beck, S., Lambeau, G., Scholz-Pedretti, K., Gelb, M. H., Janssen, M. J., Edwards, S. H., Wilton, D. C., Pfeilschifter, J., &Kaszkin, M. (2003). Potentiation of tumor necrosis factor alpha-induced secreted phospholipase A2 (sPLA2)-IIA expression in mesangial cells by an autocrine loop involving sPLA2 and peroxisome proliferator-activated receptor alpha activation. *J Biol Chem, 278*(32), 29799-29812. doi:10.1074/jbc.M211763200

Behnert, A., Fritzler, M. J., Teng, B., Zhang, M., Bollig, F., Haller, H., Skoberne, A., Mahler, M., &Schiffer, M. (2013). An anti-phospholipase A2 receptor quantitative immunoassay and epitope analysis in membranous nephropathy reveals different antigenic domains of the receptor. *PLoS One, 8*(4), e61669. doi:10.1371/journal.pone.0061669

Bobart, S. A., De Vriese, A. S., Pawar, A. S., Zand, L., Sethi, S., Giesen, C., Lieske, J. C., &Fervenza, F. C. (2019). Noninvasive diagnosis of primary membranous nephropathy using phospholipase A2 receptor antibodies. *Kidney Int, 95*(2), 429-438. doi:10.1016/j.kint.2018.10.021

Bomback, A. S., &Fervenza, F. C. (2018). Membranous Nephropathy: Approaches to Treatment. *Am J Nephrol, 47 Suppl 1*, 30-42. doi:10.1159/000481635

Bonanni, A., Vaglio, A., Bruschi, M., Sinico, R. A., Cavagna, L., Moroni, G., Franceschini, F., Allegri, L., Pratesi, F., Migliorini, P., Candiano, G., Pesce, G., Ravelli, A., Puppo, F., Martini, A., Tincani, A., &Ghiggeri, G. M. (2015). Multi-antibody composition in lupus nephritis: isotype and antigen specificity make the difference. *Autoimmun Rev, 14*(8), 692-702. doi:10.1016/j.autrev.2015.04.004

Border, W. A., Ward, H. J., Kamil, E. S., &Cohen, A. H. (1982). Induction of membranous nephropathy in rabbits by administration of an exogenous cationic antigen. *J Clin Invest, 69*(2), 451-461. doi:10.1172/jci110469

Borza, D. B. (2016). Alternative Pathway Dysregulation and the Conundrum of Complement Activation by IgG4 Immune Complexes in Membranous Nephropathy. *Front Immunol, 7*, 157. doi:10.3389/fimmu.2016.00157

Borza, D. B., Zhang, J. J., Beck, L. H., Jr., Meyer-Schwesinger, C., &Luo, W. (2013). Mouse models of membranous nephropathy: the road less travelled by. *Am J Clin Exp Immunol, 2*(2), 135-145.

Boskovic, J., Arnold, J. N., Stilion, R., Gordon, S., Sim, R. B., Rivera-Calzada, A., Wienke, D., Isacke, C. M., Martinez-Pomares, L., &Llorca, O. (2006). Structural model for the mannose receptor family uncovered by electron microscopy of Endo180 and the mannose receptor. *J Biol Chem, 281*(13), 8780-8787. doi:10.1074/jbc.M513277200

Bradford, C. M., Ramos, I., Cross, A. K., Haddock, G., McQuaid, S., Nicholas, A. P., &Woodroofe, M. N. (2014). Localisation of citrullinated proteins in normal appearing white matter and lesions in the central nervous system in multiple sclerosis. *J Neuroimmunol, 273*(1-2), 85-95. doi:10.1016/j.jneuroim.2014.05.007

Brenchley, P. E., Coupes, B., Short, C. D., O'Donoghue, D. J., Ballardie, F. W., &Mallick, N. P. (1992). Urinary C3dg and C5b-9 indicate active immune disease in human membranous nephropathy. *Kidney Int, 41*(4), 933-937. doi:10.1038/ki.1992.143

Brooks-Worrell, B., Gersuk, V. H., Greenbaum, C., &Palmer, J. P. (2001). Intermolecular antigen spreading occurs during the preclinical period of human type 1 diabetes. *J Immunol, 166*(8), 5265-5270. doi:10.4049/jimmunol.166.8.5265

Bruner, B. F., Vista, E. S., Wynn, D. M., Harley, J. B., &James, J. A. (2010). Anti-neutrophil cytoplasmic antibodies target sequential functional proteinase 3 epitopes in the sera of patients with Wegener's granulomatosis. *Clin Exp Immunol, 162*(2), 262-270. doi:10.1111/j.1365-2249.2010.04251.x

Bruner, B. F., Vista, E. S., Wynn, D. M., &James, J. A. (2011). Epitope specificity of myeloperoxidase antibodies: identification of candidate human immunodominant epitopes. *Clin Exp Immunol, 164*(3), 330-336. doi:10.1111/j.1365-2249.2011.04372.x

Bruschi, M., Carnevali, M. L., Murtas, C., Candiano, G., Petretto, A., Prunotto, M., Gatti, R., Argentiero, L., Magistroni, R., Garibotto, G., Scolari, F., Ravani, P., Gesualdo, L., Allegri, L., &Ghiggeri, G. M. (2011). Direct characterization of target podocyte antigens and auto-antibodies in human membranous glomerulonephritis: Alfa-enolase and borderline antigens. *J Proteomics, 74*(10), 2008-2017. doi:10.1016/j.jprot.2011.05.021

Bullich, G., Ballarin, J., Oliver, A., Ayasreh, N., Silva, I., Santin, S., Diaz-Encarnacion, M. M., Torra, R., &Ars, E. (2014). HLA-DQA1 and PLA2R1 polymorphisms and risk of idiopathic membranous nephropathy. *Clin J Am Soc Nephrol, 9*(2), 335-343. doi:10.2215/CJN.05310513

Burnette, W. N. (1981). "Western blotting": electrophoretic transfer of proteins from sodium dodecyl sulfate--polyacrylamide gels to unmodified nitrocellulose and radiographic detection with antibody and radioiodinated protein A. *Anal Biochem, 112*(2), 195-203. doi:10.1016/0003-2697(81)90281-5

C

Cao, L., Shi, X., Chang, H., Zhang, Q., &He, Y. (2015). pH-Dependent recognition of apoptotic and necrotic cells by the human dendritic cell receptor DEC205. *Proc Natl Acad Sci U S A, 112*(23), 7237-7242. doi:10.1073/pnas.1505924112

Cattran, D. C., Appel, G. B., Hebert, L. A., Hunsicker, L. G., Pohl, M. A., Hoy, W. E., Maxwell, D. R., Kunis, C. L., &North America Nephrotic Syndrome Study, G. (2001). Cyclosporine in patients with steroid-resistant membranous nephropathy: a randomized trial. *Kidney Int, 59*(4), 1484-1490. doi:10.1046/j.1523-1755.2001.0590041484.x

Cattran, D. C., Pei, Y., Greenwood, C. M., Ponticelli, C., Passerini, P., &Honkanen, E. (1997). Validation of a predictive model of idiopathic membranous nephropathy: its clinical and research implications. *Kidney Int, 51*(3), 901-907.

Cestele, S., Schiavon, E., Rusconi, R., Franceschetti, S., &Mantegazza, M. (2013). Nonfunctional NaV1.1 familial hemiplegic migraine mutant transformed into gain of function by partial rescue of folding defects. *Proc Natl Acad Sci U S A, 110*(43), 17546-17551. doi:10.1073/pnas.1309827110

Chen, S., Liu, Z., Chen, J., &Wu, J. (2011). Study on improvement of extracellular production of recombinant Thermobifida fusca cutinase by Escherichia coli. *Appl Biochem Biotechnol, 165*(2), 666-675. doi:10.1007/s12010-011-9286-z

Chen, Y., Deng, Y., Ni, Z., Chen, N., Chen, X., Shi, W., Zhan, Y., Yuan, F., Deng, W., &Zhong, Y. (2013). Efficacy and safety of traditional chinese medicine (Shenqi particle) for patients with idiopathic membranous nephropathy: a multicenter randomized controlled clinical trial. *Am J Kidney Dis, 62*(6), 1068-1076. doi:10.1053/j.ajkd.2013.05.005

Chen, Y. M., Zhou, Y., Go, G., Marmerstein, J. T., Kikkawa, Y., &Miner, J. H. (2013). Laminin beta2 gene missense mutation produces endoplasmic reticulum stress in podocytes. *J Am Soc Nephrol, 24*(8), 1223-1233. doi:10.1681/ASN.2012121149

Coenen, M. J., Hofstra, J. M., Debiec, H., Stanescu, H. C., Medlar, A. J., Stengel, B., Boland-Auge, A., Groothuismink, J. M., Bockenhauer, D., Powis, S. H., Mathieson, P. W., Brenchley, P. E., Kleta, R., Wetzels, J. F., &Ronco, P. (2013). Phospholipase A2 receptor (PLA2R1) sequence variants in idiopathic membranous nephropathy. *J Am Soc Nephrol, 24*(4), 677-683. doi:10.1681/ASN.2012070730

Cornaby, C., Gibbons, L., Mayhew, V., Sloan, C. S., Welling, A., &Poole, B. D. (2015). B cell epitope spreading: mechanisms and contribution to autoimmune diseases. *Immunol Lett, 163*(1), 56-68. doi:10.1016/j.imlet.2014.11.001

Corthay, A., Backlund, J., Broddefalk, J., Michaelsson, E., Goldschmidt, T. J., Kihlberg, J., &Holmdahl, R. (1998). Epitope glycosylation plays a critical role for T cell recognition of type II collagen in collagen-induced arthritis. *Eur J Immunol, 28*(8), 2580-2590. doi:10.1002/(SICI)1521-4141(199808)28:08<2580::AID-IMMU2580>3.0.CO;2-X

Cosio, F. G., &Cattran, D. C. (2017). Recent advances in our understanding of recurrent primary glomerulonephritis after kidney transplantation. *Kidney Int, 91*(2), 304-314. doi:10.1016/j.kint.2016.08.030

Couser, W. G. (2017). Primary Membranous Nephropathy. *Clin J Am Soc Nephrol, 12*(6), 983-997. doi:10.2215/CJN.11761116

Couser, W. G., Steinmuller, D. R., Stilmant, M. M., Salant, D. J., &Lowenstein, L. M. (1978). Experimental glomerulonephritis in the isolated perfused rat kidney. *J Clin Invest, 62*(6), 1275-1287. doi:10.1172/JCI109248

Csorba, T. R., Lyon, A. W., &Hollenberg, M. D. (2010). Autoimmunity and the pathogenesis of type 1 diabetes. *Crit Rev Clin Lab Sci, 47*(2), 51-71. doi:10.3109/10408361003787171

Cui, Z., Xie, L. J., Chen, F. J., Pei, Z. Y., Zhang, L. J., Qu, Z., Huang, J., Gu, Q. H., Zhang, Y. M., Wang, X., Wang, F., Meng, L. Q., Liu, G., Zhou, X. J., Zhu, L., Lv, J. C., Liu, F., Zhang, H., Liao, Y. H., Lai, L. H., Ronco, P., &Zhao, M. H. (2017). MHC Class II Risk Alleles and Amino Acid Residues in Idiopathic Membranous Nephropathy. *J Am Soc Nephrol, 28*(5), 1651-1664. doi:10.1681/ASN.2016020114

Cupillard, L., Mulherkar, R., Gomez, N., Kadam, S., Valentin, E., Lazdunski, M., &Lambeau, G. (1999). Both group IB and group IIA secreted phospholipases A2 are natural ligands of the mouse 180-kDa M-type receptor. *J Biol Chem, 274*(11), 7043-7051. doi:10.1074/jbc.274.11.7043

Cusick, M. F., Libbey, J. E., &Fujinami, R. S. (2012). Molecular mimicry as a mechanism of autoimmune disease. *Clin Rev Allergy Immunol, 42*(1), 102-111. doi:10.1007/s12016-011-8293-810.1007/s12016-011-8294-7

Cybulsky, A. V., Rennke, H. G., Feintzeig, I. D., &Salant, D. J. (1986). Complement-induced glomerular epithelial cell injury. Role of the membrane attack complex in rat membranous nephropathy. *J Clin Invest, 77*(4), 1096-1107. doi:10.1172/JCI112408

D

Dabade, T. S., Grande, J. P., Norby, S. M., Fervenza, F. C., &Cosio, F. G. (2008). Recurrent idiopathic membranous nephropathy after kidney transplantation: a surveillance biopsy study. *Am J Transplant, 8*(6), 1318-1322. doi:10.1111/j.1600-6143.2008.02237.x

Dahan, K., Debiec, H., Plaisier, E., Cachanado, M., Rousseau, A., Wakselman, L., Michel, P. A., Mihout, F., Dussol, B., Matignon, M., Mousson, C., Simon, T., Ronco, P., &Group, G. S. (2017). Rituximab for Severe Membranous Nephropathy: A 6-Month Trial with Extended Follow-Up. *J Am Soc Nephrol, 28*(1), 348-358. doi:10.1681/ASN.2016040449

Dahan, K., Gillion, V., Johanet, C., Debiec, H., &Ronco, P. (2018). The Role of PLA2R Antibody in Treatment of Membranous Nephropathy. *Kidney Int Rep, 3*(2), 498-501. doi:10.1016/j.ekir.2017.10.013

Dahnrich, C., Komorowski, L., Probst, C., Seitz-Polski, B., Esnault, V., Wetzels, J. F., Hofstra, J. M., Hoxha, E., Stahl, R. A., Lambeau, G., Stocker, W., &Schlumberger, W. (2013). Development of a standardized ELISA for the determination of autoantibodies against human M-type phospholipase A2 receptor in primary membranous nephropathy. *Clin Chim Acta, 421*, 213-218. doi:10.1016/j.cca.2013.03.015

Dardik, R., &Lahav, J. (1989). Multiple domains are involved in the interaction of endothelial cell thrombospondin with fibronectin. *Eur J Biochem, 185*(3), 581-588. doi:10.1111/j.1432-1033.1989.tb15153.x

Darrah, E., &Andrade, F. (2018). Rheumatoid arthritis and citrullination. *Curr Opin Rheumatol, 30*(1), 72-78. doi:10.1097/BOR.0000000000000452

De Vriese, A. S., Glassock, R. J., Nath, K. A., Sethi, S., &Fervenza, F. C. (2017). A Proposal for a Serology-Based Approach to Membranous Nephropathy. *J Am Soc Nephrol, 28*(2), 421-430. doi:10.1681/ASN.2016070776

Debiec, H., Guigonis, V., Mougenot, B., Decobert, F., Haymann, J. P., Bensman, A., Deschenes, G., &Ronco, P. M. (2002). Antenatal membranous glomerulonephritis due to anti-neutral endopeptidase antibodies. *N Engl J Med, 346*(26), 2053-2060. doi:10.1056/NEJMoa012895

Debiec, H., Hanoy, M., Francois, A., Guerrot, D., Ferlicot, S., Johanet, C., Aucouturier, P., Godin, M., &Ronco, P. (2012). Recurrent membranous nephropathy in an allograft caused by IgG3kappa targeting the PLA2 receptor. *J Am Soc Nephrol, 23*(12), 1949-1954. doi:10.1681/ASN.2012060577

Debiec, H., Lefeu, F., Kemper, M. J., Niaudet, P., Deschenes, G., Remuzzi, G., Ulinski, T., &Ronco, P. (2011). Early-childhood membranous nephropathy due to cationic bovine serum albumin. *N Engl J Med, 364*(22), 2101-2110. doi:10.1056/NEJMoa1013792

Debiec, H., Nauta, J., Coulet, F., van der Burg, M., Guigonis, V., Schurmans, T., de Heer, E., Soubrier, F., Janssen, F., &Ronco, P. (2004). Role of truncating mutations in MME gene in fetomaternal alloimmunisation and antenatal glomerulopathies. *Lancet, 364*(9441), 1252-1259. doi:10.1016/S0140-6736(04)17142-0

Debiec, H., &Ronco, P. (2011). PLA2R autoantibodies and PLA2R glomerular deposits in membranous nephropathy. *N Engl J Med, 364*(7), 689-690. doi:10.1056/NEJMc1011678

Debiec, H., &Ronco, P. (2014). Immunopathogenesis of membranous nephropathy: an update. *Semin Immunopathol, 36*(4), 381-397. doi:10.1007/s00281-014-0423-y

Debiec, H., Valayannopoulos, V., Boyer, O., Noel, L. H., Callard, P., Sarda, H., de Lonlay, P., Niaudet, P., &Ronco, P. (2014). Allo-immune membranous nephropathy and recombinant aryl sulfatase replacement therapy: a need for tolerance induction therapy. *J Am Soc Nephrol, 25*(4), 675-680. doi:10.1681/ASN.2013030290

Dennis, E. A., Cao, J., Hsu, Y. H., Magrioti, V., &Kokotos, G. (2011). Phospholipase A2 enzymes: physical structure, biological function, disease implication, chemical inhibition, and therapeutic intervention. *Chem Rev, 111*(10), 6130-6185. doi:10.1021/cr200085w

Derksen, V., Huizinga, T. W. J., &van der Woude, D. (2017). The role of autoantibodies in the pathophysiology of rheumatoid arthritis. *Semin Immunopathol, 39*(4), 437-446. doi:10.1007/s00281-017-0627-z

DeVoss, J. J., &Anderson, M. S. (2007). Lessons on immune tolerance from the monogenic disease APS1. *Curr Opin Genet Dev, 17*(3), 193-200. doi:10.1016/j.gde.2007.04.001

Doi, T., Mayumi, M., Kanatsu, K., Suehiro, F., &Hamashima, Y. (1984). Distribution of IgG subclasses in membranous nephropathy. *Clin Exp Immunol, 58*(1), 57-62.

Dolla, G. (2017). *PLA2R1 et THSD7A, deux auto-antigènes de la glomérulonéphrite extra-membraneuse (GEM) : caractérisation des formes solubles, des épitopes, et rôles biomarqueurs.* (Thèse de doctorat en Sciences de la vie et de la santé), Université Nice-Sophia Antipolis,

Donadio, J. V., Jr., Torres, V. E., Velosa, J. A., Wagoner, R. D., Holley, K. E., Okamura, M., Ilstrup, D. M., &Chu, C. P. (1988). Idiopathic membranous nephropathy: the natural history of untreated patients. *Kidney Int, 33*(3), 708-715.

Dong, Y., Cao, L., Tang, H., Shi, X., &He, Y. (2017). Structure of Human M-type Phospholipase A2 Receptor Revealed by Cryo-Electron Microscopy. *J Mol Biol, 429*(24), 3825-3835. doi:10.1016/j.jmb.2017.10.019

Doyle, H. A., &Mamula, M. J. (2001). Post-translational protein modifications in antigen recognition and autoimmunity. *Trends Immunol, 22*(8), 443-449.

Drickamer, K. (1999). C-type lectin-like domains. *Curr Opin Struct Biol, 9*(5), 585-590.

Drickamer, K., &Fadden, A. J. (2002). Genomic analysis of C-type lectins. *Biochem Soc Symp*(69), 59-72.

Du, F. H., Mills, E. A., &Mao-Draayer, Y. (2017). Next-generation anti-CD20 monoclonal antibodies in autoimmune disease treatment. *Auto Immun Highlights, 8*(1), 12. doi:10.1007/s13317-017-0100-y

Du, Y., Li, J., He, F., Lv, Y., Liu, W., Wu, P., Huang, J., Wei, S., &Gao, H. (2014). The diagnosis accuracy of PLA2R-AB in the diagnosis of idiopathic membranous nephropathy: a meta-analysis. *PLoS One, 9*(8), e104936. doi:10.1371/journal.pone.0104936

E

East, L., &Isacke, C. M. (2002). The mannose receptor family. *Biochim Biophys Acta, 1572*(2-3), 364-386.

Edwards, J. C., &Cambridge, G. (2001). Sustained improvement in rheumatoid arthritis following a protocol designed to deplete B lymphocytes. *Rheumatology (Oxford), 40*(2), 205-211. doi:10.1093/rheumatology/40.2.205

Engelholm, L. H., Ingvarsen, S., Jurgensen, H. J., Hillig, T., Madsen, D. H., Nielsen, B. S., &Behrendt, N. (2009). The collagen receptor uPARAP/Endo180. *Front Biosci (Landmark Ed), 14*, 2103-2114.

Engvall, E., &Perlmann, P. (1971). Enzyme-linked immunosorbent assay (ELISA). Quantitative assay of immunoglobulin G. *Immunochemistry, 8*(9), 871-874. doi:10.1016/0019-2791(71)90454-x

Espinosa-Hernandez, M., Ortega-Salas, R., Lopez-Andreu, M., Gomez-Carrasco, J. M., Perez-Saez, M. J., Perez-Seoane, C., &Aljama-Garcia, P. (2012). C4d as a diagnostic tool in membranous nephropathy. *Nefrologia, 32*(3), 295-299. doi:10.3265/Nefrologia.pre2012.Feb.11224

F

Farinha, C. M., King-Underwood, J., Sousa, M., Correia, A. R., Henriques, B. J., Roxo-Rosa, M., Da Paula, A. C., Williams, J., Hirst, S., Gomes, C. M., &Amaral, M. D. (2013). Revertants, low temperature, and correctors reveal the mechanism of F508del-CFTR rescue by VX-809 and suggest multiple agents for full correction. *Chem Biol, 20*(7), 943-955. doi:10.1016/j.chembiol.2013.06.004

Farquhar, M. G., Vernier, R. L., &Good, R. A. (1957). An electron microscope study of the glomerulus in nephrosis, glomerulonephritis, and lupus erythematosus. *J Exp Med, 106*(5), 649-660. doi:10.1084/jem.106.5.649

Feenstra, K., van den Lee, R., Greben, H. A., Arends, A., &Hoedemaeker, P. J. (1975). Experimental glomerulonephritis in the rat induced by antibodies directed against tubular antigens. I. The natural history: a histologic and immunohistologic study at the light microscopic and the ultrastructural level. *Lab Invest, 32*(2), 235-242.

Fervenza, F. C., Abraham, R. S., Erickson, S. B., Irazabal, M. V., Eirin, A., Specks, U., Nachman, P. H., Bergstralh, E. J., Leung, N., Cosio, F. G., Hogan, M. C., Dillon, J. J., Hickson, L. J., Li, X., Cattran, D. C., &Mayo Nephrology Collaborative, G. (2010). Rituximab therapy in idiopathic membranous nephropathy: a 2-year study. *Clin J Am Soc Nephrol, 5*(12), 2188-2198. doi:10.2215/CJN.05080610

Fervenza, F. C., Appel, G. B., Barbour, S. J., Rovin, B. H., Lafayette, R. A., Aslam, N., Jefferson, J. A., Gipson, P. E., Rizk, D. V., Sedor, J. R., Simon, J. F., McCarthy, E. T., Brenchley, P., Sethi, S., Avila-Casado, C., Beanlands, H., Lieske, J. C., Philibert, D., Li, T., Thomas, L. F., Green, D. F., Juncos, L. A., Beara-Lasic, L., Blumenthal, S. S., Sussman, A. N., Erickson, S. B., Hladunewich, M., Canetta, P. A., Hebert, L. A., Leung, N., Radhakrishnan, J., Reich, H. N., Parikh, S. V., Gipson, D. S., Lee, D. K., da Costa, B. R., Juni, P., Cattran, D. C., &Investigators, M. (2019). Rituximab or Cyclosporine in the Treatment of Membranous Nephropathy. *N Engl J Med, 381*(1), 36-46. doi:10.1056/NEJMoa1814427

Fiancette, R., Vincent, C., Donnard, M., Bordessoule, D., Turlure, P., Trimoreau, F., &Denizot, Y. (2009). Genes encoding multiple forms of phospholipase A(2) are expressed in immature forms of human leukemic blasts. *Leukemia, 23*(6), 1196-1199. doi:10.1038/leu.2009.36

Floege, J., &Amann, K. (2016). Primary glomerulonephritides. *Lancet, 387*(10032), 2036-2048. doi:10.1016/S0140-6736(16)00272-5

Floege, J., Barbour, S. J., Cattran, D. C., Hogan, J. J., Nachman, P. H., Tang, S. C. W., Wetzels, J. F. M., Cheung, M., Wheeler, D. C., Winkelmayer, W. C., Rovin, B. H., &Conference, P. (2019). Management and treatment of glomerular diseases (part 1): conclusions from a Kidney Disease: Improving Global Outcomes (KDIGO) Controversies Conference. *Kidney Int, 95*(2), 268-280. doi:10.1016/j.kint.2018.10.018

Floreani, A., Leung, P. S., &Gershwin, M. E. (2016). Environmental Basis of Autoimmunity. *Clin Rev Allergy Immunol, 50*(3), 287-300. doi:10.1007/s12016-015-8493-8

Francis, J. M., Beck, L. H., Jr., &Salant, D. J. (2016). Membranous Nephropathy: A Journey From Bench to Bedside. *Am J Kidney Dis, 68*(1), 138-147. doi:10.1053/j.ajkd.2016.01.030

Fresquet, M., Jowitt, T. A., Gummadova, J., Collins, R., O'Cualain, R., McKenzie, E. A., Lennon, R., &Brenchley, P. E. (2015). Identification of a major epitope recognized by PLA2R autoantibodies in primary membranous nephropathy. *J Am Soc Nephrol, 26*(2), 302-313. doi:10.1681/ASN.2014050502

Fresquet, M., Jowitt, T. A., McKenzie, E. A., Ball, M. D., Randles, M. J., Lennon, R., &Brenchley, P. E. (2017). PLA2R binds to the annexin A2-S100A10 complex in human podocytes. *Sci Rep, 7*(1), 6876. doi:10.1038/s41598-017-07028-8

Fresquet, M., Lennon, R., &Brenchley, P. E. (2015). The Effect of Anti-PLA2R Autoantibodies on Human Podocytes *In Vitro* [ASN Kidney Week 2015, Poster Abstract: FR-PO354]. *J Am Soc Nephrol, 26*, 435A.

Fresquet, M., Rhoden, S. J., Jowitt, T. A., McKenzie, E. A., Roberts, I., Lennon, R., &Brenchley, P. E. (2019). Autoantigens PLA2R and THSD7A in membranous nephropathy share a common epitope motif in the N-terminal domain. *J Autoimmun*, 102308. doi:10.1016/j.jaut.2019.102308

Frump, A. L., Lowery, J. W., Hamid, R., Austin, E. D., &de Caestecker, M. (2013). Abnormal trafficking of endogenously expressed BMPR2 mutant allelic products in patients with heritable pulmonary arterial hypertension. *PLoS One, 8*(11), e80319. doi:10.1371/journal.pone.0080319

G

Galvin, N. J., Vance, P. M., Dixit, V. M., Fink, B., &Frazier, W. A. (1987). Interaction of human thrombospondin with types I-V collagen: direct binding and electron microscopy. *J Cell Biol, 104*(5), 1413-1422. doi:10.1083/jcb.104.5.1413

Georges, E., Johanet, C., Plaisier, E., Debiec, H., Ronco, P., &Dahan, K. (2019). Efficacy of Rituximab in a Patient With Partial Clinical Remission and Persistent Circulating PLA2R-Ab. *Kidney Int Rep, 4*(7), 1027-1030. doi:10.1016/j.ekir.2019.03.002

Gilhus, N. E., Tzartos, S., Evoli, A., Palace, J., Burns, T. M., &Verschuuren, J. (2019). Myasthenia gravis. *Nat Rev Dis Primers, 5*(1), 30. doi:10.1038/s41572-019-0079-y

Glassock, R. J. (2003). Diagnosis and natural course of membranous nephropathy. *Semin Nephrol, 23*(4), 324-332.

Glassock, R. J. (2009). Human idiopathic membranous nephropathy--a mystery solved? *N Engl J Med, 361*(1), 81-83. doi:10.1056/NEJMe0903343

Godel, M., Grahammer, F., &Huber, T. B. (2015). Thrombospondin type-1 domain-containing 7A in idiopathic membranous nephropathy. *N Engl J Med, 372*(11), 1073. doi:10.1056/NEJMc1500130

Gomez, A. M., Van Den Broeck, J., Vrolix, K., Janssen, S. P., Lemmens, M. A., Van Der Esch, E., Duimel, H., Frederik, P., Molenaar, P. C., Martinez-Martinez, P., De Baets, M. H., &Losen, M. (2010). Antibody effector mechanisms in myasthenia gravis-pathogenesis at the neuromuscular junction. *Autoimmunity, 43*(5-6), 353-370. doi:10.3109/08916930903555943

Goumenos, D. S. (2008). What have we learned from the use of ciclosporin A in the treatment of nephrotic patients with idiopathic membranous nephropathy? *Expert Opin Pharmacother, 9*(10), 1695-1704. doi:10.1517/14656566.9.10.1695

Granata, F., Petraroli, A., Boilard, E., Bezzine, S., Bollinger, J., Del Vecchio, L., Gelb, M. H., Lambeau, G., Marone, G., &Triggiani, M. (2005). Activation of cytokine production by secreted

phospholipase A2 in human lung macrophages expressing the M-type receptor. *J Immunol, 174*(1), 464-474. doi:10.4049/jimmunol.174.1.464

Griveau, A., Devailly, G., Eberst, L., Navaratnam, N., Le Calve, B., Ferrand, M., Faull, P., Augert, A., Dante, R., Vanacker, J. M., Vindrieux, D., &Bernard, D. (2016). The PLA2R1-JAK2 pathway upregulates ERRalpha and its mitochondrial program to exert tumor-suppressive action. *Oncogene, 35*(38), 5033-5042. doi:10.1038/onc.2016.43

Guo, N. H., Krutzsch, H. C., Negre, E., Vogel, T., Blake, D. A., &Roberts, D. D. (1992). Heparin- and sulfatide-binding peptides from the type I repeats of human thrombospondin promote melanoma cell adhesion. *Proc Natl Acad Sci U S A, 89*(7), 3040-3044. doi:10.1073/pnas.89.7.3040

Gupta, A., &Quigg, R. J. (2015). Glomerular Diseases Associated With Hepatitis B and C. *Adv Chronic Kidney Dis, 22*(5), 343-351. doi:10.1053/j.ackd.2015.06.003

Gutierrez, J. M., &Lomonte, B. (2013). Phospholipases A2: unveiling the secrets of a functionally versatile group of snake venom toxins. *Toxicon, 62*, 27-39. doi:10.1016/j.toxicon.2012.09.006

H

Haddad, G., &Kistler, A. (2017). An *In Vitro* Model of Idiopathic Membranous Nephropathy Reveals PLA2R- and Complement-Dependent Pathways of Podocyte Injury [ASN Kidney Week 2017, Poster Abstract: TH-PO020]. *J Am Heart Assoc, 28*, 109.

Hallstrand, T. S., Chi, E. Y., Singer, A. G., Gelb, M. H., &Henderson, W. R., Jr. (2007). Secreted phospholipase A2 group X overexpression in asthma and bronchial hyperresponsiveness. *Am J Respir Crit Care Med, 176*(11), 1072-1078. doi:10.1164/rccm.200707-1088OC

Hallstrand, T. S., Lai, Y., Henderson, W. R., Jr., Altemeier, W. A., &Gelb, M. H. (2012). Epithelial regulation of eicosanoid production in asthma. *Pulm Pharmacol Ther, 25*(6), 432-437.

Hallstrand, T. S., Lai, Y., Ni, Z., Oslund, R. C., Henderson, W. R., Jr., Gelb, M. H., &Wenzel, S. E. (2011). Relationship between levels of secreted phospholipase A(2) groups IIA and X in the airways and asthma severity. *Clin Exp Allergy, 41*(6), 801-810. doi:10.1111/j.1365-2222.2010.03676.x

Hanasaki, K., &Arita, H. (2002). Phospholipase A2 receptor: a regulator of biological functions of secretory phospholipase A2. *Prostaglandins Other Lipid Mediat, 68-69*, 71-82.

Hanasaki, K., Yokota, Y., Ishizaki, J., Itoh, T., &Arita, H. (1997). Resistance to endotoxic shock in phospholipase A2 receptor-deficient mice. *J Biol Chem, 272*(52), 32792-32797. doi:10.1074/jbc.272.52.32792

Hang, L. M., &Nakamura, R. M. (1997). Current concepts and advances in clinical laboratory testing for autoimmune diseases. *Crit Rev Clin Lab Sci, 34*(3), 275-311. doi:10.3109/10408369708998095

Hayashi, N., Okada, K., Matsui, Y., Fujimoto, K., Adachi, H., Yamaya, H., Matsushita, M., &Yokoyama, H. (2018). Glomerular mannose-binding lectin deposition in intrinsic antigen-related membranous nephropathy. *Nephrol Dial Transplant, 33*(5), 832-840. doi:10.1093/ndt/gfx235

Hayter, S. M., &Cook, M. C. (2012). Updated assessment of the prevalence, spectrum and case definition of autoimmune disease. *Autoimmun Rev, 11*(10), 754-765. doi:10.1016/j.autrev.2012.02.001

He, Y., &Bjorkman, P. J. (2011). Structure of FcRY, an avian immunoglobulin receptor related to mammalian mannose receptors, and its complex with IgY. *Proc Natl Acad Sci U S A, 108*(30), 12431-12436. doi:10.1073/pnas.1106925108

Henderson, W. R., Jr., Chi, E. Y., Bollinger, J. G., Tien, Y. T., Ye, X., Castelli, L., Rubtsov, Y. P., Singer, A. G., Chiang, G. K., Nevalainen, T., Rudensky, A. Y., &Gelb, M. H. (2007). Importance of group X-secreted phospholipase A2 in allergen-induced airway inflammation and remodeling in a mouse asthma model. *J Exp Med, 204*(4), 865-877. doi:10.1084/jem.20070029

Herwig, J., Skuza, S., Sachs, W., Sachs, M., Failla, A. V., Rune, G., Meyer, T. N., Fester, L., &Meyer-Schwesinger, C. (2019). Thrombospondin Type 1 Domain-Containing 7A Localizes to the Slit Diaphragm and Stabilizes Membrane Dynamics of Fully Differentiated Podocytes. *J Am Soc Nephrol, 30*(5), 824-839. doi:10.1681/ASN.2018090941

Heymann, W., Hackel, D. B., Harwood, S., Wilson, S. G., &Hunter, J. L. (1959). Production of nephrotic syndrome in rats by Freund's adjuvants and rat kidney suspensions. *Proc Soc Exp Biol Med, 100*(4), 660-664. doi:10.3181/00379727-100-24736

Hiesberger, T., Hodits, R., Ullrich, R., Exner, M., Kerjaschki, D., Schneider, W. J., &Nimpf, J. (1996). Receptor-associated protein and members of the low density lipoprotein receptor family share a common epitope. An extended model for the development of passive Heymann nephritis. *J Biol Chem, 271*(46), 28792-28797. doi:10.1074/jbc.271.46.28792

Higashino, K., Ishizaki, J., Kishino, J., Ohara, O., &Arita, H. (1994). Structural comparison of phospholipase-A2-binding regions in phospholipase-A2 receptors from various mammals. *Eur J Biochem, 225*(1), 375-382.

Higashino Ki, K., Yokota, Y., Ono, T., Kamitani, S., Arita, H., &Hanasaki, K. (2002). Identification of a soluble form phospholipase A2 receptor as a circulating endogenous inhibitor for secretory phospholipase A2. *J Biol Chem, 277*(16), 13583-13588. doi:10.1074/jbc.M108752200

Hiki, Y., Kobayashi, Y., Itoh, I., &Kashiwagi, N. (1984). Strong association of HLA-DR2 and MT1 with idiopathic membranous nephropathy in Japan. *Kidney Int, 25*(6), 953-957.

Hirayama, K., Ebihara, I., Yamamoto, S., Kai, H., Muro, K., Yamagata, K., Kobayashi, M., &Koyama, A. (2002). Predominance of type-2 immune response in idiopathic membranous nephropathy. Cytoplasmic cytokine analysis. *Nephron, 91*(2), 255-261. doi:10.1159/000058401

Hladunewich, M. A., Troyanov, S., Calafati, J., Cattran, D. C., &Metropolitan Toronto Glomerulonephritis, R. (2009). The natural history of the non-nephrotic membranous nephropathy patient. *Clin J Am Soc Nephrol, 4*(9), 1417-1422. doi:10.2215/CJN.01330209

Hofstra, J. M., Beck, L. H., Jr., Beck, D. M., Wetzels, J. F., &Salant, D. J. (2011). Anti-phospholipase A(2) receptor antibodies correlate with clinical status in idiopathic membranous nephropathy. *Clin J Am Soc Nephrol, 6*(6), 1286-1291. doi:10.2215/CJN.07210810

Hofstra, J. M., Debiec, H., Short, C. D., Pelle, T., Kleta, R., Mathieson, P. W., Ronco, P., Brenchley, P. E., &Wetzels, J. F. (2012). Antiphospholipase A2 receptor antibody titer and subclass in idiopathic membranous nephropathy. *J Am Soc Nephrol, 23*(10), 1735-1743. doi:10.1681/ASN.2012030242

Hofstra, J. M., Fervenza, F. C., &Wetzels, J. F. (2013). Treatment of idiopathic membranous nephropathy. *Nat Rev Nephrol, 9*(8), 443-458. doi:10.1038/nrneph.2013.125

Hofstra, J. M., &Wetzels, J. F. (2010). Alkylating agents in membranous nephropathy: efficacy proven beyond doubt. *Nephrol Dial Transplant, 25*(6), 1760-1766. doi:10.1093/ndt/gfq017

Hoxha, E., Beck, L. H., Jr., Wiech, T., Tomas, N. M., Probst, C., Mindorf, S., Meyer-Schwesinger, C., Zahner, G., Stahl, P. R., Schopper, R., Panzer, U., Harendza, S., Helmchen, U., Salant, D. J., &Stahl, R. A. (2017). An Indirect Immunofluorescence Method Facilitates Detection of Thrombospondin Type 1 Domain-Containing 7A-Specific Antibodies in Membranous Nephropathy. *J Am Soc Nephrol, 28*(2), 520-531. doi:10.1681/ASN.2016010050

Hoxha, E., Harendza, S., Zahner, G., Panzer, U., Steinmetz, O., Fechner, K., Helmchen, U., &Stahl, R. A. (2011). An immunofluorescence test for phospholipase-A(2)-receptor antibodies and its clinical usefulness in patients with membranous glomerulonephritis. *Nephrol Dial Transplant, 26*(8), 2526-2532. doi:10.1093/ndt/gfr247

Hoxha, E., Kneissler, U., Stege, G., Zahner, G., Thiele, I., Panzer, U., Harendza, S., Helmchen, U. M., &Stahl, R. A. (2012). Enhanced expression of the M-type phospholipase A2 receptor in glomeruli correlates with serum receptor antibodies in primary membranous nephropathy. *Kidney Int, 82*(7), 797-804. doi:10.1038/ki.2012.209

Hoxha, E., Thiele, I., Zahner, G., Panzer, U., Harendza, S., &Stahl, R. A. (2014). Phospholipase A2 receptor autoantibodies and clinical outcome in patients with primary membranous nephropathy. *J Am Soc Nephrol, 25*(6), 1357-1366. doi:10.1681/ASN.2013040430

Hoxha, E., Zahner, G., Reinhard, L., &Stahl, R. A. (2018). PLA2R1 Epitope Recognition Patterns and Clinical Outcome in Patients with Membranous Nephropathy [ASN Kidney Week 2018, Poster Abstract: SA-PO342]. *J Am Heart Assoc, 29*, 823.

Hu, P., Xuan, Q., Hu, B., Lu, L., &Qin, Y. H. (2013). Anti-neutral endopeptidase, natriuretic peptides disarrangement, and proteinuria onset in membranous nephropathy. *Mol Biol Rep, 40*(4), 2963-2967. doi:10.1007/s11033-012-2367-4

Huang, C. C., Lehman, A., Albawardi, A., Satoskar, A., Brodsky, S., Nadasdy, G., Hebert, L., Rovin, B., &Nadasdy, T. (2013). IgG subclass staining in renal biopsies with membranous glomerulonephritis indicates subclass switch during disease progression. *Mod Pathol, 26*(6), 799-805. doi:10.1038/modpathol.2012.237

Huang, J., Attwe, A., Marcos, E., Amsellem, V., Breau, M., Kebe, K., Houssaini, A., Validire, P., Maitre, B., Vindrieux, D., Bernard, D., &Adnot, S. (2016). Genetic Inactivation of the Phospholipase A2 Receptor (PLA2R1) Protects Against Lung Cell Senescence in Chronic Obstructive Pulmonary Disease (COPD) [Poster Abstract at the American Thoracic Society 2016 International Conference]. *Am J Respir Crit Care Med, 193*, A2325. doi:10.1164/ajrccm-conference.2016.193.1_MeetingAbstracts.A2325

Hunley, T. E., Corzo, D., Dudek, M., Kishnani, P., Amalfitano, A., Chen, Y. T., Richards, S. M., Phillips, J. A., 3rd, Fogo, A. B., &Tiller, G. E. (2004). Nephrotic syndrome complicating alpha-glucosidase replacement therapy for Pompe disease. *Pediatrics, 114*(4), e532-535. doi:10.1542/peds.2003-0988-L

I

Ishizaki, J., Hanasaki, K., Higashino, K., Kishino, J., Kikuchi, N., Ohara, O., &Arita, H. (1994). Molecular cloning of pancreatic group I phospholipase A2 receptor. *J Biol Chem, 269*(8), 5897-5904.

Iwakura, T., Fujigaki, Y., Katahashi, N., Sato, T., Ishigaki, S., Tsuji, N., Naito, Y., Isobe, S., Ono, M., Sakao, Y., Tsuji, T., Ohashi, N., Kato, A., Miyajima, H., &Yasuda, H. (2016). Membranous Nephropathy with an Enhanced Granular Expression of Thrombospondin Type-1 Domain-containing 7A in a Pregnant Woman. *Intern Med, 55*(18), 2663-2668. doi:10.2169/internalmedicine.55.6726

J

Jacob, S., Viegas, S., Leite, M. I., Webster, R., Cossins, J., Kennett, R., Hilton-Jones, D., Morgan, B. P., &Vincent, A. (2012). Presence and pathogenic relevance of antibodies to clustered acetylcholine receptor in ocular and generalized myasthenia gravis. *Arch Neurol, 69*(8), 994-1001. doi:10.1001/archneurol.2012.437

Janeway, C. J., Travers, P., Walport, M., &Shlomchik, M. (2011). The complement system and innate immunity. In Immunobiology: The Immune System in Health and Disease. (5th Edition ed.). New York: Garland Science. Retrieved from https://www.ncbi.nlm.nih.gov/books/NBK10757/.

Jarad, G., &Miner, J. H. (2009). Update on the glomerular filtration barrier. *Curr Opin Nephrol Hypertens, 18*(3), 226-232.

Jefferson, J. A., Pippin, J. W., &Shankland, S. J. (2010). Experimental Models of Membranous Nephropathy. *Drug Discov Today Dis Models, 7*(1-2), 27-33. doi:10.1016/j.ddmod.2010.11.001

Jiang, W., Swiggard, W. J., Heufler, C., Peng, M., Mirza, A., Steinman, R. M., &Nussenzweig, M. C. (1995). The receptor DEC-205 expressed by dendritic cells and thymic epithelial cells is involved in antigen processing. *Nature, 375*(6527), 151-155. doi:10.1038/375151a0

Jones, D. B. (1957). Nephrotic glomerulonephritis. *Am J Pathol, 33*(2), 313-329.

Joshi, M., Burbelo, P. D., Waldman, M. A., Gordon, S. M., Thurlow, J. S., &Olson, S. W. (2018). Pre-Diagnostic Evaluation of Anti-Phospholipase A2 Receptor Antibodies in Primary Membranous Nephropathy [ASN Kidney Week 2018, SA-PO341]. *J Am Soc Nephrol, 29*, 823.

K

Kaminitz, A., Stein, J., Yaniv, I., &Askenasy, N. (2007). The vicious cycle of apoptotic beta-cell death in type 1 diabetes. *Immunol Cell Biol, 85*(8), 582-589. doi:10.1038/sj.icb.7100093

Kanigicherla, D., Gummadova, J., McKenzie, E. A., Roberts, S. A., Harris, S., Nikam, M., Poulton, K., McWilliam, L., Short, C. D., Venning, M., &Brenchley, P. E. (2013). Anti-PLA2R antibodies measured by ELISA predict long-term outcome in a prevalent population of patients with idiopathic membranous nephropathy. *Kidney Int, 83*(5), 940-948. doi:10.1038/ki.2012.486

Kanigicherla, D. A., Short, C. D., Roberts, S. A., Hamilton, P., Nikam, M., Harris, S., Brenchley, P. E., &Venning, M. C. (2016). Long-term outcomes of persistent disease and relapse in primary membranous nephropathy. *Nephrol Dial Transplant, 31*(12), 2108-2114. doi:10.1093/ndt/gfv435

Kao, L., Lam, V., Waldman, M., Glassock, R. J., &Zhu, Q. (2015). Identification of the immunodominant epitope region in phospholipase A2 receptor-mediating autoantibody binding in idiopathic membranous nephropathy. *J Am Soc Nephrol, 26*(2), 291-301. doi:10.1681/ASN.2013121315

Kawa, S., Kitahara, K., Hamano, H., Ozaki, Y., Arakura, N., Yoshizawa, K., Umemura, T., Ota, M., Mizoguchi, S., Shimozuru, Y., &Bahram, S. (2008). A novel immunoglobulin-immunoglobulin interaction in autoimmunity. *PLoS One, 3*(2), e1637. doi:10.1371/journal.pone.0001637

KDIGO Guidelines. (2012). Chapter 7: Idiopathic membranous nephropathy. *Kidney Int Suppl (2011), 2*(2), 186-197. doi:10.1038/kisup.2012.20

Kerjaschki, D., Exner, M., Ullrich, R., Susani, M., Curtiss, L. K., Witztum, J. L., Farquhar, M. G., &Orlando, R. A. (1997). Pathogenic antibodies inhibit the binding of apolipoproteins to megalin/gp330 in passive Heymann nephritis. *J Clin Invest, 100*(9), 2303-2309. doi:10.1172/JCI119768

Kerjaschki, D., &Farquhar, M. G. (1982). The pathogenic antigen of Heymann nephritis is a membrane glycoprotein of the renal proximal tubule brush border. *Proc Natl Acad Sci U S A, 79*(18), 5557-5561. doi:10.1073/pnas.79.18.5557

Kerjaschki, D., &Farquhar, M. G. (1983). Immunocytochemical localization of the Heymann nephritis antigen (GP330) in glomerular epithelial cells of normal Lewis rats. *J Exp Med, 157*(2), 667-686. doi:10.1084/jem.157.2.667

Kerjaschki, D., Miettinen, A., &Farquhar, M. G. (1987). Initial events in the formation of immune deposits in passive Heymann nephritis. gp330-anti-gp330 immune complexes form in epithelial coated pits and rapidly become attached to the glomerular basement membrane. *J Exp Med, 166*(1), 109-128. doi:10.1084/jem.166.1.109

Kerjaschki, D., Schulze, M., Binder, S., Kain, R., Ojha, P. P., Susani, M., Horvat, R., Baker, P. J., &Couser, W. G. (1989). Transcellular transport and membrane insertion of the C5b-9 membrane attack complex of complement by glomerular epithelial cells in experimental membranous nephropathy. *J Immunol, 143*(2), 546-552.

Kilpatrick, D. C. (1998). Phospholipid-binding activity of human mannan-binding lectin. *Immunol Lett, 61*(2-3), 191-195.

Kilpatrick, D. C. (2002). Animal lectins: a historical introduction and overview. *Biochim Biophys Acta, 1572*(2-3), 187-197.

Kim, H. J., Kim, K. S., Kim, S. H., Baek, S. H., Kim, H. Y., Lee, C., &Kim, J. R. (2009). Induction of cellular senescence by secretory phospholipase A2 in human dermal fibroblasts through an ROS-mediated p53 pathway. *J Gerontol A Biol Sci Med Sci, 64*(3), 351-362. doi:10.1093/gerona/gln055

Kim, S., Chin, H. J., Na, K. Y., Kim, S., Oh, J., Chung, W., Noh, J. W., Lee, Y. K., Cho, J. T., Lee, E. K., Chae, D. W., Progressive Renal, D., Medical, I., &Genomics Research, m. (2011). Single nucleotide polymorphisms in the phospholipase A2 receptor gene are associated with genetic susceptibility to idiopathic membranous nephropathy. *Nephron Clin Pract, 117*(3), c253-258. doi:10.1159/000320194

Kimura, Y., Miura, N., Debiec, H., Morita, H., Yamada, H., Banno, S., Ronco, P., &Imai, H. (2017). Circulating antibodies to alpha-enolase and phospholipase A2 receptor and composition of glomerular deposits in Japanese patients with primary or secondary membranous nephropathy. *Clin Exp Nephrol, 21*(1), 117-126. doi:10.1007/s10157-016-1235-2

Kini, R. M., &Evans, H. J. (1989). A model to explain the pharmacological effects of snake venom phospholipases A2. *Toxicon, 27*(6), 613-635.

Klouda, P. T., Manos, J., Acheson, E. J., Dyer, P. A., Goldby, F. S., Harris, R., Lawler, W., Mallick, N. P., &Williams, G. (1979). Strong association between idiopathic membranous nephropathy and HLA-DRW3. *Lancet, 2*(8146), 770-771. doi:10.1016/s0140-6736(79)92118-4

Knoppova, B., Reily, C., Maillard, N., Rizk, D. V., Moldoveanu, Z., Mestecky, J., Raska, M., Renfrow, M. B., Julian, B. A., &Novak, J. (2016). The Origin and Activities of IgA1-Containing Immune Complexes in IgA Nephropathy. *Front Immunol, 7*, 117. doi:10.3389/fimmu.2016.00117

Kolko, M., Bruhn, T., Christensen, T., Lazdunski, M., Lambeau, G., Bazan, N. G., &Diemer, N. H. (1999). Secretory phospholipase A2 potentiates glutamate-induced rat striatal neuronal cell death in vivo. *Neurosci Lett, 274*(3), 167-170. doi:10.1016/s0304-3940(99)00709-0

Kon, S. P., Coupes, B., Short, C. D., Solomon, L. R., Raftery, M. J., Mallick, N. P., &Brenchley, P. E. (1995). Urinary C5b-9 excretion and clinical course in idiopathic human membranous nephropathy. *Kidney Int, 48*(6), 1953-1958. doi:10.1038/ki.1995.496

Kuo, M. W., Wang, C. H., Wu, H. C., Chang, S. J., &Chuang, Y. J. (2011). Soluble THSD7A is an N-glycoprotein that promotes endothelial cell migration and tube formation in angiogenesis. *PLoS One, 6*(12), e29000. doi:10.1371/journal.pone.0029000

Kurien, B. T., &Scofield, R. H. (2008). Autoimmunity and oxidatively modified autoantigens. *Autoimmun Rev, 7*(7), 567-573. doi:10.1016/j.autrev.2008.04.019

Kuroki, A., Iyoda, M., Shibata, T., &Sugisaki, T. (2005). Th2 cytokines increase and stimulate B cells to produce IgG4 in idiopathic membranous nephropathy. *Kidney Int, 68*(1), 302-310. doi:10.1111/j.1523-1755.2005.00415.x

Kuroki, Y., Honma, T., Chiba, H., Sano, H., Saitoh, M., Ogasawara, Y., Sohma, H., &Akino, T. (1997). A novel type of binding specificity to phospholipids for rat mannose-binding proteins isolated from serum and liver. *FEBS Lett, 414*(2), 387-392.

L

Lai, K. N., Li, P. K., Lui, S. F., Au, T. C., Tam, J. S., Tong, K. L., &Lai, F. M. (1991). Membranous nephropathy related to hepatitis B virus in adults. *N Engl J Med, 324*(21), 1457-1463. doi:10.1056/NEJM199105233242103

Lai, W. L., Yeh, T. H., Chen, P. M., Chan, C. K., Chiang, W. C., Chen, Y. M., Wu, K. D., &Tsai, T. J. (2015). Membranous nephropathy: a review on the pathogenesis, diagnosis, and treatment. *J Formos Med Assoc, 114*(2), 102-111. doi:10.1016/j.jfma.2014.11.002

Lambeau, G., Ancian, P., Barhanin, J., &Lazdunski, M. (1994). Cloning and expression of a membrane receptor for secretory phospholipases A2. *J Biol Chem, 269*(3), 1575-1578.

Lambeau, G., Ancian, P., Nicolas, J. P., Beiboer, S. H., Moinier, D., Verheij, H., &Lazdunski, M. (1995). Structural elements of secretory phospholipases A2 involved in the binding to M-type receptors. *J Biol Chem, 270*(10), 5534-5540. doi:10.1074/jbc.270.10.5534

Lambeau, G., Barhanin, J., Schweitz, H., Qar, J., &Lazdunski, M. (1989). Identification and properties of very high affinity brain membrane-binding sites for a neurotoxic phospholipase from the taipan venom. *J Biol Chem, 264*(19), 11503-11510.

Lambeau, G., &Gelb, M. H. (2008). Biochemistry and physiology of mammalian secreted phospholipases A2. *Annu Rev Biochem, 77*, 495-520. doi:10.1146/annurev.biochem.76.062405.154007

Lambeau, G., Schmid-Alliana, A., Lazdunski, M., &Barhanin, J. (1990). Identification and purification of a very high affinity binding protein for toxic phospholipases A2 in skeletal muscle. *J Biol Chem, 265*(16), 9526-9532.

Land, J., Rutgers, A., &Kallenberg, C. G. (2014). Anti-neutrophil cytoplasmic autoantibody pathogenicity revisited: pathogenic versus non-pathogenic anti-neutrophil cytoplasmic autoantibody. *Nephrol Dial Transplant, 29*(4), 739-745. doi:10.1093/ndt/gft416

Larsen, C. P., Cossey, L. N., &Beck, L. H. (2016). THSD7A staining of membranous glomerulopathy in clinical practice reveals cases with dual autoantibody positivity. *Mod Pathol, 29*(4), 421-426. doi:10.1038/modpathol.2016.32

Larsen, C. P., Messias, N. C., Silva, F. G., Messias, E., &Walker, P. D. (2013). Determination of primary versus secondary membranous glomerulopathy utilizing phospholipase A2 receptor staining in renal biopsies. *Mod Pathol, 26*(5), 709-715. doi:10.1038/modpathol.2012.207

Larsen, C. P., Trivin-Avillach, C., Coles, P., Collins, A. B., Merchant, M., Ma, H., Wilkey, D. W., Ambruzs, J. M., Messias, N. C., Cossey, L. N., Rosales, I. A., Wooldridge, T., Walker, P. D., Colvin, R. B., Klein, J., Salant, D. J., &Beck, L. H., Jr. (2018). LDL Receptor-Related Protein 2 (Megalin) as a Target Antigen in Human Kidney Anti-Brush Border Antibody Disease. *J Am Soc Nephrol, 29*(2), 644-653. doi:10.1681/ASN.2017060664

Le Petit, J. C., Laurent, B., &Berthoux, F. C. (1982). HLA-DR3 and idiopathic membranous nephritis (IMN) association. *Tissue Antigens, 20*(3), 227-228.

Le, W. B., Shi, J. S., Zhang, T., Liu, L., Qin, H. Z., Liang, S., Zhang, Y. W., Zheng, C. X., Jiang, S., Qin, W. S., Zhang, H. T., &Liu, Z. H. (2017). HLA-DRB1*15:01 and HLA-DRB3*02:02 in PLA2R-Related Membranous Nephropathy. *J Am Soc Nephrol, 28*(5), 1642-1650. doi:10.1681/ASN.2016060644

Lee, T., Derebail, V. K., Kshirsagar, A. V., Chung, Y., Fine, J. P., Mahoney, S., Poulton, C. J., Lionaki, S., Hogan, S. L., Falk, R. J., Cattran, D. C., Hladunewich, M., Reich, H. N., &Nachman, P. H. (2016). Patients with primary membranous nephropathy are at high risk of cardiovascular events. *Kidney Int, 89*(5), 1111-1118. doi:10.1016/j.kint.2015.12.041

Leehey, D. J., Casini, T., &Massey, D. (2010). Remission of membranous nephropathy after therapy with Astragalus membranaceus. *Am J Kidney Dis, 55*(4), 772. doi:10.1053/j.ajkd.2010.01.012

Lhotta, K., Wurzner, R., &Konig, P. (1999). Glomerular deposition of mannose-binding lectin in human glomerulonephritis. *Nephrol Dial Transplant, 14*(4), 881-886. doi:10.1093/ndt/14.4.881

Li, J., Sullivan, J. A., &Ni, H. (2018). Pathophysiology of immune thrombocytopenia. *Curr Opin Hematol, 25*(5), 373-381. doi:10.1097/MOH.0000000000000447

Li, N., Aoki, V., Hans-Filho, G., Rivitti, E. A., &Diaz, L. A. (2003). The role of intramolecular epitope spreading in the pathogenesis of endemic pemphigus foliaceus (fogo selvagem). *J Exp Med, 197*(11), 1501-1510. doi:10.1084/jem.20022031

Lionaki, S., Derebail, V. K., Hogan, S. L., Barbour, S., Lee, T., Hladunewich, M., Greenwald, A., Hu, Y., Jennette, C. E., Jennette, J. C., Falk, R. J., Cattran, D. C., Nachman, P. H., &Reich, H. N. (2012). Venous thromboembolism in patients with membranous nephropathy. *Clin J Am Soc Nephrol, 7*(1), 43-51. doi:10.2215/CJN.04250511

Liu, D., Zhang, J., Shi, Y., &Liu, Z. (2019). Gene polymorphism and risk of idiopathic membranous nephropathy. *Life Sci, 229*, 124-131. doi:10.1016/j.lfs.2019.05.010

Liu, L. Y., Lin, M. H., Lai, Z. Y., Jiang, J. P., Huang, Y. C., Jao, L. E., &Chuang, Y. J. (2016). Motor neuron-derived Thsd7a is essential for zebrafish vascular development via the Notch-dll4 signaling pathway. *J Biomed Sci, 23*(1), 59. doi:10.1186/s12929-016-0277-9

Liu, Y., Chirino, A. J., Misulovin, Z., Leteux, C., Feizi, T., Nussenzweig, M. C., &Bjorkman, P. J. (2000). Crystal structure of the cysteine-rich domain of mannose receptor complexed with a sulfated carbohydrate ligand. *J Exp Med, 191*(7), 1105-1116. doi:10.1084/jem.191.7.1105

Liu, Y., Li, X., Ma, C., Wang, P., Liu, J., Su, H., Zhuo, H., Kong, X., Xu, D., &Xu, D. (2018). Serum anti-PLA2R antibody as a diagnostic biomarker of idiopathic membranous nephropathy: The optimal cut-off value for Chinese patients. *Clin Chim Acta, 476*, 9-14. doi:10.1016/j.cca.2017.11.006

Liu, Y. H., Chen, C. H., Chen, S. Y., Lin, Y. J., Liao, W. L., Tsai, C. H., Wan, L., &Tsai, F. J. (2010). Association of phospholipase A2 receptor 1 polymorphisms with idiopathic membranous nephropathy in Chinese patients in Taiwan. *J Biomed Sci, 17*, 81. doi:10.1186/1423-0127-17-81

Lleo, A., Invernizzi, P., Gao, B., Podda, M., &Gershwin, M. E. (2010). Definition of human autoimmunity--autoantibodies versus autoimmune disease. *Autoimmun Rev, 9*(5), A259-266. doi:10.1016/j.autrev.2009.12.002

Llorca, O. (2008). Extended and bent conformations of the mannose receptor family. *Cell Mol Life Sci, 65*(9), 1302-1310. doi:10.1007/s00018-007-7497-9

Ludwig, R. J., Vanhoorelbeke, K., Leypoldt, F., Kaya, Z., Bieber, K., McLachlan, S. M., Komorowski, L., Luo, J., Cabral-Marques, O., Hammers, C. M., Lindstrom, J. M., Lamprecht, P., Fischer, A., Riemekasten, G., Tersteeg, C., Sondermann, P., Rapoport, B., Wandinger, K. P., Probst, C., El Beidaq, A., Schmidt, E., Verkman, A., Manz, R. A., &Nimmerjahn, F. (2017). Mechanisms of Autoantibody-Induced Pathology. *Front Immunol, 8*, 603. doi:10.3389/fimmu.2017.00603

Luo, R., Wang, Y., Xu, P., Cao, G., Zhao, Y., Shao, X., Li, Y. X., Chang, C., Peng, C., &Wang, Y. L. (2016). Hypoxia-inducible miR-210 contributes to preeclampsia via targeting thrombospondin type I domain containing 7A. *Sci Rep, 6*, 19588. doi:10.1038/srep19588

M

Ma, H., Beck, L. H., &Salant, D. J. (2011). Membranous Nephropathy-Associated Anti-Phospholipase A2 Receptor IgG4 Autotantibodies Active the Lectin Complement Pathway [ASN Kidney Week 2011, Oral Abstract: FR-OR257]. *J Am Heart Assoc, 22*, 62A.

Ma, H., Salant, D. J., &Beck., L. H. (2015). Autoantibodies Target Multiple Epitopes in THSD7A in Primary Membranous Nephropathy [ASN Kidney Week, Poster Abstract: FR-PO966]. *J Am Soc Nephrol, 26*, 589A.

Ma, H., Sandor, D. G., &Beck, L. H., Jr. (2013). The role of complement in membranous nephropathy. *Semin Nephrol, 33*(6), 531-542. doi:10.1016/j.semnephrol.2013.08.004

Maguer-Satta, V., Besancon, R., &Bachelard-Cascales, E. (2011). Concise review: neutral endopeptidase (CD10): a multifaceted environment actor in stem cells, physiological mechanisms, and cancer. *Stem Cells, 29*(3), 389-396. doi:10.1002/stem.592

Makker, S. P., &Tramontano, A. (2006). Differential capacity of anti-RAP and anti-megalin antibodies to produce progressive passive Heymann nephritis - implications for the pathogenesis of idiopathic human membranous glomerulonephritis. *J Pathol, 210*(3), 282-287. doi:10.1002/path.2058

Malek, V., &Gaikwad, A. B. (2017). Neprilysin inhibitors: A new hope to halt the diabetic cardiovascular and renal complications? *Biomed Pharmacother, 90*, 752-759. doi:10.1016/j.biopha.2017.04.024

Malito, E., Hulse, R. E., &Tang, W. J. (2008). Amyloid beta-degrading cryptidases: insulin degrading enzyme, presequence peptidase, and neprilysin. *Cell Mol Life Sci, 65*(16), 2574-2585. doi:10.1007/s00018-008-8112-4

Martinez-Pomares, L. (2012). The mannose receptor. *J Leukoc Biol, 92*(6), 1177-1186. doi:10.1189/jlb.0512231

Martinez-Prat, L., Palterer, B., Vitiello, G., Parronchi, P., Robinson, W. H., &Mahler, M. (2019). Autoantibodies to protein-arginine deiminase (PAD) 4 in rheumatoid arthritis: immunological and clinical significance, and potential for precision medicine. *Expert Rev Clin Immunol*, 1-15. doi:10.1080/1744666X.2020.1668778

Masutani, K., Taniguchi, M., Nakashima, H., Yotsueda, H., Kudoh, Y., Tsuruya, K., Tokumoto, M., Fukuda, K., Kanai, H., Hirakata, H., &Iida, M. (2004). Up-regulated interleukin-4 production by peripheral T-helper cells in idiopathic membranous nephropathy. *Nephrol Dial Transplant, 19*(3), 580-586. doi:10.1093/ndt/gfg572

Matzaraki, V., Kumar, V., Wijmenga, C., &Zhernakova, A. (2017). The MHC locus and genetic susceptibility to autoimmune and infectious diseases. *Genome Biol, 18*(1), 76. doi:10.1186/s13059-017-1207-1

McAdoo, S. P., &Pusey, C. D. (2017). Anti-Glomerular Basement Membrane Disease. *Clin J Am Soc Nephrol, 12*(7), 1162-1172. doi:10.2215/CJN.01380217

McCall, A. S., Bhave, G., Pedchenko, V., Hess, J., Free, M., Little, D. J., Baker, T. P., Pendergraft, W. F., 3rd, Falk, R. J., Olson, S. W., &Hudson, B. G. (2018). Inhibitory Anti-Peroxidasin Antibodies in Pulmonary-Renal Syndromes. *J Am Soc Nephrol, 29*(11), 2619-2625. doi:10.1681/ASN.2018050519

McCluskey, J., Farris, A. D., Keech, C. L., Purcell, A. W., Rischmueller, M., Kinoshita, G., Reynolds, P., &Gordon, T. P. (1998). Determinant spreading: lessons from animal models and human disease. *Immunol Rev, 164*, 209-229. doi:10.1111/j.1600-065x.1998.tb01222.x

McGrogan, A., Franssen, C. F., &de Vries, C. S. (2011). The incidence of primary glomerulonephritis worldwide: a systematic review of the literature. *Nephrol Dial Transplant, 26*(2), 414-430. doi:10.1093/ndt/gfq665

McLean, M. H., Dieguez, D., Jr., Miller, L. M., &Young, H. A. (2015). Does the microbiota play a role in the pathogenesis of autoimmune diseases? *Gut, 64*(2), 332-341. doi:10.1136/gutjnl-2014-308514

Melander, M. C., Jurgensen, H. J., Madsen, D. H., Engelholm, L. H., &Behrendt, N. (2015). The collagen receptor uPARAP/Endo180 in tissue degradation and cancer (Review). *Int J Oncol, 47*(4), 1177-1188. doi:10.3892/ijo.2015.3120

Melchers, F., &Rolink, A. R. (2006). B cell tolerance--how to make it and how to break it. *Curr Top Microbiol Immunol, 305*, 1-23. doi:10.1007/3-540-29714-6_1

Mellors, R. C., Ortega, L. G., &Holman, H. R. (1957). Role of gamma globulins in pathogenesis of renal lesions in systemic lupus erythematosus and chronic membranous glomerulonephritis, with an observation on the lupus erythematosus cell reaction. *J Exp Med, 106*(2), 191-202. doi:10.1084/jem.106.2.191

Menschikowski, M., Hagelgans, A., Nacke, B., Jandeck, C., Sukocheva, O., &Siegert, G. (2015). Epigenetic control of phospholipase A2 receptor expression in mammary cancer cells. *BMC Cancer, 15*, 971. doi:10.1186/s12885-015-1937-y

Menschikowski, M., Platzbecker, U., Hagelgans, A., Vogel, M., Thiede, C., Schonefeldt, C., Lehnert, R., Eisenhofer, G., &Siegert, G. (2012). Aberrant methylation of the M-type phospholipase A(2) receptor gene in leukemic cells. *BMC Cancer, 12*, 576. doi:10.1186/1471-2407-12-576

Mentzel, S., van Son, J. P., Dijkman, H. B., Wetzels, J. F., &Assmann, K. J. (1999). Induction of albuminuria in mice: synergistic effect of two monoclonal antibodies directed to different domains of aminopeptidase A. *Kidney Int, 55*(4), 1335-1347. doi:10.1046/j.1523-1755.1999.00362.x

Meyer-Schwesinger, C., Dehde, S., Klug, P., Becker, J. U., Mathey, S., Arefi, K., Balabanov, S., Venz, S., Endlich, K. H., Pekna, M., Gessner, J. E., Thaiss, F., &Meyer, T. N. (2011). Nephrotic

syndrome and subepithelial deposits in a mouse model of immune-mediated anti-podocyte glomerulonephritis. *J Immunol, 187*(6), 3218-3229. doi:10.4049/jimmunol.1003451

Meyer-Schwesinger, C., Lambeau, G., &Stahl, R. A. (2015). Thrombospondin type-1 domain-containing 7A in idiopathic membranous nephropathy. *N Engl J Med, 372*(11), 1074-1075. doi:10.1056/NEJMc1500130

Mishina, H., Watanabe, K., Tamaru, S., Watanabe, Y., Fujioka, D., Takahashi, S., Suzuki, K., Nakamura, T., Obata, J. E., Kawabata, K., Yokota, Y., Inoue, O., Murakami, M., Hanasaki, K., &Kugiyama, K. (2014). Lack of phospholipase A2 receptor increases susceptibility to cardiac rupture after myocardial infarction. *Circ Res, 114*(3), 493-504. doi:10.1161/CIRCRESAHA.114.302319

Mishra, D., Singh, S., &Narayan, G. (2016). Role of B Cell Development Marker CD10 in Cancer Progression and Prognosis. *Mol Biol Int, 2016*, 4328697. doi:10.1155/2016/4328697

Mitchell, J. A., Knowles, R. B., Kirkby, N. S., Reed, D. M., Edin, M. L., White, W. E., Chan, M. V., Longhurst, H., Yaqoob, M. M., Milne, G. L., Zeldin, D. C., &Warner, T. D. (2018). Kidney Transplantation in a Patient Lacking Cytosolic Phospholipase A2 Proves Renal Origins of Urinary PGI-M and TX-M. *Circ Res, 122*(4), 555-559. doi:10.1161/CIRCRESAHA.117.312144

Moodie, F. D., Leaker, B., Cambridge, G., Totty, N. F., &Segal, A. W. (1993). Alpha-enolase: a novel cytosolic autoantigen in ANCA positive vasculitis. *Kidney Int, 43*(3), 675-681. doi:10.1038/ki.1993.97

Morello, J. P., Petaja-Repo, U. E., Bichet, D. G., &Bouvier, M. (2000). Pharmacological chaperones: a new twist on receptor folding. *Trends Pharmacol Sci, 21*(12), 466-469.

Morita, M., Mii, A., Shimizu, A., Yasuda, F., Shoji, J., Masuda, Y., Ohashi, R., Nagahama, K., Kaneko, T., &Tsuruoka, S. (2015). Glomerular endothelial cell injury and focal segmental glomerulosclerosis lesion in idiopathic membranous nephropathy. *PLoS One, 10*(4), e0116700. doi:10.1371/journal.pone.0116700

Moudgil, K. D. (1998). Diversification of response to hsp65 during the course of autoimmune arthritis is regulatory rather than pathogenic. *Immunol Rev, 164*, 175-184. doi:10.1111/j.1600-065x.1998.tb01219.x

Muller, G. A., Muller, C., Liebau, G., Kompf, J., Ising, H., &Wernet, P. (1981). Strong association of idiopathic membranous nephropathy (IMN) with HLA-DR 3 and MT-2 without involvement of HLA-B 18 and no association to BfF1. *Tissue Antigens, 17*(3), 332-337.

Murakami, M., &Lambeau, G. (2013). Emerging roles of secreted phospholipase A(2) enzymes: an update. *Biochimie, 95*(1), 43-50. doi:10.1016/j.biochi.2012.09.007

Murakami, M., Sato, H., Miki, Y., Yamamoto, K., &Taketomi, Y. (2015). A new era of secreted phospholipase A(2). *J Lipid Res, 56*(7), 1248-1261. doi:10.1194/jlr.R058123

Murakami, M., Taketomi, Y., Sato, H., &Yamamoto, K. (2011). Secreted phospholipase A2 revisited. *J Biochem, 150*(3), 233-255. doi:10.1093/jb/mvr088

Murtas, C., Bruschi, M., Candiano, G., Moroni, G., Magistroni, R., Magnano, A., Bruno, F., Radice, A., Furci, L., Argentiero, L., Carnevali, M. L., Messa, P., Scolari, F., Sinico, R. A., Gesualdo, L., Fervenza, F. C., Allegri, L., Ravani, P., &Ghiggeri, G. M. (2012). Coexistence of different circulating anti-podocyte antibodies in membranous nephropathy. *Clin J Am Soc Nephrol, 7*(9), 1394-1400. doi:10.2215/CJN.02170312

Myers, L. K., Myllyharju, J., Nokelainen, M., Brand, D. D., Cremer, M. A., Stuart, J. M., Bodo, M., Kivirikko, K. I., &Kang, A. H. (2004). Relevance of posttranslational modifications for the arthritogenicity of type II collagen. *J Immunol, 172*(5), 2970-2975. doi:10.4049/jimmunol.172.5.2970

N

Nakahara, K., Takahashi, H., Okuse, C., Shigefuku, R., Yamada, N., Murao, M., Matsunaga, K., Koike, J., Yotsuyanagi, H., Suzuki, M., Kimura, K., &Itoh, F. (2010). Membranous nephropathy associated with chronic hepatitis B occurring in a short period after acute hepatitis B virus infection. *Intern Med, 49*(5), 383-388. doi:10.2169/internalmedicine.49.2812

Nakatsue, T., Koike, H., Han, G. D., Suzuki, K., Miyauchi, N., Yuan, H., Salant, D. J., Gejyo, F., Shimizu, F., &Kawachi, H. (2005). Nephrin and podocin dissociate at the onset of proteinuria in experimental membranous nephropathy. *Kidney Int, 67*(6), 2239-2253. doi:10.1111/j.1523-1755.2005.00328.x

Nangaku, M., Shankland, S. J., &Couser, W. G. (2005). Cellular response to injury in membranous nephropathy. *J Am Soc Nephrol, 16*(5), 1195-1204. doi:10.1681/ASN.2004121098

Napper, C. E., Dyson, M. H., &Taylor, M. E. (2001). An extended conformation of the macrophage mannose receptor. *J Biol Chem, 276*(18), 14759-14766. doi:10.1074/jbc.M100425200

Nicolas, J. P., Lambeau, G., &Lazdunski, M. (1995). Identification of the binding domain for secretory phospholipases A2 on their M-type 180-kDa membrane receptor. *J Biol Chem, 270*(48), 28869-28873. doi:10.1074/jbc.270.48.28869

Nolin, J. D., Ogden, H. L., Lai, Y., Altemeier, W. A., Frevert, C. W., Bollinger, J. G., Naika, G. S., Kicic, A., Stick, S. M., Lambeau, G., Henderson, W. R., Jr., Gelb, M. H., &Hallstrand, T. S. (2016). Identification of Epithelial Phospholipase A2 Receptor 1 as a Potential Target in Asthma. *Am J Respir Cell Mol Biol, 55*(6), 825-836. doi:10.1165/rcmb.2015-0150OC

O

Ohashi, P. S., &DeFranco, A. L. (2002). Making and breaking tolerance. *Curr Opin Immunol, 14*(6), 744-759. doi:10.1016/s0952-7915(02)00406-5

P

Pan, Y., Wan, J., Liu, Y., Yang, Q., Liang, W., Singhal, P. C., Saleem, M. A., &Ding, G. (2014). sPLA2 IB induces human podocyte apoptosis via the M-type phospholipase A2 receptor. *Sci Rep, 4*, 6660. doi:10.1038/srep06660

Passerini, P., Malvica, S., Tripodi, F., Cerutti, R., &Messa, P. (2019). Membranous Nephropathy (MN) Recurrence After Renal Transplantation. *Front Immunol, 10*, 1326. doi:10.3389/fimmu.2019.01326

Pedchenko, V., Bondar, O., Fogo, A. B., Vanacore, R., Voziyan, P., Kitching, A. R., Wieslander, J., Kashtan, C., Borza, D. B., Neilson, E. G., Wilson, C. B., &Hudson, B. G. (2010). Molecular architecture of the Goodpasture autoantigen in anti-GBM nephritis. *N Engl J Med, 363*(4), 343-354. doi:10.1056/NEJMoa0910500

Pedchenko, V., Vanacore, R., &Hudson, B. (2011). Goodpasture's disease: molecular architecture of the autoantigen provides clues to etiology and pathogenesis. *Curr Opin Nephrol Hypertens, 20*(3), 290-296. doi:10.1097/MNH.0b013e328344ff20

Pepys, M. B., &Butler, P. J. (1987). Serum amyloid P component is the major calcium-dependent specific DNA binding protein of the serum. *Biochem Biophys Res Commun, 148*(1), 308-313.

Pickford, A. R., Potts, J. R., Bright, J. R., Phan, I., &Campbell, I. D. (1997). Solution structure of a type 2 module from fibronectin: implications for the structure and function of the gelatin-binding domain. *Structure, 5*(3), 359-370.

Polanco, N., Gutierrez, E., Covarsi, A., Ariza, F., Carreno, A., Vigil, A., Baltar, J., Fernandez-Fresnedo, G., Martin, C., Pons, S., Lorenzo, D., Bernis, C., Arrizabalaga, P., Fernandez-Juarez, G., Barrio, V., Sierra, M., Castellanos, I., Espinosa, M., Rivera, F., Oliet, A., Fernandez-Vega, F., Praga, M., &Grupo de Estudio de las Enfermedades Glomerulares de la Sociedad Espanola de, N. (2010). Spontaneous remission of nephrotic syndrome in idiopathic membranous nephropathy. *J Am Soc Nephrol, 21*(4), 697-704. doi:10.1681/ASN.2009080861

Ponticelli, C., Altieri, P., Scolari, F., Passerini, P., Roccatello, D., Cesana, B., Melis, P., Valzorio, B., Sasdelli, M., Pasquali, S., Pozzi, C., Piccoli, G., Lupo, A., Segagni, S., Antonucci, F., Dugo, M., Minari, M., Scalia, A., Pedrini, L., Pisano, G., Grassi, C., Farina, M., &Bellazzi, R. (1998). A randomized study comparing methylprednisolone plus chlorambucil versus methylprednisolone plus cyclophosphamide in idiopathic membranous nephropathy. *J Am Soc Nephrol, 9*(3), 444-450.

Ponticelli, C., &Glassock, R. J. (2014). Glomerular diseases: membranous nephropathy--a modern view. *Clin J Am Soc Nephrol, 9*(3), 609-616. doi:10.2215/CJN.04160413

Ponticelli, C., Zucchelli, P., Imbasciati, E., Cagnoli, L., Pozzi, C., Passerini, P., Grassi, C., Limido, D., Pasquali, S., Volpini, T., &et al. (1984). Controlled trial of methylprednisolone and chlorambucil in idiopathic membranous nephropathy. *N Engl J Med, 310*(15), 946-950. doi:10.1056/NEJM198404123101503

Ponticelli, C., Zucchelli, P., Passerini, P., Cesana, B., Locatelli, F., Pasquali, S., Sasdelli, M., Redaelli, B., Grassi, C., Pozzi, C., &et al. (1995). A 10-year follow-up of a randomized study with methylprednisolone and chlorambucil in membranous nephropathy. *Kidney Int, 48*(5), 1600-1604.

Poole, B. D., Scofield, R. H., Harley, J. B., &James, J. A. (2006). Epstein-Barr virus and molecular mimicry in systemic lupus erythematosus. *Autoimmunity, 39*(1), 63-70. doi:10.1080/08916930500484849

Poole, B. D., Templeton, A. K., Guthridge, J. M., Brown, E. J., Harley, J. B., &James, J. A. (2009). Aberrant Epstein-Barr viral infection in systemic lupus erythematosus. *Autoimmun Rev, 8*(4), 337-342. doi:10.1016/j.autrev.2008.12.008

Pourcine, F., Dahan, K., Mihout, F., Cachanado, M., Brocheriou, I., Debiec, H., &Ronco, P. (2017). Prognostic value of PLA2R autoimmunity detected by measurement of anti-PLA2R antibodies combined with detection of PLA2R antigen in membranous nephropathy: A single-centre study over 14 years. *PLoS One, 12*(3), e0173201. doi:10.1371/journal.pone.0173201

Pozdzik, A., Brocheriou, I., David, C., Touzani, F., Goujon, J. M., &Wissing, K. M. (2018). Membranous Nephropathy and Anti-Podocytes Antibodies: Implications for the Diagnostic Workup and Disease Management. *Biomed Res Int, 2018*, 6281054. doi:10.1155/2018/6281054

Praga, M., Barrio, V., Juarez, G. F., Luno, J., &Grupo Espanol de Estudio de la Nefropatia, M. (2007). Tacrolimus monotherapy in membranous nephropathy: a randomized controlled trial. *Kidney Int, 71*(9), 924-930. doi:10.1038/sj.ki.5002215

Pratesi, F., Moscato, S., Sabbatini, A., Chimenti, D., Bombardieri, S., &Migliorini, P. (2000). Autoantibodies specific for alpha-enolase in systemic autoimmune disorders. *J Rheumatol, 27*(1), 109-115.

Prunotto, M., Carnevali, M. L., Candiano, G., Murtas, C., Bruschi, M., Corradini, E., Trivelli, A., Magnasco, A., Petretto, A., Santucci, L., Mattei, S., Gatti, R., Scolari, F., Kador, P., Allegri, L., &Ghiggeri, G. M. (2010). Autoimmunity in membranous nephropathy targets aldose reductase and SOD2. *J Am Soc Nephrol, 21*(3), 507-519. doi:10.1681/ASN.2008121259

Pungercar, J., &Krizaj, I. (2007). Understanding the molecular mechanism underlying the presynaptic toxicity of secreted phospholipases A2. *Toxicon, 50*(7), 871-892. doi:10.1016/j.toxicon.2007.07.025

Q

Qin, H. Z., Zhang, M. C., Le, W. B., Ren, Q., Chen, D. C., Zeng, C. H., Liu, L., Zuo, K., Xu, F., &Liu, Z. H. (2016). Combined Assessment of Phospholipase A2 Receptor Autoantibodies and Glomerular Deposits in Membranous Nephropathy. *J Am Soc Nephrol, 27*(10), 3195-3203. doi:10.1681/ASN.2015080953

Qin, X. S., Liu, J. H., Lyu, G. T., Peng, M. L., Yang, F. N., Qin, D. C., Li, Y. Z., &Liu, Y. (2017). Variants in the Promoter Region of HLA-DQA1 were Associated with Idiopathic Membranous Nephropathy in a Chinese Han Population. *Chin Med J (Engl), 130*(14), 1677-1682. doi:10.4103/0366-6999.209884

R

Ramachandran, R., Kumar, V., Kumar, A., Yadav, A. K., Nada, R., Kumar, H., Kumar, V., Rathi, M., Kohli, H. S., Gupta, K. L., Sakhuja, V., &Jha, V. (2016). PLA2R antibodies, glomerular PLA2R deposits and variations in PLA2R1 and HLA-DQA1 genes in primary membranous nephropathy in South Asians. *Nephrol Dial Transplant, 31*(9), 1486-1493. doi:10.1093/ndt/gfv399

Raychaudhuri, S., Sandor, C., Stahl, E. A., Freudenberg, J., Lee, H. S., Jia, X., Alfredsson, L., Padyukov, L., Klareskog, L., Worthington, J., Siminovitch, K. A., Bae, S. C., Plenge, R. M., Gregersen, P. K., &de Bakker, P. I. (2012). Five amino acids in three HLA proteins explain most of the association between MHC and seropositive rheumatoid arthritis. *Nat Genet, 44*(3), 291-296. doi:10.1038/ng.1076

Raychowdhury, R., Niles, J. L., McCluskey, R. T., &Smith, J. A. (1989). Autoimmune target in Heymann nephritis is a glycoprotein with homology to the LDL receptor. *Science, 244*(4909), 1163-1165. doi:10.1126/science.2786251

Reichert, L. J., Koene, R. A., &Wetzels, J. F. (1998). Prognostic factors in idiopathic membranous nephropathy. *Am J Kidney Dis, 31*(1), 1-11.

Reinhard, L., Zahner, G., Menzel, S., Koch-nolte, F., Stahl, R. A., &Hoxha, E. A Novel ELISA Allows Exact PLA2R1 Domain-Specific Autoantibody Quantification in Sera from Patients with Membranous Nephropathy [ASN Kidney Week 2019, Poster Abstract: FR-PO812]. *J Am Soc Nephrol*(30), 650.

Remuzzi, G., Chiurchiu, C., Abbate, M., Brusegan, V., Bontempelli, M., &Ruggenenti, P. (2002). Rituximab for idiopathic membranous nephropathy. *Lancet, 360*(9337), 923-924. doi:10.1016/S0140-6736(02)11042-7

Rhoden, S. J., Lausecker, F., Fresquet, M., Adamson, A., Jowitt, T. A., Brenchley, P. E., &Lennon, R. (2018). Generating a Mouse Model of Membranous Nephropathy (MN) [ASN Kidney Week 2018, SA-PO339]. *J Am Soc Nephrol, 29*, 823.

Rigopoulou, E. I., Roggenbuck, D., Smyk, D. S., Liaskos, C., Mytilinaiou, M. G., Feist, E., Conrad, K., &Bogdanos, D. P. (2012). Asialoglycoprotein receptor (ASGPR) as target autoantigen in liver autoimmunity: lost and found. *Autoimmun Rev, 12*(2), 260-269. doi:10.1016/j.autrev.2012.04.005

Rispens, T., Ooievaar-De Heer, P., Vermeulen, E., Schuurman, J., van der Neut Kolfschoten, M., &Aalberse, R. C. (2009). Human IgG4 binds to IgG4 and conformationally altered IgG1 via Fc-Fc interactions. *J Immunol, 182*(7), 4275-4281. doi:10.4049/jimmunol.0804338

Ritz, S. A. (2010). Air pollution as a potential contributor to the 'epidemic' of autoimmune disease. *Med Hypotheses, 74*(1), 110-117. doi:10.1016/j.mehy.2009.07.033

Roccatello, D., Sciascia, S., Di Simone, D., Solfietti, L., Naretto, C., Fenoglio, R., Baldovino, S., &Menegatti, E. (2016). New insights into immune mechanisms underlying response to Rituximab in patients with membranous nephropathy: A prospective study and a review of the literature. *Autoimmun Rev, 15*(6), 529-538. doi:10.1016/j.autrev.2016.02.014

Rodas, L. M., Matas-Garcia, A., Barros, X., Blasco, M., Vinas, O., Llobell, A., Martin, N., &Quintana, L. F. (2019). Antiphospholipase 2 receptor antibody levels to predict complete spontaneous remission in primary membranous nephropathy. *Clin Kidney J, 12*(1), 36-41. doi:10.1093/ckj/sfy005

Rodien, P., Madec, A. M., Ruf, J., Rajas, F., Bornet, H., Carayon, P., &Orgiazzi, J. (1996). Antibody-dependent cell-mediated cytotoxicity in autoimmune thyroid disease: relationship to

antithyroperoxidase antibodies. *J Clin Endocrinol Metab, 81*(7), 2595-2600. doi:10.1210/jcem.81.7.8675583

Rodriguez, E. F., Cosio, F. G., Nasr, S. H., Sethi, S., Fidler, M. E., Stegall, M. D., Grande, J. P., Fervenza, F. C., &Cornell, L. D. (2012). The pathology and clinical features of early recurrent membranous glomerulonephritis. *Am J Transplant, 12*(4), 1029-1038. doi:10.1111/j.1600-6143.2011.03903.x

Rojas-Rivera, J. E., Carriazo, S., &Ortiz, A. (2019). Treatment of idiopathic membranous nephropathy in adults: KDIGO 2012, cyclophosphamide and cyclosporine A are out, rituximab is the new normal. *Clin Kidney J, 12*(5), 629-638. doi:10.1093/ckj/sfz127

Ronco, P., &Debiec, H. (2015). Membranous nephropathy: A fairy tale for immunopathologists, nephrologists and patients. *Mol Immunol, 68*(1), 57-62. doi:10.1016/j.molimm.2015.07.003

Ronco, P., &Debiec, H. (2015). Pathophysiological advances in membranous nephropathy: time for a shift in patient's care. *Lancet, 385*(9981), 1983-1992. doi:10.1016/S0140-6736(15)60731-0

Ronco, P., &Debiec, H. (2017). A podocyte view of membranous nephropathy: from Heymann nephritis to the childhood human disease. *Pflugers Arch, 469*(7-8), 997-1005. doi:10.1007/s00424-017-2007-x

Rondas, D., Crevecoeur, I., D'Hertog, W., Ferreira, G. B., Staes, A., Garg, A. D., Eizirik, D. L., Agostinis, P., Gevaert, K., Overbergh, L., &Mathieu, C. (2015). Citrullinated glucose-regulated protein 78 is an autoantigen in type 1 diabetes. *Diabetes, 64*(2), 573-586. doi:10.2337/db14-0621

Roozendaal, C., Zhao, M. H., Horst, G., Lockwood, C. M., Kleibeuker, J. H., Limburg, P. C., Nelis, G. F., &Kallenberg, C. G. (1998). Catalase and alpha-enolase: two novel granulocyte autoantigens in inflammatory bowel disease (IBD). *Clin Exp Immunol, 112*(1), 10-16. doi:10.1046/j.1365-2249.1998.00528.x

Rosenzwajg, M., Languille, E., Debiec, H., Hygino, J., Dahan, K., Simon, T., Klatzmann, D., &Ronco, P. (2017). B- and T-cell subpopulations in patients with severe idiopathic membranous nephropathy may predict an early response to rituximab. *Kidney Int, 92*(1), 227-237. doi:10.1016/j.kint.2017.01.012

Roth, A. J., Ooi, J. D., Hess, J. J., van Timmeren, M. M., Berg, E. A., Poulton, C. E., McGregor, J., Burkart, M., Hogan, S. L., Hu, Y., Winnik, W., Nachman, P. H., Stegeman, C. A., Niles, J., Heeringa, P., Kitching, A. R., Holdsworth, S., Jennette, J. C., Preston, G. A., &Falk, R. J. (2013). Epitope specificity determines pathogenicity and detectability in ANCA-associated vasculitis. *J Clin Invest, 123*(4), 1773-1783. doi:10.1172/JCI65292

Rouault, M., Le Calvez, C., Boilard, E., Surrel, F., Singer, A., Ghomashchi, F., Bezzine, S., Scarzello, S., Bollinger, J., Gelb, M. H., &Lambeau, G. (2007). Recombinant production and properties of binding of the full set of mouse secreted phospholipases A2 to the mouse M-type receptor. *Biochemistry, 46*(6), 1647-1662. doi:10.1021/bi062119b

Roy, S., Biswas, S., Saroha, A., Sahu, D., &Das, H. R. (2013). Enhanced expression and fucosylation of ficolin3 in plasma of RA patients. *Clin Biochem, 46*(1-2), 160-163. doi:10.1016/j.clinbiochem.2012.10.028

Rozenberg, I., Kotliroff, A., Zahavi, T., &Benchetrit, S. (2018). Outcome of Idiopathic Membranous Nephropathy: A Retrospective Study. *Isr Med Assoc J, 20*(3), 186-189.

Ruggenenti, P., Cravedi, P., Chianca, A., Perna, A., Ruggiero, B., Gaspari, F., Rambaldi, A., Marasa, M., &Remuzzi, G. (2012). Rituximab in idiopathic membranous nephropathy. *J Am Soc Nephrol, 23*(8), 1416-1425. doi:10.1681/ASN.2012020181

Ruggenenti, P., Debiec, H., Ruggiero, B., Chianca, A., Pelle, T., Gaspari, F., Suardi, F., Gagliardini, E., Orisio, S., Benigni, A., Ronco, P., &Remuzzi, G. (2015). Anti-Phospholipase A2 Receptor Antibody Titer Predicts Post-Rituximab Outcome of Membranous Nephropathy. *J Am Soc Nephrol, 26*(10), 2545-2558. doi:10.1681/ASN.2014070640

Rutenber, E., &Robertus, J. D. (1991). Structure of ricin B-chain at 2.5 A resolution. *Proteins, 10*(3), 260-269. doi:10.1002/prot.340100310

S

Saeed, M., Beggs, M. L., Walker, P. D., &Larsen, C. P. (2014). PLA2R-associated membranous glomerulopathy is modulated by common variants in PLA2R1 and HLA-DQA1 genes. *Genes Immun, 15*(8), 556-561. doi:10.1038/gene.2014.50

Salant, D. J. (2019). Unmet challenges in membranous nephropathy. *Curr Opin Nephrol Hypertens, 28*(1), 70-76. doi:10.1097/MNH.0000000000000459

Salant, D. J., Belok, S., Madaio, M. P., &Couser, W. G. (1980). A new role for complement in experimental membranous nephropathy in rats. *J Clin Invest, 66*(6), 1339-1350. doi:10.1172/JCI109987

Salant, D. J., &Cybulsky, A. V. (1988). Experimental glomerulonephritis. *Methods Enzymol, 162*, 421-461. doi:10.1016/0076-6879(88)62096-9

Salant, D. J., Quigg, R. J., &Cybulsky, A. V. (1989). Heymann nephritis: mechanisms of renal injury. *Kidney Int, 35*(4), 976-984. doi:10.1038/ki.1989.81

Schieppati, A., Mosconi, L., Perna, A., Mecca, G., Bertani, T., Garattini, S., &Remuzzi, G. (1993). Prognosis of untreated patients with idiopathic membranous nephropathy. *N Engl J Med, 329*(2), 85-89. doi:10.1056/NEJM199307083290203

Schmidt, E., Kasperkiewicz, M., &Joly, P. (2019). Pemphigus. *Lancet, 394*(10201), 882-894. doi:10.1016/S0140-6736(19)31778-7

Scholz-Pedretti, K., Gans, A., Beck, K. F., Pfeilschifter, J., &Kaszkin, M. (2002). Potentiation of TNF-alpha-stimulated group IIA phospholipase A(2) expression by peroxisome proliferator-activated receptor alpha activators in rat mesangial cells. *J Am Soc Nephrol, 13*(3), 611-620.

Schulze, M., Donadio, J. V., Jr., Pruchno, C. J., Baker, P. J., Johnson, R. J., Stahl, R. A., Watkins, S., Martin, D. C., Wurzner, R., Gotze, O., &et al. (1991). Elevated urinary excretion of the C5b-9 complex in membranous nephropathy. *Kidney Int, 40*(3), 533-538. doi:10.1038/ki.1991.242

Scott, R. P., &Quaggin, S. E. (2015). Review series: The cell biology of renal filtration. *J Cell Biol, 209*(2), 199-210. doi:10.1083/jcb.201410017

Seifert, L., Hoxha, E., Eichhoff, A. M., Zahner, G., Dehde, S., Reinhard, L., Koch-Nolte, F., Stahl, R. A. K., &Tomas, N. M. (2018). The Most N-Terminal Region of THSD7A Is the Predominant Target for Autoimmunity in THSD7A-Associated Membranous Nephropathy. *J Am Soc Nephrol, 29*(5), 1536-1548. doi:10.1681/ASN.2017070805

Seikrit, C., Ronco, P., &Debiec, H. (2018). Factor H Autoantibodies and Membranous Nephropathy. *N Engl J Med, 379*(25), 2479-2481. doi:10.1056/NEJMc1805857

Seitz-Polski, B., Dahan, K., Debiec, H., Rousseau, A., Andreani, M., Zaghrini, C., Ticchioni, M., Rosenthal, A., Benzaken, S., Bernard, G., Lambeau, G., Ronco, P., &Esnault, V. L. M. (2019). High-Dose Rituximab and Early Remission in PLA2R1-Related Membranous Nephropathy. *Clin J Am Soc Nephrol, 14*(8), 1173-1182. doi:10.2215/CJN.11791018

Seitz-Polski, B., Debiec, H., Rousseau, A., Dahan, K., Zaghrini, C., Payre, C., Esnault, V. L. M., Lambeau, G., &Ronco, P. (2018). Phospholipase A2 Receptor 1 Epitope Spreading at Baseline Predicts Reduced Likelihood of Remission of Membranous Nephropathy. *J Am Soc Nephrol, 29*(2), 401-408. doi:10.1681/ASN.2017070734

Seitz-Polski, B., Dolla, G., Payre, C., Girard, C. A., Polidori, J., Zorzi, K., Birgy-Barelli, E., Jullien, P., Courivaud, C., Krummel, T., Benzaken, S., Bernard, G., Burtey, S., Mariat, C., Esnault, V. L., &Lambeau, G. (2016). Epitope Spreading of Autoantibody Response to PLA2R Associates with Poor Prognosis in Membranous Nephropathy. *J Am Soc Nephrol, 27*(5), 1517-1533. doi:10.1681/ASN.2014111061

Seitz-Polski, B., Dolla, G., Payre, C., Tomas, N. M., Lochouarn, M., Jeammet, L., Mariat, C., Krummel, T., Burtey, S., Courivaud, C., Schlumberger, W., Zorzi, K., Benzaken, S., Bernard, G., Esnault, V. L., &Lambeau, G. (2015). Cross-reactivity of anti-PLA2R1 autoantibodies to rabbit and mouse PLA2R1 antigens and development of two novel ELISAs with different diagnostic performances in idiopathic membranous nephropathy. *Biochimie, 118*, 104-115. doi:10.1016/j.biochi.2015.08.007

Seitz-Polski, B., Payre, C., Ambrosetti, D., Albano, L., Cassuto-Viguier, E., Berguignat, M., Jeribi, A., Thouret, M. C., Bernard, G., Benzaken, S., Lambeau, G., &Esnault, V. L. (2014). Prediction of membranous nephropathy recurrence after transplantation by monitoring of anti-PLA2R1 (M-type phospholipase A2 receptor) autoantibodies: a case series of 15 patients. *Nephrol Dial Transplant, 29*(12), 2334-2342. doi:10.1093/ndt/gfu252

Sekula, P., Li, Y., Stanescu, H. C., Wuttke, M., Ekici, A. B., Bockenhauer, D., Walz, G., Powis, S. H., Kielstein, J. T., Brenchley, P., Investigators, G., Eckardt, K. U., Kronenberg, F., Kleta, R., &Kottgen, A. (2017). Genetic risk variants for membranous nephropathy: extension of and association with other chronic kidney disease aetiologies. *Nephrol Dial Transplant, 32*(2), 325-332. doi:10.1093/ndt/gfw001

Sethi, S., Debiec, H., Madden, B., Charlesworth, M. C., Morelle, J., Gross, L., Ravindran, A., Buob, D., Jadoul, M., Fervenza, F. C., &Ronco, P. (2019). Neural epidermal growth factor-like1 protein (NELL-1) associated membranous nephropathy. *Kidney International*. doi:10.1016/j.kint.2019.09.014

Sethi, S., Madden, B. J., Debiec, H., Charlesworth, M. C., Gross, L., Ravindran, A., Hummel, A. M., Specks, U., Fervenza, F. C., &Ronco, P. (2019). Exostosin 1/Exostosin 2-Associated Membranous Nephropathy. *J Am Soc Nephrol, 30*(6), 1123-1136. doi:10.1681/ASN.2018080852

Shah, P., Tramontano, A., &Makker, S. P. (2007). Intramolecular epitope spreading in Heymann nephritis. *J Am Soc Nephrol, 18*(12), 3060-3066. doi:10.1681/ASN.2007030342

Shah, S., Wu, E., Rao, V. K., &Tarrant, T. K. (2014). Autoimmune lymphoproliferative syndrome: an update and review of the literature. *Curr Allergy Asthma Rep, 14*(9), 462. doi:10.1007/s11882-014-0462-4

Shamriz, O., Mizrahi, H., Werbner, M., Shoenfeld, Y., Avni, O., &Koren, O. (2016). Microbiota at the crossroads of autoimmunity. *Autoimmun Rev, 15*(9), 859-869. doi:10.1016/j.autrev.2016.07.012

Sis, B., Tasanarong, A., Khoshjou, F., Dadras, F., Solez, K., &Halloran, P. F. (2007). Accelerated expression of senescence associated cell cycle inhibitor p16INK4A in kidneys with glomerular disease. *Kidney Int, 71*(3), 218-226. doi:10.1038/sj.ki.5002039

Skoberne, A., Behnert, A., Teng, B., Fritzler, M. J., Schiffer, L., Pajek, J., Lindic, J., Haller, H., &Schiffer, M. (2014). Serum with phospholipase A2 receptor autoantibodies interferes with podocyte adhesion to collagen. *Eur J Clin Invest, 44*(8), 753-765. doi:10.1111/eci.12292

Spicer, S. T., Tran, G. T., Killingsworth, M. C., Carter, N., Power, D. A., Paizis, K., Boyd, R., Hodgkinson, S. J., &Hall, B. M. (2007). Induction of passive Heymann nephritis in complement component 6-deficient PVG rats. *J Immunol, 179*(1), 172-178. doi:10.4049/jimmunol.179.1.172

Sribar, J., Oberckal, J., &Krizaj, I. (2014). Understanding the molecular mechanism underlying the presynaptic toxicity of secreted phospholipases A(2): an update. *Toxicon, 89*, 9-16. doi:10.1016/j.toxicon.2014.06.019

Stahl, P., Schlesinger, P. H., Sigardson, E., Rodman, J. S., &Lee, Y. C. (1980). Receptor-mediated pinocytosis of mannose glycoconjugates by macrophages: characterization and evidence for receptor recycling. *Cell, 19*(1), 207-215. doi:10.1016/0092-8674(80)90402-x

Stahl, P. R., Hoxha, E., Wiech, T., Schroder, C., Simon, R., &Stahl, R. A. (2017). THSD7A expression in human cancer. *Genes Chromosomes Cancer, 56*(4), 314-327. doi:10.1002/gcc.22440

Stanescu, H. C., Arcos-Burgos, M., Medlar, A., Bockenhauer, D., Kottgen, A., Dragomirescu, L., Voinescu, C., Patel, N., Pearce, K., Hubank, M., Stephens, H. A., Laundy, V., Padmanabhan, S., Zawadzka, A., Hofstra, J. M., Coenen, M. J., den Heijer, M., Kiemeney, L. A., Bacq-Daian, D., Stengel, B., Powis, S. H., Brenchley, P., Feehally, J., Rees, A. J., Debiec, H., Wetzels, J. F., Ronco, P., Mathieson, P. W., &Kleta, R. (2011). Risk HLA-DQA1 and PLA(2)R1 alleles in idiopathic membranous nephropathy. *N Engl J Med, 364*(7), 616-626. doi:10.1056/NEJMoa1009742

Stehle, T., Audard, V., Ronco, P., &Debiec, H. (2015). Phospholipase A2 receptor and sarcoidosis-associated membranous nephropathy. *Nephrol Dial Transplant, 30*(6), 1047-1050. doi:10.1093/ndt/gfv080

Stoddard, S. V., Welsh, C. L., Palopoli, M. M., Stoddard, S. D., Aramandla, M. P., Patel, R. M., Ma, H., &Beck, L. H., Jr. (2019). Structure and function insights garnered from in silico modeling of the thrombospondin type-1 domain-containing 7A antigen. *Proteins, 87*(2), 136-145. doi:10.1002/prot.25640

Svobodova, B., Honsova, E., Ronco, P., Tesar, V., &Debiec, H. (2013). Kidney biopsy is a sensitive tool for retrospective diagnosis of PLA2R-related membranous nephropathy. *Nephrol Dial Transplant, 28*(7), 1839-1844. doi:10.1093/ndt/gfs439

Syam, N., Chatel, S., Ozhathil, L. C., Sottas, V., Rougier, J. S., Baruteau, A., Baron, E., Amarouch, M. Y., Daumy, X., Probst, V., Schott, J. J., &Abriel, H. (2016). Variants of Transient Receptor Potential Melastatin Member 4 in Childhood Atrioventricular Block. *J Am Heart Assoc, 5*(5). doi:10.1161/JAHA.114.001625

T – U

Takahashi, S., Watanabe, K., Watanabe, Y., Fujioka, D., Nakamura, T., Nakamura, K., Obata, J. E., &Kugiyama, K. (2015). C-type lectin-like domain and fibronectin-like type II domain of phospholipase A(2) receptor 1 modulate binding and migratory responses to collagen. *FEBS Lett, 589*(7), 829-835. doi:10.1016/j.febslet.2015.02.016

Takekoshi, Y., Tanaka, M., Miyakawa, Y., Yoshizawa, H., Takahashi, K., &Mayumi, M. (1979). Free "small" and IgG-associated "large" hepatitis B e antigen in the serum and glomerular capillary walls of two patients with membranous glomerulonephritis. *N Engl J Med, 300*(15), 814-819. doi:10.1056/NEJM197904123001502

Tamaru, S., Mishina, H., Watanabe, Y., Watanabe, K., Fujioka, D., Takahashi, S., Suzuki, K., Nakamura, T., Obata, J. E., Kawabata, K., Yokota, Y., Murakami, M., Hanasaki, K., &Kugiyama, K. (2013). Deficiency of phospholipase A2 receptor exacerbates ovalbumin-induced lung inflammation. *J Immunol, 191*(3), 1021-1028. doi:10.4049/jimmunol.1300738

Tampoia, M., Migliucci, F., Villani, C., Abbracciavento, L., Rossini, M., Fumarulo, R., Gesualdo, L., &Montinaro, V. (2018). Definition of a new cut-off for the anti-phospholipase A2 receptor (PLA2R) autoantibody immunoassay in patients affected by idiopathic membranous nephropathy. *J Nephrol, 31*(6), 899-905. doi:10.1007/s40620-018-0533-z

Tavakolpour, S. (2017). Towards personalized medicine for patients with autoimmune diseases: Opportunities and challenges. *Immunol Lett, 190*, 130-138. doi:10.1016/j.imlet.2017.08.002

Taylor, M. E., Conary, J. T., Lennartz, M. R., Stahl, P. D., &Drickamer, K. (1990). Primary structure of the mannose receptor contains multiple motifs resembling carbohydrate-recognition domains. *J Biol Chem, 265*(21), 12156-12162.

Taylor, M. E., &Drickamer, K. (2019). Mammalian sugar-binding receptors: known functions and unexplored roles. *FEBS J, 286*(10), 1800-1814. doi:10.1111/febs.14759

Taylor, R. P., &Lindorfer, M. A. (2008). Immunotherapeutic mechanisms of anti-CD20 monoclonal antibodies. *Curr Opin Immunol, 20*(4), 444-449. doi:10.1016/j.coi.2008.05.011

Thiri, M., Honda, K., Kashiwase, K., Mabuchi, A., Suzuki, H., Watanabe, K., Nakayama, M., Watanabe, T., Doi, K., Tokunaga, K., &Noiri, E. (2016). High-density Association Mapping and Interaction Analysis of PLA2R1 and HLA Regions with Idiopathic Membranous Nephropathy in Japanese. *Sci Rep, 6*, 38189. doi:10.1038/srep38189

Timmermans, S. A., Abdul Hamid, M. A., Cohen Tervaert, J. W., Damoiseaux, J. G., van Paassen, P., &Limburg Renal, R. (2015). Anti-PLA2R Antibodies as a Prognostic Factor in PLA2R-Related Membranous Nephropathy. *Am J Nephrol, 42*(1), 70-77. doi:10.1159/000437236

Tomas, N. M., Beck, L. H., Jr., Meyer-Schwesinger, C., Seitz-Polski, B., Ma, H., Zahner, G., Dolla, G., Hoxha, E., Helmchen, U., Dabert-Gay, A. S., Debayle, D., Merchant, M., Klein, J., Salant, D. J., Stahl, R. A. K., &Lambeau, G. (2014). Thrombospondin type-1 domain-containing 7A in idiopathic membranous nephropathy. *N Engl J Med, 371*(24), 2277-2287. doi:10.1056/NEJMoa1409354

Tomas, N. M., Hoxha, E., Reinicke, A. T., Fester, L., Helmchen, U., Gerth, J., Bachmann, F., Budde, K., Koch-Nolte, F., Zahner, G., Rune, G., Lambeau, G., Meyer-Schwesinger, C., &Stahl, R. A. (2016). Autoantibodies against thrombospondin type 1 domain-containing 7A induce membranous nephropathy. *J Clin Invest, 126*(7), 2519-2532. doi:10.1172/JCI85265

Tomas, N. M., Meyer-Schwesinger, C., von Spiegel, H., Kotb, A. M., Zahner, G., Hoxha, E., Helmchen, U., Endlich, N., Koch-Nolte, F., &Stahl, R. A. K. (2017). A Heterologous Model of Thrombospondin Type 1 Domain-Containing 7A-Associated Membranous Nephropathy. *J Am Soc Nephrol, 28*(11), 3262-3277. doi:10.1681/ASN.2017010030

Tomura, S., Kashiwabara, H., Tuchida, H., Shishido, H., Sakurai, S., Miyajima, T., Tsuji, K., &Takeuchi, J. (1984). Strong association of idiopathic membranous nephropathy with HLA-DR2 and MT1 in Japanese. *Nephron, 36*(4), 242-245. doi:10.1159/000183162

Towbin, H., Staehelin, T., &Gordon, J. (1979). Electrophoretic transfer of proteins from polyacrylamide gels to nitrocellulose sheets: procedure and some applications. *Proc Natl Acad Sci U S A, 76*(9), 4350-4354. doi:10.1073/pnas.76.9.4350

Tramontano, A., Knight, T., Vizzuso, D., &Makker, S. P. (2006). Nested N-terminal megalin fragments induce high-titer autoantibody and attenuated Heymann nephritis. *J Am Soc Nephrol, 17*(7), 1979-1985. doi:10.1681/ASN.2005101144

Tramontano, A., &Makker, S. P. (2004). Conformation and glycosylation of a megalin fragment correlate with nephritogenicity in Heymann nephritis. *J Immunol, 172*(4), 2367-2373. doi:10.4049/jimmunol.172.4.2367

Tryggvason, K., &Patrakka, J. (2006). Thin basement membrane nephropathy. *J Am Soc Nephrol, 17*(3), 813-822. doi:10.1681/ASN.2005070737

Tryggvason, K., &Wartiovaara, J. (2005). How does the kidney filter plasma? *Physiology (Bethesda), 20*, 96-101. doi:10.1152/physiol.00045.2004

V

Val-Bernal, J. F., Garijo, M. F., Val, D., Rodrigo, E., &Arias, M. (2011). C4d immunohistochemical staining is a sensitive method to confirm immunoreactant deposition in formalin-fixed paraffin-embedded tissue in membranous glomerulonephritis. *Histol Histopathol, 26*(11), 1391-1397. doi:10.14670/HH-26.1391

Valesini, G., Gerardi, M. C., Iannuccelli, C., Pacucci, V. A., Pendolino, M., &Shoenfeld, Y. (2015). Citrullination and autoimmunity. *Autoimmun Rev, 14*(6), 490-497. doi:10.1016/j.autrev.2015.01.013

Van Damme, B. J., Fleuren, G. J., Bakker, W. W., Vernier, R. L., &Hoedemaeker, P. J. (1978). Experimental glomerulonephritis in the rat induced by antibodies directed against tubular antigens. V. Fixed glomerular antigens in the pathogenesis of heterologous immune complex glomerulonephritis. *Lab Invest, 38*(4), 502-510.

van de Logt, A. E., Dahan, K., Rousseau, A., van der Molen, R., Debiec, H., Ronco, P., &Wetzels, J. (2018). Immunological remission in PLA2R-antibody-associated membranous nephropathy: cyclophosphamide versus rituximab. *Kidney Int, 93*(4), 1016-1017. doi:10.1016/j.kint.2017.12.019

van de Logt, A. E., Fresquet, M., Wetzels, J. F., &Brenchley, P. (2019). The anti-PLA2R antibody in membranous nephropathy: what we know and what remains a decade after its discovery. *Kidney Int*. doi:10.1016/j.kint.2019.07.014

van de Logt, A. E., Hofstra, J. M., &Wetzels, J. F. (2015). Serum anti-PLA2R antibodies can be initially absent in idiopathic membranous nephropathy: seroconversion after prolonged follow-up. *Kidney Int, 87*(6), 1263-1264. doi:10.1038/ki.2015.34

van den Brand, J. A., Hofstra, J. M., &Wetzels, J. F. (2012). Prognostic value of risk score and urinary markers in idiopathic membranous nephropathy. *Clin J Am Soc Nephrol, 7*(8), 1242-1248. doi:10.2215/CJN.00670112

van der Neut Kolfschoten, M., Schuurman, J., Losen, M., Bleeker, W. K., Martinez-Martinez, P., Vermeulen, E., den Bleker, T. H., Wiegman, L., Vink, T., Aarden, L. A., De Baets, M. H., van de Winkel, J. G., Aalberse, R. C., &Parren, P. W. (2007). Anti-inflammatory activity of human IgG4

antibodies by dynamic Fab arm exchange. *Science, 317*(5844), 1554-1557. doi:10.1126/science.1144603

Vanacore, R., Pedchenko, V., Bhave, G., &Hudson, B. G. (2011). Sulphilimine cross-links in Goodpasture's disease. *Clin Exp Immunol, 164 Suppl 1*, 4-6. doi:10.1111/j.1365-2249.2011.04356.x

Vanderlugt, C. J., &Miller, S. D. (1996). Epitope spreading. *Curr Opin Immunol, 8*(6), 831-836.

Vanderlugt, C. L., &Miller, S. D. (2002). Epitope spreading in immune-mediated diseases: implications for immunotherapy. *Nat Rev Immunol, 2*(2), 85-95. doi:10.1038/nri724

Vaughan, R. W., Demaine, A. G., &Welsh, K. I. (1989). A DQA1 allele is strongly associated with idiopathic membranous nephropathy. *Tissue Antigens, 34*(5), 261-269.

Venkatesha, S., Durai, M., &Moudgil, K. D. (2015). Chapter 4 - Epitope Spreading in Autoimmune Diseases. In *Infection and Autoimmunity (Second Edition)* (Second Edition ed., pp. 45-68): Academic Press.

Vignesh, P., Rawat, A., Sharma, M., &Singh, S. (2017). Complement in autoimmune diseases. *Clin Chim Acta, 465*, 123-130. doi:10.1016/j.cca.2016.12.017

Villanueva, E. B., Little, J. P., Lambeau, G., &Klegeris, A. (2012). Secreted phospholipase A(2) group IIA is a neurotoxin released by stimulated human glial cells. *Mol Cell Neurosci, 49*(4), 430-438. doi:10.1016/j.mcn.2012.02.006

Vindrieux, D., Augert, A., Girard, C. A., Gitenay, D., Lallet-Daher, H., Wiel, C., Le Calve, B., Gras, B., Ferrand, M., Verbeke, S., de Launoit, Y., Leroy, X., Puisieux, A., Aubert, S., Perrais, M., Gelb, M., Simonnet, H., Lambeau, G., &Bernard, D. (2013). PLA2R1 mediates tumor suppression by activating JAK2. *Cancer Res, 73*(20), 6334-6345. doi:10.1158/0008-5472.CAN-13-0318

Vindrieux, D., Devailly, G., Augert, A., Le Calve, B., Ferrand, M., Pigny, P., Payen, L., Lambeau, G., Perrais, M., Aubert, S., Simonnet, H., Dante, R., &Bernard, D. (2014). Repression of PLA2R1 by c-MYC and HIF-2alpha promotes cancer growth. *Oncotarget, 5*(4), 1004-1013. doi:10.18632/oncotarget.1681

Vivarelli, M., Emma, F., Pelle, T., Gerken, C., Pedicelli, S., Diomedi-Camassei, F., Klaus, G., Waldegger, S., Ronco, P., &Debiec, H. (2015). Genetic homogeneity but IgG subclass-dependent clinical variability of alloimmune membranous nephropathy with anti-neutral endopeptidase antibodies. *Kidney Int, 87*(3), 602-609. doi:10.1038/ki.2014.381

von Haxthausen, F., Reinhard, L., Pinnschmidt, H. O., Rink, M., Soave, A., Hoxha, E., &Stahl, R. A. K. (2018). Antigen-Specific IgG Subclasses in Primary and Malignancy-Associated Membranous Nephropathy. *Front Immunol, 9*, 3035. doi:10.3389/fimmu.2018.03035

W

Wahren-Herlenius, M., &Dorner, T. (2013). Immunopathogenic mechanisms of systemic autoimmune disease. *Lancet, 382*(9894), 819-831. doi:10.1016/S0140-6736(13)60954-X

Wakui, H., Imai, H., Komatsuda, A., &Miura, A. B. (1999). Circulating antibodies against alpha-enolase in patients with primary membranous nephropathy (MN). *Clin Exp Immunol, 118*(3), 445-450. doi:10.1046/j.1365-2249.1999.01080.x

Waldman, M., &Austin, H. A., 3rd. (2012). Treatment of idiopathic membranous nephropathy. *J Am Soc Nephrol, 23*(10), 1617-1630. doi:10.1681/ASN.2012010058

Wang, B., Zuo, K., Wu, Y., Huang, Q., Qin, W. S., Zeng, C. H., Li, L. S., &Liu, Z. H. (2011). Correlation between B lymphocyte abnormality and disease activity in patients with idiopathic membranous nephropathy. *J Int Med Res, 39*(1), 86-95. doi:10.1177/147323001103900111

Wang, C. H., Chen, I. H., Kuo, M. W., Su, P. T., Lai, Z. Y., Wang, C. H., Huang, W. C., Hoffman, J., Kuo, C. J., You, M. S., &Chuang, Y. J. (2011). Zebrafish Thsd7a is a neural protein required for angiogenic patterning during development. *Dev Dyn, 240*(6), 1412-1421. doi:10.1002/dvdy.22641

Wang, C. H., Su, P. T., Du, X. Y., Kuo, M. W., Lin, C. Y., Yang, C. C., Chan, H. S., Chang, S. J., Kuo, C., Seo, K., Leung, L. L., &Chuang, Y. J. (2010). Thrombospondin type I domain containing 7A (THSD7A) mediates endothelial cell migration and tube formation. *J Cell Physiol, 222*(3), 685-694. doi:10.1002/jcp.21990

Wang, J., Cui, Z., Lu, J., Probst, C., Zhang, Y. M., Wang, X., Qu, Z., Wang, F., Meng, L. Q., Cheng, X. Y., Liu, G., Debiec, H., Ronco, P., &Zhao, M. H. (2017). Circulating Antibodies against Thrombospondin Type-I Domain-Containing 7A in Chinese Patients with Idiopathic Membranous Nephropathy. *Clin J Am Soc Nephrol, 12*(10), 1642-1651. doi:10.2215/CJN.01460217

Wang, L., Wang, F. S., &Gershwin, M. E. (2015). Human autoimmune diseases: a comprehensive update. *J Intern Med, 278*(4), 369-395. doi:10.1111/joim.12395

Wang, W., Fan, S., Li, G., Wang, A. Y., Hong, D., Zhong, X., &Wang, L. (2018). Interaction between PLA2R1 and HLA-DQA1 variants contributes to the increased genetic susceptibility to membranous nephropathy in Western China. *Nephrology (Carlton)*. doi:10.1111/nep.13536

Warren, S. J., Arteaga, L. A., Rivitti, E. A., Aoki, V., Hans-Filho, G., Qaqish, B. F., Lin, M. S., Giudice, G. J., &Diaz, L. A. (2003). The role of subclass switching in the pathogenesis of endemic pemphigus foliaceus. *J Invest Dermatol, 120*(1), 104-108. doi:10.1046/j.1523-1747.2003.12017.x

West, A. P., Jr., Herr, A. B., &Bjorkman, P. J. (2004). The chicken yolk sac IgY receptor, a functional equivalent of the mammalian MHC-related Fc receptor, is a phospholipase A2 receptor homolog. *Immunity, 20*(5), 601-610.

Wiebke, S., Sachs, M., C., M.-S., &Meyer-Schwesinger, A. G. (2018). The Proteasomal Degradation System Plays a Prominent Role in Podocyte Protein Homeostasis [ASN Kidney Week 2018, Poster Abstract: SA-PO377]. *J Am Soc Nephrol, 29*, 832.

Wu, K., Yuan, J., &Lasky, L. A. (1996). Characterization of a novel member of the macrophage mannose receptor type C lectin family. *J Biol Chem, 271*(35), 21323-21330. doi:10.1074/jbc.271.35.21323

X

Xu, J., Hu, X., Xie, J., &Chen, N. (2015). Management of Membranous Nephropathy in Asia. *Kidney Dis (Basel), 1*(2), 119-125. doi:10.1159/000437288

Xu, X., Wang, G., Chen, N., Lu, T., Nie, S., Xu, G., Zhang, P., Luo, Y., Wang, Y., Wang, X., Schwartz, J., Geng, J., &Hou, F. F. (2016). Long-Term Exposure to Air Pollution and Increased Risk of Membranous Nephropathy in China. *J Am Soc Nephrol, 27*(12), 3739-3746. doi:10.1681/ASN.2016010093

Y

Yalow, R. S., &Berson, S. A. (1960). Plasma insulin concentrations in nondiabetic and early diabetic subjects. Determinations by a new sensitive immuno-assay technic. *Diabetes, 9*, 254-260. doi:10.2337/diab.9.4.254

Yokota, Y., Ikeda, M., Higashino, K., Nakano, K., Fujii, N., Arita, H., &Hanasaki, K. (2000). Enhanced tissue expression and elevated circulating level of phospholipase A(2) receptor during murine endotoxic shock. *Arch Biochem Biophys, 379*(1), 7-17. doi:10.1006/abbi.2000.1849

Z

Zaghrini, C. (2019). *THSD7A, le second auto-antigène de la glomérulonéphrite extra-membraneuse : nouveau test diagnostique et identification des épitopes immunodominants* (Thèse de doctorat en Sciences de la vie et de la santé), Université Nice-Sophia Antipolis,

Zaghrini, C., Seitz-Polski, B., Justino, J., Dolla, G., Payre, C., Jourde-Chiche, N., Van de Logt, A. E., Booth, C., Rigby, E., Lonnbro-Widgren, J., Nystrom, J., Mariat, C., Cui, Z., Wetzels, J. F. M., Ghiggeri, G., Beck, L. H., Jr., Ronco, P., Debiec, H., &Lambeau, G. (2019). Novel ELISA for thrombospondin type 1 domain-containing 7A autoantibodies in membranous nephropathy. *Kidney Int, 95*(3), 666-679. doi:10.1016/j.kint.2018.10.024

Zahner, G., Hoxha, E., &Stahl, R. A. (2012). The Generation of Inducible Podocyte Specific Human Phospholipase A2 Receptor-1 Transgenic Mice [ASN Kidney Week 2012, Poster Abstract: FR-PO874]. *J Am Soc Nephrol, 23*, 568A.

Zahner, G., Meyer-Schwesinger, C., Tomas, N. M., Hoxha, E., Wiech, T., &Stahl, R. A. (2014). Development, and Morphologic Characteriziation of a Mouse Model of Membranous Nephropathy Involving the Human Phospholipase A2 Receptor [ASN Kidney Week 2014, Oral Abstract: FR-OR085]. *J Am Soc Nephrol, 25*, 66A.

Zelensky, A. N., &Gready, J. E. (2003). Comparative analysis of structural properties of the C-type-lectin-like domain (CTLD). *Proteins, 52*(3), 466-477. doi:10.1002/prot.10626

Zelensky, A. N., &Gready, J. E. (2004). C-type lectin-like domains in Fugu rubripes. *BMC Genomics, 5*(1), 51. doi:10.1186/1471-2164-5-51

Zelensky, A. N., &Gready, J. E. (2005). The C-type lectin-like domain superfamily. *FEBS J, 272*(24), 6179-6217. doi:10.1111/j.1742-4658.2005.05031.x

Zhang, M. F., Huang, J., Zhang, Y. M., Qu, Z., Wang, X., Wang, F., Meng, L. Q., Cheng, X. Y., Cui, Z., Liu, G., &Zhao, M. H. (2019). Complement activation products in the circulation and urine of primary membranous nephropathy. *BMC Nephrol, 20*(1), 313. doi:10.1186/s12882-019-1509-5

Zhang, X. D., Cui, Z., &Zhao, M. H. (2018). The Genetic and Environmental Factors of Primary Membranous Nephropathy: An Overview from China. *Kidney Dis (Basel), 4*(2), 65-73. doi:10.1159/000487136

Zhang, Z., Shi, Y., Yang, K., Crew, R., Wang, H., &Jiang, Y. (2017). Higher frequencies of circulating ICOS(+), IL-21(+) T follicular helper cells and plasma cells in patients with new-onset membranous nephropathy. *Autoimmunity, 50*(8), 458-467. doi:10.1080/08916934.2017.1385775

Zhao, C. N., Xu, Z., Wu, G. C., Mao, Y. M., Liu, L. N., Qian, W., Dan, Y. L., Tao, S. S., Zhang, Q., Sam, N. B., Fan, Y. G., Zou, Y. F., Ye, D. Q., &Pan, H. F. (2019). Emerging role of air pollution in autoimmune diseases. *Autoimmun Rev, 18*(6), 607-614. doi:10.1016/j.autrev.2018.12.010

Zvaritch, E., Lambeau, G., &Lazdunski, M. (1996). Endocytic properties of the M-type 180-kDa receptor for secretory phospholipases A2. *J Biol Chem, 271*(1), 250-257. doi:10.1074/jbc.271.1.250